Ministry of Energy, Mines and Petroleum Resources
Oil and Gas Division
Resource Development and Geoscience Branch

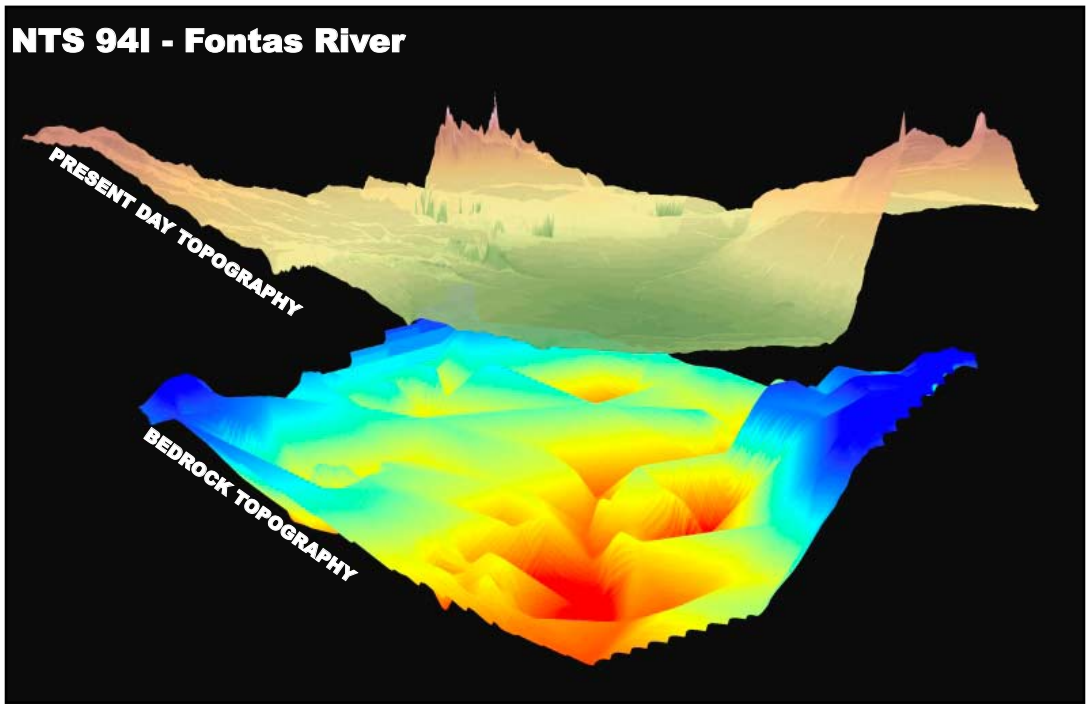

Summary of Activities 2004

BRITISH COLUMBIA
The Best Place on Earth

TABLE OF CONTENTS

Western Canada Sedimentary Basin

Best, M.E., Levson, V.M. and McConnell, D.
Sand and Gravel Mapping in Northeast British Columbia Using Airborne Electromagnetic Surveying Methods 1

Ibrahimbas, A. and Riediger, C.
Hydrocarbon Source Rock Potential as Determined by Rock-Eval VI/TOC Pyrolysis, N.E. B.C. and N.W. Alberta 7

Johnsen, T., Ferbey, T., Levson, V.M. and Kerr, B.
Quaternary Geology and Aggregate Potential of the Fort Nelson Airport Area 19

Levson, V.M., Ferbey, T., Kerr, B., Johnsen, T., Bednarski, J., Smith, R., Blackwell, J. and Jonnes, S.
Quaternary Geology and Aggregate Mapping in Northeast British Columbia: Applications for Oil and Gas Exploration and Development 29

Ryan, B.
The CBM Resource of Some Prospective Areas of the Crowsnest Coalfield 41

Ryan, B., Todoschuck, T. and Lane, B.
A Note on the Market Potential of Low-Volatile Bituminous Coal, Willow Creek Property, Northeastern British Columbia 57

Interior Basins

Hayes, M., Ferri, F. and Morii, S.
Interior Basins Strategy 71

Best, M.E.
Qualitative Interpretation of Potential Field Profiles: Southern Nechako Basin 75

English, J.M., Fowler, M., Johnston, S.T., Mihalynuk, M.G. and Wight, K.L.
Thermal Maturity in the Central Whitehorse Trough, Northwest British Columbia 81

Ferri, F., Osadetz, K. and Evenchick C.
Petroleum Source Rock Potential of Lower to Middle Jurassic Clastics, Intermontane Basins, British Columbia 89

Osadetz, K.G., Jiang, C., Evenchick, C.A., Ferri, F., Stasiuk, L.D., Wilson, N.S.F. and Hayes, M. Sterane
Compositional Traits of Bowser and Sustut Basin Crude Oils: Indications for Three Effective Petroleum Systems 101

Wight, K.L., English, J.M. and Johnston, S.T.
Structural Relationship Between the Laberge Group and Sinwa Formation on Copper Island, Southern Atlin Lake, Northwest British Columbia 117

Coal Bed Gas and CO_2 Sequestration

Ryan, B.
Unique Aspects of British Columbia CBM Geology: Influences on Produceability 125

Ryan, B. and Richardson, D.
The Potential for CO_2 Sequestration in British Columbia Coal Seams 141

Voormeij, D.A. and Simandl, G.J.
Ultramafic Rocks in British Columbia: Delineating Targets for Mineral Sequestration of CO_2 161

Library and Archives Canada Cataloguing in Publication Data
British Columbia. Resource Development and Geoscience Branch.
Summary of activities. –- 2004 -

Annual.
Issued also in CD ROM.
ISSN 1913-1275 = Summary of activities (British Columbia. Resource Development and Geoscience Branch. Print)

1. British Columbia. Resource Development and Geoscience Branch - Periodicals. 2. Geology, Economic - British Columbia - Periodicals. 3. Geology - British Columbia - Periodicals. I. Title. II. Title: Summary of activities ... Resource Development and Geoscience Branch.

TN177.B7B74 553. 09711’05 C2007-960048-4

Additional copies of this digital report can be obtained from:
Crown Publications
521 Fort Street,
Victoria, British Columbia,
Canada, V8W 1E7
http://www.crownpub.bc.ca/

or individual articles can be acquired at: http://www.em.gov.bc.ca/subwebs/oilandgas/pub/pub.htm

Cover: Preliminary reconstruction of the bedrock topography of NTS map area 94 I based on data from about 400 wireline-geophysical logs. Depth to bedrock varies from a few metres to as much as 280 metres. Buried bedrock valleys are interpreted as Late Tertiary to Pleistocene paleochannels that could be suitable targets for gas exploration. View towards southwest. For more information, see article by Levson, et al., (this volume).

In referencing articles within this publication, please use the format in the following example:

Ryan, B. and Richardson, D. (2004): The Potential for CO_2 Sequestration in British Columbia Coal Seams; in Summary of Activities 2004, BC Ministry of Energy and Mines, pages 137-156.

FOREWORD

Energy plays a vital role in achieving the goals and needs of our society. It is also a global issue that will challenge humanity's ingenuity in the coming decades. BC Ministry of Energy and Mines, in partnerships with communities, universities, governments, First Nations and other groups, will play an important role in developing British Columbia's energy future.

In 2002, the province of British Columbia released a new energy plan: "Energy for our Future: A Plan for BC". The British Columbia Government's approach to energy is multi-tiered, and includes conservation, efficiency and supply diversification. The latter embraces traditional sources such as hydroelectric, natural gas, oil and coal, together with renewable energy like geothermal, wind, solar and others.

To help maximize the benefits of British Columbia's endowment of energy resources, the BC Ministry of Energy and Mines is expanding geoscience activities related to hydrocarbons (including carbon management) and other energy sources. This inaugural volume presents the results of this new work. Staff from the BC Ministry of Energy and Mines' Oil and Gas Division, Resource Development and Geoscience Branch, contributed the majority of the articles contained in the volume.

The Geological Survey of Canada is a partner in several of the ongoing energy-related research projects within British Columbia. Geological Survey of Canada staff have co-authored or written several of the articles which discuss results from major projects in the Bowser Basin, Whitehorse Trough and aggregate mapping in the northeast part of the province. University research projects also play an important role.

Some of the highlights of this volume are:

- Hydrocarbon source rock potential in northeastern British Columbia
- Indications of three effective petroleum systems in the Bowser Basin
- Aggregate mapping in northeastern British Columbia and its oil and gas potential
- Potential CO_2 sequestration of coals and ultramafic rocks
- Unique aspects of coal bed gas geology in British Columbia
- Thermal maturity of the central Whitehorse Trough

Over the past two years the Resource Development and Geoscience Branch has published numerous Open Files and other products, including descriptions of tight and deep Devonian gas plays for the northeastern part of the province. The branch has also continued to improve and add new information to its website.

I sincerely thank all the authors for the long hours devoted towards these contributions. Special thanks go to Filippo Ferri for his dedication and vision. His perseverance and extra efforts paid off by the production of this volume. Collectively, their efforts made this first volume very successful. Our energetic, emerging Branch embraces change and continuous improvement and we look forward to serving a broad array of clients. To comment on any of these papers or to provide more general feedback, please contact Derek Brown at (250) 952-0432 or Derek.brown@gems6.gov.bc.ca.

Derek Brown
Executive Director,
Resource Development and Geoscience Branch
Ministry of Energy and Mines

TABLE OF CONTENTS

Western Canada Sedimentary Basin

Best, M.E., Levson, V.M. and McConnell, D.
Sand and Gravel Mapping in Northeast British Columbia Using Airborne Electromagnetic Surveying Methods 1

Ibrahimbas, A. and Riediger, C.
Hydrocarbon Source Rock Potential as Determined by Rock-Eval VI/TOC Pyrolysis, N.E. B.C. and N.W. Alberta 7

Johnsen, T., Ferbey, T., Levson, V.M. and Kerr, B.
Quaternary Geology and Aggregate Potential of the Fort Nelson Airport Area 19

Levson, V.M., Ferbey, T., Kerr, B., Johnsen, T., Bednarski, J., Smith, R., Blackwell, J. and Jonnes, S.
Quaternary Geology and Aggregate Mapping in Northeast British Columbia: Applications for Oil and Gas Exploration and Development 29

Ryan, B.
The CBM Resource of Some Prospective Areas of the Crowsnest Coalfield 41

Ryan, B., Todoschuck, T. and Lane, B.
A Note on the Market Potential of Low-Volatile Bituminous Coal, Willow Creek Property, Northeastern British Columbia 57

Interior Basins

Hayes, M., Ferri, F. and Morii, S.
Interior Basins Strategy 71

Best, M.E.
Qualitative Interpretation of Potential Field Profiles: Southern Nechako Basin 75

English, J.M., Fowler, M., Johnston, S.T., Mihalynuk, M.G. and Wight, K.L.
Thermal Maturity in the Central Whitehorse Trough, Northwest British Columbia 81

Ferri, F., Osadetz, K. and Evenchick C.
Petroleum Source Rock Potential of Lower to Middle Jurassic Clastics, Intermontane Basins, British Columbia 89

Osadetz, K.G., Jiang, C., Evenchick, C.A., Ferri, F., Stasiuk, L.D., Wilson, N.S.F. and Hayes, M. Sterane
Compositional Traits of Bowser and Sustut Basin Crude Oils: Indications for Three Effective Petroleum Systems 101

Wight, K.L., English, J.M. and Johnston, S.T.
Structural Relationship Between the Laberge Group and Sinwa Formation on Copper Island, Southern Atlin Lake, Northwest British Columbia 117

Coal Bed Gas and CO_2 Sequestration

Ryan, B.
Unique Aspects of British Columbia CBM Geology: Influences on Produceability 125

Ryan, B. and Richardson, D.
The Potential for CO_2 Sequestration in British Columbia Coal Seams 141

Voormeij, D.A. and Simandl, G.J.
Ultramafic Rocks in British Columbia: Delineating Targets for Mineral Sequestration of CO_2 161

SAND AND GRAVEL MAPPING IN NORTHEAST BRITISH COLUMBIA USING AIRBORNE ELECTROMAGNETIC SURVEYING METHODS

Melvyn E. Best
Bemex Consulting International
5288 Cordova Bay Road
Victoria, B.C. V8Y 2L4

Victor Levson
Resource Development and Geoscience Branch, BC Ministry of Energy and Mines,
6th Flr-1810 Blanshard St., Victoria, BC, Canada, V8W 9N3

Doug McConnell
Fugro Airborne Surveys
200, 517 10th Ave. S.W.

KEYWORDS: Sand and gravel deposits, airborne electromagnetic (EM), resistivity, geophysics, Kotcho area, northeast BC

INTRODUCTION

The Ministry of Energy and Mines recently initiated, as part of the provincial Oil and Gas Development Strategy, a regional geological assessment of aggregate resources in northeast British Columbia. The area identified for this project (Figure 1) was selected because subsurface data collected during seismic shot hole drilling in the region indicated that gravels were present under 1 to 2 m of overburden. Aggregate deposits are extremely rare in this area, with the closest known deposits occurring many tens of kilometres distant. The study area occurs along the Kotcho winter road, about 40 km east of the Sierra-Yoyo-Desan (SYD) Road.

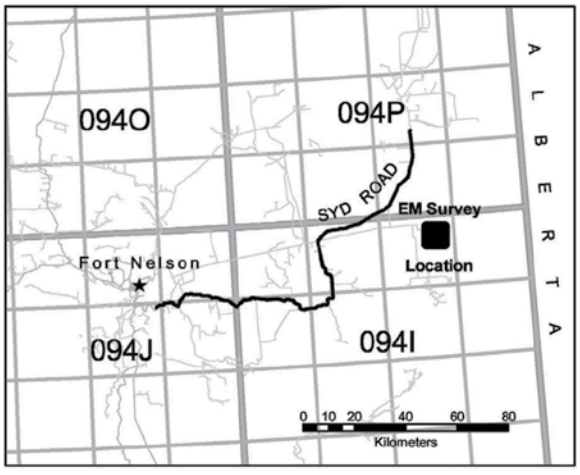

Figure 1. Map of the survey location relative to the Sierra-Yoyo-Desan (SYD) Road.

After initial identification of the area from the shot hole data, the Ministry of Energy and Mines contracted a geotechnical aggregate investigation in the region. The results of the study identified an area approximately 700 m long by 100 to 400 m wide that contained an estimated 410 000 m2 of sandy gravel (Dewer and Polysou, 2003). Excavations in the vicinity of the deposit showed gravels underlying silt-rich sediments. The buried sands and gravels were encountered in 10 test pits in an elongated, southwest-trending area, oblique to present surface stream channels. In the core of the deposit, the sands and gravels are at least 5 m thick, and in 6 of the test holes the base of the deposit was not encountered. Surprisingly, the water table was encountered in only 1 test hole at the south-easternmost edge of the deposit.

The gravel deposit occurs along a gentle south-easterly slope in an area with very little surface topography, and there is little or no geomorphic indication that subsurface gravels are present. The sands and gravels are overlain by silts and clays generally 1 to 2 m thick but locally up to 5 m thick. These sediments are interpreted to be glaciolacustrine in origin. Even though much of the area has been logged, and surface features are readily visible, air photographic interpretation alone would not have detected this deposit.

The present study was initiated to test the effectiveness of using airborne electromagnetic (EM) data for detecting such buried gravel deposits. The objectives of the EM study were threefold: 1) to determine whether the buried gravels could be detected remotely, 2) to attempt to trace the extent of the gravel deposit beyond the field tested boundaries, and 3) to locate any other aggregate sources in the area, either directly adjacent to the known deposit or within the general region. To accomplish these objectives, a detailed survey (Figure 1) with a 100 m line spacing was conducted directly over the known deposit, and a larger area (approximately 25 km2 in size—the total black area shown in Figure 1) was

covered with a 200 m line spacing (Cain, 2004).

Fugro Airborne Surveys was contracted to carry out a multi-frequency helicopter EM and magnetic survey using the RESOLVE™ EM system. The processed data include 5 apparent resistivity grids generated from the horizontal coplanar coils at frequencies of 380, 1400, 6200, 25 000 and 115 000 Hz. Fugro also generated apparent resistivity cross sections (differential resistivity) and resistivity inversion cross sections along several lines. The data set includes a series of magnetic grids as well (total field magnetic, vertical derivative, several high pass filters, with and without reduction to the pole; i.e., RTP).

This paper discusses the EM data sets and integrates them into a possible resistivity model of the subsurface within the survey area.

RESISTIVITY OF ROCKS AND GLACIAL SEDIMENTS

Approximate resistivity ranges for sedimentary rocks and glacial sediments are given in Figure 2. Note resitivity has units of ohm metres (ohm-m), and conductivity (which is the inverse of resistivity) has units of siemens per metre (S/m). In some instances these ranges could even be larger than those shown in Figure 2. The resistivity range for sandstone overlaps that of sand and gravel, and that of till overlaps both sandstone and sand and gravel.

The main factors that determine the resistivity of a rock or sediment are 1) porosity, 2) resistivity of pore fluid(s), and 3) percentage of conducting minerals (clays, graphite, sulphides) contained within the mineral grains. The influence of pore water on the resistivity of a rock or sediment can be determined from Archie's Law (Archie, 1942):

$$\rho_b = \rho_f \Phi^{-m} S_w^{\ 2} \qquad (1)$$

where ρ_b and ρ_f are the resistivity of the bulk material and of the fluid respectively, Φ is the porosity, and m is the cementation factor (usually between 1.5 and 2.0). The water saturation within the pores is S_w (assuming the other fluid in the pores is resistive; for example, oil or air). $S_w = 1$ when the pores are filled with 100% water.

Archie's Law implies that for a given pore fluid, the larger the porosity the larger the bulk resistivity. This equation does not take into account conducting mineral grains such as clay, graphite, and sulphides. Such conducting grains, if they are electrically connected, will lower the bulk resistivity of a rock or sediment from that predicted by Archie's Law.

When the conducting mineral grains are isolated from one another, no current will flow within the mineral grains. In this case the current will flow through the water in the pores, and the bulk resistivity is determined from Archie's Law. On the other hand, if there are continuous conducting pathways within the mineral grains, some of the current will flow within the pore water and some of the current will flow within the conducting mineral grains. The bulk resistivity of the material will therefore be less than that predicted by Archie's Law. Indeed, in the case of clay, the bulk resistivity can result almost entirely from conducting clay minerals rather than pore water.

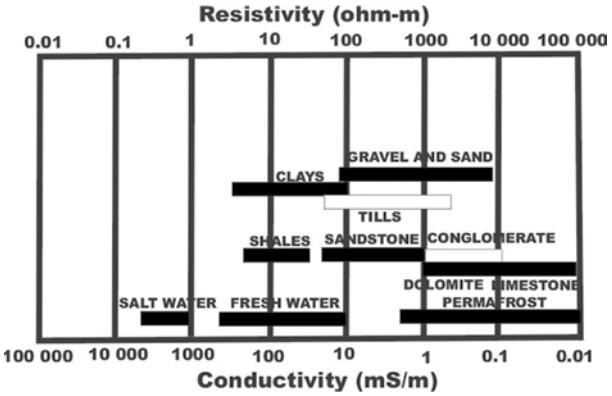

Figure 2. Resistivity ranges for rocks and glacial sediments (modified from Palacky and Stevens, 1990).

DESCRIPTION OF DATA

Resistivity Sections

Figures 3 and 4 are resistivity sections computed for lines 10110 to 10180. The upper diagram of each line was generated using apparent resistivity data from the horizontal coplanar configurations (differential resistivity). The estimated depth of the differential resistivity sections at each frequency and for a given position along a line is equal to the skin depth computed from the apparent resistivity value at that position. The lower section on each line is a layered earth inversion (in this case 4 layers) computed using the in-phase and quadrature data at all 5 frequencies.

The apparent resistivity is calculated from the normalized in-phase and quadrature values of the secondary magnetic field by assuming the earth is homogeneous with a resistivity equal to the apparent resistivity ρ_a. For a given frequency f and transmitter-receiver separation S, the apparent resistivity computed from the in-phase and quadrature values depends on the height above ground. As the height increases, the in-phase and quadrature values decrease in a predictable way, and hence the apparent resistivity will change accordingly.

The apparent resistivity is therefore considered to be an approximate measure of the average resistivity of the earth to a depth equal to the skin depth (δ).

$$\delta\ (\text{m}) = 503\ (\rho_a/f)^{½} \qquad (2)$$

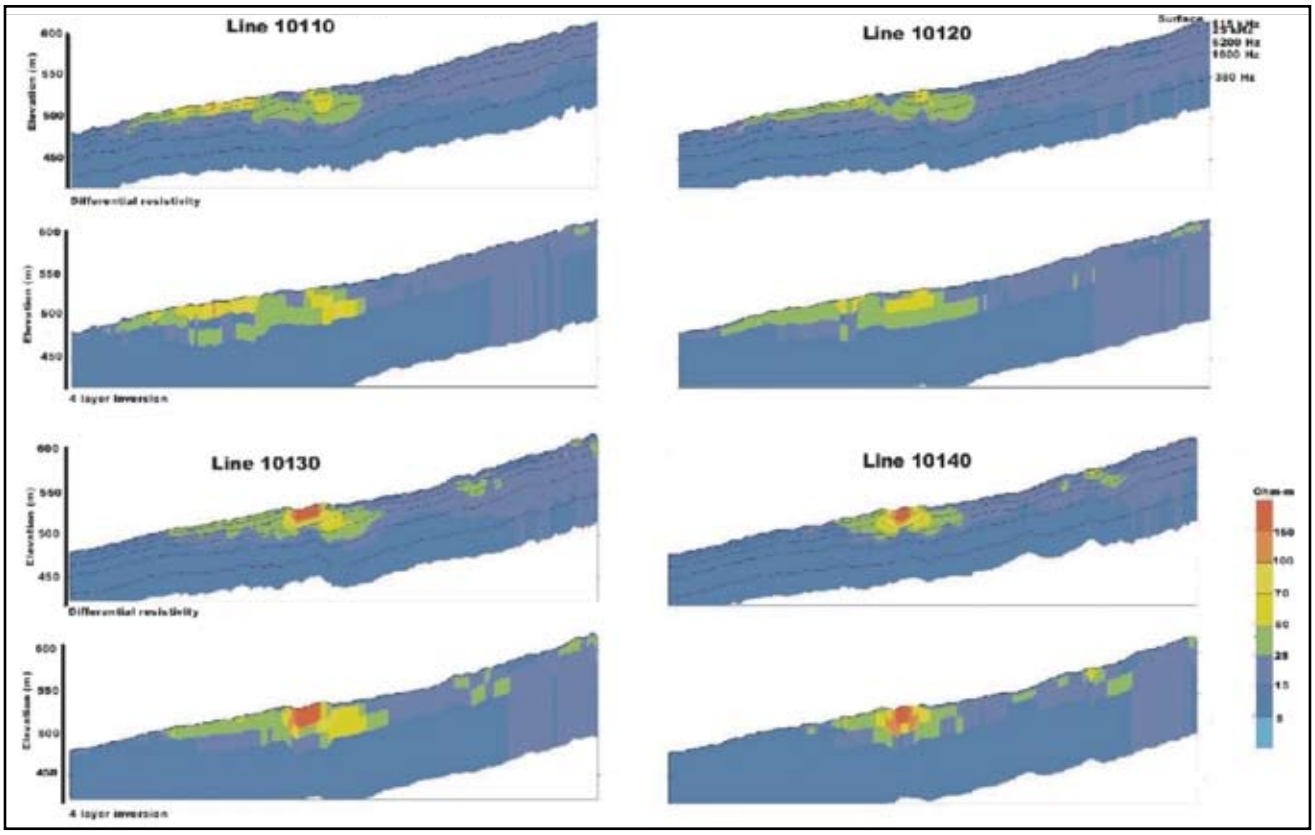

Figure 3. Resistivity cross sections for lines 10110 to 10140. The upper diagram of each line is the differential resistivity and the lower diagram is the 4-layer inversion as described in the text. North is to the right.

For a given resistivity, the skin depth decreases as the frequency increases. Consequently the highest frequency of 115 000 Hz represents the average resistivity at the shallow depths, while the lowest frequency of 380 Hz represents the average resistivity at the deepest depth the RESOLVE system can image.

The earth is generally not homogeneous but more complex. This is why the computed resistivity is called an apparent resistivty. As an example, consider a two-layer earth with the upper-layer resistivity equal to 100 ohm-m and the lower-layer resistivity equal to 5 ohm-m. The skin depth of the upper layer at 115 000 Hz and 380 Hz is 14.8 m and 258 m, respectively. If the upper layer is 20 m thick, then the apparent resistivity at 115 000 Hz will be close to the upper resistivity of 100 ohm-m and at 380 Hz would be approximately equal to the lower layer resistivity of 5 ohm-m. On the other hand, if the upper layer is only 5 m thick, the apparent resistivity at 115 000 Hz would be between 100 and 5 ohm-m—in other words, a weighted average of the upper and lower resistivities since the upper-layer skin depth is nearly 3 times the layer thickness. The apparent resistivity at 380 Hz would still be approximately equal to 5 ohm-m.

Notice the similarity between the upper and lower sections in Figures 3 and 4 for each of the lines, even though the upper resistivity section is computed assuming the earth is a homogeneous half-space at each frequency. This happens because the resistivity structure of the earth is either homogeneous (as observed on most of the lines) or is approximately two-layered with the upper layer more resistive.

Apparent Resistivity Maps

The upper resistivity in Figure 5 is the apparent resistivity calculated from the high-frequency (115 kHz) horizontal coplanar coils, and the lower map is the apparent resistivity calculated from the low-frequency coils (380 Hz). These maps illustrate the spatial variability of the average conductivity at shallow (115 kHz) and deep (380 Hz) depths.

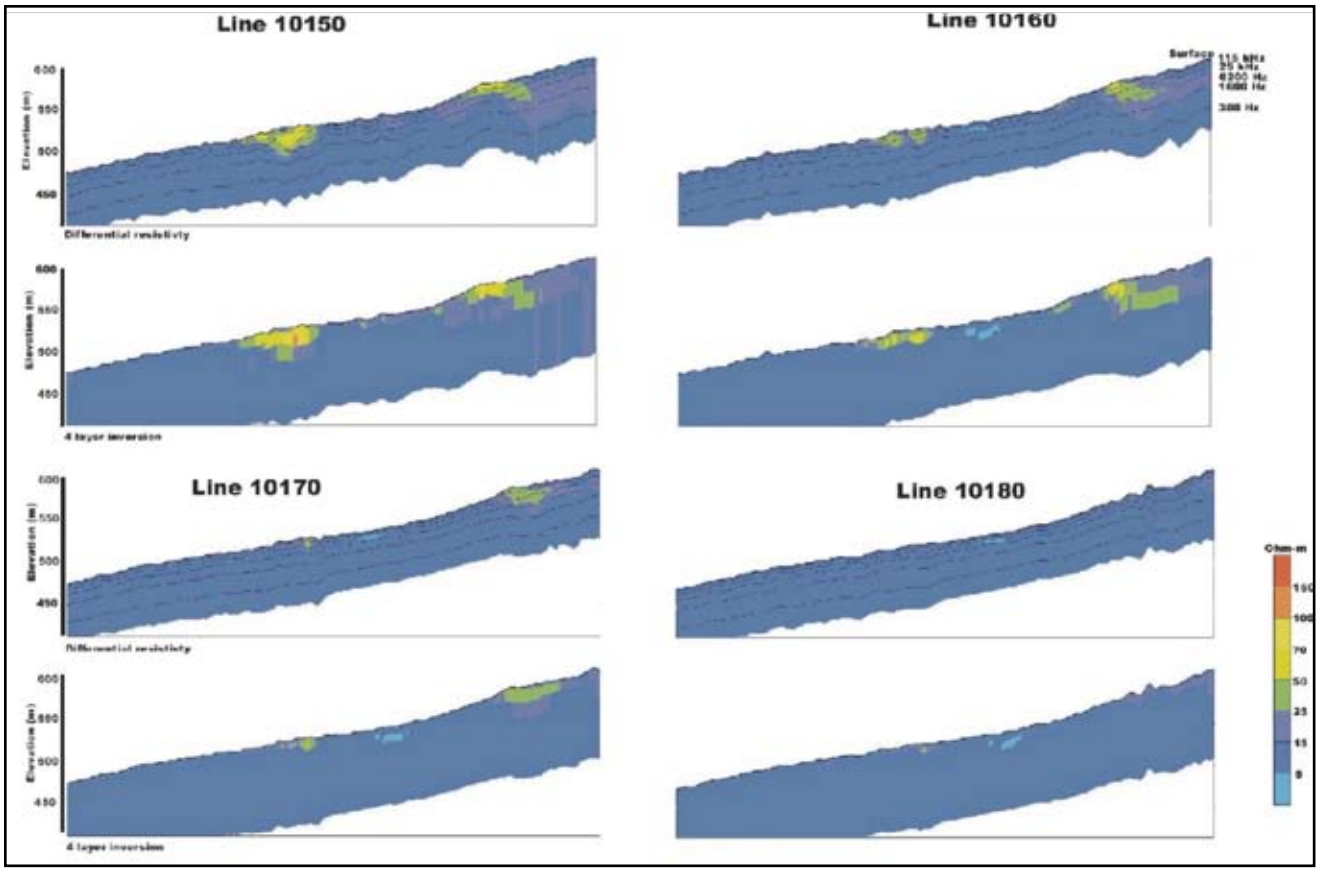

Figure 4. Resistivity cross sections from lines 10150 to 10180. The upper diagram of each line is the differential resistivity and the lower diagram is the 4-layer inversion as described in the text. North is to the right.

INTERPRETATION OF DATA

Apparent Resistivity Maps

As discussed, the 5 apparent resistivity maps represent resistivity values averaged over 5 different subsurface depths, depending on the frequency. These maps exhibit several interesting features worth noting (Figure 5). There is a resistivity high (Zone A) located in the northern part of the survey area between lines 10130 and 10180 that is prominent at frequencies between 115,000 and 6200 Hz. At lower frequencies the resistivity of this feature merges with the background resistivity values. This feature is related to the sand and gravel deposit outlined by trenching.

There is a resistive feature (Zone B) between lines 10060 and 10160 that starts near the southern boundary of the survey area and continues north to the middle of the survey. This resistive feature is most prominent on the 3 highest frequencies, similar to Zone A.

An approximately north-south boundary (with an east-west jog at approximately the midpoint of the survey) separates higher resistivity values to the west from lower resistivity values to the east. This boundary is located between lines 10180 and 10120 (Figure 5) and is visible on all 5 apparent resitivity maps. The eastern edges of Zones A and B are coincident with this boundary. It is not clear what this boundary represents geologically since it is observed on all 5 frequencies.

In addition to Zones A and B, there are 2 other resistive zones that can be seen on the higher frequencies (Figure 5). Zone C is along the northern boundary of the survey area between lines 10150 and 10110, and Zone D lies between lines 10240 and 10280. Both these features are more diffuse than Zones A and B, but the resistivity values are comparable.

Resistivity Sections

Resistivity sections between lines 10110 and 10180 provide information on the depth extent of Zones A and B (Figures 3 and 4). Zone A appears on lines 10130 to 10170, and zone B appears on lines 10110 to 10170. Zone C is most prominent on lines 10060 to 10100, although there is a hint of this resistive feature on lines 1010 and 10120. Zone D does not appear on any of these processed lines.

The background resistivity values (away from the resistivity features and at depth under the resistive features)

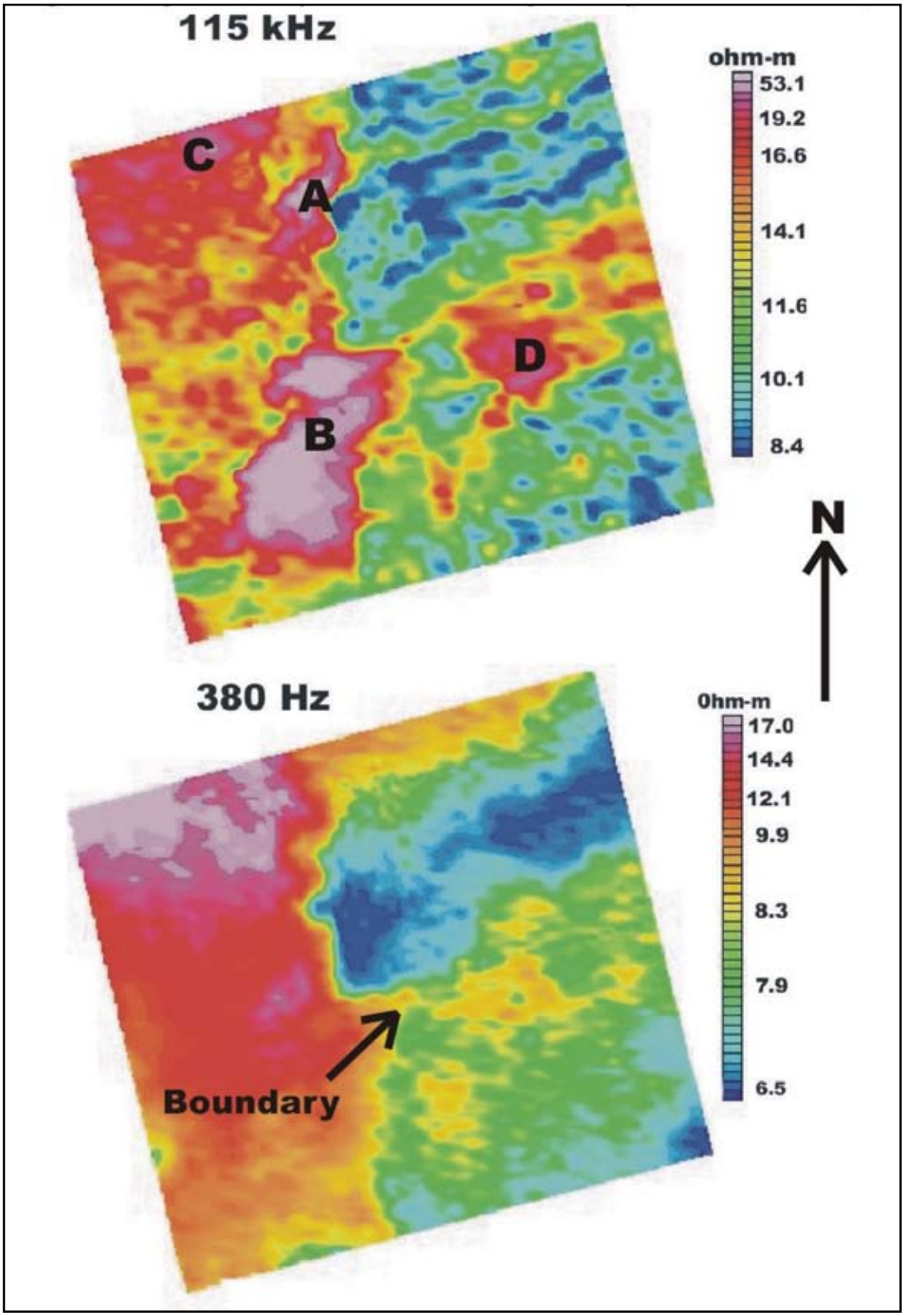

Figure 5. Apparent resistivity maps for frequencies of 115 kHz (upper diagram) and 380 Hz (lower diagram) . The 4 resistivity areas discussed in the text are labeled A to D in the upper diagram.

are low (less than 15 ohm-m) and most likely associated with shale or clay. The resistivity of the resistive features computed from the layered earth inversions generally have values greater than 50 ohm-m, although the outer fringes are somewhat less resistive (greater than 25 ohm-m). These values correspond either to sand and gravel or to sandstone. Sandstone bedrock is known to exist in the area, so there could be knobs of sandstone protruding through shale and/or till.

Once drilling or trenching confirms the presence of sand and gravel in any of these resistive features, we can assume that the entire area containing the resistive anomaly will most likely be composed of sand and gravel. The thicker regions of resistive Zones A and B are estimated to be between 25 and 35 m deep but do thin towards the edges. This is deeper than the trenching carried out to date. The depths from the resistivity cross sections can be used in conjunction with the apparent resistivity maps to estimate the total volume of sand and gravel in place.

RESULTS

On the high-frequency data reflecting the shallow geology, 4 main areas of high resistivity were identified in the survey. Zone A coincided remarkably well with the area of shallow buried gravels as mapped out by the field investigations. The northern and southern areas of Zone B are much larger and became the focus of recent reconnaissance-scale ground investigations. During these recent studies, both areas were found to contain sand and gravel. At least 4 m of sand and gravel under 1 to 2 m of overburden were encountered in test pits in the centre of these areas. Further work is required to outline these deposits in detail and to investigate the potential of Zones C and D. The results strongly indicate that high-resolution EM surveys can be an effective tool for mapping buried sand and gravel deposits.

SUMMARY AND CONCLUSIONS

Airborne EM was effective in mapping sand and gravel deposits in the Kotcho area of British Columbia. The areal extent of the known deposit (from seismic shot hole data and trenching) was mapped, and the total area containing sand and gravel was extended. The resistivity cross sections also provided an estimate of the depth of the sand and gravel deposit.

The survey outlined 2 other resistivity features as discussed above (Zones C and D). Unfortunately the resistivity range for sand and gravel overlaps the resistivity range for sandstone. Since sandstone may outcrop in this area, follow-up drilling or trenching is required to determine the material causing these anomalous resistivity features.

REFERENCES

Archie, G.E., 1942, The electrical resistivity log as an aid in determining some reservoir characteristics: *AIME*, 146, 54-67.

Cain, M.J. (2004): RESOLVE survey for the *British Columbia Geological Survey*; Fugro Airborne Surveys, Report 3091, 22 pages.

Dewer, D. and Polysou, N. (2003): Area 10 (Kotcho East) gravel investigation - Sierra-Yoyo-Desan Road area, North-eastern British Columbia; *Amec Earth and Environmental Limited,* Report No. KX04335, 13 pages.

Palacky, G.J., and Stevens, L.E., 1990, Mapping of Quaternary sediments in northeastern Ontario using ground electromagnetic methods: *Geophysics*, 55, 1595-1604.

HYDROCARBON SOURCE ROCK POTENTIAL AS DETERMINED BY ROCK-EVAL 6/TOC PYROLYSIS, NORTHEAST BRITISH COLUMBIA AND NORTHWEST ALBERTA

By A. Ibrahimbas[1] and C. Riediger[1,2]

KEYWORDS: Hydrocarbon source rocks, organic geochemistry, thermal maturity, petroleum systems.

ABSTRACT

The potential for conventional and/or unconventional hydrocarbon exploration requires the presence of organic-rich, thermally mature rock units containing oil- or gas-prone kerogen. This potential is poorly known in large parts of northeast BC and northern Alberta due to a paucity of organic geochemical studies.

Here, we investigate Lower Triassic to Lower Cretaceous potential source rocks within a large area of northeast BC and northwest Alberta (118° to 124°W and 57° to 58°N). Hydrocarbon source rock parameters, including type and amount of kerogen, and thermal maturity of these formations, are assessed by analyzing 74 core samples from 23 wells using Rock-Eval 6/TOC pyrolysis.

In general all units are immature in northwest Alberta, with increasing maturity to the west, where they become overmature. The Lower Triassic Montney Formation contains Type II kerogen with TOC (total organic carbon) values up to 4.2 wt.%, suggesting that this unit generated significant amounts of hydrocarbons where it is mature.

The base of the Doig Formation comprises a highly radioactive zone, the "Phosphate Zone", which contains Type II kerogen with TOC values up to 11 wt.%. This interval is an excellent hydrocarbon source rock.

The Upper Triassic Baldonnel and Pardonet Formations are late mature to overmature where sampled. The Baldonnel Formation contains up to 1.4 wt.% TOC, indicating only poor to fair source rock potential. The Pardonet Formation is overmature and contains residual TOC values up to 2.8 wt.%, which suggests this marine unit may have initially been a good source rock for hydrocarbons but is now spent.

The Lower Jurassic Gordondale Member comprises Type II kerogen with TOC values up to 10.45 wt.%, indicating that this unit is an excellent hydrocarbon source rock. The Lower Cretaceous Wilrich Shale is also of interest, as it has been suggested as a potential target for shale gas exploration. This unit is immature to mature within the study area. It contains Type III kerogen with TOC values up to 4.28 wt.%.

Future investigation will involve one-dimensional basin modeling in order to understand the amount and timing of hydrocarbon generation from these units with respect to timing of trap formation and accumulation of hydrocarbons.

INTRODUCTION

Hydrocarbon prospectivity in the Western Canada Sedimentary Basin (WCSB), or in any basin, hinges on the availability of oil- and/or gas-prone rock units that have generated and expelled hydrocarbons. Potential and proven hydrocarbon source rock intervals of Mesozoic age are known throughout much of the WCSB, with most available data from the Alberta portion of the basin (e.g., Creaney and Allan, 1990; Creaney et al., 1994). Results of the previous works are summarized in Table 1.

However, in the area of this study, bounded by 57° and 58°N latitude and 118° and 124°W longitude (Figure 1), there are few data available pertaining to hydrocarbon source rock potential. Furthermore, little is known of the thermal maturity of Paleozoic and Mesozoic strata in this area, and such information is critical for predicting what type of hydrocarbons, if any, may have been generated.

This paper reports the results of hydrocarbon source rock characterization of six formations of interest within the study area, namely, the Montney Formation, the "Phosphate Zone" at the base of the Doig Formation, the Baldonnel and the Pardonet Formations, the Gordondale Member (for discussion of the Gordondale, formerly Nordegg, terminology, see Asgar-Deen et al., in press), and Wilrich Formation (Figure 2). Samples were collected from cores in BC and Alberta and were analyzed by Rock-Eval 6/TOC pyrolysis.

Future investigation will involve one-dimensional quantitative basin modeling in order to understand the amount and timing of hydrocarbon generation relative to trap formation and the accumulation of hydrocarbons.

[1]*University of Calgary*
[2]*Corresponding author (e-mail: riediger@ucalgary.ca)*

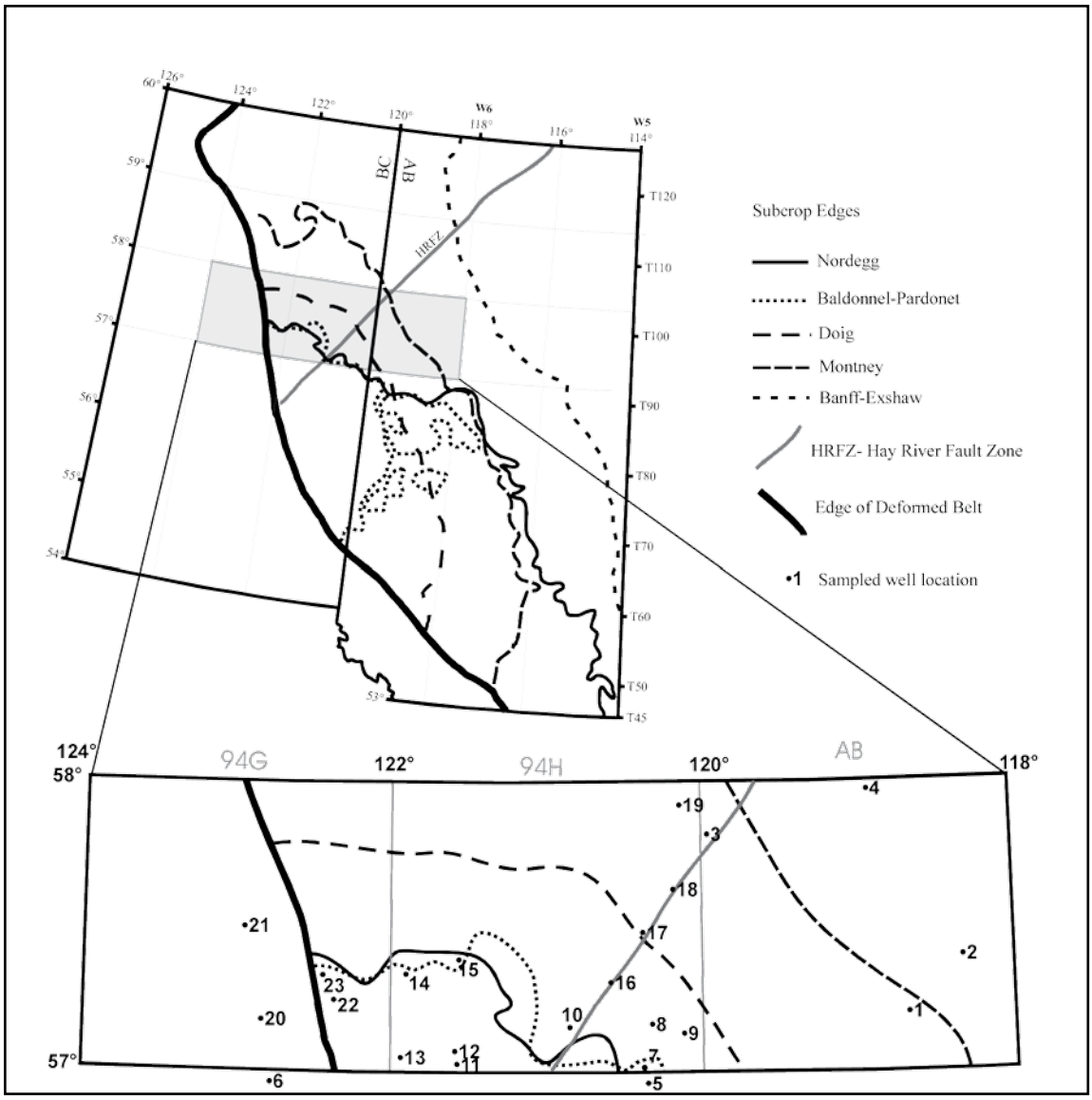

Figure 1. Map showing the study area, core sample locations, and the subcrop edges of the formations of interest (compiled from Richards et al., 1994; Edwards et al., 1994; Poulton et al., 1994).

STRATIGRAPHY

Devonian to Cretaceous stratigraphy in the study area is shown in Figure 2. Potential hydrocarbon source rock intervals are highlighted by shading. We use the new Gordondale Member terminology to refer to the organic-rich, fine-grained strata that are laterally equivalent to the Nordegg Member. These relationships are described by Asgar-Deen (2003) and Asgar-Deen et al. (in press).

Although the Devonian-Mississippian Exshaw Formation is a well-known and proven source rock for hydrocarbons, the lack of core through this zone precluded acquisition of samples during this study. However, Rock-Eval/TOC analyses of drill cuttings samples are planned.

Details of the stratigraphy shown in Figure 2 are not given here, but interested readers can find this information in the appropriate chapters of the Geological Atlas of the Western Canada Sedimentary Basin (Mossop and Shetson, 1994).

TABLE 1. PREVIOUS STUDIES OF ROCK-EVAL/TOC DATA SHOWING THE TOC'S AND THE KEROGEN TYPES OF THE UNITS OF INTEREST (*TOC VALUES WILL VARY, DEPENDING ON MATURITY)

Unit	*TOC range (average)(wt. %)	Kerogen Type	References
Wilrich	0.45-2.05 (1.4)	Type III	Faraj, 2003;Ibrahimbas, (Unpublished results)
Gordondale	0.55-28 (5)	Type I/IIS	Riediger et al., 1990b; Asgar-Deen, 2003; Faraj, 2003
Pardonet	0.26-6.5 (0.94)	Type II	Riediger, 1997; Carrelli, 2002
Baldonnel	0.14-2.08 (<1)	Type II	Riediger 1997; Carrelli 2002
Phosphate Zone	1.12-11 (3.6)	Type II	Riediger et al.,1990a; 1990b; Creaney and Allan, 1992; Faraj, 2003
Montney	0.8-4.7 (1.3)	Type II	Riediger et al., 1990a; 1990b; Hankel, 2001; Faraj, 2003

METHODOLOGY

For this study, 74 core samples were taken from 23 well locations (Figure 1). Samples were selected based on core availability within the zones of interest in the study area. Each sample was crushed to a fine powder prior to analysis. All samples were weighed to 100 mg and subjected to Rock-Eval 6/TOC analysis in order to determine the kerogen type, TOC content, and thermal maturity, which are the main parameters for characterizing a hydrocarbon source rock. Analyses were conducted at the Organic Geochemistry Labs of the Geological Survey of Canada (Calgary). Measured parameters include S1 (mg HC/g rock), S2 (mg HC/g rock), S3 (mg CO_2/g rock), Tmax (°C), and TOC (wt.%) (see Table 2). Several additional parameters, including HI (hydrogen index, S2/TOCx100), OI (oxygen index, S3/TOCx100), and PI (production index, S1/[S1+S2]) are calculated from these measured values and are shown in Table 2. Pyrolysis experiments were repeated for some samples at lower sample weight to ensure that the Rock-Eval/TOC detector was not overloaded by generated hydrocarbons during the original runs.

Details of the analytical procedure and discussion of Rock-Eval parameters are available in Espitalié et al. (1977), Peters (1986), and Snowdon et al. (1998). Peters (1986) and Peters and Cassa (1994) provide a summary of interpretive guidelines for Rock-Eval data.

RESULTS AND DISCUSSION

Rock-Eval 6/TOC results are summarized in Table 2. Of the 7 potential hydrocarbon source rocks shown in Figure 2, geochemical data from only the Montney, Phosphate Zone, Baldonnel/Pardonet, Gordondale, and Wilrich intervals are reported. As noted previously, no samples from the Exshaw Formation were collected for this study due to a lack of core through this zone.

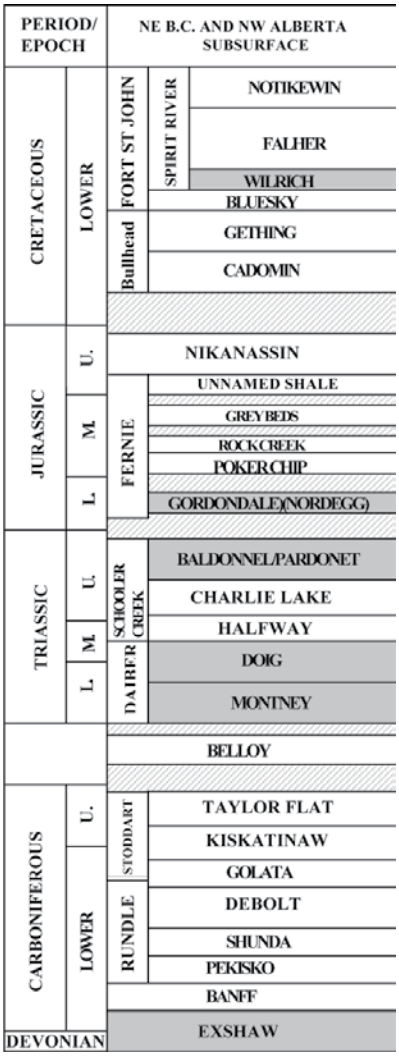

Figure 2. Stratigraphic chart of the study area (compiled from Richards et al., 1994; Henderson et al., 1994; Edwards et al., 1994; Poulton et al., 1994; Hayes et al., 1994). Potential source rocks are highlighted by shading.

However, geochemical data from well cuttings will be incorporated in the second phase of the study.

In this section, the thermal maturity and amount and type of organic matter are discussed. Interpretive guidelines from Peters (1986) and Peters and Cassa (1994) are used to evaluate the hydrocarbon source rock potential of each unit, and these guidelines are reproduced in Table 3. In Table 4, thermal maturity, TOC content, HI, and kerogen type are summarized for each unit.

Thermal Maturity

Rock-Eval Tmax data given in Table 2 are used to assess thermal maturity in the study area. Each unit is mapped individually in Figure 3 because variations in kerogen type affect the Tmax values (Peters, 1986). The overall maturity trend in the study area shows that the maturity of the units increases from east to west towards the Cordilleran deformation front. All units are thermally mature throughout the central part of the study area (Beatton River NTS map area 94H). Most of the studied units are immature in Alberta and are overmature in the Trutch map area (94G).

TOC Content, Kerogen Type, and Hydrocarbon Source Rock Potential

The ranges of TOC values for each unit are summarized in Table 4. Histograms showing the TOC variation for each unit with mean TOC values and standard deviations are also given in Figure 4. The plot of S2 against TOC for immature to early mature samples is used to determine the proportion of the inert carbon in the TOC measured by pyrolysis (Conford et al., 1998). During pyrolysis, only the labile kerogen will generate hydrocarbons to be recorded in S2 peak. Thus by discounting the proportion of inert carbon, it is possible to obtain a more accurate HI (S2/TOCx100) value from the slope of the best fitted lines of S2 versus TOC data (Figure 5). A bivariate plot of HI vs. OI (pseudo-Van Krevelen diagram) is also commonly used to assess the kerogen type (Figure 6).

In this section, information on TOC and kerogen type for each unit are used to evaluate the hydrocarbon source rock potential based on criteria outlined in Table 3.

The TOC values for the Montney Formation range from 0.51 to 4.18 wt.%, with a mean value of 2.01 wt.% (std. dev. = 1.24) (Figure 4). It contains 0.35 wt.% inert carbon (Figure 5), hence the proportion of organic carbon content that has the capacity to generate hydrocarbons ranges from 0.16 to 3.83 wt.%, with a mean value of 1.66 wt.%. The unit yields HI values of 43 to 450 mg HC/g TOC, which is typical for oil- and gas-prone Type II kerogen (Figure 6). Considering only the immature samples, adjusted HI_0 (original HI prior to maturation) is 571 mg HC/g TOC. These TOC and HI_0 values indicate good to very good source rock potential in the Montney Formation.

The "Phosphate Zone" has high TOC values ranging from 1.76 to 10.98 wt.% (Table 4), with a mean value of 6.14 wt.% (std. dev.=3.35) (Figure 4). The amount of the inert carbon in the "Phosphate Zone" is also high, with a value of 1.4 wt.% (Figure 5); therefore, the true organic carbon content of the unit is then between 0.4 and 9.6 wt.%. The unit comprises Type II oil- and gas-prone kerogen with HI values ranging from 189 to 489 mg HC/g TOC (263 to 645 mg HC/g TOC after discarding the effect of inert carbon [Figure 5]). The unit has excellent source rock potential.

The TOC values for Pardonet and Baldonnel Formations are fair to moderate. The samples are all overmature, and hence original kerogen type cannot be determined from geochemical data. However, these are marine carbonate units and thus likely contained Type II kerogen. This interpretation is also supported by the results of a previous study by Carrelli (2002) on these formations. The residual TOC values for Pardonet Formation range 0.97 to 2.79 wt.%, with a mean value of 1.73 wt.% (std. dev. = 0.60). Bordenave et al. (1993) suggested that overmature Type II source rocks would have lost 50% of their original TOC due to generation and expulsion of hydrocarbons. Hence, the original TOC values for Pardonet Formation were likely over 4 wt.%. The TOC values measured from the Baldonnel Formation range from 0.65 to 1.39 wt.%, which, by the same reasoning, were likely 1 to 2 wt.% originally. The Pardonet Formation had fair to good initial source rock potential, and the Baldonnel Formation had poor to fair initial source rock potential.

The Gordondale Member contains high TOC values ranging from 0.66 to 10.45 wt.% (mean = 5.71 wt.%, std. dev. = 2.66) (Figure 4). The unit yields HI values of 26 to 273 mg HC/g TOC and OI values of 3 to 23 mg CO_2/g TOC (Figure 6), and the high degree of maturity precludes a precise assessment of the organic matter type. Riediger et al. (1990b) and Asgar-Deen (2003) proposed this unit having Type I/IIS kerogen; therefore, the unit most likely comprises Type II kerogen, considering its marine origin. This interval has excellent source rock potential where mature.

The TOC values of the Wilrich Shale ranges from 1.08 to 4.28 wt.% (mean = 2.12 wt.%, std. dev. = 0.91) (Figure 4). After considering the approximately 0.5 wt.% inert carbon (Figure 5), it will contain 0.58 to 3.78 wt.% TOC with a mean value of 1.62 wt.%. The unit contains Type III, gas-prone kerogen, with HI values ranging from 138 to 393 mg HC/g TOC (Figure 6). The mean value of HI is 235 mg HC/g TOC after eliminating the effect of 0.5 wt.% inert carbon. The TOC and HI values indicate that the unit has good to very good source rock potential for gas generation.

TABLE 2. ROCK EVAL/TOC RESULTS FROM CORE SAMPLES IN THE STUDY AREA

(+REPEAT RUN AT LOWER SAMPLE WEIGHT)

Unit	Well #	Well ID	Depth (m)	Tmax (°C)	S1 (mg HC/ g rock	S2 (mgHC/ g rock)	S3 (mg CO_2/ g rock)	PI S1/ (S1+S2)	TOC (wt.%)	HI (mgHC/ g TOC)	OI (mgCO/ g TOC)
Wilrich	1	11-17-94-5W6	932.2	431	1.65	4.28	0.49	0.28	2.36	182	21
	2	7-25-96-4W6	827	428	1.06	3.15	0.38	0.25	1.96	161	19
	4	10-36-103-7W6	698.9	431	1.58	2.83	0.4	0.36	1.97	144	20
			704.8	429	0.59	4.8	0.44	0.11	3.16	153	14
	16	D-69-A/94-H-7	1100.5	441	0.22	2.69	0.16	0.08	1.83	148	9
			1103.1	442	0.3	2.84	0.16	0.10	1.83	156	9
	17	A-43-K/94-H-8	1194.5	438	0.14	1.49	0.27	0.09	1.08	139	25
			1196	438	0.27	2.84	0.26	0.09	1.47	194	18
	19	B-81-G/94-H-16	809.5	436	0.18	1.7	0.23	0.10	1.23	138	19
			811.4	437	1.06	16.8	0.18	0.06	4.28	393	4
Gordondale	5	A-58-K/94-A-16	1010.9	439	1.08	6.27	0.09	0.15	3.03	208	3
			1012.4	441	2.05	6.53	0.06	0.24	2.4	273	3
			1013.5	438	1	4.3	0.06	0.19	2.05	210	3
	11	A-43-A/94-H-4	1277.6	461	2.93	8.48	0.18	0.26	7.29	119	2
			1277.6	461	2.71	8.34	0.2	0.25	7.35	116	3
			1279.1	454	1.13	2.99	0.23	0.27	3.55	85	6
			1281.1	464	1.85	6.02	0.23	0.24	4.14	74	3
	12	D-93-A/94-H-4	1262.5	460	0.64	1.08	0.12	0.37	1.48	74	8
			1264.1	456	1.46	6.82	0.3	0.18	6.32	109	5
			1265.6	463	2.27	8.47	0.33	0.21	8.91	97	4
			1267.1	446	3.8	8.19	0.26	0.32	5.94	139	4
			1268.6	443	6.21	10.19	0.26	0.38	6.85	150	4
			1270.1	448	6.77	12.77	0.2	0.35	7.84	165	3
			1271.6	449	2.93	5.58	0.21	0.34	3.87	146	5
			1273.1	448	1.78	3.3	0.15	0.35	2.35	142	6
	13	D-65-D/94-H-4	1387.4	472	0.62	1.56	0.16	0.28	5.18	31	3
			1388.4	481	0.52	2.93	0.31	0.15	8.12	37	4
			1389.2	484	0.3	2.36	0.35	0.11	5.89	42	6
			1389.9	484	0.25	2.05	0.38	0.11	5.25	41	7
			1390.6	484	0.18	0.77	0.2	0.19	3.03	26	7
			1391.8	484	0.32	1.37	0.37	0.19	4.98	29	7
			1392.4	484	0.62	3.34	0.3	0.16	9.48	37	3
			1393	480	0.68	3.35	0.29	0.17	10.45	33	3
	14	A-5-E/94-H-6	1145.5	452	0.25	1.12	0.3	0.18	1.33	85	23
	15	B-54-H/94-H-5	1218.7	443	0.49	2.23	0.12	0.18	2.19	102	5
	22	C-86-C/94-G-8	1426.9	456	0.22	0.16	0.21	0.58	0.66	24	32
			1429.1	453	0.19	0.18	0.18	0.51	0.58	31	31
Pardonet	6	A-77-K/94-B-15	1050.4	480	0.27	0.84	0.15	0.24	1.73	51	9
			1055.8	461	0.36	0.42	0.19	0.46	1.83	23	10
			1059.3	471	0.21	0.39	0.17	0.35	1.16	34	15
			1061.8	468	0.33	0.34	0.21	0.49	1.34	26	16
	23	D-99-F/94-G-8	1316.6	468	0.65	1.44	0.15	0.31	2.29	64	7
			1317.6	464	0.53	0.92	0.11	0.37	0.97	96	11
			1319.1	466	0.73	1.6	0.15	0.31	2.79	58	5
Baldonnel	6	A-77-K/94-B-15	1065.1	472	0.14	0.24	0.16	0.37	0.86	29	19
	12	D-93-A/94-H-4	1274.1	452	0.52	0.56	0.13	0.48	0.98	57	13

TABLE 2. ROCK EVAL/TOC RESULTS (CONTINUED).

Unit	Well #	Well ID	Depth (m)	Tmax (°C)	S1 (mg HC/ g rock	S2 (mgHC/ g rock)	S3 (mg CO_2/ g rock)	PI (S1/ (S1+S2))	TOC (wt.%)	HI (mgHC/ g TOC)	OI (mgCO_2/ g TOC)
	22	C-86-C/94-G-8	1434.4	469	0.56	0.77	0.17	0.42	1.39	57	12
			1439.8	464	0.69	0.63	0.2	0.52	1.02	63	20
			1443.2	478	0.74	0.63	0.16	0.54	0.65	98	25
Phosphate Zone	8	A-78-F/94-H-1	1069.2	447	0.99	10.21	0.22	0.09	2.95	346	7
			1073.4	445	0.93	9.02	0.21	0.09	2.63	343	8
			1075	443	0.76	5.9	0.19	0.11	1.9	311	10
			1076.4	437	1.29	14.51	0.23	0.08	5.26	277	4
	9	D-48-H/94-H-1	1051.3	425	0.01	0.05	0.31	0.17	0.12	42	258
			1053.8	438	0.9	12.44	0.3	0.07	2.65	469	11
			1056	433	1.78	28.61	0.33	0.06	5.86	489	6
	10	D-72-E/94-H-2	1176.3	443	1.57	3.9	0.18	0.29	1.76	189	3
			1180.6	443	1.62	9.93	0.18	0.14	5.27	189	3
			*1180.6	441	1.59	9.79	0.21	0.14	5.02	196	4
			1182.9	442	1.64	15.9	0.2	0.09	7.73	207	3
			*1182.9	442	1.57	15.49	0.18	0.09	7.58	206	2
			1186.1	445	2.01	25.17	0.22	0.07	10.98	231	2
			*1186.1	445	2.08	24.62	0.21	0.08	10.79	230	2
			1187.4	444	2.14	25.68	0.18	0.08	10.95	236	2
			*1187.4	445	2.1	25.13	0.2	0.08	10.76	235	2
Montney	3	6-36-101-13W6	908.3	288	2.75	0.7	0.26	0.8	0.51	137	51
	7	D-13-D/94-H-1	1133.2	447	1.19	8.8	0.17	0.12	4.03	219	4
			1134.8	447	0.83	5.18	0.19	0.14	2.37	219	8
	18	D-45-G/94-H-9	905.8	431	0.8	4.8	0.23	0.14	1.23	390	19
			909.2	433	0.33	2.91	0.19	0.1	0.82	355	23
			914.5	439	0.41	9.09	0.26	0.04	2.02	450	13
			917.4	435	0.36	5.4	0.22	0.06	1.28	422	17
	20	D-88-F/94-G-2	2130.8	490	0.02	0.02	0.11	0.5	0.87	2	13
			2131.3	490	0	0.01	0.08	0	0.64	2	13
			2132.4	-40	0	0	0.15	0	0.4	0	38
			2133.1	500	0	0	0.1	0	0.43	0	23
	21	C-80-L/94-G-7	869.9	477	0.67	2.02	0.26	0.25	4.18	50	6
			873.4	466	0.48	0.69	0.18	0.41	1.63	43	11

TABLE 3. HYDROCARBON SOURCE ROCK EVALUATION PARAMETERS FOR ROCK-EVAL/TOC PYROLYSIS DATA (MODIFIED FROM PETERS, 1986). **(TABLE 3 (C) INCLUDES RANGES OF VITRINITE REFLECTANCE THAT ARE APPROXIMATELY EQUIVALENT TO ROCK-EVAL TMAX VALUES. VITRINITE REFLECTANCE DATA ARE NOT USED IN THIS STUDY)**

Petroleum Potential	Organic Matter		
	TOC	Rock-Eval Pyrolysis	
	(wt.%)	S1	S2
	0-0.5	0-0.5	0-2.5
	0.5-1	0.5-1	2.5-5
	1-2	1-2	5-10
	2-4	2-4	10-20
	>4	>4	>20

(A) Parameters for describing the petroleum potential of an immature source rock.

TABLE 3. HYDROCARBON SOURCE ROCK EVALUATION PARAMETERS (CONTINUED).

Kerogen Type	HI (mg HC/g TOC)	S2/S3
I	>600	>15
II	300-600	10-15
II/III	200-300	5-10
III	50-200	1-5
IV	<50	<1

(B) Parameters for describing kerogen type (quality) of an immature source rock.

Stage of Thermal Maturity for Oil	Maturation: Vitrinite Reflectance Ro (%)	Maturation: Rock-Eval Tmax (°C)
Immature	0.2-0.6	<435
Mature		
Early	0.6-0.65	435-445
Peak	0.65-0.9	445-450
Late	0.9-1.35	450-470
Postmature	>1.35	>470

(C) Parameters for describing the level of thermal maturation.

TABLE 4. SUMMARY OF ROCK-EVAL/TOC DATA FROM CORE SAMPLES (RAW DATA)

UNIT (number of samples)	DEPTH (m)	Tmax (°C) range	TOC (wt.%)	HI (mg HC/g TOC)	Kerogen Type	Source Rock Potential
WILRICH (10)	809.5-1196	428-442	1.08-4.28	138-393	Type III	Good to very good (gas only)
GORDONDALE (27)	1010.9-1429.1	438-484	0.66-10.45	26-273	Type II	Excellent (oil+gas)
PARDONET (7)	1050.4-1319.1	461-480	0.97-2.79	23-96	Type II	Fair to good (oil+gas)
BALDONNEL (5)	1065.1-1443.2	452-478	0.65-1.39	29-98	Type II	Poor to fair (oil+gas)
PHOSPHATE ZONE (12)	1051.3-1187.4	433-447	1.76-10.98	189-489	Type II	Excellent (oil+gas)
MONTNEY (13)	869.9-2133.1	431-500	0.51-4.18	43-450	Type II	Good to very good (oil+gas)

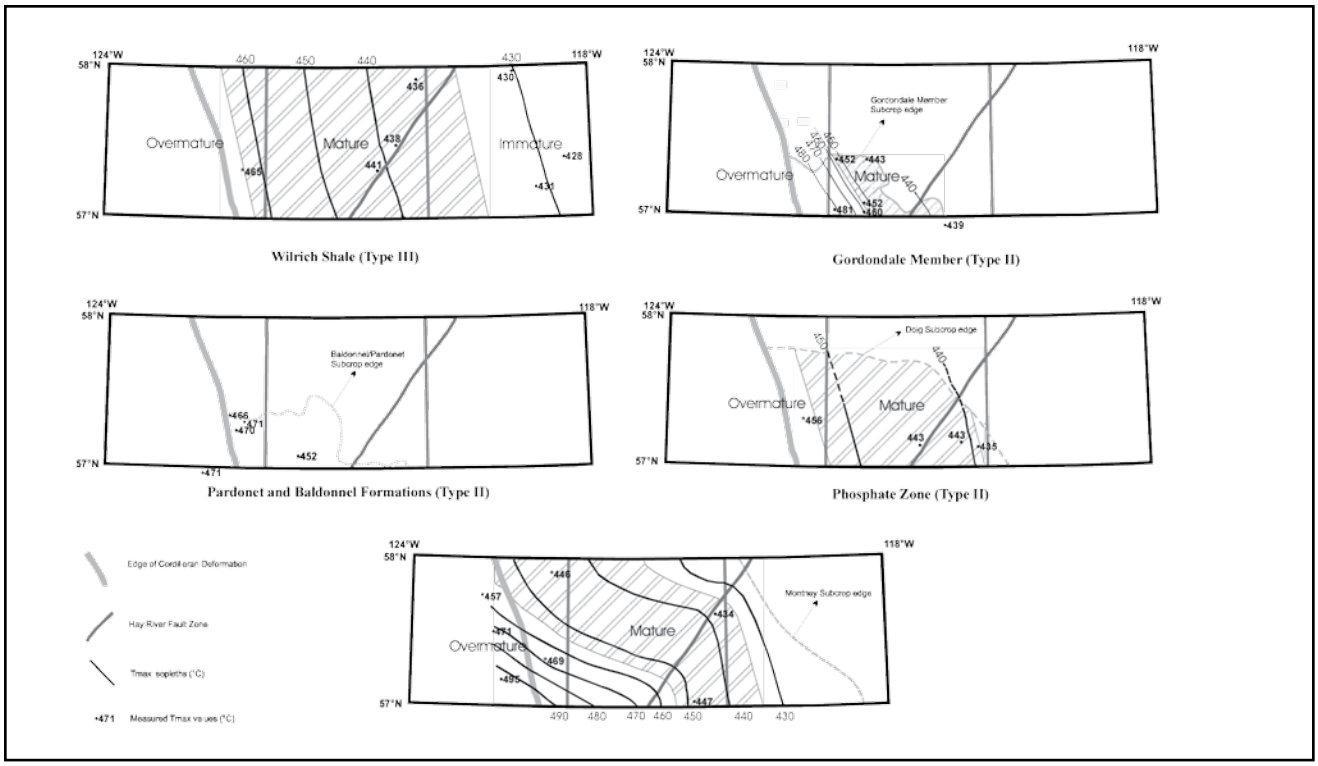

Figure 3. The thermal maturity distribution of each unit based on Rock-Eval Tmax values (ºC). * Tmax values from unpublished results (Dr. Larry Lane [GSC, Calgary], personal communication, 2003).

CONCLUSIONS

Six units of Early Triassic to Early Cretaceous age have been assessed for their hydrocarbon source potential in the study area. A total of 74 samples from 23 wells were analyzed by Rock-Eval 6/TOC pyrolysis.

The Montney Formation within the study area is thermally immature to overmature with increasing maturity from northeast to southwest. It contains Type II kerogen with TOC values up to 4.18 wt.%. This suggests that the Montney Formation may have generated significant amounts of hydrocarbons where it is mature in the BC part of the study area.

The highly radioactive "Phosphate Zone" at the base of the Doig Formation contains Type II kerogen with TOC values up to 10.98 wt.%. The maturity increases from east to west, and it is mature in the Beatton River map area (94H). The high TOC values suggest that this unit has excellent hydrocarbon source potential where mature.

The Baldonnel and Pardonet Formations are overmature in the west part of the study area where sampled. Both likely comprise Type II kerogen, although the high degree of maturity precludes a direct assessment of kerogen type. The Baldonnel Formation has TOC values up to 1.39 wt.%, suggesting that it had poor to fair initial source rock potential. The Pardonet Formation has TOC values up to 2.8 wt.%, which suggests that it had fair to good initial hydrocarbon generation potential when mature.

The Gordondale Member samples vary from peak mature to overmature. It contains Type II kerogen with TOC values up to 10.45 wt.%, suggesting that it is an excellent source rock where mature.

The Wilrich Shale contains Type III kerogen with TOC values up to 4.28 wt.%. Therefore, it has good to very good generation potential for gas. It is immature in the east part of the study area with increasing maturity to west.

The next step in this project is to apply one-dimensional basin modeling to understand the amount and timing of hydrocarbons generated from these units, which will then be correlated with the timing of trap formation and accumulation of the hydrocarbons in the study area.

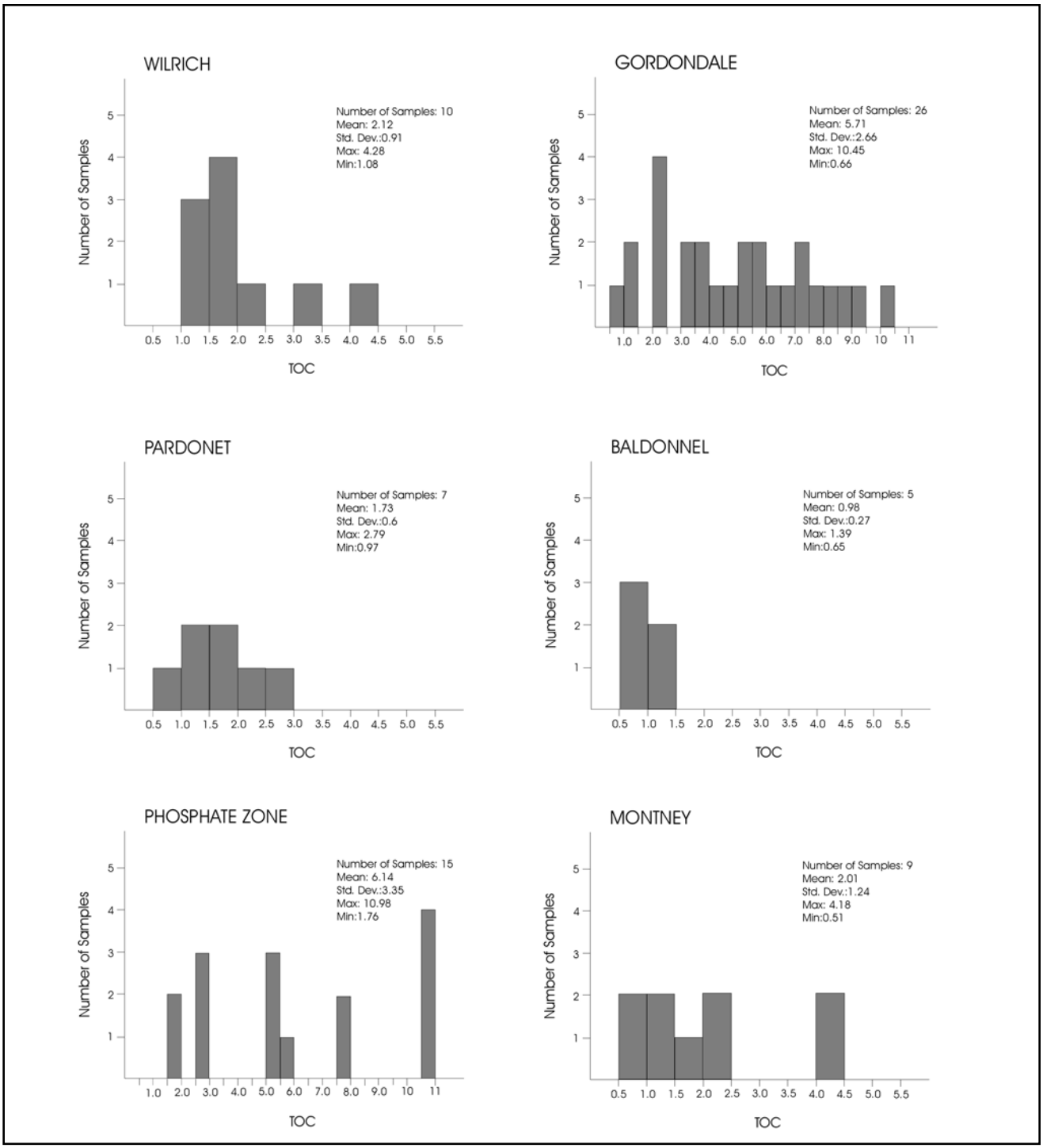

Figure 4. TOC histograms for the units with mean and standard deviation values. Note scale change for organically-richer units ("Phosphate Zone" and Gordondale Member).

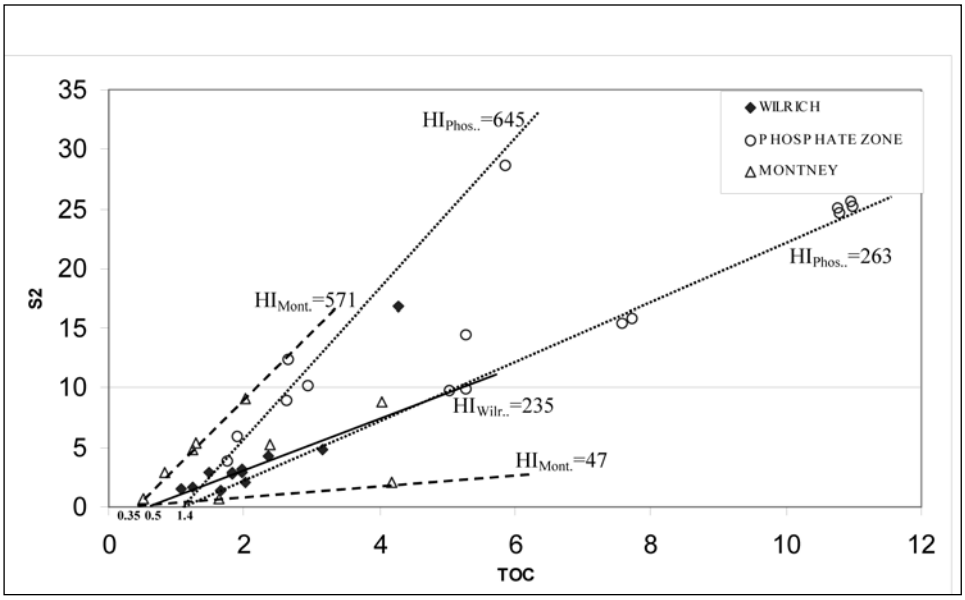

Figure 5. Rock-Eval pyrolysis S2 versus TOC, showing hydrogen index (HI) and inert carbon content of the units that have immature to early mature samples.

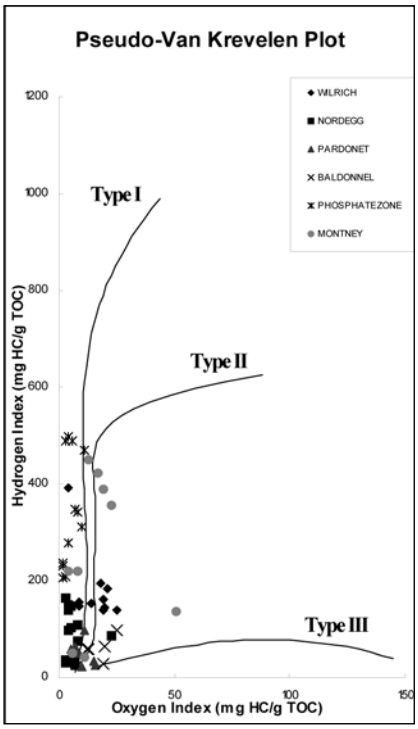

Figure 6. Pseudo-Van Krevelen diagram, showing Rock-Eval hydrogen index vs. oxygen index for the sampled units.

ACKNOWLEDGEMENTS

We wish to acknowledge Mark Hayes and Kevin Pederson of the BC Ministry of Energy and Mines and the BC Ministry of Energy and Mines Geology Facility-Core Lab in Charlie Lake for funding and logistical support for this project. Ross Stewart and the Organic Geochemistry Labs at GSC Calgary are gratefully acknowledged for providing the Rock-Eval VI/TOC pyrolysis data. Dr. Larry Lane is gratefully acknowledged for discussions of geology of the study area and access to his geochemical dataset.

REFERENCES

Asgar-Deen, M., 2003, Stratigraphy, Sedimentology and Paleogeography of the Lower Jurassic Nordegg Member (Gordondale Member), west-central Alberta, Canada. *Unpublished M.Sc. Thesis, Department of Geology and Geophysics, University of Calgary*, 206 pages.

Asgar-Deen, M., Hall, R., and Riediger, C.L., In press. The Gordondale Member: designation of a new member in the Fernie Formation to replace the informal "Nordegg Member" nomenclature of the subsurface of west-central Alberta. *Canadian Bulletin of Petroleum Geology.*

Bordenave, M.L., Espitalié, J., LePlat, P., Oudin, J.L., and Vandenbroucke, M., 1993. Screening techniques for source rock evaluation. Chapter II.2. In: *Applied Petroleum Geochemistry*. M.L. Bordenave (ed.). Éditions Technip, pages 217-278.Carrelli, G.G., 2002, Geology and source rock potential of the upper Triassic Baldonnel and Pardonet formations, northeastern British Columbia. *Unpublished MSc. Thesis, University of Calgary*, 2002, 335 pages. Cornford, C., Gardner, P., and Burgess, C, 1998, Geochemical truths in large data sets. I: Geochemical screening data. *Organic Geochemistry*, v.29, no.1-3, pages 519-530.

Creaney, S., and Allan, J., 1990, Hydrocarbon generation and migration in the Western Canada Sedimentary Basin. In: Classic Petroleum Provinces. J.Brooks (ed.) *Geological Society Special Publication*, No.50, pages 189-202.

Creaney, S., and Allan, J, 1992, Petroleum systems in the Foreland Basin of Western Canada. In: Foreland Basins and Foldbelts. R.W. Macqueen and D.A. Leckie (ed.). *American Association of Petroleum Geologists*, Memoir 55, pages 279-306.

Creaney, S., Allan, J., Cole, K., Brooks, P.W., Fowler, M.G., Osadetz, K.G., Snowdon, L.R., and Riediger C.L., 1994, Petroleum generation and migration in the Western Canada Sedimentary Basin. In: Geological Atlas of Western Canada Sedimentary Basin. G.D. Mossop and I. Shetsen (comps.), Calgary*, Canadian Society of Petroleum Geologists and Alberta Research Council*, pages 455-468.

Edwards, D.E., Barclay, J.E., Gibson, D.W., Kvill, G.E., Halton, E., 1994, Triassic strata of the Western Canada Sedimentary Basin. In: Geological Atlas of Western Canada Sedimentary Basin. G.D. Mossop and I. Shetsen (comps.), Calgary, *Canadian Society of Petroleum Geologists and Alberta Research Council*, pages 259-276.

Espitalié, J., Laporte, J.L., Madec, M., Marquis, F., Leplat, P., Paulet, J., and Boutefeu, A., 1977, Méthode rapide de caractérisation des roches de méres de leur potentiel pétrolier et de leur degré d'évolution. *Institut Francais Pétrolier Revue*, v.32, pages 23-42.

Faraj, B., 2003, Shale gas potential of selected formations from the WCSB of Western Canada. In: *5th Annual Unconventional Gas and Coalbed Methane Conference Proceedings*, 2003, Calgary.

Handerson, C.M., Richards, B.C., Barclay, J.E., 1994, Permian strata of the Western Canada Sedimentary Basin. In: Geological Atlas of Western Canada Sedimentary Basin. G.D. Mossop and I. Shetsen (comps.), Calgary, *Canadian Society of Petroleum Geologists and Alberta Research Council*, pages 251-258.

Hankel R., 2001, Source rock and oil geochemistry and conodont biostratigraphy of the Triassic Lower Montney Formation in the Peace River Arch area, west-central Alberta. *Unpublished MSc. Thesis, University of Calgary*, 2001, 61 pages. Fennell, J.W., 1994, Cretaceous Mannville Group of the Western Canada Sedimentary Basin. In: Geological Atlas of Western Canada Sedimentary Basin. G.D. Mossop and I. Shetsen (comps.), Calgary, Canadian Society of Petroleum *Society of Petroleum Geologists and Alberta Research Council*, pages 317-334.

Hayes, B.J.R., Cristopher, J.E., Rosenthal, L., Los, G., McKercher, B., Minken, D.F., Tremblay, Y.M., Ibrahimbas, A., (Unpublished data), Hydrocarbon source rock potential of the Wilrich Shale. *Unpublished data for the 701 Course Project, University of Calgary*, 2003, 50 pages.

Mossop G.D., and Shetsen, I., (compilers), 1994. Geological Atlas of Western Canada Sedimentary Basin. Calgary, *Canadian Society of Petroleum Geologists and Alberta Research Council*, 510 pages.

Peters, K.E., and Cassa, M.R., 1994, Applied Source Rock Geochemistry. In: The petroleum system- from source to trap; L.B. Magoon and W.G. Dow (ed.). *American Association of Petroleum Geologists*, Memoir 60, pages 93-117.

Peters, K.E., 1986, Guidelines for evaluating petroleum source rocks using programmed pyrolysis. *American Association of Petroleum Geologists Bulletin*, v.70, pages 318-329.

Poulton, T.P., Christopher, J.E., Hayes, B.J.R., Losert, J., Tittemore, J., Gilchrist, R.D., 1994, Jurassic and Lowermost Cretaceous strata of the Western Canada Sedimentary Basin. In: Geological Atlas of Western Canada Sedimentary Basin. G.D. Mossop and I. Shetsen (comps.), Calgary, *Canadian Society of Petroleum Geologists and Alberta Research Council*, pages 297-316.

Richards, B.C., Barclay, J.E., Bryan, D., Hartling, A., Henderson, C.M., Hinds, R.C., 1994, Carboniferous strata of the Western Canada Sedimentary Basin. In: Geological Atlas of Western Canada Sedimentary Basin. G.D. Mossop and I. Shetsen (comps.), Calgary, *Canadian Society of Petroleum Geologists and Alberta Research Council*, pages 221-250.

Riediger, C.L., 1997, Geochemistry of potential hydrocarbon source rocks of Triassic age in the Rocks Mountain Foothills of northeastern British Columbia and west-central Alberta. *Bulletin of Canadian Petroleum Geology*, v.45(4), pages 719-741.

Riediger, C.L., Fowler, M.G., Brooks, P.W., and Snowdon, L.R., 1990a, Triassic oils and potential Mesozoic source rocks, Peace River Arch area, Western Canada Basin. *Organic Geochemistry*, v.16, pages 295-305.

Riediger, C.L., Fowler, M.G., Snowdon, L.R., Goodarzi, F., and Brooks, P.W., 1990b, Source rock analysis of the Lower Jurassic "Nordegg Member" and oil-source rock correlations, northwestern Alberta and northeastern British Columbia. *Bulletin of Canadian Petroleum Geology*, v.38A, pages 236-249.

Snowdon, L.R., Fowler, M.G., and Riediger, C.L., 1998. Interpretation of organic geochemical data. *CSPG Short Course Notes*, November 5-6, 1998, Calgary, Alberta.

QUATERNARY GEOLOGY AND AGGREGATE POTENTIAL OF THE FORT NELSON AIRPORT AREA

T. Johnsen[1], T. Ferbey[1], V. M. Levson[1] and B. Kerr[1]

KEYWORDS: Surficial geology, aggregate, Sierra-Yoyo-Desan Road, Clarke Lake Bypass, Fort Nelson

INTRODUCTION

A key component of the British Columbia Oil and Gas Development Strategy (OGDS) is a comprehensive road infrastructure plan aimed at promoting better access to resources through improved infrastructure. The completion of road infrastructure improvements, such as the upgrade of Sierra-Yoyo-Desan (SYD) Resource Road and construction of Clarke Lake Bypass Road in the Fort Nelson area, northeast British Columbia (Fig. 1), are expected to promote longer drilling seasons, accelerate exploration and production programs, and increase industry and provincial government revenues. It has been estimated that 2 000 000 m^3 of aggregate material are needed for this initial road infrastructure improvement program. A study was conducted to evaluate existing local sources of aggregate material along SYD Road that could be used for this project (Thurber, 2000), and it was determined that existing aggregate reserves were largely depleted.

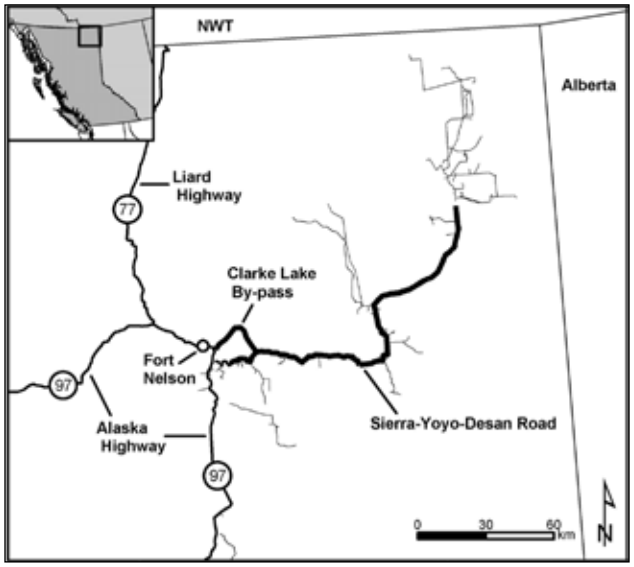

Figure 1: Location of Fort Nelson and major roadways in northeast British Columbia

To meet the aggregate needs for this initial improvement project and future resource and lease-road construction, a surficial mapping program was initiated to systematically explore for new, local aggregate sources in northeast British Columbia (see Levson *et al.*, this volume). Initial test-pit programs were conducted in spring 2003, with follow-up work and reconnaissance-scale fieldwork and preliminary aerial photograph mapping conducted during summer 2003. To date, four main aggregate resources have been identified within the SYD Road corridor, with a total resource of approximately 5 000 000 m^3 of granular material. This effort has also identified numerous other areas that are believed to have potential to host granular deposits but that require further work to sufficiently evaluate.

One such area is within the Fort Nelson airport area, approximately 8 km northeast of the Fort Nelson town site (Figs. 2, 3). This area is of particular interest due to its proximity to the Clarke Lake Bypass Road right-of-way. This report summarizes findings from detailed surficial mapping and test pitting conducted within Fort Nelson airport area.

PROJECT BACKGROUND

SYD Road is a high-grade, all-weather road located east of Fort Nelson and accessed from mile 293 of Alaska Highway. It extends 180 km to the east and northeast ending at the North Helmet airstrip in the Helmet District (Fig. 1). During the majority of summer and a good portion of winter, this resource road supports drilling, well tie-in, wellhead servicing, and well production activities in the area. As such, this road can experience high volumes of heavy oil-field service traffic, which has been increasing due to increased oil and gas exploration and production activities in the area. The volume of traffic on the SYD Road is greater than on the Alaska Highway. Current plans include upgrading and widening of the SYD Road to meet increased demands of this critical resource road. SYD Road provides access to resources that generate $200 to $300 million per year in direct revenue to the province.

As part of this infrastructure improvement project, a new 21 km road is to be constructed from Fort Nelson to the SYD, including a new two-lane bridge crossing of the Fort Nelson River—the Clarke Lake Bypass (Fig. 1). This will eliminate the need to use the narrow BC Rail train bridge and a set of switchbacks. This transportation project will improve safety and access, reduce travel time, and reduce maintenance costs of the road and of vehicles using the road.

[1]*British Columbia Ministry of Energy and Mines*

Finding aggregate deposits that are local can generate great savings. Aggregates account for 30% to 50% of road construction and maintenance costs in northeast BC. As well, costs of transportating aggregate can be prohibitive. For example, for the SYD project, rail transportation costs of aggregate from Fort St. John to Fort Nelson and truck transportation costs from Fort Nelson to the SYD are approximately $\$85/m^3$. Two million cubic metres of aggregate is needed for the 180 km SYD Road upgrade, totalling $170 million. If transportation costs were lowered by just $\$1/m^3$, a savings of $2 million could be generated. It is expected that if local sources of aggregate were found, total aggregate costs could be reduced significantly. Therefore to help minimize road construction costs, Quaternary geology and aggregate potential mapping was completed close to the Clarke Lake Bypass in the Fort Nelson airport area.

STUDY AREA

The study area includes part of the Fort Nelson airport area and is comprised of the area south and east of the main runway, down to the floodplain of Fort Nelson River below (Fig. 3). The study area is located within the Fort Nelson Lowland physiographic region, a flat to very gently rolling area with very little relief (Holland 1976).

The Fort Nelson airport area can be locally divided into three physiographic units: plain, valley side, and valley bottom (inset, Fig. 3). Fort Nelson airport is situated on a near-level plain above Muskwa Valley. This plain continues north and west but has been incised by McConachie Creek, which flows east into Fort Nelson River just north of airport property. This plain is moderately well drained, typically supporting stands of white spruce (*Picea glauca*) and rare lodgepole pine (*Pinus contorta* var. *latifolia*), but does have areas where black spruce (*Picea mariana*) bogs dominate. Closer to the valley sides, trembling aspen (*Populus tremuloides)* is common. Valley sides are steep and terraced; terrace flats are typically 25 to 150 m wide and up to 1000 m long. Terrace flats and risers support white spruce and trembling aspen stands almost exclusively and typically are well drained. The valley bottom setting is flat and moderately to poorly drained. Trembling aspen and balsam poplar (*Populus balsamifera ssp. balsamifera*) stands are more common here, with large blocks having been logged in recent years.

The Fort Nelson airport has had a long and complex land-use history. During the early 1940s it served as a base for the United States Army and Air Force for various staging and training exercises. As a result, much of the area, although now grown over with trees and vegetation, has been disturbed. Evidence of disturbance includes overgrown roads, building foundations, and excavations. These disturbances have made interpretation of aerial photographs and field observations challenging.

BEDROCK GEOLOGY

The Fort Nelson area is underlain by gently dipping marine shales and siltstones of the Lower Cretaceous Buckinghorse Formation of the Fort St. John Group (Okulitch *et al.*, 2002; Thompson, 1977). This formation has a minor component of sandstone. There are no bedrock exposures within the study area. Buckinghorse Formation rocks can however be seen in steep cutbanks south of the Fort Nelson airport area along Fort Nelson River.

Grading laterally and vertically from these rocks are coarser-grained sandstones and siltstones of the Lower Cretaceous Sikanni Formation. To the north of Fort Nelson and northwest of the Fort Nelson airport, Sikanni Formation rocks form a topographic high. Exposures of these rocks are common in road cuts north of town and in areas cleared for agricultural purposes. A similar topographic high is seen east of the airport property, across Fort Nelson River. In both cases these prominent topographic features rise approximately 150 m above the surrounding area.

This sequence of rocks is interpreted to be a transgressive/regressive cycle from marine shales into alluvial-deltaic sandstones, mudstones, conglomerates, and coal. This cycle is repeated three times in the stratigraphy and is attributed to orogenic activity within the Columbian Orogen (Stott, 1975; Thompson, 1977).

QUATERNARY HISTORY AND LANDFORMS

The last ice sheets to have covered northeastern British Columbia and adjacent Alberta have left a record of their presence in the existing landforms and surficial deposits: streamlined forms, meltwater channels, erratics and drift sheets, and traces of former ice-dammed lakes (Mathews 1980). Many of these landforms have been unmodified since the close of the Late Wisconsinan glaciation.

During deglaciation, 13 500 to 10 000 years before present, the Laurentide Ice Sheet retreated generally to the northeast (Mathews 1980). A series of ice-dammed and topographically dammed glacial lakes and meltwater channels developed. Within the Fort Nelson area, a number of meltwater channels and likely recessional moraines that have been mapped as part of this project record the retreat of the Laurentide Ice Sheet (Fig. 2). Moraines are arcuate-shaped in plan view, with northwest-southeast to north-south orientations and with their concave sides facing northeast to east. The recessional moraines are associated with a number of meltwater channels. A moderate-sized meltwater channel now occupied by Jackfish Creek (approximately 25 km south of Fort Nelson) occurs on the north-northeast edge of a topographic high (Fig. 2). Presumably the position of this meltwater channel was related to the presence of ice to

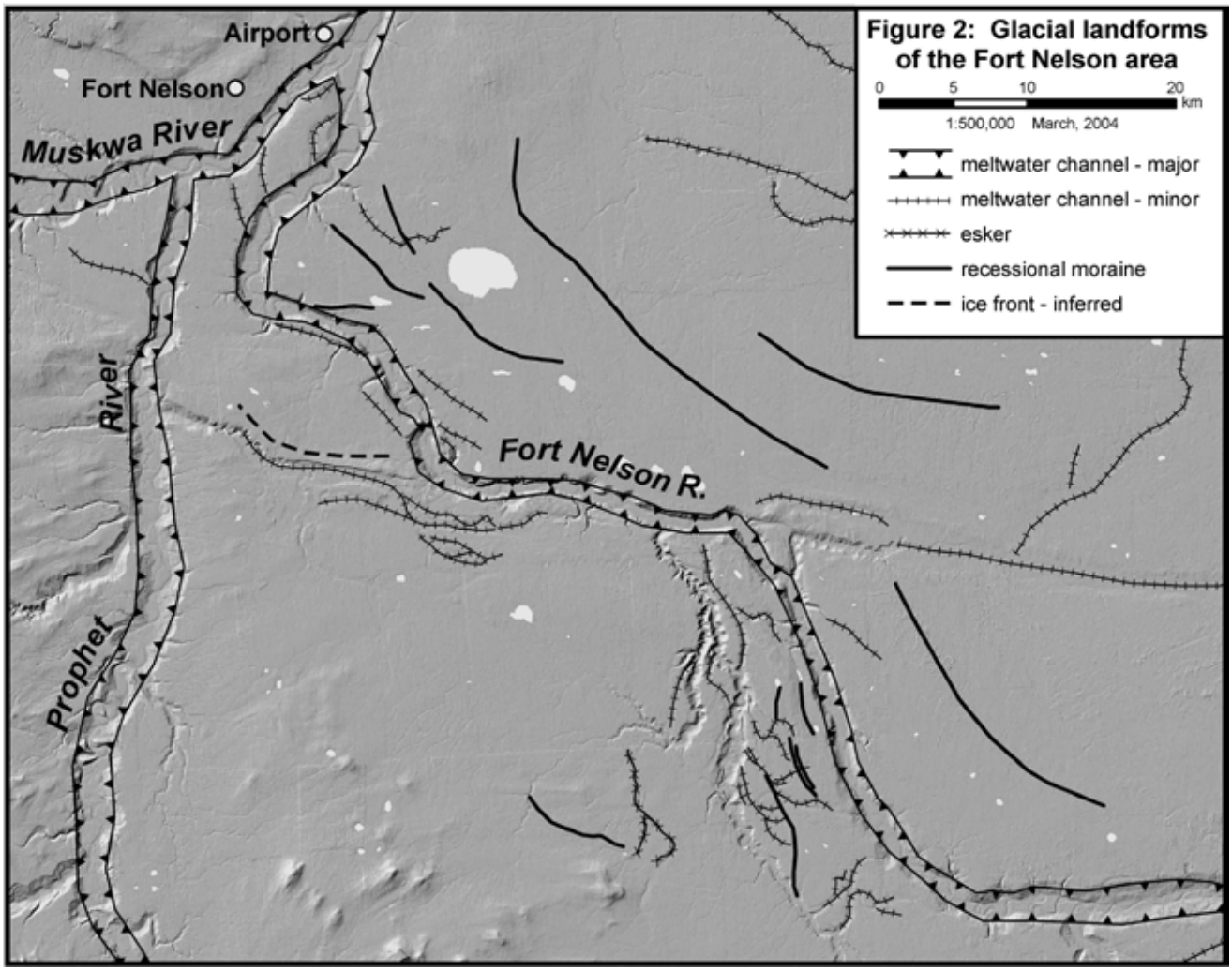

the north-northeast (mapped as an inferred ice front, Fig. 2), otherwise the channel would have developed at a lower elevation. Taken together these observations confirm the general northeast retreat of the Laurentide Ice Sheet within the Fort Nelson area and the importance of this pattern of retreat to the development of meltwater channels, some of which are being mined for aggregate.

The Fort Nelson airport area is located at the confluence of two major meltwater channels (each approximately 2 km wide and approximately 90 m deep) now occupied by the Muskwa and Fort Nelson Rivers (Mathews 1980; Fig. 2). These rivers are smaller in width and much more sinuous than the valleys they occupy. These channels once carried much larger volumes of water and sediment during deglaciation. These conditions led to the transport and deposition of gravel during deglaciation; consequently, there should be aggregate deposits associated with these meltwater systems, particularly at higher elevations within the valleys and on the adjacent plain. Aggregate deposits and landforms on the plain may also be associated with earlier stages of glaciation, when sediments were transported and deposited underneath (subglacial), within (englacial), or atop (supraglacial) former ice sheets. Shallow boreholes that were completed as part of an environmental baseline study for the Fort Nelson airport property indicate that drift thickness can be greater 7 m thick (Transport Canada 1998).

METHODS

Results from a previously conducted reconnaissance test-pit program by Atco Airports Ltd. indicated the occurrence of granular material on Fort Nelson airport property. This information stimulated interest in this area as a host to aggregate deposits. To further assess the area's potential to host such a deposit, British Columbia Ministry of Energy and Mines (MEM) personnel carried out detailed aerial photograph and field surveys.

MEM personnel made observations at 46 field stations, using hand augers and shovels. In areas of tree blowdown, natural exposures in tree-root wads were also utilized to determine subsurface sediment types. To characterize the study area and subsurface sediments, various data were collected: topographic position; dominant tree, shrub, and herb species; exposure height; unit thickness; and sediment texture, structure, and paleoflow. Black and white 1:10 000 and 1:40 000 scale aerial photographs were used throughout the various stages of this study.

Other data collected and compiled for this study included test-pit logs from the original test-pit program conducted by Atco Airports Ltd., subsurface borehole logs (Transport Canada 1998), and test-pit results from an investigation of Clarke Lake Bypass Road right-of-way (Thurber Engineering, unpublished). Following the methodology of Howes and Kenk (1997), detailed surficial geology mapping was completed using these data and 1:10 000 scale black and white aerial photographs.

A test-pitting program was initiated in December 2003 to assess the aggregate potential of the area. Using a Kobelco 220LC tracked excavator, 2 to 5 metre deep pits were excavated at 18 sites on Fort Nelson airport property. At each pit, sediments were described in detail and classified using both the Wentworth scale and the Modified Unified System of Soil Classification. Granular material was sampled from select sites for various laboratory analyses. Following procedures set by Cunningham (1990), sieve analyses, degradation tests (susceptibility of aggregates to mechanical breakdown), and sand equivalent tests (presence or absence of plastic fines) were completed on these samples.

RESULTS AND INTERPRETATION

Surficial geology

The results of surficial geology mapping are shown in Figure 3. Figure 4 summarizes test-pit log data and is classified as indicating either granular or non-granular material. Granular material of less than 1 metre thickness is mapped as non-granular. Granular sediments have grain sizes greater than and including fine sand (greater than 125 μm diameter, Wentworth scale).

The reader is referred to Howes and Kenk (1997) for detailed explanation of surficial geology map labels (Fig. 3). Due to the scale of mapping and the limited data, considerable variation in sediments may occur that is not reflected in the mapping. More confidence in interpretation is given to those polygons containing field data.

Four main types of deposits are found: fluvial (F), glaciofluvial (F^G), organic (O) and morainal (M). Secondary types include colluvium (C) and anthropogenic (A) deposits. Given the long land use history of the study area, many additional areas could be labelled as anthropogenic.

The valley-bottom physiographic area (inset, Fig. 3) includes active fluvial plains that contain flood channels, levees, and scroll bars. The Muskwa River is boxed between valley walls, causing the meander loops to appear boxed-shaped rather than gently looped-shaped in plan view. The area was visited during high water, when dramatic rates of bank erosion were observed. Surface sediments within the fluvial plain are dominantly silt and sand. The Muskwa River is transporting and depositing gravel today and likely did so in the past. Thus, gravel deposited from previous paths of the Muskwa River channel generally occurs beneath these finer-grained deposits. Buried gravels were locally observed along the modern cut banks of the Muskwa River.

The valley-side physiographic area (inset, Fig. 3) includes abandoned river terrace flats and terrace risers of the Muskwa River. These landforms were created during Muskwa River incision. The slopes of terrace risers vary considerably. Terrace flats vary in width from approximately 25 to 150 m. Gravel was observed at the bases of blown-down trees in the southwestern-most terrace flat, which indicates that when the Muskwa River was at this elevation it was transporting gravel. Elsewhere on the same terrace flat, two small swamps (Op) were observed in aerial photographs, suggesting that the sediments immediately underlying these swamps are fine-grained. It is unknown whether these fine-grained sediments are underlain by coarse-grained sediments. Fluvial terraces in the middle and northwest portion of the study area that are at a somewhat similar elevation may contain gravel and/or sand.

The terrace that is crossed by the Clarke Lake Bypass is composed of very fine-grained surficial sediments, likely overbank fines from the ancient Muskwa River. Swamps (Op) on this terrace further suggest that most of the feature is surfaced by fine-grained sediments. The slope above this terrace flat is composed dominantly of morainal material (till). Some of this material appears to have been reworked by mass wasting processes.

The plain physiographic area is an area of very low relief and contains glaciofluvial (F^G), organic (O), till (M), and anthropogenic (A) sediments. Deposits of glaciofluvial sediments are discontinuous and occur as elongate deposits rather than as continuous sheets. Portions of these deposits also have gentle elongate hill morphology, with hill crests aligned southwest-northeast. These observations suggest that these sediments were deposited by water flowing in conduits within glacial ice.

Glaciofluvial deposits are surrounded by organic sediments (bogs). Presumably these organic deposits are under-

Figure 3: Quaternary Geology, Fort Nelson Airport area
0 250 500 1,000 m
Projection: Albers Equal Area Conic (NAD83)
March 2004
Generalized Surficial Material
Organic
Fluvial
Glaciofluvial
Morainal (Till)
Anthropogenic
Roads
Streams
Fort Nelson River
Clarke Lake By-pass
Fort Nelson Airport
Nelson Main Line
Airport Drive
Muskwa River
zsFtm/zsMtm
Fta
szFp
gA'
Op
cdFtj
Ft
dM
Mj/dC'jh
cdFt
czFts-F
czFt
M-V
gsFt
Ftj
szFts-F
sgFtj
F-V
gFt
gF-V
F°
F° /A'
Hillshade map of area and local physiographic units
1 km
area of detail
Plain
Valley side
Valley bottom
N

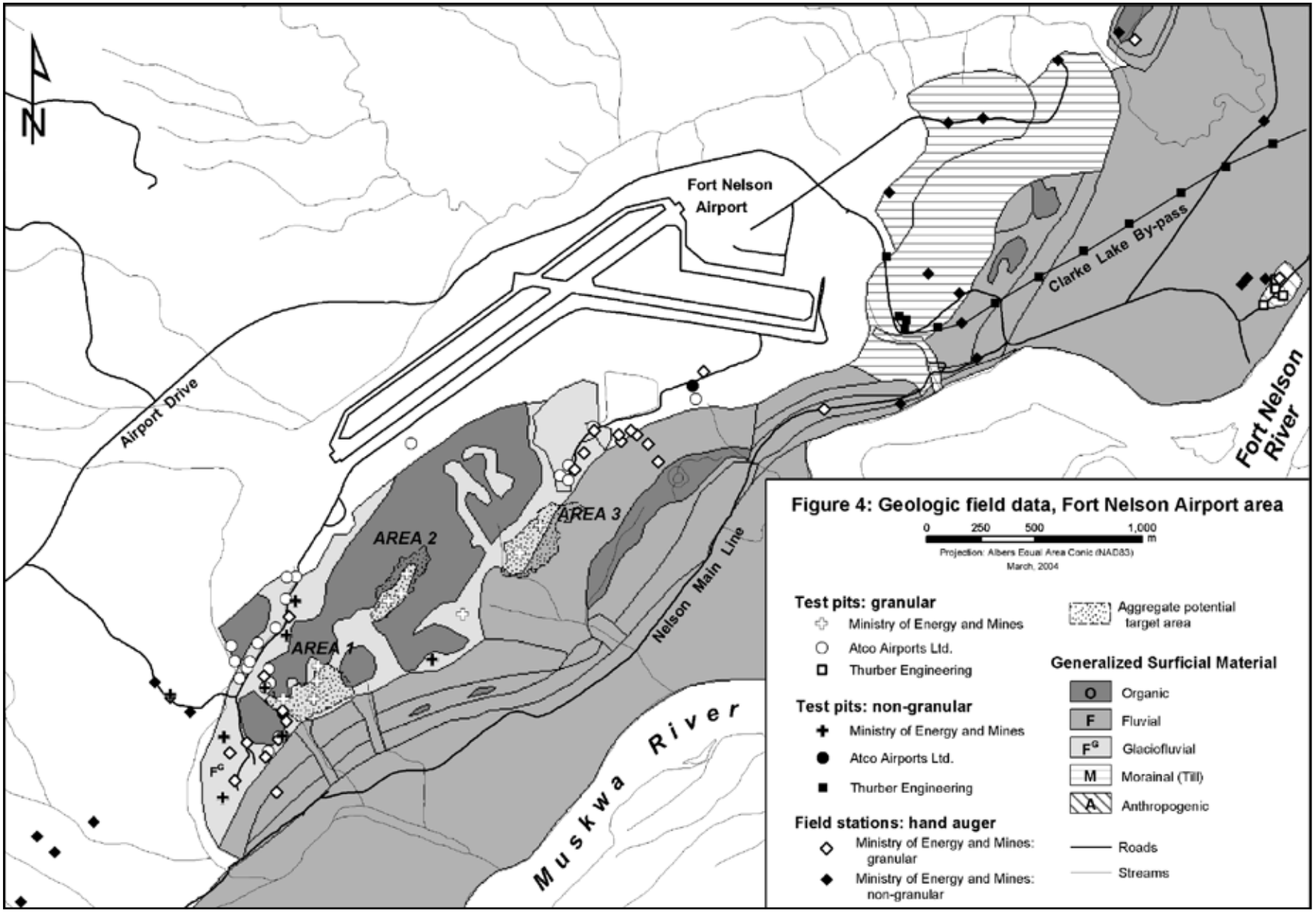
N
Fort Nelson Airport
Clarke Lake By-pass
Airport Drive
Fort Nelson River
AREA 1
AREA 2
AREA 3
Nelson Main Line
Muskwa River
Figure 4: Geologic field data, Fort Nelson Airport area
0 250 500 1,000 m
Projection: Albers Equal Area Conic (NAD83)
March, 2004
Test pits: granular
Ministry of Energy and Mines
Atco Airports Ltd.
Thurber Engineering
Test pits: non-granular
Ministry of Energy and Mines
Atco Airports Ltd.
Thurber Engineering
Field stations: hand auger
Ministry of Energy and Mines: granular
Ministry of Energy and Mines: non-granular
Aggregate potential target area
Generalized Surficial Material
O Organic
F Fluvial
F^G Glaciofluvial
M Morainal (Till)
A Anthropogenic
Roads
Streams

lain by till or thin beds of sand and gravel overlying till. Till is at the surface in the northeast portion of the study area; it is relatively clast rich and massive, with a silty clay matrix. Elsewhere till was observed to underlie glaciofluvial sediments (MEM test pits 3, 5, 8, 9, 11, 13, 15, 23, 53, 56, 57). Anthropogenic deposits are more common than indicated in Figures 3 and 4. Deposits of this type include piles of overburden, granular material, and buried garbage.

DISCUSSION ON GRANULAR DEPOSITS

Test pits were concentrated in the plain physiographic area because this area (i) has known gravel deposits and (ii) has numerous roads that provide relatively easy access for an excavator.

A total of 18 test pits were completed over 3 days (Fig. 4, Table 1). Seven samples were collected for analysis: gradation, degradation, and sand equivalent tests (Cunningham 1990). Based on test-pit data and lab analyses, three areas have been identified that may be of interest for mining granular material: Area 1 includes MEM test pits 11 and 12; Area 2 includes MEM test pits 20, 54 and 56; and Area 3 includes test pits 32 and 57 (Fig. 4).

Area 1

Test pits 11 and 12 in Area 1 lie above and northeast of an old pit face approximately 3 m high and 100 m long with a southeast aspect. Adjacent and southeast of this old pit face is evidence of an old clearing that was likely the site of previous aggregate mining. Area 1 had thicknesses of 2.6 m, more than 2.1 m, and 0.5 m of horizontally stratified gravel in test pits 11, 12, and 53, respectively (Table 1).

Results from degradation and sand equivalent tests indicate that material from test pit 11 meets Ministry of Transportation (MOT) specifications for all granular materials. Based on 4 gradation curves, the granular material in Area 1 is best suited for use as select granular sub-base (SGSB; Ministry of Transportation 2000). Due to disturbances related to land use history, it is difficult to estimate the volume of granular material in Area 1 (Fig. 4).

Area 2

This area is an elongate ridge of approximately 2 m relief, trending southwest-northeast and including test pits 20, 54, and 56. Test pit 20 contained more than 4.4 m of cross-bedded sandy gravel, test pit 54 contained 2.0 m of sandy gravel overlying 0.5 m sand and silt, and test pit 56 contained 1.3 m of sandy, pebbly gravel overlying till (Table 1). This landform is possibly an esker as (i) it has an elongate, hill morphology, (ii) it is composed of granular material, some of which is cross-bedded (approximately 30° dip), and (iii) it is located on the plain. Alternatively the ridge could be a fluvial bar related to high-elevation deposition from the Muskwa River during deglaciation. A number of pine trees, indicating a relatively dry site, occur at test pit 20. This is also the pit with the thickest gravels in the study area. The water table was not encountered.

Results from degradation and sand equivalent tests indicate that gravel from test pit 11 meets MOT specifications for all granular materials and appears best suited for use as SGSB. This classification is based on only two gradation curves, not the mean of four as required by provincial government standard (Ministry of Transportation 2000). Fracture count data (i.e., the number of fractured or naturally occurring angular clasts in specific grain-size fractions) is not required for classifying SGSB material as this material can be produced by direct excavation (i.e., pit-run). However, other MOT granular material classifications, such as high-fines granular surfacing aggregate (HFGSA) or 25 mm well-graded coarse base aggregate (WGCBA), require minimum 50% fracture count after processing. Fracture count tests were not conducted on Area 2 samples; it is therefore not known whether Area 2 sediments would meet the minimum fracture count requirement for these other granular material classifications.

A preliminary granular material volume estimate of 20 000 m^3 has been calculated. This volume was derived using the average thickness of gravels in the three test pits (2.3 m) and a conservative area estimate.

Area 3

Test pits 32 and 57 are located on a broad elongate ridge trending southwest-northeast. Sediments in test pit 32 and 57 are composed of more than 4.6 m and 2.0 m of cross-bedded fine sand, respectively (Table 1). As there was no gravel in these pits, degradation and sand equivalent tests were not completed. Based on one gradation curve, the granular material in Area 3 is not suitable for SGSB. Further testing and additional gradation results may therefore prove Area 3 sediments appropriate for use as SGSB material.

A highly preliminary granular material volume estimate of 50 000 m^3 has been calculated using a conservative area estimate and the average thickness (3.3 m) of granular material in two test pits.

EVALUATION OF MAPPING

Based on test-pit information, only minor changes were required to the surficial geology mapping. Many locations in the plain physiographic area were disturbed, indicating that anthropogenic activity was more common than

TABLE 1. SUMMARY OF MINISTRY OF ENERGY AND MINES TEST PIT DATA

Test Pit #	Depth (m)	Granular material (m) [1]	Description of granular material [2]	Overburden thickness (m)	Water table depth (m)	Sample collected
1	4.0	none	n/a	n/a	none	
3	4.0	0.3-0.8	sandy silty gravel (CL-GM)	0.3 soil	none	
5	3.5	0.6-1.6	pebble cobble gravel (GP)	0.6 soil and fine sand	none	
8	2.0	0-0.5	sandy gravel (GW)	none	none	
9	3.4	1-3.4	0.5 m silty sandy gravel (GP) underlain by 0.8 m pebble gravel (GP)	1.0 road fill and organics	2.3	yes
10	2.5	none	n/a	n/a	none	
11	3.0	0.2-2.8	pebbly cobble gravel (GM)	0.2 soil	2.5	yes
12	2.5	0.4->2.5	sandy gravel (GM)	0.4 soil	2.5	yes
13	2.0	0.5-1.0	silty sandy gravel (GM)	0.5 soil	none	
15	2.5	0.5-1	sandy gravel (GM)	0.5 soil	none	
20	4.5	0.1->4.5	sandy gravel (GM)	0.1 soil	~3.5	yes
23	2.8	0.2-4.5	silty fine sand (SM)	0.2 soil	none	
32	4.8	0.2->4.8	fine sand (SW)	0.2 soil	none	yes
53	2.8	1.8-2.3	silty sandy gravel (GM)	1.8 silt	2.3	yes
54	2.8	0.2-2.2	sandy gravel (GM)	0.2 soil	1.8	
55	2.0	0.4->2.0	gravelly coarse sand (SP)	0.4 soil	1.5	
56	2.0	0-1.3	sandy pebble gravel (GP)	none	none	yes
57	2.5	0.3-2.3	fine sand (SP-GM)	0.3 soil	none	

[1] Depth range

[2] Description after Wentworth grain size classification. Codes in brackets follow the Modified Unified Soil Classification System

is indicated in Figures 3 and 4. Historical activity included aggregate mining, as indicated above.

CONCLUSIONS

The Fort Nelson airport area is host to sediments deposited during and following the last glaciation. These sediments are of morainal, glaciofluvial, fluvial, organic, and anthropogenic origin. Reconnaissance test-pit results suggest that three areas on the Fort Nelson airport property have potential to host aggregate deposits. Detailed air photograph mapping, ground surveys, and a high density test-pit program are required to further assess the quality and volume of granular material present in these areas. As well, there may be other areas within the Fort Nelson airport area that warrant further aggregate potential investigations; for example, the area north of Area 3 and fluvial terrace flats on the valley side.

ACKNOWLEDGEMENTS

We gratefully acknowledge Northern Rockies Regional District and Atco Airports Ltd. for granting access and permission to conduct the test-pit program on the Fort Nelson airport property. Jim Ogilvie of Atco Airports Ltd. generously shared his knowledge of aggregate sightings and test-pit data. Field data was collected with the support of Sheila Jonnes, Jacqueline Blackwell, and Don McClenagan

REFERENCES

Cunningham, D., Editor. 1990. Manual of test procedures, soils and mineral aggregates. British Columbia Ministry of Transportation and Highways.

Howes, D.E. and Kenk, E. 1997. Terrain classification system for British Columbia (version 2): a system for the classification of surficial materials, landforms and geological processes of British Columbia. Ministry of Environment, Lands and Parks, Province of British Columbia, 101 p.

Holland, S.S. 1976. Landforms of British Columbia, a physiographic outline. Bulletin 48. British Columbia Department of Mines and Petroleum Resources. 138 p.

Mathews, W.H. 1980. Retreat of the last ice sheets in northeastern British Columbia and adjacent Alberta. Geological Survey, Bulletin 331. Geological Survey of Canada. 22 p.

Ministry of Transportation. 2000. Section 202 – granular surfacing, base and sub-bases, *In* Standard Specifications for Highway Construction, Volume 1, 586 p.

Stott, D.F. 1975. The Cretaceous system in northeastern British Columbia, *In* Caldwell, W.G.E. (ed.) The Cretaceous system in the Western Interior of North America – selected aspects. Geological Association of Canada, Special Paper 13: 441-467.

Thompson, R.I. 1977. Geology of Beatton River, Fontas River and Petitot River map-areas, northeastern British Columbia. Geological Survey of Canada, Paper 75-11, 8 p.

Transport Canada. 1998. Fort Nelson airport environmental baseline study: Volume 2. Completed by Beatty Franz and Associated Ltd.

QUATERNARY GEOLOGY AND AGGREGATE MAPPING IN NORTHEAST BRITISH COLUMBIA: APPLICATIONS FOR OIL AND GAS EXPLORATION AND DEVELOPMENT

By Victor M. Levson[1], Travis Ferbey[1], Ben Kerr[1], Timothy Johnsen[1], Jan Bednarski[2], Rod Smith[2], Jacqueline Blackwell[1] and Sheila Jonnes[1]

KEYWORDS: Quaternary geology, aggregate potential, shallow gas, Quaternary gas, diamonds, Northeast British Columbia

INTRODUCTION

Rapidly expanding oil and gas development in northeast British Columbia has resulted in a dramatic increase in the need for new geoscientific data in the region. In the field of Quaternary geology, there are two main applications of these data: 1) the identification of aggregate resources for petroleum development roads, and 2) the provision of a stratigraphic framework for the "Quaternary gas" exploration play. A third application of Quaternary geology studies in the region relates to the evaluation of diamond potential. This latter component was included in this study because of the increasingly important significance of diamonds in the mineral exploration sector in northern Canada and because of the associated potential for development of new economic activity in the region.

Quaternary geology studies were initiated in northeasternmost British Columbia (Figure 1) by the Ministry of Energy and Mines in 2002, primarily in response to the critical need for aggregate (sand and gravel) in the region. Access roads to new and rapidly developing gas fields require substantial volumes of aggregate for road construction, improvement, and maintenance. Current infrastructure developments in the region include a major upgrade of the Sierra-Yoyo-Desan (SYD) Road, the construction of a bypass route to the Clarke Lake Road, and a number of new petroleum development road proposals. The Quaternary geology mapping program is also intended to support future exploration and development within northeast British Columbia, including construction of the proposed Northern Link Road (between SYD and Rainbow Lake, Alberta, Figure 1).

Objectives

The main objectives of this study are to

- conduct regional geological inventories of aggregate resources in the vicinity of existing and planned resource roads in northeast British Columbia;
- conduct site-specific investigations to define sand and gravel reserves along the SYD Road, the Clarke Lake Bypass, and new petroleum development roads;
- investigate the natural gas reservoir potential of Quaternary/Tertiary paleovalleys; and
- conduct reconnaissance-scale investigations of diamond potential in the region.

Previous Studies

Few Quaternary geology studies have been conducted previously in the region northeast of Fort Nelson. They have mainly included a regional investigation of ice retreat during the last glaciation (Mathews, 1980) and an unpublished airphoto interpretation study of terrain features and potential aggregate deposits by Mollard (1984a,b). The soils of the Fort Nelson area were mapped by Valentine (1971). The bedrock geology of northeasternmost British Columbia was mapped by Thompson (1977) and Stott (1982).

Study area

The study area occurs within the boreal plains region of northeast British Columbia and includes the area between the Alberta border and the Alaska highway, extending north from Fort St. John to the Northwest Territories. The main areas of focus for the 2003 field season (Figure 1) were the Fontas River and Petitot River map areas (NTS 94 I and P, respectively) and the eastern half of the Fort Nelson map area (NTS 94 J). Results of some of the work conducted in the Fort Nelson area are provided elsewhere in this volume (see paper by Johnsen et al.)

[1]*British Columbia Ministry of Energy and Mines, Resource Development and Geoscience Branch, Victoria, British Columbia*
[2]*Geological Survey of Canada*

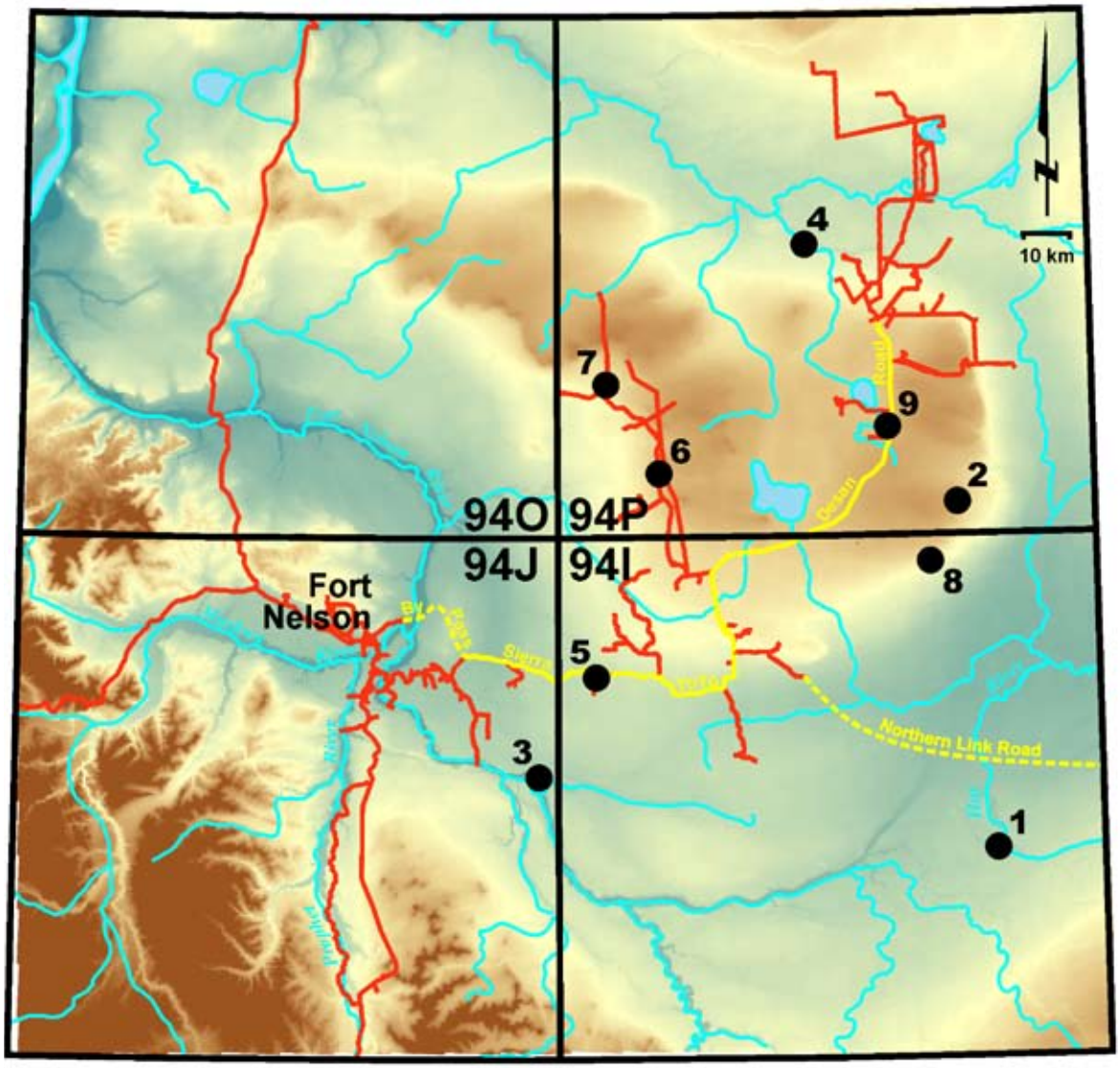

Figure 1. Location map of study area. Numbered sites are discussed in the text.

Low-relief topography and clay-rich soils dominate the study region, resulting in poor drainage and a shallow water table in most areas. Lakes, marshes, fens, and peat bogs with scattered black spruce are common. Areas that are elevated, even slightly, above the regional water table are largely forested, with the dominant tree species being aspen, pine, and white spruce.

PLEISTOCENE GEOLOGY

During the Pleistocene, glaciers advanced westward up the regional slope into northeast British Columbia and dammed rivers draining eastward off the Rocky Mountains. This resulted in the widespread deposition of glacial lake sediments over pre-existing Quaternary deposits and hence the dominance of clay-rich soils. In addition, the local bedrock is dominated by shales and other fine-textured rocks and, consequently, the derived glacial sediments are rich in clay. These fine-grained Pleistocene deposits are common at the surface and are one reason why shallow aggregate deposits are relatively rare in the region.

The dominant surficial materials in the study area are organic deposits and clay tills. Elevated areas that support a tree cover are invariably underlain by morainal deposits, whereas organic materials and glaciolacustrine sediments dominate lower, more poorly drained areas. Morainal landforms include low-relief till plains, rolling moraines, crevasse-fill ridges, flute ridges, recessional moraines, and interlobate moraines. Glaciofluvial landforms are relatively uncommon and include eskers, kames, fans, deltas, and terraces. The latter occur mainly within the Kimea Creek-Petitot River meltwater channel system.

During deglaciation, numerous meltwater channels were incised by streams generally flowing westward from the retreating Laurentide ice sheet. Sands and gravels were locally deposited in association with meltwater channels,

but many appear to be entirely erosional and may have formed subglacially. Some recently discovered aggregate deposits underlying stony diamicton along channel flanks are interpreted to be subglacial channel deposits overlain by meltout till (Figure 2). Although large surficial deposits of aggregate are rare, one exceptionally large glaciofluvial fan-delta (Figure 3; see Site 1, Figure 1 for location) was discovered on the east side of the Fontas River map area (NTS 94 I). This feature covers an area of approximately 100 km^2 and is likely the single largest sand and gravel deposit in northeast British Columbia. An indication of the enormous size of the fan is that it was first noticed on a satellite image. A measured section in the fan showed 7 m of well-rounded, quartzite-rich gravels overlain by 5 m of well-sorted sands. The thick sand cap has been largely removed in many areas by erosion of the Hay River, which dissects the fan. The best target areas for coarse aggregate are thus along lower terraces of the river where it cuts the fan. These sands and gravels overlie approximately 5 m of clay-rich diamicton interpreted to be basal till.

Dating of Pleistocene sediments in the area has been facilitated by the discovery of an interglacial peat underlying a thin till and oxidized sandy unit in the Spruce Road area (Site 2, Figure 1). The peat contains abundant plant matter, including many wood fragments, as well as numerous pelecypod and gastropod fossils. Radiocarbon analyses on two wood pieces yielded dates of more than 38 690 radiocarbon years before present (BP) (Beta 183832) and more than 40 590 radiocarbon years BP (Beta 183831). Another fragment of wood recovered from gravels stratigraphically underlying till in the Elleh Creek area (Site 3, Figure 1) was dated at 24 400±150 radiocarbon years BP (Beta 183598). Collectively, these dates and the associated stratigraphy provide new constraints on the Pleistocene history of the region and indicate that ice-free conditions probably existed from before 40 ka until after about 24 ka BP.

AGGREGATE STUDIES

Aggregate resources in northeast British Columbia are relatively rare outside of major river valleys. Existing deposits in many areas of active petroleum road development have been largely depleted (Thurber Engineering, 2001, 2002) while demand is increasing. The region northeast of Fort Nelson is an area of particularly active exploration and

Figure 2. Sands and gravels in the Nogah Road area, interpreted to be subglacial channel deposits, underlying thin, stony, meltout till. The gravels overlie thick, clay-rich, basal till at most locations.

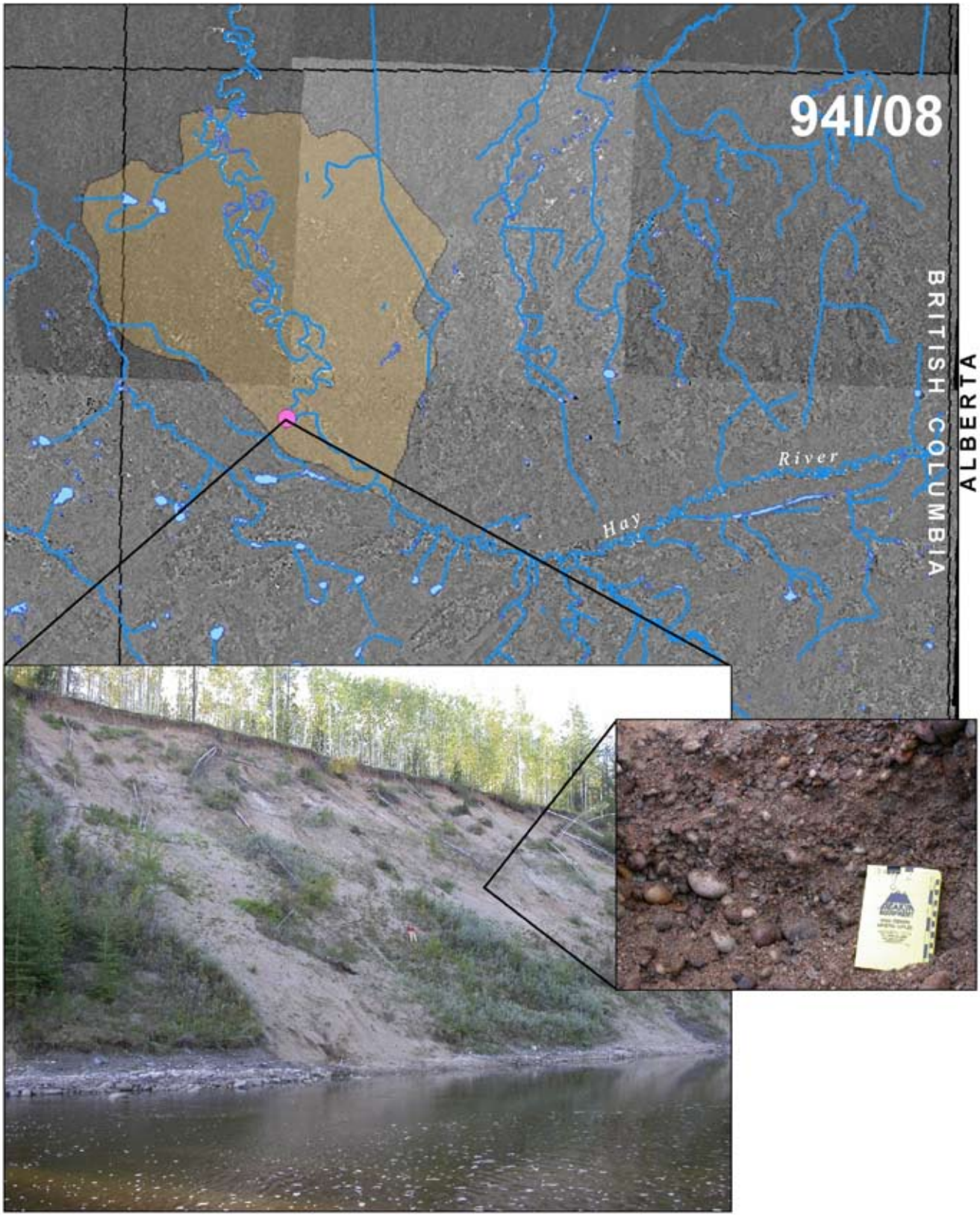

Figure 3. Large glaciofluvial fan-delta exposed along the Hay River. The orange polygon approximately delineates the extent of this fan. Inset photographs were taken at a section on Hay River where this fan-delta has been incised. Note person for scale.

development. For example, EnCana Corporation has described plans to drill about 100 new wells per year for the next several years on the Greater Sierra gas field, which is nearly 300 km long (Daily Oil Bulletin, June 2002). Road improvements in this area would reduce the requirement to impose road bans in the spring, allowing for an extended drilling season. The chronic shortage of aggregate has resulted in high prices and even the need for shipping of gravel into the region by train from Fort St. John.

To meet this need, a program was initiated as part of the British Columbia Oil and Gas Development Strategy (OGDS) to systematically explore for new, local aggregate sources in northeast British Columbia. The program includes both regional and site-specific aggregate evaluations. The identification of regional sand and gravel resources will provide the necessary information for developing a long-term strategy to ensure that roads in the region are capable of supporting the future demands of industry. Improved access and transportation cost savings to resource companies will also enhance viability of projects and encourage exploration investment, leading to new discoveries. The identification and evaluation of site-specific reserves will ensure an aggregate supply not only of adequate volume, but also of good quality. Sampling and laboratory testing will identify the areas of best aggregate quality for the various types of road improvement.

A key component of the OGDS is a comprehensive road infrastructure plan aimed at promoting better access to resources through improved infrastructure. The completion of road improvements, such as the upgrade of the SYD Road and construction of the Clarke Lake Bypass Road in the Fort Nelson area, is expected to promote longer drilling seasons, accelerate exploration and production programs, and increase industry and provincial revenues.

It has been estimated that the current upgrade of the SYD Road will require two million cubic metres of aggregate for the initial road infrastructure improvement program. However, a study completed by Thurber Engineering (2002) indicated that existing aggregate resources along the SYD Road were largely depleted. Four of the ten reserves investigated were completely depleted, and only three had more than 100 thousand m^3 of aggregate remaining. To meet this need, a program was initiated to systematically explore for new, local aggregate sources in the region.

Initial aggregate evaluations in the fall of 2002 focused on an airphoto study and brief field investigation of the SYD corridor (Blyth *et al.*, 2003). From this preliminary work, fourteen sites with aggregate potential were identified, including sites in the Kimea Creek (Figure 4), Hoffard Creek, Courvoisier Creek, Komie Road (Figure 5), Kotcho East (Figure 6), and Sahdoanah Creek areas (Sites 4 to 9, respectively, Figure 1).

As a follow-up to the airphoto study, ground investigations were conducted in the winter of 2003 at 9 sites (Dewar and Polysou, 2003a). A total of 458 test pits were excavated, and granular materials were encountered in 235 of these pits at 8 of the sites. Two additional areas, where bedrock was inferred to be shallow, were also investigated. Bedrock was encountered in all 15 test pits at the sites, although the quality of the rock appeared to be suitable only for general borrow material. Detailed investigations conducted at 4 sites included field sampling and laboratory testing (124 sieve analyses, 10 sand equivalent tests, and 10 degradation tests). Sieve tests were completed on an additional 47 samples from 3 other sites. The results of the sampling program and laboratory analyses are provided by Dewar and Polysou (2003b, c, d, e).

The 4 areas investigated in detail are referred to here as the Kimea, Kotcho East, Komie North, and Elleh sites. These sites have a total inferred resource of approximately 5 000 000 m^3 of granular material: Komie North (more than 300 000 m^3), Kimea (more than 3 000 000 m^3), Kotcho East (approximately 450 000 m^3) and Elleh (more than 1 000 000 m^3). The Kimea deposit is one of several prospective glaciofluvial terraces (Figure 4) within a large meltwater channel system extending along parts of Kimea Creek and Petitot River. The Komie North deposit is interpreted to be an ice-contact delta (Figure 5). The origin of the Kotcho East deposit (Figure 6) is enigmatic because it is entirely buried and has virtually no surface expression. It may be a raised delta or part of a proximal glaciofluvial stream deposit. The Elleh deposit is interpreted to consist mainly of advance-phase glaciofluvial deposits but also locally includes interglacial sands and gravels deeper in the deposit, where the 24 ka BP radiocarbon age was obtained. Late-glacial (retreat-phase) gravels, which stratigraphically overlie till, also occur in the area at the surface.

Electromagnetic Surveys

Subdued topography, extensive muskeg, and a general scarcity of glaciofluvial landforms make the use of traditional aggregate mapping techniques, such as aerial photograph interpretation, relatively ineffective for locating new deposits in many parts of the study area. In addition, sand and gravel deposits in the area are commonly blanketed by glaciolacustrine and glacial sediments. As a result, new subsurface investigations and geophysical techniques are being tested and used to identify these buried aggregate deposits. Data sources include down-hole geophysical logs, water-well logs, seismic shot hole data, and conductor pipe logs. Airborne aeromagnetic surveys, high-resolution electromagnetic (EM) surveys, light detection and ranging (LIDAR), and other remote sensing techniques are also being used in exploring for buried aggregate deposits. In this section we briefly report on the results of a high-resolution airborne EM survey of a buried gravel deposit in the Kotcho East area (NTS map area 93I/15).

Figure 4. Exposure of glaciofluvial terrace gravels in the Kimea Creek area. The deposit is within a large meltwater channel system extending along the Kimea Creek and Petitot River valleys. Note shovel in foreground for scale.

The survey was centred on a deposit originally discovered during a follow-up field investigation of buried gravels reported from seismic shot hole logs. Excavations in the vicinity of the reported occurrence show gravels underlying silt-rich sediments (Figure 6). The buried sands and gravels were encountered in 10 test pits in an elongated southwest-trending area, oblique to present surface stream channels. The sands and gravels occur along a gentle southeasterly slope with no obvious geomorphic indications of their presence. They are overlain by silts and clays generally 1 to 2 m thick but locally up to 5 m thick. These sediments are interpreted to be glaciolacustrine in origin. In the inferred core of the paleochannel, the sands and gravels are at least 5 m thick, and in 6 of the test holes the base of the channel was not encountered. Surprisingly, the water table was encountered in only one test hole at the southeasternmost edge of the deposit.

An airborne EM survey was conducted over this area to evaluate the utility of the method for mapping shallow gravel deposits, to attempt to trace the extent of the Kotcho East gravel deposit beyond the field-tested boundaries, and to identify any new gravel targets in the region. To accomplish these goals, a detailed survey with 100 m line spacing was flown over the Kotcho deposit and 200 m line spacing was flown over a larger area (about 25 km^2) around the known deposit. The survey employed the helicopter RESOLVE multicoil multifrequency EM system supplemented by two high-sensitivity cesium magnetometers and a GPS electronic navigation system. The EM system was located in a bird flown at an average height of 39 m above the ground. Apparent resistivity maps were produced from the 400, 1500, 6400, 25 000, and 115 000 Hz data.

Results (Figure 7) show that three main areas of high resistivity were identified in the survey on the high-frequency data, which best reflects the shallow geology. The northernmost area coincided remarkably well with the area of shallow buried gravels as mapped out by the field investigations. The southern two areas are much larger and will be the focus of future ground investigations. Preliminary testing indicates that these other areas of high resistivity are also sand and gravel deposits. The results of this work strongly indicate that high-resolution EM surveys can be an

Figure 5. Planar cross-bedded gravels exposed in the Komie North deposit, interpreted to be deltaic forset gravels.

effective tool for mapping buried sand and gravel deposits in the study region. A more detailed discussion of the results of this survey is provided elsewhere in this volume (see paper by Best *et al*.).

PALEOCHANNEL MAPPING

Reconstructions of the three-dimensional architecture of thick Quaternary sequences in northeast British Columbia and northwest Alberta have recently become of interest for several reasons. First, natural gas exploration companies have been investigating shallow gas targets in the region (see below). Secondly, rapidly expanding oil and gas infrastructure has depleted local surface aggregate supplies and created a critical need for identification of subsurface gravel deposits. Thirdly, shallow groundwater aquifers are used for agricultural purposes, as drinking water sources, and as possible discharge sites for waters extracted during coalbed methane operations. In addition, shallow aquifers are susceptible to contamination as development expands in the region. All of these applications have resulted in the need for an improved understanding of the Quaternary stratigraphy of the region. The main geological characteristic of shared importance to all these applications is the presence of relatively large bodies of granular sediment in a variety of paleochannel settings in the subsurface.

The depth and geometry of sand and gravel sequences of either glaciofluvial or interglacial origin in these paleovalleys is key to aquifer mapping and aggregate studies. Large, laterally continuous units can form significant aquifers at nearly any depth within the buried valleys; however, sand and gravel units must occur relatively close to surface and have a thin overburden to be of economic significance as aggregate resources. The greatest potential for shallow gravels is in smaller paleochannels that were tributary to the larger paleovalleys. Mapping these channel deposits is relatively difficult and often requires higher-resolution geophysics or dense borehole data.

Preliminary reconstruction of the bedrock topography—the first step in identification and mapping of paleochannels—has been completed using water-well logs and oil and gas well records (e.g., Figure 8). More detailed mapping of these buried features is being accomplished in

Figure 6. Test pit exposure of sands and gravels in the Kotcho East deposit buried by surficial silts. Test pit is approximately 1.5 m wide.

some areas by interpretation of geophysical data, including high-resolution aeromagnetics, resistivity surveys, seismic profiling, and ground-penetrating radar.

QUATERNARY/TERTIARY GAS

Interest in Quaternary gas was highlighted in the study region by development of the Sousa Quaternary gas field near High Level, Alberta. That field has successfully been producing gas since 1998 from paleochannel sediments underlying late Quaternary glacial deposits. The sands and gravels that form the reservoir are believed to be of early Quaternary age, although a Late Tertiary age is also possible. The cap for the gas is thick clay-rich glacial tills and glaciolacustrine sediments. Numerous wells have been drilled into Quaternary sediments and completed at depths of less than 300 m. One field in Alberta has yielded more than 4 billion cubic feet (bcf) of gas, with one well producing up to 4.4 million cubic feet per day (mmcf/d) (Canadian Discovery Digest, 2000).

Northeast British Columbia has a similar geological and glacial history to that of northwest Alberta, where these producing shallow gas fields have been developed, and, as such, the region has similar potential to host Quaternary gas. In order to identify potential paleochannel areas, the British Columbia Ministry of Energy and Mines is currently mapping the regional bedrock topography of NTS map areas 94 I (Figure 9) and 94 P. To date, about 1000 wireline-geophysical logs have been used to map the surface of the bedrock (Upper Cretaceous Dunvegan Formation conglomerates,

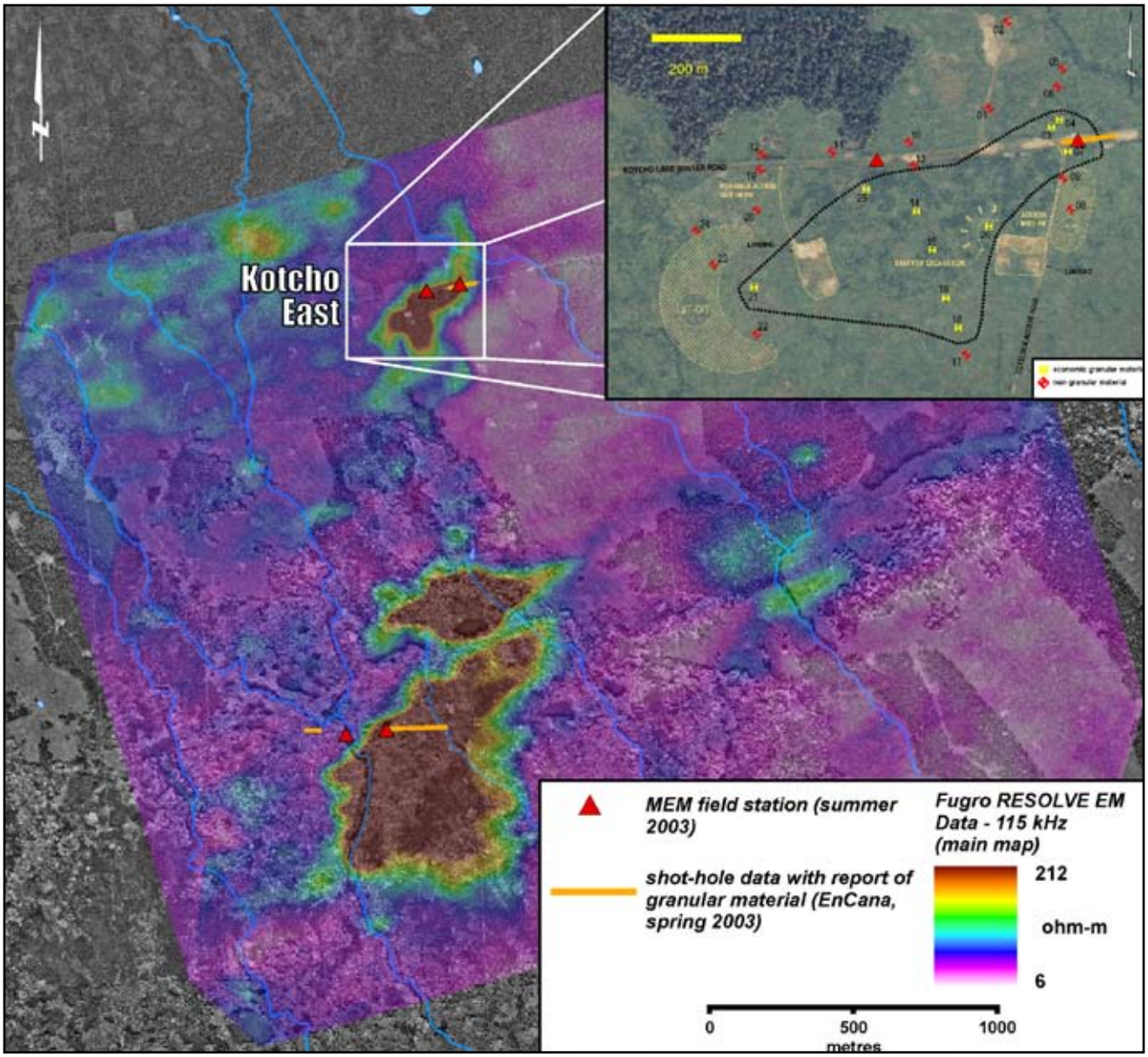

Figure 7. Results of an electromagnetic survey in the Kotcho East area. An area of high resistivity (in the north) corresponds closely with a known sand and gravel deposit (as determined by field investigations shown in the inset). Preliminary testing indicates that the large areas of high resistivity in the south are also sand and gravel deposits.

sandstones, and shales and Lower Cretaceous Fort St. John Group shales and sandstones). Where possible, lithologic and sedimentologic descriptions in nearby conductor pipe and water-well logs have been used to verify bedrock picks (Figure 8). Drift thickness in these map sheets varies from a few metres to as much as 280 m. Bedrock valleys and areas with granular material overlying bedrock indicate the presence of Late Tertiary to Pleistocene paleochannels that could be suitable targets for gas exploration.

Quaternary/Tertiary gas occurrences appear to be mainly in areas distant from deeply incised, large modern valleys. The reservoir sediments are buried by thick sequences of Middle to Late Pleistocene deposits of relatively low permeability. The westward advance of Laurentide glaciers up the regional slope in successive Quaternary glaciations effectively dammed eastward-draining rivers and deposited thick sequences of glaciolacustrine sediments and clay tills derived from local Mesozoic shales. Large paleovalleys in the Fort St. John area are up to a few hundred metres deep and a few kilometres wide and make significant exploration targets. Preliminary mapping indicates that a number of smaller buried paleovalleys in the Fontas River and Petitot River map areas are likely present (Figure 1). The proximity of these paleovalleys to producing Quaternary gas fields in Alberta as well as the similar geological setting suggest that this region has similar potential for new gas discoveries.

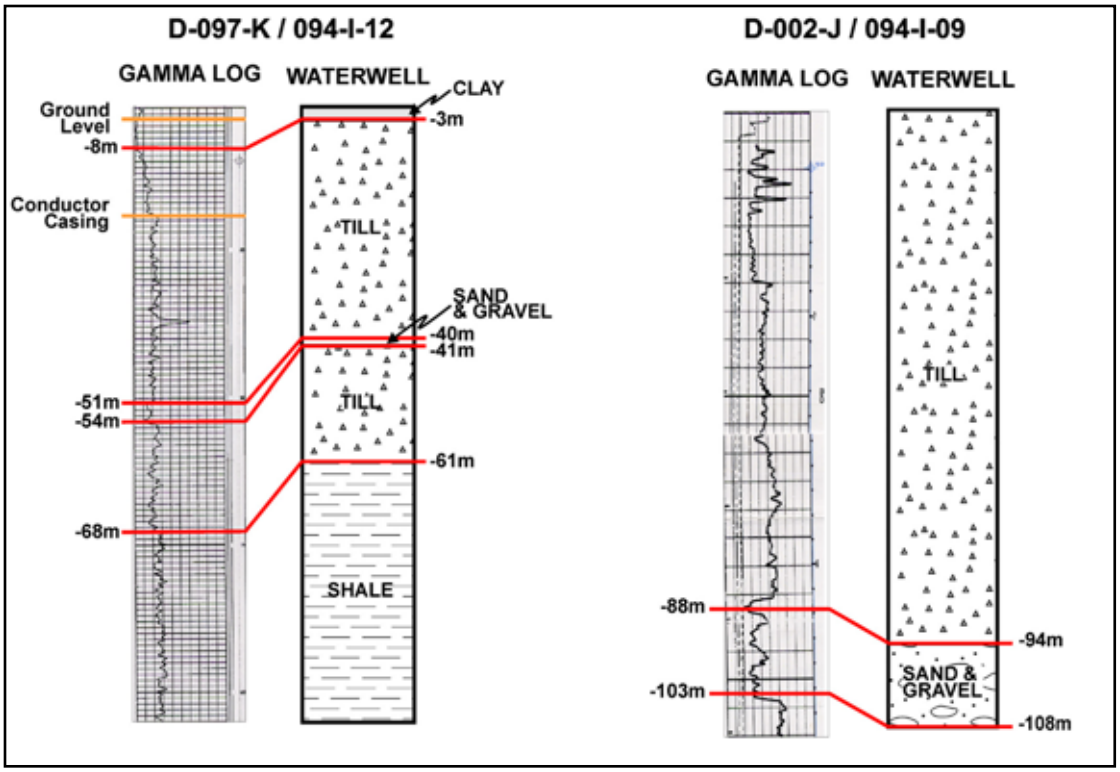

Figure 8. Examples of water-well logs and nearby oil and gas well geophysical logs used in the identification and mapping of Quaternary stratigraphy, subsurface aggregates, bedrock topography, and paleochannels.

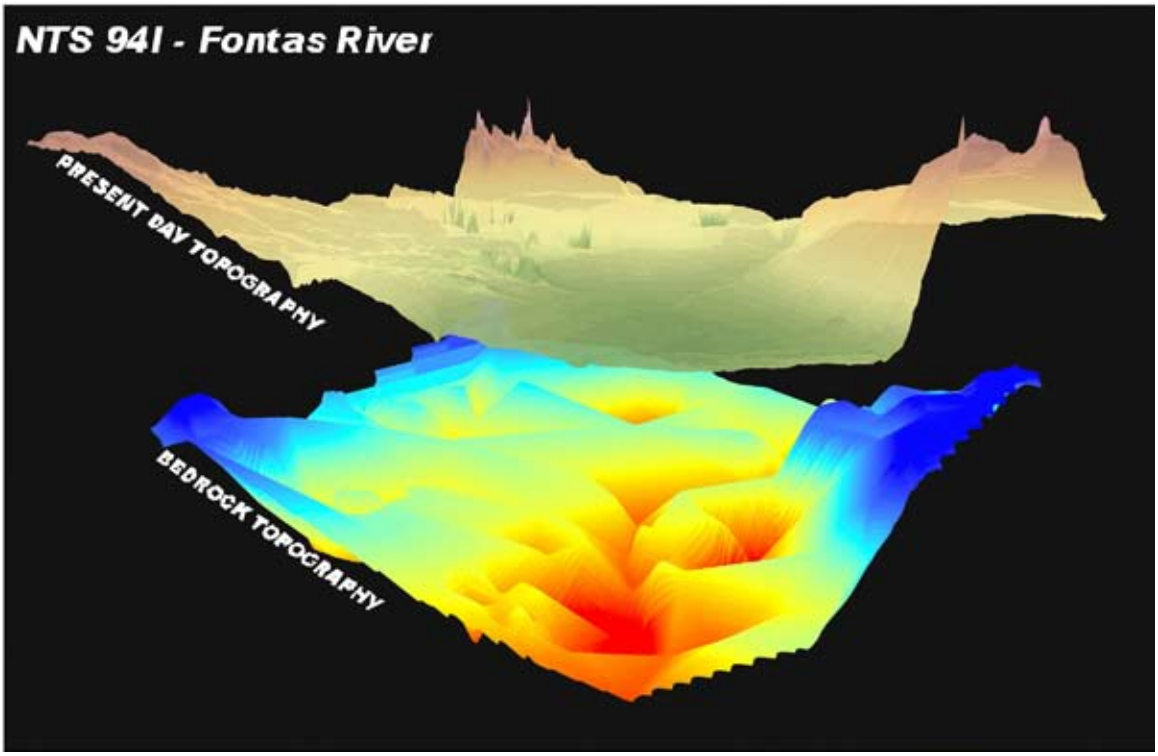

Figure 9. Preliminary reconstruction of the bedrock topography (lower panel) and surface relief (upper panel) of NTS map area 94 I based on data from about 400 wireline-geophysical logs. View is towards the southwest. Depth to bedrock varies from a few metres to as much as 280 m. Buried bedrock valleys are interpreted as Late Tertiary to Pleistocene paleochannels that are possible targets for gas exploration

DIAMOND POTENTIAL

A secondary component of recent Quaternary geoscience studies in northeast British Columbia involves the evaluation of the regional diamond potential. Sedimentary rocks in the area are underlain by Precambrian basement with possible Slave craton equivalents, but the diamond potential of the region is largely unknown. As part of the 2003 Quaternary geology program, reconnaissance sampling of glaciofluvial deposits was conducted. Glaciofluvial sediments were selected as a sampling medium because of their potential to reflect relatively large drainage areas compared to modern fluvial deposits. Bulk samples were collected and concentrates were produced in the laboratory using heavy liquids. Kimberlite indicator minerals have been detected at a number of sites. Microprobe analyses are in progress to evaluate possible sources for the indicator minerals.

CONCLUSIONS

Recent Quaternary geology investigations in the boreal plains in northeasternmost British Columbia have been initiated in response to the need for more information on the surficial geology of the region. The main demand has come from a rapidly expanding oil and gas road infrastructure and an accompanying critical need for the identification of aggregate deposits. Gravels close to surface with minimal overburden are preferred, but such deposits are relatively rare in northeast British Columbia. In addition, techniques commonly used for identifying gravel deposits, such as geomorphological mapping, are relatively ineffective in the region due to the widespread forest cover and subdued topography. Additionally, ground-based exploration techniques are too costly and time-consuming for covering vast areas of investigation such as the plains region of northeast British Columbia. As a consequence, Quaternary mapping programs in the region have focused on the collection of subsurface borehole and geophysical data as well as airborne aeromagnetic, high-resolution electromagnetic, and LIDAR survey data.

The result of this work has led to the discovery of several new aggregate occurrences in the region. To date, 4 main aggregate deposits have been investigated in detail within the study area, with a total resource of approximately 5 million m^3 of granular material. One of these deposits was completely buried and could not be detected by traditional airphoto mapping techniques. It was initially discovered from seismic shot hole data and was subsequently mapped using an airborne high-resolution electromagnetic survey. Several other occurrences have been investigated to various levels of detail. One of the most significant of these in terms of size is a large fan-delta in the Hay River that covers an area of approximately 100 km^2 and contains a maximum known thickness of 22 m of sand and gravel.

Mapping of buried channels in northeast British Columbia has recently become of interest because of the discovery of natural gas in Quaternary paleochannel sediments in northwest Alberta. Sands and gravels of probable Early Quaternary or Late Tertiary age form the reservoirs, which are capped by thick Pleistocene glaciolacustrine deposits and clay-rich tills that act as cap 'rocks'. Preliminary bedrock topography mapping in the study area suggests that paleochannels with gas potential are present. Finally, the discovery of kimberlite indicator minerals at several sites in the study area suggests that northeast British Columbia has diamond potential and that further diamond exploration in the region is warranted.

ACKNOWLEDGEMENTS

The authors would like to acknowledge John Pawlowicz, Mark Fenton, and Roger Paulen of the Alberta Geological Survey and Alain Plouffe of the Geological Survey of Canada, who provided many valuable ideas during the course of this work; their collaboration and contributions are greatly appreciated. The cooperation and advice of Tyson Pylypiw and Doug Anderson from Encana Corporation, Doug McConnnell of Fugro, and Doug Dewar of Amec are also greatly appreciated.

REFERENCES

Blyth, H., Levson, V. and Savinkoff, P. (2003): Sierra-Yoyo-Desan aggregate potential mapping; British Columbia Ministry of Energy and Mines, fourteen 1:50 000-scale map sheets.

Cain, M.J. (2004): RESOLVE survey for the British Columbia Geological Survey; *Fugro Airborne Surveys,* Report 3091, 22 pages.

Canadian Discovery Digest (2001): Sousa 111 2W6 Quaternary Gas; Exploration Review, Canadian Discovery Digest, January/ February 2001 Report, pages 25-39.

Dewer, D. and Polysou, N. (2003a): Project overview report: Sierra-Yoyo-Desan Road area gravel investigation, Northeastern British Columbia; *AMEC Earth and Environmental Limited*, Report No. KX04335-KX04395, 14 pages.

Dewer, D. and Polysou, N. (2003b): Field and laboratory work-Summary Report (Areas 1,2,3,4,5,5A,7,7A): Sierra-Yoyo-Desan Road gravel investigation, Northeastern British Columbia; *AMEC Earth and Environmental Limited,* Report No. KX04335-KX04395, 19 pages.

Dewer, D. and Polysou, N. (2003c): Area 8 (Komie North) gravel investigation - Sierra-Yoyo-Desan Road area, Northeastern British Columbia; *AMEC Earth and Environmental Limited,* Report No. KX04335, 19 pages.

Dewer, D. and Polysou, N. (2003d): Area 9 (Kimea) gravel investigation - Sierra-Yoyo-Desan Road area, Northeastern British Columbia; *AMEC Earth and Environmental Limited,* Report No. KX04335, 25 pages.

Dewer, D. and Polysou, N. (2003e): Area 10 (Kotcho East) gravel investigation - Sierra-Yoyo-Desan Road area, Northeastern British Columbia; *AMEC Earth and Environmental Limited,* Report No. KX04335, 13 pages.

Mathews, W.H. (1980): Retreat of the last ice sheets in Northeastern British Columbia and adjacent Alberta; *Geological Survey of Canada*, Bulletin 331, 22 pages.

Mollard, D.G. (1984a): Office airphoto study for the mapping of sand/gravel prospects in Kotcho Lake area, Northeastern British Columbia; *JD Mollard and Associates Ltd.*, 9 pages.

Mollard, D.G. (1984b): Terrain and surface geology map; Kotcho Area, British Columbia; *JD Mollard and Associates Ltd.*, 9 pages.

Stott, D.F. (1982): Lower Cretaceous Fort St. John Group and Upper Cretaceous Dunvegan Formation of the foothills and plains of Alberta, British Columbia, District of MacKenzie and Yukon Territory, Geological Survey of Canada, Bulletin 328, 124 pages.

Thompson, R.I. (1977): Geology of Beatton River, Fontas River and Petitot River map areas, Northeastern British Columbia; *Geological Survey of Canada*, Paper 75-11, 8pp.

Thurber Engineering (2001): Sierra-Yoyo-Desan Road gravel inventory; report to British Columbia Ministry of Energy and Mines, Oil and Gas Initiative Branch, 14 pages.

Thurber Engineering (2002): Sierra-Yoyo-Desan Road gravel inventory; supplementary report to British Columbia Ministry of Energy and Mines, Oil and Gas Initiative Branch, 9 pages.

Valentine, K.W.G. (1971): Soils of the Fort Nelson Area of British Columbia; *British Columbia Soil Survey, Canada Department of Agriculture,* Report No. 12, 60 pages.

THE COALBED METHANE RESOURCE OF SOME PROSPECTIVE AREAS OF THE CROWSNEST COALFIELD

By Barry Ryan[1]

KEYWORDS: Coal rank, gas contents, coal thicknesses, Mist Mountain Formation

INTRODUCTION

The majority of literature refers to the extraction of coalbed methane (CBM) from coal. This is not scientifically correct as the gas extracted from coal is a mixture of methane, carbon dioxide, and other gases. The British Columbia government is adopting the term coalbed gas (CBG). The abbreviations CBM and CBG both refer to the commercial gas extracted from coal at depth. To avoid confusion with existing scientific literature, this paper uses the term CBM.

The Crowsnest coalfield is located between the Elk River and Michel Creek drainages and covers a total area of about 600 km^2. A major pipeline, which trends north-south through the coalfield (Figure 1), connects the Alberta gas fields with the US market. This pipeline has been expanded from the original 36-inch Trans Canada pipeline and is now twinned with a 48-inch Foothills pipeline following the same right-of-way. An 8-inch pipeline, which branches off the main line in the northeast corner of the coalfield, serves the towns of Sparwood and Elkford and some of the mines. A second 8-inch pipeline branches off at Morrissey and serves the town of Fernie. Title to the gas rights in the coalfield is in part with the crown and in part unassigned at this time. This paper summarizes existing mapping data, coal quality, and coal resource data. It also attempts to delineate the resource potential of areas where the crown has clear title; this means disregarding areas where various companies have at least freehold coal rights.

The Crowsnest coalfield has been mapped by a number of geologists. One of the earliest was Newmarch (1953), who provided a preliminary map of the coalfield and detailed geology of the Coal Creek area, which was compiled at a time when the mines in the creek were still operating. Price (1961) produced a regional map of the Crowsnest coalfield, which also provides strike and dip information. The area was mapped using orthophotos in the period 1977 to 1981 by a number of personnel from the British Columbia Ministry of Mines (Pearson *et al.,* 1977; Pearson and Grieve, 1978, 1980). These maps outline seam trends and provide structural information. Recently, a compilation of the mapping and construction of geological sections was completed by Johnson and Smith (1991). Other recent studies such as Dawson *et al.* (1998) have used these maps and accompanying sections. Monahan (2002), as part of an assessment of the oil and gas potential of the area, produced a revised map using existing mapping and well data.

The map from Johnson and Smith is reproduced here (Figure 1) with additional information, which includes approximate delineation of various land blocks, areas in which the Mist Mountain Formation is at least in part at a depth of less than 1000 m, and fold axial plunge data transferred from Price (1961). In addition, geological sections from Johnson and Smith (1991) are reproduced with some additional sections to give a spacing of 5 km for sections through the coalfield (Figure 2). The 1000 m depth line is shown on the sections.

There are a number of publications that deal with coal quality and surface and underground coal resources of the coalfield. A summary paper (Pearson and Grieve, 1985) discusses coal quality. Coal rank in the coalfield varies from high-volatile bituminous to low-volatile bituminous, with higher rank coals in the southwest part of the basin. There is also evidence that rank increases down dip into the core of the major syncline that crosses Morrissey Creek

Johnson and Smith (1991) were the first to estimate the CBM resource of the coalfield, and they calculated a value of 12 trillion cubic feet (Tcf). They used an average gas versus depth curve derived from data from the San Juan Basin. In 1990, a number of companies drilled stratigraphic test holes in the southern part of the coalfield (Dawson *et al*., 2000) (Figure 3). A best-fit curve to all desorption data (Figure 4) resulting from this drilling in the coalfield indicates a lower total resource for the coalfield of 6.7 Tcf.

To date, the only assessment that covers parts of the coalfield is that by Dawson et al. (1998), who assessed the CBM resource potential of the two Dominion Blocks (Block 73 in the north and Block 82 in the south; Figure 1). These blocks have a total area of 202 km2 (Block 73, 20.2 km2; Block 82, 182.1 km2). Dawson et al. (1998) considered gas contents to vary from 10.9 to 20.1 cm3/g (350 to 650 standard cubic feet per tonne [scf/t]). They estimated a total resource for the two blocks of 6.57 Tcf to a depth of 1000 m. The northern Block 73 having 0.65 Tcf (93% shallower than 1000 m) and Block 82 having 5.92 Tcf (62% shallower

[1] *Resource Development and Geosciences Branch, BC Ministry of Energy and Mines, barry.ryan@gems4.gov.bc.ca*

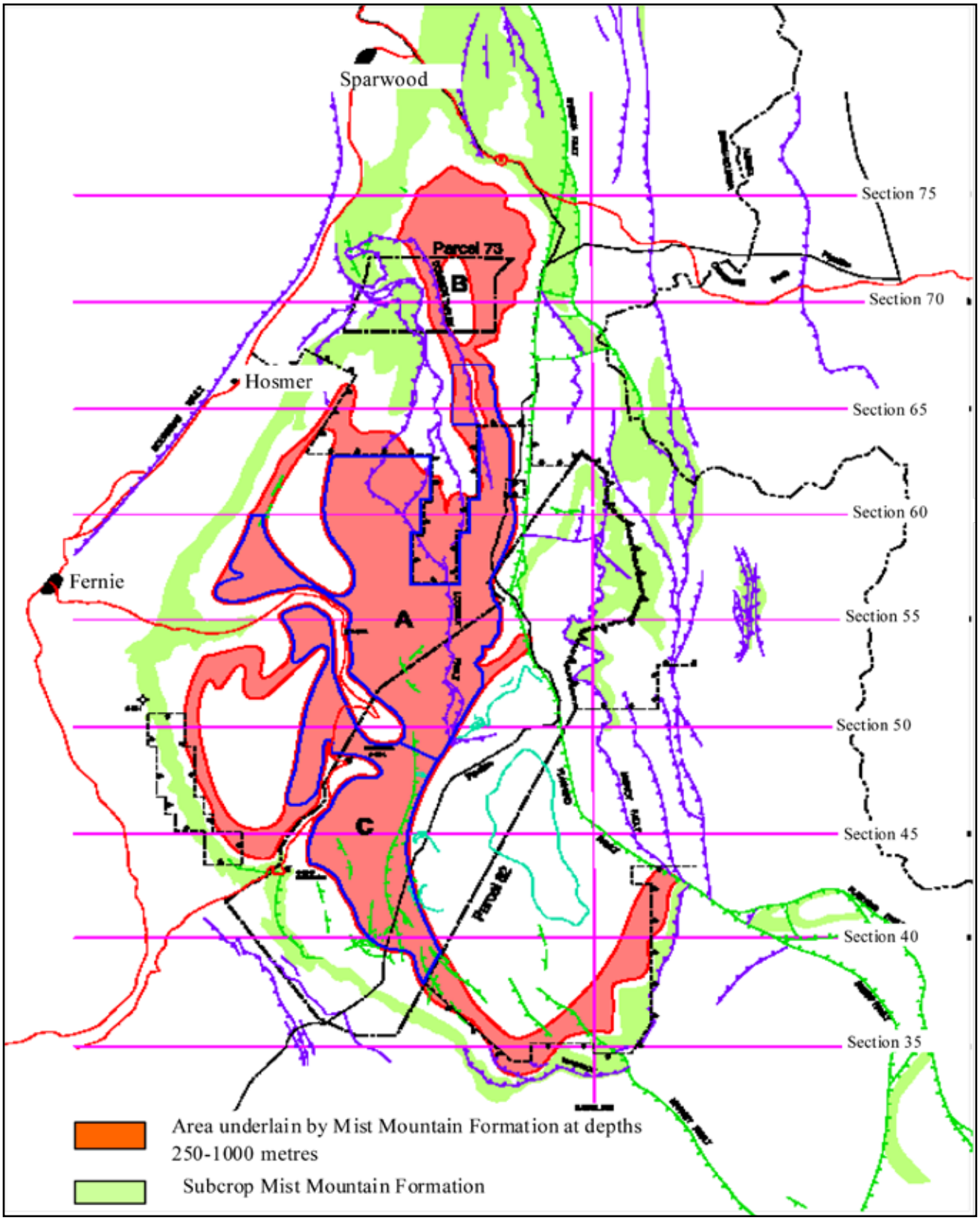

Figure 1. Outline of the Crowsnest coalfield. CBM resources of areas A, B, and C discussed in text.

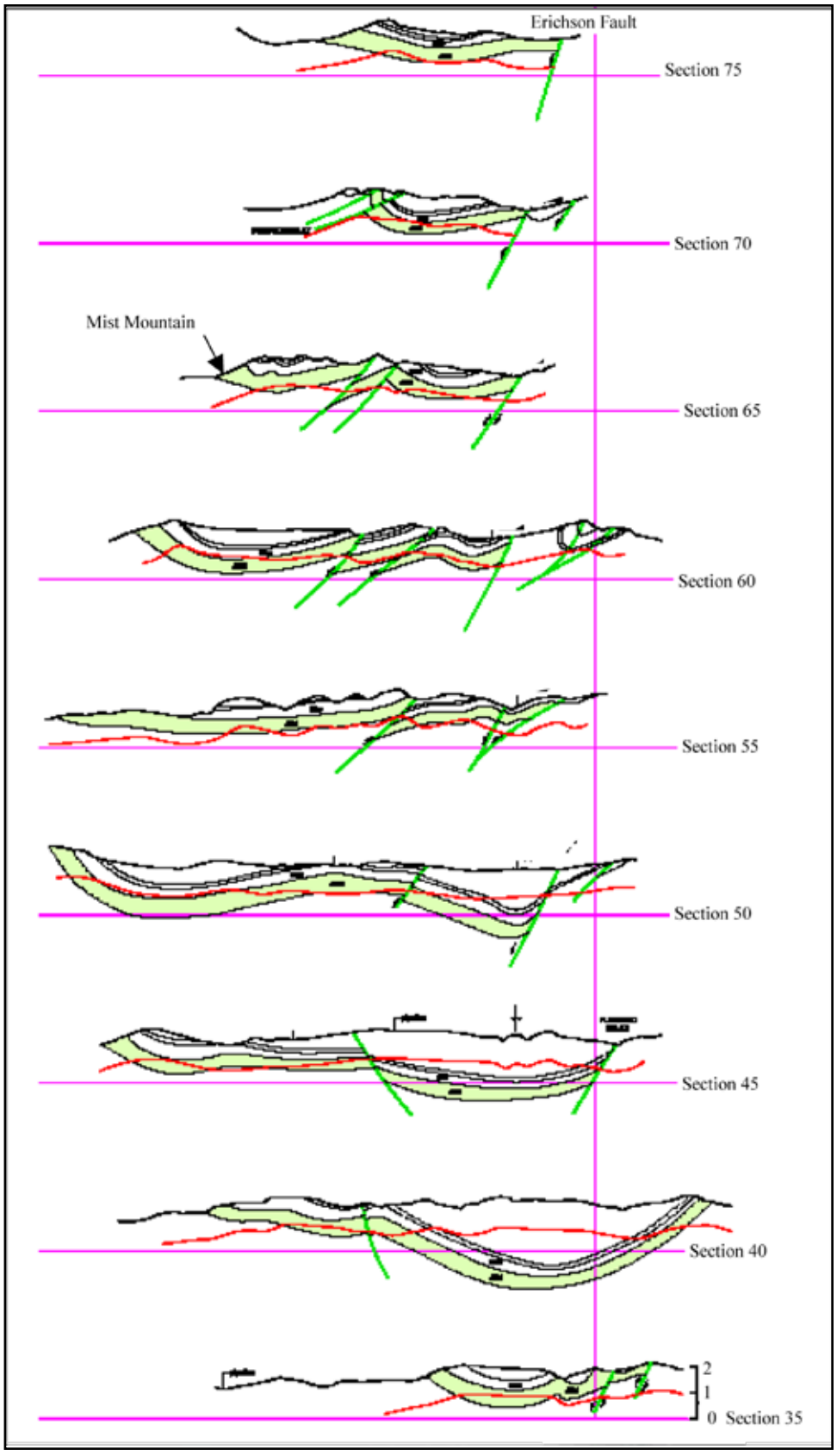

Figure 2. Schematic sections of Crowsnest coalfield.

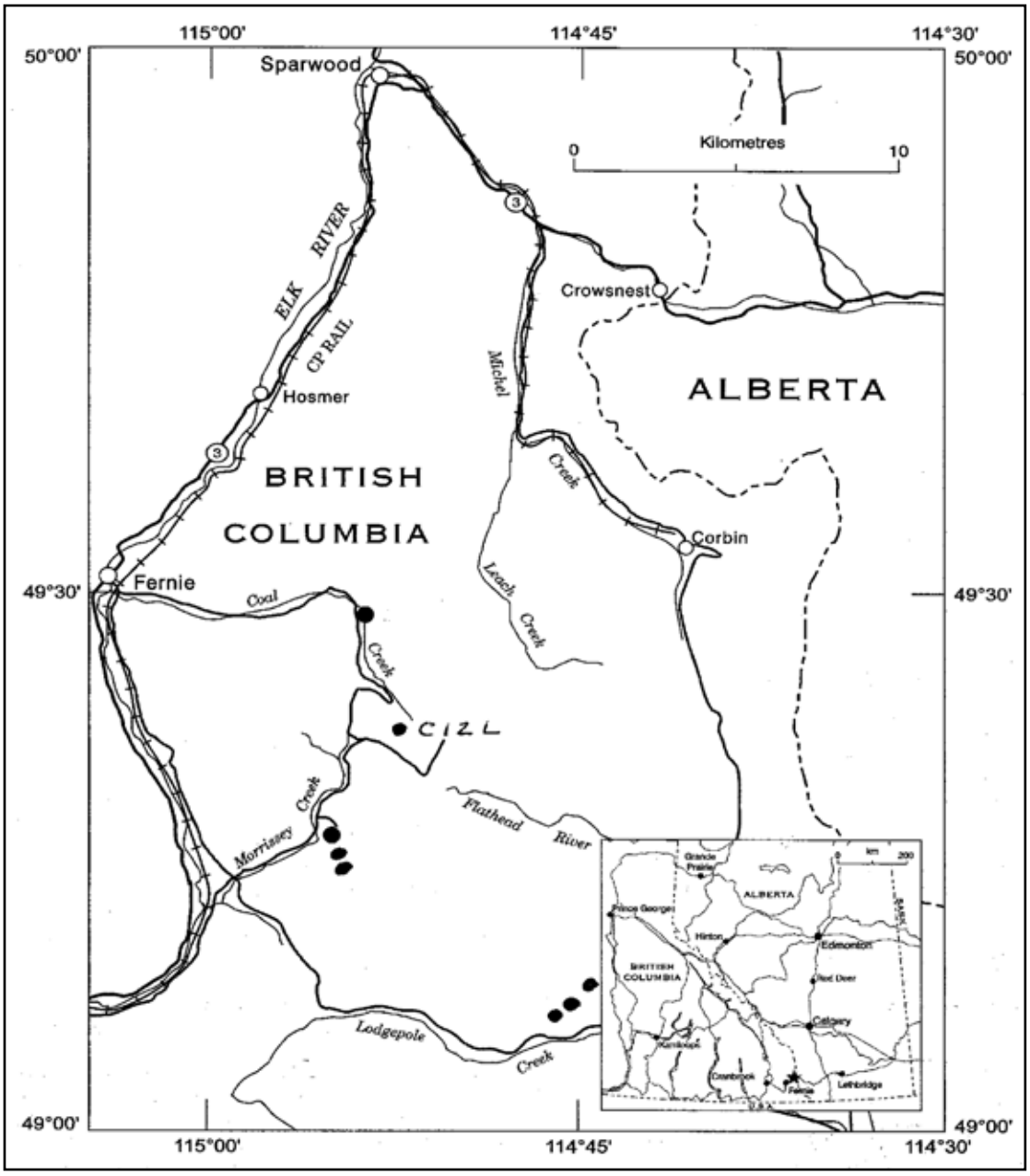

Figure 3. Location of stratigraphic test holes drilled in 1990; data from Dawson et al. (2000).

than 1000 m), providing a resource shallower than 1000 m of 4.28 Tcf. They used estimated gas contents of 16 and 18 cm^3/g applied to all seams (Table 1). The specific seam thickness and gas content values used by Dawson *et al.* (1998) seem to be high, based on available desorption data (Figure 4) and on cumulative coal thickness data for the Crowsnest coalfield as a whole (Table 2).

Dawson *et al.* (1998) used the seam designation applied to the northern part of the Crowsnest coalfield where the basal seam is number 10. Some papers (for example, Newmarch, 1953) designate the basal seam in the Crowsnest coalfield as 1 Seam and count up section. People checking literature on coal in southeast BC should make sure they know the specific seam designation being used in each paper.

STRATIGRAPHY

Any estimation of the depth to the Mist Mountain Formation requires at least some knowledge of the thickness of overlying formations and of the regional dips. In the Crowsnest coalfield, formations above the Mist Mountain include the Elk Formation and Blairmore Group (Figure 5), which includes the basal Cadomin Formation and overlying lower and middle Blairmore rocks. Most authors

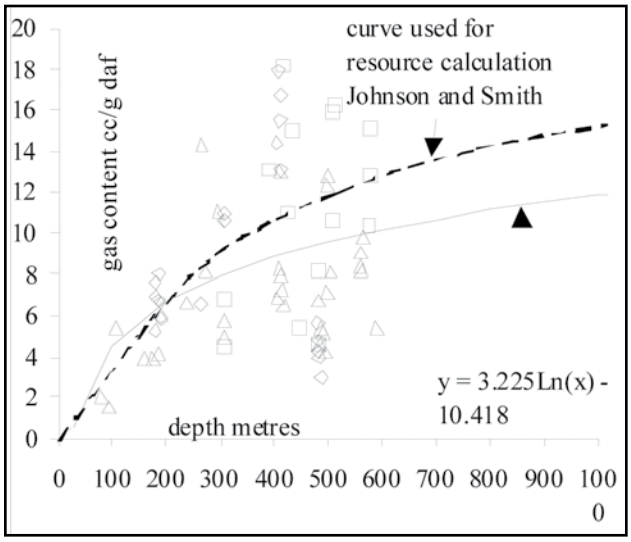

Figure 4. Desorption data for Crowsnest coalfield. Squares are for hole C12L, diamonds from Mobile Chevron holes, and triangles from Saskoil holes.

indicate that the Elk and Mist Mountain Formations thin to the east. Table 3 summarizes some of the thickness information available in a number of papers.

Newmarch (1953) indicates that the Kootenay Group, which includes the Elk and Mist Mountain Formations, varies in thickness along the western margin of the coalfield from 1097 m at Michel to 686 m at Hosmer and 625 m at Fernie. The Kootenay Group is described as 305 to 777 m thick (Crabb, 1957). It thins to the east in the Lewis Thrust block (Price 1964) and is 1076 m at Coal Creek, 488 m at Mt Taylor, and 396 m 12.1 km northeast from the mouth of Lodgepole Creek (Price, 1961).

The Mist Mountain Formation at Coal Creek is described as 645 m thick (Gibsons, 1985) or 629 m thick (Newmarch, 1953). Gibsons (1985) states that it is up to 625 m thick in southeast BC. Pearson and Grieve (1978) provide a number of Mist Mountain sections for the western and southern margins of the coalfield (Table 3) that range from 657 to 490 m in thickness. The overlying Elk Formation varies in thickness up to 488 m (Gibson, 1977; Jansa, 1972).

The Cadomin Formation forms the base of the Blairmore Group and ranges up to 170 m thick (White and Leckie, 2000). The formation is 137 to 168 m thick on the east side of the McEvoy syncline and 184 m thick at Coal Creek. The Blairmore group thins to the east and Crabb (1957) provides thicknesses of 700 m on the west and 300 m on the east. Price (1961) quotes thicknesses of 365 to 2000 m.

The Blairmore Group is overlain by the upper Cretaceous Crowsnest Formation (mainly alkaline volcanics), which is 40 to 100 m thick below the Lewis Thrust but does not occur within the thrust sheet.

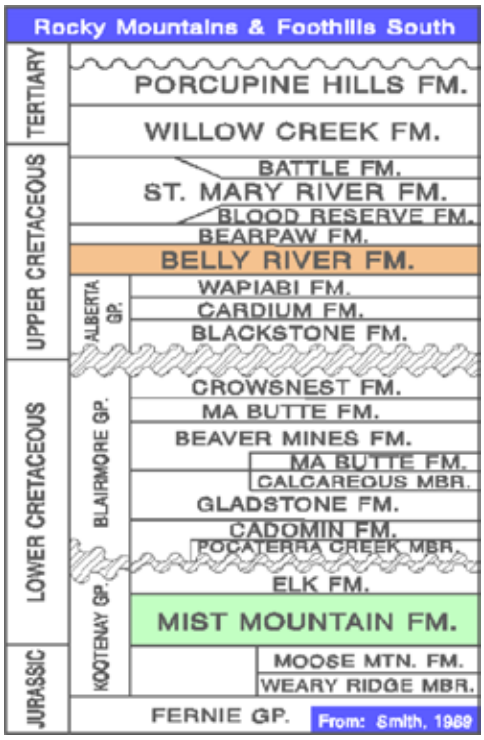

Figure 5: Statigraphic table from Smith (1989).

Outcrops of the Upper Cretaceous Alberta Group survive in the Crowsnest coalfield only in the core of the McEvoy syncline, where it is up to 229 m thick.

Stratigraphic thickness data is essential for estimating depth to the prospective seams in the Mist Mountain Formation. However, thicknesses need to be adjusted to take account of bed dips. As mentioned, strike and dip data are available on a number of published maps and are not reproduced in Figure 1. A simple nomograph (Figure 6), in conjunction with Table 3, provides estimates of drill depth to seams in the Mist Mountain Formation.

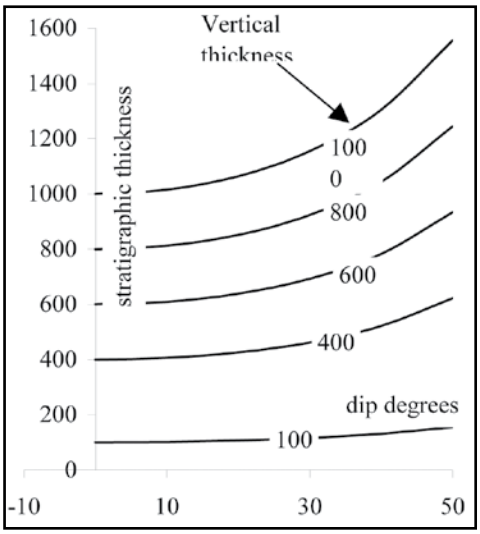

Figure 6. Nomograph of vertical thickness from dip and stratigraphic thickness.

TABLE 1. DOMINION BLOCKS CBM RESOURCE SUMMARY*

block 73

section	A-A	500-1000	metres	A-A	1000-1500		A-A	>1500	
	thick	gas	bcf	thick	gas	bcf	thick	gas	bcf
Elk	1.37	18	9.87	1.37	18	5.17			
1	2.07	18	16.09	2.07	18	7.1			
2U	2.44	18	15.82	2.44	18	7.37	2.44	18	3.84
2L	5.64	18	34.25	5.64	18	16.5	5.64	18	12.95
3	13.71	18	54.79	13.71	18	32.35	13.71	18	72.91
5U	7.32	18	28.79	7.32	18	15.89	7.32	18	41.23
5L	1.52	18	5.88	1.52	18	2.97	1.52	18	9.04
7U	3.66	18	13.13	3.66	18	3.45	3.66	18	27.29
7L	1.52	18	5.5	1.52	18	1.24	1.52	18	13.88
8U	3.5	18	14.87				3.5		27.64
8L	7.32	18	29.71				7.32		58.96
9	20.09	18	60.69				20.09		194.7
10U	3.05	18	8.83				3.05		30.23
10L	6.1	18	17.27				6.1		61.23
totals	79.31		315.49	39.25		92.04	75.87		553.9

Block 83

	Mt Taylor		A-A						
seam	250-500			500-1000			1000-1500		
	thick	gas	bcf	thick	gas	bcf	thick	gas	bcf
1	2.86	16.6	0	2.86	18	6.14	2.86	18	3.61
2	2.13	16.6	0	2.13	18	5.66	2.13	18	1.62
3	7.68	16.6	0	7.68	18	21.84	7.68	18	4.1
4	1	16.6	0.27	1	18	3.18			
5	10.61	16.6	6.19	10.61	18	30.63			
6	1.16	16.6	0.7	1.16	18	3			
7	5.39	16.6	3.11	5.39	18	12.13			
8	13.23	16.6	9.56	13.23	18	23.87			
9	5.79	16.6	4.37	5.79	18	7.66			
10	1.31	16.6	1.16	1.31	18	1.2			
B	2.47	16.6	2.32	2.47	18	1.74			
totals	53.63		27.68	53.63		117.05			9.33

	Mt Taylor		B-B						
seam	500-1000			1000-1500			>1500		
	thick	gas	bcf	thick	gas	bcf	thick	gas	bcf
1	2.86	18	23.47	2.86	18	13.75	2.86	18	6.34
2	2.13	18	16.31	2.13	18	9.34	2.13	18	3.29
3	7.68	18	25.83	7.68	18	33.28	7.68	18	7.48
4	1	18	5.25	1	18	4.26			
5	10.61	18	60.11	10.61	18	42.66			
6	1.16	18	8.57	1.16	18	3.51			
7	5.39	18	45.79	5.39	18	8.56			
8	13.23	18	121.93						
9	5.79	18	49.5						
10	1.31	18	10.24						
B	2.47	18	15.85						
totals	53.63		382.85	30.83		115.36	12.67		17.11

*from Dawson *et al.* (1998).

TABLE 1. CONTINUED

Block 83

	Lookout C-C								
seam	250-500			500-1000			1000-1500		
	thick	gas	bcf	thick	gas	bcf	thick	gas	bcf
1				33.8	18	116.67	33.8	18	63.37
2				5.2	18	27.67	5.2	18	3.41
3				12.2	18	72.98			
5	9	16	20.07	9	18	39.79			
6	4.8	16	14.17	4.8	18	18			
9	2.5	16	6.82	2.5	18	6.14			
10	1.8	16	4.97	1.8	18	3.63			
totals	18.1		46.03	69.3		284.88	39		66.78

	Lookout D-D					
seam	1000-1500			>1500		
	thick	gas	bcf	thick	gas	bcf
1				12.11	18	161.36
2				14.4	18	191.87
3	3.55	18	10.72	3.55	18	35.51
4	11.04	18	55.58	11.04	18	91.89
5	13.07	18	156.16	13.07	18	23.69
7	1	18	13.32			
9	1.7	18	22.65			
10	1	18	13.32			
totals	31.36		271.75			504.32
south extension	54.17	18	612.83	54.17	18	573.65
totals		total	884.58	54.17		1077.97

	Pipeline C-C		
seam	500-1000		
	thick	gas	bcf
1	33.8	18	1410.14
2	5.2	18	216.94
3	12.2	18	508.98
5	9	18	375.48
6	4.8	18	200.26
9	2.5	18	104.3
10	1.8	18	75.1
totals	69.3		2891.2

total <1000 metres 3.42 tcf
total 5.77 tcf

TABLE 2
CUMULATIVE COAL THICKNESSES FOR SECTIONS IN THE CROWSNEST COALFIELD.

seam	Fernie Ridge	Morrissey Ridge	Coal Creek	Hosmer Ridge	West Lodgepole	North Lodgepole	Mclatchie Creek	martin Ridge	Parcel 73
11	4.48	0.00	2.44						
10	2.44	2.32	2.44						
9	3.23	3.38	3.20						
8	6.22	2.19	1.37	1.52					
7	2.99	5.09	0.30	5.79	5.94			1.52	
6	2.77	2.41	0.76	10.67	2.65			6.00	6.10
5	7.25	3.72	5.49	1.83	8.08	6.40		5.43	1.50
4	3.41	4.15	3.81	2.13	6.89	5.79	7.62	2.20	
3	4.02	9.57	2.44	11.58	9.33	7.92	7.47	8.35	11.30
2	6.71	5.49	7.62	5.79				8.02	18.89
1	4.30	7.22	6.10	6.10	14.02	12.19	6.64		
			3.05						
			3.66						
total coal	**47.82**	**45.54**	**42.68**	**45.42**	**46.91**	**32.31**	**21.73**	**31.53**	**37.79**

note seam 11=B seam

TABLE 3
SUMMARY OF STRATIGRAPHIC THICKNESSES FOR JURA-CRETACEOUS UNITS.

location	thickness metres	
		Blairmore Group
Coal Creek	610	Lower Blairmore Price, R.A. (1961)
McEvoy Syncline	365-2000	Blairmore Price, R.A. (1961)
west	700	Blairmore Crabb, J. (1957)
east	305	Blairmore Crabb, J. (1957)
		Cadomin Formation
Coal Creek	185	Jansa, L. (1972)
Michel	731	Jansa, L. (1972)
Coal Creek	32	McLean, J. R. (1977)
		Kootenay Group
lodgepole	549	Price, R.A. (1961)
Mt Taylor	465	Price, R.A. (1964)
West	700	Crabb, J. (1957)
East	305	Crabb, J. (1957)
		Elk Formation
SE BC	up to 488	Gibson, D.W. (1977)
Michel	483	Jansa, L. (1972)
Coal Creek	519	Jansa, L. (1972)
		Mist Mountian Fomraion
Lodgepole	490	Pearson, D.E. and Grieve, D.A. (1978)
Flathead	604	Pearson, D.E. and Grieve, D.A. (1978)
Morrissey Creek	663	Pearson, D.E. and Grieve, D.A. (1978)
Morrissey Ridge	460	Pearson, D.E. and Grieve, D.A. (1978)
Coal Creek	616	Pearson, D.E. and Grieve, D.A. (1978)
Coal Creek	645	Gibson, D.W. (1985)
Coal Creek	617	Jansa, L. (1972)
Coal Creek	629	Newmarch, C.B. (1953)
Fernie Ridge	634	Pearson, D.E. and Grieve, D.A. (1978)
Hosmer	657	Pearson, D.E. and Grieve, D.A. (1978)
Sparwood Ridge	628	Pearson, D.E. and Grieve, D.A. (1978)
Michel	645	Jansa, L. (1972)

COAL SECTIONS

There has been very limited exploration in the centre of the coalfield where the Mist Mountain Formation does not outcrop; consequently; most of the information on seam thickness and cumulative coal thickness in the Mist Mountain Formation comes from mapping, exploration, and mining along the western and southern margin of the coalfield. There are a number of partial coal sections described for the purpose of estimating mineable reserves. It is probable that in many cases these sections do not document all coal in the formation, so that cumulative coal thicknesses probably represent minimum values. Data (Table 2 and Figure 7) indicate that cumulative coal thicknesses range from 40 to 50 m on the west and from 30 to 40 m on the east. Seams generally decrease in thickness up section, and the third or second seam from the base is usually the thickest.

COAL RANK AND MACERAL DATA

Coal rank varies from high-volatile bituminous to low-volatile bituminous, increasing down dip to the east and along strike to the south (Pearson and Grieve, 1985). There is also evidence that rank increases down dip into the core of the major syncline that crosses Morrissey Creek. If rank increases down dip into major synclines, then upward migration of biogenic methane may saturate up-dip lower-rank coal within a seam, leaving the deeper, higher-rank parts of a seam undersaturated. Obviously production from a shallow saturated seam with lower gas content is more economic than production from a deeper undersaturated seam with higher gas content. Rank gradients (ΔRmax/100 m) range from 0.01 to 0.12 (Figure 8).

Adsorption characteristics of seams are controlled by environmental factors (depth and temperature) and physical properties such as rank and maceral content. Jura-Cretaceous coals in southeast BC differ from many coals now producing CBM in that they have high and variable contents of organic inert macerals on a mineral-matter-free-basis (mmfb). These are grouped under the name inerts and include in part the macerals, fusinite, semifusinite, inertodetrinite, and macrinite. Various subvarieties of the vitrinite maceral make up the rest of the seam on a mineral-matter-free basis. The inert macerals, when compared to the vitrinite macerals, are characterized by lower adsorption ability, higher diffusivity and greater strength. The inert maceral content of seams (mmfb) varies and tends to increase down section with rank (Figure 9), though it is usually the second or third seam above the base of the section that contains the highest inert maceral content. There is also a tendency for the upper parts of seams to be vitrinite-rich. The lower parts of seams with higher inertinite content will have better diffusivity and may be less sheared.

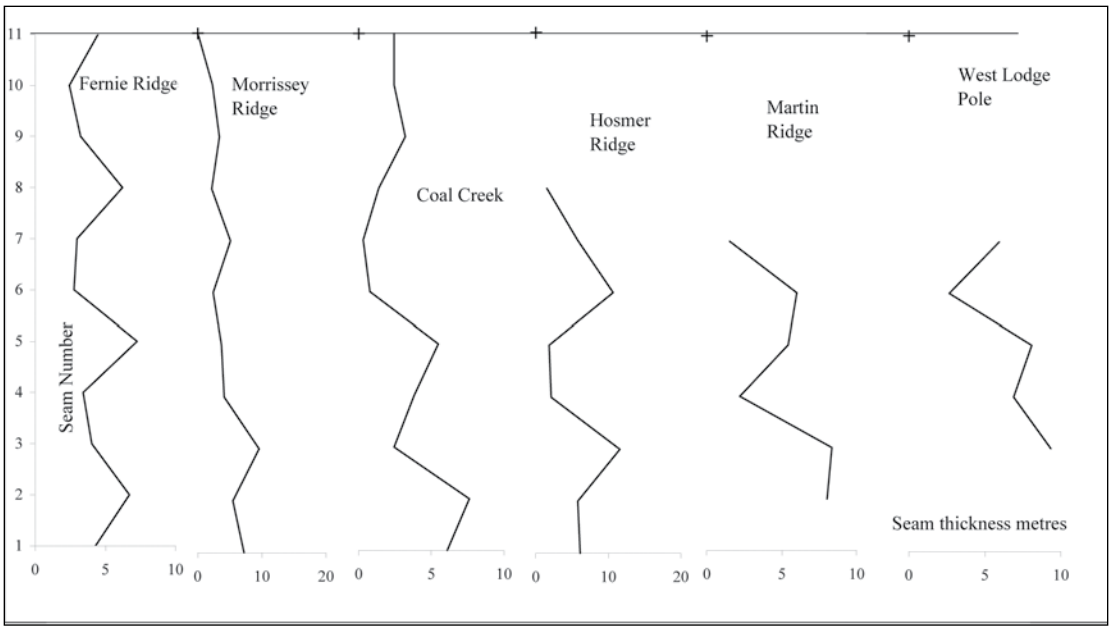

Figure 7. Plot of seam thicknesses by seam number.

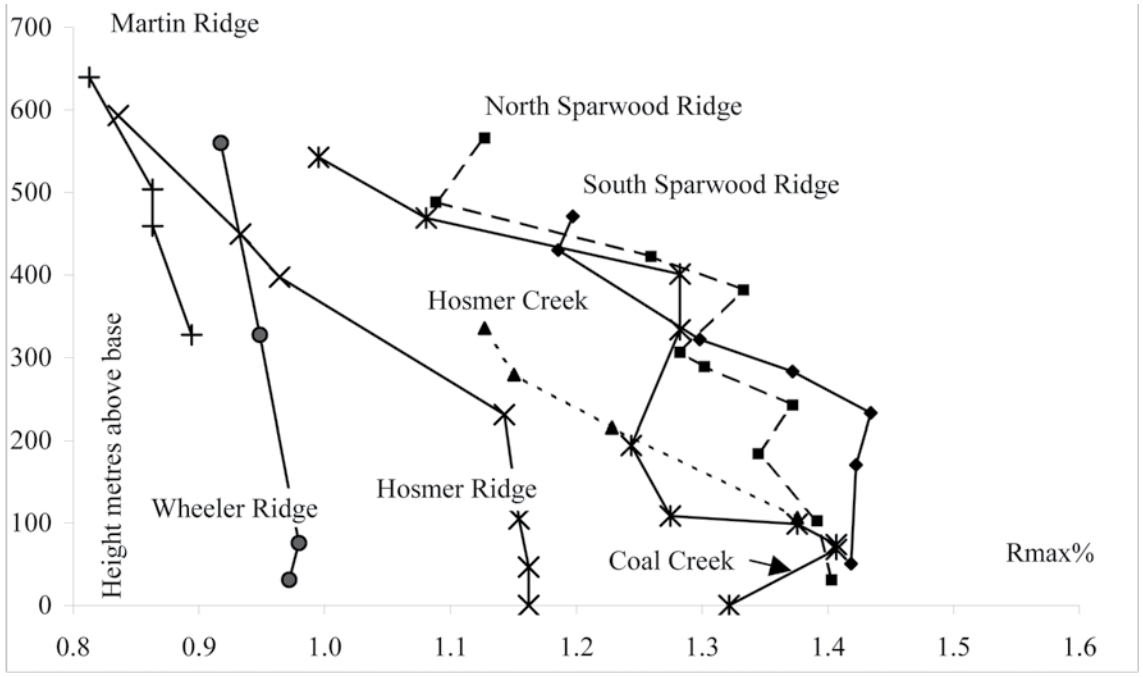

Figure 8. Rank gradients in the Crowsnest coalfield.

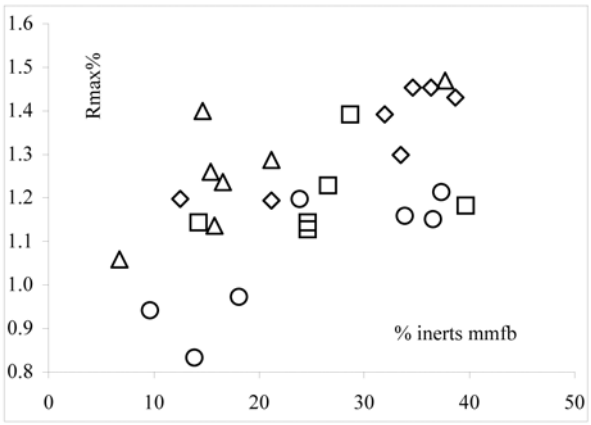

circle=Hosmer Ridge triangle =Sparwood North
square=Hosmer Creek diamonds=Sparwwod South

Figure 9. Variation in inerts content (mmfb) with rank.

CBM RESOURCE AREA

Experience in moderately deformed coals indicates that, except in unusual structural environments, reasonable permeability (greater than 2 mD) does not extend below about 1000 m. Areas where at least the top of the Mist Mountain Formation is less than 1000 m from surface are outlined on the map derived from Johnson and Smith (Figure 1) and in the accompanying sections (Figure 2).

The eastern margin of the Crowsnest coalfield is in part defined by the Erickson/Flathead normal fault system, which, by down-dropping the Kootenay Group on the west by 1000 to 3000 m, has preserved the coalfield. A simplified structural model of the coalfield is represented by two thrust blocks, each containing a north-trending syncline. The Sparwood syncline (Dawson *et al*., 1998) in the north and the McEvoy syncline in the south (Price, 1961) are the dominant structures in the block below the Lookout/Dominion thrust and above the Erickson/Flathead normal fault. Above the Lookout/Dominion thrust, the tight Hosmer syncline (Dawson *et al*., 1998) is cut off by a thrust north of Hosmer. To the south the syncline opens up, has very flat limbs, and merges with the flat limb of the McEvoy syncline.

Within these two synclinal trends, there are obviously areas where seams are too shallow to contain gas. This depth depends on topography and groundwater flow patterns. Ideally, groundwater flow should be down dip and away from seam outcrop. Generally, seams below 200 m and not intersected close to valley walls or above valley floor should contain gas; consequently, areas where Mist Mountain Formation seams are within 200 to 1000 m of surface are most prospective for CBM. There is insufficient structural control to accurately delineate the 200 m depth to the Mist Mountain Formation. As a conservative approximation, the formation is assumed to be at a depth greater than 200 m wherever it was overlain by the full thickness of the Elk Formation, which varies in thickness up to 488 m (Gibson, 1977). This line is easy to mark on Figure 1 and, with data from the sections (Figure 2), helps to delineate the area prospective for CBM. Figure 1 also locates the two Dominion Blocks (73 and 82) and areas where companies have freehold coal rights. Data are derived from standard 1:50 000 topographic maps and Grieve and Kilby (1989).

It appears that potential exists in three areas where the crown has gas rights. These areas are

a) the headwaters of Bray and Martin Creeks.

b) Dominion Block 73.

c) west of Dominion Block 82 and the southwest part of the block.

Area A

The main area where the BC government has the gas rights covers the headwaters of Bray and Martin Creeks, north of Coal Creek (Figure 1). The area includes parts of Block 82 and skirts the freehold blocks in the centre of the coalfield. The area is about 93 km^2. The area overlies the west limb of the Coal Creek syncline, which is traced north from the headwaters of Coal Creek. In the north it plunges to the southwest at 10° to 30° (Armstrong *et al*., 1976), with dips on the limbs increasing to the north. In the south, the syncline plunges to the north (Price 1961). The Dominion thrust progressively cuts off the east limb of the syncline and it is not present in Dominion Block 73.

The west limb of the syncline is steep and overridden by a number of thrusts. There are probably more thrusts than are mapped, and they will tend to seal seams so that up-dip migration of gas to the west will be limited and water movement in seams will probably be along the up-plunge direction of the syncline, either to the north or south. Steeply dipping seams below thrusts probably initially developed west-dipping shear surfaces that, as the seam is rotated, become near horizontal. A vertical hole drilled into these seams will intersect an extended apparent thickness of coal with near-horizontal fractures. Fracing of these seams at shallow depth will open up the fractures in directions extending along strike to the north and south. Drainage areas may extend along strike and not up and down dip. Holes may access structural traps below west-dipping thrusts. Also, as hydrostatic pressure is decreased, the effective lithostatic pressure will be somewhat reduced because of the increased amount of low-density coal in the vertical column.

Mining occurred from 1908 to 1914 west of an area near Hosmer Creek. Portals were driven through the Fernie Formation into the Mist Mountain Formation, which contains at least 10 seams, and the basal Number 1 Seam was mined for a time. The Mist Mountain Formation is

described as 762 m thick with 79 m of coal (Armstrong, *et al.,* 1976); however, these may be apparent rather than true thicknesses, based on thicknesses quoted elsewhere (Tables 2 and 3), which indicate true cumulative coal thicknesses ranging from 45 m at Hosmer to 31 m on Martin Ridge. The rank at Hosmer Creek ranges from 0.95% to 1.19%, with a gradient of 0.12 ΔRmax per 100 m and to the east on Martin Ridge from 0.83% to 0.91% (gradient 0.03 ΔRmax per 100 m). To the north in Dominion Block 73, rank of the basal seam is 1.16% (Grieve and Kilby, 1989). In the past, there was a lot of exploration and mining to the south in the Coal and Morrissey Creeks and adjacent areas. In these areas, the Mist Mountain section contains between 45 and 48 m of coal dispersed in about 11 seams.

Gulf Canada drilled a 590 m stratigraphic test hole (hole C12L, Dawson *et al*., 2000) (Figure 3) south of the area at the head waters of Martin and Coal Creeks. The hole intersected 24.4 m of coal in the top 280 m of the Mist Mountain Formation. It was drilled west of a major thrust into an area where the Mist Mountain Formation is flat dipping. Gas contents indicate that coals are undersaturated, but gas contents were higher than they were in holes drilled by other companies further to the south. Data for coals near the bottom of the hole indicate that coals are close to saturated. These seams are in the mid part of the Mist Mountain Formation section. The lowermost coal was the thickest, and this may correspond to Seam 5 in the Morrissey and Fernie Ridge sections, in which case the coal remaining lower in the section would be between 18 and 24 m cumulative thickness, providing a possible total cumulative thickness between 42 and 48 m.

No detailed estimates of the coal resources in Area A (delineated in Figure 1) exist. However, mining studies estimate a coal resource on Hosmer Ridge of about 700 million tonnes to 760 m. Alternatively, the resource can be estimated by utilizing the area of 93 km^2 and a cumulative coal thickness of 45 m; this provides an estimated coal resource of 5200 million tonnes.

The average gas content of the Gulf Canada hole is about 10 cm^3/g on an as-received basis. This is probably a low average value to use for resource estimates; however, the value of 18 cm^3/g used by Dawson *et al.* (1998) may be high. Using the lower gas content of 10 cm^3/g provides an estimated in-place resource of about 1.6 Tcf.

Area B

The Dominion Block 73 covers an area of 20.23 km^2. Dawson *et al.* (1998) calculated a CBM potential resource of 0.32 Tcf to 1000 m (Table 1). They provide a 750 m thick stratigraphic section of Mist Mountain that appears to contain over 70 m of cumulative coal. Grieve and Kilby (1989) identified a section of 480 m, which excludes seams number 1 and 2 and contains 37.8 m of coal up to and including 3 Seam. The basal seam has a rank of 1.16%, but ranks appear to increase down dip and definitely increase to the south.

Structurally, most of Block 73 is in a thrust block below the Dominion/Lookout thrust and east of area A. The structural style is similar to that of area A, being a syncline with steep-dipping west limb and shallow east limb. Opportunities for thrust-generated traps in the steep-dipping west limb exist. The syncline is along the trend of the McEvoy syncline to the south and Sparwood syncline to the north. The Sparwood syncline trends across Michel Creek to the north, where it becomes the Elk syncline in the Elkview coal mine north of Highway 3 at the north end of the Crowsnest coalfield.

The coal potential was analyzed by Grieve and Kilby (1989), who used seams with a cumulative thickness of 37.8 m in their study. The thickness of coal available for CBM resource calculations is probably between this thickness and that used by Dawson *et al.* (1998). They provide a total coal resource in the block of about 1 billion tonnes, which agrees with the estimate provided by Latour (1970). The tonnage estimated to be shallower than 1000 m is 550 million tonnes. Dawson *et al.* (1998) used an average gas content of 18 cm^3/g for all coal deeper than 250 m and calculated a gas resource of 0.32 Tcf. Using a lower gas content of 10 cm^3/g (320 scf/t), this resource decreases to 0.18 Tcf.

Area C

In the south, the southern extension of the Hosmer syncline is ill-defined, and dips west of Morrissey Ridge are flat. There is an extensive area where the Mist Mountain Formation is flat dipping and, at least in part, shallower than 1000 m. There are also some areas where the formation on the west limb of the McEvoy syncline is shallower than 1000 m. In this area, the offset on the Lookout/Dominion thrust reverses, and it is shown on sections in the south as a normal fault (Figures 1 and 2). If this interpretation is correct, then the southern area west of the fault should have experienced extension at the time of faulting and may still have better permeability on cleats.

Most of Area C is within Block 82 with some of the area on the southwestern margin of the block. The total area is about 51 km^2. Block 82 has a CBM resource potential of 3.42 Tcf to 1000 m (Dawson *et al,* 1998), and most of this is in the Pipeline area (Table 1) in the southwest, where the pipeline crosses the area trending north through the coal field. The centre and northern part of the block is underlain by the McEvoy syncline, which is cored by the Blairmore Formation and younger rocks. Based on the presence of these formations and their thicknesses, the Mist Mountain Formation is over 1000 m deep in the core of the syncline.

In the southwest of Block 82, there is an area where the east limb of the southern extension of Coal Creek syncline is flat and partially within the 1000 m depth window. Small changes in the structural interpretation could change the resource assessment significantly.

Saskoil (Dawson *et al.,* 2000) drilled two holes in 1991 in the Lodgepole Creek area. The holes were drilled near the subcrop in different parts of the Mist Mountain Formation. By combining the data from the holes, it appears that in the area, the full Mist Mountain section is 500 m thick and contains a cumulative coal thickness of 63 m. To the west, the cumulative coal in the section at Coal Creek is 42.7 m and at Morrissey Ridge is 45.5 m.

The rank of coal to the west under Fernie and Morrissey Ridges ranges from low-volatile bituminous to high-volatile bituminous (Figure 8). The vitrinite reflectance values are 1.45% for the basal seam at Morrissey Creek, decreasing to 1.38% at Coal Creek. However, rank appears to increase down dip to the east into the syncline (Pearson and Grieve, 1978).

Gas contents of samples from the holes drilled by Saskoil were low but are probably not representative of contents further to the northeast. For the purposes of calculation, an assumed gas content of 10 cm^3/g (320 scf/t) is used. This is considerably lower than the value used by Dawson *et al.* (1998), but is approximately the average gas content for samples from hole C12 L drilled by Gulf (Figure 3).

Based on an area of 51 km^2, 50 m cumulative coal, and a gas content of 10 cm^3/g, the CBM resource is 1 Tcf.

ESTIMATED RESOURCE AVAILABLE ON CROWN LANDS

The total resource estimated in the three areas is 2.78 Tcf (Table 4). This is an estimate of the gas resource available in all the coal in the section to a depth of 1000 m. It is derived using a conservative gas content value but assumes that all the area outlined is underlain by the full coal section, and this is probably an optimistic assumption. Other than the order of magnitude size of the 2.78 Tcf resource and the general areas to which it is assigned, not too much significance should be attached to its value. Companies interested in fine-tuning estimates of the resource potential in the coalfield should use the process and references outlined in this paper as a guide and complete their own assessment. In terms of the available reserve, this will depend on the presence of permeability and on the number of seams in the section that can be economically drained of gas.

COAL QUALITY AND IMPLICATIONS FOR CBM PRODUCTION

If higher-rank coals are to achieve gas saturation or near gas saturation at present depths, then it is probable that a large component of the gas will be biogenic. One should therefore consider the conditions that favour generation and retention of biogenic gas, which is generated on coal surfaces and then penetrates the microporosity to be adsorbed. Excessive water movement will limit the ability of biogenic gas to migrate into coal microporosity and to be adsorbed. Some seams in the Crowsnest coalfield are sheared, which increases surface area available for bacteria but limits the ability of a seam to maintain permeability when hydrostatic pressure is decreased. In situations where biogenic gas is generated down dip within a syncline limb, introduction of hot CO_2 could initiate up-dip movement of water, CO_2 in solution, and methane without any decrease in hydrostatic pressure. Hot CO_2 would be readily available from a coal-fired power plant.

Coal petrography varies, and seams lower in the section contain more inertinite on a mineral-matter-free basis. However, it is often the third seam above the Moose Mountain Member that contains the most inertinite (Pearson and Grieve, 1978). The inertinite content of seams varies from hanging wall to footwall, with the lower parts of seams having consistently higher inertinite contents (Pearson and Grieve, 1985). As a maceral group, inertinite is stronger than vitrinite and resists shearing better. It has lower adsorption abilities and higher diffusivities. These properties may be advantageous for CBM recovery. In thick seams that are initially undersaturated, but in which biogenic methane is being generated in the microfractures of the coal, inert macerals will reach re-saturation sooner because of lower demands and better diffusivity of methane from microfractures into the micropores. A seam may therefore be partitioned with the lower inertinite-rich part being satu-

TABLE 4. CBM RESOURCES WHERE THE CROWN HAS GAS RIGHTS.

	Reference	gas content cc/g	tonnage billion tonnes	total gas tcf
Area A	south of Dominion Block 73	10	2.2	0.7
Area B	Dominion Block 73	10	560	0.18
Area C	part of Dominion Block 82 and area to west	10	6.55	2.1
		total	**568.75**	**2.98**

rated at a moderate gas content and the upper vitrinite-rich part being undersaturated, possibly with the same gas content. Completion in the whole seam may result in no gas reaching surface, because gas released from one part of the seam may be adsorbed by another part. Completion in the inertinite-rich lower part of the seam may result in immediate gas production. The higher diffusivity and strength of the inertinite should help it maintain fracture opening and permeability despite the fact that there is probably less matrix shrinkage to aid permeability.

In the Elk Formation, there are some thin coal seams, which are generally less than 1 m thick and are characterized by high liptinite contents. They are often referred to as needle coals because of their structure, which derives from a high algae content. They tend to be better developed near the Mist Mountain contact. Coals of this type generate large quantities of thermogenic methane at ranks of 0.6% to 1.0%. The liptinite macerals are not very microporous, so that they have lower adsorption abilities than other macerals. However, the maceral is less brittle than vitrinite and tends to withstand deformation better. In areas where the Mist Mountain is below prospective depths, the overlying Elk Formation, which contains a higher sand content than the Mist Mountain Formation, may well contain free gas in sandstones and adsorbed gas in thin coal seams.

HISTORICAL DATA

In 1939, the Minister of Mines Report states that in the Coal Creek Number 1 Colliery "a considerable amount of methane is given off this amounting to an average of 1250,000 cubic feet in 24 hours". Elsewhere in the report, it states that ventilation was 74 300 cubic feet per minute. The numbers suggest that the methane content in the mine air was upwards of 1%. McCulloch *et al.* (1975) indicate that there is an approximate empirical relationship between the amount of methane per tonne released for a mature mine and the in-place gas content of the coal (Figure 10). The relation predicts that the in-place gas content (cm^3/g) is one-seventh the gas emission per tonne of mined coal. In 1939, coal production in the East Kootenays was about 500 000 tonnes, and production from the Number 1 East Colliery, Coal Creek, was 124 616 tons (Newmarch, 1953). If this tonnage is assigned to the Number 1 mine, and it operated for 300 days in the year, then the predicted gas content is over 13 cm^3/g. The Number 1 seam (lowest in the section) was reported to be the gassiest seam mined. There are a number of reports indicating that the coal from the Coal Creek Collieries was gassy and dusty.

The Carbonado Colliery (6.5 km up Morrissey Creek from the Elk River), which opened in 1902, is described as being very gassy and prone to outbursts. It was closed in 1909 after a number of severe gas outbursts. Other reports indicate that seams low in the section were very fractured and produced a lot of fine coal.

There are very limited public data on CO_2 concentrations in coals in the Crowsnest coalfield. A report (Rice, 1918) provides some analyses. In 1916, five

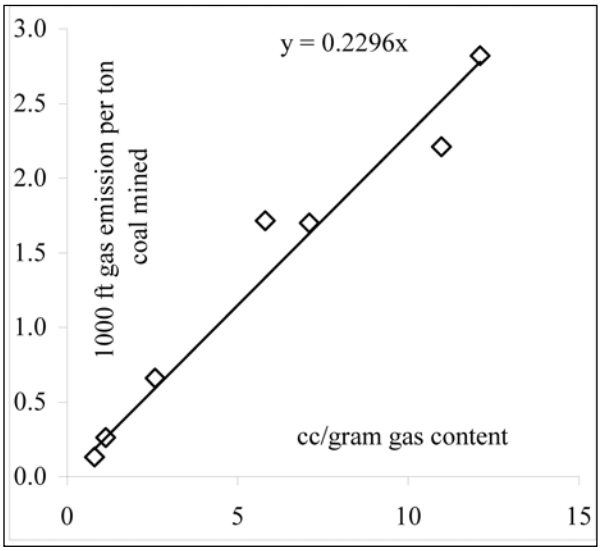

Figure 10. Relationship of gas released in underground mine and adsorbed gas content plot; derived from McCulloch *et al*. (1975).

samples were collected from the working face in the underground Coal Creek Colliery and placed into sealed jars (Table 5). When the gas was analyzed, it was apparent that all had leaked; however, the CO_2 content may be estimated from the $CO_2/(CH_4+CO_2)$ ratio, and it appears that, except for one sample, CO_2 contents were probably less than 5% (data are reported as cm^3 per 100 g, equivalent to mole fractions). Based on the trace of the Bourgeau thrust relative to the outcrop of the basin (Monahan, 2002), it appears that seams in the Mist Mountain Formation in the Crowsnest may not have been as close to carbonates in the overlying Bourgeau thrust plate as seams in the Elk Valley coalfield were and may therefore have lower CO_2 concentrations.

TABLE 5
ESTIMATED GAS COMPOSITION.

sample	CH_4	CO_2	O_2	N_2	$CO_2/(CO_2+CH_4)$
17	64.1	1.4	1	33.5	2.1
18	24.6	0.9	4.4	70.1	3.5
19	27	1.2	3.2	68.6	4.3
20	15.8	0.4	1.2	82.6	2.5
21	0.3	1.6	20	78.1	84.2

Data from Rice (1918). Composition of gas in coal samples, volume percent. Samples from working faces of Coal Creek Colliery (1916), Coal Creek, Crowsnest coalfield.

COAL DEFORMATION AND IMPLICATIONS FOR CBM PRODUCTION

The Crowsnest coalfield is folded into a series of north-trending anticlines and synclines, which generally have steep-dipping west limbs and shallower-dipping east limbs. Folds open to the south, indicating less east-west compression of the coalfield in that direction. They are contained in a number of north-trending blocks defined by thrusts and normal faults. On the east, the major fault system is composed of the Erickson and Flathead normal faults, and on the west, it is the Lookout/Dominion thrust system. The folds reverse plunge through the basin, with the McEvoy syncline in the south forming a distinct basin, and the Coal Creek syncline forming a basin under Fernie Ridge. The map of Price (1961) indicates a number of plunge reversals for folds; it is not clear whether these are related to a later phase of cross folding or are controlled by changes in stratigraphic thickness. Obviously if they are related to a later stage of cross folding, then this could cause extension and improved permeability in areas where the cores of synclines or anticlines form culminations.

The Crowsnest coalfield forms part of the Lewis Thrust sheet, which in southeastern BC was transported between 140 and 200 km at a rate of about 1.5 cm per year (Osadetz *et al*., 2003). Movement took place in the period from 74 to 59 Ma, as is indicated by profound cooling in the thrust block at about 75 Ma (Osadetz *et al*., 2003). This movement is documented by analyzing the displacement on the thrust plane; however, there was also probably bedding plane slip within the thrust sheet, which would, over the estimated 7 km thickness of the sheet, (Osadetz *et al.,* 2003) account for more displacement.

Some of this additional displacement is hidden in the Fernie Formation, in that rocks below the Fernie Formation are more folded than are the overlying Kootenay Group and fold geometries are offset (Price 1961). Additional displacement almost certainly occurred along coal seams. Bedding plane movement along seams will increase coal fragmentation, and its amount will not be related to the degree of any subsequent folding. If the coal was maturing through high-volatile bituminous rank at the time of thrust displacement, it would be very susceptible to bedding-plane slip.

In-seam shearing related to Lewis Thrust movement and not to folding produces fine coal and inhibits the formation of cleats or destroys those that have formed. It plays a key role in limiting permeability and causing production problems. It is therefore important to consider what factors might limit the amount of shearing in seams. Some examples of seams that may resist shearing are:

- Thinner seams
- Seams rich in inert macerals or liptinite
- Seams that attain high rank before thrusting started
- Seams with higher ash content
- Seams with clay-poor hanging walls and footwalls.

There have been a number of studies of coal seam deformation in the northern part of the Crowsnest coalfield. Norris (1965) studied A Seam in underground A-North mine at the north end of the coalfield. This seam is approximately 420 m above the basal Balmer or 10 Seam in the Mist Mountain Formation. He describes the seam as being highly sheared, with abundant shear surfaces and intrastratal folds. Joints tended to strike north or northwest with evidence of early minor extension faults cut off by renewed bedding-plane slip. He does not directly discuss cleats or the degree of shearing in the seam, but the impression is left that the seam is highly sheared and fragmented.

Bustin (1982) studied the lowest seam in the Mist Mountain Formation in a number of underground coal mines (Balmer North, Five Panel, and Six Panel) at the north end of the Crowsnest coalfield. In the Balmer North mine, the best-developed cleats formed acute angles to bedding, striking northwest and dipping shallowly to the southeast. Cleat surfaces were polished and striated. Other cleat sets were measured but did not have a consistent orientation through the mine. Cleats in the Five and Six Panel mines are more consistent with a set striking north to northwest with a steep dip to the west. These cleats are subperpendicular to bedding and trend parallel to the regional fold axis. All fractures and most cleats in the seam appear to have a tectonic influence, with surfaces polished and often showing evidence of shearing. However, their orientations are not easily related to a regional stress field. Thrusting probably started with differential movement between the roof and floor (Norris, 1965) that disrupted earlier extension faults. As seam thickening and thrusting progressed, exogenetic fractures with fold axis-parallel trends and variable dips to the west developed in the coal.

SUMMARY

The Crowsnest coalfield is an area of 600 km^2 underlain by the Jura-Cretaceous Mist Mountain Formation, which contains from 30 to 60 cumulative metres of high-volatile to low-volatile bituminous coal. The combination of area and cumulative coal guarantees a large resource of coalbed methane, which has been estimated at 12 Tcf. However, outlining a resource is a far cry from defining a reserve. The coalfield forms part of the Lewis Thrust sheet and has therefore had a protracted deformational history, which started with thrusting followed by folding in the late Cretaceous and continued with extension on north-trending major faults in the Tertiary. The thrusting caused shearing within some seams that is unrelated to the amount of subsequent folding. This has probably limited permeability and generated fine coal that will make production more difficult.

Successful production will probably rely on understanding the interplay between deformation coal quality and location in specific structures. With these caveats in mind, the more prospective area is where the Mist Mountain Formation is in the depth window of approximately 200 to 1000 m. The Crown has clear title to the CBM in part of this area (Figure 1), and it is within this sub-area that a more detailed assessment of the CBM resources has been made. The value of about 3 Tcf defines the size of a box within which, hopefully, reserves can be located.

A number of ideas relating structure, coal quality, and CBM are proposed that may help explorationists zero in on areas where reserves are located.

ACKNOWLEDGEMENTS

Bob Morris was kind enough to read the manuscript and correct some of the more obvious errors in the original draft.

REFERENCES

Armstrong, W.M., Fyles, J.T., Guelke, C.B., MacGregor, E.R., Peel, A.L., Thompson, A.R. and Warren, L.H. (1976) Coal in British Columbia, A technical Appraisal*; Coal task Force,* Report of the Technical Committee.

Bustin, R.M. (1982): Geological factors affecting roof conditions in some underground coal mines in the southeastern Canadian Rocky Mountains; *Geological Survey of Canada,* Paper 80-34.

Crabb, J. (1957): a summary of the geology of the Crowsnest coalfields and adjacent areas; *Alberta Society of Petroleum Geology* 7th annual field conference Guide book

Dawson, F.M. Marchioni, D.L. Anderson, T.C. and McDougall, W.J. (2000): An assessment of coalbed methane exploration projects in Canada; *Geological Survey of Canada,* Bulletin 549.

Dawson, F.M., Lawrence, G.F. and Anderson, T.C. (1998): Coalbed methane resource assessment of the Dominion coal blocks southeast British Columbia; *Geological Survey of Canada,* Open File 3549.

Gibson, D.W. (1977): Sedimentary facies in the Jura-Cretaceous Kootenay Formation, Crowsnest Pass area southwestern Alberta and southeastern British Columbia, Bulletin of the *Canadian Petroleum Geology*, Volume 25, pages 767-789.

Grieve, D.A. and Kilby, W.E. (1989): Geology and coal resources of the Dominion coal block southeastern *British Columbia; Ministry of Energy and Mines,* paper 1989-4.

Jansa, L. (1972): Depositional history of the coal-bearing Upper Jurassic-Lower Cretaceous Kootenay Formation Southern Rocky Mountains, Canada*; Geological Society of America,* Bulletin, Volume 83, pages 3199-3222.

Johnson, D.G.S. and Smith, L.A. (1991): Coalbed Methane in southeastern British Columbia; *British Columbia Ministry of Energy and Mines, Petroleum Geology Branch,* Special paper 1991-1.

Latour, B.A. (1970): Coal deposits of the dominion government coal block Fernie area British Columbia*; Department of Energy Mines and Resource, Geological Survey of Canada,* Report.

McLean, J,R. (1977): The Cadomin Formation Stratigraphy, sedimentology and tectonic implications; Bulletin of the *Canadian Petroleum Geology*, Volume 25, pages 792-827.

McCulloch, C.M., Levine, J.R. Kissell, F.N., and Deul, M. (1975): Measuring the methane content of bituminous coals; United States department of the *Interior Bureau of Mines* report 8043.

Monahan, P. (2002): The Geology and oil and gas potential of the Fernie-Elk Valley Area, southeastern *British Columbia, Ministry of Energy and Mines.*

Newmarch, C.B. (1953): Geology of the Crowsnest Coal Basin; *British Columbia Department of Mines*, Bulletin Number 33.

Norris, D.K. (1965): Structural analysis of part of the north A-North Coal Mine Michel, British Columbia; Geological Survey of Canada, Paper 64-24.

Osadetz, K.G., Kohn, B.P. Kohn, Feinstein, S. and R. A. Price (2003): Aspects of foreland belt thermal and geological history in southern Canadian Cordillera from fission-track data, *Petroleum Geology Special Paper 2002-2*

Pearson, D.E. and Grieve, D.A. (1977): Coal Investigations, Crowsnest coalfield; *BC Ministry of Energy and Mines* pages 47-54.

Pearson, D.E. and Grieve, D.A. (1978): Petrographic evaluation of the Crowsnest Coalfield; *Canadian Institute of Mining and Metallurgy,* Annual General meeting Vancouver 1978.

Pearson, D.E. and Grieve, D.A. (1978): Preliminary geological map of the Crowsnest Coalfield, west part*; BC Ministry of Energy and Mines*, Preliminary Map 27.

Pearson, D.E., Gigliotti, F.B. Ollerenshaw, N.C., and Grieve, D.A. (1977): Preliminary map of the Crowsnest coalfield northwest part; *BC Ministry of Energy and Mines,* Preliminary Map 24.

Pearson, D.E. and Grieve, D.A (1980): Coal measures of the Crowsnest coalfield; *BC Ministry of Energy and Mines*, Preliminary Map 42.

Pearson, D.E. and Grieve, D.A (1985): Rank variation, coalification pattern and coal quality in the Crowsnest Coalfield, British Columbia; *Canadian Institute of Mining and Metallurgy* Bulletin, Volume 78, pages 39-46.

Price, R.A. (1961): Fernie map area east half Alberta and British Columbia 82G E1/2; *Geological Survey of Canada,* Paper 61-24.

Price, R.A. (1964): Flathead map area British Columbia and Alberta; Memoir 336.

Rice, G.S. (1918): Bumps and outbursts of gas in the mines of the Crowsnest Pass Coalfield, British Columbia Department of Mines, Bulletin Number 2.

Smith, G.G. (1989): Coal resources of Canada; *Geological Survey of Canada,* Paper 89-4.

White, J.M. and Leckie, D.A. (2000): the Cadomin and Dalhousie formations of SW Alberta and SE British Columbia; age sedimentology and tectonic implications; *Canadian Society of Exploration Geologists* Conference 2000, abstract.

A NOTE ON THE MARKET POTENTIAL OF LOW-VOLATILE BITUMINOUS COAL, WILLOW CREEK PROPERTY, NORTHEASTERN BRITISH COLUMBIA

By Barry Ryan[1], Ted Todoschuk[2] and Bob Lane[3]

KEYWORDS: Low-volatile coking coal, Willow Creek property, low-volatile pulverized coal injection (PCI), coke oven blends.

INTRODUCTION

The international coking coal market is very competitive and is segmented into many non-interchangeable coal products. Two products that are more in demand than many are low-volatile bituminous high-rank coking coal for blends into coke ovens and low-volatile bituminous coal for pulverization and injection into blast furnaces (pulverized coal injection or PCI coal). The Willow Creek property contains coal that may be suitable for these two markets. The higher-priced market is the low-volatile coking coal market, where up to 30% of this coal can be added into coal blends for coke ovens. This is a higher-priced market than the PCI market, and it is advantageous for mines if possible to switch from the low-volatile PCI market to the low-volatile coking coal market. Low-volatile coking coal is also in short supply as reserves in the US and other countries are running out. This note looks at the possible use of 7 Seam from the Willow Creek property in northeastern British Columbia as a low-volatile component in a standard coke oven blend. The Willow Creek property is located 40 km west of Chetwynd (Figure 1) and overlies seams in the Gething Formation.

THE WILLOW CREEK PROPERTY

There are two coal-bearing formations in the Peace River coalfield (Table 1). Coal from the younger Gates Formation was mined at the Quintette and Bullmoose mines (both now closed). There is active exploration of the formation in the Wolverine River area by Western Canadian Coal Corporation and Northern Energy and Mining Incorporated.

Coal from the older Gething Formation was mined briefly in the early 1900s but has not hosted any major coalmines. However, there is a long history of exploration in the formation, and coal was first reported in the formation by the explorer Alexander Mackenzie in 1793. The formation trends northwest across the Pine River about 40 km west of Chetwynd (Figure 1), and in this general area there have been a number of exploration projects. North of the Pine River, seams in the Gething Formation are generally medium-volatile in rank. South of the river in the Willow Creek area, rank increases and some seams are low-volatile bituminous. Further to the south, the rank of seams in the formation increases to semi-anthracite. The quality of seams in the Gething Formation has been discussed in a number of exploration reports and is summarized in Ryan (1997). Coal in the formation is characterized by low ash contents and variable inert maceral content. Sulphur and phosphorus contents are generally low, and rheology depends on rank and maceral content.

TABLE 1: GENERALIZED LOWER CRETACEOUS STRATIGRAPHY.

Pine River Area.			metres
Jurassic to lower Cretaceous	FORT ST JOHNS GROUP	CRUISER FORMATION marine shale	115
		GOODRICH FORMATION fine grained sandstone and shale	350
		HASLAR FORMATION marine shale	260
		BOULDER CREEK FORMATION sandstone and conglomerates	150
		HULCROSS FORMATION grey marine shale	100
		GATES FORMATION non marine sandstones and coal seams	110
		MOOSEBAR FORMATION marine shale	250
	BULLHEAD GROUP	GETHING FORMATION non marine sediments and coal	500
		CADOMIN FORMATION conglomerates	150

[1] *Resource Development and Geosciences Branch, B.C.Ministry of Energy and Mines, barry.ryan@gems4. gov.bc.ca*
[2] *Dofasco Canada*
[3] *Mines Branch, B.C. Ministry of Energy and Mines*

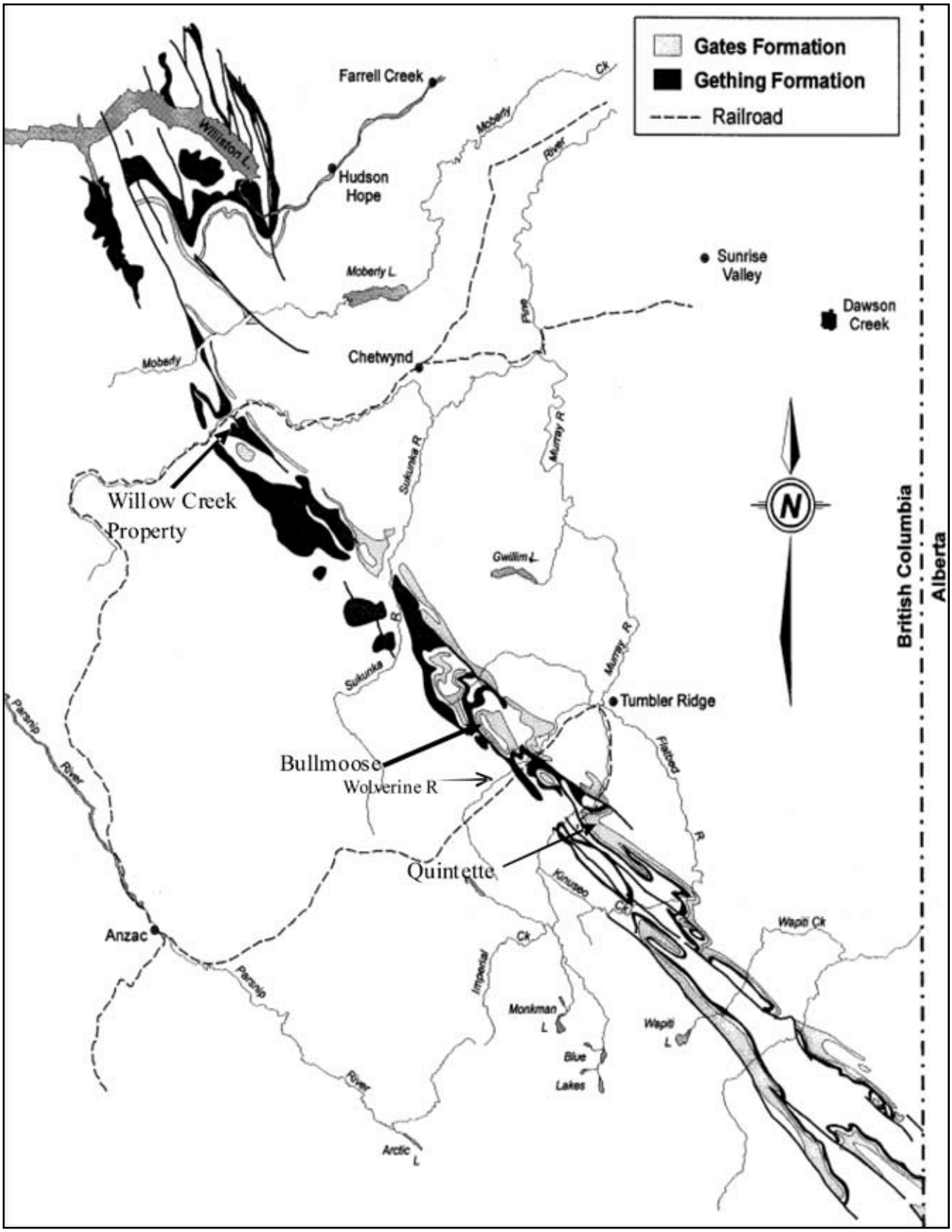

Figure 1. Location map for the Willow Creek property Pine Valley Coal Corporation, northeast British Columbia.

The area adjacent to and south of the Pine River has for some time been referred to as the Willow Creek property, which was explored in the early 1980s as a potential underground mine. Interest waned, and it was not till the mid 1990s that exploration was renewed with the intent of developing a small low strip-ratio open-pit mine. In 1993, Globaltex acquired control of the property and now has in place a British Columbia "Project Approval Certificate" and "Mine Permit". The company has continued development work in conjunction with a number of partners.

The operating company for the property is now called Pine Valley Mining Corporation, and they have conducted various mine feasibility studies that are based on mining the uppermost 9 seams in the Gething Formation (Table 2). These seams are numbered from 1 Seam near the top of the formation to 9 Seam, which occurs in the mid part of the formation at a depth stratigraphicaly about 300 m below 1 Seam. The rank of seams ranges from about 1.3% Rmax to 1.7% Rmax, with 6 and 7 Seams, which are thick, having ranks in the range of 1.6 to 1.67%. Raw-ash contents range from 15% to 7% and are generally low (Table 3). These seams, especially 7 Seam (which makes up a major part of the reserves), have the potential to be marketed as a low-volatile PCI coal or as a low-volatile blend coal in coke-oven blends.

The studies indicate that there are proven in-place reserves of about 15 million tonnes at an in-place strip ratio of about 3.6 to 1 bcm/t (bank cubic metre of overburden per tonne of coal). This is sufficient to justify an output level of some 900 000 to 1.5 million tonnes per year. In addition, there are identified resources in nearby areas that may significantly increase proven reserves and annual production in the future.

In the last few years, a number of raw coal bulk samples were excavated and coal shipped to Japan for test marketing. To date about 125 000 tonnes have been mined from an area referred to as the Peninsular Pit, where seams 6 and 7 outcrop. A rail spur capable of handling up to 25 coal cars and connected to the BC Rail Prince George line was constructed in the Pine Valley. At the moment, run-of-mine coal is screened and shipped raw. A 37 000 tonne test shipment was sold in 2001, and in 2002 a larger shipment of about 84 000 tonnes was shipped. Work performed to date suggests that up to 1.0 million tonnes of very low strip-ratio coal (estimated at 1.8:1) in the Peninsula Pit can be mined and sold on a raw coal basis without incurring material coal dilution or recovery problems.

The company's current plan is to start mining in this area and then move into more steeply dipping coal measures within the Willow Central and Willow North areas. Construction of a coal preparation plant is planned to coincide with the move to the Willow Central and Willow North areas.

7 SEAM COAL QUALITY AND SAMPLE COLLECTION

The carbonization sample was collected from the outcrop face of the small 7 Seam test pit (Peninsular Pit) in winter. The snow and cold made sampling and access difficult. Sufficient fist-sized or larger fragments of the seam were collected from parts of the seam ranging from hanging wall to footwall to fill a 45 gallon drum. The drum was shipped to Canmet carbonization laboratories at Bells Corners, Ontario. Pilot oven coking tests and related analyses were performed by Gransden and Price (2003), and the results are summarized in the next section. In addition, small grab samples of bright and dull bands were collected to check for oxidation.

The bright and dull samples were analysed for oxidation using the "Alkali Extraction" test that is now recognized by American Standards for Testing Materials (test D5263-93[2001]). The test measures the amount of humic acid developed as a result of natural weathering. The test is only applicable to mid-rank coals from high-volatile to low-volatile bituminous. Lower rank coals have humic acids that are naturally occurring at the rank, and high rank coals are resistant to this type of chemical action but can be damaged by other weathering processes. Because of the high rank of 7 Seam, bright samples, which are not representative of the whole seam, were analysed because these would be most sensitive to this type of weathering. Transmittance results (Table 4) range from 90% to 95%, indicating that the seam is not oxidized and there are marginal free swelling index (FSI) values, ranging from 1 to 1.5.

In the Willow Creek area, the raw-ash content for 7 Seam averages 5% and ranges from 1% to 39%, based on exploration drilling. The FSI values range from 0 to 3 and the variations appear to be related to varying inert maceral content and not ash content. This is based on a plot of ash versus FSI with the data coded based upon volatile matter (VM) dry mineral-matter-free (dmmf) values (Figure 2). Oxidation increases the volatile matter content (VM dmmfb) of samples; therefore, low FSI data points with high VM dmmf values are probably oxidized, whereas low FSI data points with low VM dmmf values probably represent samples with high inert maceral contents. It is clear in Figure 2 that samples with high VM dmmfb have, on average, higher FSI values than those with low VM dmmfb values.

Petrography on previous samples of 7 Seam (Table 5) indicates that 7 Seam contains from 40% to 60% vitrinite macerals, being mostly collodetrinite. It was not possible to do a petrographic analysis of the 7 Seam sample collected for the pilot coke-oven test before it was shipped to Canmet, because the sample was crushed by Canmet. Petrographic analyses of the carbonization sample by Canmet and the author indicate that the coal has a very low content of finely

TABLE 2. STRATIGRAPHIC SECTION, WILLOW CREEK AREA.

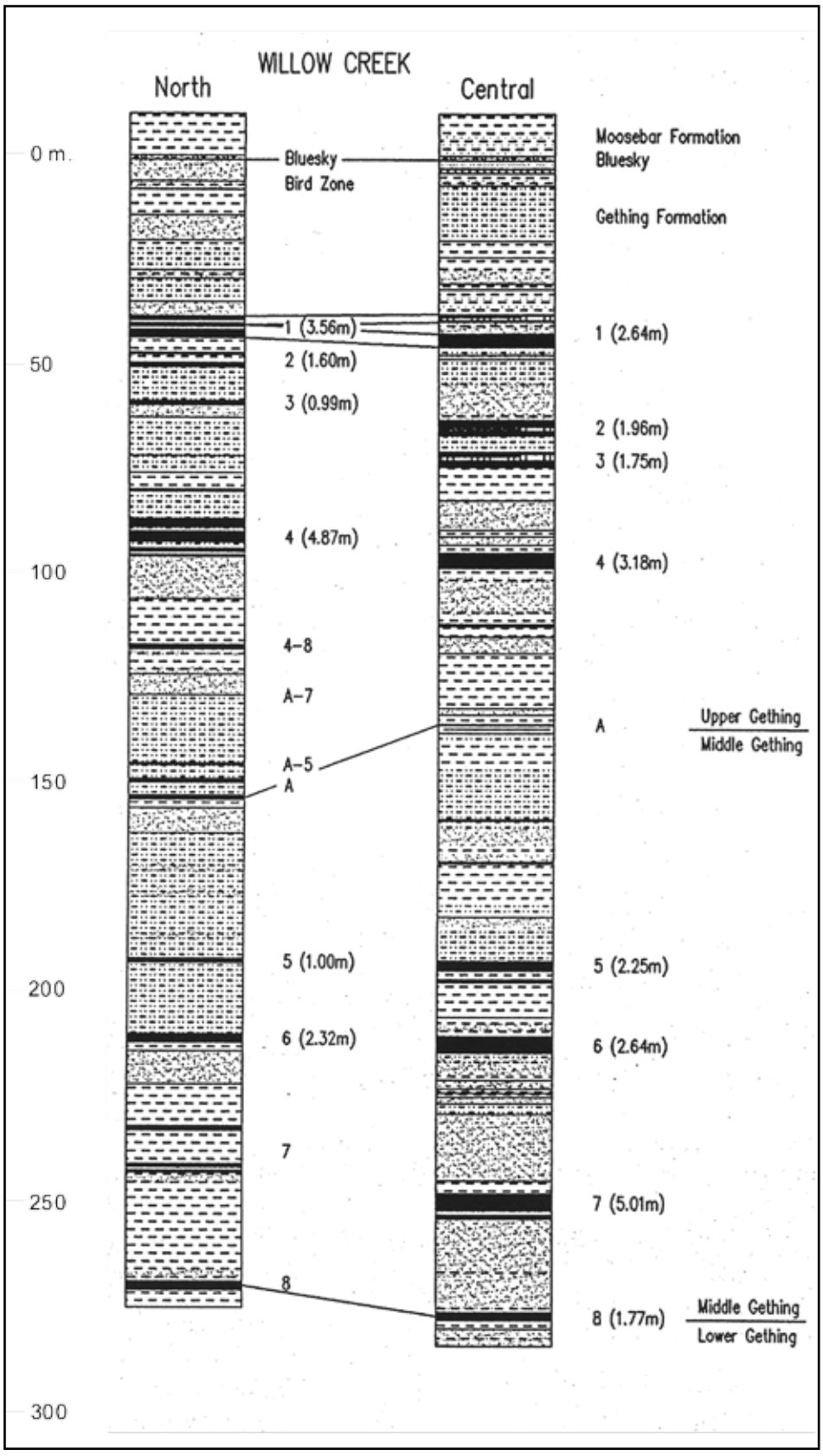

(P.C. KEVIN JAMES)

TABLE 3. AVERAGE QUALITY AND THICKNESS FOR SEAMS AT WILLOW CREEK.

Seam	metres from Moosbar	thickness north metres	thickness central metres	raw ash% DB	VM% DB	CV cals/g	Megajoules/kg	Sulphur%	FSI raw data	Rmax%
1	40	3.56	2.64	7.9	23.5	7870	32.95	0.5	4.5	1.28
2	55	1.6	1.96	14.5	23	7734	32.38	0.59	6	1.33
3	70	1	1.75	8.7	21.1	7729	32.36	0.43	2	1.34
4	100	4.87	3.18	10.1	20	7688	32.19	0.48	3	1.4
A	140	?	?	?	?	?	?	?	?	1.49
5	190	1	2.25	8.3	16.9	7898	33.07	0.7	1	?
6	210	2.32	2.64	7.3	16.3	7957	33.31	0.62	1	?
7	250	?	5.01	8	16.1	7897	33.06	0.65	1.5	1.67
8	280	?	1.77	?	?	?	?	?	?	?
9	?	?	?	?	?	?	?	?	?	?

TABLE 4. PROXIMATE ANALYSES FOR 7 SEAM AND "ALKALI EXTRACTION" TEST FOR SAMPLE OXIDATION.

		H_2O% AR	VM% DB	Ash% DB	FC% DB	FSI	Sulphur%	HGI	Alkali exctraction
WC 2002	8 bright	0.74	17.23	3.4	79.38	1.5			93.3
WC 2002	9 bright	0.7	17.14	3.48	79.38	1.5			91.7
WC 2002	10 bright	0.65	16.58	11.13	72.29	1.5			95
WC 2002	1 dull	0.56	14.47	3.09	82.44	1			90
bulk 1			15.31	4.73	79.96		0.53	70	
bulk 2			15.65	4.23	76.72		0.53		
product quality			16.4	4	79.6	1	0.55	70	
Canmet 7 seam			14.7	2.93	82.4	0.5	0.48		95.5

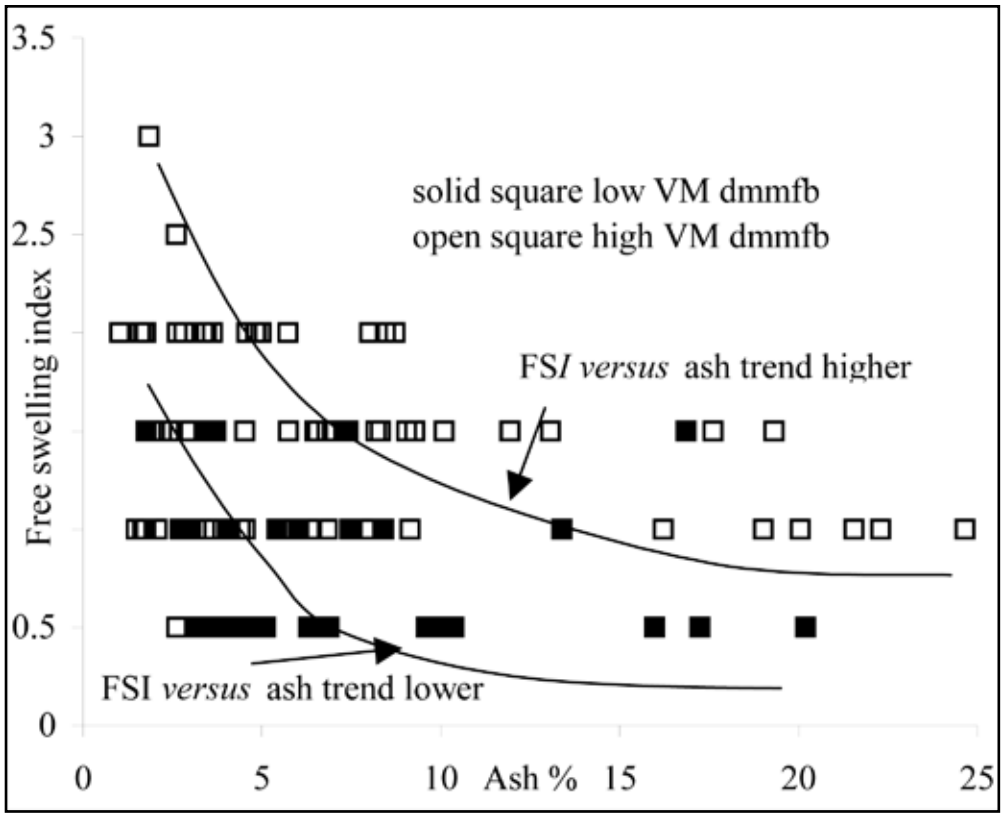

Figure 2. Ash versus FSI data for 7 Seam; from coal assessment report 690, British Columbia Ministry of Energy and Mines library.

TABLE 5. PETROGRAPHY OF 7 SEAM SAMPLES COLLECTED IN 2001.

						VOLUME PERCENTS						Petrography for samples 300 point count.							
Description	length cm	H2O% AR	VM% DB	Ash% DB	FC% DB	telinite	collotelinite	collodetrinite	vitrodetrinite	pseudovitrinite	total reactives	semifusinite	fusinite	inertodetrinite	macrinite	micrinite	total inerts	mineral matter	weight ash%
C	163	4.3	12.7	1.8	85.5	2	6	37	0	2	48	33	1	1	7	6	48	3	5.1
C	111	3.1	12.4	12.7	74.9	0	19	39	2	1	61	10	2	2	9	6	29	10	16.3
C	70	5.1	12.5	2.4	85.1	8	3	32	1	3	47	23	2	0	19	6	50	2	4.0
bright		2.7	14.9	1.7	83.4	2	12	50	1	15	80	8	0	2	6	1	17	1	2.3
dull		3.6	13.1	1.4	85.4	4	13	36	0	4	58	23	2	2	9	4	40	2	4.0
bright		6.7	14.8	13.2	72.1	24	21	34	1	0	81	1	1	2	1	0	5	13	20.5
dull		2.9	12.7	3.8	83.5	2	7	44	0	0	53	14	0	2	20	9	45	3	4.5

C=channel sample bright and dull are grab samples of lithotypes

dispersed mineral matter and a moderate to high content of inert organic material. The Canmet petrographic analysis, after the sample was crushed at Bells Corners, measured 76% semifusinite, which is partitioned as 50% reactive and 50% inert, providing a total reactive maceral content of 58.5% but with a very low percentage of vitrinite (Table 6). The petrographic analysis by the author identified more vitrinite macerals (mainly collodetrinite) with dispersed macrinite and inertodetrinite and less semifusinite. However the proportions of inert and reactive macerals are similar (54% by the author and 58.4% by Canmet). Identification of macerals is a somewhat interpretative process; Canmet appears to identify reactive semifusinite, whereas the author identifies it as high-reflecting collodetrinite. Previous petrographic analyses on channel samples and bright and dull grab samples indicate the range of petrography in the seam (Table 5).

TABLE 6. PETROGRAPHY OF THE 7 SEAM SAMPLES USED IN THE PILOT COKE-OVEN TEST AND PETROGRAPHY OF OTHER LOW-VOLATILE COALS USED IN COKE-OVEN BLENDS.

	7 seam			other low-volatile seams			
	PVCL	Ryan	NrCan ref 3	Jellinbah ref 1	Smoky River ref 2	US low vol from ref 1	US low vol range from-to from ref 2
vitrinite	28.5		15	79.3	61.8	79.3	
telinite		1					
collo telinite		10					
collo detrinite		41					
vitro detrinite		2					
reactive semifusinite	30	0	37.9		13		
total reactives	**58.5**	**54**	**52.9**	**79.3**	**74.8**	**79.3**	**79.8-66.7**
semifusinite	30	25	37.9	13.4	13	13.4	
micrinite	2.2	1	0.7		4.3		
macrinite	0	11	0				
fusinite	7.5	0	6.8		4		
inertodetrinite	0	6	0	4.6		4.6	
mineral matter	1.8	4	1.7	2.6	3.9	2.6	2.4-4.8
total inerts	**41.5**	**47**	**47.1**	**20.6**	**25.2**	**20.6**	**11.7-28.5**
Rmax	**1.68**	**1.64**	**1.68**	**1.7**	**1.62**	**1.7**	**1.54-1.72**
sulphur	0.5		0.48	0.83	0.42	0.83	
HGI	70			96		96	
VM dry			14.72	19.3	17.4	19.3	17.8-20.5
FSI			0.5	2	7	4.5	
Fluidity			0	0	2		58-455
total dilatation			0	7	10	46	15-79

1=Caldeira and Stainly (2002); 2=Fawcett and Dawson (1990)
3=Gransden and Price (2003)

Schapiro *et al.* (1961) introduced a way to predict cold coke strength using coal petrography. The method, which considers one-third of the inert macerals as reactive, is used extensively when pilot coke-oven test data are not available. Canmet considers 50% of the inert macerals to be reactive, based on studies of Cretaceous Western Canadian coals. However, these methods presuppose that petrography is the main influence and that other factors such as coking conditions and the way the different macerals are intermixed do not also play a major role in influencing cold coke strength. Coin *et al*. (1997) suggest that rank is the overriding factor and petrography is not very important in influencing cold coke strength. Pearson (1998) suggests that petrography can be useful in predicting cold coke strength but that the proportion of inert macerals that is reactive varies with rank (measured using random reflectance of vitrinite, Rrand) and vitrinite content. For 7 Seam the random reflectance cut-off that separates reactive from nonreactive inert macerals is 1.76%, based on the equation of Pearson (1998):

cut-off reflectance = Rrand*0.99+0.24

The reactive cut-off converges on the Rrand value as rank increases, and this means that there is a tendency to increase the proportion of inerts designated as reactive as rank increases. This is obviously important for high-rank coals with high inert maceral contents. One should be very careful in deciding if they have coking potential based only on an interpretation of petrography. A comparison of Australian Gondwana coals with western Canadian Cretaceous coals appears to indicate that the proportion of inert macerals that is reactive is also dependent on the origin of the coal (Figure 3; Pearson, 1998). In fact it appears that the reactive cut-off is higher at the same rank for Australian coals than it is for western Canadian coals. Diessel (1996) did not find a difference between inert material in Australian and US Carboniferous coals.

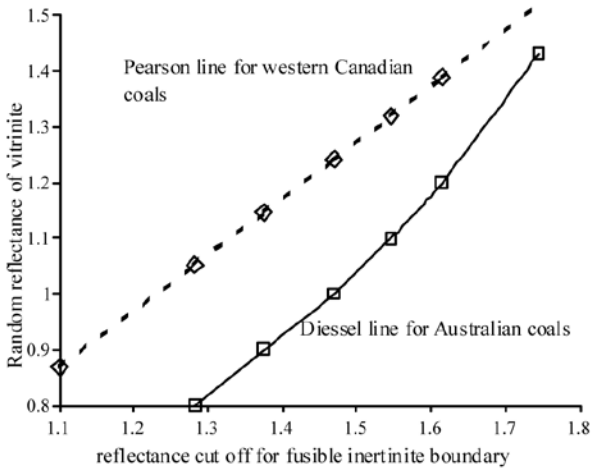

Figure 3. Relationship between reactive semifusinite and rank; Figure modified from Pearson (1998).

TABLE 7. ASH OXIDE ANALYSES FOR 7 SEAM AND OTHER SEAMS ON THE PROPERTY.

Sample	Ash %	SiO_2 %	TiO_2 %	Al_2O_3 %	Fe_2O_3 %	MgO %	CaO %	Na_2O %	K_2O %	P_20_5 %	Ba(4) %	B/A ratio
7 sm Pilot oven sample	2.4	63.00	0.95	23.29	2.48	0.33	1.10	1.97	1.12	1.70	0.65	0.08
7sm central P1	4.5	69.94	0.82	21.22	1.8	0.9	1.04	1	2.35	0.8		0.08
7 Seam data from Coal assessment report 690	5.48	24.65	13.99	0.71	35.68	2.97	7.07	2.1	0.48	2.13		1.23
	6.48	67.7	18.27	0.75	3.5	1.1	2.07	1.54	2.53	0.27		0.12
	6.31	69	20.85	1.41	0.79	0.35	0.95	1.16	1.81	1.57		0.06
Seam1	3.26	54.92	24.17	2.68	1.67	0.78	3.98	2.31	0.37	4.73		0.11
Seam 1	8.52	62.91	8.13	0.32	13.12	1.09	5.18	1.41	0.24	0.49		0.29
Seam 2	3.59	59.62	25.52	1.88	2.43	0.7	3.11	2.91	1.57	1.09		0.12
Seam 4	2.59	23.05	16.65	0.71	9.27	2.75	21.08	2.56	0.49	2.45		0.89
Seam 4	5.21	56.86	26.79	1.06	1.88	0.92	2.69	1.58	0.73	4.07		0.09
Seam 5	4.77	66.84	19.85	0.49	2.15	0.62	1.06	1.37	2.29	0.48		0.09
Seam 6	4.33	64.14	23.68	1.08	1.17	0.54	1.4	1.48	1.45	1.81		0.07
Seam 6	5.95	61.52	23.69	0.99	2.75	1	1.68	1.83	2.41	1.4		0.11

The ash chemistry of the 7 Seam sample was analysed, and previous analyses exist for seams on the property (Table 7), mainly from Coal Assessment Report 690, which is in the Ministry of Energy and Mines library. The data generally indicate a very basic ash with low base-to-acid ratio. Occasional samples have siderite in them, which increases the Fe2O3 concentration in the ash. All base elements are in low concentration, except for moderate concentrations of K and Na. Phosphorous contents are low and, based on an average ash content of 5%, represent a concentration about 0.03% phosphorous in the total sample. The low ash content of the samples will ensure that the effects of the base oxides will be negligible in any blend.

PILOT COKE-OVEN TEST RESULTS

The 45 gallon drum of 7 Seam sample was crushed at Bells Corners to 80% less than 3 mm. A split of the sample was returned to the author for petrographic and ash-oxide analysis. A second split was analysed for proximate and ultimate analysis and, in addition, rheology (Table 8 and 9). In order to test the applicability of using 7 Seam as a blend in coke ovens, it was necessary to obtain a suite of coals that make up a normal coke-oven blend, to coke the blend, and then to make up a new blend with 10% of 7 Seam replacing the low-volatile component in the standard blend before doing a second coke test.

Dofasco Inc. provided three coals, and these coals were mixed in the proportions 28% low-volatile (Rmax 1.7%), 35% high-volatile (Rmax 1%), and 37% medium-volatile (Rmax 1.08%) in preparation for a pilot coke-oven test on a standard coke-oven blend. A second blend was prepared in which the Dofacso coals contributed 18% low-volatile, 37% high-volatile, and 35% medium-volatile, with the balance being made up with 10% 7 Seam. Component seam proportions and proximate and ultimate analyses of the two blends are in Table 8. The addition of 10% 7 Seam decreased the ash and volatile content of the blend. The rheology data for the two blends (Table 9) indicate that the addition of 7 Seam has had no measurable effect on Gieseler plasticity but has had a detrimental affect on dilatation, which has decreased from 112% to 69%.

The pilot coke-oven tests and related analyses were performed by Gransden and Price (2003). The two blends were coked in the Canmet 18 inch oven, which takes a sample load of 350 kg of blended coal. The coal was charged at 3% moisture and 80% less than 3 mm. The coking conditions were those used for other pilot coke-oven tests and are contained in Table 10.

TABLE 8. BLEND PROPORTIONS AND PROXIMATE AND ULTIMATE ANALYSES OF THE TWO BLENDS AND 7 SEAM THAT WERE COKED IN THE PILOT OVEN BY CANMET.

	Base Blend	7Seam blend	7 Seam
Low-volatile Rmax 1.7%	28	18	
medium-volatile Rmax 1.08%	35	35	
high-volatile Rmax 0.99%	37	37	
7 Seam	0	10	100
Coal proximate analysis			
ash% db	6.43	6	2.93
Volatile matter db%	29.85	28.22	14.72
fixed carbon db%	63.72	65.78	82.35
Sulphur db%	0.89	0.83	0.48
Ultimate analysis			
Carbon	81.95	82.92	88.28
hydrogen	4.84	4.84	3.84
nitrogen	1.55	1.52	1.22
ash% db	6.43	6	2.93
Oxygen by dif	4.34	3.89	3.25
Coke proximate analysis			
ash% db	8.46	7.84	
Volatile matter db%	0.46	0.5	
fixed carbon db%	91.08	91.66	
Sulphur db%	0.71	0.65	

TABLE 9. RHEOLOGY OF THE TWO BLENDS AND OF 7 SEAM.

	Base Blend	7Seam blend	7 Seam
Low-volatile Rmax 1.7%	28	18	
medium-volatile Rmax 1.08%	35	35	
high-volatile Rmax 0.99%	37	37	
7 Seam	0	10	100
FSI	7.5	7	0.5
Gieseler Plasticity			
Initial softening temp °C	42	403	
Fusuion temp °C	415	416	
Max fluid temp °C	445	443	493
Final fluid temp °C	485	486	
Solidification temp °C	491	492	
melting range temp °C	83	83	
Max fluiditiy ddpm	2422	2547	0.1
Dilitation			
Softening temp °C	376	374	
Max contration temp °C	417	419	
Max dilatation temp °C	470	468	
Contraction	24	28	
Dilation	106	63	

The quality of the coke produced by the blend with 10% of 7 Seam was the same as or not as good as the standard blend on a number of counts. Coke strength after reaction and coke reactivity index were unchanged within the limits of the measurements (Table 9). However, cold coke strength decreased markedly. On the plus side, maximum wall pressure and maximum gas pressure both decreased. The ash and sulphur contents of the coke decreased.

The poor performance of 7 Seam in the blend is probably the result of a combination of the low percent of active reactives and the high rank. Coke textures (Table 11) confirm a noticeable decrease in the reactive components of the 7 Seam blend as coke inerts increase by about 6%. It was unfortunate that the petrographic composition could not be checked prior to coking. There is a distinct possibility that in other areas the seam will have higher reactives content or lower rank. It is also possible that either the upper or lower part of the seam has a higher reactive content and could be mined separately for a coke-oven blend market. Six Seam, which is about 30 m above 7 Seam, may provide a better candidate for blending.

TABLE 10. CARBONIZATION CONDITIONS AND RESULTS FOR THE TWO COKE TESTS.

	Base Blend	7Seam blend
Low-volatile Rmax 1.7%	28	18
medium-volatile Rmax 1.08%	35	35
high-volatile Rmax 0.99%	37	37
7 Seam	0	10
moisture %	2.6	2.4
Minus 3.35 mm %	81.2	81
ASTM bulk density Kg/m3	778	782
Oven bulk density Kg/m3	824	823
Coking time h:min	18:30	18:05
Final centre temp °C	1068	1064
Time to 900 °C	14:55	14:30
Time to 950 °C	15:30	15:05
Time to 1000 °C	16:05	15:50
Max wall pressure Kpa	7.7	5.0
Max gas pressure Kpa	14.8	3.4
Coke yield %	75.7	76.5
100 mm sieve %	0.0	0.8
75 mm sieve %	5.7	8.2
50 mm sieve %	43.6	42.2
37.5 mm sieve %	79.5	77.1
25 mm sieve %	92.7	91.9
19 mm sieve %	94.7	94.5
12.5 mm sieve %	95.7	95.8
Passsing 12.5 mm sieve %	4.3	4.2
Mean coke size	50.2	50.3
ASG	0.954	0.987
Stability	61.0	57.3
Hardness	67.0	65.2
I 10	19.3	20.7
I 20	78.5	77.0
I 40	49.4	42.6
CSR %	55.0	56.6
CRI %	30.7	28.8

TABLE 11. COKE TEXTURES FOR THE TWO BLENDS.

	Base Blend	7Seam blend
Low-volatile Rmax 1.7%	28	18
medium-volatile Rmax 1.08%	35	35
high-volatile Rmax 0.99%	37	37
7 Seam	0	10
isotropic	0.00	0.94
incipient	1.85	2.62
circular fine	41.08	37.83
circular medium	1.18	1.50
circular coarse	0.00	0.00
total circular	**44.11**	**41.95**
lenticular fine	20.54	18.35
lenticular medium	2.86	3.00
lenticular coarse	0.51	0.75
total lenticular	**23.91**	**22.10**
ribbon coarse	3.03	4.12
ribbon medium	3.70	2.62
ribbon fine	11.62	8.80
total ribbon	**18.35**	**15.54**
fusinite	0.17	0.37
semi-fusinite	3.37	10.67
unidentified inerts	10.10	7.68
altered vitrinite	0.00	0.00
green coke	0.00	0.00
depositional carbon	0.00	0.75
petroleum coke	0.00	0.00
breeze	0.00	0.00
total inerts	**13.64**	**19.48**
blend Rmax%	1.16	1.14
low vol	21.54	19.77
medium vol	27.39	26.98
high vol	51.07	53.26

MARKET OPPORTUNITIES FOR PCI AND LOW VOLATILE PCI

A large percent of the reserves in the Willow Creek area are derived from 6 and 7 Seams. The rank of these seams is low-volatile bituminous, and they have moderate and variable inert maceral content. On average, they do not exhibit good coking characteristics, and consequently coal on the property is considered suitable for thermal or pulverized coal injection (PCI) purposes. There are two important ratios to consider when discussing PCI. The first is the the PCI ratio (kg/t)—the amount of PCI coal used for each tonne of hot metal produced. The second is the coke replacement ratio—the ratio of weight of PCI coal for weight of coke; i.e., the reduction in coke requirement divided by the amount of PCI coal used.

The coke replacement ratio varies with the rank of coal used and ranges from about 0.6 for high-volatile low-rank coals to nearly 1 for low-volatile high-rank coals. The rate is in part related to the hydrogen content of the fuel. Hydrogen is an effective reductant but has a cooling effect in the raceway at the base of the blast furnace where it is injected. This limits the amount of hydrogen-rich fuels (natural gas) that can be injected. Higher coke replacement ratios are achieved with coal rather than oil and gas. The hydrogen content of coal decreases as rank increases, so the coke replacement ratio increases as rank increases (Figure 4). This has been pointed out by a number of authors (Hutny *et al*., 1991), and more recently by Stainlay (2003). There is, therefore, an expanding market for PCI coal and especially for high-rank low-volatile bituminous coal.

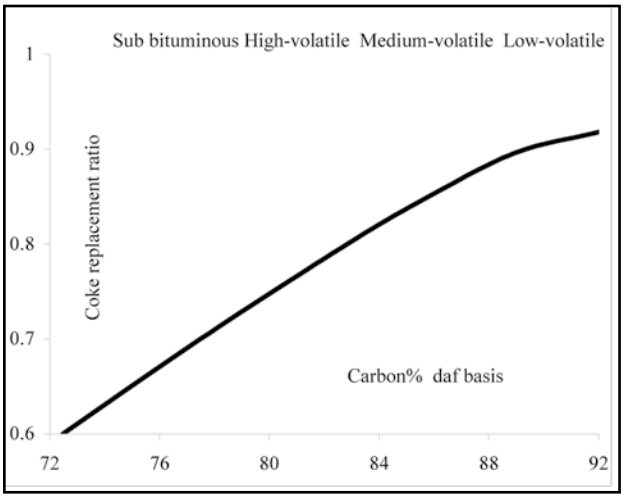

Figure 4. Coke replacement ratio versus coal rank.

It requires 1.2 to 1.5 tonnes of coal to make a tonne of coke, so if the coke replacement ratio is 0.75, the coal replacement ratio is at least 0.75 x 1.2; i.e., 1.0 or more. However, PCI coal sells for much less than coking coal. Prices vary but are often only 70% of the price of premium coking coal. Obviously there is the potential for considerable savings for the blast furnace operator. Based on the price variation, it is to the advantage of the operator to use low-volatile coals for PCI to save even more money.

The burning characteristics of high-rank low-volatile PCI coal in the blast furnace are different from low-rank high-volatile coals, but once the blast furnace is adapted there can be a considerable saving in requirement for higher-priced coking coal. At the moment the majority of blast furnaces have converted to PCI, and the global average injection rate is 96 kg/t. The present demand is about 31 million tonnes, and this is expected to grow to 42 million tonnes by 2010 (Stainlay, 2003). The increase in consumption will be caused by more conversions and an increase in the PCI rate from about 100 to maybe as high as 200 kg/t. This increase in PCI rate will in part be achieved by switching from high- to low-volatile PCI coals. The maximum PCI rate reported is from China, where a rate of about 280 kg/t was achieved using anthracite.

Traditionally, the main component of coking coal blends for coke ovens has been medium-volatile bituminous coals with good rheology and ash chemistry. As science and international coal trade developed, it was found that a mixture of coals would result in an optimum blend whose composition plotted in the optimum blend field of various diagrams (for example, the MOF diagram). As few single coals plotted in the field, most steel mills moved to at least a ternary blend of low-, medium-, and high-volatile coals. High-volatile coals add fluidity to the blend, and low-volatile coals improve coke yield at the expense of increasing coke-oven pressure. Low-volatile coals represent a balancing act between increasing rank and preservation of rheology, which is destroyed as rank increases. The three-component blend of coals for coke ovens has become the norm in recent years; however, reserves of low-volatile coal are becoming depleted, especially in the US (Kolijn and Khan, 2003). Steel mills looking to maintain a low-volatile component in their coke-oven blends will have limited opportunities in the future.

In Australia, the Jellinbah mine mines a low-volatile seam (Table 6), which is being marketed as a PCI product and as a possible blend component in coke ovens (Calderia and Stanlay, 2003). The coal is higher rank than 7 Seam but also has a much higher reactives content.

Low-volatile coals can be replaced in the coal blend with medium-volatile coals, especially if the amount of high-volatile coal is also reduced (Kolijn and Khan, 2003). This can maintain coke quality and coke yield because of the reduction in amounts of both low- and high-volatile coal and has the added advantage of reducing oven pressure.

REGIONAL AVAILABILITY OF LOW-VOLATILE COALS IN BRITISH COLUMBIA

The rank of coals in the Gething Formation was studied by a number of authors (Marchioni and Kalkreuth, 1992; Karst and White, 1979). The rank of the formation decreases to the northeast into the Western Canadian Sedimentary Basin and is generally medium-volatile bituminous along the trend of the Rocky Mountain Foothills. Within this trend, there are three areas where the rank is low-volatile bituminous (Figure 5; adapted from Marchioni and Kalkreuth, 1992). The northernmost underlies the subcrop area of the Willow Creek, Lossan, and Burnt River properties (Figure 5). To the south along the trend of the foothills, another area is east of the town of Tumbler Ridge and at depth within the Gething Formation. The third area is to the southeast in Alberta. The best opportunity for low-volatile mineable coal resources is in the area around Willow Creek and to the southeast.

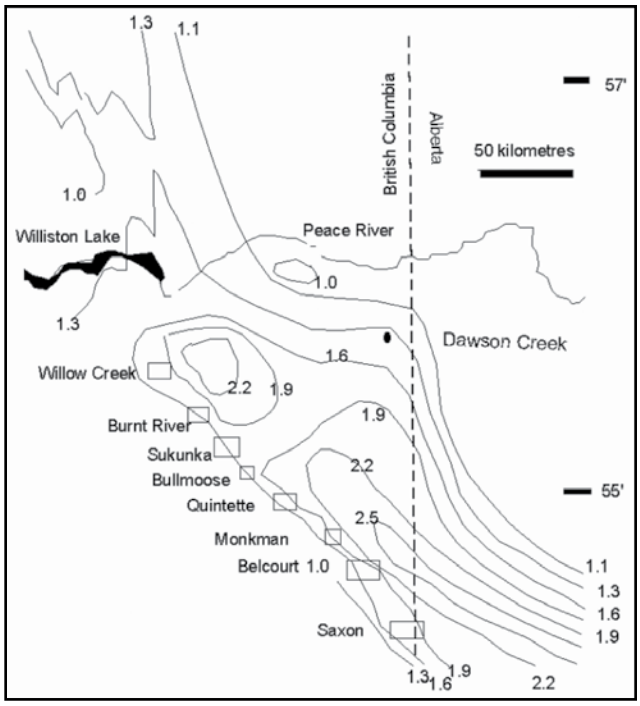

Figure 5. Reflectance isograds for the top of the Gething Formation; adapted from Machioni and Kalkreuth (1992).

The Mist Mountain coal section in Morrissey Ridge area in the southwest part of the Crowsnest coalfield (southeast British Columbia) contains low-volatile coal (Pearson and Grieve, 1985). Coal in the area was mined in the period from 1902 to 1906 in the Carbonado Mine. The coal was used as single component in beehive ovens but it did not make good coke, and this was in part the reason for the failure of the mine.

Outside British Columbia, the Smoky River mine (now closed) in Alberta exported a low-volatile coking coal (Table 6). The coal has a similar rank to 7 Seam but a higher reactive maceral content and much better FSI. The mine is expected to re-open as the Grande Cache mine in the near future.

CONCLUSIONS

The internationally traded coal market will remain very competitive in the long term, especially when China re-enters the coking coal and coke export markets in a big way. However, there are two brands of coking coal that are presently in demand and will probably remain in an under-supply situation. These are low-volatile coal for PCI and low-volatile coal for coke-oven blends. The latter commands a higher price. British Columbia has limited potential to take advantage of these markets. The best opportunities are at Willow Creek and possibly in other parts of the Gething Formation. There are also possibilities in the southeast corner of the Crowsnest coalfield in southeastern British Columbia.

This limited test did not indicate that 7 Seam from the Willow Creek property could be used in a coke-oven blend; however, it appears that the sample may not have been representative. When the mine is in production, sampling will be easier and channel samples may indicate better potential for samples to use in additional coke-oven tests.

ACKNOWLEDGEMENTS

Age and the expanding breadth of coal science, including coalbed methane, ensures that the senior author cannot pretend to be more than a generalist in his field. This short report has benefited considerably from conversations with John Gransden.

REFERENCES

Caldeira, J.G. and Stainly R.S. (2002): The challenge to use extremely low-volatile Australian weak coking coals in the production of good quality cokes; 2002 Iron making Conference Proceedings, pages 405-415.

Coin C.D.A., and Broome, A.J. (1997): Coke Quality Prediction from Pilot Scale Ovens and Plant Data, International Coal Conference, Calgary, September 1997, pages 325-333.

Diessel C.E.K. (1996): Inertinite; ACARP Report, Australian Coal Research Limited, Issue No2, July 1996.

Fawcett, D.A., and Dawson, R.F. (1990): Unique blending properties of Smoky River coal; American Institute of Mining Engineering, Iron Making Conference Detroit, March 1990, pages 110-108.

Gransden, J. and Price, J.T. (2003): Carbonization Project Report 7 Seam coal in a coke makers blend; Canmet Energy technology Centre, Job No. 3586R

Hutny, W.P., Lee, G.K. and Price, J.T. (1991): Fundamentals of coal combustion during injection into a blast furnace; Prog. Energy Combustion Sciences, Volume 17, pages 373-395.

Karst, R. and White, G.V. (1979): Coal Rank Distribution within the Bluesky-Gething Stratigraphic Horizon of Northeast B.C.; in Geological Fieldwork 1979, B.C. Ministry of Energy, Mines and Petroleum Resources, Paper 80-1, pages 103-107.

Kolijn, C. J. and Khan, M.A. (2003) Medium-volatile coal-The solution for coke oven blends with reduced low-volatile coal content; ACE Steel technology, July 2003, pages 42-49.

Marchioni, D. and Kalkreuth, W. (1992): Vitrinite reflectance and thermal maturity in Cretaceous strata of the Peace River Arch region west central Alberta and adjacent British Columbia; Geological Survey of Canada, Open file 2576.

Pearson, D. and Grieve, D.A. (1985): Rank variation, coalification pattern and coal quality in the Crowsnest Coalfield, British Columbia; Canadian Institute of Mining and Metallurgy, Bulletin, Volume 78, pages 39-46.

Pearson, D. (1998): Fusible inertinites in Coking Coals; 1998 (Toronto) ICSTI/ Iron making Conference Proceedings, pages 753-755.

Pine Valley Mining Corporation (2001): Willow Creek Project raw coal production study; Amendment to Permit C-153. British Columbia Ministry of Energy and Mines.

Ryan, B.D. (1997): Coal quality variations in the Gething Formation northeast British Columbia; British Columbia Ministry of Energy and Mines Geological Fieldwork 1996:1 pages 373-397.

Schapiro, N., Gray R.J., and Eusner, G.R. (1961): The use of coal petrography in coke making, J.Inst. Fuel. Volume. 37, 1961, pages 234-242.

Stainlay, R. (2003): PCI- current status and prospects for growth; Asia Steel International Conference, Jamshedpur, India - April 2003.

INTERIOR BASINS STRATEGY

By M. Hayes, F. Ferri and S. Morii

Resource Development and Geoscience Branch, B.C. Ministry of Energy and Mines,
6th Flr-1810 Blanshard St., Victoria, BC, Canada, V8W 9N3

KEYWORDS: oil, gas, hydrocarbons, Intermontane, Interior Basins, Nechako, Bowser, Whitehorse Trough.

INTRODUCTION

The government of British Columbia, through the Ministry of Energy and Mines, has a Service Plan goal of achieving a 17% increase in natural gas production and a 31% increase in the number of wells drilled over the next three fiscal years. (*B.C. Ministry of Energy And Mines*: Service Plan [2004/5–2006/7]). One of the key Ministry strategies developed to realize this goal involves improving knowledge of the province's petroleum geology in order to identify new energy development opportunities within British Columbia. The aim of this strategy is to realize B.C.'s ultimate hydrocarbon potential within its relatively under-explored portion of the Western Canada Sedimentary Basin (WCSB) and see development of commercial oil and gas production within its interior and offshore basins. The achievement of these goals will benefit all British Columbians through increases in oil and gas royalties and tenure disposition fees and the creation of new employment opportunities.

The Resource Development and Geoscience Branch is mandated to identify, quantify, and promote the hydrocarbon potential of onshore regions of British Columbia. In addition, the branch undertakes community relations initiatives, including those with First Nations, in areas of hydrocarbon potential.

In onshore regions outside of the WCSB, oil and gas potential occurs primarily within Mesozoic and Cenozoic clastic sediments of the Interior Basins. The main areas include, from north to south, the Whitehorse Trough, the Bowser and Sustut Basins, and the Nechako Basin (Figure 1). In addition, there are several small Tertiary basins (e.g., Hat Creek) and the onshore portions of the Georgia Basin. Although some of these areas have seen limited subsurface exploration (e.g., Bowser and Nechako Basins), they remain 'frontier basins' because of infrastructure challenges and lack of extensive geological information.

Recent publications on the oil and gas resource potential of the intermontane basins suggests upwards of 18.8 trillion cubic feet (tcf; 5.3 x 10^{11} m^3) of gas and 7.6 billion barrels (bb; 1.2 x 10^9 m^3) of oil (Hannigan *et al*., 1994; 1995; 2001). In light of this, the B.C. Ministry of Energy and Mines has undertaken several initiatives to better quantify this potential resource and attract industry investment.

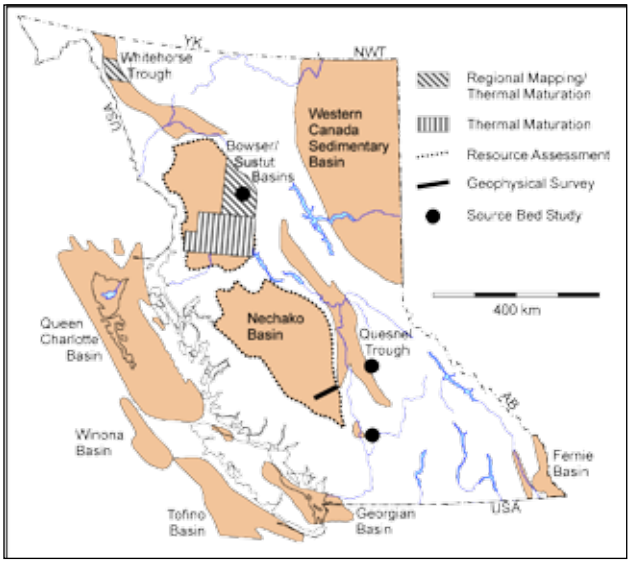

Figure 1. Map of British Columbia showing the outline of its major petroleum basins and location of projects within the Intermontane Basins funded entirely, or in part, by the Resource Development and Geoscience Branch of the B.C. Ministry of Energy and Mines.

NEW INITIATIVES

The Resource Development and Geoscience Branch (RDGB) has initiated or supported several projects within these areas, leading to the capture of new energy-related geoscience information. Projects have started in the Whitehorse Trough and Bowser-Sustut and Nechako Basins.

Whitehorse Trough

In central Whitehorse Trough, English *et al.* (2003, 2004), through a grant to the University of Victoria and in conjunction with the RDGB, have gathered baseline thermal maturation and source rock potential data as part of a more regional mapping program. These new Rock-Eval data have been released as two open file reports (Fowler, 2003, 2004).

Nechako Area and Quesnel Trough

In 2002, the RDGB commissioned Petrel Robertson Ltd. to produce a report on the petroleum exploration potential of the Nechako-Chilcotin area (Hayes, 2002). This paper summarizes current information about surface and subsurface geology and outlines several areas of varying hydrocarbon potential.

Subsequent to this, RDGB entered into a working agreement with the Geological Survey of Canada for a new petroleum resource assessment of the Nechako Basin. This is an ongoing project and has produced several milestone products, including Rock-Eval and total organic content (TOC) analysis of subsurface samples from all interior wells (Osadetz *et al.*, 2003) and new strip logs of all interior wells, incorporating digital well logs and qualitative porosity and permeability descriptions (Thornsteinsson *et al*., in press). In addition, a new heat-flow model is being generated, which, together with new and current information, will be integrated into a new resource assessment.

The lack of a recognized source horizon was one of the shortcomings listed by Hayes (2002) for the Nechako Basin, and this is generally the case for all Interior basins. Ferri (2004) addresses, in part, this issue through sampling of organic-rich Jurassic and Cretaceous sediments within the Quesnel Trough and within the Bowser and Sustut Basins.

The RDGB also acquired new high-resolution gravity and magnetic data along a 30 km transect immediately west of Williams Lake (Figure 1; *see* Best, 2004). The purpose of this survey was to validate the presence of a gravity low delineated by data obtained by Canadian Hunter Exploration Ltd. in the early 1980s (Salt, 1980). One interpretation is that this gravity low represents a thick sequence of sediments, possibly of Tertiary age.

Bowser-Sustut Basins

The Bowser and Sustut Basins potentially represent the largest petroleum exploration target area within the Intermontane region (Figure 1). This area has received renewed interest in the last few years as a result of new thermal maturation data indicating that large portions of these basins are within the oil and gas window (Evenchick *et al.*, 2002). Prior to this, much of the area, particularly the Bowser Basin, was considered to be over-mature with respect to oil and in the upper end of the gas window (Hannigan *et. al.*, 1995). This new data suggests the potential for hydrocarbon resources beyond those described in the report by Hannigan *et al.* (1995).

In light of this new information, the B.C. Ministry of Energy and Mines embarked on a program to better quantify potential resources through the acquisition of new geoscience information. Part of this strategy involved collaborative research with the Geological Survey of Canada, leading to a new resource assessment of the basins. An uplift history of the northern two-thirds of the Bowser and Sustut Basins is being modeled, based on apatite fission track analysis from several localities within the basins (O'Sullivan *et al.*, 2004). Sampling during acquisition of data points for this study led to the discovery of oil staining in several samples, analysis of which suggests the presence of two petroleum systems (Osadetz *et al.*, 2003). Further examination of catalogued surface and subsurface samples and core recognized more oil staining (Osadetz *et al.*, 2004; Evenchick *et al.*, 2004). These occurrences also confirmed the new thermal model generated for these areas.

These new data, together with the impetus from the British Columbia government for more energy-related information in the area, led the Canadian government to initiate a multi-year, multi-million dollar program to better define the geology and energy resources of the Bowser and Sustut Basins ("Integrated Petroleum Resource Potential and Geoscience Studies of the Bowser and Sustut Basins"; *see* Evenchick *et al.*, 2004). The province is a partner in this new project, which runs from 2003 to 2007.

REFERENCES

Best, M. (2004): Gravity and Magnetic Survey, Nechako Basin Study, Acquisition and Processing Phase; B.C. Ministry of Energy and Mines; Petroleum Geology Open File 2004-1.

English, J.M., Mihalynuk, M.G., Johnston, S.T., Orchard, M.J., Fowler, M. and L.J. Leonard (2003): Atlin TGI, Part VI: Early to Middle Jurassic Sedimentation, Deformation and a Preliminary Assessment of Hydrocarbon Potential, Central Whitehorse Trough and Northern Cache Creek Terrane; in Geological Fieldwork 2002, B.C. Ministry of Energy and Mines, Paper 2003-1, pages 187-201.

English, J.M., Fowler, M., Johnston, S.T., Mihalynuk, M.G. and Wight, K.L. (2004): Thermal Maturity in the Central Whitehorse Trough, Northwest British Columbia; Resource Development and Geoscience Branch, B.C. Ministry of Energy and Mines, Summary of Activities 2004, this volume.

Evenchick, C.A., Hayes, M.C., Buddell, K.A. and Osadetz, K.G. (2002): Vitrinite and Bitumen Reflectance Data and Preliminary Organic Maturity Model for the Northern two thirds of the Bowser and Sustut basins, North-central British Columbia; B.C. Ministry of Energy and Mines, Petroleum Geology Open File 2002-1.

Evenchick, C.A., Ferri, F., Mustard, P.S., McMechan, M., Osadetz, K.G., Stasiuk, L., Wilson, N.S.F, Enkin, R.J., Hadlari, T. and McNicoll, V.J. (2004): Recent Results and Activities of the Integrated Petroleum Resource Potential and Geoscience Studies of the Bowser and Sustut Basins Project, British Columbia; in Current Research, Geological Survey of Canada, 2003-A13, 11 pages.

Ferri, F. (2004): Potential Source Rock Characterization, Intermontane Basins, British Columbia; Resource Development and Geoscience Branch, B.C. Ministry of Energy and Mines, Summary of Activities 2004, this volume.

Fowler, M. (2003): Atlin TGI - Rock EVAL VII Program Pyrolysis Results from Whitehorse Trough; B.C. Ministry of Energy and Mines, Geofile 2003-1.

Fowler, M. (2004): Rock-Eval VI analysis of samples from the central Whitehorse Trough by the Geological Survey of Canada, Calgary in partnership with the B.C. Ministry of Energy and Mines; B.C. Ministry of Energy and Mines, Petroleum Geology Open File 2004-2.

Hannigan, P., Lee, P.J., Osadetz, K.G., Dietrich, J.R. and Olsen-Heise, K. (1994): Oil and Gas Resource Potential of the Nechako-Chilcotin Area of British Columbia; B.C. Ministry of Energy and Mines, Geofile 2001-6.

Hannigan, P., Lee, P.J., and Osadetz, K. (1995): Oil and Gas Resource Potential of the Bowser-Whitehorse area of British Columbia; B.C. Ministry of Energy and Mines, Geofile 2001-5.

Hannigan, P., Dietrich, J.R., Lee, P.J. and Osadetz, K.G. (2000): Hydrocarbon Resources of Pacific Margin Basins; in Canadian Society of Exploration Geophysicists, Annual Meeting, Program and Abstracts.

Hannigan, P., Dietrich, J.R., Lee, P.J. and Osadetz, K.G. (2001): Petroleum Resource Potential of Sedimentary Basins on the Pacific Margin of Canada; Geological Survey of Canada, Bulletin 564, 72 pages.

Hayes, B. (2002): Petroleum Exploration Potential of the Nechako Basin, British Columbia; B.C. Ministry of Energy and Mines, Petroleum Geology Special Paper 2002-3.

O'Sullivan, P.B., Donelick, R.A., Osadetz, K.G., Evenchick, C.A. and Ferri, F. (2004): Apatite Fission Track Data for Northern Two Thirds of the Bowser Basin; B.C. Ministry of Energy and Mines, Petroleum Geology Open File 2004-3.

Osadetz, K.G., Evenchick, C.A., Ferri, F., Stasiuk, L., Obermajer, D.M. and Wilson, N.S F. (2003): Molecular composition of Crude Oil Stains from Bowser Basins in Geological Fieldwork 2002, B.C. Ministry of Energy and Mines, Paper 2003-1, pages 257-264.

Osadetz, K.G., Jiang, C., Evenchick, C.A., Ferri, F., Stasiuk, L.D., Wilson, N.S.F. and Hayes, M. (2004): Sterane compositional traits of Bowser and Sustut basin crude oils: Indications for three effective petroleum systems; Resource Development and Geoscience Branch, B.C. Ministry of Energy and Mines, Summary of Activities 2004, this volume.

Salt, W.T. (1980): Gravity Survey of the Big Creek Area; B.C. Ministry of Energy and Mines, Geological and Geophysical Report 2393.

Thornsteinsson, E.T., Osadetz, K.G., Ferri, F. and Hayes, M. (in press): Stratigraphy and Lithology of Petroleum Wells within the Bowser Basin and Nechako area; B.C. Ministry of Energy and Mines, Petroleum Geology Open File 2004-4.

QUALITATIVE INTERPRETATION OF POTENTIAL FIELD PROFILES: SOUTHERN NECHAKO BASIN

By Melvyn E. Best

Bemex Consulting International
5288 Cordova Bay Road

KEYWORDS: potential fields, gravity, magnetics, Nechako Basin, petroleum exploration, Big Creek-Riske Creek gravity/magnetic profile

INTRODUCTION

The Nechako Basin (Figure 1) is one of several interior basins within British Columbia. Although the potential for economic quantities of hydrocarbons exists within the basin (Hannigan et. al., 1994), only limited exploration has been carried out. Quaternary surficial sediments and Tertiary volcanic outcrop cover large areas of the basin, limiting surface geological mapping and potentially creating problems in acquiring seismic data. In addition, volcanic rocks within the sedimentary section can cause seismic acquisition and processing problems. The presence of these volcanic rocks also complicates the interpretation of seismic and magnetic data.

Several companies explored for oil and gas within the Nechako Basin prior to 1980, but no commercial quantities were found. In the early 1980s Canadian Hunter Exploration carried out an exploration program consisting of a regional gravity survey, a limited number of two-dimensional seismic lines, and the drilling of several wells (Robertson, 2002). As no economic accumulations of hydrocarbons were encountered during drilling, they abandoned the play. No additional exploration activity has been conducted since that time.

As part of the BC government's initiative for economic development within British Columbia, Bemex Consulting International was awarded a contract to carry out ground gravity and magnetic surveys in the southern Nechako Basin. The purpose of the survey is to promote the basin's potential and to illustrate how integrated potential field data can provide constraints on basin structure, sediment thickness, and volcanic structures within the sedimentary section. An approximate east-west profile was selected for this survey based on the regional gravity data collected by Canadian Hunter. Data collected along this profile included gravity, total field magnetic and the vertical gradient of the total field. Elevations and UTM coordinates were acquired along the profile as well.

This report describes the data acquisition and processing steps for the ground geophysical survey and presents a preliminary qualitative interpretation of these profiles.

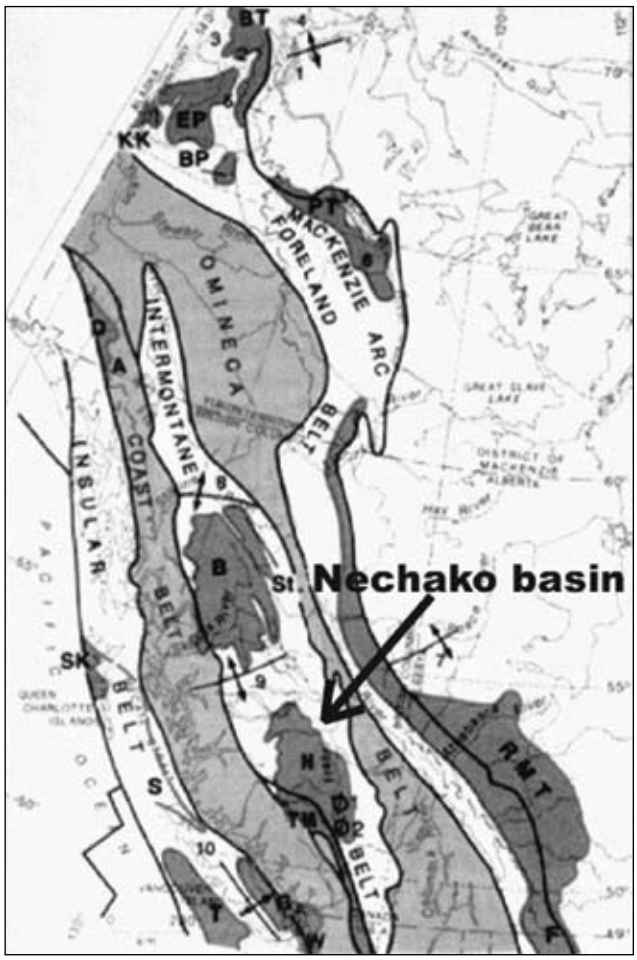

Figure 1. Morphological Belts of the Canadian Cordillera, showing the position of the Nechako Basin and related tectonic elements (from Yorath, 1991). Note: B = Bowser Basin, N = Nechako Basin.

ACQUISITION AND PROCESSING

Ground gravity and magnetic data were collected along a 33 km profile at approximately 330 m and 165 m spacing, respectively. The data were collected along the road that connects Riske Creek and Big Creek (Figure 2). The loca-

tion of the profile was chosen to cross a significant gravity low centred near Big Creek that was observed on the Canadian Hunter regional gravity survey.

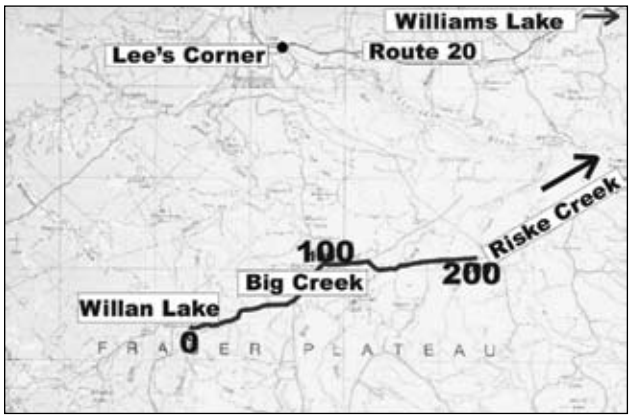

Figure 2. Location of profile along Big Creek–Riske Creek Road (from NTS 92O). The profile goes from station 0 in the west near Willan Lake to station 200 in the east.

A Lacoste-Romberg gravity meter was used to measure the relative change in gravity between each station. Measurements at several stations were repeated approximately 4 hours apart to correct for instrument and tidal drift. Relative elevations were measured at each gravity station using a laser level. These relative elevations were then tied to a known elevation above sea level near station 122. UTM coordinates (NAD 83) were obtained from BC Terrain Resource Information Mapping (TRIM) maps at a scale of 1:50 000.

A GEM rover gradiometer was used to measure the magnetic field and the vertical gradient of the magnetic field at each gravity station and approximately midway between each gravity station. A second GEM magnetometer was used as a base station. Several base stations were located along the profile, depending on where the roving survey was being conducted that day.

Processing of the gravity data consisted of drift corrections, latitude corrections, free-air elevation corrections, and Bouguer elevation corrections. (A Bouguer density of 2350 kg/m3 (2.35 g/cc) was determined from tests carried out over areas with significant topographic relief. The density is consistent with the density used for the Canadian Hunter survey). Terrain corrections up to and including ring D (Hammer, 1939) were also computed. The overall accuracy of the gravity data is estimated to be ±0.60 mGal or better.

The total magnetic field data were corrected for diurnal variations using the base station readings. No other corrections were applied to the total magnetic field data and the vertical gradient of the total magnetic field data.

Plots of the corrected gravity data, elevation above sea level, and corrected magnetic field data are given in Figure 3. More details on data acquisition and processing can be found in Best (2004).

REGIONAL SETTING

The Nechako Basin is a Mesozoic forearc basin (Yorath, 1991) located in the Intermontane Belt of the southern Canadian Cordillera (Figure 1). Spatially, the Nechako Basin is bounded by the Skeena Arch to the north, the Fraser River Fault System to the east, and the Coast Mountain plutons to the west (Figure 1).

The tectonic history of the Nechako Basin is complex. Its structural geology is poorly understood, due largely to extensive Quaternary sediments covering the surface and large areas of Tertiary volcanic outcrop. Outcrops of deformed Mesozoic sediments are present,but isolated within the basin proper. More continuous outcrop occurs along the western flank (Petrel Robertson, 2002).

The Nechako Basin sediments were derived from bordering uplifts related to contraction during terrane accretion (Gabrielse et al.., 1991). The Takla and Hazelton Groups, comprising volcanic and sedimentary strata, were deposited during Triassic and Early-Middle Jurassic time. The formation of the Skeena Arch (Yorath, 1991) during the Middle Jurassic (?) segregated the Nechako Basin from the Bowser Basin to the north.

In Middle Jurassic to Early Cretaceous time, the Intermontane and Insular super-terranes were accreted to each other and to North America. (Gabrielse and Yorath, 1991). Sedimentation from the resulting uplifts was shed both west into the Nechako Basin and other intermontane basins and east into the Rocky Mountain Fold Belt. Transpressional tectonics dominated until the Eocene, at which time there was a change to a regime of dextral transtension (Price, 1994) and an episode of associated magmatism.

Deformation styles in the Nechako Basin were affected by both lithological contrasts and tectonics. Deformation of Stikine and Cache Creek rocks can be related to early Mesozoic accretionary prisms and subduction zones. Structures related to the early Mesozoic include folds and (northwest-trending) thrust faults, which verge either east or west, depending on position in the Intermontane Belt (Gabrielse, 1991; Price, 1994). Major transcurrent faults (related to Eocene extension) cut and bound the basin.

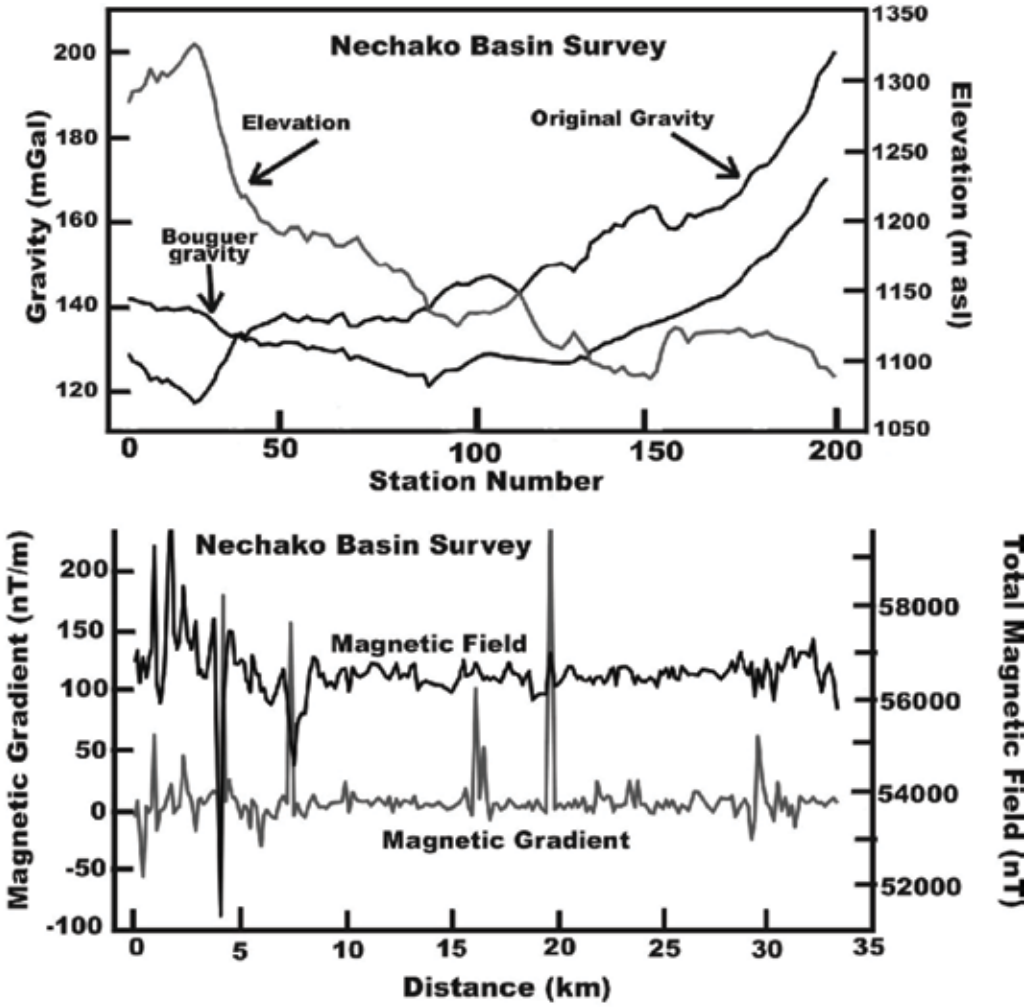

Figure 3. Elevation above sea level, corrected gravity, and corrected magnetic data versus distance (km) from station zero. Station number is shown on the upper diagram with station zero at the western end of the Big Creek–Riske Creek profile.

PRELIMINARY INTERPRETATION OF GRAVITY AND MAGNETIC PROFILES

The final processed gravity and magnetic data are shown in Figure 3. The gravity profile confirms the presence of a low near Big Creek with a magnitude comparable to that of the low on the regional Canadian Hunter gravity map (Petrel Robertson, 2002). This feature has an approximate width of 20 to 25 km.

A plot of a linear regional gravity trend passing through stations 0 and 200 of the final gravity data is provided in Figure 4(a). Although a linear regional trend may not be the best choice, it is as good a choice as any for this single profile. Figure 4(b) is the residual gravity data after the linear regional trend has been subtracted from the gravity data.

There are several features worth noting along the gravity profile in Figure 4(b). A gravity low centred near 14.5 km has a width of approximately 800 m and a magnitude of 3 to 4 mGal. This feature may be related to a paleochannel associated with Big Creek since the profile is closest to the creek at this location. A broader low with a magnitude of 3 to 4 mGal centred around 21 km has a width of approximately 3 to 4 km. Neither of these local lows appears to be associated with elevation changes (Figure 3).

The gravity low that crosses the entire profile has a magnitude of approximately 35 mGal. Negative gravity anomalies are caused by material of higher density surrounding lower density rocks centred over the negative anomaly. There are an infinite number of models that can fit the gravity data.

One tempting model is to assume a fault-related grabben filled with low-density sedimentary rocks. Figure 5 is an example of such a density model that fits the general shape of the residual gravity anomaly. In this case it is a 3 to 4 km thick, low-density body (0.3 g/cc lower than the surrounding rock) centred over the gravity low. The top of the body in this case is only a few hundred metres below the surface.

Unfortunately a change in volcanic rock type (density) could also cause such a gravity low. Without additional information we cannot be sure of the model.

The total magnetic field data and vertical gradient are also shown in Figure 3. The average value of the total magnetic field is approximately 57 500 nT between stations 0 and 36 (0 and 6 km). There are large variations within the magnetic field (from 52 000 to 60 000 nT) along this same segment of the profile. These large magnetic field values are associated with higher elevation and are likely related to shallow basalt flows. This may explain, at least in part, the tendency towards higher gravity values in that region.

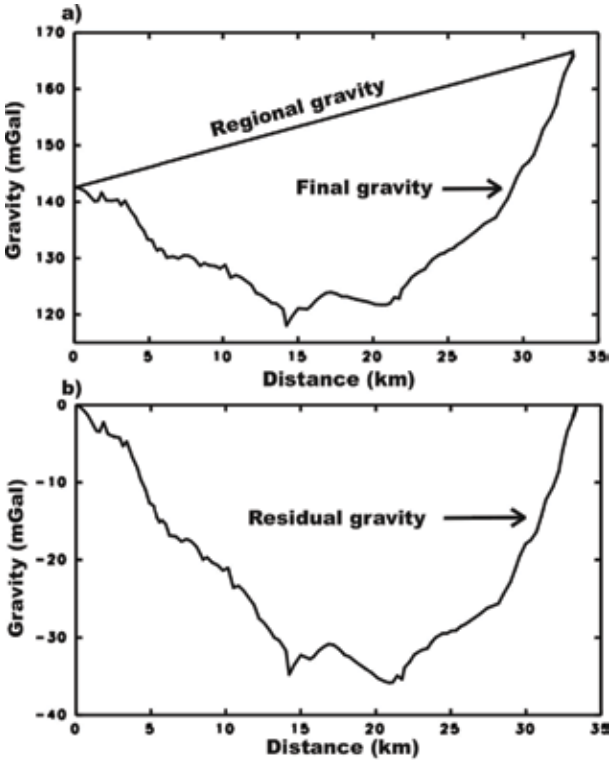

Figure 4. Regional residual gravity separation. a) Bouguer gravity and linear regional gravity. b) Residual gravity (regional minus Bouguer).

The rest of the profile has an average total field value closer to 56 500 nT, with less variation in the magnetic field magnitude. The magnetic features from station 36 to the end of the line at station 200 are therefore likely deeper than the magnetic features between station 0 and station 36. The deeper magnetic features are coincident with the gravity low, which perhaps indicates that sediments may exist above the magnetic basement in this area.

RECOMMENDATIONS FOR FURTHER INTERPRETATION

The qualitative description of the gravity and magnetic profiles presented above is quite limited. However, if the gravity and magnetic profiles are studied in conjunction with regional potential field data, a more detailed interpretation can be provided.

Consequently we recommend integrating the above profiles with regional potential field data (GSC regional aeromagnetic data and the Canadian Hunter regional gravity data) to carry out a preliminary interpretation of the southern portion of the Neshkoro basin, particularly in the vicinity of the regional gravity low.

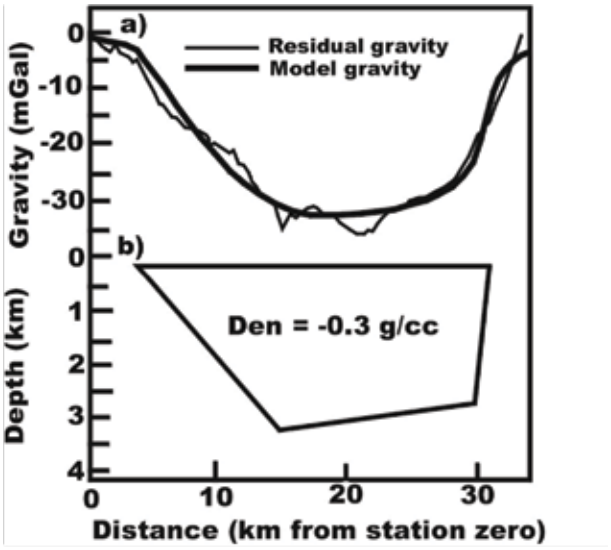

Figure 5. Example of two-dimensional gravity modelling. a) Model versus residual gravity data. b) Depth model assuming a density contrast between the host rock and gravity anomaly of −0.3 g/cc.

In addition to the regional potential field data, the interpretation should incorporate geological information as well as all available well and seismic data. One or more of the Canadian Hunter seismic lines that cross or are close to the regional gravity low should be incorporated into the interpretation (they should be reprocessed first, if the digital data is available). The seismic and well data can be used to provide depth constraints for the quantitative interpretation of the gravity and magnetic data.

REFERENCES

Best, M.E., 2004, Gravity and Magnetic survey, Nechako basin study, acquisition and processing phase: Petroleum Geology Open File 2004-1, British Columbia Ministry of Energy and Mines.

Gabrielse, H., 1991, Structural styles : Chapter 2 in Geology of the Cordilleran Orogen of Canada: H. Gabrielse and C.J. Yorath (ed.): Geological Survey of Canada, no. 4, p. 329-371 (also Geological Society of America, The Geology of North America, v. G-2).

Gabrielse3, H., and Yorath, C.J., 1991, Tectonic synthesis: Chapter18 in Geology of the Cordilleran Orogen of Canada: H. Gabrielse and C.J. Yorath (ed.): Geological Survey of Canada, no. 4, p. 329-371 (also Geological Society of America, The Geology of North America, v. G-2).

Gabrielse, H., Monger, J.W.H., Wheeler, J.O., and Yorath, C.J., 1991, Part A, Morphological belts, tectonic assemblages, and terranes: in Geology of the Cordilleran Orogen of Canada: H. Gabrielse and C.J. Yorath (ed.): Geological Survey of Canada, no. 4, p. 329-371 (also Geological Society of America, The Geology of North America, v. G-2).

Hammer, S., 1939, Terrain corrections for gravimeter stations: Geophysics, 4, 184.

Hannigan, P., Lee, P.J., Osadetz, K.G., Dietrich, J.R., and Olsen-Heise, K., 1994, Oil and gas resource potential of the Nechako-Chilcoten area of British Columbia: Report, Petroleum Resource Subdivision, Geological Survey of Canada.

Robertson, P., 2002, Petroleum exploration potential of the Nechako basin, British Columbia: Petroleum Geology Special Paper 2002-3, British Columbia Ministry of Energy and Mines.

Price. R.A., 1994, Cordilleran tectonics in the evolution of the western Canada sedimentary basin: Chapter 2 in Geolgocial Atlas of the Western Canada Sedimentary Basin, Mossop, G., and Shetsin, I. (eds.), Alberta Research Council and the Canadian Society of Petroleum Geologists, Calgary.

Yorath, C.J., 1991, Upper Jurassic to Paleogene assemblages: Chapter 9 in Geology of the Cordilleran Orogen of Canada: H. Gabrielse and C.J. Yorath (ed.): Geological Survey of Canada, no. 4, p. 329-371 (also Geological Society of America, The Geology of North America, v. G-2).

THERMAL MATURITY IN THE CENTRAL WHITEHORSE TROUGH, NORTHWEST BRITISH COLUMBIA

By J.M. English[1], M. Fowler[2], S.T. Johnston[1], M.G. Mihalynuk[3] and K.L. Wight[1]

KEYWORDS: Whitehorse Trough, Laberge Group, Sinwa Formation, Atlin Lake, Tulsequah, regional geology, organic maturation, programmed pyrolysis, vitrinite reflectance.

INTRODUCTION

The Whitehorse Trough is an early Mesozoic marine sedimentary basin that extends from southern Yukon to Dease Lake in British Columbia. Early studies recognised the potential of the low-grade sedimentary rocks of the Whitehorse Trough to host hydrocarbon accumulations (e.g., Gilmore, 1985; Hannigan et al., 1995; National Energy Board, 2001). These assessments were based on data from samples collected in southern Yukon (Gilmore, 1985; National Energy Board, 2001), and indicate that the region is gas-prone. It is not known if potential hydrocarbon traps were filled and preserved, as none have been drilled. Structural complexity decreases and metamorphic grade is lower in the British Columbia portion of the Whitehorse Trough. On the basis of flat-lying Eocene volcanic rocks of the Sloko Group, no widespread deformation postdates Early Eocene time (Mihalynuk, 1999). Undeformed Middle Jurassic plutons that intrude structures within the Whitehorse Trough in British Columbia constrain deformation to between about 174 and 172 Ma (the age of youngest deformed strata and oldest cross-cutting plutons, respectively; e.g., Mihalynuk et al., 1999; Mihalynuk et al., in press). Such a simple deformation history limits the possibility of post-generation hydrocarbon escape. Previous assessments of source rock potential in British Columbia were based on extrapolation of data from the Yukon portion of the Whitehorse Trough. The objective of this paper is to determine the level of organic maturation and the source rock potential in this portion of the Whitehorse Trough.

GEOLOGICAL BACKGROUND

The Whitehorse Trough is an elongate arc-marginal sedimentary basin and is believed to represent submarine-fan deposition in a forearc basin that received detritus from the Upper Triassic Stuhini and Lower Jurassic Hazelton magmatic arcs to the west and southwest during Upper Triassic to Middle Jurassic time (e.g., Tempelman-Kluit, 1979; Dickie and Hein, 1995; Hart et al., 1995; Johannson et al., 1997; Figure 1); the Stuhini Group is known as the Lewes River Group in Yukon (Wheeler, 1961). The Whitehorse Trough is juxtaposed along the Nahlin Fault with oceanic crustal rocks to the northeast, including thick platformal carbonate and argillaceous chert successions of the northern Cache Creek Terrane. The Laberge Group of the Whitehorse Trough ranges in age from Lower Sinemurian to Middle Bajocian; proximal conglomeratic strata onlap onto Upper Triassic volcanic and carbonate rocks of the Stuhini Group to the south and southwest (e.g., Souther, 1971; Monger et al., 1991). Whitehorse Trough strata within the study area include carbonate rocks of the Upper Triassic Sinwa Formation and interbedded sandstone, siltstone, and argillite of the Lower Jurassic Inklin Formation.

Contraction of the Whitehorse Trough occurred in the Middle Jurassic when the Cache Creek Terrane was emplaced over it during an accretionary event (e.g., Thorstad and Gabrielse, 1986; Mihalynuk, 1999). The timing of this deformational event is constrained by the age of the youngest blueschist in the Cache Creek Terrane (French Range, approximately 174 Ma: Mihalynuk et al., in press) and the age of the oldest post-deformational stitching intrusions (approximately 172 Ma: Mihalynuk et al., 1992; Mihalynuk et al., 2003; Bath, 2003). A Middle Jurassic southwest-vergent fold and thrust belt is developed in the Whitehorse Trough that includes the regional-scale King Salmon Thrust. During this deformation, the Cache Creek Terrane was thrust westward over the Whitehorse Trough and the Stikine arc. During Bajocian time, chert-pebble conglomerates derived from the Cache Creek Terrane were deposited across the Whitehorse Trough and the more southerly Middle-Upper Jurassic Bowser Basin (Ricketts et al., 1992; Mihalynuk et al., in press).

THERMAL MATURITY IN THE CENTRAL WHITEHORSE TROUGH

Systematic sample collection for programmed pyrolysis was undertaken in the central Whitehorse Trough in order to assess the level of organic maturation and source rock potential of this basin. Programmed pyrolysis of whole rock using the Rock-Eval 6 system provides information on the type, maturity, and quantity of associated organic matter (Behar et al., 2001; Lafargue,

[1] *University of Victoria*
[2] *Geological Survey of Canada (Calgary)*
[3] *B.C. Ministry of Energy and Mines*

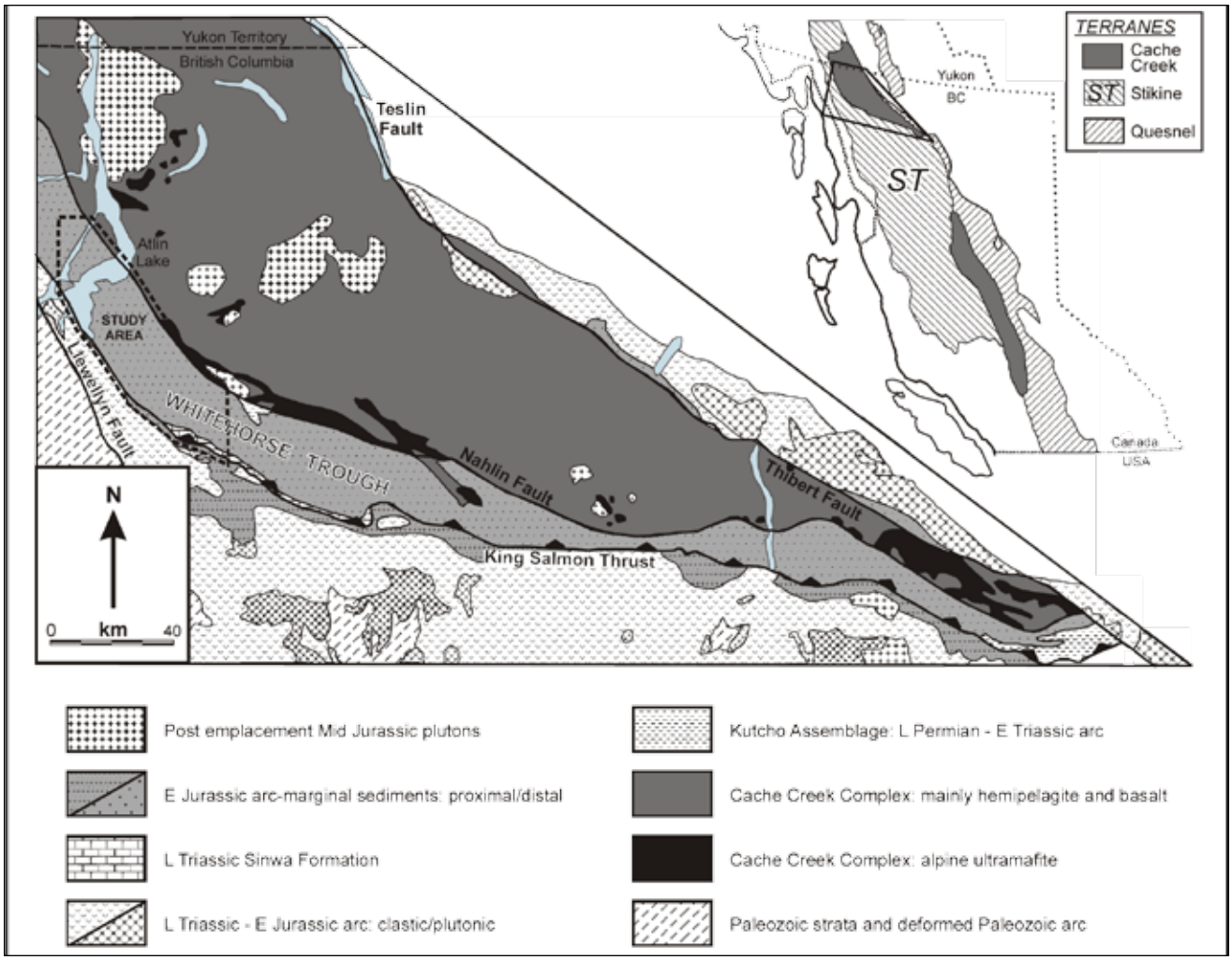

Figure 1. Map of British Columbia showing the distribution of the primary components of the Intermontane Belt in the northern Canadian Cordillera (top right) and a regional geologic map (main). This geology map does not include post-Middle Jurassic rock units. The central Whitehorse Trough study area is outlined by a dashed box.

et al., 1998). Aliquots of sediment samples were dried and powdered for Rock-Eval/TOC analysis at the Geological Survey of Canada, Calgary (GSCC). A Vinci Technologies Rock-Eval 6 instrument was used. Duplicate analyses of samples were carried out to test reproducibility of data. Each sample of about 100 mg of finely ground source rock is put in a furnace at 300°C, raised to 850°C, and then allowed to cool. The hydrocarbons liberated during heating are analysed by a flame ionisation detector, which separates the components into two parameters (Figure 2). The first peak, denoted S1 (mg $_{HC}$/g rock), indicates 'free bitumen' already in the sample. The second peak, denoted S_2 (mg HC/g rock), results from thermal breakdown of kerogen. The Rock-Eval 6 S_3 parameter (mgCO2/g or mg CO/g rock) represents the oxygen-bearing compounds released at the same time as the S_1 peak added to that obtained between 300° and 400°, as measured by an infrared cell. The temperature corresponding to the maximum of the S_2 peak (T_{max}) is an indicator of source rock maturity, although this value is only reliable when S_2 is greater than 0.2 (Peters, 1986) and is also affected by organic matter type. An indication of source rock richness is given by the sum of the first two peaks ($S_1 + S_2$). Other parameters determined include the

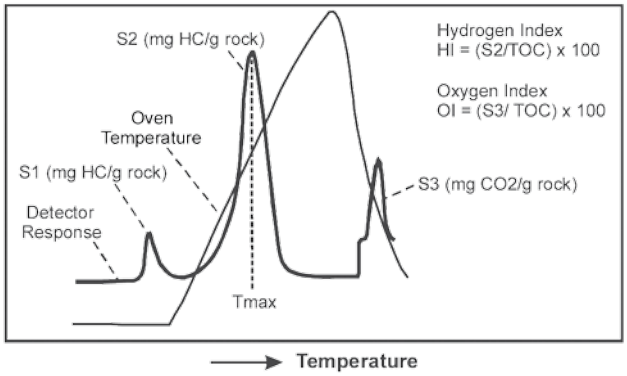

Figure 2. Schematic pyrogram illustrating the liberation of hydrocarbon during heating of the rock sample. Determined parameters include S_1, S_2, S_3, T_{max}, and the hydrogen and oxygen indices.

hydrogen index (S_2/TOC) and the oxygen index (S_3/TOC); these parameters are used to determine the type of organic matter present in a low maturity potential source rock.

The complete Rock-Eval pyrolysis dataset may be obtained at the British Columbia Geological Survey (BCGS) website (Fowler, 2004). Source rocks with total organic carbon (TOC) contents of 0% to 0.5%, 0.5% to 1%, 1% to 2%, and greater than 2% are considered poor, fair, good, and very good, respectively (Peters, 1986). Using this classification, most samples, including all samples from the Sinwa Formation, are classified as poor to fair source rocks, with 22% classified as good, and 8% classified as very good (Figure 3). The good and very good source rocks within the Inklin Formation appear to occur dominantly in Pliensbachian successions.

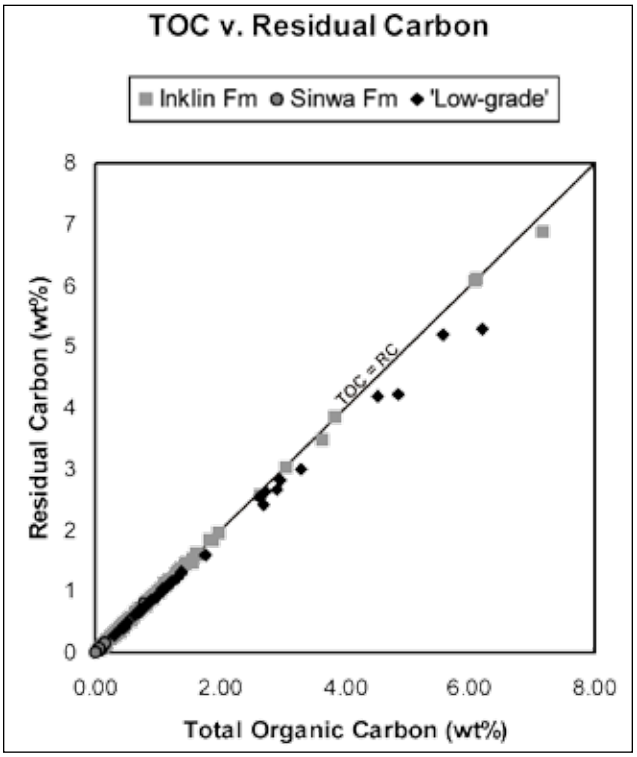

Figure 3. Plot of total organic carbon (TOC) versus residual carbon for samples from the central Whitehorse Trough. 'Low-grade' samples form a subset of the Inklin Formation samples, for which S_2 > 0.2 and T_{max} < 480°C.

However, most authors now believe that a TOC content of greater than 1% and likely a minimum of 2% is needed for the generation and expulsion of liquid hydrocarbons (Hunt, 1996; Meyer and Nederlof, 1984; Peters and Moldowan, 1993; Thomas and Clouse, 1990). Thus, few of the Whitehorse Trough samples are likely to have been oil-prone source rocks. TOC is almost equal to residual carbon in the majority of samples (Figure 3), indicating that there is little generative potential left in these rocks. Therefore, depending on organic matter type in these samples originally, they may have had much higher initial TOC contents. Consequently, samples presently having a TOC content of at least 1% could have been hydrocarbon source rocks assuming they originally contain oil-prone Type I or II organic matter.

The organic matter type in a source rock can be determined by plotting hydrogen index against the oxygen index (Espitalié et al., 1977; Figure 4). None of the potential source rocks sampled in the central Whitehorse Trough are oil prone; the majority are inert (low hydrogen index) due to the lack of generative potential, while the rest are gas prone (Figure 4). The lack of generative potential is mostly a function of high thermal maturity. From a spatial standpoint, samples that are gas prone and have generative potential are from the northeastern flank of the central Whitehorse Trough. This belt of rock is interpreted to represent the structurally and stratigraphically highest units within the Laberge Group in this region and is interpreted to continue northeast beneath the structurally overlying Cache Creek Terrane.

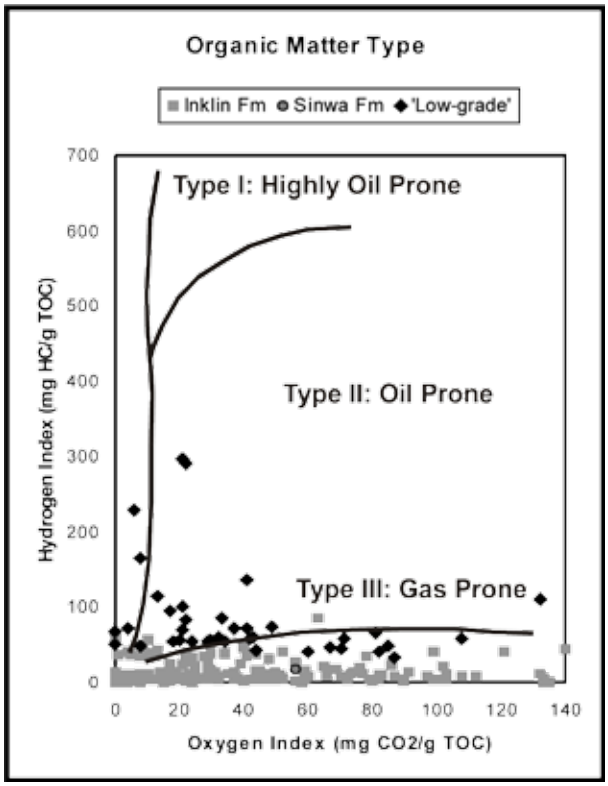

Figure 4. Plot of hydrogen index versus oxygen index for samples from the central Whitehorse Trough. 'Low-grade' samples form a subset of the Inklin Formation samples, for which S_2 > 0.2 and T_{max} < 480°C. The organic matter type in a source rock can be determined from this plot (Espitalié et al., 1977).

Tmax can be used as an indicator of thermal maturation as long as S_2 is greater than 0.2. Unfortunately, for the majority of samples, this qualifier rules out the interpretation of the pyrolysis data for maturation purposes. Once again, qualifying samples tend to come from the northeastern flank of the Whitehorse Trough, and these samples are within the oil and gas windows (Figure 5). Although T_{max} values of samples with S_2 less than 0.2 must be viewed cautiously, it can be graphically shown that most samples from the southwestern flank of the Whitehorse Trough are overmature (Figure 5). Distribution of mature and overmature areas of the central Whitehorse Trough can been seen by contouring Tmax values (Figure 6) and is consistent with limited available vitrinite reflectance data (Table 1).

The vitrinite reflectance values suggest that potential source rocks along the northeastern flank of the central Whitehorse Trough are almost immature. If these vitrinite reflectance data are accurate, this may imply that there was little hydrocarbon potential in the basin even originally, as these 'low maturity' samples have low hydrogen index values. Higher levels of organic maturation along the southwestern flank of the central Whitehorse Trough may reflect increased structural burial of these strata or contact metamorphism during Eocene magmatism.

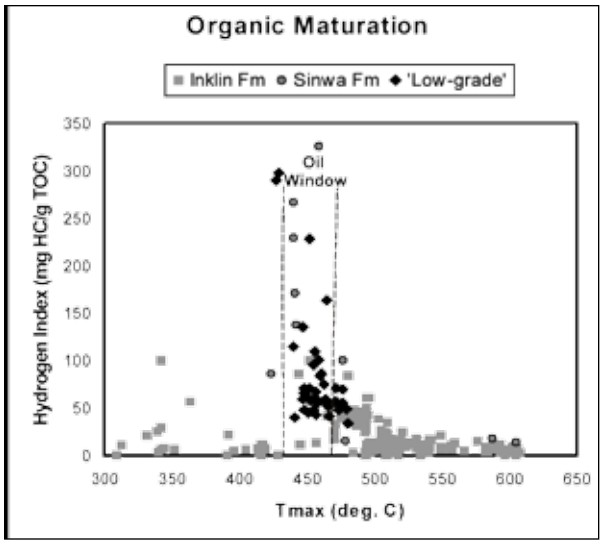

Figure 5. Plot of hydrogen index versus T_{max} for samples from the central Whitehorse Trough. 'Low-grade' samples form a subset of the Inklin Formation samples, for which S_2 > 0.2 and T_{max} < 480°C. Due to low S_2 values, T_{max} values for the majority of other Inklin Formation samples are suspect and are dominantly overmature.

TABLE 1. VITRINITE REFLECTANCE DATA FROM THE ATLIN AREA, NW BRITISH COLUMBIA.

Sample Number	Age	NAD	Easting	Northing	$R_o$max
GGAJ-92-59-2T	Late Pliensbachian	27	571625	6578475	0.6
GGAJ-92-56-T	Early Pliensbachian	27	568200	6576600	0.85
GGAJ-92-184-T	Early Pliensbachian	27	568575	6575975	0.85
GGAJ-92-119-T	Late Sinemurian	27	566725	6559450	1.45
GGAJ-92-177-T	Early Sinemurian	27	562950	6576175	1.54
GGAJ-92-45-T	Early? Sinemurian	27	566300	6574850	1.62
ABA02-13-1	na	83	602818	6543186	1.45
FCO02-1-2c	na	83	605002	6540947	2.36
JEN02-5-7	na	83	588036	6557555	0.85
JEN02-6-2a	na	83	588883	6557054	0.98
JEN02-19-9e	na	83	590287	6547881	1.87
LLE02-10-7	na	83	586892	6546875	1.79
MMI02-6-1-1	na	83	588017	6552900	1.07
MMI02-7-5-2	na	83	588090	6551600	1.65
MMI02-19-4-6	na	83	593505	6549108	2.05
MMI02-20-6	na	83	593040	6546960	1.79
ORO02-6-1c	na	83	589770	6555472	0.92
STJ02-3-3a	na	83	591257	6553403	1.05

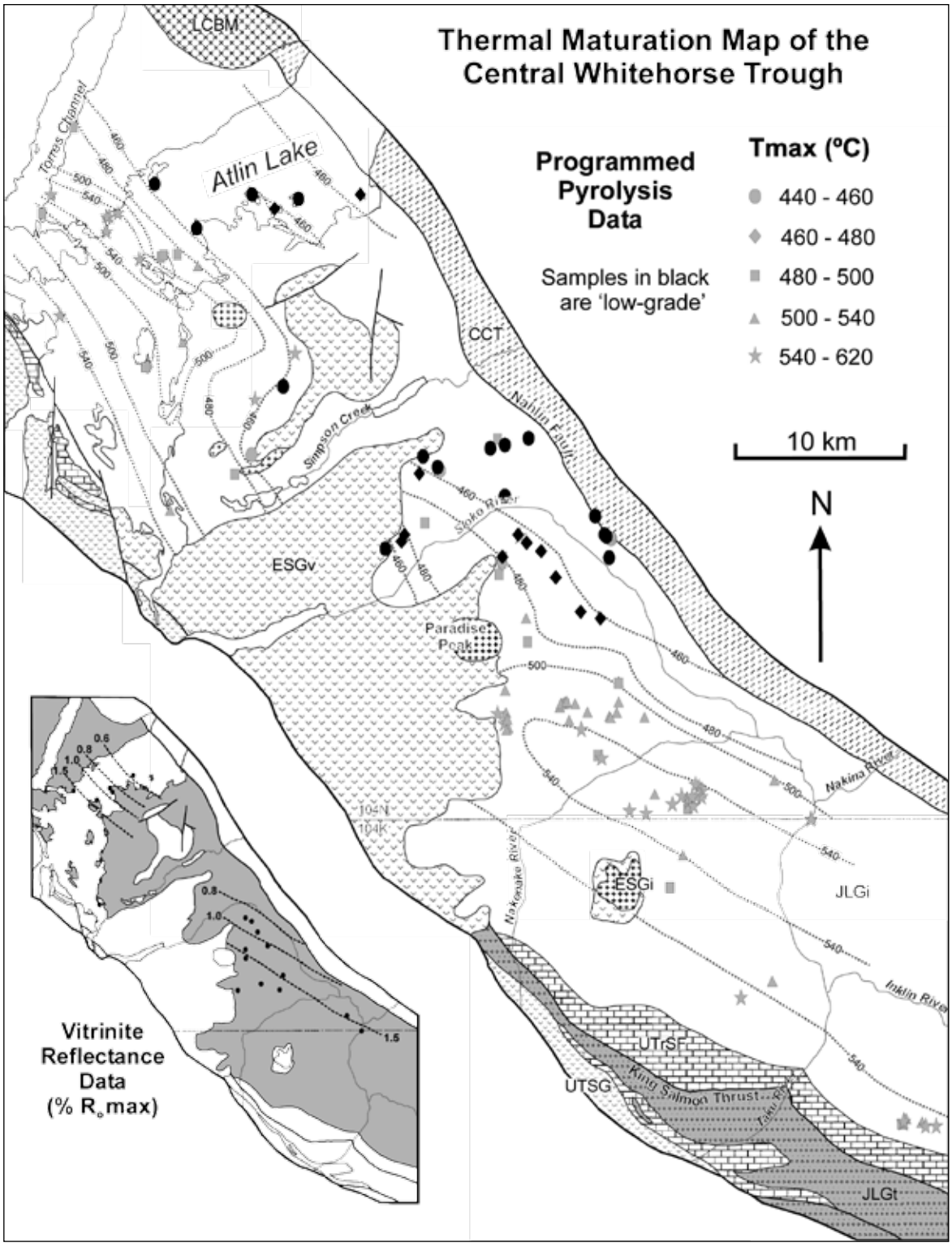

Figure 6. Contoured thermal maturation map for the central Whitehorse Trough based on T_{max} values. Note: T_{max} values are poorly constrained for relatively 'high-grade' samples due to the low (< 0.2) S_2 values; despite this, all samples with S_2 values > 0.03 were plotted as a crude representation of maturation levels in the region. Vitrinite reflectance data shown in Table 1. Abbreviations: CCT – Cache Creek Terrane; ESGi – Eocene Sloko Group intrusions; ESGv – Eocene Sloko Group volcanics; JLGi – Jurassic Laberge Group Inklin Formation; JLGt – Jurassic Laberge Group Takwahoni Formation; LCBM – Late Cretaceous Birch Mountain pluton; UTrSF – Upper Triassic Sinwa Formation; UTSG – Upper Triassic Stuhini Group.

SUMMARY

The Whitehorse Trough is an early Mesozoic marine sedimentary basin that extends from southern Yukon to Dease Lake in British Columbia. Strata within the central Whitehorse Trough include carbonate rocks of the Upper Triassic Sinwa Formation and interbedded sandstone, siltstone, and argillite of the Lower Jurassic Inklin Formation. Programmed pyrolysis data indicate that potential source rocks in the Inklin Formation are gas prone and are within the oil and gas windows along the northeastern flank of the central Whitehorse Trough.

ACKNOWLEDGEMENTS

This research was funded by a University of Victoria Fellowship to J. English, an NSERC Discovery Grant to S.T. Johnston, an NSERC Undergraduate Student Research Award to K. Wight, and by the Geological Survey of Canada and the British Columbia Ministry of Energy and Mines. Thanks to the rest of the bedrock geology mappers who worked in the Whitehorse Trough as part of this project: Fabrice Cordey, Lucinda Leonard, Adam Bath, Lee Ferreira, Jacqueline Blackwell, Fionnuala Devine, and Oliver Roenitz. Thanks to Lucinda Leonard for assistance in drafting figures. Thanks also to Norm Graham at Discovery Helicopters for logistical assistance. Figure 6 was prepared with the GMT software (Wessel and Smith, 1995).

REFERENCES

Bath, A. (2003): Atlin TGI, Part IV: Middle Jurassic granitic plutons within the Cache Creek terrane and their aureoles: Implications for terrane emplacement and deformation; in Geological Fieldwork 2002: B.C. Ministry of Energy and Mines, Paper 2003-1, pages 51-55.

Behar, F., Beaumont, V. and Penteado, H. L. D. B. (2001): Rock-Eval 6 Technology: Performances and Developments; Oil & Gas Science and Technology, Volume 56, pages 111-134.

Dickie, J. R. and Hein, F. J. (1995): Conglomeratic fan deltas and submarine fans of the Jurassic Laberge Grup, Whitehorse Trough, Yukon Territory, Canada: fore-arc sedimentation and unroofing of a volcanic island arc complex; Sedimentary Geology, Volume 98, pages 263-292.

Espitalié, J., Madec, M., Tissot, B., Mennig, J. J. and Leplat, P. (1977): Source rock characterisation method for petroleum exploration; Proceedings of the 9th Annual Offshore Technology Conference, Volume 4, pages 439-448.

Fowler, M. (2004): Rock-Eval VI analysis of samples from the central Whitehorse Trough; Energy-Resource Development and Geoscience Branch, B.C. Ministry of Energy and Mines, Petroleum Geology Open File 2004-2.

Gabrielse, H. (1998): Geology of Cry Lake and Dease Lake map areas, north-central British Columbia; Geological Survey of Canada, Bulletin 504, 147 pages.

Gilmore, R. G. (1985): Whitehorse field party; unpublished report; Petro-Canada, 16 pages.

Hannigan, P., Lee, P. J. and Osadetz, K. G. (1995): Oil and gas potential of the Bowser - Whitehorse area of British Columbia; unpublished report; *Institute of Sedimentary and Petroleum Geology*, 47 pages plus appendices.

Hart, C. J. R., Dickie, J. R., Ghosh, D. K. and Armstrong, R. L. (1995): Provenance constraints for Whitehorse Trough conglomerate: U-Pb zircon dates and initial Sr ratios of granitic clasts in Jurassic Laberge Group, Yukon Territory; in Jurassic magmatism and tectonics of the North American Cordillera, Miller, D. M. and Busby, C., Boulder, Colorado, Geological Society of America, Special Paper 299, pages 47-63.

Hunt, J. M. (1996): Petroleum Geochemistry and Geology; W.H. Freeman and Company, New York, 743 pages.

Johannson, G. G., Smith, P. L. and Gordey, S. P. (1997): Early Jurassic evolution of the northern Stikinian arc: evidence from the Laberge Group, northwestern British Columbia; *Canadian Journal of Earth Sciences*, Volume 34, pages 1030-1057.

Lafargue, E., Marquis, F. and Pillot, D. (1998): Rock-Eval 6 applications in hydrocarbon exploration, production and soils contamination studies; *Oil & Gas Science and Technology*, Volume 53, pages 421-437.

Meyer, B. L. and Nederlof, M. H. (1984): Identification of source rocks on wire-line logs by density/resistivity and sonic transit time/resistivity crossplots; *American Association of Petroleum Geologists Bulletin*, Volume 68, pages 121-129.

Mihalynuk, M. G. (1999): Geology and mineral resources of the Tagish Lake area (NTS 104M/8, 9, 10E, 15 and 104N/12W) northwestern British Columbia; *B.C. Ministry of Energy, Mines and Petroleum Resources*, Bulletin 105, 217 pages.

Mihalynuk, M. G., Erdmer, P., Ghent, E. D., Archibald, D. A., Friedman, R. M., Cordey, F., Johannson, G. G. and Beanish, J. (1999): Age constraints for emplacement of the northern Cache Creek terrane and implications of blueschist metamorphism; *in* Geological Fieldwork 1998, *B.C. Ministry of Energy, Mines and Petroleum Resources*, Paper 1999-1, pages 127-141.

Mihalynuk, M. G., Erdmer, P., Ghent, E. D., Cordey, F., Archibald, D., Friedman, R. M. and Johannson, G. G. (in press): Subduction to obduction of coherent French Range blueschist - In less than 2.5 Myrs?; *Geological Society of America Bulletin*.

Mihalynuk, M. G., Johnston, S. T., English, J. M., Cordey, F., Villeneuve, M. E., Rui, L. and Orchard, M. J. (2003): Atlin TGI, Part II: Regional geology and mineralization of the Nakina area (NTS 104N/2W and 3); *in* Geological Fieldwork 2002, *B.C. Ministry of Energy and Mines*, Paper 2003-1, pages 9-37.

Mihalynuk, M. G., Smith, M. T., Gabites, J. E., Runkle, D. and Lefebure, D. (1992): Age of emplacement and basement character of the Cache Creek terrane as constrained by new isotopic and geochemical data; *Canadian Journal of Earth Sciences*, Volume 29, pages 2463-2477.

Monger, J. W. H., Wheeler, J. O., Tipper, H. W., Gabrielse, H., Harms, T., Struik, L. C., Campbell, R. B., Dodds, C. J., Gehrels, G. E. and O'Brien, J. (1991): Upper Devonian to Middle Jurassic assemblages - Part B. Cordilleran terranes; *in* Geology of the Cordilleran Orogen in Canada, The Geology of North America, Gabrielse, H. and Yorath, C. J., Denver, Colorado, *Geological Society of America*, pages 281-327.

National Energy Board (2001): Petroleum resource assessment of the Whitehorse Trough, Yukon Territory, Canada; *Yukon Energy Resources Branch*, 50 pages.

Peters, K. E. (1986): Guidelines for evaluating petroleum source rock using programmed pyrolysis; *The American Association of Petroleum Geologists Bulletin*, Volume 70, pages 318-329.

Peters, K. E. and Moldowan, J. M. (1993): The Biomarker Guide; Prentice-Hall, Eaglewood Cliffs, New Jersey, 363 pages.

Ricketts, B. D., Evenchick, C. A., Anderson, R. G. and Murphy, D. C. (1992): Bowser basin, northern British Columbia : Constraints on the timing of initial subsidence and Stikinia - North America terrane interactions; Geology, Volume 20, pages 1119-1122.

Souther, J. G. (1971): Geology and mineral deposits of Tulsequah map-area, British Columbia; Geological Survey of Canada, Memoir 362, 84 pages.

Tempelman-Kluit, D. J. (1979): Transported cataclasite, ophiolite and granodiorite in Yukon : evidence of arc-continent collision; Geological Survey of Canada, Paper 79-14, 27 pages.

Thomas, M. M. and Clouse, J. A. (1990): Primary migration by diffusion through kerogen: II. Hydrocarbon diffusivities in kerogen; Geochimica et Cosmochimica Acta, Volume 54, pages 2781-2792.

Thorstad, L. E. and Gabrielse, H. (1986): The Upper Triassic Kutcho Formation, Cassiar Mountains, north-central British Columbia; Geological Survey of Canada, Paper 86-16, 53 pages.

Wessel, P. and Smith, W. H. F. (1995): New version of the Generic Mapping Tools released; Eos, Volume F359.

Wheeler, J. O. (1961): Whitehorse map-area, Yukon Territory (105D); Geological Survey of Canada, Memoir 312, 156 pages.

PETROLEUM SOURCE ROCK POTENTIAL OF LOWER TO MIDDLE JURASSIC CLASTICS, INTERMONTANE BASINS, BRITISH COLUMBIA

Filippo Ferri
Resource Development and Geoscience Branch, BC Ministry of Energy and Mines,
6th Flr-1810 Blanshard St., Victoria, BC, Canada, V8W 9N3

Kirk Osadetz
Geological Survey of Canada: Calgary, 3303 33 St. NW, Calgary, AB, Canada, T2L 2A7

Carol Evenchick
Geological Survey of Canada: Pacific, 101-605 Robson St. Vancouver, BC, Canada, V6B 5J3

KEYWORDS: petroleum source rocks, petroleum, crude oil, natural gas, Bowser Basin, Quesnel Trough, Nechako Basin, Sustut Basin, Intermontane, Interior Basins, Canadian Cordillera, Jurassic

INTRODUCTION

The presence of suitable petroleum source rocks is a necessary condition for the presence of an effective total petroleum system, which constrains the petroleum potential of under-explored basins such as those within the Intermontane region of British Columbia (Curiale, 1994). Hayes (2002), in his report on the crude oil and natural gas potential of the Nechako Basin of British Columbia, indicated that a major issue for the basin was the lack of recognition of a good petroleum source rock horizon. This perception is applicable to all the Intermontane basins due to the limited amount of crude oil and natural gas exploration activity and a subsequent lack of relevant information.

This paper summarizes some of our current understanding of Early and Middle Jurassic stratigraphy within parts of the Intermontane region of the Canadian Cordillera that may have petroleum source rock potential. It also provides an update on the activities undertaken by the Resource Development and Geoscience Branch (RDGB) of the British Columbia Ministry of Energy and Mines to address the issue through recognition and basic characterization of potential source bed horizons within the Intermontane region. This is part of a much larger collaborative program, which began in 2001, between the Geological Survey of Canada (GSC) and the RDGB to look at energy-related aspects of the Intermontane Basins. The RDGB is also collaborating with the GSC on a new, multiyear initiative, which started in 2003, entitled "Integrated Petroleum Resource Potential and Geoscience Studies of the Bowser and Sustut Basins".

Subsurface characterization of potential Cretaceous and Tertiary petroleum source rocks within the Nechako area has been documented by Hunt (1992) and Hunt and Bustin (1997). Osadetz et al. (2003) obtained Rock-Eval pyrolytic and total organic content (TOC) data for well cuttings from all bore holes within the Nechako and Bowser Basins. Evenchick et al. (2003) reported bleeding crude oil from paleomagnetic coring operations in fine-grained clastics that may be either migrated petroleum or residual crude oil stains in potential petroleum source rocks. The purpose of the present study was to sample potential source-bed horizons of Early and Middle Jurassic age in areas where subsurface data is lacking. In addition, the following brief summary on the extent of potential source-bed horizons of this age within certain parts of the Canadian Cordillera indicates these units are potentially regionally distributed.

The author, as part of the regional mapping program examining Bowser Lake and Sustut Group rocks within the western portion of the McConnell Creek map area (NTS 094D; see Evenchick et al., 2003), sampled potential petroleum source rock horizons in this area (Figures 1 and 2). In addition, one week was spent examining possible source beds on the east side of the Nechako area within the Quesnel Trough (Figures 1, 3, and 4). Twenty-five samples were collected in the McConnell Creek area, and 12 samples were taken from the Quesnel Trough. Further sampling is planned in both regions during the 2004 field season.

Current research in the Bowser Basin has recognized crude oil staining in surface and subsurface samples of the Bowser and Sustut Groups (Osadetz *et al.,* 2004, 2003; Evenchick *et al.*, 2003). The data suggest the presence of at least 3 source-bed horizons, one of Jurassic to Cretaceous age, another within carbonate sequences of Paleozoic age, and a third of fresh-water origin. Data in this paper, in part, reviews sampling undertaken in the field in an attempt to locate the stratigraphic horizons responsible for the staining.

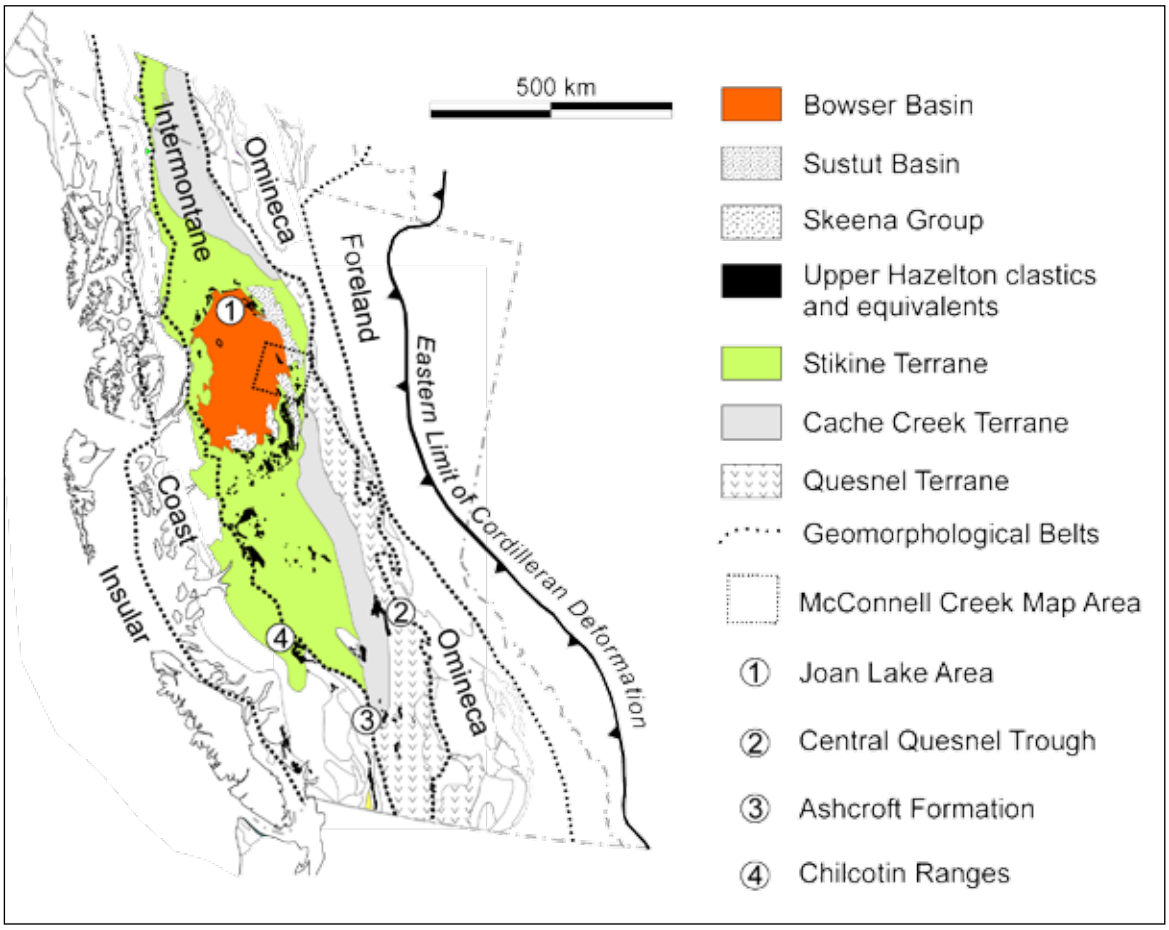

Figure 1. Geomorphological belts of the Canadian Cordillera together with selected terranes and locations of areas mentioned in text or shown in subsequent diagrams. The regional distribution of Early to Middle Jurassic clastics is also indicated. Base map modified from Osadetz et al., 2003.

In Bowser-Sustut and Quesnel Trough areas, the focus of sampling was within black carbonaceous sequences of Early to Middle Jurassic age, which are believed to underlie coarser clastic units of the basins. This stratigraphic interval encompasses the Toarcian-Aalenian time period, which on a worldwide scale is inferred to record an interval of anoxic water conditions resulting in enhanced preservation of accumulated organic material (Jenkyns, 1988).

Worldwide oceanic anoxic events are documented at several stratigraphic levels within Jurassic and Cretaceous sedimentary rocks. In addition to the Toarcian, these include intervals within the Aptian-Albian, Cenomanian-Turonian, and Santonian ages (Jenkyns, 1980, 1988). Most of these time periods are well represented within the Western Canada Sedimentary Basin and have contributed a large proportion of the petroleum within known pools (e.g., First and Second White Speckled Shale, Base of Fish Scales zone, and Fernie Formation; see Creaney et al., 1994).

BOWSER AND SUSTUT BASINS

The Bowser and Sustut Basins are overlap assemblages deposited on an allochthonous terrane of the Canadian Cordillera. Located in north-central British Columbia, they are found within the northern part of the Intermontane Belt and sit on Devonian to Jurassic rocks of Stikinia (Figure 1).

There are 3 main successions within these basins: the Middle Jurassic to mid-Cretaceous Bowser Lake Group, the Lower to mid-Cretaceous Skeena Group, and the mid- to Upper Cretaceous Sustut Group. Bowser Lake strata represent a southwestward-prograding delta to distal submarine fan sequence and contain marine to nonmarine sediments (Evenchick et al., 2001). Skeena rocks, located along the southern part of Bowser Basin, are inferred to have been deposited in marine to nonmarine deltaic environments, but their relationship to Bowser Lake stratigraphy is uncertain (Tipper and Richards, 1976). The Sustut Group is inferred to have been deposited in fluvial to lacustrine environments (Eisbacher, 1974) that existed in a foreland basin east of deforming Bowser Lake strata (Evenchick and Thorkelson, in press).

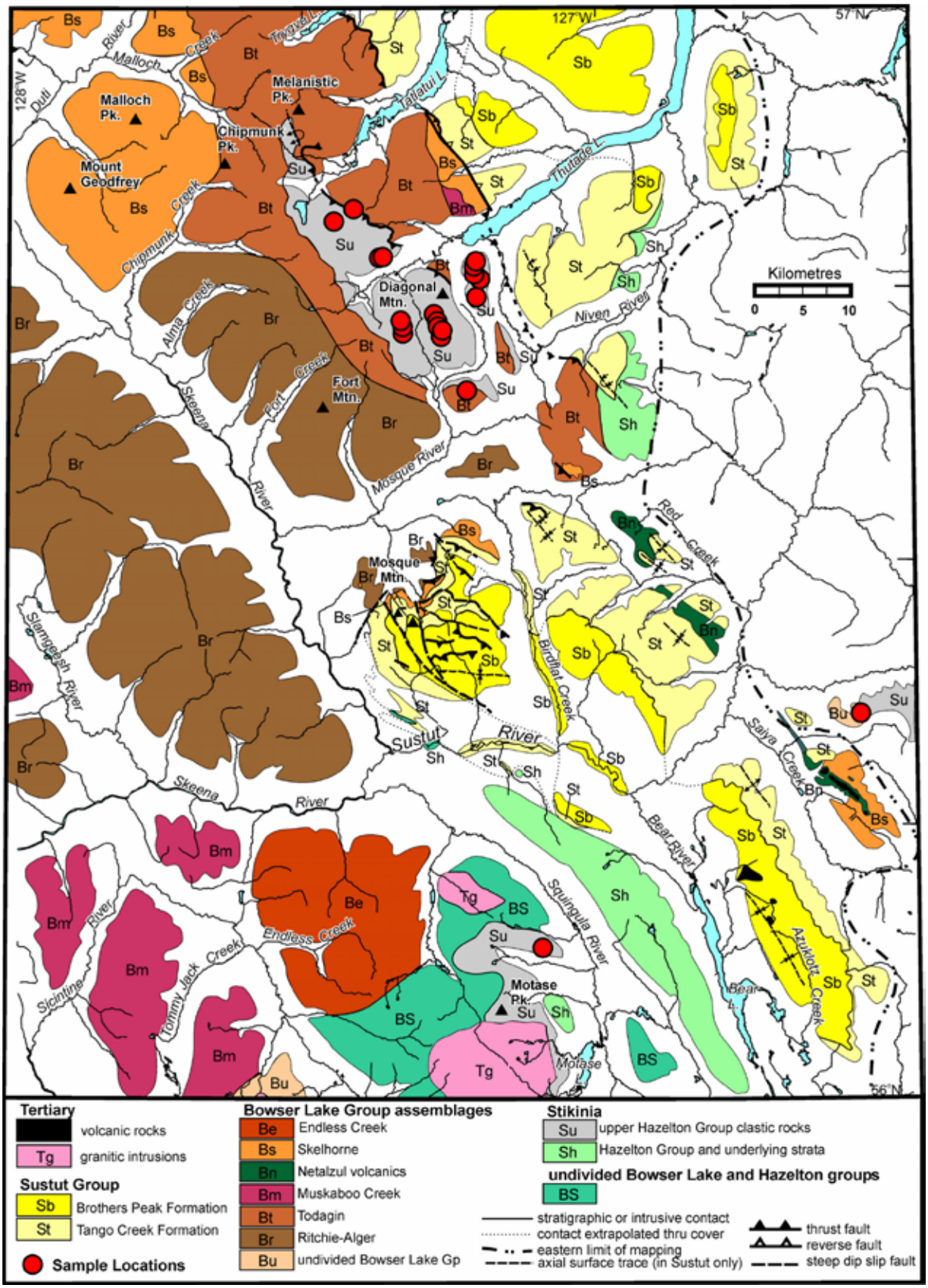

Figure 2. Generalized geology of the McConnell Creek map area, showing sample locations. Modified from Evenchick et al., 2003.

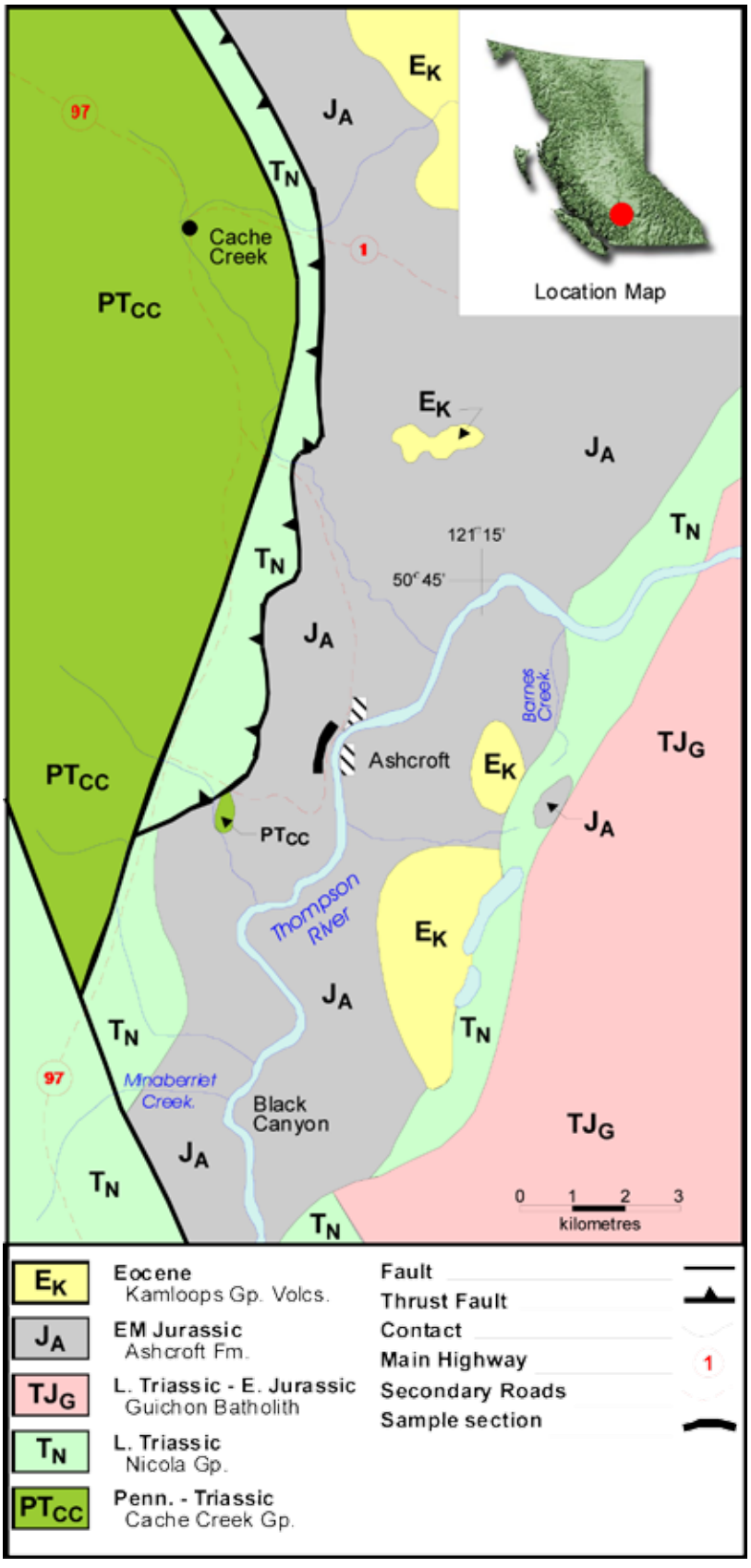

Figure 3. Generalized geology map of the Ashcroft area, showing extent of Ashcroft Formation and sample locations. Modified from Travers, 1978.

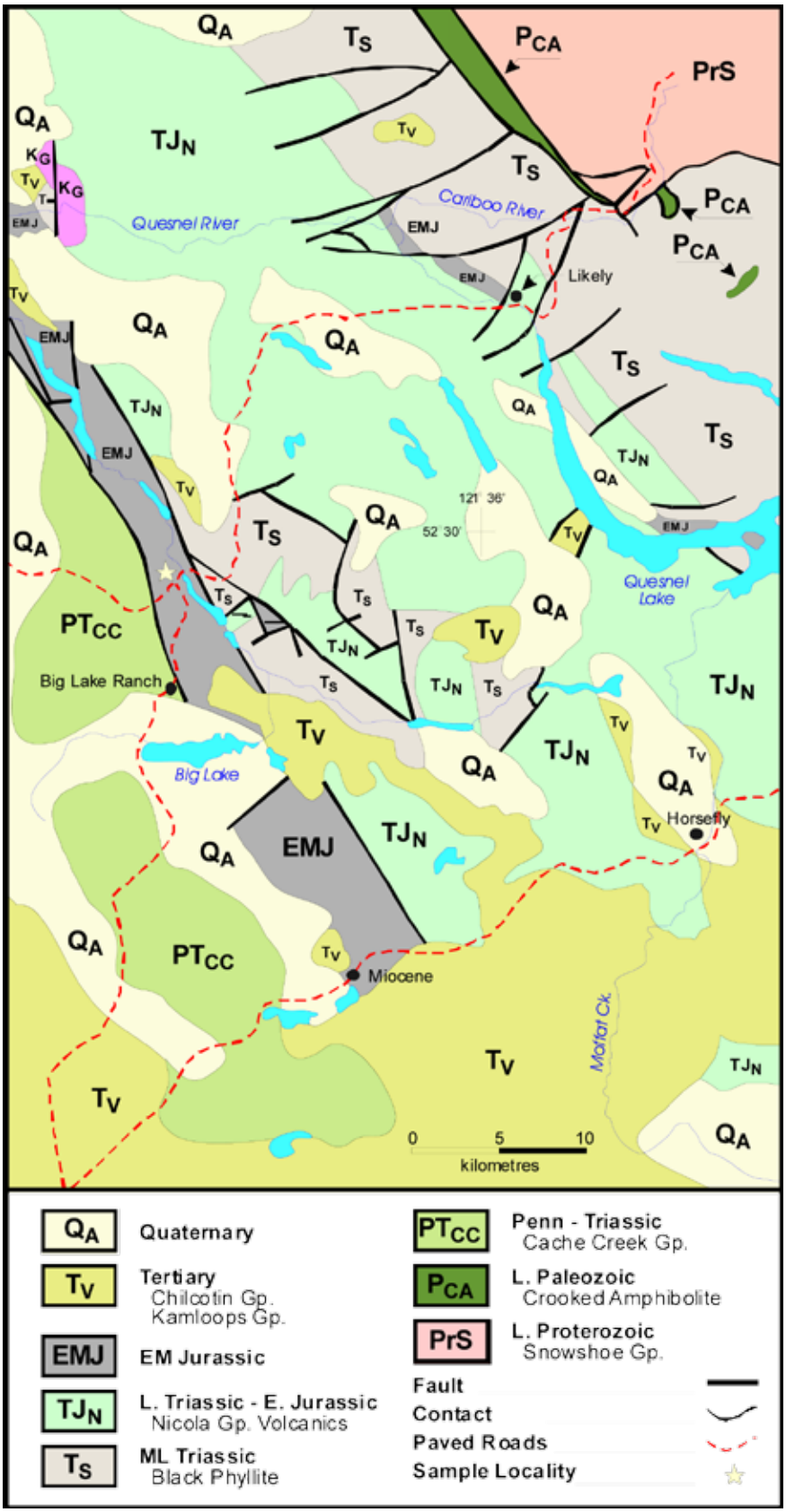

Figure 4. Generalized geology of Quesnel Terrane west of Quesnel Lake, showing sample location and distribution of Early to Middle Jurassic clastics.

Bowser, Skeena, Sustut, and underlying Stikinia rocks are deformed into dominantly northwest-trending fold and thrust structures comprising the Skeena Fold Belt (Evenchick, 1991). Evenchick (1991) demonstrated that this thin-skinned structural belt of mid-Cretaceous age contains a well-developed triangle zone at its northeastern margin within Sustut strata.

Potential Source Beds

In the area of the Bowser and Sustut Basins, black organic-rich shales have been recognized within the Lower to Middle Jurassic sediments of the upper Hazelton Group (Thomson et al., 1986). In addition, slope and submarine fan facies of the Bowser Lake Group contain abundant sections of black shale that may have elevated organic contents.

Effective Mesozoic and Paleozoic petroleum source rocks are postulated based on analysis of crude oil stains from surface and subsurface samples of Bowser and Sustut lithologies (Evenchick *et al.*, 2003; Osadetz *et al.*, 2003, 2004). Indirect confirmation of a Paleozoic source horizon is indicated by crude oil staining in cored paleomagnetic samples taken from Permian and Triassic sequences (Evenchick *et al.*, 2003). Stikine Assemblage strata contain black carbonaceous sequences of Devonian-Mississippian age (Logan *et al.*, 2000) similar in composition to other time-equivalent sequences throughout Cordilleran terranes and within the miogeocline (e.g., Exshaw and Bakken Formations).

HAZELTON GROUP

Strata of the Bowser Lake Group overlie fine-grained clastic sedimentary rocks of the upper Hazelton Group (Figure 2). This latter succession is dominantly a volcanic sequence of broadly Early to Middle Jurassic age (Tipper and Richards, 1976). Although upper Hazelton clastics are well developed below the Bowser Lake Group, these rocks locally grade into dominantly volcanic sequences.

Terminology of the Hazelton Group varies along the basin margins. In the northwestern part of the basin, upper clastics are termed the Spatsizi Formation (Evenchick and Thorkelson, in press) whereas further west, in the Eskay Creek and Forrest Kerr areas, this horizon contains 3 facies with varying proportions of volcanic rocks and is referred to as the Salmon River Formation (Anderson, 1993; Logan et al., 2000). In southern Bowser Basin, Tipper and Richards (1976) subdivided upper Hazelton clastics into the Nilkitkwa and Smithers Formations.

Upper Hazelton Group clastic rocks span Early Pliensbachian to Bajocian-Bathonian times in the northern Bowser Basin (Thomson, et al., 1986; Evenchick et al., 2001). Volcanic rocks become increasingly voluminous northward in Spatsizi River map area (Thomson et al., 1986). There, upper Hazelton Group rocks have been formally assigned to the Spatsizi Formation (Evenchick and Thorkelson, in press). In the Joan Lake area of this map region, Thomson et al. (1986) initially assigned these rocks to group status and defined the Joan, Wolf Den, Melisson, Abou, and Quock Formations. Although subdivision of this horizon is possible in the Joan Lake area, Evenchick and Thorkelson (ibid.) suggested this succession be lowered to formation status (and the constituent formations to members) because it was difficult to recognize all units on a regional scale, and strata in similar stratigraphic positions around the Bowser Basin are formations in the Hazelton Group.

In the Joan Lake area, Upper Pliensbachian to Middle Toarcian Wolf Den and Aalenian Abou Members are dominanted by black to dark grey shales which, together with their faunal assemblages, suggest anoxic water conditions (Thomson et al., 1986). The Bajocian Quock Member, with its distinctive sections of interlayered black siliceous carbonaceous siltstone, shale, and light-coloured ash tuff ("pyjama beds"), are also inferred to have been deposited in anaerobic conditions. Thomson et al. (ibid.) describe parts of these lithologies as containing up to 20% organic material. The authors speculated this horizon would have acted as an excellent petroleum source rock and noted its well-placed stratigraphic position at the base of the Bowser Lake sequence.

Although the members of the Spatsizi Formation in the Joan Lake area may represent a restrictive facies of the upper Hazelton Group, the overall basinal, anoxic conditions (as inferred for upper Hazelton clastics around the margins of the Bowser Basin and within structural windows or culminations) suggests that these organic-rich lithologies may underlie much of the basin (Thomson et al., 1986).

MCCONNELL CREEK MAP AREA (094D)

The author spent approximately 5 weeks in the western and central parts of the McConnell Creek map area as part of a provincial-federal cooperative regional mapping program (Evenchick et al., 2003). During this time, sections of the upper Hazelton Group were examined and sampled in the Diagonal Mountain and Motasse Peak areas for characterization of organic content. In addition, parts of the lower Bowser Lake Group together with black siltstone or shales in the Ritchie-Alger and Todagin assemblages were also sampled.

Upper Hazelton rocks in this area have been previously described by Tipper and Richards (1976), Jeletzky (1976), Evenchick and Porter (1993), Jakobs (1993), and Evenchick et al. (2003). The largest area covered by these rocks in the western McConnell Creek map sheet is roughly centred on Diagonal Mountain. The total thickness of the

upper Hazelton Group is difficult to determine as the base is not exposed; however, the exposed section is conservatively in the order of 300 m thick. The dominant lithology is variably cleaved, rusty- to orange-weathering, blocky, dark grey to black siliceous siltstones and shales with variable proportions of thin bedded white to pinkish tuff (Photo 1). These tuffaceous lithologies comprise the typical Toarcian to Bajocian sections of the upper Hazelton Group seen around the Bowser Basin and are informally referred to as the "pyjama beds". The amount of tuff is variable within sections exposed in the Diagonal Mountain area, but is usually less than 30% of the section where present. Tuff varies from less than 1 mm to 10 cm thick and, although usually homogenous, can display graded bedding or ripple marks. Parts of the sequence are composed almost entirely of dark grey to black, platy siltstone or shale. Some sections are blue-grey in colour and quite carbonaceous.

Minor lithologies include light grey- to grey-weathering calcareous siltstone exhibiting a dark grey-brown colour on fresh surface and brown to grey-brown weathering, grey micritic to clastic limestone up to 30 cm thick, which forms lenses up to several metres in length. Sections of this sequence are rusty-weathering and contain several percent authigenic (or detrital?) pyrite. Pyrite is best developed within tuffaceous sections, although it is also present in siliceous siltstone. The anoxic conditions inferred for this sequence, together with the abundance of pyrite, suggests the potential to host sedimentary exhalative mineral deposits.

The contact between the upper Hazelton clastics and overlying Bowser Lake Group is transitional (Evenchick et al., 2003; Jakobs, 1993). Interbedded tuff is lost up-section, and the siliceous nature of the siltstone disappears, resulting in well-cleaved, rusty- to brown-weathering shales and slate up to 20 m thick. The first thin beds of chert(?) sandstone are observed at the top of this lithology, together with the first indications of bioturbation in shale and siltstone. Sandstone becomes more abundant up-section and the percentage of rusty-weathering horizons decreases. The contact has been placed at the top of the rusty-weathering section, occurring some 100 m above the first sandstone horizon and approximately 15 m below the base of the first chert-pebble conglomerate typical of the Bowser Lake Group (Evenchick et al., 2003).

The present interpretation of the upper contact for the Hazelton Group would make it as young as late Bathonian (*see* Evenchick *et al.*, 2001; 2003). Evenchick *et al.* (2003) argue that, considering the Oxfordian ages for the Bowser Lake Group in the area, the age of this contact may be younger and within the Callovian. The oldest ages for the Hazelton Group in the Diagonal Mountain area are Toarcian (Evenchick *et al.*, 2001). Palfy *et al.* (2000) reported an age of 167.2 +10.5 –0.4 Ma for tuff sampled from "pyjama beds" approximately 4.5 km south-southeast of Diagonal Mountain.

Photo 1. Typical interlayered tuff and dark grey to black siliceous siltstone of the "pyjama beds", upper Hazelton Group clastics, McConnell Creek map area.

Lithologies at Diagonal Mountain are similar to those of the Quock Member (Thomson et al., 1986). Based on fossil ages (Evenchick et al., 2001), sections at Diagonal Mountain would also be equivalent age to units of the Abou, Melisson, and Wolf Den Members. The lack of shallower-water lithologies at Diagonal Mountain (represented by the Melisson Member) suggests that this unit was either removed below the Late Toarcian unconformity or that it was not deposited. Descriptions of the Wolf Den, Abou, and Quock Members are entirely consistent with lithologies observed at Diagonal Mountain, although they are not distributed in a simple stratigraphy that can be mapped.

At Motasse Peak, the Hazelton Group also contains the striped, interlayered siltstone and tuff as described in the Diagonal Mountain area. Tuff is also lost up-section, resulting in rusty-weathering siltstone and shale. The recognition of the upper contact is difficult because of the thick section of rusty-weathering siltstones and shales together with a lack of coarse clastic lithologies typical of the basal Bowser Lake Group. There is no definite break in the rusty nature of the siltstone lithologies. This may be due to the presence of nearby Tertiary intrusions, in conjunction with structural complication.

Ritchie-Alger and Todagin assemblages represent coeval slope and submarine fan assemblages, respectively, of Late Jurassic to Early Cretaceous age. These units have an abundance of dark grey and black fine-grained lithologies that may have accumulated abundant organic matter. The Todagin assemblage contains dark grey- and black-weathering siltstone and shale, which are not as dominant within the Ritchie-Alger. These units also are inferred to have been deposited in turbiditic deposits and higher-energy sequences of chert sandstone and conglomerate, which are more voluminous in the Ritchie-Alger assemblage than they are in the Todagin (Evenchick et al., 2001; 2003).

Siltstone units are typically orange-brown to dark grey-weathering and massive to thickly bedded. They can display poor cleavage, but are typically blocky- to crumbly-weathering. They commonly contain thin orange-brown weathering laminae, which are commonly bioturbated. Nodules or discontinuous horizons of orange-weathering grey limestone up to several tens of centimeters thick are also present within sections of the siltstone. Several horizons (up to 5 m thick) of rusty-weathering black siltstone were also observed in these units.

QUESNEL TROUGH

The senior author spent several days sampling sections of organic-rich shale within parts of the Quesnel Trough. These localities are described by Macauley (1984) as potential oil shale horizons based on descriptions of earlier workers. These sections are within Lower to Middle Jurassic fine clastic rocks, similar in composition to the upper Hazelton Group, and include the Ashcroft Formation in the south and an unnamed sequence near the town of Likely. Both units overlie Triassic to Jurassic arc sequences of the Quesnel Terrane and are considered part of the overlap succession.

Ashcroft Formation

The Ashcroft Formation is well exposed in the area of Ashcroft and comprises approximately 1200 to 1600 m of carbonaceous shale, siltstone, and minor sandstone and conglomerate (Travers, 1978; Duffell and McTaggart, 1952). Exposures east of Ashcroft are believed to be nonmarine in origin (McMillan, 1974; Monger, 1982). Conglomerate, although a minor constituent, is distinctive by its polymict nature, containing clasts derived from ancestral North America and the Cache Creek and Quesnel Terranes (Travers, 1978; Duffell and McTaggart, 1952). The unit rests unconformably on the volcanics of Quesnellia and possibly the Cache Creek Terrane (Travers, 1978; Monger, 1982).

The age of the Ashcroft Formation is broadly Early to Middle Jurassic, and a compilation of fossil localities show this succession to be possibly Sinemurian to Callovian in age (Monger and Lear, 1989; Travers, 1978). Fossils collected near the base of the unit are possibly Sinemurian in age (Travers, 1978, Frebold and Tipper, 1969) and range up to Bajocian at the same locality (Monger and Lear, 1989). Along the eastern, nonmarine part of the sequence, fossil data suggest an unconformity between Pliensbachian and Callovian lithologies (Travers, 1978). Travers (1978) inferred that the western succession of Ashcroft strata were deposited during an interval of continuous sedimentation between Sinemurian and Callovian time, based on the lack of regolith and channel conglomerate associated with the unconformity in eastern sections. This may be true; however, no fossils of Toarcian or Bathonian age have been recovered from this area, which could indicate non-deposition, erosion, or lack of data.

McMillan (1974) describes up to 10 m of fetid, dark grey crystalline limestone in the Barnes Creek area, which he believed to be of bioclastic origin. In other sections along the creek, fetid limestone occurs as clasts within conglomerate deposited above a regolith. Associated shales, as elsewhere in the Ashcroft Formation, are black and carbonaceous. The section here contains Callovian fossils.

Duffel and McTaggart (1952) describe thick sections of black carbonaceous shale, which contain Callovian age fossils, in Black Canyon and near the mouth of Minaberriet Creek. This may have been the locality of the suspected oil shale. Recently, similar carbonaceous sequences were sampled along the highway into Ashcroft. Further sampling is planned for this area during 2004.

The Ashcroft Formation was sampled near the town of Ashcroft, where the unit is well exposed in road and railway cuts (Figure 3). Travers (1978) shows this sequence as being an overturned panel along the footwall of a thrust carrying the Nicola Group. No fossil data is available at this locality, although fossil collections to the south, along strike, are Pliensbachian or Sinemurian and Bajocian (Monger and Lear, 1989).

At this locality, the Ashcroft Formation consists of platy and blocky, rusty-weathering, dark grey to black siliceous siltstone. Cleavage is well developed locally but is commonly a spaced parting. Non-siliceous siltstone units typically exhibit blue-grey weathering and yellow salt residue. Discontinuous light-coloured bands were observed (tuffaceous?) and locally contained authigenic pyrite crystals. Some horizons are quite coarse and texturally approach a sandstone. Interbedded with these typical siliceous siltstone sequences are sections of black, crumbly, sooty (carbonaceous) siltstone and shale ranging from 5 to 10 m thick. These graphitic horizons locally contain 2 to 5 cm thick beds of pale to medium grey micritic limestone. The entire section at this locality is at least 100 m thick. Both lithologies were sampled at several points along the section. Results of organic petrographic and anhydrous pyrolysis analysis of these samples will be reported subsequently.

Central Quesnel Trough

Oil shales were described southwest of Likely in the early part of the 20th century (Robertson, 1904, 1905; Ells, 1925; Macauley, 1984). Analysis of these rocks demonstrated that they contain appreciable amounts of kerogen, and one report indicated a potential value of 25 litres/tonne for producible liquid petroleum (see Macauley, 1984). Macauley (ibid.) suggested that, based on descriptions and local geology, the unit that was sampled was probably part of the Lower to Middle Jurassic clastic succession overlying arc sequences of Quesnellia (Figure 4).

These Lower to Middle Jurassic sediments are considered overlap assemblages as they contain coarse clastics in their upper parts with cobbles derived from Cache Creek and Quesnel Terrane and ancestral North American sources, indicating that they formed after amalgamation of these terranes. This succession is also shown to overlap both Cache Creek and Quesnel Terrane rocks northwest and southeast of Likely (Tipper, 1978).

Panteleyev et al. (1996) detailed the geology and metallogenic nature of central Quesnel Terrane. Units described by these authors that could have been the source of the early samples include the fine-grained Pliensbachian to Aalenian siltstones and shales (Units 5 and 6). The older Upper Triassic "Black Phyllite", although composed of dark fine-grained clastics, is generally of too high a metamorphic grade (greenschist and higher) to contain any residual kerogen.

These Pliensbachian to Aalenian sediments contain sections of thin-bedded dark grey to grey calcareous siltstone, siltstone, and sandstone in the lower part. Polymictic conglomerate occurs in the top of the sequence and can also be interbedded with the finer lithologies. A Pliensbachian to possibly Toarcian age is suggested for the lower fine-grained unit, whereas Aalenian ammonites were extracted from interbedded fine-grained lithologies within the upper conglomeratic sequence (Panteleyev et al., 1996; Poulton and Tipper, 1991). The thickness of these sections is not reported, although structural sections, based on the geology of Panteleyev et al. (1996), would suggest several hundred metres.

Numerous sections were visited in 2003, based on mapping by Panteleyev et al. (1996), but due to the recessive nature of the units and limited time available, only one exposure was found on a road cut along the main highway, near Beaver Lake. This exposure consists of black sooty siltstone and dark grey to black calcareous siltstone. Both lithologies appear to be quite organic rich. The entire section at this locality was some 10 m thick. Results of organic petrographic and anhydrous pyrolysis analyses of these samples will be reported subsequently.

REGIONAL IMPLICATIONS

Sampling of Lower to Middle Jurassic organic-rich horizons within the Stikine and Quesnel terranes has shown these lithologies to be quite similar, not only in age but in overall composition. Both sequences were deposited after underlying terranes coalesced and amalgamated to ancestral North America, suggesting that sedimentary basins may have been contiguous.

Deep-water, fine-grained sediments of Early to Middle Jurassic age (Toarcian to Bajocian) appear to be widespread within the Canadian Cordillera and overlie many of the allochthonous terranes (Monger et al., 1991; Poulton and Tipper, 1991). These units are characterized by dark shales and siltstones interbedded with varying amounts of volcanics and coarser clastics. They are found within northern and central Stikine Terrane (Tipper and Richards, 1976), along the Chilcotin Ranges underlying rocks of the Tyaughton Trough (Umhoefer and Tipper, 1998; Figure 1) and eastward within the Quesnel Terrane (Panteleyev et al., 1996). Clearly the deeper-water conditions leading to the deposition of these sediments were extensive in the Canadian Cordillera, although punctuated by several volcanic episodes. The present configuration of these depocentres is a result of dextral strike-slip motion since the Cretaceous along major terrane-bounding faults (Gabrielse, 1991).

Lower to Middle Jurassic black shales within both

northern Stikine Terrane and Quesnellia are inferred to have been deposited in anaerobic depositional conditions. This time period brackets a major worldwide anoxic event (Jenkyns, 1988), which suggests that many of these sedimentary sequences within the Canadian Cordillera were also deposited in these environments. These low-oxygen conditions are conducive to the preservation of organic matter. To the east, within the Western Canada Sedimentary Basin, shale, siltstone, and carbonate of the Fernie Group were deposited during the same time period and are inferred to have been deposited under similar conditions. These rocks have proven to be one of the major petroleum source horizons within this basin.

The wide geographic distribution of Lower and Middle Jurassic fine-grained sediments suggests these units underlie coarser, clastic successions of the Interior Basins. Furthermore, the implied anoxic depositional environment recorded by these Lower and Middle Jurassic clastics suggests that these successions, under the right conditions, could have been sources of petroleum that migrated into overlying clastics.

ACKNOWLEDGEMENTS

The senior author would like to thank Chris Slater, Angelique Magee, Jamel Joseph, and Gareth Smith for excellent field assistance within the McConnell Creek map area. Our stay in this area was made much more comfortable by the hospitality of Arleyene and Dennis Farnworth of Steelehead Valhalla Lodge. Many thanks to Tom Brooks, Daryll Adzich, Ryan Hines, and Craig Kendell of Canadian Helicopters for dependable and safe flying.

REFERENCES

Anderson, R.G. (1993): A Mesozoic Stratigraphic and Plutonic Framework for northwestern Stikinia (Iskut River area), northwestern British Columbia, Canada; *in* G. Dunne and K. McDougall, (*eds*.), Mesozoic Paleogeography of the Western United States--II, S*ociety of Economic Palaeontologists and Mineralogists*, Pacific Section, Volume 71, pages 477-494.

Creaney, S., Allan, J., Cole, K.S., Fowler, M.G., Brooks, P.W., Osadetz, K.G., Macqueen, R.W., Snowdon, L.R., Riediger, C. (1994): Petroleum Generation and Migration in the Western Canada Sedimentary Basin; *in* Geological Atlas of the Western Canada Sedimentary Basin. G.D. Mossop and I. Shetsen (*comp*.), Calgary, Canadian Society of Petroleum Geologists and Alberta Research Council, pages 455-468.

Curiale, J.A. 1994. Correlation of Oils and Source Rocks - A Conceptual and Historical Prospective; *in*: Magoon, L.B., Dow, W.G. (*Editors.*), The Petroleum system-from Source to Trap. American Association of Petroleum Geologists, Memoir 60, pages 251-260.

Duffell, S. and McTaggart, K.C. (1952): Ashcroft Map-area, British Columbia; *Geological Survey of Canada*, Memoir 262, 122 pages.

Eisbacher, G.H. (1974): Sedimentary History and Tectonic Evolution of the Sustut and Sifton Basins, North-central British Columbia; *Geological Survey of Canada*, Paper 73-31, 57 pages.

Ells, S.C. (1925): Oil Shales of Canada; *in* Shale Oil, R.H. McKee (*ed.*), *American Chemical Society*, Monograph Series No. 25, The Chemical Catalog Company Inc., New York, pages 57-58.

Evenchick, C.A. (1991): Geometry, Evolution and Tectonic Framework of the Skeena Fold Belt, North-central British Columbia; *Tectonics*, Volume 10, pages 527-546.

Evenchick, C.A. and Thorkelson, D.J. (in press):Geology of the Spatsizi River Map Area, North-central British Columbia; *Geological Survey of Canada*, Bulletin 577.

Evenchick, C.A. and Proter, J.S. (1993): Geology of West McConnell Creek Map Area, British Columbia; *in* Current Research, Part A, *Geological Survey of Canada*, Paper 93-1A, pages 47-55.

Evenchick, C.A., Poulton, T.P., Tipper, H.W. and Braidek, I., (2001): Fossils and Facies of the Northern Two-thirds of the Bowser Basin, British Columbia; *Geological Survey of Canada*, Open File 3956.

Evenchick, C.A., Ferri, F., Mustard, P.S., McMechan, M., Osadetz, K.G., Stasiuk, L., Wilson, N.S.F, Enkin, R.J., Hadlari, T. and McNicoll, V.J. (2003): Recent Results and Activities of the Integrated Petroleum Resource Potential and Geoscience Studies of the Bowser and Sustut Basins Project, British Columbia; *in* Current Research, *Geological Survey of Canada*, 2003-A13, 11 pages.

Frebold, H. and Tipper, H.W. (1969): Lower Jurassic Rocks and Fauna near Ashcroft, British Columbia and Their Relation to Some Granitic Plutons (92-I); *Geological Survey of Canada*, Paper 69-23, 20 pages.

Gabrielse, H. (1991): Structural Styles, Chapter 17 *in* Geology of the Cordilleran Orogen in Canada, H. Gabrielse and C.J. Yorath (*ed.*.); *Geological Survey of Canada*, Geology of Canada, No. 4, pages 571-675.

Hayes, B. (2002): Petroleum Exploration Potential of the Nechako Basin, British Columbia; *B.C. Ministry of Energy and Mines*, Petroleum Geology Special Paper 2002-3.

Hunt, J.A. (1992): Stratigraphy, Maturation and Source Rock Potential of Cretaceous Strata in the Chilcotin-Nechako Region of British Columbia; *University of British Columbia*, Masters Thesis, 448 pages.

Hunt, J.A. and Bustin, R.M. (1997): Thermal Maturation and Source Rock Potential of Cretaceous Strata in the Chilcotin-Nechako Region, South-Central British Columbia; *Bulletin of Canadian Petroleum Geology*, Volume 45, pages 239-248.

Jakobs, G. (1993): Jurassic Stratigraphy of the Diagonal Mountain Area, McConnell Creek Map Area, North-Central British Columbia; *in* Report of Activities, Part A; *Geological Survey of Canada*, Paper 93-1, pages 43-46.

Jeletzky, O.L. (1976): Preliminary Report on Stratigraphy and Depositional History of Middle to Upper Jurassic Strata in McConnell Creek Map Area, (94D West Half), British Columbia *in* Report of Activities, Part A, *Geological Survey of Canada*, Paper 76-1A, pages 63-67.

Jenkyns, H.C. (1980): Cretaceous Anoxic Events: from Continents to Oceans; *Journal of the Geological Society of London*, Volume 137, pages 171-188.

Jenkyns, H.C. (1988): The Early Toarcian (Jurassic) Anoxic Event: Stratigraphic, Sedimentary and Geochemical Evidence; *American Journal of Science*, Volume 288, pages 101-151.

Logan, J.M., Drobe, J.R. and McClelland, W.C. (2000): Geology of the Forrest Kerr-Mess Creek Area, Northwestern British Columbia; *B.C. Ministry of Energy and Mines*; Bulletin 104, 164 pages.

Macauley, G. (1984): Geology of the Oil Shale Deposits of Canada; *Geological Survey of Canada*, Paper 81-25, 65 pages.

McMillan, W.J. (1974): Stratigraphic Section from the Jurassic Ashcroft Formation and Triassic Nicola Group Contiguous to the Guichon Creek Batholith; *in* Geological Fieldwork, *Geological Department of Mines and Petroleum Resources*; pages 27-34.

Monger, J.W.H. (1982): Geology of the Ashcroft Map Area, Southwestern British Columbia; *in* Current Research, Part A, Paper 82-1, pages 293-297.

Monger, J.W.H. and Lear, S. (1989): Geology, Ashcroft, British Columbia, *Geological Survey of Canada*, Preliminary Map 42-1989.

Monger, J.W.H., Wheeler, J.O., Tipper, H.W., Gabrielse, H., Harms, T., Struik, L.C., Campbell, R.B., Dodds, C.J., Gehrels, G.E. and O'Brien, J. (1991): Part B. Cordilleran Terranes *in* Upper Devonian to Middle Jurassic Assemblages, Chapter 8 of Geology of the Cordilleran Orogen in Canada, H. Gabrielse and C.J. Yorath (*ed.*); *Geological Survey of Canada*, Geology of Canada, No. 4, pages 281-327.

Osadetz, K.G., Snowdon, L.R., and Obermajer, M. (2003): ROCK-EVAL/TOC results from 11 Northern British Columbia boreholes. *Geological Survey of Canada*, Open File 1550 and *B.C. Ministry of Energy and Mines*, Petroleum Geology Open File 2003-1.

Osadetz, K.G., Evenchick, C.A., Ferri, F., Stasiuk, L., Obermajer, D.M. and Wilson, N.S F. (2003): Molecular composition of Crude Oil Stains from Bowser Basins *in* Geological Fieldwork 2002, *B.C. Ministry of Energy and Mines*, Paper 2003-1, pages 257-264.

Osadetz, K.G., Jiang, C., Evenchick, C. A., Ferri, F., Stasiuk, L. D., Wilson, N. S. F. and Hayes, M. (2004): Sterane Compositional Traits of Bowser and Sustut Basin Crude Oils: Indications for Three Effective Petroleum Systems; *Resource Development and Geoscience Branch, BC Ministry of Energy and Mines,* Summary of Activities 2004.

Pálfy, J., Mortensen, J.K., Smith, P.L., Friedman, R.M., McNicoll, V. and Villeneuve, M. (2000): New U-Pb Zircon Ages Integrated with Ammonite Biochronology from the Jurassic of the Canadian Cordillera; *Canadian Journal of Earth Sciences*; Volume 37, pages 549-567.

Panteleyev, A, Bailey, D.G., Bloodgood, M.A. and Hancock, K.D. (1996): Geology and Mineral Deposits of the Quesnel River-Horsefly Map Area, Central Quesnel Trough, British Columbia; *Ministry of Employment and Investment*, Bulletin 97, 156 pages.

Poulton, T.P. and Tipper, H.W. (1991): Aalenian Ammonites and Strata of Western Canada; *Geological Survey of Canada*, Bulletin 411, 71 pages.

Robertson, J. (1904): Progress of Mining – Oil Shales; *British Columbia Department of Mines*, Annual Report, 1903, page 24.

Robertson, J. (1905): Progress of Mining – Oil Shales; *British Columbia Department of Mines*, Annual Report, 1904, pages 23-24.

Thomson, R.C., Smith, P.L. and Tipper, H.W. (1986): Lower to Middle Jurassic (Pliensbachian to Bajocian) Stratigraphy of the Northern Spatsizi Area, North-central British Columbia; *Canadian Journal of Earth Science,* Volume 23, pages 1963-1973.

Tipper, H.W. (1978): Northeastern Part of Quesnel (93B) Map-Area, British Columbia, *in* Current Research, Part A, *Geological Survey of Canada*, Paper 78-1, pages 67-68.

Tipper, H.W. and Richards, T.A. (1976): Jurassic Stratigraphy and History of North-central British Columbia; *Geological Survey of Canada*, Bulletin 270, 73 pages.

Travers, W.B. (1978): Overturned Nicola and Ashcroft Strata and Their Relation to the Cache Creek Group, Southwestern Intermontane Belt, British Columbia; *Canadian Journal of Earth Science*, Volume 15, pages 99-116.

Umhoefer, P.J. and Tipper, H.W. (1998): Stratigraphy, Depositional Environment, and Tectonic Setting of the Upper Triassic to Middle Jurassic Rocks of the Chilcotin Ranges, Southwestern British Columbia; *Geological Survey of Canada*, Bulletin 519, 58 pages.

STERANE COMPOSITIONAL TRAITS OF BOWSER AND SUSTUT BASIN CRUDE OILS: INDICATIONS FOR THREE EFFECTIVE PETROLEUM SYSTEMS

By K.G. Osadetz[1], C. Jiang[2] ,C. A. Evenchick[3], F. Ferri[4], L. D. Stasiuk[1], N. S. F. Wilson[1] and M. Hayes[4]

KEYWORDS: Crude oil, natural gas, petroleum stains, seepages, Bowser-Sustut Basins, organic geochemistry, solvent extracts, biomarkers, steranes, terpanes, gas chromatography-mass spectrometry.

ABSTRACT

Crude oils extracted from Bowser Lake and Sustut Groups have distinctive compositions that are inferred to be indicative of at least three effective petroleum systems that have generated, expelled, and accumulated crude oil. Compositional differences among the three effective petroleum systems are illustrated by compositional variations of steranes, complicated molecules that have retained structural similarities to their inferred biological precursor, cholesterol. Oil stains occur widely, both geographically and stratigraphically. One compositional oil family is inferred to be derived from Stikine Assemblage, the sub-Hazelton succession. This petroleum is derived from pre-Jurassic marine carbonate source rocks deposited in hypersaline to mesohaline environments. A second compositional oil family is derived from Mesozoic open-marine source rocks that are inferred to be within the upper Hazelton or lower Bowser Lake Group, as the lowest stratigraphic occurrence of these oils lies in marine-slope deposits of the Bowser clastic wedge. A third oil family, which is inferred to be derived from lacustrine Mesozoic source rocks, occurs in northern Bowser and Sustut Basins, where it is probably derived from thick, often coaly, nonmarine Bowser Lake successions. The occurrence and composition of these crude oils expand the petroleum prospectivity of the Bowser and Sustut Basins by reducing petroleum system risks and indicating a possible petroleum system for Hazelton Group, which is now attributed petroleum potential.

INTRODUCTION

This report results from work performed as part of the project "Integrated Petroleum Resource Potential and Geoscience Studies of the Bowser and Sustut Basins", a collaborative research project of the BC Ministry of Energy and Mines (Oil and Gas Emerging Opportunities and Geoscience Branch) and the Geological Survey of Canada (Evenchick *et al.*, 2003). The current multiyear project is multidisciplinary in scope and broad in geographic coverage, including the length and breadth of both the Bowser and Sustut Basins. Primary activities include geological framework and energy resource studies and petroleum resource assessment.

Previous petroleum assessment work of the region identified substantial petroleum potential while recognising that there are several poorly understood but significant risks (Hannigan *et al.*, 1995). That study showed that there were significant play-level risks associated with the inferred petroleum potential of the Bowser Basin. More recent GSC/BCMEM research resulted in a profound shift in perceptions of organic and thermal maturity patterns in the Bowser and Sustut Basins (Evenchick *et al.*, 2002). The first regional organic maturity dataset illustrates that large areas, including the lowest stratigraphic levels of the Bowser Basin, have sufficiently low organic maturity levels to be favourable for the formation and preservation of crude oil. This fundamentally changed previous views that considered the high thermal maturity of some of the stratigraphically highest coals as a negative indication for hydrocarbon potential in all stratigraphic levels and all the geographic regions of the basins. The recent discovery of petroleum seepages and stains within the basin (Osadetz *et al.*, 2003a) provides information that eliminates play-level risks associated with petroleum system function and reservoir occurrence. The results presented herein indicate that there are at least three operational petroleum systems, each with sources and crude oils of different molecular composition and stratigraphic characteristics operating in Bowser and Sustut Basins. The results are consistent with the revised observations and models of thermal maturity and history. Integration of these data, models, and interpretations will increase the robustness of petroleum resource assessments in this potential frontier petroleum province.

[1]*Geological Survey of Canada: Calgary, 3303 33 St. NW, Calgary, AB, Canada, T2L 2A7*
[2]*Humble Geochemical Services Division, 218 Higgins Street, Humble, Texas 77338 U.S.A.*
[3]*Geological Survey of Canada: Pacific, 101-605 Robson St. Vancouver, BC, Canada, V6B 5J3;*
[4]*Resource Development and Geoscience Branch, BC Ministry of Energy and Mines, PO Box 9323, 6th Floor, 1810 Blanshard St., Victoria, BC, Canada, V8W 9N3*

REGIONAL GEOLOGICAL OVERVIEW

The Bowser and Sustut Basins are located in north-central British Columbia (Figure 1) in the Intermontane Belt of the Canadian Cordillera, a region of sedimentary diagenesis or low metamorphic grade (mainly greenschist facies) relative to the adjacent Omineca and Coast metamorphic and plutonic belts. They overlie Devonian to early Middle Jurassic strata of the allochthonous terrane Stikinia.

The basins comprise 3 stratigraphic successions with overlapping ages. The Bowser Lake Group is the lowest, ranging from upper Middle Jurassic to mid-Cretaceous. It constitutes a major clastic depositional wedge that includes strata deposited in distal submarine fan, slope, shallow-marine shelf, deltaic, fluvial, and lacustrine environments (e.g., Tipper and Richards, 1976; Evenchick *et al.*, 2001). It was deposited directly on Stikinia, a volcanic arc that includes Jurassic upper Hazelton Group clastic successions. The Lower to mid-Cretaceous Skeena Group occurs south of the Bowser Lake Group, with uncertain stratigraphic relationships. Skeena Group strata were deposited in marine and nonmarine environments and are intercalated with volcanic successions (Tipper and Richards, 1976). The mid- to Upper Cretaceous Sustut Group, a fluvial and lacustrine foreland basin succession, unconformably onlaps the Hazelton and Bowser Lake Groups that are deformed in older Skeena Fold Belt structures. The Skeena Fold Belt subsequently involved and deformed the Sustut Group (Eisbacher, 1974; Figure 2).

All 3 successions and underlying Stikinia are deformed in the Skeena Fold Belt, a thin-skinned contractional fold and thrust belt of Cretaceous and possibly early Tertiary age (Evenchick 1991). Northeast-vergent open to closed folds of about 100 to 1000 m wavelengths are the dominant structures at exposed levels, but larger wavelength folds often outlined by anticlinoria and synclinoria in Bowser Lake Group are associated with structural culminations and depressions inferred to be controlled by the involvement of Stikine Assemblage volcanic and clastic strata. The fold hinges trend northwest dominantly, but domains of northeast fold hinge trends occur in western Skeena Fold Belt (ibid.). Hinterland-verging thrusts in the vicinity of the boundary between Bowser Basin and Sustut Basin (Evenchick and Thorkelson, in press) define a triangle zone (Gordy *et al.*, 1977), similar to major productive and prospective structures in many thrust and fold belts (MacKay *et al.*, 1996).

CRUDE OIL OCCURRENCE

New field work and the analysis of existing samples have identified, extracted, and characterized 20 crude oil occurrences from locations in Bowser and Sustut Basins (Table 1, Figure 2). Numerous additional indications of crude oil staining and petroleum fluid inclusions occur within the Bowser and Sustut Basins, but only 20 samples (Table 1) are characterized here. Petroleum occurrences include:

1. Tsatia Mountain (NAD 27, UTM Zone V E442468 N6380068), a breeched oil field in Muskaboo Creek Assemblage Bowser Lake Group (GSC Extract X9693 and X9694; Osadetz *et al.*, 2003);
2. Sandstone in the roof of the triangle zone north of Cold Fish Lake (NAD 27, UTM Zone V E511100 N6396070), Tango Creek Formation, Sustut Group (GSC Extract 9746);
3. Footwall of the Crescent Fault near the confluence of Buckinghorse Creek and Spatsizi River (NAD 27, UTM Zone V E525670 N6366320), Eaglenest (deltaic) Assemblage of the Bowser Lake Group (GSC Extract X9731);
4. Amoco Ritchie well a-3-J/104-A-6, one of the only 2 petroleum exploration wells in the basin, shows extensive oil stains, which were extracted from samples at depths of 644.8 m, 1321.9 m, 1439.7 m, and 2055.8 m (2115.7', 4337.0', 4723.4', and 6745.0') (GSC Extracts X9742-X9745);
5. Twelve diverse samples from the northern Bowser and Sustut Basins (between 57.4284° N to 57.7803°N and 127.7689° W to 130.0625° W; GSC Extracts X9790 to X9801);
6. New field examples of rocks, potentially stained with crude oil, that were identified during sample drilling for paleomagnetic samples (Evenchick *et al.*, 2003). Oil films were present in the circulating fluid during paleomagnetic sampling of all Stikinia rocks sampled at Oweegee Dome. Oil films were present in a large number of lithologies through this antiformal culmination, including limestone, volcanic flows, volcaniclastic turbidites and conglomerates in Hazelton Group and lower units, as well as from Bowser Lake Group sandstone at Mount Ritchie (Figure 2, ibid.). These samples remain to be extracted and characterized, but they might reasonably be expected to resemble oil samples from the Ritchie wells;
7. Confirmed flammable natural gas seeps of biogenic methane into Tatogga Lake (Osadetz *et al.*, 2003), which will be reported elsewhere (Evenchick *et al.*, in prep).

All these indications demonstrate that petroleum (both crude oil and natural gas) occurs in Bowser and Sustut Basins. The existing resource assessment suggests that significant petroleum resources and large pool sizes can be expected (Hannigan *et al.*, 1995), but only exploratory drilling will confirm the existence of a significant undiscovered petroleum resource.

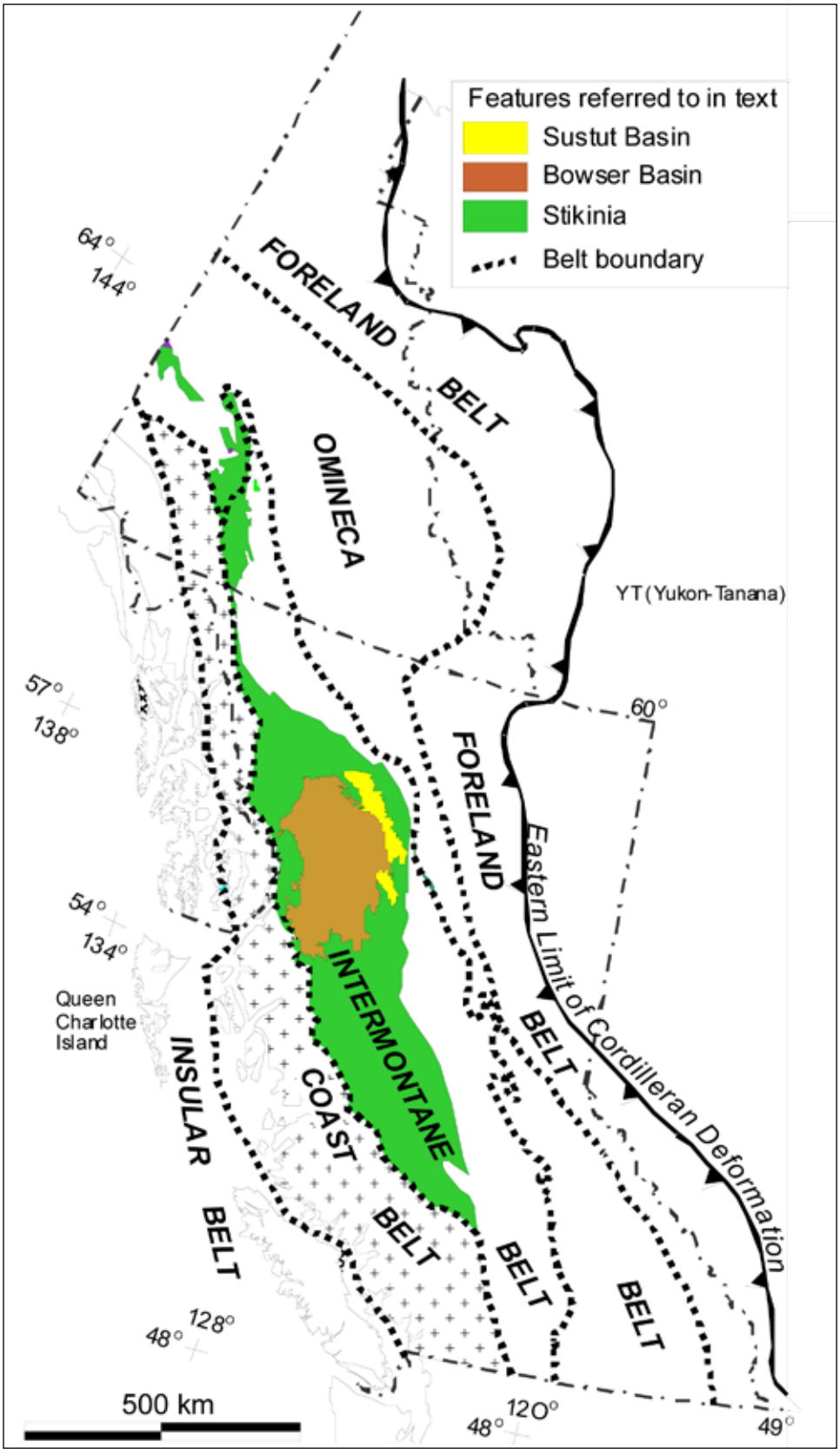

Figure 1. Location of the Bowser and Sustut Basins on a base map showing the morphogeological belts of the Canadian Cordillera.

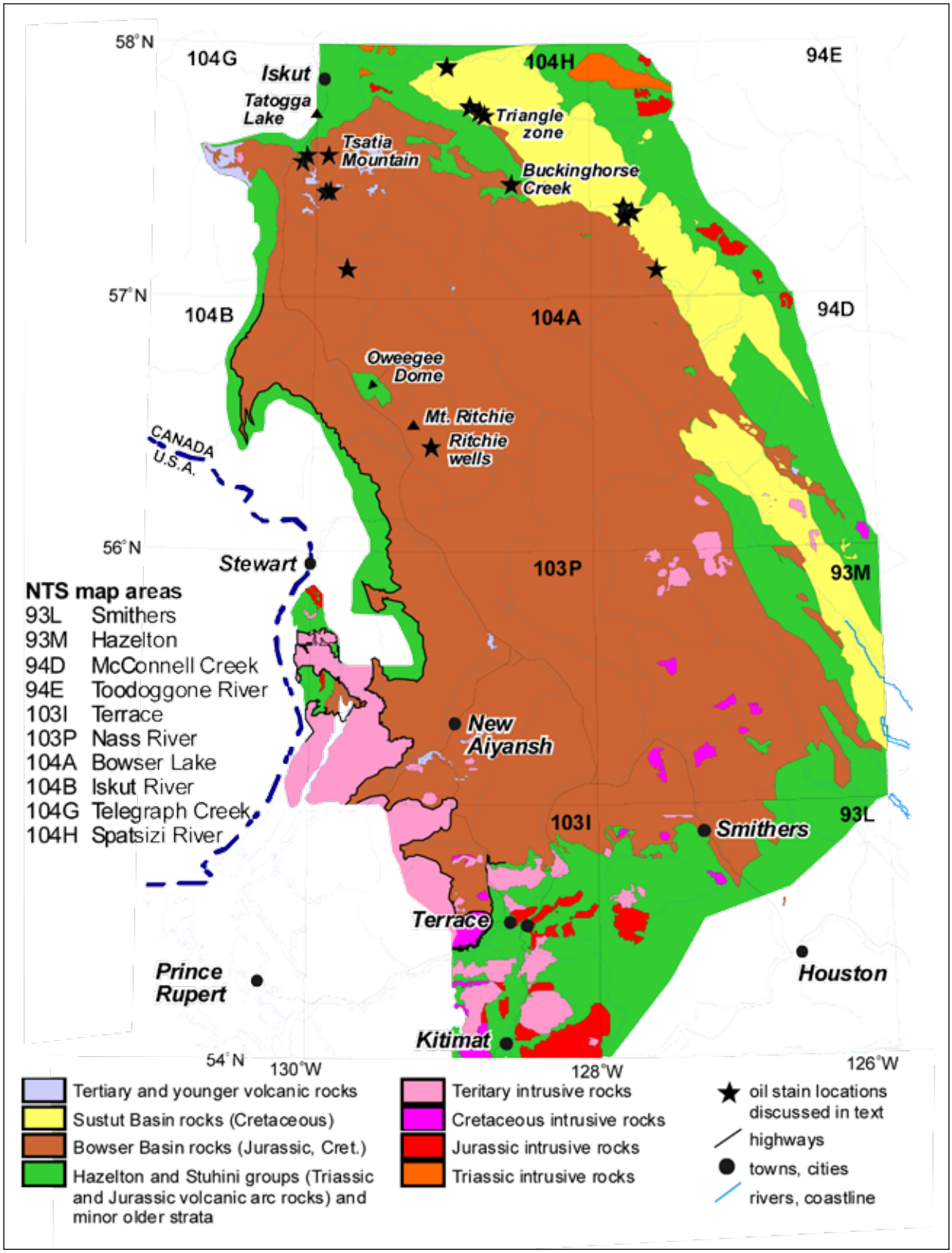

Figure 2. The locations of select crude oil samples discussed in text shown on a regional map of the Bowser and Sustut Basins. The locations of all samples are listed in Table 1.

TABLE 1. CRUDE OIL STAIN AND FLUID INCLUSION SAMPLE LOCATIONS.

Extract #	Latitude (°N)	Longitude (°W)	Depth	Map Unit
X9693	57.5613	129.9616	outcrop	Bowser Lake Gp; Muskaboo Creek Assemblage
X9694	57.5613	129.9616	outcrop	Bowser Lake Gp; Muskaboo Creek Assemblage
X9731	57.4408	128.5724	outcrop	Bowser Lake Gp; Eaglenest Assemblage
X9742	56.4188	129.1531	644.8 m	Bowser Lake Group
X9743	56.4188	129.1531	1321.9 m	Bowser Lake Group
X9744	56.4188	129.1531	1439.6 m	Bowser Lake Group
X9745	56.4188	129.1531	2055.8 m	Bowser Lake Group
X9746	57.5613	129.9616	outcrop	Sustut Group; Tango Creek Fm.
X9790	57.9247	129.1408	outcrop	Sustut Group; Tango Creek Fm.
X9791	57.5559	130.0481	outcrop	Bowser Lake Gp; Todagin Assemblage
X9792	57.1124	129.7686	outcrop	Bowser Lake Gp; Todagin Assemblage
X9793	57.4284	129.9309	outcrop	Bowser Lake Gp; Skelhorne Assemblage
X9794	57.4322	129.8974	outcrop	Bowser Lake Gp; Skelhorne Assemblage
X9795	57.3179	127.7667	outcrop	Sustut Group; Tango Creek Fm.
X9796	57.3137	127.7329	outcrop	Sustut Group; Tango Creek Fm.
X9797	57.1170	127.5309	outcrop	Bowser Lake Gp; Eaglenest Assemblage
X9798	57.7310	128.7963	outcrop	Sustut Group; Brothers Peak Fm.
X9799	57.7803	128.8793	outcrop	Sustut Group; Brothers Peak Fm.
X9800	57.5460	130.0625	outcrop	Bowser Lake Gp; Skelhorne Assemblage
X9801	57.3060	127.7689	outcrop	Sustut Group; Tango Creek Fm.

PETROLEUM CHARACTERIZATION USING MOLECULAR COMPOSITIONAL TRAITS

Crude oil compositional characteristics reflect kerogen paleoecology, depositional environments, diagenesis, and maturity. Differential expulsion, migration, and post-accumulation effects (processes like catagenesis, biodegradation, and water washing) can also affect crude oil composition (Peters and Moldowan, 1993; Waples and Machihara, 1990; Seifert and Moldowan, 1986, 1981, 1978); therefore, it is important to distinguish source characteristics from migration and post-accumulation effects before inferring depositional and diagenetic characteristics directly from crude oils. Extracts studied herein exhibit three distinguishable and distinctive compositional associations, or family groups, defined by persistent compositional characteristics that are exhibited by a variety of fractions and compounds, but which are especially well-illustrated by steranes, the focus of this discussion.

Phytolic acid side-chains from chlorophyll molecules indicate a particular phototrophism. The acyclic isoprenoid compounds pristane (Pr) and phytane (Ph), which are ubiquitous compounds in crude oils, are commonly derived from these side chains of chlorophyll molecules, although other sources for these compounds exist (Figure 3; Volkman and Maxwell, 1986). Low Pr/Ph ratios are commonly inferred to indicate water column anoxia, especially when accompanied by even-odd n-alkane predominance (Welte and Waples, 1973). High Pr/Ph ratios are commonly interpreted as indicative of oxic water columns (Volkman and Maxwell, 1986).

Steranes, both regular and rearranged, are common biological markers in oils. Acid clays in the depositional environment can control early diagenetic reactions that result in sterane rearrangement via unsaturated intermedi-

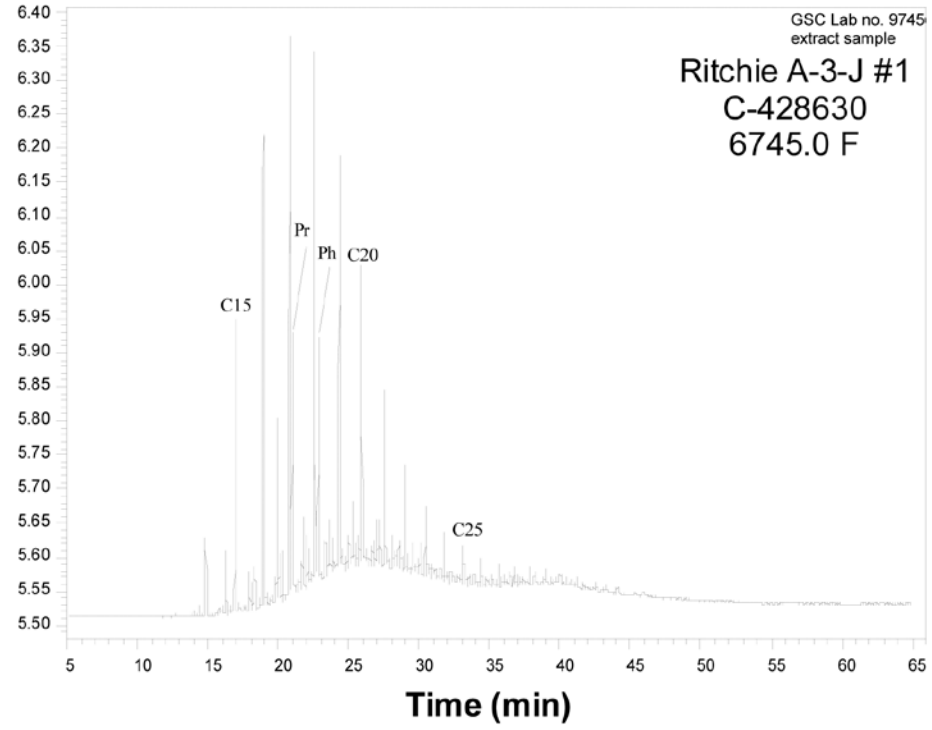

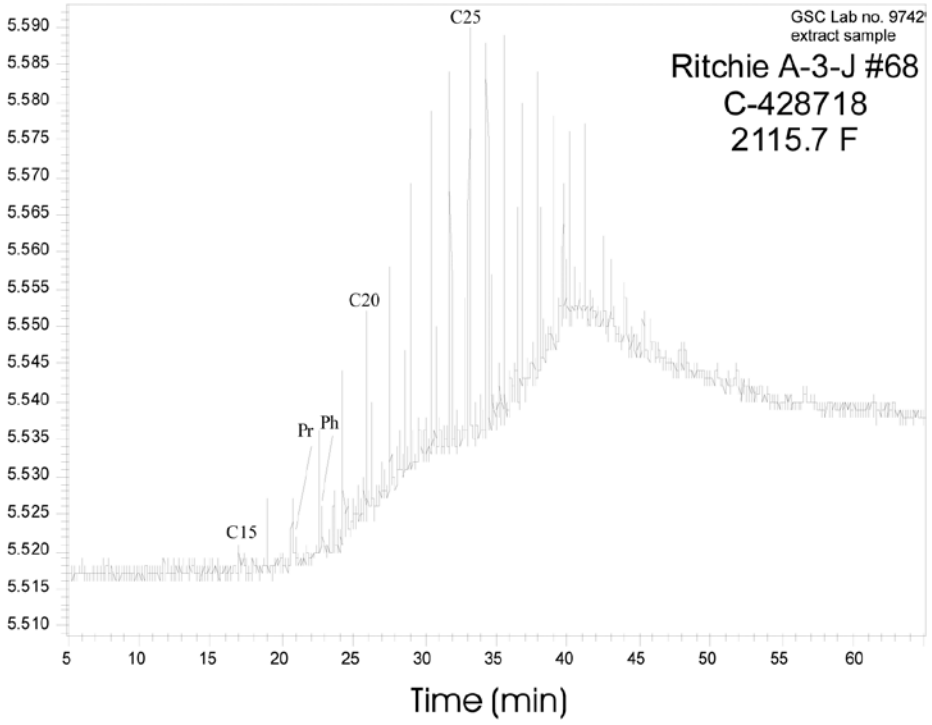

Figure 3. Illustrative saturate fraction gas chromatograms (SFGC) of two solvent extract samples from the Ritchie A-3-J well at 2055.8 m (6745.0', top) and 644.8 m (2115.7', bottom) (Figure 2). All figures show detector response (y axis) as a function of time since injection on the chromatographic column (x axis). The obvious SFGC compositional differences between these two samples are interpreted as due primarily to biodegradation of the shallower crude oil sample by aerobic bacteria.

ates to produce diasteranes (Figure 4; Sieskind et al, 1979; Rubinstein et al., 1975). Low relative diasterane abundances, like those in some carbonate-sourced petroleum systems, are generally interpreted to indicate a clay-starved depositional environment (i.e., a "carbonate" source rock), although many "carbonate" source rocks have ratios of diasterane to regular sterane like those attributed to "clastic" source rocks (Osadetz et al., 1992). A biological source of diasteranes is unlikely, but the association of anomalously high diasteranes in carbonate rocks with evaporitic depositional environments suggests a relationship (Clark and Philp, 1989).

Strongly reducing depositional environments are required to preserve organic matter and form kerogen in sedimentary petroleum source rocks. Since strongly reducing conditions can persist below the sediment-water interface, even in the absence of water column anoxia, euxinic sediments do not directly indicate water column environmental conditions. However, some biological compounds of source rock kerogen, notably phytoloic acid side-chains of chlorophyll and bactirohopane-tetrol, are commonly inferred to be affected by reduction and oxidation reactions in the water column prior to, or at the earliest stages of, their incorporation into the sediment (Peters and Moldowan, 1993). Peters and Moldowan (1991) suggest that C32 to C34 hopane prominences could result from either redox reactions controlled by the depositional environment or from precursor molecules other than bacteriohopane-tetrol. The first alternative is preferred because C34 hopane and C35 hopane prominence commonly follows source rock depositional environment and paleoecology (Osadetz et al., 1992). This results in a water column chemistry indicator that is preserved in compounds that are a common trace component of crude oils (Figure 5; Peters and Moldowan, 1991). The higher the carbon number of predominant extended hopanes, the stronger and more persistant the water column anoxia.

RESULTS

Select gross and molecular compositional results of the 20 samples examined appear in Table 2. All subsequent illustrations of gas chromatograms and mass chromatograms show detector response (y axis) as a function of time since injection on the chromatographic column (*x* axis).

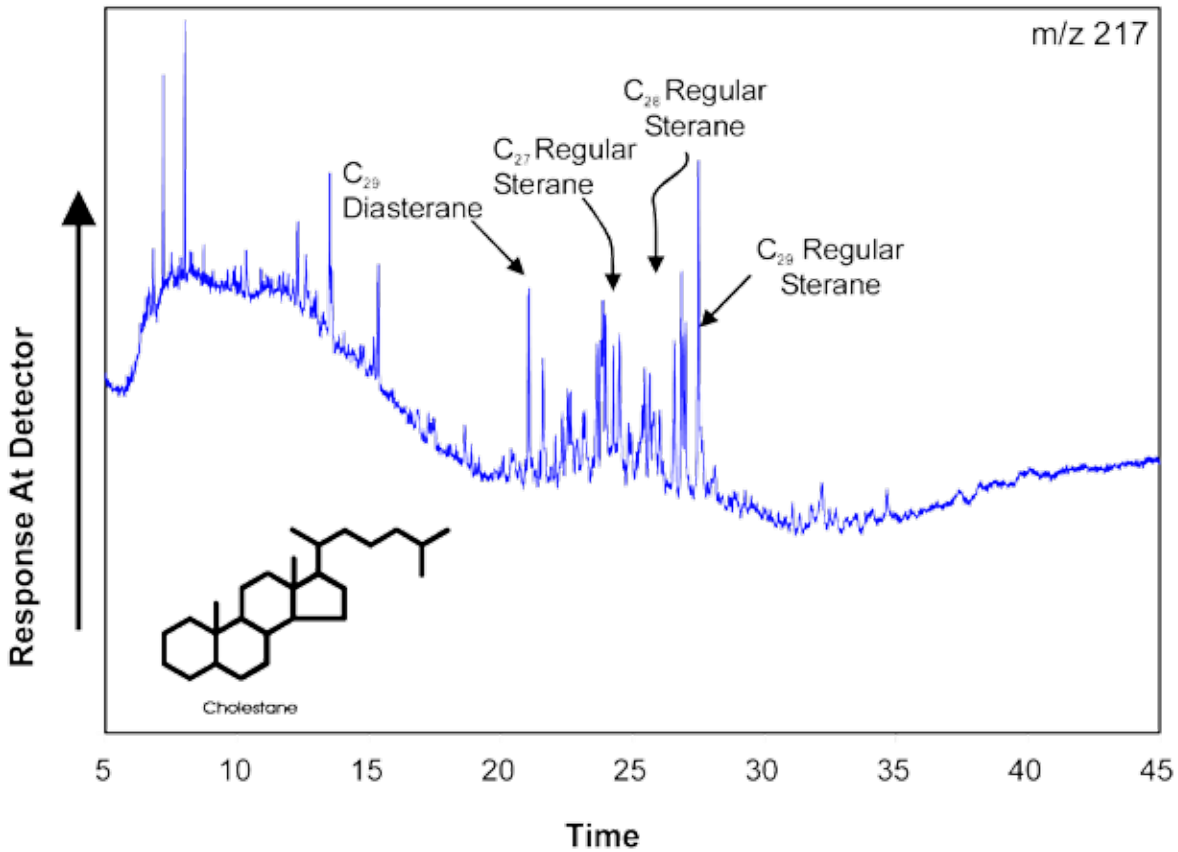

Figure 4. An example m/z 217 mass chromatogram showing the relative abundance of both regular and rearranged steranes (or diasteranes) in solvent extract sample X9693, from a sample of Muskaboo Creek Assemblage bioclastic sandstone at Tsatia Mountain.

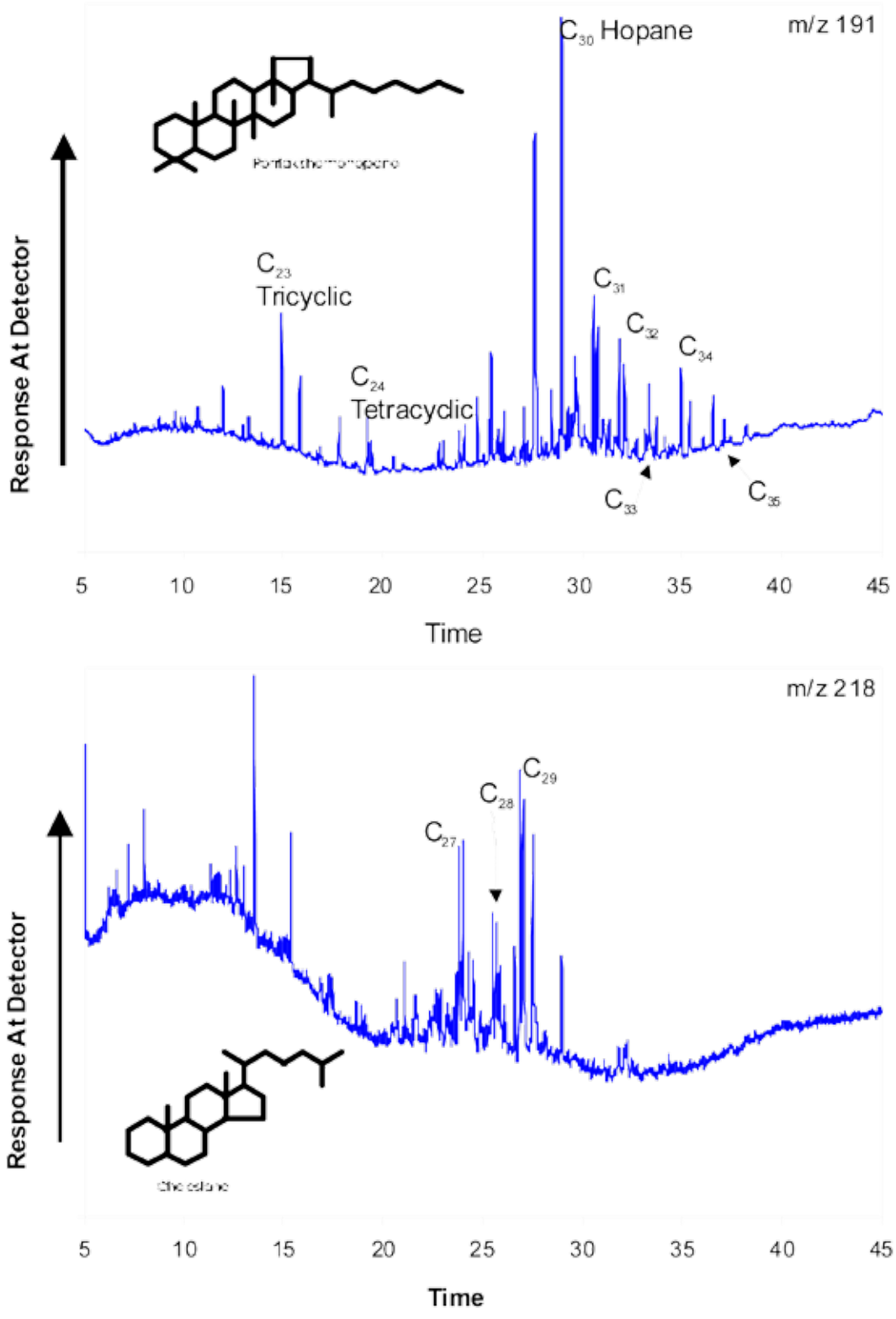

Figure 5. An example m/z 191 (terpanes, top) and 218 (regular steranes, bottom) mass chromatogram in solvent extract sample X9693, from Muskaboo Creek Assemblage bioclastic sandstone at Tsatia Mountain.

Compounds are identified by both standard elution order and by full scan triple sector GCMS operating in MS-MS mode. All samples have been characterized optically or petrographically as being stains or petroleum fluid inclusions. The low hydrocarbon yields and low HC% values are due to the small recoverable volumes (Table 2). This is expected, considering the exposure of both outcrops and old well cuttings to processes of dissipation and alteration resulting from their exposure to the elements, especially in light of the inferred low densities and expected volatility of the hydrocarbons (Osadetz *et al.*, 2002).

SELECT CRUDE OIL MOLECULAR COMPOSITIONAL TRAITS

Molecular compositional differences among the samples are diverse, but they can be characterized by consideration of select compound variations. The observed variations are interpreted using standard techniques and previous studies to distinguish variations due to the alteration (specifically biodegradation) so that other variations due primarily to source can be isolated and interpreted. The variation of biological marker compounds (like steranes and terpanes) within the sample set are observed and interpreted to be unaffected by alteration, allowing interpretation of compositional variations attributed to source rock age (regular steranes, Grantham and Wakefield, 1988), lithology (diasteranes/regular steranes, Seiskind *et al.*, 1979; hopane prominence, Osadetz *et al.*, 1992), and depositional environment (Peters and Moldowan, 1991) that form the basis of compositional family and petroleum system definition.

Figure 3 illustrates the range of saturate fraction gas chromatogram (SFGC) compositions observed in the samples. Both samples are from the Ritchie A-3-J well at 2055.8 m (6745.0'; Figure 3, top) and 644.8 m (2115.7'; Figure 3, bottom; Figure 2) and both have similar biological marker compositions. Solvent extract X9745 (top) exhibits a normal crude oil response dominated by normal alkanes derived from cell wall phospholipids and the irregular isoprenoid, most noticeably pristane (Pr) and phytane (Ph). The low amplitude baseline hump defines the envelope of a complicated mixture of co-eluting compounds. Solvent extract X9742 (bottom) exhibits a biodegraded crude oil response dominated by normal alkanes that are paired, for samples with longer elution times than nC_{20}, with a homologous series of alkylcyclohexanes and methylalkylcyclohexanes that were identified by GC-MS-MS experiments not discussed herein. Sample X9742 also exhibits a high amplitude baseline hump of more complicated co-eluting compounds. Note especially the relative change between the two samples in response of the hump to compounds eluting prior to and after nC_{20}. The sterane compositions of these two samples are essentially similar (Table 2, Figures 4, 5, 6), illustrating that the composition of the lower molecular weight saturate fraction has been altered by the preferential removal of normal alkanes. Such compositional variations are commonly inferred to be indicative of biodegradation (Peters and Moldowan, 1993; Osadetz *et al.*, 1992).

The sample set compositional variation can be illustrated using a few key compounds. The most illustrative variations are shown by the regular and rearranged steranes (Figure 4). An example m/z 217 mass chromatogram showing the relative abundance of regular and rearranged

TABLE 2. SELECT GROSS AND MOLECULAR COMPOSITIONAL RESULTS FROM BOWSER BASIN CRUDE OILS.

Sample No.	TOC (%)	(ppm of rock)	Extract (% of TOC)	HC (%)	R+A (%)	Sat/Aro	Pr/Ph	C_{29} St Dia/Reg	% C_{27}	% C_{28}	% C_{29}	C_{27}/C_{29}	C_{28}/C_{29}
X9693	BD	2385	N/A	10.8	85.0	1.0	N/A	0.22	26	21	53	0.49	0.40
X9694	BD	22500	N/A	8.9	80.0	1.0	N/A	0.26	32	19	48	0.67	0.39
X9731	BD	N/A	N/A	N/A	N/A	N/A	N/A	0.76	42	26	31	1.35	0.83
X9742	BD	5500	N/A	4.6	87.7	0.3	N/A	0.54	30	29	40	0.76	0.73
X9743	0.10	396	40	7.9	86.8	2.0	N/A	0.56	25	33	42	0.59	0.80
X9744	0.01	771	771	10.7	57.1	0.8	0.44	0.64	22	33	44	0.50	0.75
X9745	5.05	579	1	27.3	58.2	0.6	1.11	0.55	26	34	40	0.66	0.86
X9746	0.05	1179	236	5.4	75.0	4.0	0.69	0.52	30	29	41	0.73	0.71
X9790	4.69	4442	9	4.7	90.6	0.1	1.29	0.57	16	18	66	0.24	0.28
X9791	0.88	1897	22	3.6	86.4	1.0	0.86	0.65	41	27	31	1.32	0.87
X9792	0.74	2857	39	3.9	85.0	0.4	0.67	0.76	41	27	32	1.28	0.86
X9793	1.07	4080	38	4.9	73.5	0.3	0.97	0.61	40	27	33	1.22	0.83
X9794	19.15	9238	5	6.2	90.2	0.7	1.67	0.38	21	24	55	0.38	0.43
X9795	8.07	8600	11	7.4	84.5	0.2	4.49	0.27	7	19	73	0.10	0.26
X9796	3.26	6657	20	8.2	82.0	0.4	2.59	0.32	16	22	62	0.26	0.35
X9797	43.28	29875	7	15.7	83.7	0.2	4.56	0.23	5	25	70	0.07	0.35
X9798	0.78	4903	63	2.0	89.5	0.5	0.7	0.54	36	26	37	0.97	0.71
X9799	0.53	3448	65	12.0	81.5	0.3	0.56	0.37	25	30	46	0.53	0.64
X9800	0.52	1832	35	8.1	84.3	0.9	1.04	0.77	38	27	35	1.10	0.77
X9801	3.19	3701	12	10.2	86.3	0.3	1.87	0.19	9	19	72	0.13	0.27

steranes (or diasteranes) in solvent extract sample X9693 is from Muskaboo Creek Assemblage at Tsatia Mountain. Steranes are derived from cholestane-like molecules that act as common cell wall rigidifiers in eukaryotic organisms. The presence of diasteranes is an indicator of depositional environment and source rock lithology (Sieskind et al, 1979; Rubinstein et al., 1975).

Two important groups of biological marker are the terpanes (m/z 191; Figure 5, top) and regular steranes (m/z 218; Figure 5, bottom). Their occurrence is also illustrated by mass chromatograms from solvent extract sample X9693, from Muskaboo Creek Assemblage at Tsatia Mountain. The m/z 191 mass chromatogram illustrates terpanes, which are primarily derived from bacteriohopanetetrol, a cell wall rigidifier in prokaryotic organisms (Peters and Moldown, 1993). The ratio of similar carbon number hopanes in the homologous group of compounds that occurs to the right of the C_{30} hopane peak as annotated double peaks is controlled by physical conditions of the depositional environment (Peters and Moldowan, 1991). This sample shows that C_{34} hopanes are prominent, due to the accumulation of the source rock in an environment where anhydrite of gypsum was accumulating (Osadetz *et al.*, 1992). The m/z 218 mass chromatogram illustrates regular steranes that were probably derived primarily from cholesterol. The ratio of C_{28} to C_{29} steranes is known to increase with geological age in marine depositional environments, due to biochemical evolution in the marine biosphere (Grantham and Wakefield, 1998). The observed ratio of C_{28}/C_{29} steranes, combined with the standard interpretation of the m/z 191 mass chromatogram, indicates that the source rock of this oil stain is a sub-Hazelton Group carbonate deposited in submarine hypersaline to mesohaline environments and probably occuring in the underlying Stikine succession.

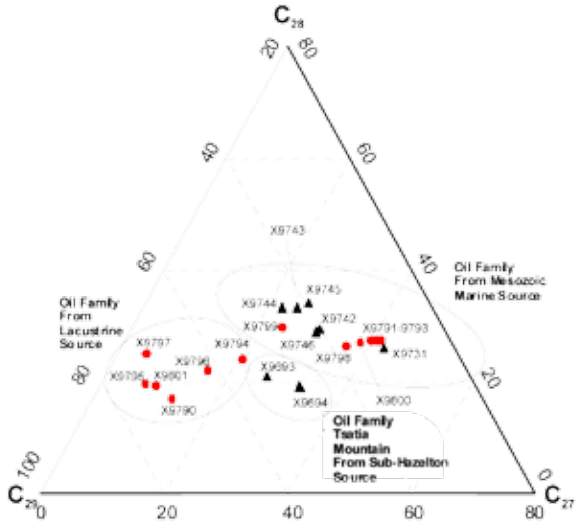

Figure 6. A ternary diagram illustrating compositional variations and affinities of all 20 solvent extract samples using the relative abundance of C_{27}-C_{28}-C_{29} regular steranes (Table 2). The three oil families are identified.

A ternary diagram shows the variations and affinities of all 20 samples using the relative abundance of C27-C28-C29 regular steranes (Figure 6, Table 2). The biodegradation of some oils (Figure 3) does not affect regular sterane compositions, such that observed variations can be attributed primarily to source rock compositional differences. This figure illustrates the presence of the three oil families identified. One, composed of two extracts from Tsatia Mountain (X9693, X9694), is inferred using terpane and sterane compositional characteristics to be derived from a carbonate source in the underlying Stikine succession, as discussed above. Using similar standard interpretations (Peters and Moldowan, 1993), we interpret the steranes and terpanes of the other samples. The second compositional family includes samples from the Amoco Ritchie a-3-J/104-A-6 well at depths of 644.8 m, 1321.9 m, 1439.7 m, and 2055.8 m (2115.7', 4337.0', 4723.4', and 6745.0') (GSC Extracts X9742-X9745), the Tango Creek Formation sample from the Triangle zone (GSC Extract X9746), the Eaglenest assemblage sample from Buckinghorse Creek (GSC Extract X9731), as well as six samples from other locations in the northern Bowser Basin region (GSC Extracts X9791-93 and X9798-80, Table 1) that have compositional characteristics that suggest derivation from a Mesozoic open-marine source rock. This potential source facies probably lies in the upper Hazelton or lower Bowser Lake Groups, as the lowest stratigraphic occurrence of these oils lies in slope and shelf facies of the Bowser Lake Group. A third oil family composed of 6 samples from the group of 12 diverse samples from northern Bowser Basin (GSC Extracts X9790, X9794-97 and X9801) is distinguished by having lower C27 regular steranes and generally higher C29 regular steranes compared to all other samples. This oil compositional family is inferred to have a nonmarine, possibly lacustrine, source in Bowser Lake or Sustut Groups (Peters and Moldowan, 1993). The transitional positions of samples X9794 and X9796 do not preclude the possibility that they could be mixtures of the two oil families inferred to have Mesozoic source rocks. This is possible, since the geographic ranges of the two end-member compositions of the Mesozoic marine and nonmarine source oils overlap; however, other evidence presented below suggests that mixing is not important.

A cross plot of the ratio C29 diasteranes to regular steranes and ratio of regular C28 steranes to C29 steranes (Figure 7) shows additional compositional variations within families using variation of diasteranes/regular steranes (Sieskind et al, 1979; Rubinstein et al., 1975). Those oils inferred to have a nonmarine Mesozoic source have an overlapping range of diaterane/regular sterane ratios to those inferred to have Mesozoic marine sources; however, the range of nonmarine source oil compositions is illustrated by X9790, which is one of the samples that is most different from the oils inferred to have marine Mesozoic sources. Therefore, it is unlikely that the samples X9794 and X9796 are mixtures of any significant proportion. A cross plot of the ratio

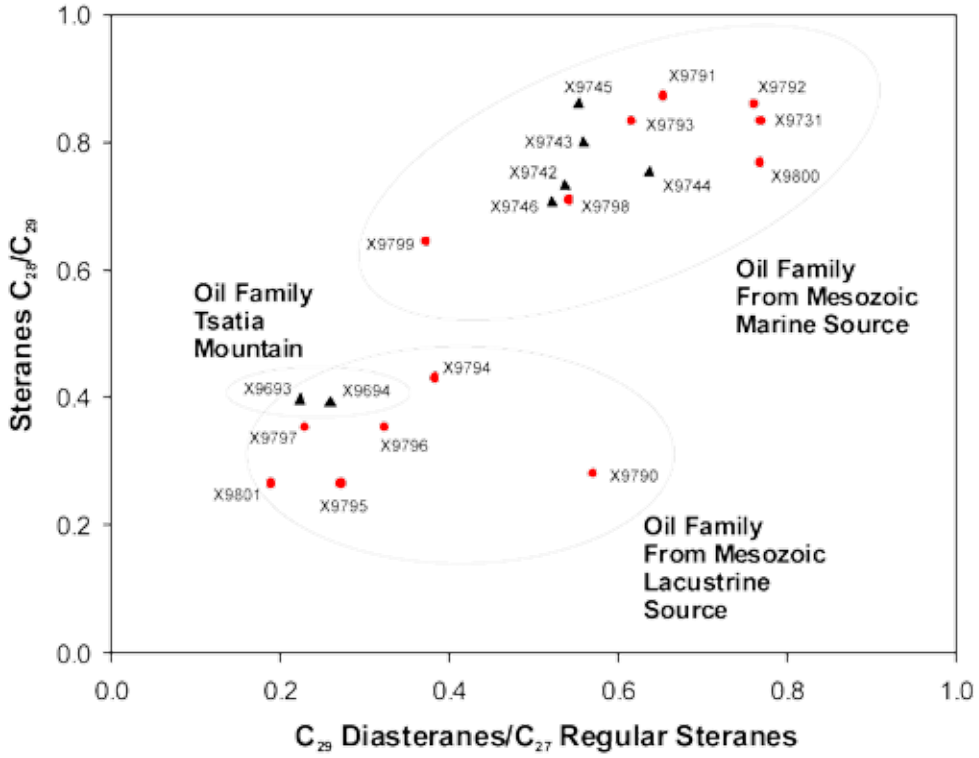

Figure 7. A cross plot of the ratios C_{29} diasteranes to C_{27} regular steranes and ratio of regular C_{28} steranes to C_{29} steranes showing that the compositional variations within families, as typified by the variation of diasteranes/regular steranes.

C29 diasteranes to regular steranes and the ratio of pristane to phytane from the SFGC illustrates that the compositional distinction between the two interpreted Mesozoic oil families is also reflected by other compositional traits (Figure 8). Insufficient pristane and phytane were observed in the oils inferred to be sourced from the Stikine Assemblage strata (X9693; X9694) to allow their characterization using pristane and phytane; however, they are distinguished from most Mesozoic sourced oils by their generally higher saturate to aromatic hydrocarbon ratio (Table 2).

DISCUSSION

The interpretation that biodegradation has altered the composition of some crude oils at or near the surface is important but not surprising. The Amoco Ritchie a-3-J/104-A-6 well has a porous interval containing a resistive fluid that is either "by-passed petroleum pay" or fresh water. The nature of the wireline-log resistivity anomaly is not diagnostic. Some crude oil extracts from this well are clearly biodegraded (Figure 3) as a result of aerobic bacterial degradation that implies a connection with oxygenated (probably fresh and meteoric) water, which, like hydrocarbons, is electrically resistive. In the same well, Koch (1973) reported other petroleum shows, including both dry and wet gas in cuttings samples at depths less than 792 m (2600') where the gas detector indicated more than 40 units, compared to background readings of 10 to 20 units. Therefore, the nature of the resistivity anomaly in the well remains unresolved. Regardless, the combined observations are important since the wireline logs indicate the presence of porous zones in some of the deepest strata in Bowser Lake Group, while the oil stains indicate an effective petroleum system in the same region. The results are consistent with the revised thermal maturity model (Evenchick *et al.*, 2002).

The analysis of the molecular composition of these oil stains and seepages has identified at least three distinct compositional crude oil families. One oil family is inferred to be derived from carbonate source rocks in underlying Stikinia. The second and third oil families, one of which has the characteristics of a marine source, and the other of which has compositional characteristics of a nonmarine or lacustrine source, are inferred to be derived from Jurassic or younger sources in the Hazelton-Bowser-Sustut successions. The source rocks of these petroleum systems have not been identified explicitly, nor have the oils been correlated to solvent extracts from potential source rocks, although potential source rock intervals have been identified in a variety of stratigraphic positions (Evenchick et al., 2002; Osadetz et al., 2003b). However, the significant number of petroleum stains and their association with structures that could be traps for petroleum (as at the Ritchie well, Tsatia Mountain, and in the roof of the triangle zone) all point

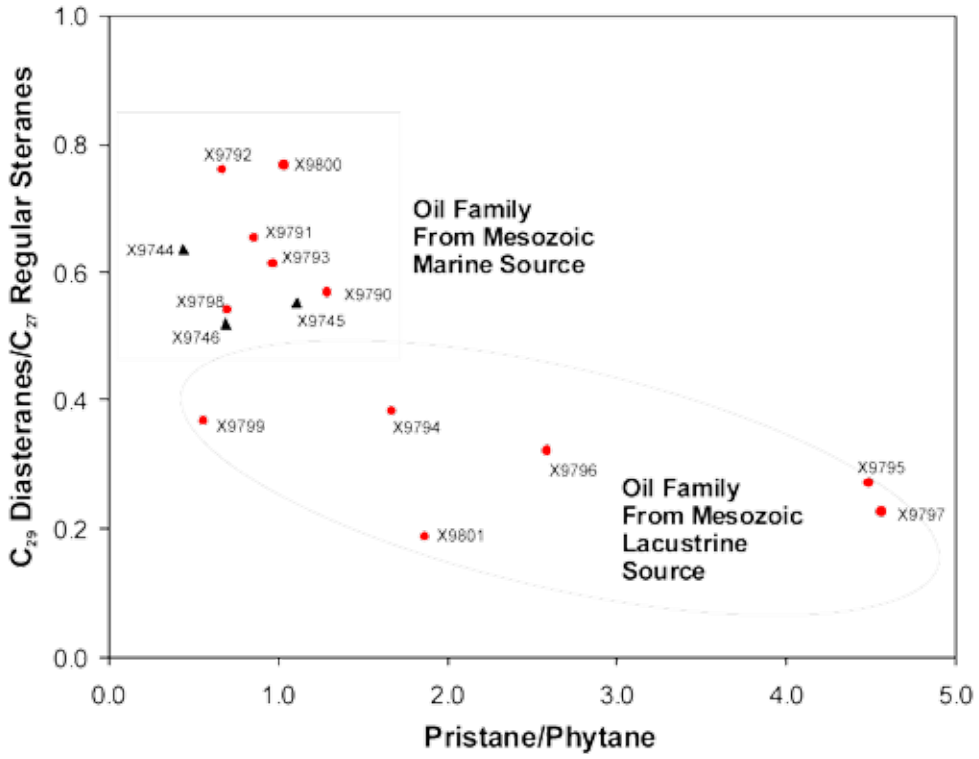

Figure 8: A cross plot of the ratio C_{29} diasteranes to C_{27} regular steranes and ratio of pristane (Pr) and phytane (Ph) from the saturate fraction gas chromatogram (SFGC) that illustrates how compositional distinctions between the two Mesozoic oil families is reflected by additional compositional traits.

toward a complete removal of play-level risks for both petroleum system and reservoir. This suggests that a revised petroleum assessment would be even more encouraging than the existing one (Hannigan et al., 1995).

CONCLUSIONS

Oil stains occur widely, both geographically and stratigraphically, with only the northern half of these basins being investigated. Twenty crude oil stains and petroleum fluid inclusions have been extracted from Bowser Lake and Sustut Group rocks, and their compositions have been characterized. The molecular compositions of these samples are interpreted to show that there are at least three compositionally distinct oil families representative of three effective petroleum systems in Bowser and Sustut Basins.

Molecular compositional differences can be characterized by sterane compositional variations using standard techniques and previous studies, once the effects of alteration (specifically biodegradation) are discounted. One compositional oil family is inferred derived from the sub-Hazelton succession. A second compositional oil family derived from normal Mesozoic marine source rocks is inferred derived from the upper Hazelton or lower Bowser Lake Groups. A third oil family derived from lacustrine Mesozoic source rocks is inferred to occur in the Bowser Lake Group.

The occurrence and composition of these crude oils expand the petroleum prospectivity of Bowser Basin by reducing petroleum system risks and indicating a possible petroleum system for Hazelton Group. The preservation of crude oils is also a strong confirmation of the revised thermal maturity model for the basin (Evenchick et al., 2002). Existing petroleum resource assessments (Hannigan et al., 1995) do not attribute petroleum potential to sub-Bowser successions, indicating a need for revision.

ACKNOWLEDGEMENTS

We thank Sneh Achal, Rachel Robinson, and Marina Milovic for their technical assistance in the production of the data employed here. GSC colleagues Mark Obermajer, Maowen Li, and David Ritcey provided helpful discussions and technical assistance in the preparation of this paper. This is Geological Survey of Canada contribution #2003313.

APPENDIX 1: ANALYTICAL PROCEDURES

Anhydrous Pyrolysis

Rock-Eval/TOC is a useful screen for recognizing sources and stained lithologies. Rock samples suspected or identified as having crude oil stains or petroleum fluid inclusions were pyrolyzed using Rock-Eval/TOC (Table 2) to determine total organic carbon content (Table 2; Espitalie et al., 1985; Peters, 1986; Tissot and Welte, 1978, p. 443-447). The Rock-Eval/TOC analysis gives five parameters: S1, S2, S3, TOC, and Tmax. The S1 parameter measures free or adsorbed hydrocarbons volatilized at moderate temperatures (300° C). S2 measures the hydrocarbons liberated during a ramped heating (300° C to 550° C at 25oC/min.). The S3 parameter measures organic CO_2 generated from the kerogen during rapid heating (300° C to 390° C at 25° C/min.). Milligrams of product per gram of rock sample, the equivalent to kilograms per tonne, is the measure of all these parameters. Total Organic Carbon (TOC) is measured and reported in weight percent. Tmax, the temperature corresponding to the S2 peak maximum temperature, is measured in oC.

Rock-Eval/TOC parameters have significance only above threshold TOC, S1, and S2 values. If TOC is less than about 0.3%, then all parameters have questionable significance and the experiment suggests no potential. Oxygen index (OI = S3/TOC), has questionable significance if TOC is less than about 0.5%. OI values greater than 150 mg/g TOC can result from either low TOC determination or from a mineral matrix CO_2 contribution during pyrolysis. Both Tmax and production index (PI = S1/[S1+S2]) have questionable significance if S1 and S2 values are less than about 0.2. Results can be affected by mineral matrix effects; these either retain generated compounds, generally lowering the S1 or S2 peaks while increasing Tmax, or liberate inorganic CO_2 and increase S3 and OI. Mineral matrix effects are important if TOC, S1, and S2 are low—an effect not significant in this study.

Solvent Extract Gross Composition

The amount and composition of solvent extractable bituminous material, including crude oil stains and petroleum fluid inclusions, was obtained by extracting the bitumen from the rock sample using the Soxhlet technique (Table 2). Solvent extracts were fractionated using packed column chromatography, following a method effectively similar to that published by Snowdon (1978). The resulting gross composition can be used to identify crude oil stains or to characterize source rock richness and maturity. Normalized solvent extract hydrocarbon (HC) yield, quoted in milligrams of extract per gram of organic carbon (mg/g TOC), is a richness indicator. HC yields of less than 30 mg/g TOC suggest no source rock potential. Those between 30 and 50 mg/g TOC suggest marginal potential. HC yields between 50 and 80 mg/g TOC show good potential. Greater values indicate excellent potential. Hydrocarbon percentage criteria for maturity are commonly independent of OM type and lithology. Stained samples are those with more than 55% HCs, and lower values are characteristic of petroleum source rocks if sufficient material is available, which is not the case for this study. Less than 20% HCs characterizes thermally immature sources; 25% to less than 45% HCs is the interval of marginal maturity; higher values occur during the the main HC generation stage.

Solvent Extract Molecular Composition

The extractable bitumen was de-asphalted by adding an excess of pentane (40 volumes) and then fractionating using open-column liquid chromatography. Saturate hydrocarbons were analysed using gas chromatography (GC) and gas chromatography-mass spectrometry (GCMS). A Varian 3700 FID gas chromatograph was used with a 30 m DB-1 column coated with OV-1 and helium as the mobile phase. The temperature was programmed from 50° C to 280° C at a rate of 4° C/min and then held for 30 min at the final temperature. The eluting compounds were detected and quantitatively determined using a hydrogen flame ionization detector. The resulting saturate fraction chromatograms (SFGC) were integrated using Turbochrom software. GCMS was performed in both single ion monitoring and full scan modes on both saturate and aromatic hydrocarbon fractions of solvent extracts, although only select saturate fraction compositional characteristics obtained from single ion monitoring experiments are reported here. Single ion monitoring GCMS experiments were performed on a VG 70SQ mass spectrometer with a HP gas chromatograph attached directly to the ion source (30 m DB-5 fused silica column used for GC separation), or under similar analytical conditions. The temperature, initially held at 100° C for 2 min, was programmed at 40° C/min to 180° C and at 4° C/min to 320° C, then held for 15 min at 320° C. The mass spectrometer was operated with a 70 eV ionization voltage, 300 mA filament emission current and interface temperature of 280° C. Terpane and sterane ratios reported herein were calculated using m/z 191 and m/z 217 and m/z 218 mass chromatograms.

REFERENCES

Clark, J. P., and Philp, R. P. (1989): Geochemical characterization of evaporite and carbonate depositional environments and correlation of associated crude oils in the Black Creek Basin, Alberta. *Bulletin of Canadian Petroleum Geology*, v. 37, no. 4., pages 401-416.

Eisbacher, G.H.(1974): Sedimentary history and tectonic evolution of the Sustut and Sifton basins, north-central British Columbia; *Geological Survey of Canada*, Paper 73-31, 57 pages.

Espitalie, J., Deroo, G. and Marquis, F. (1985): Rock Eval Pyrolysis and Its Applications. Preprint; Institut Francais du Petrole, Geologie No. 27299, 72 p. English translation of, La pyrolyse Rock-Eval et ses applications, Premiere, Deuxieme et Troisieme Parties, in *Revue de l'Institut Francais du Petrole,* v. 40, p. 563-579 and 755-784; v. 41, pages 73-89.

Evenchick, C.A. (1991): Geometry, evolution, and tectonic framework of the Skeena Fold Belt, north-central British Columbia; *Tectonics*, v. 10, page 527-546.

Evenchick, C.A., Poulton, T.P., Tipper, H.W., and Braidek, I. (2001): Fossils and facies of the northern two-thirds of the Bowser Basin, northern British Columbia; *Geological Survey of Canada,* Open File 3956.

Evenchick, C.A., Ferri, F., Mustard, P.S., McMechan, M., Osadetz, K. G., Enkin, R., Hadlari, T., and McNicoll, V. J. (2003): Recent results and activities of the Integrated Petroleum Resource Potential and Geoscience Studies of the Bowser and Sustut Basins project; in *Current Research, Geological Survey of Canada, A-13*, 11 pages.

Evenchick, C.A., Hayes, M.C., Buddell, K.A., and Osadetz, K.G. (2002): Vitrinite reflectance data and preliminary organic maturity model for the northern two thirds of the Bowser and Sustut basins, north-central British Columbia. Geological Survey of Canada, Open File 4343 and *B.C. Ministry of Energy and Mines*, Petroleum Geology Open File 2002-1.

Evenchick, C.A., Osadetz, K.G., Ferri, F., Mayr, B., and Snowdon, L. R., (in prep.): A Natural Seepage of Biogenic Methane in the Intermontane Belt (Bowser Basin) of the Canadian Cordillera. *Bulletin of Canadian Petroleum Geology,* v. XX, no. X., p. XXX-XXX.

Evenchick, C.A. and Thorkelson, D.J. (in press): Geology of the Spatsizi River map area, north-central British Columbia, *Geological Survey of Canada Bulletin* 577.

Gordy., P.L., Frey, F.R., and Norris, D.K. (1977): Geological guide for the C.S.P.G. 1977 Waterton - Glacier Park Field Conference. - *Candian Society of Petroleum Geologists*, Calgary.Grantham, P. J., and Wakefield, L. L.(1988): Variations in the sterane carbon number distributions of marine source rock derived crude oils through geological time, *Organic Geochemistry*, v. 12, no. 1, pages 61-73.

Hannigan P. K., Lee, P. J. and Osadetz, K. G. (1995): Oil and gas resource potential of the Bowser-Whitehorse area of British Columbia, *Report to BCEMR,* March 1995, 72 pages.

Koch, N. G. (1973): Central Cordilleran Region; in R. G. McCrossan ed., The Future Petroleum Provinces of Canada - Their Geology and Potential, *Canadian Society of Petroleum Geologists*, Memoir 1, pages 37-71.

MacKay, P. A., Varsek, J. L., Kubli, T. E., Dechesne, R. G., Newson, A. C., Reid, J. P. (1996): Triangle Zones and Tectonic Wedges. *Bulletin of Canadian Petroleum Geology,* v.44, No.2, pages. I-1-I-5.

Osadetz, K.G., Evenchick, C. A. , Ferri, F. , Stasiuk, L. D., and Wilson, N. S. F. (2003a): Indications for effective petroleum systems in Bowser and Sustut basins, north-central British Columbia. *in* Geological fieldwork, 2002; *B.C. Ministry of Energy and Mines*, Paper 2003-1, pages 257-264.

Osadetz, K.G., Snowdon, L.R., and Obermajer, M. (2003b): ROCK-EVAL/TOC results from 11 Northern British Columbia boreholes. *Geological Survey of Canada*, Open File 1550 and *B.C. Ministry of Energy and Mines*, Petroleum Geology Open File 2003-1 (CD-ROM).

Osadetz, K. G., Brooks, P. W., and Snowdon, L. R. (1992): Oil families and their sources in Canadian Williston Basin (southeastern Saskatchewan and southwestern Manitoba). *Bulletin of Canadian Petroleum Geology*, 40, pages 254-273.

Peters, K. E. (1986): Guidelines for evaluating petroleum source rock using programmed pyrolysis. *American Association of Petroleum Geologists*, Bulletin, v. 70/3, p. 318-329.

Peters, K. E., and Moldowan, J. M. (1993): *The Biomarker Guide,* Prentic-Hall, Englewood Cliffs, N. J., 363 pages.

Peters, K. E., and Moldowan, J. M. (1991): Effects of source, thermal maturity, and biodegradation on the distribution and isomerization of homohpanes in petroleum. *Organic Geochemistry*, v. 17, no. 1, pages 47-61.

Rubinstein, I., Sieskind, O., and Albercht, P. (1975): Rearranged sterenes in a shale: occurrence of simulated formation. *Journal of the Chemical Society*, Perkin Transactions I, pages 1833-1835.

Seifert, W. K., and Moldowan, M. J. (1986): Use of biological markers in petroleum exploration; in R. B. Johns (ed.), Biological Markers in the Sedimentary Record. Amsterdam: Elsevier, pages 261-290.

Seifert, W. K., and Moldowan, J. M. (1981): Paleoreconstruction of biological markers. *Geochimica et Cosmochimica Acta,* v. 45, pages 783-794.

Seifert, W. K., and Moldowan, J. M. (1978): Applications of steranes, terpanes and monoaromatics to the maturation, migration and source of crude oils. *Geochimica et Cosmochimica Acta,* v. 42, pages 77-95.

Sieskind, O., Joly, G., and Alberecht, P. (1979): Simulation of the geochemical transformation of sterols: superacid effect of clay minera. *Geochimica et Cosmochimica Acta,* V. 43, pages 1675-1679.

Snowdon, L. R. (1978): Organic geochemistry of the Upper Cretaceous/Tertiary delta complexes of the Beaufort Mackenzie Sedimentary Basin. *Geological Survey of Canada,* Bulletin 291.

Tipper, H.W. and Richards, T.A. (1976): Jurassic stratigraphy and history of north-central British Columbia*; Geological Survey of Canada,* Bulletin 270, 73 pages.

Tissot, B. P., and Welte, D. H. (1978): Petroleum formation and occurrence; Springer-Verlag, Berlin, 538 pages.

Volkman, J. K., and Maxwell, J. R. (1986): Acyclic isoprenoids as biological markers; in R. B. Johns (ed.), Biological Mrakers in the Sedimentary Record. Methods in Geochemistry and Geophysics, 24, Amsterdam: Elsevier, pages 1-42.

Waples, D. W., and Machihara, T. (1990): Application of sterane and triterpane biomarkers in petroleum exploration. *Bulletin of Canadian Petroleum Geology*, v. 38, pages 357-380.

Welte, D. H., and Waples, D. W. (1973): Uber die Bevorzugung geradzahliger n-Alkane in *Sedimentgesteinen. Naturwissenschaften,* v. 60, pages 516-517.

STRUCTURAL RELATIONSHIP BETWEEN THE LABERGE GROUP AND SINWA FORMATION ON COPPER ISLAND, SOUTHERN ATLIN LAKE, NORTHWEST BRITISH COLUMBIA

by Kara L. Wight, Joseph M. English and Stephen T. Johnston

University of Victoria

KEYWORDS: king salmon thrust, whitehorse trough, llewellyn fault, atlin lake, copper island fault

INTRODUCTION

The Whitehorse Trough is an elongate Mesozoic arc-marginal volcano-sedimentary basin that extends from central Yukon to Dease Lake in northwest British Columbia (Figure 1). The Whitehorse Trough contains volcaniclastic and carbonate strata of the Upper Triassic Stuhini Group and siliciclastic strata of the Lower to Middle Jurassic Laberge Group (Figure 2). Major structures within the southern Whitehorse Trough include the Llewellyn and Nahlin Faults and the southwest-vergent King Salmon Thrust.

The King Salmon Thrust carries the Upper Triassic Sinwa Formation (Stuhini Group) and Lower Jurassic Inklin Formation (Laberge Group) in its hanging wall over top of more proximal facies of the Laberge Group to the southwest (Souther, 1971; Figure 1). Regional mapping suggests that the King Salmon Thrust extends northwards into the southern Atlin Lake region (e.g., Wheeler and McFeely, 1991). The major structure in the Atlin Lake region is, however, the Llewellyn Fault (Wheeler and McFeely, 1991), a steep north-northwest-trending strike-slip fault of largely Triassic to Cretaceous age (Mihalynuk, 1999). The fault that marks the southwest limit of the Laberge Group in the southern Atlin Lake region (herein called the Copper Island Fault) has previously been interpreted to be the northern extension of the King Salmon Thrust. Both the King Salmon Thrust and the Copper Island Fault trend northwest. The main goal of this paper is to determine whether the Copper Island Fault in the southern Atlin Lake region is an extension of the King Salmon Thrust or whether it is a separate and possibly younger structure. To address this question, a detailed geological mapping program was undertaken on Copper Island in southern Atlin Lake. Mapping focused on determining the nature of the Copper Island Fault and its relationship to other regional structures and on documenting the structure and stratigraphy of adjacent strata of the Laberge Group.

The goals of this paper are to (1) describe the stratigraphy and structure of Copper Island, (2) construct and discuss the structural cross sections for Copper Island, and (3) establish whether the Copper Island Fault is a northern continuation of the King Salmon Thrust (as previously assumed) or a separate entity.

GEOLOGICAL BACKGROUND

Early Mesozoic arc-marginal volcano-sedimentary rocks of the Whitehorse Trough include conglomerate, siltstone, sandstone, and greywacke that were deposited in a deep-marine setting of submarine fans and conglomeratic fan deltas (e.g., Dickie and Hein, 1995; Johannson et al., 1997). Laberge Group sediments were derived from the unroofing of the Stikine magmatic arc and Yukon-Tanana Terrane to the west and southwest (Dickie and Hein, 1995; Johnston et al., 1996; Johannson et al., 1997) and are divisible into a distal sandstone facies in the northeast (Inklin Formation) and a proximal conglomeratic facies in the southwest (Souther, 1971; Monger et al., 1991).

The marine Inklin Formation consists of a roughly 3 km thick succession of interbedded greywacke, shale, and siltstone with minor conglomerate (Johannson et al., 1994), interpreted as the distal facies of coalescing submarine fans and conglomeratic fan deltas (Dickie and Hein, 1995). In the southern Atlin Lake area, the Inklin Formation ranges in age from Early Sinemurian to Late Pliensbachian (Johannson et al., 1997). In the southern Whitehorse Trough, the conglomeratic facies of the Laberge Group onlaps the Upper Triassic volcanic and carbonate rocks of the Stuhini Group (Souther, 1971). In the southern Atlin area, the distal Laberge Group facies are faulted against the Stuhini Group strata by the Copper Island Fault, and the proximal conglomeratic facies of the Laberge Group are missing.

The Whitehorse Trough was tectonically shortened during the Middle Jurassic as a result of a collisional event that involved the westward emplacement of the Cache Creek Terrane over the Whitehorse Trough and Stikine Terrane (Mihalynuk, 1999). Structures of the central Whitehorse Trough are dominated by southwest-vergent folds and thrusts (English et al., 2003). The age of the fold and thrust belt development is constrained as mainly Middle Jurassic on the basis of biostratigraphy (Tipper, 1978) and between 174 and 172 Ma based on isotopic cooling age determinations (Mihalynuk et al., in press).

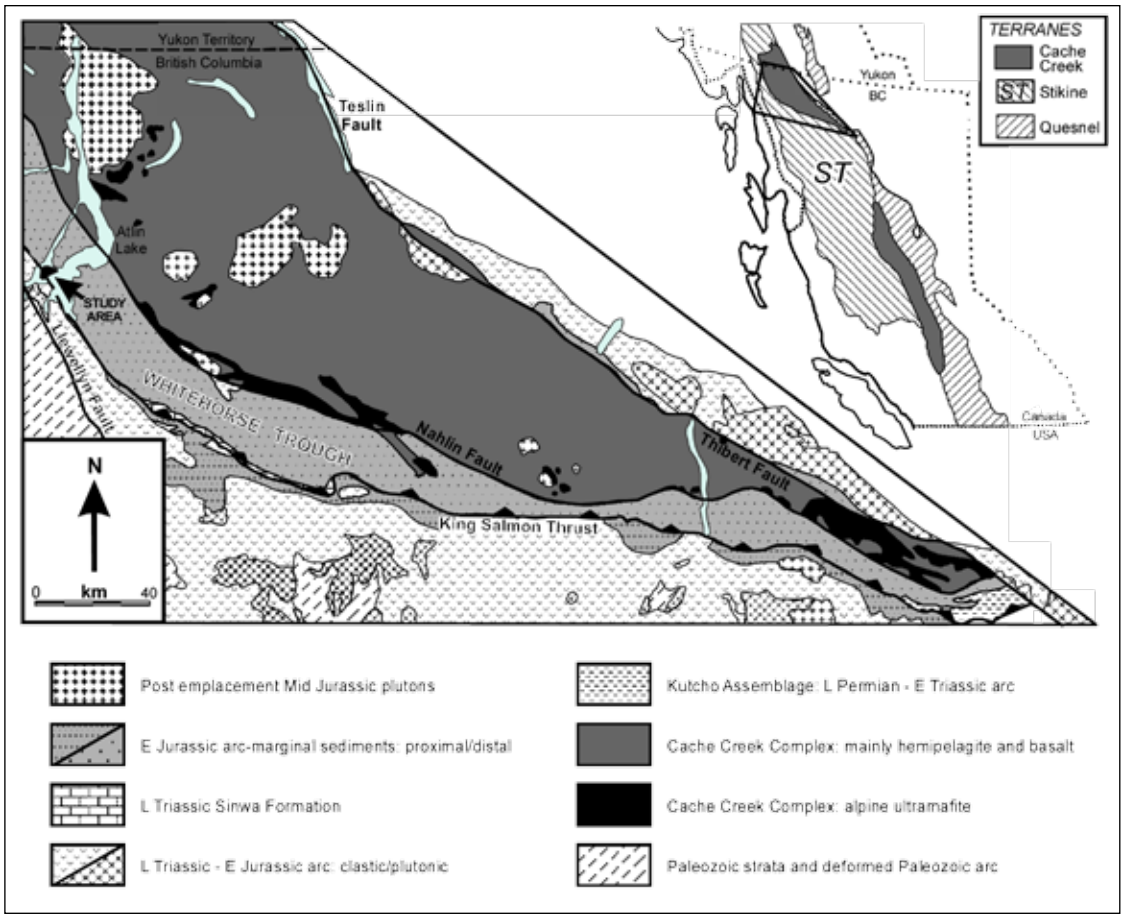

Figure 1. Location of Copper Island study area in southern Atlin Lake.

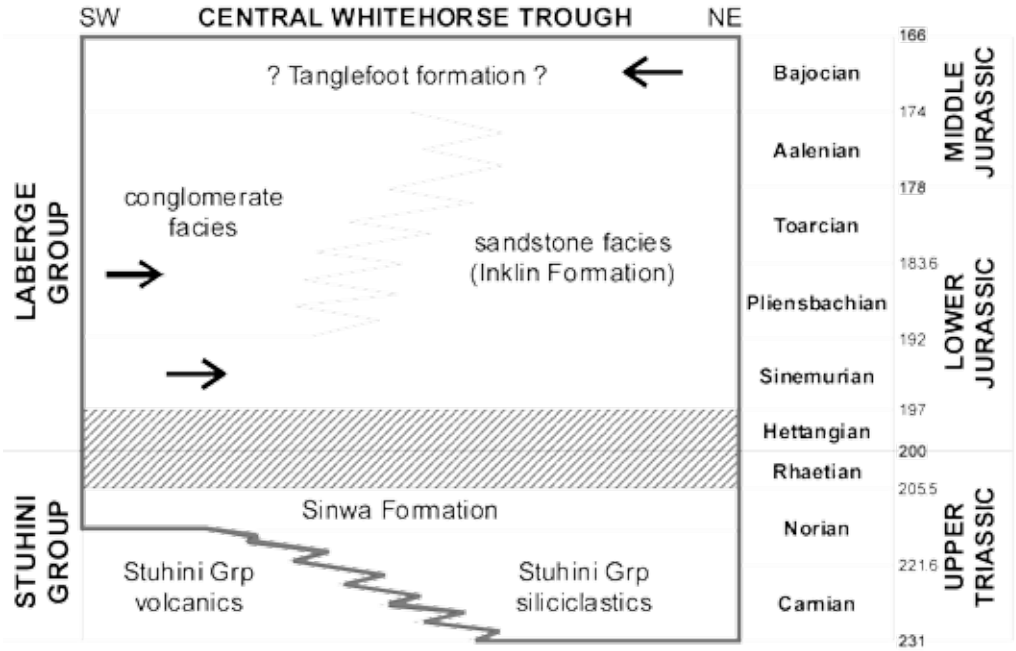

Figure 2. Stratigraphy of Laberge Group within the Whitehorse Trough. Arrows indicate paleoflow direction. Tanglefoot Formation is a chert and pebble conglomerate from the Cache Creek Terrane in Yukon (source: English et al., in review).

Two major thrust faults that developed during collision are the King Salmon Thrust and the Nahlin Fault. The Nahlin Fault bounds the northeast limit of the Whitehorse Trough at the surface (Aitken, 1959) and carries Cache Creek Terrane in its hanging wall. In the southern Whitehorse Trough, the King Salmon Thrust carries the Upper Triassic Sinwa Formation and Lower Jurassic Inklin Formation in its hanging wall over more conglomeratic facies of the Laberge Group in its footwall. The King Salmon Thrust occurs near the base of the Sinwa Formation, and subsidiary thrust faults splay from and mimic the trend and vergence of this major structure (English et al., 2003).

The northern extent of the King Salmon Thrust is, however, uncertain. In the area southeast of Atlin Lake, Early Eocene Sloko Group volcanic rocks conceal the northern continuation of the King Salmon Thrust (Aitken, 1959; Mihalynuk, 1999). A similarly positioned fault, the Copper Island Fault, occurs on the northwest side of the exposed Sloko Group through Atlin Lake and was previously interpreted as the King Salmon Thrust. The Copper Island Fault can be distinguished from the King Salmon Thrust based on its geometry and relationship to adjacent rocks. This fault may instead represent a splay of the Llewellyn Fault. The possibility that the Copper Island Fault is a strike-slip splay was investigated.

STUDY AREA

The structure and stratigraphy of the Laberge Group on Copper Island in southern Atlin Lake were used to evaluate the Copper Island Fault. The study area covers a 30 km2 region straddling the Copper Island Fault. This fault, which separates the Sinwa Formation and Inklin Formation, was mapped from the southwest shore of Atlin Lake, across Second Narrows and Copper Island, to the western shore of Torres Channel (Figure 3). At its western extent, the Copper Island Fault is plugged by a Late Cretaceous intrusion in the vicinity of Cathedral Mountain (Mihalynuk, 1999).

STRATIGRAPHY

The study area is underlain by volcanic, volcaniclastic, and carbonate strata of the Upper Triassic Stuhini Group and Lower Jurassic Inklin Formation (Figures 2 and 3). Volcanic rocks of the Stuhini Group are a minor component of the area and outcrop on the southwest corner of Copper Island.

The Norian Sinwa Formation of the Stuhini Group consists of light to dark grey massive to bedded limestone. Fossiliferous undulating light grey beds are 0.2 to 5 cm thick and interbedded with 0.25 to 2 cm thick beds of dark grey limestone. Some of these shallow marine carbonates have an extensive lattice of calcite veining and a marbled appearance near the contact zone with the Laberge Group. Some samples were fetid. In the Second Narrows region, limestone is intercalated with Late Triassic volcaniclastic strata and pyroclastic rocks of the Stuhini Group (Mihalynuk, 1999). The fault zone extending across Second Narrows marks the unexposed contact between the Sinwa Formation limestone and the Laberge Group.

Early to Late Pliensbachian greywacke, siltstone, argillite, sandstone, and minor conglomerate are characteristic of the Inklin Formation within the Laberge Group. The most common sediments on Copper Island consisted of medium grey to dark grey-green massive to graded wacke beds (more than 15% matrix) that range from 1.5 to 100 m thick, with the thickest beds exposed on the northwest shore of Copper Island. Two to three metre thick beds of these lithic wackes are commonly interbedded with argillite, siltstone and sandstones. Flame structures and convoluted and planar contacts mark the boundaries between beds. The greywacke consists of angular, poorly sorted medium to coarse sand in a 15% to 70% mud matrix. Clasts include lithic clasts (predominantly volcanic rock), feldspar, quartz, biotite, and less than 15% mafic minerals. Most beds were right way up; however, bedding of greywacke and siltstone is overturned in the central portion of Copper Island. Veins of calcite are found in the vicinity of fault zones, and orange weathering is common.

Within the Inklin Formation, there is a siliciclastic unit of medium- to coarse-grained quartz-rich wacke and sandstone that occurs as 100+ m thick beds, coarsens upwards, and displays dark orange weathering. Rip-up clasts (approximately 20 by 40 cm) and lenses of siltstone commonly are contained within the sandstone.

The 1 to 10+ m thick siltstone occurs as black to medium rusty brown 0.5 to 3 cm laminations. The bedding varies from undulating and convoluted to planar. The siltstone is subordinate within wacke-dominant sequences and is commonly interbedded with coarser orange-brown fine-grained sandstone. Bioturbation, orange weathering, and lenses of sandstone are common.

Pebble to cobble conglomerate occurs as one minor 20 m thick bed on southeast Copper Island. The clasts are dominantly rounded to subrounded volcanics, greywacke, and shale. This unit was not found outcropping in any other portion of the island. The absence of the conglomeratic facies of the Laberge Group in the southern Atlin area is different from the stratigraphy found in the footwall of the King Salmon Thrust in the Taku River area, where coarse conglomeratic facies of the Laberge Group are dominant (Souther, 1971).

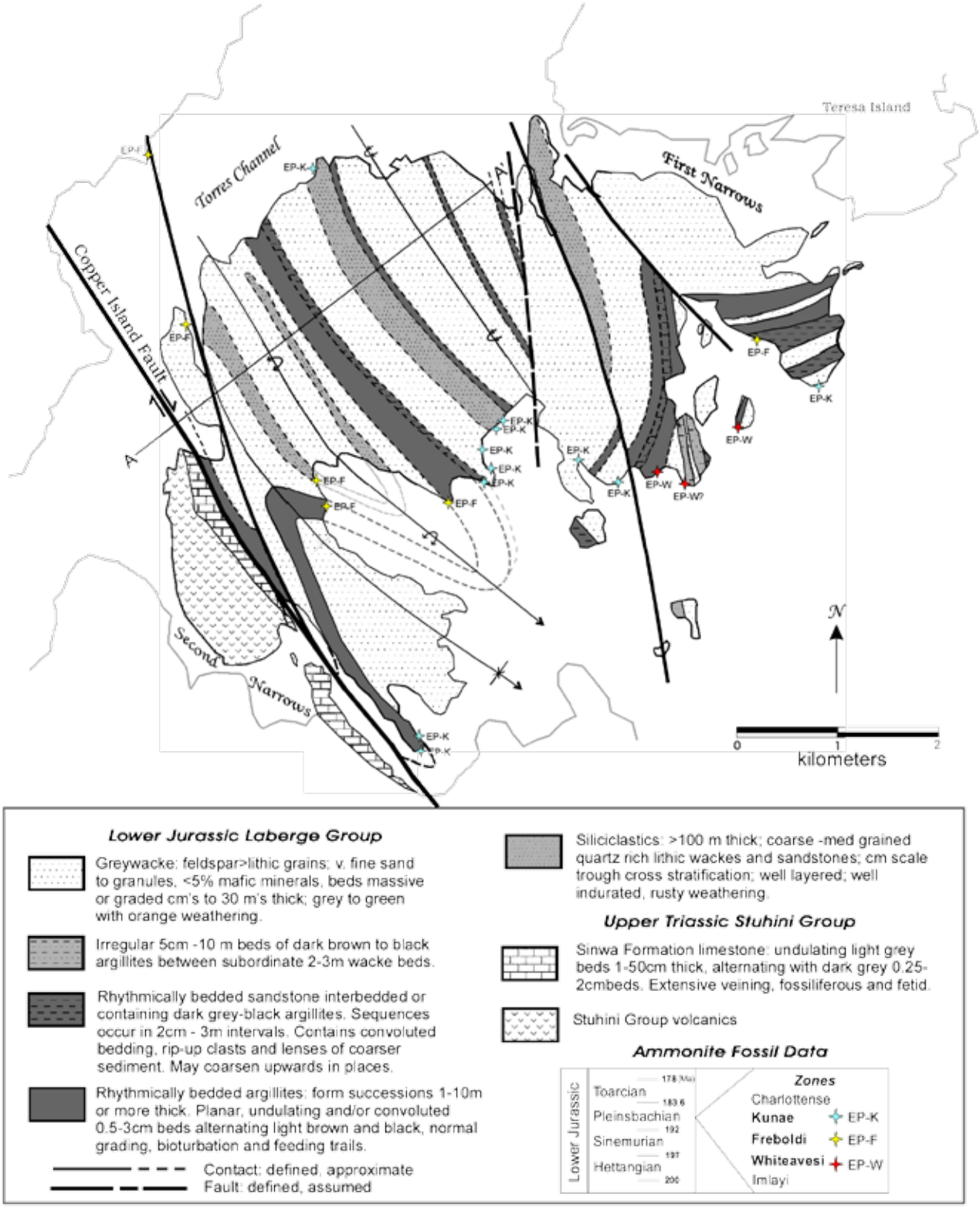

Figure 3. Bedrock geology map of Copper Island.

STRUCTURE

Copper Island is characterised by northwest-southeast trending folds and faults. One shallowly southeast-plunging syncline occurs on southwest Copper Island adjacent to the Copper Island Fault. An overturned anticline in central Copper Island shallowly plunges to the southeast (Figure 4 and 5). Minor folds perpendicular to the Copper Island Fault occur along the ridge top northeast of Second Narrows. A tight minor antiform on a centrally located island off the southeast shore of Copper Island could not be followed onto Copper Island.

The Copper Island Fault separates the Sinwa Formation to the southwest from the younger Inklin Formation to the northeast. Laberge Group siltstone adjacent to the fault contains Late Pliensbachian (Kunae Zone) ammonites (Johannson et al., 1997), and previous dating of the Sinwa Formation concludes the age to be Norian (Upper Triassic) (Souther, 1971).

Bedding attitude is variable adjacent to the Copper Island Fault. The Sinwa Formation limestone dips from subvertical to shallow in multiple orientations (e.g., 138/79; 260/60; 356/011). The Inklin strata are moderately shallow and dip inconsistently (e.g., 018/23; 226/40; 233/52; 336/54). Variability in bedding may be due to local deformation along the Copper Island Fault. The Copper Island Fault is a subvertical structure trending northwest through Second Narrows and Copper Island (Figure 3 and 5). The linear fault zone is 175 to 200 m wide and crosscuts different-aged bedding of adjacent strata. Extensively fractured rocks and slickenfibre lineations that shallowly plunge to the southeast (17°→148° and 18°→126°) are observed in the Copper Island Fault zone. The shallow orientation of the slickenfibres may indicate a largely translational motion on the Copper Island Fault.

Additional post Mid-Jurassic linear faults divide the northeast portion of Copper Island and crosscut Laberge Group bedding and the northwest-trending folds. The rocks in these faulted areas are shattered or gouged, and the faults form linear features on air photographs and commonly have intrusions along the margins of the fault zone. Intrusions often are in or directly next to narrow linear bays that formed along the fault zones. The younger faults variably cut across the folds formed in the Mid-Jurassic (Tipper, 1978; Mihalynuk, in press). Several other faults cut across Copper Island on the eastern shore, variably trending 270° to 330°. Variable orientations and the number of faults added much complexity to structural interpretation of the east portion of Copper Island. In detail, thick beds may disappear over short distances and are thought to be interrupted by a fault rather than pinched out stratigraphically.

Subvertical strike-slip faults are common in the southern Atlin Lake area and are exposed along Atlin Lake on Bastion and Griffith Islands (English et al., in review). Additionally, the subvertical Llewellyn Fault trends northwest across Llewellyn Inlet. Mihalynuk (1999) documented abundant vertical to subvertical northeast-trending faults of sinistral and dextral motion with less than 10 m offset in the Tagish Lake Area. Regionally, the subvertical Copper Island Fault continues to separate the Upper Triassic Stuhini Group and the Lower Jurassic Laberge Group to the northwest and merges with the Llewellyn Fault near Tagish Lake (based on bedrock geology map of Mihalynuk, 1999). Therefore, the Copper Island Fault represents a splay on the Llewellyn strike slip system rather than a continuation of the King Salmon Thrust.

DISCUSSION

The Copper Island Fault is commonly interpreted as an extension of the King Salmon Thrust (Wheeler and McFeely, 1991); however, these two faults may be independent structures.

In the central portion of the Whitehorse Trough near the Taku River, the Sinwa and Inklin Formations occur northeast of and in the hanging wall of the King Salmon Thrust and are carried over younger Lower Jurassic conglomeratic facies of the Laberge Group to the west (Souther, 1971). The Copper Island Fault, however, juxtaposes older, Upper Triassic Sinwa Formation limestones to the southwest, against younger, Late Pliensbachian Laberge Group strata to the northeast; Sinemurian and Early Pliensbachian strata are absent across the fault. The cutting out and structural thinning of the stratigraphic section and the juxtaposition of younger rocks to the northeast against older rocks to the southwest is the opposite of what would be expected if the Copper Island Fault were a west-verging thrust fault.

Arguably, the history of the King Salmon Thrust is similar to the history of the Nahlin Fault. The Nahlin Fault bounds the northeast margin of the Whitehorse Trough (Figure 1) and originated as a thrust fault during emplacement of the Cache Creek Terrane (Mihalynuk, 1999). As the Nahlin Fault extends into Atlin Lake area, the structure becomes vertical and displays dextral wrench displacement, perhaps due to reactivation between about 55 and 46 Ma (Mihalynuk et al., 2003). Thus, the Copper Island Fault could represent younger strike-slip motion on a northern continuation of the King Salmon Thrust; however, this remains problematic because the age relation of stratigraphy across Copper Island Fault differs from that of the King Salmon Thrust.

The steep nature of the Copper Island Fault, the variable bedding adjacent to the structure, the shallowly plunging slickenfibres, and the crosscutting of beds all suggest a translational strike-slip motion for the Copper Island Fault. In addition, the well-developed fold and thrust belt characteristic of the southern Whitehorse Trough is not seen in

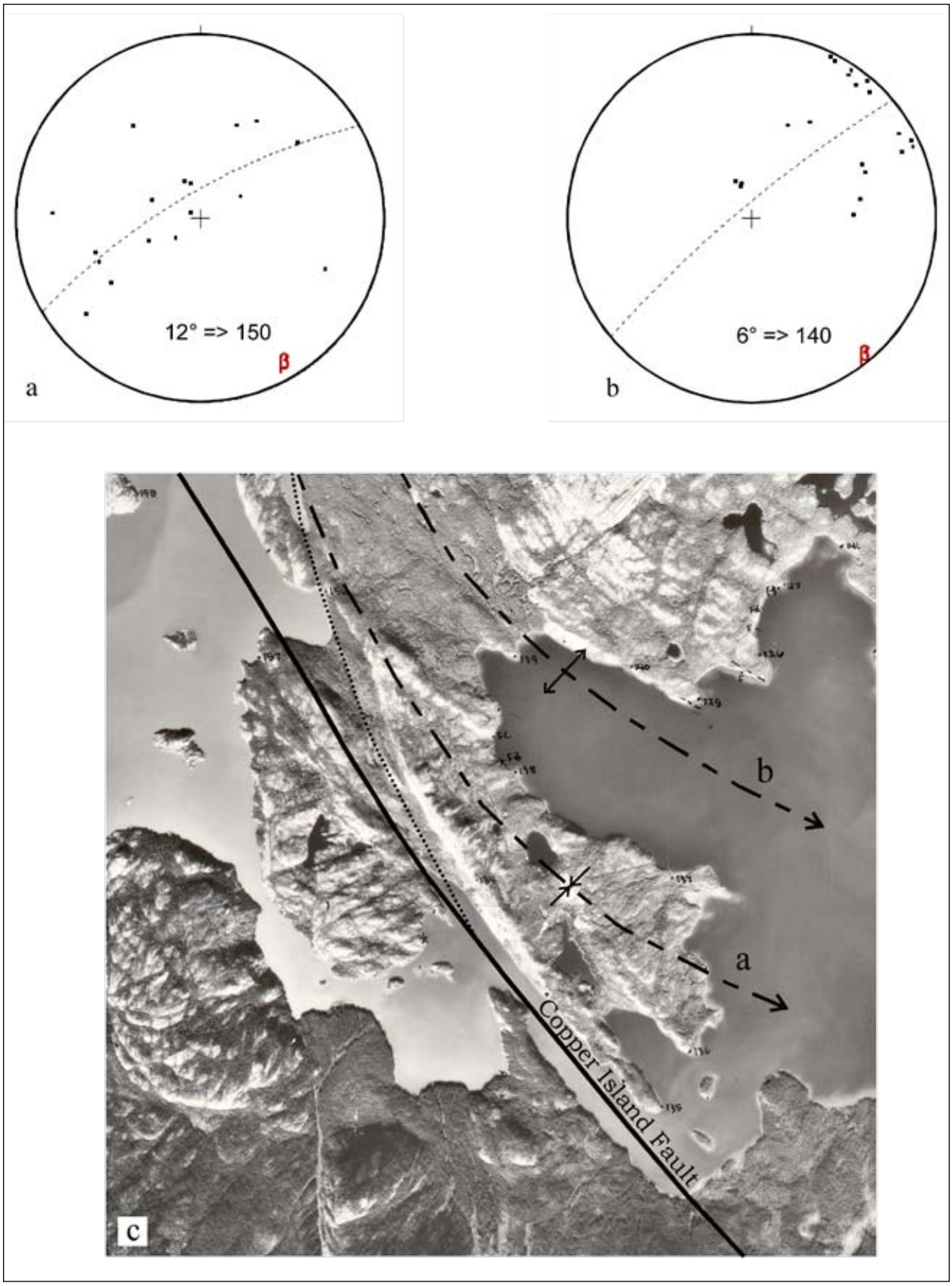

Figure 4. Syncline (a) and overturned anticline (b) plunging shallowly towards the southeast located northeast of Copper Island Fault. Compare to air photo (c) which shows the plunging nature of syncline (a) (source: BC5624 059).

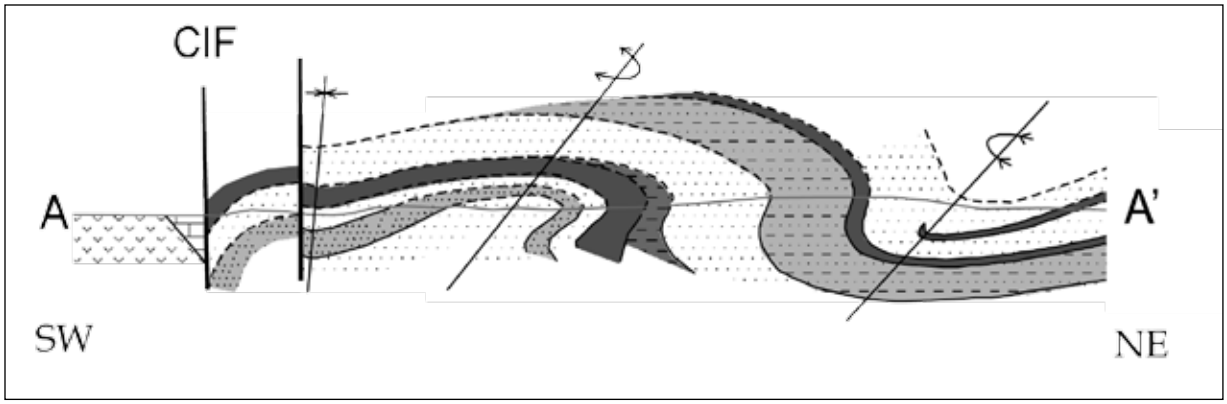

Figure 5. Cross section of western Copper Island. Central folds are overturned and have undergone further deformation perpendicular to fold axis. Note the vertical-subvertical Copper Island Fault in the SW and fault splay slightly NE of the CIF. See Figure 3 for section line and legend.

southern Atlin Lake (English et al., in review), and local and regional faults in the area are dominantly strike-slip in nature (e.g., Llewellyn Fault, Figure 1). Given that the subvertical Copper Island Fault can be traced to the northwest, continuing to separate the Stuhini Group and the Laberge Group until it merges with the Llewellyn Fault near Tagish Lake, the Copper Island Fault represents a splay of the Triassic to Cretaceous Llewellyn strike-slip system rather than a northern continuation of the King Salmon Thrust.

IMPLICATIONS FOR HYDROCARBONS

In the Taku River area, the Sinwa Formation carbonates extend to depth beneath the Laberge Group in the hanging wall of the shallow-angle King Salmon Thrust and may be a potential source rock for hydrocarbon accumulations. However, this relationship is not as clear in the southern Atlin Lake and Copper Island areas. The steep angle fault separating the Sinwa Formation from the Laberge Group may have developed during strike-slip motion, and the extent of the Sinwa Formation, and concomitant source rock potential, in the subsurface beneath the Laberge Group in the Atlin Lake area remains unconstrained (Figure 5).

CONCLUSIONS

In the southern Atlin Lake region, the subvertical Copper Island Fault separates the Upper Triassic Sinwa Formation from Late Pliensbachian sediments of the Inklin Formation. The Copper Island Fault has previously been interpreted to represent the northwestern continuation of the King Salmon Thrust. The geometry and stratigraphic relationship across the fault suggest that the Copper Island Fault is a separate and younger feature from the King Salmon Thrust and is probably characterised by strike-slip displacement. The King Salmon Thrust carries the Sinwa and Inklin Formations in its hanging wall and places them above the proximal conglomerate facies of the Laberge Group. These conglomerates are not exposed in the Atlin Lake area, and the subvertical Copper Island Fault does not display an older-over-younger relationship. Moreover, the basal Sinemurian strata of the Inklin Formation are missing across the fault. The Copper Island Fault can be traced to the northwest until it merges with the Llewellyn Fault; therefore, the Copper Island Fault represents a splay of the Llewellyn strike-slip system rather than a northern continuation of the King Salmon Thrust.

REFERENCES

Aitken, J. D. (1959): Atlin map-area, British Columbia; *Geological Survey of Canada*, Memoir 307, 89 pages.

Dickie, J. R. and Hein, F. J. (1995): Conglomeratic fan deltas and submarine fans of the Jurassic Laberge Group, Whitehorse Trough, Yukon Territory, Canada: fore-arc sedimentation and unroofing of a volcanic island arc complex; *Sedimentary Geology*, Volume 98, pages 263-292.

English, J. M., Johannson, G. G., Johnston, S. T., Mihalynuk, M. G., Fowler, M. and Wight, K. L. (in review): Structure, stratigraphy and hydrocarbon potential of the central Whitehorse Trough, northern Canadian Cordillera; *Bulletin of Canadian Petroleum Geology*.

English, J. M., Mihalynuk, M. G., Johnston, S. T., Orchard, M. J., Fowler, M. and Leonard, L. J. (2003): Atlin TGI, Part VI: Early to Middle Jurassic sedimentation, deformation and a preliminary assessment of hydrocarbon potential, central Whitehorse Trough and northern Cache Creek terrane; *in* Geological Fieldwork 2002; *B.C. Ministry of Energy and Mines*, Paper 2003-1, pages 187-201.

Johannson, G. G. (1994): Provenance constraints on Early Jurassic evolution of the northern Stikinian arc: Laberge Group, Whitehorse Trough, northwestern British Columbia; M.Sc. thesis; *University of British Columbia*, 297 pages.

Johannson, G. G., Smith, P. L. and Gordey, S. P. (1997): Early Jurassic evolution of the northern Stikinian arc: evidence from the Laberge Group, northwestern British Columbia; *Canadian Journal of Earth Sciences*, Volume 34, pages 1030-1057.

Mihalynuk, M. G. (1999): Geology and mineral resources of the Tagish Lake area (NTS 104M/8, 9, 10E, 15 and 104N/12W) northwestern British Columbia; *B.C. Ministry of Energy, Mines and Petroleum Resources*, Bulletin 105, 217 pages.

Mihalynuk, M. G., Erdmer, P., Ghent, E. D., Cordey, F., Archibald, D., Friedman, R. M. and Johannson, G. G. (in press): Subduction to obduction of coherent French Range blueschist - In less than 2.5 Myrs?; *Geological Society of America Bulletin*.

Mihalynuk, M. G., Johnston, S. T., English, J. M., Cordey, F., Villeneuve, M. E., Rui, L. and Orchard, M. J. (2003): Atlin TGI, Part II: Regional geology and mineralization of the Nakina area (NTS 104N/2W and 3); *in* Geological Fieldwork 2002, *B.C. Ministry of Energy and Mines*, Paper 2003-1, pages 9-37.

Monger, J. W. H., Wheeler, J. O., Tipper, H. W., Gabrielse, H., Harms, T., Struik, L. C., Campbell, R. B., Dodds, C. J., Gehrels, G. E. and O'Brien, J. (1991): Upper Devonian to Middle Jurassic assemblages - Part B. Cordilleran terranes; *in* Geology of the Cordilleran Orogen in Canada, The Geology of North America, Gabrielse, H. and Yorath, C. J., Denver, Colorado, *Geological Society of America*, pages 281-327.

Souther, J. G. (1971): Geology and mineral deposits of Tulsequah map-area, British Columbia; *Geological Survey of Canada*, Memoir 362, 84 pages.

Tipper, H. W. and Richards, T. A. (1976): Jurassic stratigraphy and history of north-central British Columbia; *in* Current Research Part A, *Geological Survey of Canada*, Paper 78-1a, pages 25-27.

Wheeler, J. O. and McFeely, P. (1991): Tectonic assemblage map of the Canadian Cordillera and adjacent portions of the United States of America; *Geological Survey of Canada,* Open File 1712A.

UNIQUE ASPECTS OF BRITISH COLUMBIA COALBED METHANE GEOLOGY: INFLUENCES ON PRODUCEABILITY

By Barry Ryan[1]

KEYWORDS: Elk Valley, Crowsnest and Peace River coalfields; gas composition; Lewis Thrust; deformation history.

INTRODUCTION

The majority of literature refers to the extraction of coalbed methane (CBM) from coal, which is not scientifically correct as the gas extracted from coal is a mixture of methane, carbon dioxide, and other gases. The British Columbia government is adopting the term coalbed gas (CBG). The abbreviations CBM and CBG both refer to the commercial gas extracted from coal at depth. To avoid confusion with existing scientific literature, this paper uses the term CBM.

Based on the amount of public data available, British Columbia is still in the grassroots stage of CBM exploration. In the last few years, companies have drilled a number of holes in southeast, northeast, and central British Columbia. Most of the drilling was done as part of experimental schemes, which provide a three-year confidentiality period, and consequently most of the information is still confidential. This paper therefore relies in part on coal rather than CBM data and on speculation as input for a discussion of influences of CBM geology on produceability. Under this general topic a number of observations or ideas are developed; they are related only in that they may all help in delineating prospective CBM areas.

Most of the coalfields in British Columbia have experienced some level of deformation. It is very important to understand the timing of coal maturation relative to deformation. In the simplest context, one should know whether structural traps were formed before or after generation of thermogenic methane. In the southeast of the province, the Elk Valley and Crowsnest coalfields (Figure 1) form part of the Lewis Thrust sheet, and this somewhat unique macrotectonic environment should be considered when assessing the CBM characteristics of the coalfields. This leads to a provisional comparison of the structural setting between the Peace River in the northeast and the southeastern coalfields. Finally, one of the most important aspects of CBM produceability is the recent tectonic history of coalfields and how it may improve permeability and interrelate with coal properties.

COMMENTS ON THE TIMING OF DEFORMATION AND COAL MATURATION

Coal, more than any other rock, changes during maturation. The main change is shrinkage, at first associated with loss of water, then with loss of carbon dioxide, and finally with loss of methane. There are a number of experimental ways of determining mass lost during maturation, but it can also be estimated from standard analyses of coals of different ranks. In the latter case, it is assumed that the fixed carbon component of a proximate analysis remains constant and that coal shrinkage is caused by loss of water and volatile matter. This is obviously only an approximation of what happens as coal rank increases; however, it enables a useful plot to be developed (Figure 2), which indicates that most of the water loss and coal shrinkage occur in the rank range defined by mean maximum vitrinite reflectance (Rmax) values of 0.4% to 0.7% (also represented by the transition from sub-bituminous to high-volatile bituminous). A second period of rapid shrinkage corresponds to the expulsion of thermogenic methane at a rank of about Rmax = 0.9%.

During the two periods of rapid shrinkage (Figure 2), seams are expelling water and volatile matter and may become overpressured. Under these conditions, especially during the first period, seams are most susceptible to bedding-parallel slip and thrusting. If deformation starts when seams are in the rank window Rmax = 0.4% to 0.7%, then pervasive deformation may well be localized in seams, in part because of overpressuring. Seams will be extensively sheared and may not develop cleats, or pre-existing cleats may be destroyed. Methane generated as rank continues to increase may have structural traps available, but permeability in seams may be low. On the other hand, if deformation occurs when the coal has reached higher ranks, then it is less likely to be as pervasive within seams, and pre-existing cleats may survive. Methane generated prior to development of structural traps may be lost as it is expelled with increasing rank.

The two periods of matrix shrinkage indicated in Figure 2 may correspond to cleat development. The earlier one is caused in part by compaction and loss of surface water, with some loss of CO_2 from the coal matrix. This shrinkage

[1] *Resource Development and Geosciences Branch, B.C. Ministry of Energy and Mines, barry.ryan@gems4.gov.bc.ca*

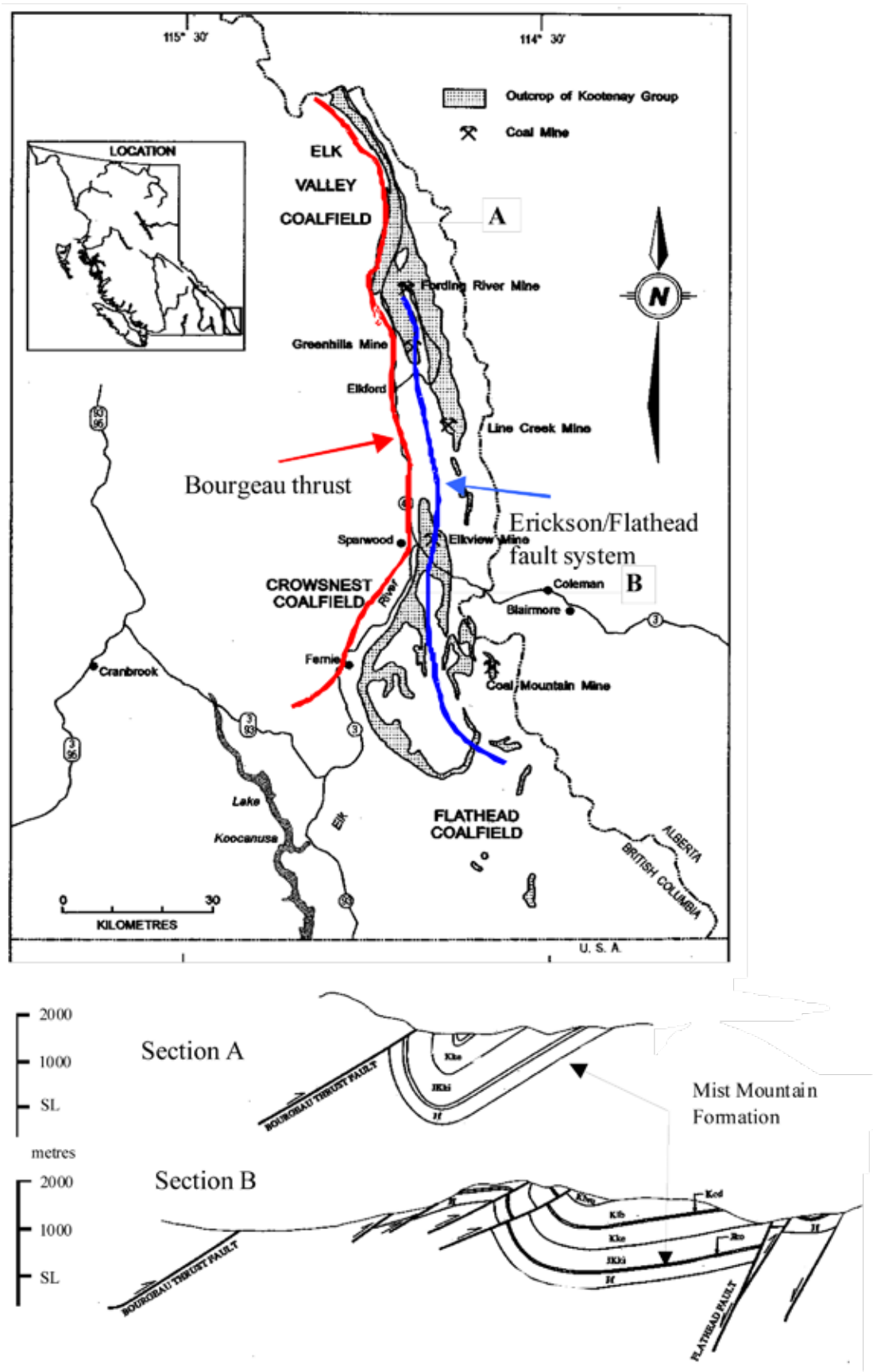

Figure 1. Structural setting of the Elk Valley and Crowsnest coalfields.

probably forms widely spaced cleats, because coal at this rank still contains, in part, a vegetation structure that will hinder the formation of closely spaced cleats. At increased rank (about Rmax = 0.9%), the coal goes through another period of rapid contraction that is caused by loss of methane from vitrinite. At this time, closely spaced cleats may form in vitrain-rich bands.

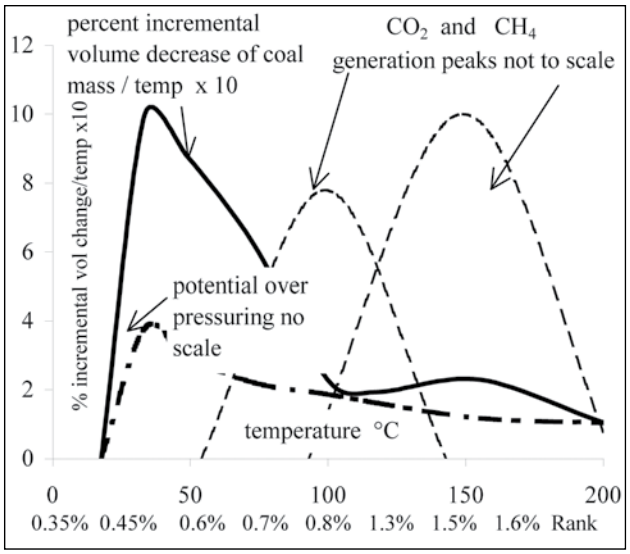

Figure 2. Matrix shrinkage and potential over-pressure as estimated from proximate analyses.

Face cleats exist in Powder River Basin coals, which have ranks of about Rmax = 0.4%. Generally, face cleats form parallel to the direction of regional compression and perpendicular to the basin axis. In that they are probably forming at fairly shallow depth (represented by a rank of about 0.4% to 0.7%), it is easy for the fold-axis-normal direction to become extensional, especially because of coal shrinkage. The regional nature of these fractures is probably accentuated because they offer pathways for water expelled from coal to escape upwards within seams to basin margins. Butt cleats that may form later during methane generation will generally be constrained to form at 90° to bedding and face cleats. These are surfaces of no or low cohesion, and therefore principle compressive stress directions must be perpendicular to them.

The spacing of face cleats decreases as rank increases up to a rank of low-volatile bituminous or semi-anthracite and then may increase (Law, 1993). If cleat development and spacing is related to the two periods of maximum shrinkage, then there should be a relationship between the plot provided by Law (1993) (Figure 3, this paper) and Figure 2. The curve in Figure 3 can be represented by a number of model points (open diamonds) that allow for the calculation of the change of cleat frequency versus rank or temperature. It is apparent that the maximum rate of change in cleat frequency is at low rank or temperature and tends to conform to the maximum period of coal shrinkage.

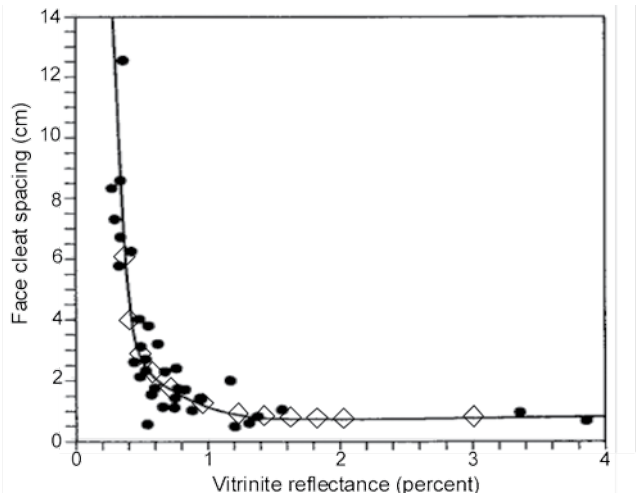

Figure 3. Spacing of face cleats versus rank (from Law, 1993); open diamonds are model points.

The generation of thermogenic methane can start at ranks as low as 0.5% in liptinite-rich coals. The gas is rich in heavier hydrocarbons, i.e., wet gas (Scott, 2001). The main stage of thermogenic methane generation starts at a rank of about 0.8% (Figure 4, from Scott, 2001), and the gas becomes progressively drier (dryness defined as C1/[C2+C3]) as rank increases. However, it will generally have lower ratios than does biogenic gas, which has high C1/(C2+C3) ratios. Coals rich in inert macerals may generate fairly dry gas (high C1/[C2+C3] ratio).

In deformed seams in British Columbia, it is important to differentiate between the effects of regional deformation (thrust faults) and local (in-seam) deformation. Regional deformation that precedes local folding probably occurs when coal rank is low, and its intensity will not vary based on location in folds. Shear joints associated with the early thrusting may not intersect bedding along fold-axis directions of later folding, and they will not vary their relative orientation with respect to bedding, depending on which limb they occur on. The simplistic geometry of shear joints related to regional shearing and local flexural flow folding is illustrated in Figures 5 and 6.

The data are plotted into lower-hemisphere stereonets as poles to bedding and poles to shear joints. It is useful to note that in the stereonets, the pole to shear joints migrates away from the pole to bedding in the direction of shearing to form an acute angle between the two poles. The orientation of shear joints related to thrusting should be regionally consistent, whereas those related to folds will change orientation depending on which limb they are on. Limited data from southeast BC indicate that the shear joints at the Greenhills coal mine on the west limb of the syncline are related to the flexural slip associated with the syncline. In other mines, the relationship is less obvious. The shear joints are, however, rotated such that they appear to be related to folds trending more to the northwest or thrusting from the southwest. (Figure 7). Face cleats appear to strike normal

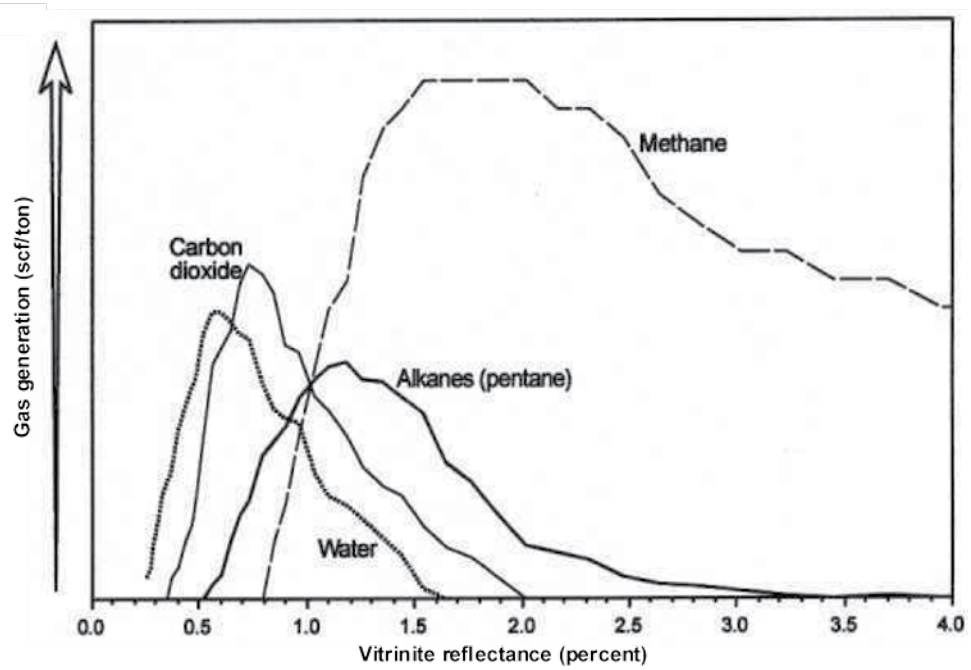

Figure 4. Generation of gases; diagram from Scott (2001).

to this early folding (or parallel to the thrusting) rather than normal to the later fold-axis direction.

In the Peace River coalfield (Figure 8), shear joints indicate northeastward thrusting or the prevalent northwest-trending folds. The properties indicated in Figure 8 are located in Figure 9. Face cleats are generally normal to the fold-axis direction, except in the north in the Gething Formation, where some trend parallel to the fold-axis direction. These cleats may in fact be axial planar features related to folding of the coal that occurred after it reached moderate rank. In the area, coal in the Gething Formation is inertinite-rich and consequently would not have shrunk as much during early coalification. Inert-rich coals that are characteristic of some Cretaceous British Columbia and Permian Australian coals may not form face cleats during early coalification and may contain fractures formed during later tectonic activity. These fractures may or may not be of extensional origin.

STRUCTURAL AND CBM HISTORY OF THE ELK VALLEY AND CROWSNEST COALFIELDS IN THE LEWIS THRUST SHEET

The Elk Valley and Crowsnest coalfields have had a complex tectonic history, in part because they are contained in the Lewis Thrust sheet (Figure 1). This unique tectonic setting, in conjunction with the Cretaceous to Early Tertiary deformation history, may be significant in terms of the produceability of the CBM resource of the coalfields.

Coal in the coalfields is contained in the Mist Mountain Formation of the Kootenay Group (Table 1), which was deposited into the miogeosyncline developed on the eastern edge of the Purcell Arch. Sediment was derived from the west as the Columbian Orogeny uplifted rocks. The Kootenay Group is separated from the overlying Blairmore Group by a disconformity that separates the Elk Formation from the overlying Cadomin conglomerate. To the north and east, there was considerable erosion associated with this unconformity, which in the Elk Valley and Crowsnest coalfields appears to be more of a disconformity.

The Mist Mountain Formation, which is Lower Cretaceous to Upper Jurassic (about 152 to 140 Ma; Mossop and Shetsen, 1994), is up to 625 m thick in southeast British Columbia (Gibson, 1985). The overlying Elk Formation varies in thickness up to 488 m (present thickness; Gibson, 1977). It is unlikely, therefore, that the coal seams in the Mist Mountain Formation were buried by much more than 1000 m at the time of the pre-Blairmore erosional event. Erosion and associated uplift probably did not have any lasting effect on gas contents of seams in the formation.

The gas contents of coals in Carboniferous rocks in the Ruhr area of Germany reflect the effects of a post-Carboniferous unconformity. Samples from just below the unconformity are close to saturated, whereas deeper coals are undersaturated. This is the opposite of what might be expected, based on degassing of the coal during erosion and uplift related to the unconformity. Freudenberg et al. (1996) suggest that shallower coals were recharged with biogenic methane generated using both CO_2 introduced during uplift and hydrogen from the coals. Seams deeper in the section are undersaturated because they were hotter, did not

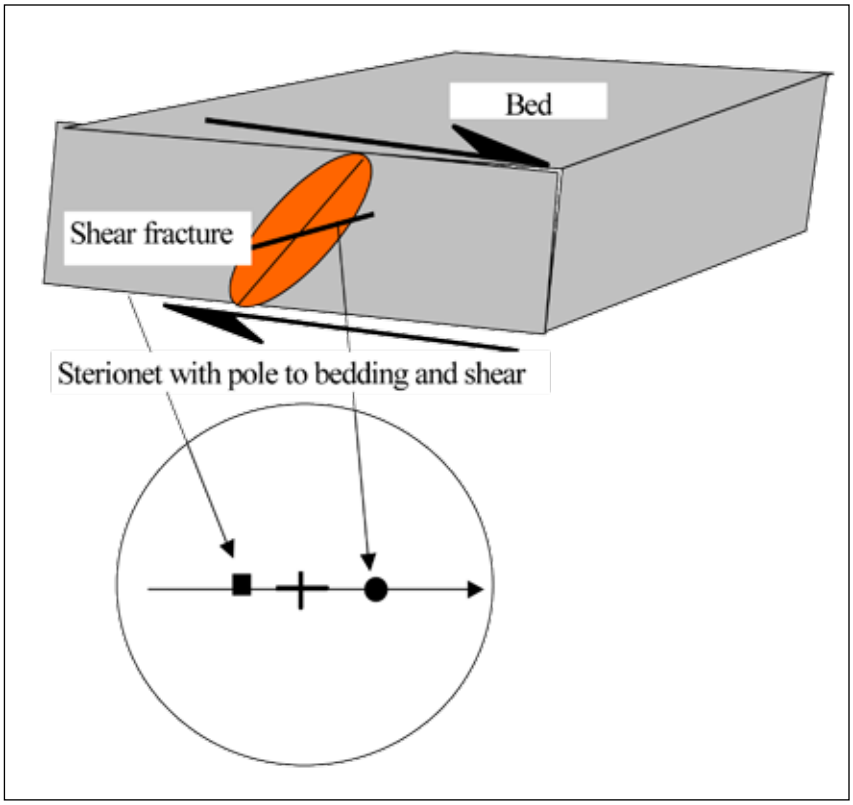

Figure 5. Orientation of shear joints in a thrust.

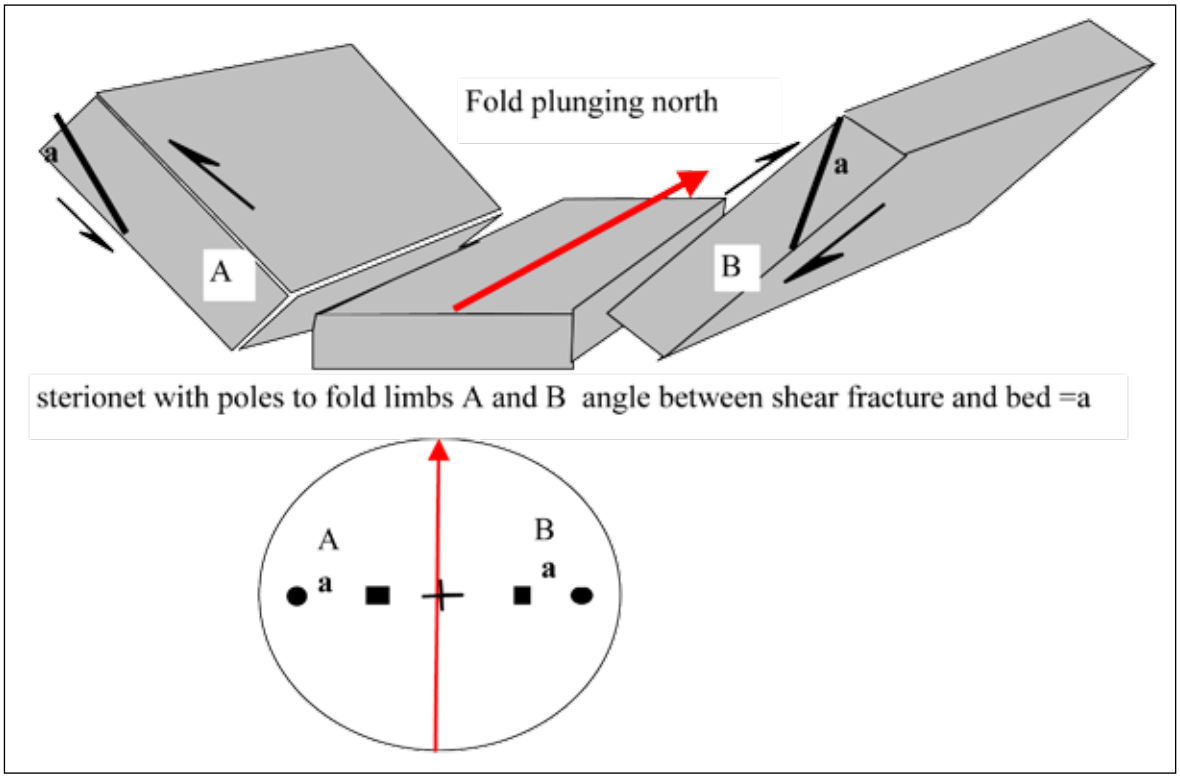

Figure 6. Orientation of shear joints in flexural flow fold.

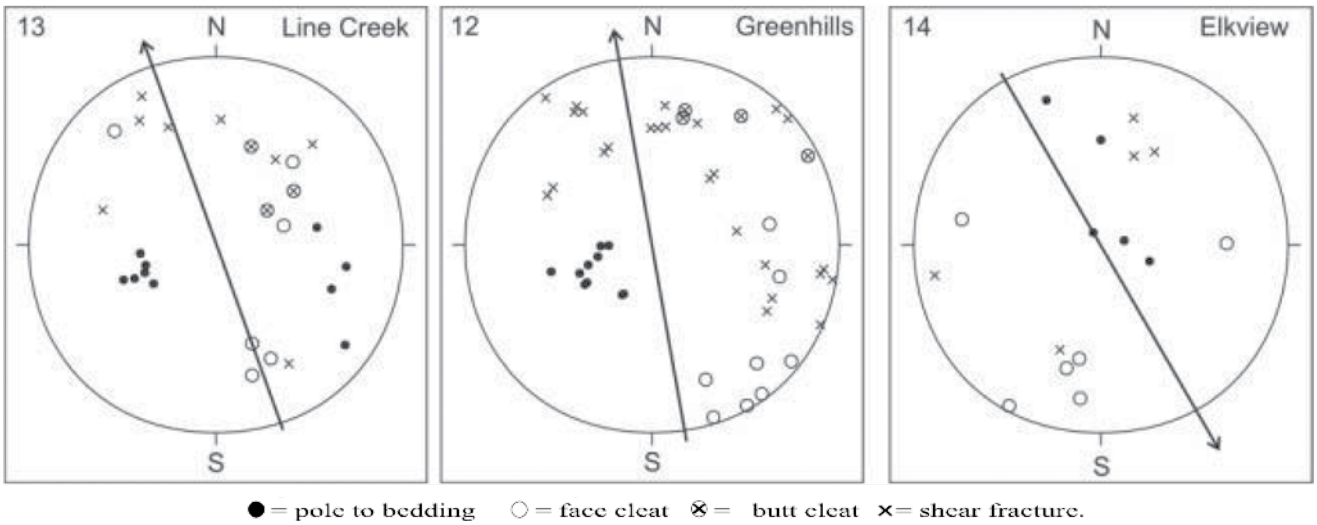

Figure 7. Sterionet of shear joints and cleats in southeast coalfields.

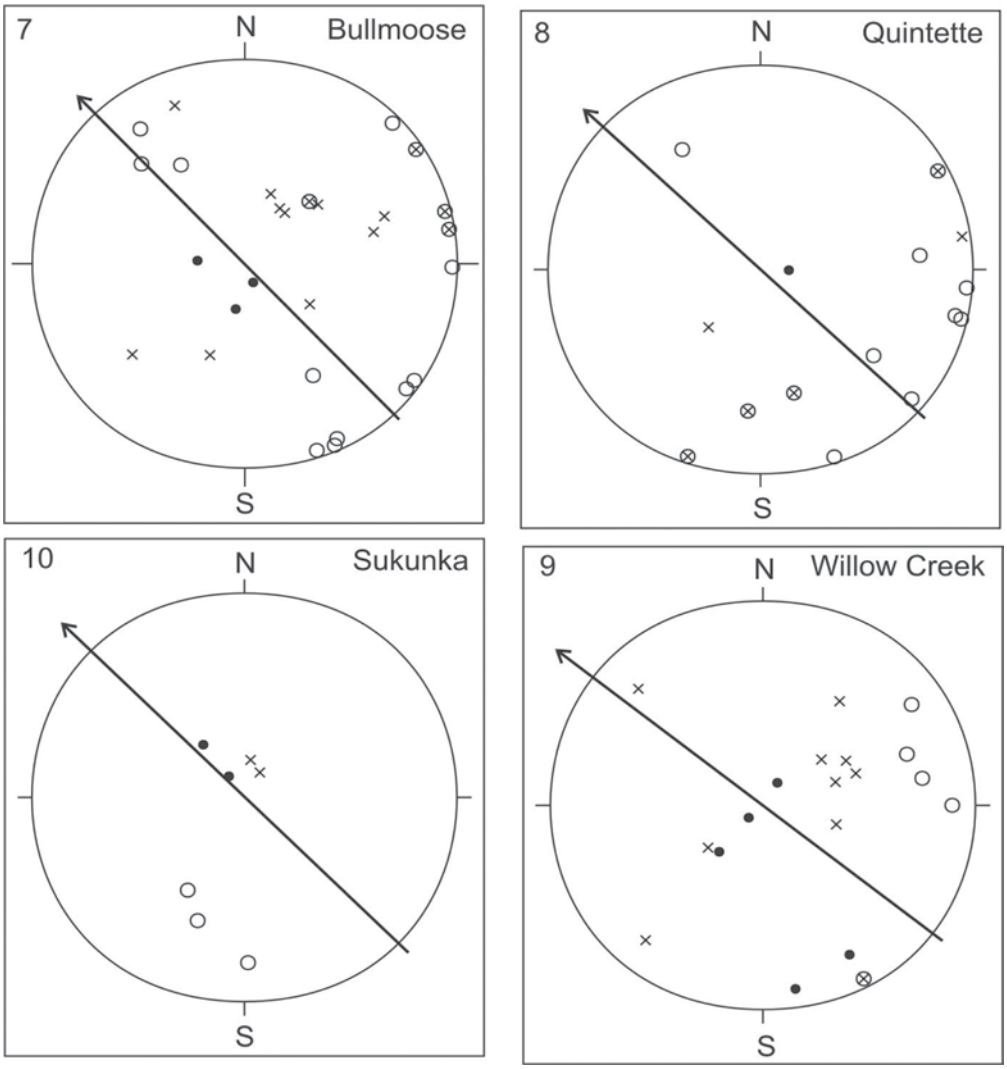

Figure 8. Sterionet of shear joints and cleats in northeast coalfields.

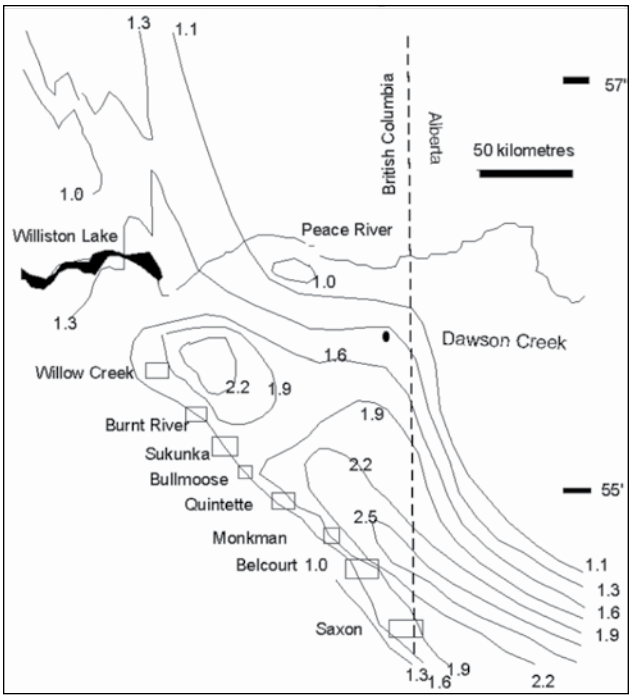

Figure 9. Reflectnace isograds for the top of the Gething Formation adapted from Machioni and Kalkreuth, (1992).

have access to CO_2, and retained a thermogenic imprint. As discussed later, it does appear that coals lower in the Mist Mountain section are undersaturated, but the explanation above cannot be used because the depth of burial of Mist Mountain coals at the time of the Cadomin unconformity was too shallow, and subsequent increase in rank would have generated sufficient methane to remove any imprint of the unconformity.

The Cadomin Formation, which is up to 170 m thick (White and Leckie, 2000), forms the base of the Lower Cretaceous Blairmore Group. It was probably deposited from about 140 to 125 Ma, based on palynology data discussed by White and Leckie (2000). There is therefore not a major time difference between the deposition of the Elk and Cadomin Formations. The Blairmore Group, which was deposited disconformably on top of the Kootenay Group, spans the time 140 to 95 Ma, and therefore deposition predates formation of the Lewis Thrust, which was active from 74 to 59 Ma (Sears, 2001). The thickness of the group ranges from 365 to 2000 m (Price, 1961). It is overlain by the Upper Cretaceous Crowsnest Formation (mainly alkaline volcanics), which is 40 to 100 m thick below the Lewis Thrust but does not occur within the thrust sheet. The formation is dated at 95 Ma using K-Ar data (Follinsbee et al., 1957), and its deposition therefore predates formation of the Lewis Thrust. Outcrops of the Upper Cretaceous Alberta Group survive in the Crowsnest coalfield in the core of the McEvoy syncline, where it is up to 230 m thick.

Prior to thrust development in the period 74 to 59 Ma, seams in the Mist Mountain Formation were probably covered by over 3000 m of rock comprised of the cumulative thickness of the Elk Formation, Blairmore Group, Crowsnest Formation, and Alberta Group. This is supposing that additional thrusts were not stacked on top of the Lewis Thrust sheet. At a depth of 3000 to 4000 m and based on normal geothermal gradients, seams in the upper part of the Mist Mountain Formation would have achieved a rank of high-volatile bituminous represented by Rmax values in the range of 0.6% to 0.8%. Seams lower in the section would have achieved higher rank. Thus at the time when Cordilleran orogenic forces to the west initiated development of the Lewis Thrust, some seams in the Mist Mountain were possibly overpressured with CO_2-laden water and in an ideal condition to participate in thrusting on all scales. Pearson and Grieves (1986) document evidence for post-folding coal maturation in the southwest corner of the Crowsnest coalfield.

The Lewis Thrust carried a thick slab, which probably consisted of over 6000 m (Price, 1962) of Paleozoic and Mesozoic rocks, eastward over rocks as young as Mesozoic. Osadetz et al. (2003) estimate the thickness at over 7 km. Movement took place during the period from 74 to 59 Ma at a rate of about 1.5 cm/yr in the Crowsnest Pass area, based on an estimated cumulative offset of between 140 and 200 km. Initiation of movement is indicated by profound cooling in the thrust block at about 75 Ma (Osadetz et al., 2003).

Thrust movement resulted in an increase in topography. It also fractured the cold and brittle thrust sheet, increasing permeability and allowing cold fluids to reach greater depths (Price et. al., 2001). This refrigeration of the thrust sheet delayed increase in rank and reduced the risk of gas loss because the decrease in temperature increased the adsorption ability of seams. However, at the time that this was occurring, the Bourgeau Thrust (Figure 1) was emplacing Paleozoic carbonates over the Lewis Thrust, and it was easy for fluids containing thermogenic CO_2 contained in the Paleozoic limestones to move downwards into the Lewis Thrust block. At the time of emplacement of the Bourgeau Thrust over the Lewis Thrust block, folds in the Lewis Thrust block would probably be largely formed and, to some extent, depth below the overlying Paleozoic limestones would in part be controlled by stratigraphy and in part by position in folds. This may explain the high CO_2 concentrations seen in some of the upper seams in the Elk Valley (Figure 10) (data from holes drilled by Norcen in 1990; Dawson et al., 2000). There is, therefore, reason to suspect that the CO_2 is thermogenic, though this cannot be confirmed without isotope data.

There are very limited public data on CO_2 concentrations in coals of the Crowsnest coalfield. A report by Rice (1918) provides some analyses. In 1916, 5 samples were collected from the working face in the underground Coal Creek Colliery and placed into sealed jars (Table 2). When

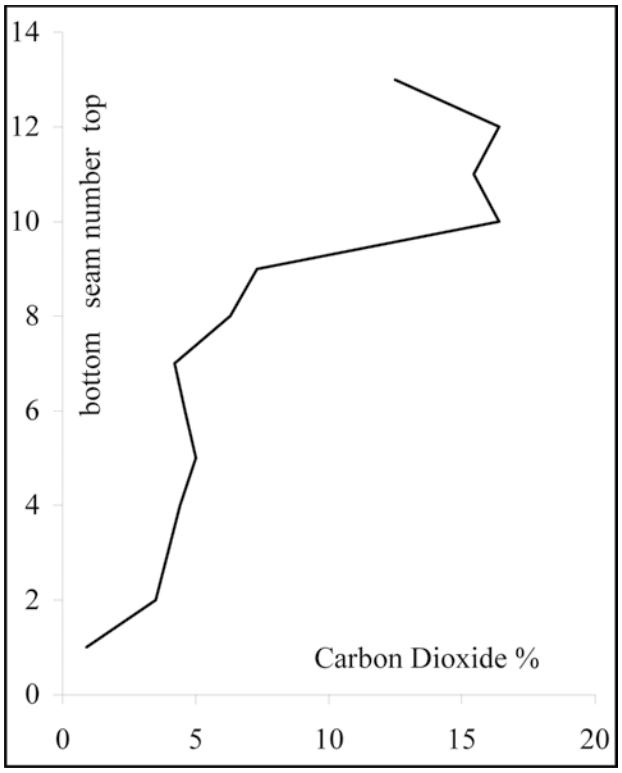

Figure 10. Elk Valley coalfield, carbon dioxide contents by seam Norcen 1990 holes Elk Valley, (Dawson et al., 2000).

the gas was analyzed, it was apparent that all had leaked; however, the CO_2 content is estimated from the CO_2/(CH_4+CO_2) ratio and it appears that, except for one sample, CO_2 contents were probably less than 5% (data are reported as cm^3 per 100 g, equivalent to mole fractions). Based on the trace of the Bourgeau Thrust relative to the outcrop of the basin (Johnson and Smith, 1991; Monahan, 2002), it appears that seams in the Mist Mountain Formation in the Crowsnest coalfield may not have been as close to the limestones in the overlying Bourgeau thrust plate or as close to the Crowsnest Volcanics as were seams in the Elk Valley coalfield; the Mist Mountain Formation may therefore have lower CO_2 concentrations.

There are no public isotope data for the methane in the Elk Valley or Crowsnest coalfields; however, some compositional data provide hints as to the origin of the gas. The ratio C1/(C2+C3) is an indication of the thermogenic component of methane; ratios less than 100 tend to indicate thermogenic methane, while ratios greater than 100 indicate biogenic methane (Wiese and Kvenvolden, 1993). This is complicated by the fact that biogenic activity can crack heavier hydrocarbons in thermogenic methane, increasing the C1/(C2+C3) ratio, and that at high ranks there may be secondary cracking of condensates to methane, which also will increase the ratio. Also, inert-rich coals probably will generate gas with higher C1/(C1+C2) ratios. These processes are illustrated in Figure 11 from Warwick *et al.* (2002).

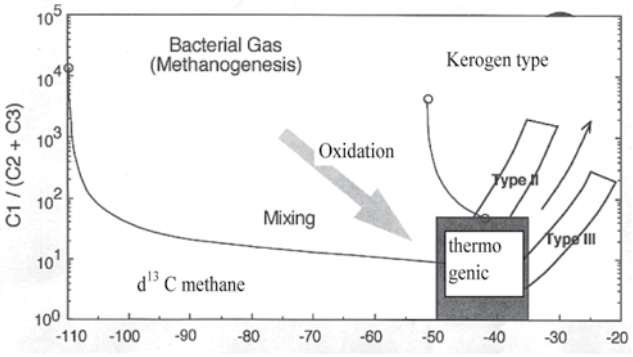

Figure 11. Isotope and gas composition diagram from Warwick et al., (2000).

In the Elk Valley, CO_2 increases as the ratio C1/(C2+C3) decreases in holes drilled by Norcen in 1990 (Figure 12) and increases for seams higher in the section (Figure 10). This tends to confirm a thermogenic origin for the CO_2. It also appears that seams lower in the section may have a biogenic imprint (high C1/[C2+C3] ratios) (Figure 13). The C1/(C2+C3) ratio varies during desorption, and it is not clear at what stage of desorption the Norcen gas samples were collected. However, gas composition data (Figure 14) collected from the hole drilled by Suncor into the Alexander syncline in the Elk Valley is for a single desorbing sample and indicates the extent that CO_2 concentrations and C1/(C2+C3) ratios can change during the desorption experiment. It is apparent that the range over which these values change within a single canister cannot explain the range in values seen in Figures 12 and 13.

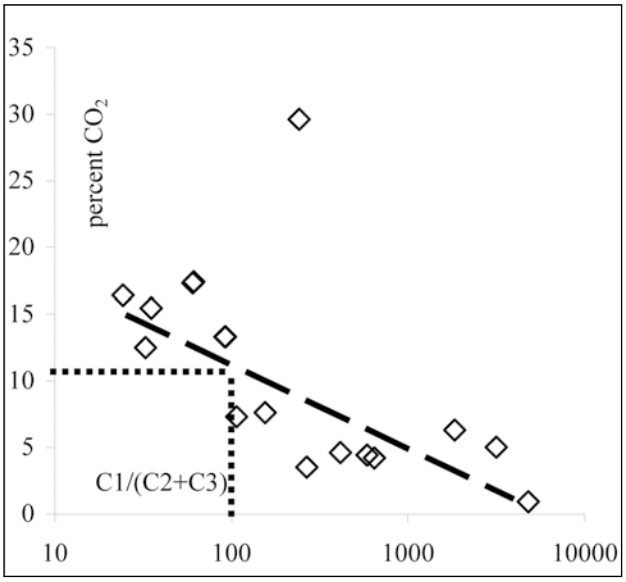

Figure 12. Elk Valley CO2 versus C1/(C2+C3) ratio for Norcen 1990 holes, Elk Valley (Dawson et al., 2000).

The very high C1/(C2+C3) ratios seen in the lower seams may indicate the presence of biogenic methane, but it is difficult to envisage a process that introduces biogenic methane into the lower seams but not into the upper seams.

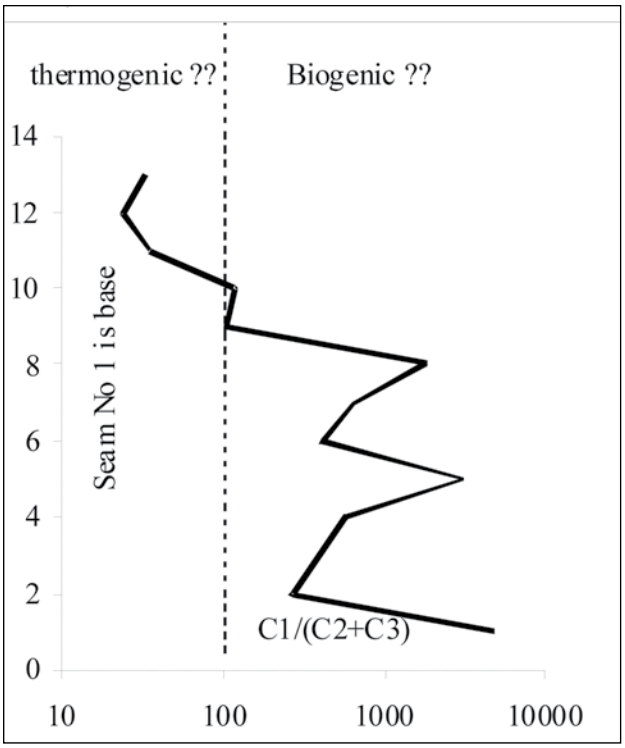

Figure 13. C1/(C2+C3) ratios versus seam number; Norcen 1990 holes, Elk Valley (Dawson et al., 2000).

Alternatively, the high ratios may indicate gas generated from liptinite-poor and inertinite-rich seams, in which case there should be a close correlation between coal seam petrography and C1/(C2+C3) ratios. Grieve (1993) provides petrographic analyses of coals at Weary Ridge in the north end of the Elk Valley coalfield close to the Norcen holes, and similar data are available for the southern end of the coalfield (Figure 15). In both cases it is clear that there is considerable variation in vitrinite content in the lower seams, and although the third seam above the base of the Mist Mountain Formation usually has a high inertinite content, other seams have variable and not necessarily low vitrinite contents. There is no clear correlation of high C1/(C2+C3) ratios with low vitrinite content. It is unlikely that petrography alone can explain the high C1/(C2+C3) ratios.

Often the degree of undersaturation of a single seam increases with depth (Figure 16). In part, the apparent near-saturation of seams higher in the section may be because they contain a mixture of CH_4 and CO_2 and the total gas contents are being compared to CH_4 isotherms. In general, partial degassing of a seam should decrease the C1/(C2+C3) ratio of the remaining gas. The high ratios are characteristic of seams irrespective of the depth at which they were sampled. The rank in the northern end of the Elk Valley coalfield is higher than it is to the south, and Rmax values range from 1.0% to over 1.6% (Grieve, 1993). It is possible that at the higher ranks, thermal cracking of the heavier hydrocarbons has increased the C1/(C2+C3) ratio.

After emplacement of the Lewis Thrust and before removal of the overlying Bourgeau Thrust sheet, Laramide heating may have been responsible for increasing the rank of Mist Mountain coals. Symons *et al.* (1999) discuss evidence for a Late Cetaceous to Tertiary Laramide heating and dolomitization event. This heating event must have ended prior to normal movement on the Flathead Fault at about 46 Ma. Evidence for post-deformation maturation is recorded in the Crowsnest coalfield by Pearson and Grieve (1985) and is evidenced in some deep drill holes (Bustin and England, 1989).

This second heating event may have affected seams low in the section more than it affected seams higher in the section. Previously generated wet gas was expelled upwards, and the increased rank was responsible for generating more gas with a much higher C1/(C2+C3) ratio. Because this event occurred after folding within the Lewis Thrust, it was possible for gas to move upwards within a single seam until the decrease in temperature allowed it to be re-adsorbed. It is important to remember that the heavier hydrocarbons have different adsorption characteristics than methane does and will be preferentially adsorbed, whereas some of the methane may escape the system. This could explain lower C1/(C2+C3) ratios for seams higher in the section or at shallower depth.

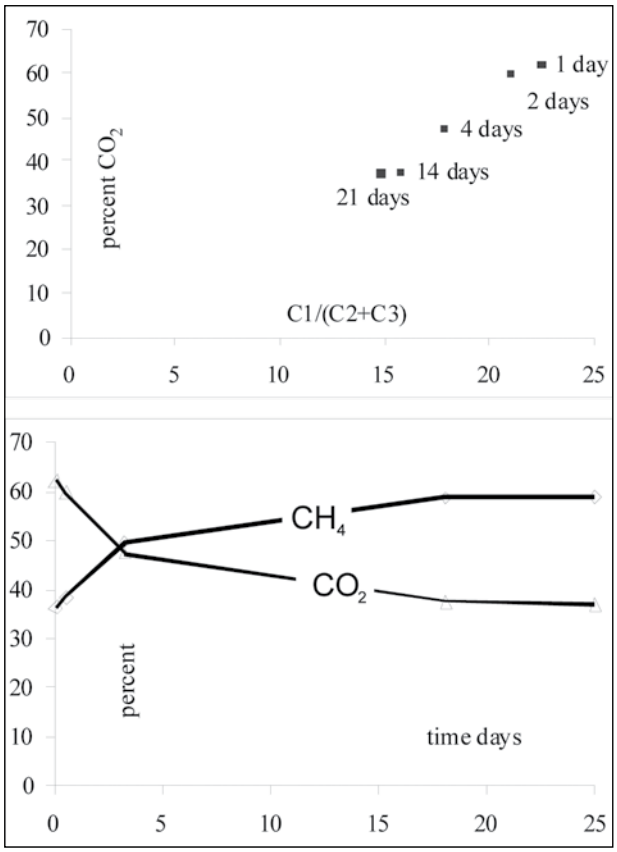

Figure 14. Data set of C1/(C2+C3) data from a single canister; numbers are days after canister sealed. Suncor data, Elk Valley coalfield (Dawson et al., 2000).

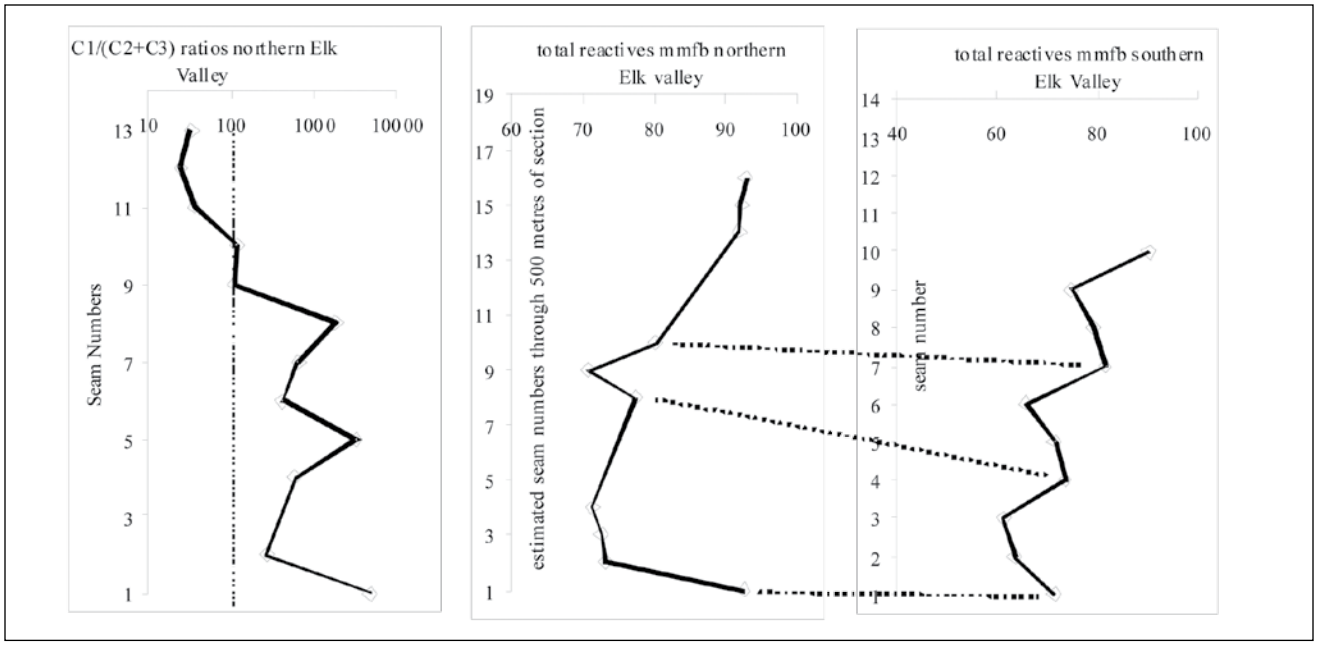

Figure 15. Petrographic variations in the Elk Valley, and C1/(C2+C3) ratios. Petrographic data from Grieve (1993). Inert-rich seams should correlate with higher C1/(C2+C3) ratios.

The increase in rank of seams at depth or lower in the section was accompanied by matrix shrinkage that temporarily improved permeability, allowing gas expelled because of increased temperature to move upwards either through the stratigraphy or along seams. The duration of the heating event was limited by the rapid unroofing of the Lewis Thrust sheet.

Any post-thrusting and post-folding maturation of coals in the Elk and Crowsnest coalfields could mean that gas expelled from coals undergoing increased maturation would have the opportunity to move into existing structural traps. There should be a clear distinction between structures that act as traps for upward-migrating thermogenic methane from those that might act as traps for biogenic gas moved in conjunction with ground water.

The onset of deformation when coal is at a rank range of 0.5% to 0.8% probably has detrimental effects on cleat development and seam permeability. The linkage results in the extensive shearing within seams and tends to destroy cleats or make their development unnecessary in terms of the coal's response to dehydration and devolatilization.

Present data indicate that permeability of seams in the Elk Valley and Crowsnest coalfields is low (Dawson et al., 2000), and it therefore becomes very important to identify areas of recent stress relief. The Erickson and Flathead fault system may be part of the same failed thrust system, in which the upper plates slipped back. If this is the case, then part of the plate may be in extension, and this would improve permeability within seams. Movement on the Lewis Thrust increases to the north across the US border, implying a clockwise rotation of the thrust sheet; this is consistent with the development of right-lateral strike-slip motion on a number of major faults. Stress environments around these faults may indicate areas of extension.

COMPARISONS BETWEEN NORTHEAST AND SOUTHEAST BRITISH COLUMBIA COALFIELDS

Coal-bearing rocks of interest to CBM exploration in the Peace River coalfield are contained in the Gething and Gates Formations (Table 3). These formations cover the age span of about 110 to 100 Ma. (Mossop and Shetsen, 1994). They overlie the Cadomin Formation and make up the second major Cordilleran-derived clastic wedge of the foreland basin. They record the first basin-wide sedimentation (Mossop and Shetsen, 1994, Chapter 17) and indicate the northeastward movement of the centre of deposition of the foreland basin. Initiation of thrusting at the craton edge caused it to subside, providing accommodation in the foredeep for the huge volume of sediments shed from the up-thrusted sheets. This thrusting predates the Lewis Thrust in the Elk Valley.

Deformation in the Peace River coalfield started later than it did in the southeast coalfields. Coalification generally preceded thrusting and folding (Kalkreuth et al., 1989), and the Gething and Gates Formations reached their maximum burial depth about 75 Ma in the west and 50 Ma to the east. This timing of maturation relative to deformation is important because it means that, in the Peace River coalfield, seams largely matured in the absence of thrusting

and therefore may have escaped a lot of in-seam shearing. In general, seams in the northeast have better cleat development than do seams in the Mist Mountain Formation. However, gas generated during coalification did not have the opportunity to be contained in structural traps. At this stage, only stratigraphic traps were effective for containing thermogenic methane expelled from seams. Later, thrusting and folding caused extensive deformation in seams in some areas but not in others.

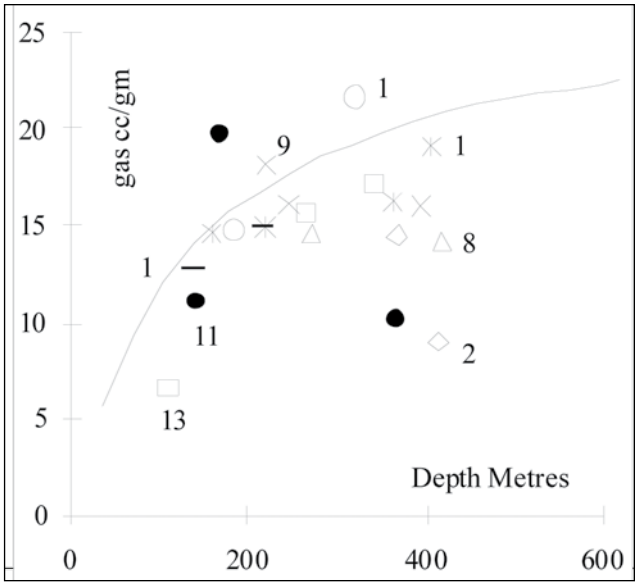

Figure 16. Desorption data from Norcen holes, 1990, Elk Valley (Dawson et al., 2000).

There are limited public desorption data available for seams in the Peace River coalfield. Data from the Gates Formation (Phillips holes drilled in 1996, Dawson *et al*., 2000) indicate that seams are nearly saturated. Also, the gas has a clear thermogenic fingerprint, based on C1/(C2+C3) ratios (Figure 17). The CO_2 concentrations are less than they are in the Norcen holes in the Elk Valley and increase as the C1/(C2+C3) ratio decreases and as depth increases. It appears that the CO_2 is of deep and thermogenic origin. Thrusting in the Peace River coalfield has not emplaced Paleozoic limestones over Cretaceous coal-bearing rocks, and there are no extrusive or intrusive magmatic rocks in the sequence, therefore access to thermogenic carbon dioxide is probably via deep faults.

There is probably semiquantative information that can be gleaned from the desorption curves. Airey (1968) modeled the shape of the desorption curve and indicated that his constant "to", which is the time to 63.2% of total desorbed gas, is strongly dependent on the degree of fracturing of the coal; this is confirmed by the work of Harris et al. (1996). Work by Gamson et al. (1996) indicates that desorption time is also dependent on coal petrology, with dull lithotypes desorbing faster. Data for Mist Mountain Formation coals indicate that they generally have desorption times (63.2% of total desorbed gas) less than 30 hours (Dawson, 1993; Feng et al., 1981). However, desorption times for Gates Formation coals from the Phillips drill program in the Peace River coalfield (Dawson et al., 2000) average over 70 hours. On a regional scale, desorption times may indicate the degree of microfracturing of coals and of pervasive deformation. On the local scale, they may correlate with a combination of petrography and fracture size. As a caution, desorption times can also be influenced by the way the desorption experiment is conducted.

In the northeast, variation in rank must be explained

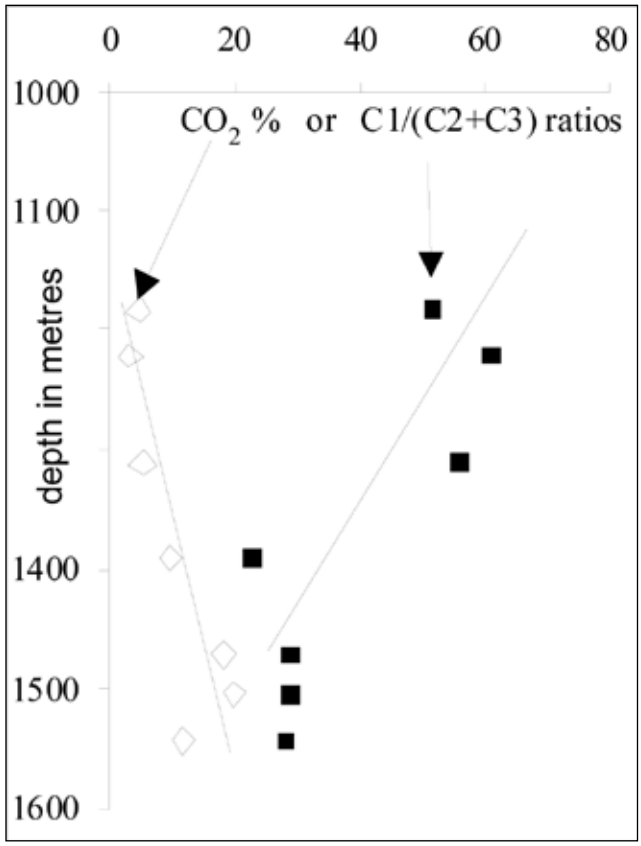

Figure 17. C1/(C2+C3) ratios for Gates Formation coals, Phillips exploration project, 1996 (Dawson et al., 2000).

by variation in stratigraphic thickness or by variation in upward heat flow, because coalification preceded deformation. There are a number of enclosed areas of high rank apparent in the Gething Formation (Marchioni and Kalkreuth, 1992) (Figure 9), and, depending on their origin, they could have implications for CBM exploration. One that is very conspicuous is located between the Willow Creek and Burnt River properties (Figure 9) and is responsible for locally increasing the rank of seams in the Gething Formation to semi-anthracite. If convective movement of fluids causes rank increase, then methane could be swept out of seams and CO_2 introduced. On the other hand if it is caused by increased burial, then there is more chance that seams will retain methane and less chance of CO2 introduction.

Convective movement of fluids should be evident by mineralization on cleat surfaces. Spears and Caswell (1986) provide estimates of the temperature of deposition for a number of diagenetic minerals found on cleats. Calcite and ankerite are deposited in the temperature range 100°C to 130°C, which corresponds to a rank of high-volatile bituminous. This represents the final expulsion of diagenetic water from seams. At this time, cleats have already formed and may be mineralized. For higher-rank coals, preservation of calcite on cleats indicates that hotter fluids associated with the higher rank did not remove calcite. The rank of the Gething and Gates Formation coals is generally higher than high-volatile bituminous, and there is calcite on face cleats in Gates coals and indications of calcite on cleats in Gething coals.

Coal ash generally has CaO contents less than 4%; higher contents often indicate the presence of carbonates on cleats, especially if a plot of ash versus CaO% indicates that CaO concentrations increase as ash contents decrease. In fact, in the absence of other data, ash chemistry data (available from existing coal studies) can provide information on the possible prevalence of carbonate on cleats. Calcite is present on cleats in the lowest seam of the Comox Formation in the Quinsam area (Ryan, 1994), whereas calcite is absent on cleats in seams from the lower part of the Mist Mountain Formation but does occur on some seams in the upper part of the formation. These cleat facies are easily separable on a CaO versus ash plot (Figure 18).

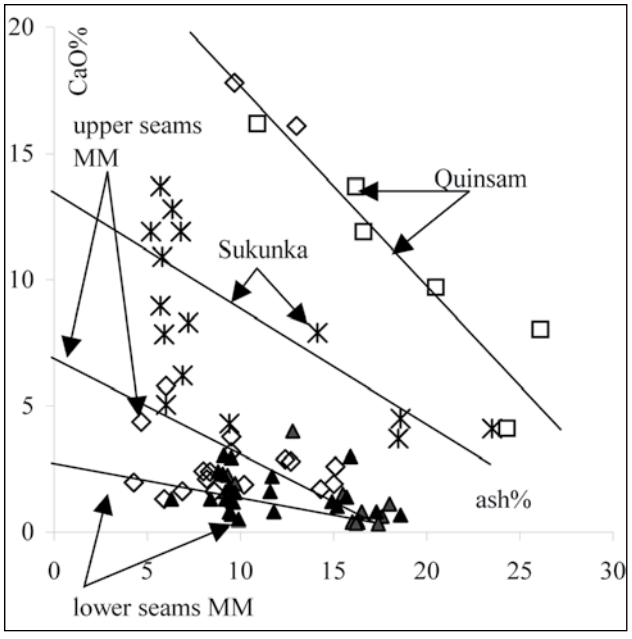

Figure 18. CaO% versus ash% for seams from the Mist Mountain, Gething, and Comox Formations.

The limited amount of CaO analysis data available for Gates and Gething coals indicates that there is probably some calcite on cleats in Gething coals from south of Willow Creek to Sukunka River and in Gates coals from Bullmoose to Belcourt. The area of high rank in the Gething Formation centred on Highhat Mountain (Marchioni and Kalkreuth, 1992) does not appear to be an area where there is unusually high or low CaO in the ash. Two analyses from the Burnt River property, which is at the centre of the area, are both under 3% CaO. A late thermal event would be expected to introduce CaO and CO_2 into the system, on one hand leaving calcite on cleats and the other replacing CO_2 with CH_4 in coal. A high-temperature thermal event may introduce CO_2 and remove CH_4 from the coal and CaO from cleats. A more detailed study of ash chemistry may lead to a better indication of whether to expect increased CO_2 in high-rank areas of the Gething Formation

THE INTERPLAY OF COAL CHARACTERISTICS AND RECENT TECTONICS

Coal preparation involves the removal of rock from the coal to reduce the ash concentration to acceptable levels for the customer. Coal is less dense than rock, and this property is used to advantage in wash plants, as is the fact that coal is generally less wettable than rock. The hydrophobicity of coal is used for cleaning fine coal by froth floatation. The wettability of coal varies with rank, largely because as rank increases, different oils and gases are expelled. This is referred to as the oil window (Dow, 1977) and is defined by Rmax values in the range of 0.5% to 1.35%. The hydrophobicity of coal attains a maximum value in the middle of the rank spectrum at ranks ranging from Rmax = 1% to 1.6% and is measured by contact angle of fluid on the coal surface (Osborne, 1988) (Figure 19).

Obviously the exact placement of the oil window depends on the petrography of samples. Samples with high liptinite contents will generate oil at lower ranks. The generation of oil at medium rank probably affects the adsorption and surface properties of coal, as discussed by Levine (1993). The most obvious effect on surface properties is that of capillary action (or wetting) as measured by contact angle. Another way of estimating the wettability of coal is to measure the difference between equilibrium moisture and air-dried moisture. This difference is probably a good measure of surface moisture, and the value also is at a minimum for the range of ranks 0.9% to 1.5% (Figure 20). The shift to higher ranks of the surface effects from the oil window probably indicates that it is the heavier oils that have the most effect on surface wetting.

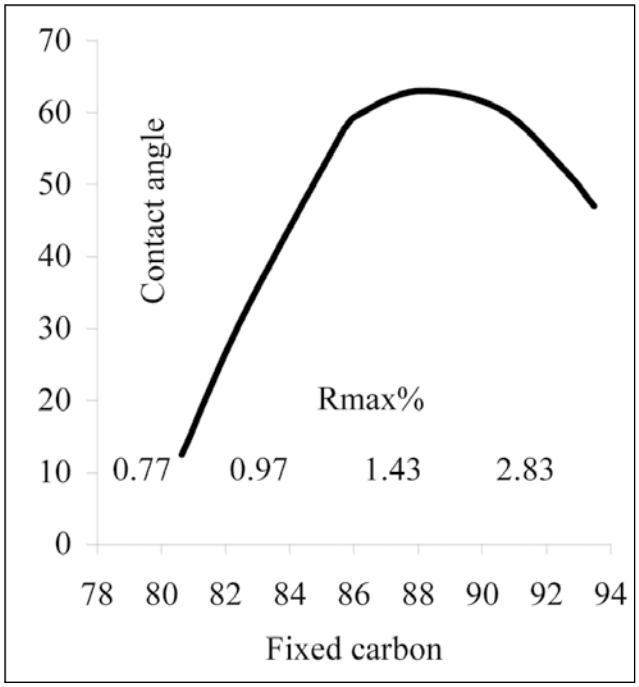

Figure 19. Contact angles of fluids on the surface of coals of different rank (Osborne, 1988).

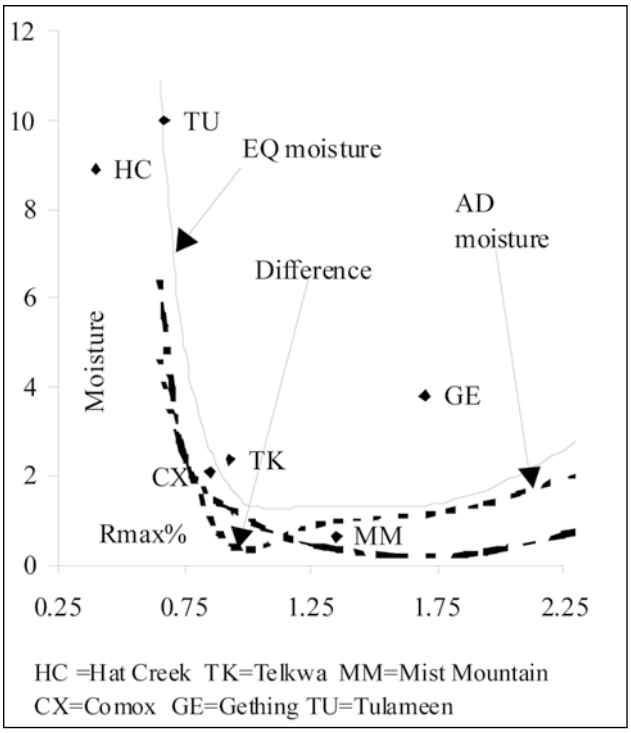

Figure 20. Contact angles of fluids on the surface of coals of different rank (Osborne, 1988).

The minimum wettability identifies coals that will have longer diffusion times but will have better relative permeability for gas because of lower water saturation on cleats than high- or low-rank coals will have. High- or low-rank coals with high wettability will have higher water saturation on cleat surfaces than will mid-rank coals and, under set conditions, will have lower relative permeability. This is because cleat surfaces of mid-rank coals can be dewatered to lower saturation values, and the relative permeability of gas approaches more closely the maximum permeability for a single fluid in the cleat system. Obviously coals in the mid-rank window may have reduced adsorption ability (Levine 1993), but cleats may contain little water and they may produce gas with minimal extraction of water.

Even with low wettability on cleat surfaces, over time cleats will probably become water-saturated. The ideal situation is one where cleats are opened up fairly recently. This would cause a decrease of pressure and desorption of gas into the cleats. Under these conditions, a seam would be saturated because the adsorbed gas would be in contact with a free gas phase. The seam may be under-pressured and gas contents may be low, but gas will be produced quickly with little water production. Obviously this requires the combination of recent stress relief, an opening of cleats (but not too much), and the correct rank window for the coal.

There are a number of areas where Tertiary stress fields are oriented such as to open cleats. However, much of Canada has the advantage of another regional event that could help open cleats. The country is undergoing isostatic rebound as a result of the removal of the continental ice sheet. Uplift amounts are in the order of tens of metres. The rapid removal of overburden pressure and resultant decompression of the more compressible units (coal) results in extension in a vertical direction and contraction in a horizontal direction. This will open cleats, and for coals with low wettability, water may not have had time to penetrate all cleat surfaces because uplift is relatively recent.

CONCLUSIONS

British Columbia contains a very large coal resource available for CBM exploration. However, much of this resource is in areas of fairly complex geology. Learning how to overcome the challenges resulting from the geology by exploration can be expensive. Sometimes, making better use of existing databases can reduce the cost.

The relative timing of deformation and the time at which the coal is the most susceptible (based on rank) to deformation is important. It affects the degree to which cleats form or are preserved in seams. Early deformation occurring when the rank is high-volatile bituminous may result in pervasive shearing of coal seams and limited development of cleats. Deformation that occurs later, after coal maturation has progressed, may cause more limited damage to cleat systems.

The orientation of cleats and fractures can help in understanding the sequence of deformation and coalification. The main problem for the geologist may be remembering long-passed structural geology courses.

Coalfields in southeast British Columbia occupy the Lewis Thrust sheet and are partially over-ridden by the Bourgeau Thrust sheet. Coal may have attained maximum rank after thrusting and consequently may have experienced in-seam deformation related to the Lewis Thrust. Thrusting also may be responsible in part for the introduction of thermogenic(?) CO_2.

In the Peace River coalfield, deformation post-dated most of the coalification, and consequently the degree of in-seam deformation is variable and in places seams retain good cleating. Rank in the Peace River coalfield is more variable than it is in the southeast. This may indicate fluid movement that could be associated with lower gas contents and introduction of CO_2. However, ash chemistry data collected from existing exploration projects do not indicate extensive fluid movement but do indicate that some cleat systems are mineralized with calcite.

After all this, it may seem that there are more problems than challenges in British Columbia. However, we may have at least one possible advantage that our neighbours to the south do not have. Isostatic rebound may be responsible for strain within seams that has opened cleats and improved permeability. This, in conjunction with high-volatile coals that resist wetting, may provide low-pressure gas-saturated systems at moderate depth.

REFERENCES

Airey, E.M. (1968): Gas emission from broken coal: an experimental and theoretical investigation*; International Journal of Rock Mechanics and Mineral Science* Volume 5, pages 475-494.

Bustin, R.M. and England, T.D.J. (1989): Timing of orogenic maturation (coalification) relative to thrust faulting in the southeastern Canadian Cordillera; *International Journal of Coal Geology*, Volume 13, pages 327-339.

Dawson, F.M. (1993): Joint venture project Fording Coal Limited; *Geological Survey of Canada,* Summary Report.

Dawson, F.M. Marchioni, D.L. Anderson, T.C. and McDougall, W.J. (200): An assessment of coalbed methane exploration projects in Canada; *Geological Survey of Canada,* Bulletin 549.

Dow, W.G. (1977): Kerogen studies and geological interpretations; *Journal of Geochemical Exploration*, Volume 7, pages 79-99.

Feng, K.K., Cheng, K.C. and Augsten, R. (1981): Methane desorption of Fording coal from Greenhills multiple seams; CANMET, Energy Research Program, Mining Research Laboratories Division report ERP/MRL 81-67(J).

Freudenberg, U. Lou, S. Schlurer, R Schutz, K and Thomas, K. (1966):Mina factors controlling coalbed methane distribution in the Ruhr district, Germany; Coalbed Methane and Coal Geology, *Geological Society*, Special Publication Number 10, pages 67-88.

Follinsbee, R.E., Ritchie, W.D. and Stansberry, G.F. (1957): The Crowsnest volcanics and Cretaceous geochronology, in 7th Annual Field Conference *Alberta Society of Petroleum Geologists,* pages 20-26.

Gamson, P., Beamish, B., and Johnson, D (1996): Coal microstructure and secondary mineralization: their effect on methane recovery; Coalbed Methane Geology, *Geological Societ,y* Special Publication Number 109, pages 165-179.

Gibson, D.W. (1985): Sedimentary facies in the Jura-Cretaceous Kootenay Formation, Crowsnest Pass area, southwestern Alberta and southeastern British Columbia; *Bulletin of Canadian Petroleum Geology*, Volume 25, pages 767-791.

Gibson, D.W. (1985): Stratigraphy, sedimentology and depositional environments of the coal-bearing Jurassic-Cretaceous Kootenay Group, Alberta and British Columbia; *Geological Survey of Canada*, Bulletin 357.

Grieve, D.A. (1993): Geology and rank distribution of the Elk Valley coalfield southeastern *British Columbia Ministry of Energy and Mines,* Bulletin 82.

Harris, I.H., Davies, A.G., Gayer, R.A. and Williams, K. (1996): Enhanced methane desorption characteristics from South Wales anthracites affected by tectonically induced fracture sets; Coalbed Methane Geology, *Geological Society*, Special Publication Number 109, pages 181-196.

Johnson, D.G.S. and Smith, L.A. (191):Coalbed Methane in southeastern British Columbia; *British Columbia Ministry of Energy and Mines, Petroleum Geology Branch*, Special Paper 1991-1.

Kalkreuth, W. Langenberg, W and McMechan, M. (1989): Regional coalification pattern of Lower Cretaceous coal-bearing strata, Rocky Mountain Foothills and foreland, Canada – implications for future exploration; *International Journal of Coal Geology*, Volume 123, pages 261-302.

Law, B.E. (1993): The Relationship Between Coal Rank and Cleat Spacing; Implications for the Prediction of Permeability in Coal; in Proceedings of the 1993 *International Coalbed Methane Symposium*, May 17-21 1993 Birmingham, Alabama, Volume 2, pages 435-442.

Levine, J.R. (1993): Coalification: The evolution of coal as source rock and reservoir rock for oil and gas; in Hydrocarbons from Coal; *American Association of Petroleum Geologists*, Series number 38, Chapter 3, pages 39-77.

Marchioni, D and Kalkreuth, W. (1992): Vitrinite reflectance and thermal maturation in Cretaceous strata of the Peace River Ach Region: West-central Alberta and adjacent British Columbia; *Geological Survey of Canada,* Open File 2576.

Monahan, P. (2002): The Geology and oil and gas potential of the Fernie-Elk Valley Area, southeastern *British Columbia Ministry of Energy and Mine,* Petroleum Geology Special Paper 2002-2.

Mossop, G.D. and Shetsen, I. (1994): Geological Atlas of the Western Canada Sedimentary Basin; Alberta Geological Survey.

Osadetz, K.G., Kohn, B.P. , Feinstein, S. and. Price, R. A. (2003): Aspects of foreland belt thermal and geological history in southern Canadian Cordillera from fission-track data.

Osborne, D.G. (1988): Coal Preparation technology; *Graham Trotman limited;* page 420.

Pearson, D.E., and Grieve, D.A. (1985): Rank variation coalification pattern and coal quality in the Crowsnest Coalfield, British Columbia; *Canadian Institute of Mining and Metallurgy,* Bulletin, Volume 78, pages 39-46.

Price, R.A. (1957): Flathead Map area, British Columbia and Alberta*; Geological Survey of Canada*, Memoir 336.

Price, R.A. (1961): Fernie map area east half, Alberta and British Columbia 82G E1/2; *Geological Survey of Canada*, Paper 61-24.

Price, R.A.,Kohn, B.P. and Feinstein, S. (2001): Deep refrigeration of a thrust and fold belt because of enhanced syntectonic penetration of meteoric water: the Lewis thrust sheet, southern Canadian Rocky Mountains; *Earth System Global Meeting* June 24-28 2001 Edinburgh International Conference Centre.

Rice, S.G. (1918): Bumps and gas outbursts of gas in mines of Crowsnest Pass Coalfield; *British Columbia Department of Mines*, Bulletin Number 2.

Ryan, B.D. (1994): Calcite in Coal from the Quinsam Coal Mine, British Columbia, Canada, Origin, Distribution and Effects on Coal Utilization; in Geological fieldwork 1994, Grant, B. and Newell, J.M., Editors, *B.C. Ministry of Energy, Mines and Petroleum Resources*, Paper 1995-1, pages 245-256.

Scott, A.R. (2001): A Coalbed methane producibility and exploration model: defining exploration fairways; 2001 *International Coalbed Methane Symposium*, Tuscaloosa, Short Course #1, chapter 5.

Sears, J.W. (2001): Emplacement and denudation history of the Lewis-Eldorado-Hoadley Thrust slab in the northern Montana Cordillera USA: Implications for steady-state orogenic processes; *American Journal of Science,* Volume 301, pages 359-373

Spears, D.A. and Caswell, S.A. (1986): Mineral matter in coals: cleat minerals and their origin in some coals from English Midlands; *International Journal of Coal Geology*, Volume 6, pages 107-125.

Symons, D.T.A., Enkin, R.J. and Cioppa, M.T. (1999): Paleomagnetism in the Western Canada Sedimentary Basin :Dating fluid flow and deformation events; *Bulletin of Canadian Petroleum Geology*, Volume 47, pages 534-547.

Warwick, P.D. Barker, C.E. and SanFilipo, J.R. (2002): Preliminary evaluation of coalbed methane potential of the Gulf Coastal Plain USA and Mexico; *Rocky Mountain Association of Geologists*, Coalbed Methane of North America II, pages 99-107.

White, J.M. and Leckie, D.A. (2000): The Cadomin and Dalhousie formations of SW Alberta and SE British Columbia; age sedimentology and tectonic implications; *Canadian Society of Exploration Geologists,* Conference 2000, abstract.

Wiese, K. and Kvenvolden, K.A. (1993): Introduction to Microbial and thermal methane*; US Geological Survey* Professional Paper 1570, pages 13-20.

THE POTENTIAL FOR CO_2 SEQUESTRATION IN BRITISH COLUMBIA COAL SEAMS

By Barry Ryan[1] and Dave Richardson[2]

KEYWORDS: Carbon dioxide phase diagram, coal macerals, carbon dioxide isotherms, coal rank.

INTRODUCTION

Most people accept that climate change resulting from human activity is a reality. The details of the causes and progress are much in dispute, but there is general consensus that increase in the concentration of carbon dioxide (CO_2) in the atmosphere is one of the causes. The amount of carbon dioxide released when any fossil fuel is burned is dependent on the ratio of carbon to hydrogen in the fuel. This ratio is a maximum for coal and a minimum for natural gas (mainly methane, CH_4), with oil having an intermediate ratio. The amount of CO_2 produced per unit of heat (in this case 10^6 BTU) for the various fossil fuels (Table 1) is a maximum for coal, but it is not zero for natural gas. The true impact of using the various fossil fuels requires an analysis of the efficiency of turning them into more useful forms of energy (often electricity or, in the case of oil, momentum). Natural gas and conventional oil reserves will be substantially depleted in the next 50 years, leaving coal as the most readily available fossil fuel. Technology that uses the energy from coal while minimizing or eliminating the release of CO_2 to the environment will become critically important; this involves sequestering CO_2 as a gas, liquid, or solid or in the adsorbed state on coal.

TABLE 1. CARBON DIOXIDE PRODUCED BY BURNING VARIOUS FOSSIL FUELS.

	oil	gas	coal
unit	barrel	cubic M	tonne
cost $US	30	5$/1000scf	25
exchange rate	0.76	0.76	0.76
cost US$ per unit	30.00	0.177	25.00
cost can$ per unit	39.47	0.23	32.89
wt of unit in kg	136.40	0.7142	1000
heat GJ per unit	6.12	0.0373	29.30
heat kcals per unit	1462007	8899	6999477
btu 10^6 per unit	5.801	0.035	27.771
kcals/kg	10719	12460	6999
GJ/tonne	44.87	52.16	29.30
cost GJ $can	6.45	6.24	1.12
cost Kcal 10^6 $can	27.0	19.8	4.7
cost btu 10^6 $can	6.81	6.58	1.18
CO2 emissions in kg from one million BTU			
coal	92.4		
oil	77.6		
gas	56.1		
Note Assumptions are made concerning heat value of each fuel and carbon content. Numbers are only approximate			

In recent years there has been a lot of discussion on the possibility of sequestering CO_2 in coal seams or using CO_2 to aid in the recovery of coalbed methane (CH_4). The basis of both these ideas is the fact that CO_2 is more strongly adsorbed onto coal surfaces than is CH_4. Once adsorbed, if temperature and pressure conditions do not change, then the CO_2 is permanently sequestered. There are of course two concerns: firstly, pressure and temperature conditions must not change, and secondly and more importantly, there are limited pressure and temperature ranges over which CO_2 is a gas. At higher temperatures and pressures, CO_2 becomes a supercritical fluid, and under these conditions it is not clear whether it is adsorbed by coal, occupies the pore spaces (acting like a fluid with very low viscosity), or infuses into the coal matrix. Under these conditions it is probably not realistic to talk of sequestering the CO_2, because it might be mobile.

Studies have looked at the potential to sequester CO_2 in a number of areas. Pashin et al. (2003) studied the Black Warrior Basin; Bachu and Stewart (2002) and Hughes (in press) have studied the potential for CO_2 sequestration in the Western Canadian Sedimentary Basin. These studies involve analysis of the coal basins and measurement of CO_2 isotherms from representative coal seams. This report is an initial study of the CO_2 sequestration potential for coals in British Columbia. BC ranks fourth of the provinces in Canada in total greenhouse gas emissions but ranks eighth in terms of tonnes of CO_2 per person per year (Figure 1). The province does not generate electricity by burning coal, so that the more obvious point sources of anthropogenic CO2 emissions are less readily identifiable in the province. In fact the largest sources of CO_2 emissions are commercial and private transportation (Table 2); the easiest way for the province to reduce CO_2 emissions may be to improve the efficiency of fuel consumption in diesel and gasoline engines. Smaller point sources may be located close to coal deposits and it may be possible to sequester in coal seams some of the CO_2 that they generate. Ideal candidates may be cement plants and natural gas processing plants, because they produce relatively pure streams of CO_2.

[1]*Resource Development and Geosciences Branch, B.C. Ministry of Energy and Mines*
[2]*Oil & Gas Titles, B.C. Ministry of Energy and Mines*

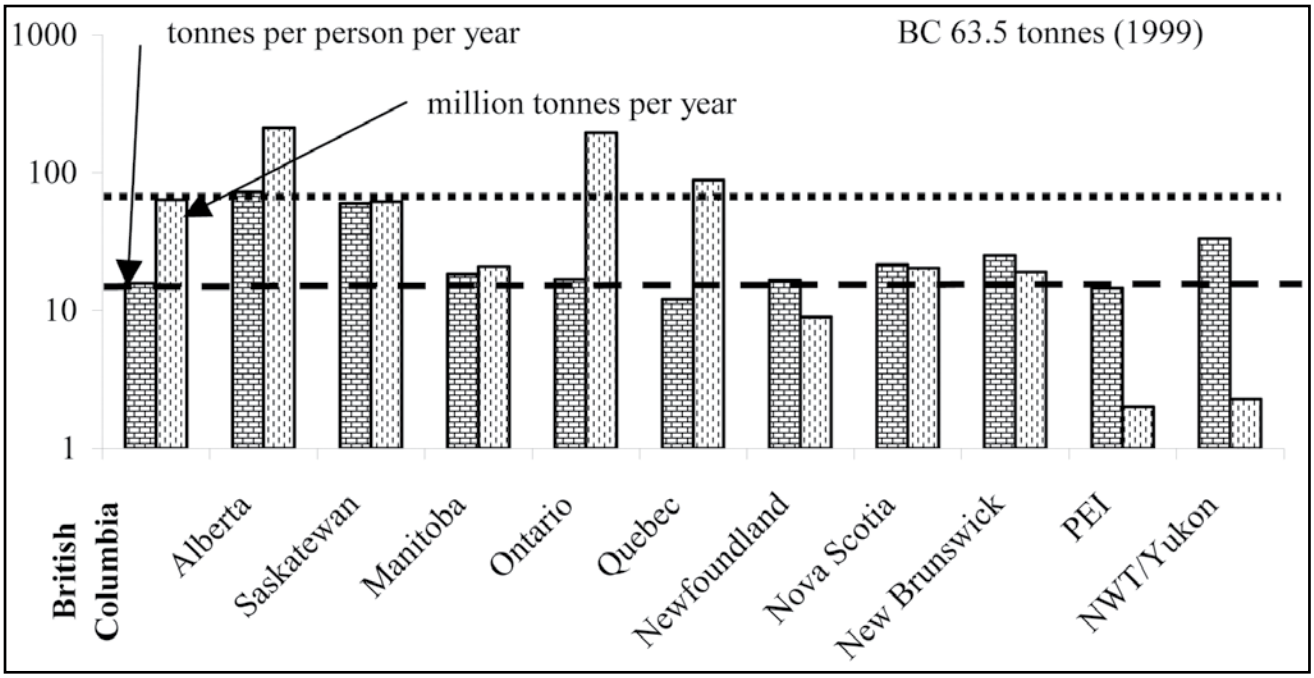

Figure 1. Total CO_2 emissions and CO_2 emissions per person for the provinces.

Data from Environment Canada 2000; Canada Greenhouse gas inventory 1990-1999.

The predominance of literature refers to the extraction of coalbed methane (CBM) from coal; this is not scientifically correct as the gas extracted from coal is a mixture of methane, carbon dioxide, and other gases. The British Columbia government is adopting the term coalbed gas (CBG). The abbreviations CBM and CBG both refer to the commercial gas extracted from coal at depth. To avoid confusion with existing scientific literature, this paper uses the term CBM.

TABLE 2. CO_2 EMISSIONS BY SOURCE IN BC FOR 1999.

			kg CO_2 equivalent
Energy	industry combustion		12.7
	transportation		26.1
	non-commercial combustion		7.95
	fugative	coal mines	0.5
		oil and gas	5.4
Industry process			2.9
Agriculture			2.6
Waste			4.9
Forestry			0.8
		total	63.85

Data from Environment Canada 2001,
Canada Greenhouse gas inventory 1990-1999.

SAMPLES AND SAMPLE LOCATIONS

Samples for this study were collected from a number of formations and from a single seam to provide some indication of the variation of CO_2 adsorption with changes in rank, maceral content, and temperature. A number of samples were collected from the Gething Formation in northeast BC at the same location as samples collected for a previous study of CH_4 adsorption characteristics (Ryan and Lane, 2002). Also in the northeast, two samples were collected from the Gates Formation at the Bullmoose Mine, which is now closed. In southeast British Columbia, one sample was collected from the Mist Mountain Formation. Two samples were collected from the Quinsam Coal mine on Vancouver Island. Tertiary coal deposits were represented by a drill core sample from the Princeton Basin.

The Gates and the Gething Formations, which are both Lower Cretaceous in age, are the two major coal-bearing formations in the Peace River coalfield in northeast BC. The formations outcrop extensively throughout the coalfield (Figure 2). Coal seams of economic interest in the Gates Formation occur exclusively south of the Sukunka River (Figure 2), and in the Gething Formation, mainly north of the Sukunka River.

The Gething Formation overlies the Cadomin Formation (Table 3), therefore it is slightly younger than the Mist Mountain Formation, which underlies the Cadomin in the southeast BC coalfields (Table 4). The Gething Formation samples were collected from the Willow Creek property, located on the south side of the Pine River about 40 km

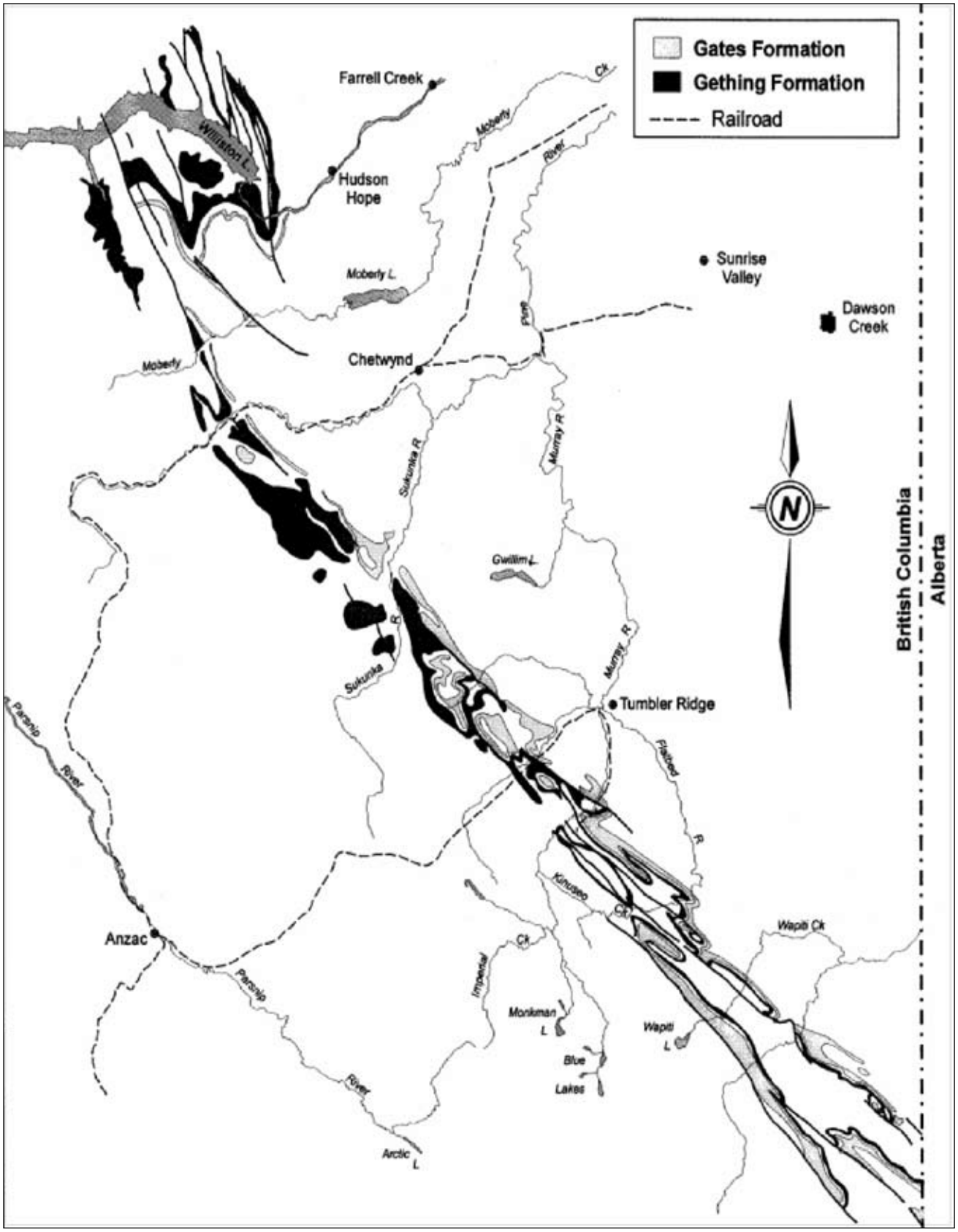

Figure 2. Outcrop pattern of the Gething and Gates Formations in the Peace River coalfield.

TABLE 3. GENERALIZED LOWER CRETACEOUS STRATIGRAPHY.

Pine River Area.			metres
Jurassic to lower Cretaceous	FORT ST JOHNS GROUP	CRUISER FORMATION marine shale	115
		GOODRICH FORMATION fine grained sandstone and shale	350
		HASLAR FORMATION marine shale	260
		BOULDER CREEK FORMATION sandstone and conglomerates	150
		HULCROSS FORMATION grey marine shale	100
		GATES FORMATION non marine sandstones and coal seams	110
		MOOSEBAR FORMATION marine shale	250
	BULLHEAD GROUP	GETHING FORMATION non marine sediments and coal	500
		CADOMIN FORMATION conglomerates	150

west of Chetwynd (Figure 2). The Pine Valley Mining Corporation plans to initiate mining in the formation at Willow Creek and has excavated a test pit. In this area, the Gething Formation has eight coal seams ranging in thickness from 1 to over 5 m and numbered from 1 downwards from the top of the formation. Six samples were collected from Seam 7-0 (Figure 3). The samples were collected from various locations in the seam, with the intention of representing a wide range of maceral composition. Samples were collected in the same area as the samples used in a previous methane adsorption study (Ryan and Lane, 2002).

The younger Gates Formation is separated from the older Gething Formation by the marine Moosebar Formation (Table 3). The formation hosts two major coalmines, both now closed. Western Canadian Coal Corporation proposes to renew mining in the formation. There are some CH_4 adsorption data available for the formation (Lamberson and Bustin, 1993) but no published CO_2 isotherm data. Samples of Gates Formation coal (B Seam) were collected from the Bullmoose Mine and from the Western Canadian Coal Corporation property (J Seam). Coal in the Gates Formation is generally restricted to 4 zones that are numbered from A counting up section to D. However, convention at the Quintette Mine and properties in the vicinity is to number the basal seam as K and with letters decreasing up section. Consequently B Seam at Bullmoose and J Seam in the Quintette area occupy similar stratigraphic levels in the Gates Formation.

The Mist Mountain Formation of Upper Jurassic to Lower Cretaceous age (Table 4) outcrops extensively in the Elk Valley and Crowsnest coalfields. The coal geology of the Elk Valley coalfield is summarized by Grieve (1993) and, to a lesser extent, Ryan (2003) has summarized the CBM potential of the Crowsnest coalfield. Both these publications list many other useful references. EnCana has drilled 17 CBM holes in the Elk Valley coalfield and at the moment is operating two pilots. As a consequence there exists a lot of CH_4 and CO_2 isotherm data, which are not yet public. Dawson *et al.* (2000) have summarized public data available for the two coalfields. In this study, Dave Endicott and Pat Gilmar (Elkview coal mine) provided a sample of the basal seam (10 Seam) from the Mist Mountain Formation.

On Vancouver Island, Upper Cretaceous coals occur in the older Comox Formation in the Comox Coal Basin and in the younger Protection and Extension Formations in the Nanaimo Coal Basin. There are four seams in the Comox Formation; unfortunately, some papers number the seams from 1 at the base, counting up to 4 at the top, and some papers start at 4 at the base, counting down to 1 at the top. The Quinsam mine extracts coal from two seams in the Comox Formation, the basal (1 Seam) and the third seam up section (3 Seam). Steve Gardner (chief geologist, Quinsam coal mine) provided samples of 1 Seam and 3 Seam.

There are a number of Tertiary coal basins in British Columbia; however, it is difficult to get fresh samples. John Hodgins of Connaught Energy provided a drill core sample from the Princeton Coal Basin. Four coal zones are contained in the Allenby Formation; the sample was collected from the lowest zone, designated as the Black-Jack, Princeton, or Blue Flame zone.

TABLE 4. GENERALIZED JURASSIC-CRETACEOUS STRATIGRAPHY, EAST KOOTENAYS .

LOWER CRETACEOUS	CADOMIN FORMATION		
JURASSIC AND CRETACEOUS	KOOTENAY GROUP	ELK FORMATION minor coal	
		MIST MOUNTAIN FORMATION coal seams	
		MORRISSEY FORMATION	MOOSE MOUNTAIN MEMBER
			WEARY RIDGE MEMBER
JURASSIC	FERNIE FORMATION	PASSAGE BEDS	

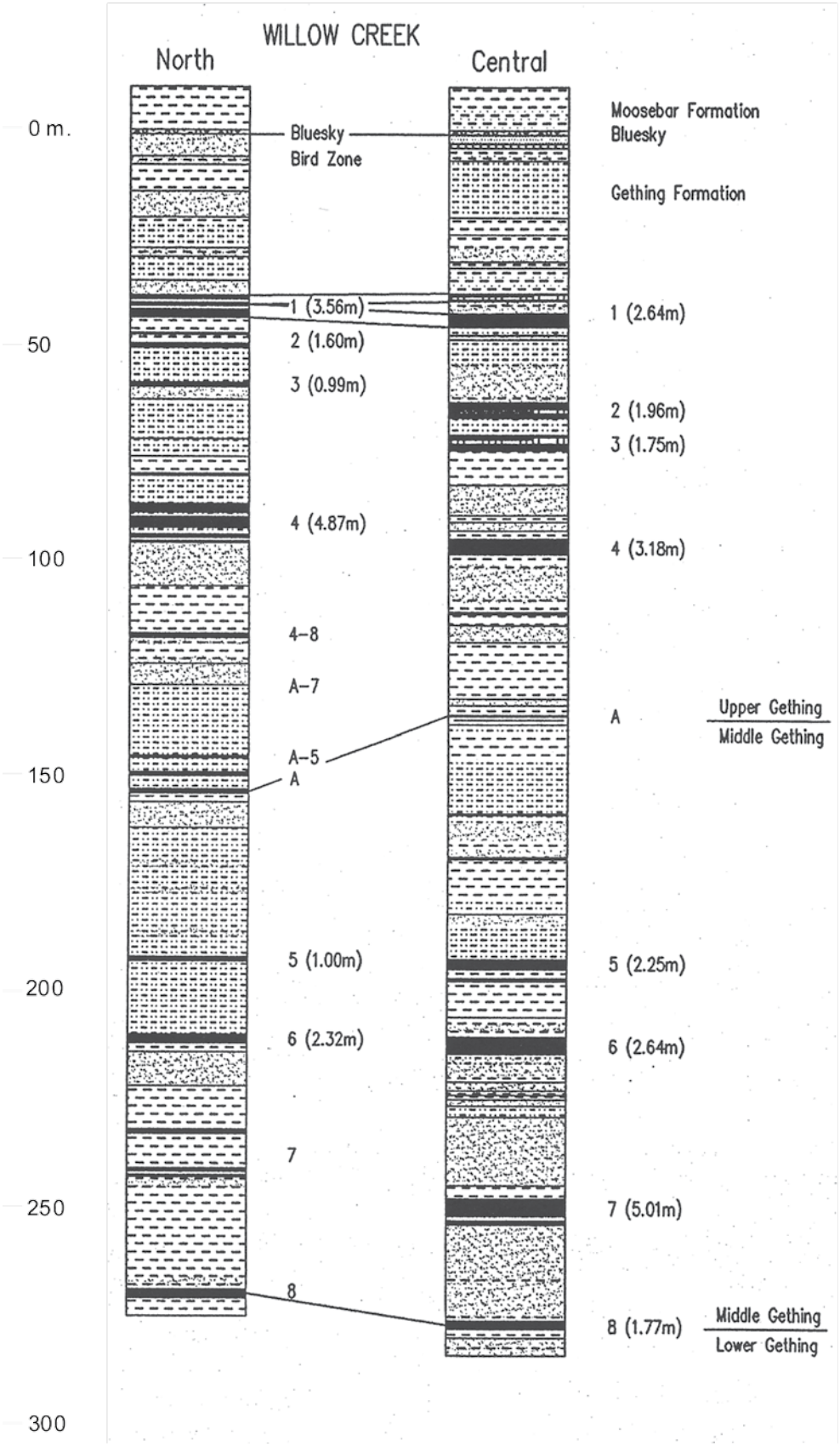

Figure 3. Stratigraphic section of the Gething Formation at the Willow Creek property (P.C. Kevin James).

SAMPLE PETROGRAPHY AND RANK

Karst and White (1979), Kalkreuth and McMechan (1988), Kalkreuth et al. (1989), and Marchioni and Kalkreuth (1992) have all discussed coal rank in the Gething Formation. Rank varies from semianthracite to high-volatile bituminous. Along the outcrop belt in the foothills, the rank is high, in places reaching semianthracite. To the north and east it decreases to high-volatile bituminous. There is some evidence that outcrops at the western outcrop edge of the formation have lower ranks. Rank was established prior to deformation and variations are related to changes in the thickness of the collective Gething and post-Gething sedimentary package (Leckie, 1983).

The rank at Willow Creek, where the samples were collected, ranges from medium- to low-volatile bituminous. The rank of the 7-Seam samples is low-volatile bituminous; Rmax = 1.64% (Table 5). Ryan (1997) and Ryan and Lane (2002) discuss the petrography of Gething Formation coal. Coal from the formation is characterized by variable reactives content and often low ash concentrations, which make it ideal for providing samples for studies investigating the influence of maceral content on adsorption of various gases. Reactive maceral contents range from approximately 80% to less than 50%. Samples (Table 5) have a high collodetrinte content, which contains fragments of non-structured inert macerals such as macrinite and inertodetrinite. Structured macerals, such as semifusinite and fusinite, are less common. Generally, compared to coals from the Mist Mountain Formation, there is less fusinite and semifusinite and consequently less preserved cell structure; this limits the possible content of dispersed mineral matter, which often fills cell lumen in these macerals. Some of the collotelinite contains the eye-shaped slits characteristic of pseudovitrinite, the origin of which is discussed by Ryan (2002).

The petrography of the three Gates Formation samples (Table 5) is similar to that of the Gething Formation samples, though the rank is lower (1.06% and 1.23%). The samples contain liptinite that is not present in the Gething samples, but they do contain pseudovitrinite that appears to be characteristic of most samples from the two formations collected from surface and at depth in drill holes. Lamberson et al. (1991) emphasize the importance of fires in forming inertinite in Gates coals. There is no obvious explanation for the variable and sometimes high content of inertinite in Gething coals. Gething coal swamps may have experienced more episodes of drying and a greater frequency of forest fires than did Gates swamps.

Grieve (1993) and others have studied the petrography of seams from the Mist Mountain. Rank varies from high-

TABLE 5. PETROGRAPHY AND MEAN MAXIMUM REFLECTANCE OF SAMPLES ANALYZED FOR CO_2 ISOTHERMS.

Data as volume percent	telinite	collo telinite	collo detrinite	vitro detrinite	liptinite	pseudo Vitrinite	semi fusinite	fusinite	macrinite	micrinite	inerto detrinite	mineral matter	Rmax %	total reactives	total inerts	TR mmfb
			Gething Formation													
7 seam -7	0	43	38	0	0	0	8	0	5	0	5	2	1.64	81	17	82
-2	0	37	52	0	0	0	1	0	0	0	3	6	1.64	90	4	96
-4	0	5	26	0	0	0	41	0	10	1	11	6	1.64	32	63	34
-3	0	3	28	0	0	0	34	0	17	1	14	2	1.64	31	67	31
-8	0	5	37	0	0	0	27	1	14	0	14	3	1.64	42	56	43
-5	0	14	39	0	0	0	35	0	3	0	5	3	1.64	53	44	55
			Gates Formation													
B seam fine	2	10	31	0	3	0	24	0	12	0	14	4	1.06	45	51	47
B seam coarse	0	3	32	0	3	0	30	0	10	0	16	5	1.06	39	57	41
J seam	0	26	26	1	0	0	18	0	5	0	8	16	1.23	53	31	63
			Mist Mountain Formation													
10 seam	0	20	25	1	0	0	26	0	6	0	8	13	1.28	46	41	53
			Comox Formation													
Quinsam 1 seam	5	18	47	0	5	1	9	0	2	0	6	9	0.68	75	17	82
Quinsam 3 seam	6	21	44	1	4	1	10	0	2	0	6	5	0.71	78	18	81
			Allenby													
Black-jack zone	1	21	57	0	7	0	0	0	0	0	0	14	0.70	85	0	100

volatile bituminous to low-volatile bituminous. Generally, seams are characterized by variable and higher inert maceral contents than are Carboniferous coals and are similar to Permian coals from Australia. They are similar in many aspects to coals in the Gething and Gates Formations, though they tend to contain more semifusinite and less macrinite than these formations. One of the more conspicuous differences is the near absence of pseudovitrinite.

The Upper Cretaceous coals on Vancouver Island are generally sub-bituminous to high-volatile A bituminous in rank. They are characterized by high vitrinite contents with moderate contents of liptinite and minor amounts of semifusinite. Psuedovitrinite is present but not common. They are less deformed than the coals in the Rocky Mountain foothills and often well cleated, though sometimes the seams low in the section have carbonate coating on cleat surfaces.

There are a number of Tertiary coal deposits varying in size from Hat Creek, which could contain 30 billion tonnes of lignite and higher-rank coals, to Coal River, which may contain about 100 million tonnes of lignite. Coal rank varies from lignite at Coal River to medium-volatile bituminous at Seaton, near the town of Smithers. Most of the Tertiary coals are sub-bituminous to high-volatile C bituminous. Coals in the Princeton Basin are sub-bituminous (Rmax = 0.7%; Table 5) and characterized by a very high percentage of vitrinite, with minor amounts of liptinite. Mineral matter is finely dispersed in the vitrinite.

SAMPLE DATA

Fifteen samples were submitted for CO_2 isotherm analysis (Table 6). The ash contents of the samples range from 1% to 20% and are generally low. Moisture contents are in the range of 2.5% to 12% and generally decrease as rank increases. The exception is the J-Seam sample, which was collected from an exploration outcrop and probably contains some oxidation. Most of the samples were analyzed at 25°C, but two were also run at 30°C. The Langmuir volumes (dry ash-free [daf] basis) range from 34 to 58 cm^3/g, though these values should not be taken as representative of the samples' adsorption ability, because at pressures over about 7.4 MPa, CO_2 is not a gas. Langmuir pressures for samples analyzed at 25°C range from 1.1 to 2.6 MPa, with a tendency to decrease as coal rank increases. The Langmuir pressures increase as temperatures of the isotherms increase.

CARBON DIOXIDE PHASE DIAGRAM AND CO_2 ADSORPTION POTENTIAL

The CO_2 phase diagram is well documented in terms of the boundaries between liquid, solid, and gas fields (Figure 4). However, the boundary between the gas and supercritical fluid fields at high temperatures and moderate pressures is less well defined and is probably represented by a zone. It is therefore difficult to determine the maximum depth at which coal can sequester CO_2 by adsorption in conditions where there is a high geothermal gradient. Figure 4 assumes that the supercritical fluid is separated from gas by a horizontal line, implying no temperature sensitivity; in fact the line should probably have a negative slope.

The vertical axis of Figure 4 is pressure, and consequently, to plot a depth tract for a stratigraphic section onto the figure one must have both temperature and pressure gradients. Once this is done, the point at which the depth tract crosses the gas-liquid or gas-critical fluid phase lines can be determined. The pressure at this point is then converted to a depth, based on the pressure gradient, and this is the maximum depth for CO_2 sequestration by adsorption on coal. By selecting a number of geothermal and pressure gradient pairs, it is possible to construct a diagram (Figure

TABLE 6. CO_2 ISOTHERM ANALYSIS RESULTS.

	as received		dry ash free						
	AR Lang Vol (cc/g)	AR Lang Pres (Mpa)	DAF Lang Vol(cc/g)	DAF Lang Pres (Mpa)	temperature (°C)	Ash (%)	as received moisture (%)	SG	Rmax
Gething									
7 seam -7	45.56	1.34	48.49	1.34	30	2.7	3.31	1.339	1.64
-7	48.15	1.23	51.25	1.23	25	2.7	3.31	1.345	1.64
-2	50.54	1.48	55.59	1.48	25	6.2	2.83	1.382	1.64
-4	54.66	1.27	57.49	1.27	25	1.1	3.85	1.338	1.64
-3	50.02	1.44	53.33	1.44	25	2.5	3.69	1.369	1.64
-8	51.95	1.44	55.69	1.44	25	2.9	3.88	1.369	1.64
-5	47.31	1.35	49.81	1.35	25	1.3	3.76	1.359	1.64
Gates									
B seam fine	31.14	1.15	34.45	1.15	25	6.9	2.74	1.370	1.06
B seam coarse	31.60	1.28	35.09	1.28	25	7.5	2.48	1.407	1.06
J seam	23.58	2.45	34.28	2.45	25	20.4	10.77	1.528	1.23
Mist Mountain									
10 seam	28.17	2.04	35.28	2.04	25	17.8	2.37	1.468	1.28
Comox									
Quinsam 1 seam	41.80	4.27	48.99	4.27	30	8.4	6.28	1.466	0.68
Quinsam 1 seam	31.40	1.32	36.80	1.32	25	8.4	6.28	1.444	0.68
Quinsam 3 seam	40.35	2.61	47.12	2.61	25	8.5	5.92	1.375	0.71
Allenby									
Black-jack zone	44.44	4.65	55.98	4.65	25	8.5	12.15	1.351	0.7

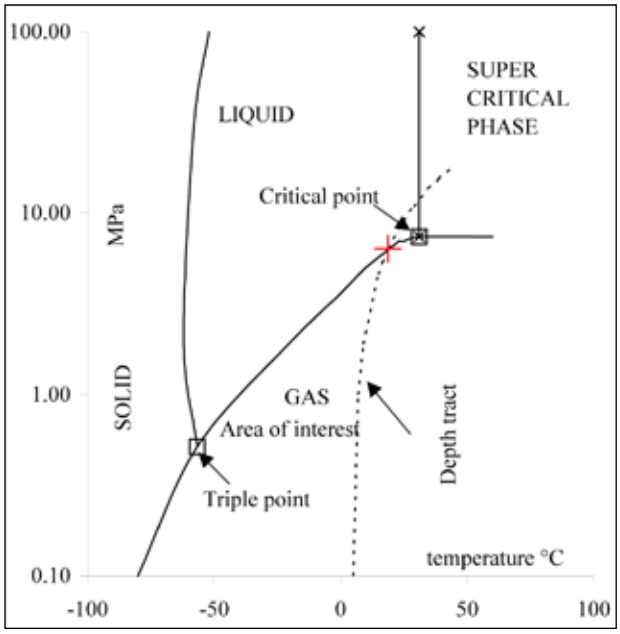

Figure 4. Carbon dioxide phase diagram.

5) in which the *x* axis is the pressure gradient and the *y* axis is the geothermal gradient and the contour lines represent the approximate maximum depths for sequestration by adsorption.

The area probably occupied by pressure and temperature gradients in BC coal basins is plotted into Figure 5, based on geothermal gradients for various coalfields in BC (Table 7). Generally, temperature data are available for holes drilled for oil and gas exploration. Often this is bottom hole temperature, so that an average temperature gradient is calculated assuming that the single temperature value is representative. Temperature gradients range from 18°C/km to 36°C/km; this compares to gradients in the Black Warrior Basin that range from 11°C/km to 22°C/km (Pashin and McIntyre, 2003). Pressure gradient information is not readily available from drill holes. If there is a normal hydrostatic gradient, the pressure gradient varies slightly based on the salinity of the water and will increase from 0.009818 MPa/m for fresh water to 0.00984 MPa/m for water with 3000 mg/L total dissolved solids. In a lot of sedimentary basins, normal hydrostatic gradients do not apply. Gradients in parts of the Western Canadian Sedimentary Basin are as low as 0.005 MPa/m. In the Black Warrior Basin, gradients range from normal (.00984 MPa/m to as low as 0.004 MPa/m and lower [Pashin and McIntyre, 2003]). In areas of complex structure such as northeast British Columbia, there can be considerable overpressuring, and hydrostatic pressure gradients can approach lithostatic gradients of 0.2 MPa/m or more.

The maximum depth of sequestration is estimated using the contour lines in Figure 5. The effect of the temperature gradient is minimal for low pressure gradients, though it increases as pressure gradients increase. The depth tract depends on the interrelationship of geothermal and pressure gradients, and the depth at which CO2 becomes supercritical or liquid can vary from about 400 m to over 1000 m. At shallow depths, conditions are defined by a low geothermal gradient matched to a high pressure gradient. At maximum depths, conditions are defined by a high geothermal gradient and low pressure gradient. These conditions may allow for adsorption of CO2 at greater depth, but the increased temperature will greatly reduce the ability of coal to adsorb any gas. The window for potential CO2 sequestration is probably below 200 m and above a depth defined in part by the CO2 phase diagram.

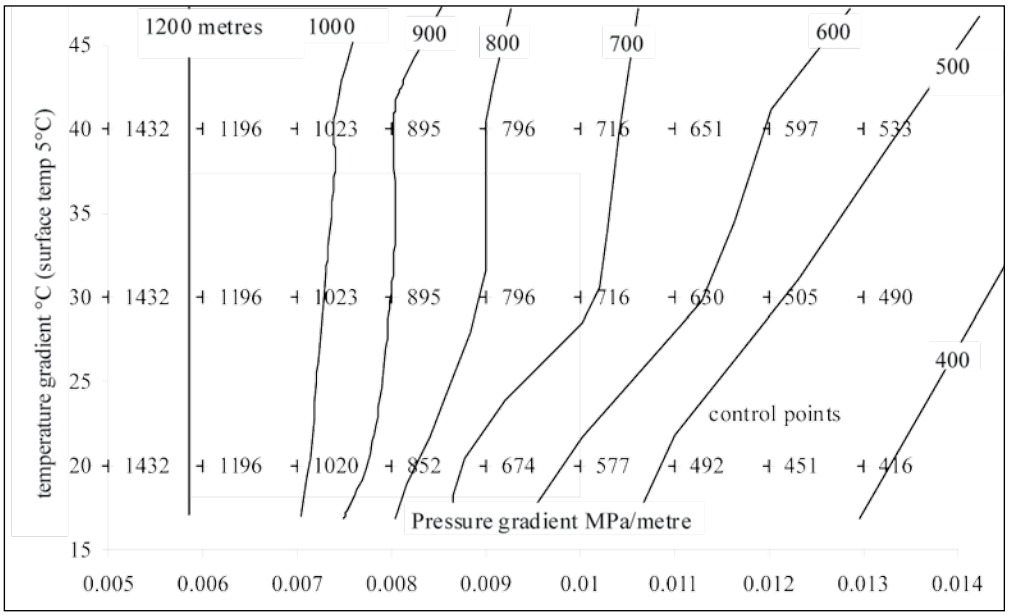

Figure 5. Diagram illustrating the approximate relationship between temperature and pressure gradients and the depth to the liquid or critical fluid fields for carbon dioxide.

TABLE 7. TEMPERATURE GRADIENTS IN COAL BASINS IN BRITISH COLUMBIA.

Region	local area	Surface temperature	gradient C /Km
SW BC	Comox	7	20.8
SW BC	Naniamo	7	27.5
SW BC	Naniamo	7	28.3
SW BC	Naniamo	7	23.3
SW BC	Naniamo	7	22.1
SE BC	Crowsnest area	8	25.4
SE BC	Crowsnest area	8	20.5
SE BC	Crowsnest area	8	18
SE BC	Elk Valley	8	23.6
SE BC	Elk Valley	8	36.2
NE BC	Bullmoose area	4	23.1
NE BC	Bullmoose area	4	30.2
NE BC	Bullmoose area	4	31.5
NE BC	Grizzly area	5	26
NE BC	Grizzly area	5	25.7
NE BC	Willow Creek	5	25.6
NE BC	Hudson Hope	5	30
NE BC	Hudson Hope	5	28.6
NE BC	Hudson Hope	5	36.4
NE BC	Hudson Hope	5	22.8

CARBON DIOXIDE AS A FREE GAS OR IN SOLUTION IN WATER OR AS A SUPER-CRITICAL FLUID

When CO_2 is injected into seams, some of the CO_2 goes into solution in the water associated with the coal. Water associated with coal occurs in three forms, defined in different ways and given different names. In simple terms, the three forms may be referred to as free and mobile water in fractures, surface water loosely bound to coal surfaces, and structural water, which forms part of the coal structure. Surface water is the difference between equilibrium moisture and inherent moisture. The amount of surface water depends on rank (Figure 6) and on the amount of porosity. The amount of CO_2 that can be held in solution in water therefore depends on rank, porosity, and temperature and pressure conditions. The solubility of CO_2 in water increases with pressure but decreases with temperature. There are numerous sources of data describing CO_2 solubility; unfortunately, there are as many combinations of units as there are

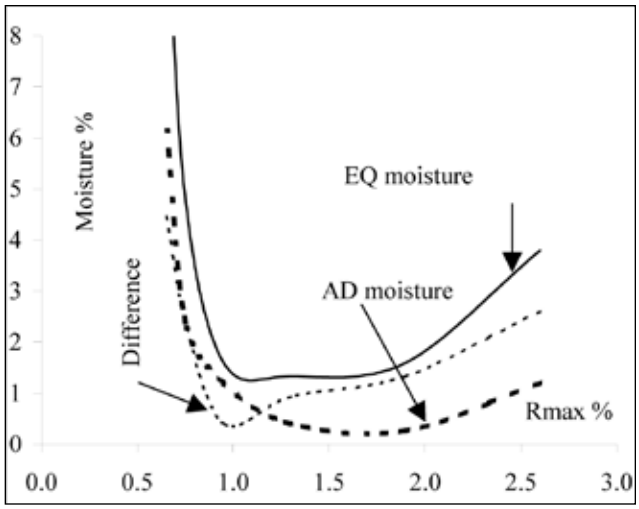

Figure 6. Air-dried, equilibrium, and free water versus rank

examples of CO_2 solubility plots. The plots (Figure 7) are adapted from Jarrell (2002) and Rightmire (1984). Based on the interplay of geothermal and temperature gradients, the amount of CO_2 held in solution ranges from about 25 to 35 m^3 gas in solution in 1 m^3 water. The actual amount held in 1 tonne of coal depends on rank and water-filled porosity. For low-rank coals, the amount of CO_2 in solution can range up to 8 cm^3/g, and for higher-rank coals probably is not more than 1 cm^3/g.

Below the critical point, CO_2 is contained in the coal by adsorption, in part by solution in the interstitial water and as free gas. The amount of CO_2 held in a free-gas phase can be estimated from the ideal gas law and ranges up to about 8 cm^3/g for 15% gas-filled porosity at a depth less than that equivalent to the critical point (Figure 8). Obviously the amount held by adsorption is much greater than that held in solution or as free gas for all ranks of coal.

The density of CO_2 gas as it approaches critical conditions is about 0.15 g/cm^3. Once CO_2 enters the supercritical phase, the density increases rapidly to about 0.7 g/cm^3 (Figure 9) and maintains this value as pressure and temperature increase as predicted by normal hydrostatic and geothermal gradients. Density tends to stay in a narrow range above the critical point because of the opposing effects of increasing pressure and increasing temperature. The rapid change in density as conditions approach the critical point makes it very difficult to determine the adsorption characteristics of CO_2 at temperatures approaching critical conditions.

GENERAL COMMENTS REGARDING ADSORPTION OF CO_2 ON COAL

As pressure increases, CO_2 becomes a liquid or a supercritical fluid as indicated by the CO_2 phase diagram (Figure 4). The diagram indicates the limited pressure-temperature

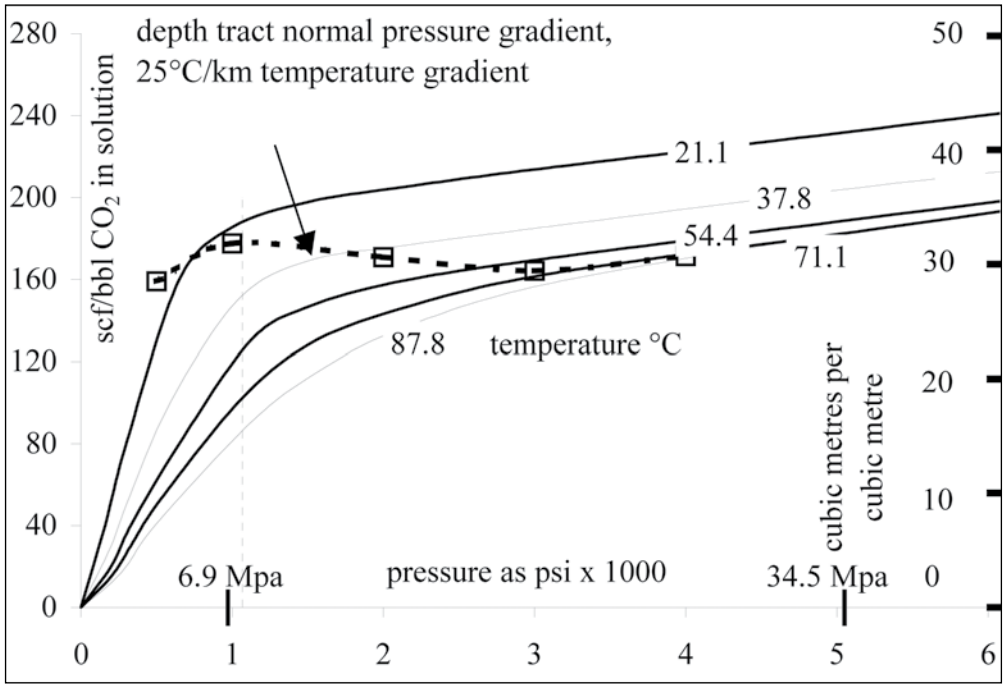

Figure 7. Plots of CO_2 solubility versus depth and temperature; data from Jarell et al. (2002) and Rightmire (1984).

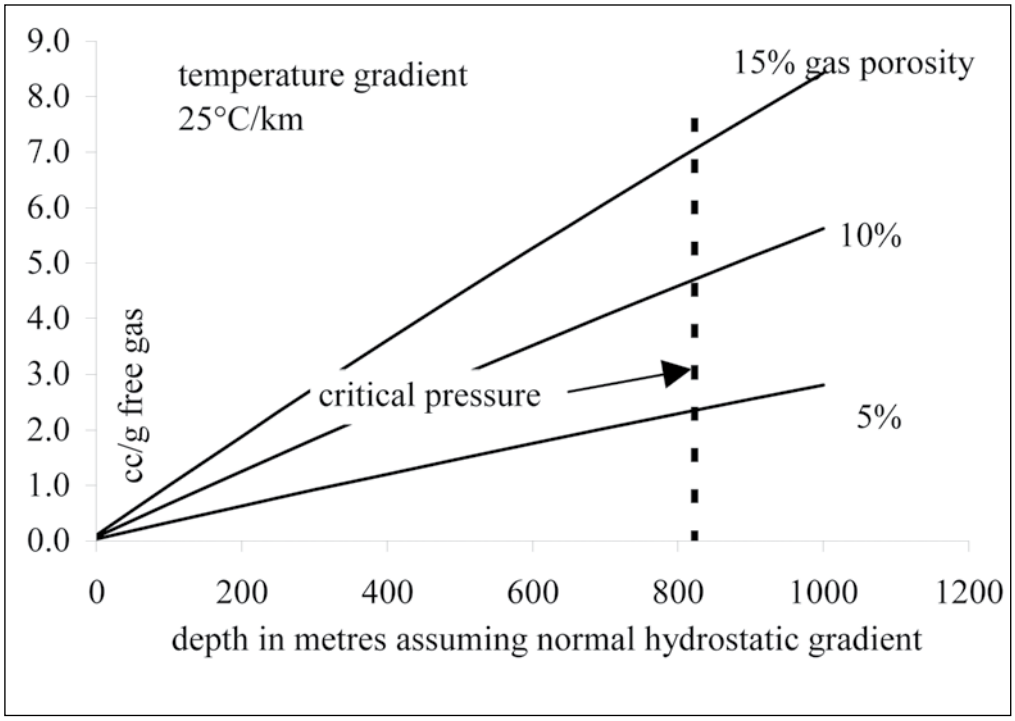

Figure 8. Potential free gas based on porosity assuming a normal hydrostatic gradient and a geothermal gradient of 25°C.

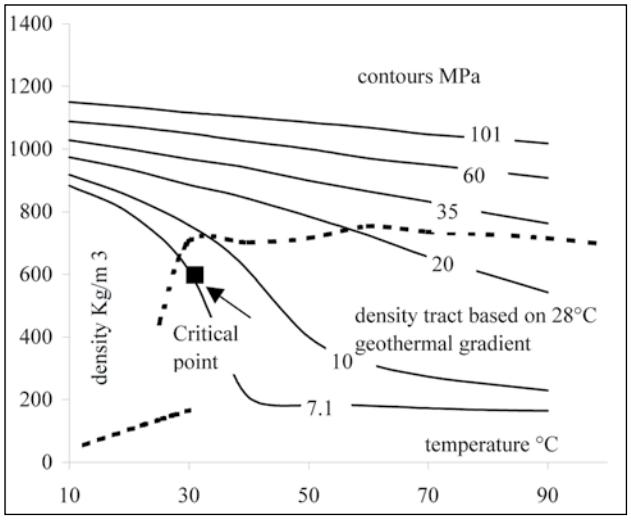

Figure 9. Density of CO_2 as a gas and in the supercritical phase; plots adapted from Bachu and Stewart (2002) and Pruess *et al.* (2001).

field in which CO_2 is a gas and therefore, based on pressure and temperature gradients, defines the depth range through which CO_2 can be sequestered by adsorption. The diagram is for pure CO_2; the addition of other gases will change the field boundaries, probably increasing the size of the gas field in terms of pressure. This is important because it may not always be cost effective to obtain a pure CO_2 gas for injection.

It is not reasonable to consider the Langmuir volume (adsorbed volume at infinite pressure) as a measure of the CO_2 adsorption ability of a sample, because CO_2 becomes a supercritical fluid at quite low pressures. It is therefore best to compare the adsorption of CO_2 at a fixed depth and not at infinite pressure. In this study isotherms were run at 25°C and 30°C, temperatures typically seen at depths of 600 to 900 m in sedimentary basins in BC. The temperature at which isotherms are run combined with temperature and pressure gradients in an area combine to provide the specific depth at which the isotherm is predicting real gas contents. Adsorption data from a number of isotherms should be compared based on calculated gas contents at this depth.

Some of the earliest investigations of the CO_2 adsorption capacity of coal were conducted by Ettinger *et al.* (1966). They recognized the stronger adsorption of CO_2 than of CH_4 onto coal and suggested that the relative adsorption of gases such as H_2S, CO_2, CH_4, N_2, and H_2O is related to their liquefaction temperature. They also pointed out that there is an increased danger of mine outbursts when coals contain a higher proportion of adsorbed CO_2. Levy *et al.* (1997) documented the difference in Langmuir volumes for nitrogen, methane, and carbon dioxide for isotherms measured on moist coal at 30°C. Working with Bowen Basin coals covering a rank range of high-volatile bituminous to low-volatile bituminous, Levy *et al.* (1997) found that the CO_2/CH_4 molar ratio for adsorbed gases decreased consistently from 1.82 to 1.37 as rank increased. They suggest that the greater adsorption of CO_2 is probably related to the increased polar nature of the molecule compared to CH_4 (Levy *et al.,* 1997).

Krooss *et al.* (2001) studied the adsorption behaviour of CO_2 at high pressures and temperatures, in part above the critical point. They discussed the difficulty of interpreting experimental results above the critical point. The density of the adsorbed phase and of the phase occupying the void in the canister are both difficult to determine. They assumed a density of 1.028 g/cm^3 for the adsorbed CO_2. In addition, the coal probably swells, which makes it even harder to correct for the component of CO_2 that is not adsorbed. Adsorption experiments do not generally confine the coal, because it is loosely packed as fine grains, and therefore they do not model the competing effects of matrix swelling and adsorption that occur in nature. In general, the results of Krooss *et al.* (2001) conform to Langmuir adsorption below the critical point, but above pressures of about 6 MPa (similar to the critical point pressure 7.47 MPa), results are inconsistent with normal adsorption. Even after data are corrected for the assumed volume of the adsorbed phase using a density of 1.028 g/cm^3, adsorption is negative. This probably indicates swelling of the coal and use of an overly large void space in the canister to correct for the non-adsorbed CO_2 phase. As Krooss *et al.* (2001) state, it is difficult to interpret the results above the critical point and even more difficult to predict what they might mean for a seam at depth.

Larsen (2004) documented the solution of CO_2 in coal over a wide range of pressure and temperature conditions extending below the critical point. Solution of CO_2 causes coal to expand but also increases the plasticity of coal. These two effects are potentially devastating to the permeability needed to inject CO_2 into coal. The amount of CO_2 dissolved in coal increases as pressure increases and as rank decreases. At pressures equivalent to depths of 150 to 200 m, about half the CO_2 contained in medium- or low-rank coals is in solution (Reucroft and Sethurarman, 1987). The softening temperature of coal appears to decrease to about 31ºC at the critical pressure (Figure 10), implying that the coal becomes a plastic solid above critical conditions of temperature and pressure.

The stronger adsorption of CO_2 affects the relative rate of desorption of CO_2 relative to CH_4, and the CO_2 content of produced gases generally increases over time. The effect is predicted by the extended Langmuir equation (Arri *et al*., 1992).

INFLUENCE OF RANK AND PETROGRAPHY ON CO_2 ADSORPTION

Adsorption of methane tends to increase as rank increases, initially rapidly and then more slowly at high ranks, though the relationship of adsorption to rank for medium-

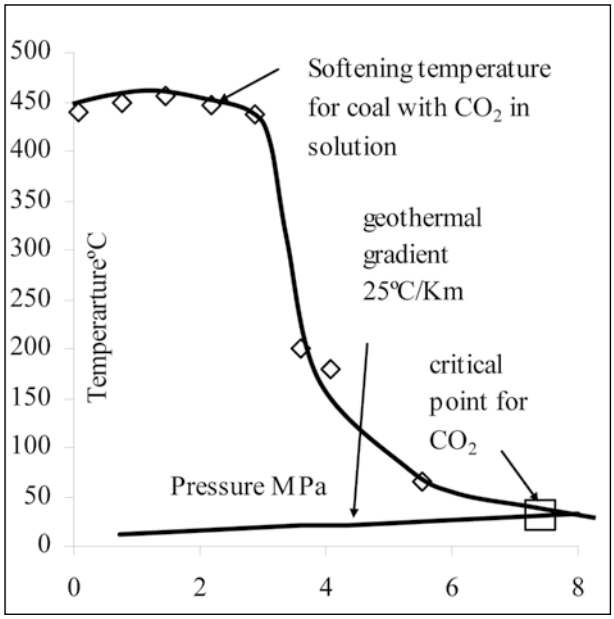

Figure 10. Softening temperature of Lower Kittanning coal (89.6% C, dry ash-free) at increasing pressure; plot adapted from Khan and Jenkins (1985) in Larsen (2004).

volatile coals is less well defined. For example, coals from the Bowen Basin (Levy *et al*., 1997) have higher adsorption capacities than coals of similar rank from the US (Levy *et al.,* 1997). Some of the variation may be caused by variable maceral content in the samples. Despite the fact that many diagrams (Ryan, 1992) imply a consistent relationship between rank and adsorption ability for CH_4, the reality is much more complicated.

Carbon dioxide adsorption capacity has a weak correlation with rank, increasing at high rank, but there are indications that adsorption is higher for lignite and sub-bituminous coals than it is for bituminous coals. This is hinted at in the data from Gluskoter *et al.* (2003) and from data in this study (Figure 11). Volume data from Gluskoter *et al.* are plotted at 300 psi and as standard cubic feet per ton (scf/t, dry ash-free [daf] basis) so that data from this study (Figure 11) are recalculated to the same pressure. Gluskoter *et al.* (2003) do not specifically identify rank by reflectance so that some assumptions are made in incorporating their data into Figure 11. However, it is obvious that both data sets imply higher adsorption for low- and high-rank coals than for medium-rank coals. The present data set was generated at 25°C. The temperature of the Gluskoter *et al.* data set is not stated.

The adsorption behaviour of CO_2 at low rank is different from that of CH_4, and this probably relates both to the distribution of micro-, meso-, and macroporosity by rank and to the stronger polarity of the CO_2 molecule compared to the CH_4 molecule. Rightmire (1984), Bustin and Clarkson (1999), and Levine (1993) have all summarized the distribution of porosity in coal (Figure 12). Total po-

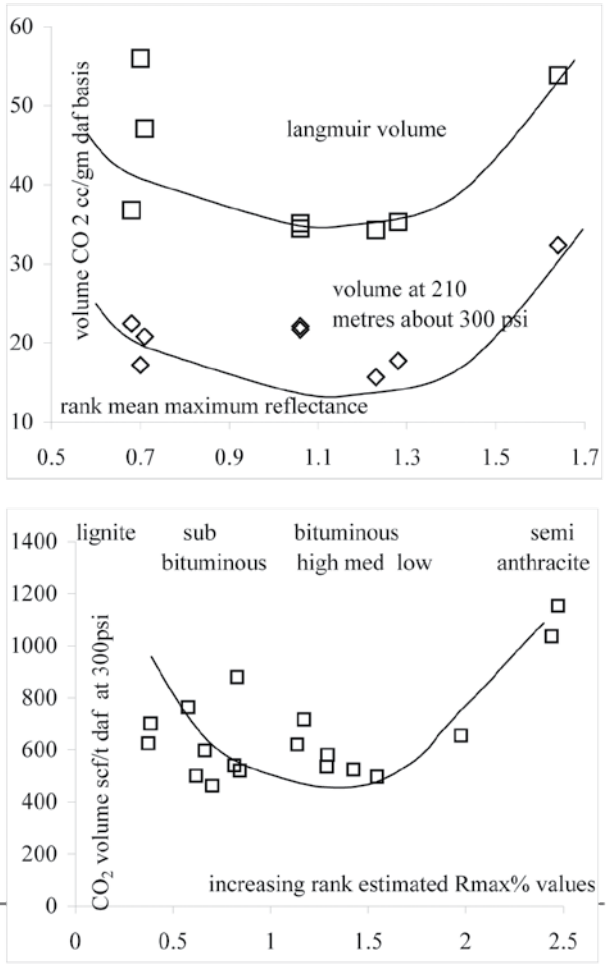

Figure 11. Carbon dioxide adsorption versus rank. Data from this study and from Gluskoter et al. (2002).

rosity is a minimum for medium-volatile rank coals, and macroporosity decreases as rank increases. At low ranks, the increased mesoporosity allows CO_2 to adsorb, possibly as a volume filling in meso-sized pores, whereas CH_4 with lower polarity forms layer adsorption in micropores. The selectivity of CO_2 over CH_4 is high, and the amount of CO_2 adsorbed high, despite low rank. As rank increases, the amount of mesoporosity decreases, CO_2 adsorption decreases, and CH_4 adsorption increases. Consequently the selectivity for CO_2 decreases. At high rank, the increase in microporosity causes increases in the adsorption of both CO_2 and CH_4 without a major increase in the selectivity for CO_2. Determining the effective porosity distribution in coals is difficult because experiments are often not done on moisture-equilibrated coal at in situ pressures. Also, the structure of low-rank coals is less predictable than that of higher-rank coals, and this results in a wider variation of porosity distribution. It is therefore hard to predict the CO_2 and CH_4 adsorption characteristics of low-rank coals.

The selectivity of CO_2 versus CH_4 of coals decreases as rank increases but may increase again at high ranks. Data

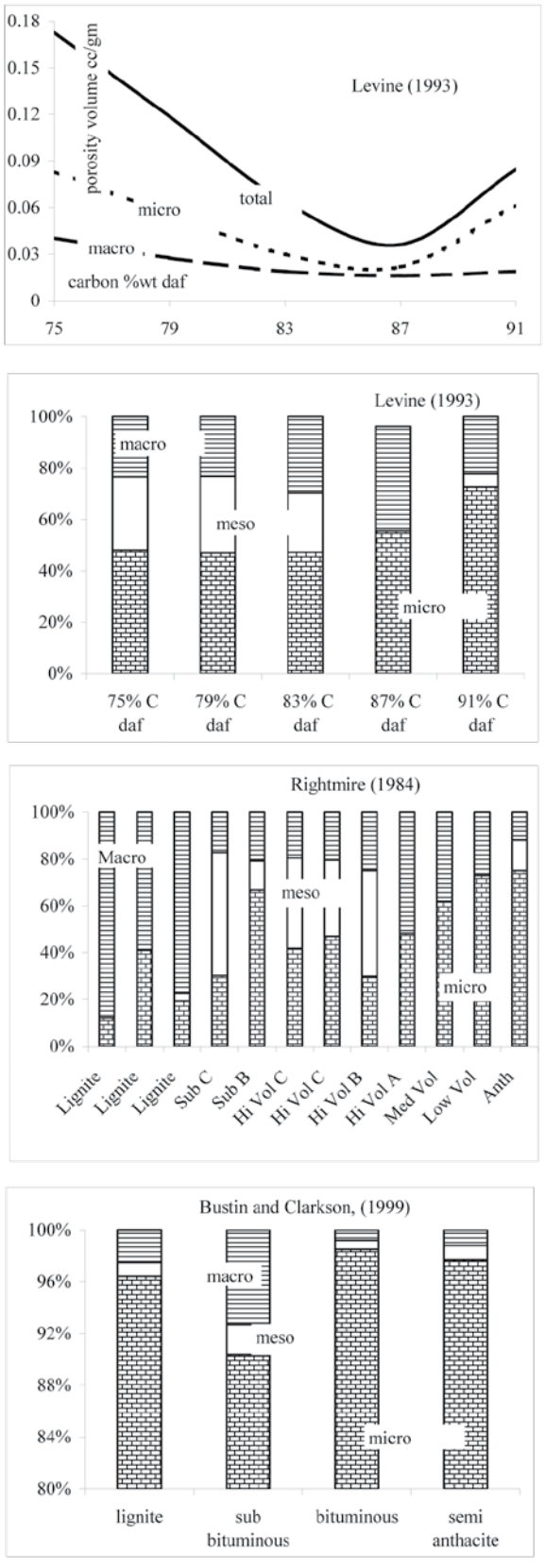

Figure 12. Distribution of porosity in coal data; adapted from Rightmire (1984), Bustin and Clarkson (1999), and Levine (1993).

from this study include only CO_2 isotherms, but in most cases CH_4 isotherms exist for the coals from previous studies, so that it is possible to construct an approximate plot of CO_2/CH_4 ratio versus rank (Figure 13). Ratios in Figure 13 are calculated at a pressure of 300 psi to conform to the data from Gluskoter *et al.* (2003), which is also reproduced in Figure 13. The ratio is very high (approaching 20) for low-rank coals and then decreases to a range of 1.5 to 2 for medium-rank coals. It might increase slightly in high-rank coals. For coals of all ranks, the volume ratio of CO_2/CH_4 decreases as pressure increases (Gluskoter *et al.,* 2003) and probably also as temperature increases.

It is important to recognize the difference between molecule-for-molecule replacement and weight-for-weight replacement when comparing the adsorption capacity of CO_2 and CH_4. If there is a one-for-one molecule replacement, then 2.75 g of CO_2 will replace 1 g of CH_4 (the ratio of the molecular weights). In terms of greenhouses gases, one is interested in sequestering a weight of CO_2, not a volume. The increased selectivity and adsorption of low-rank coals may make them better candidates for CO_2 sequestration than higher-rank coals.

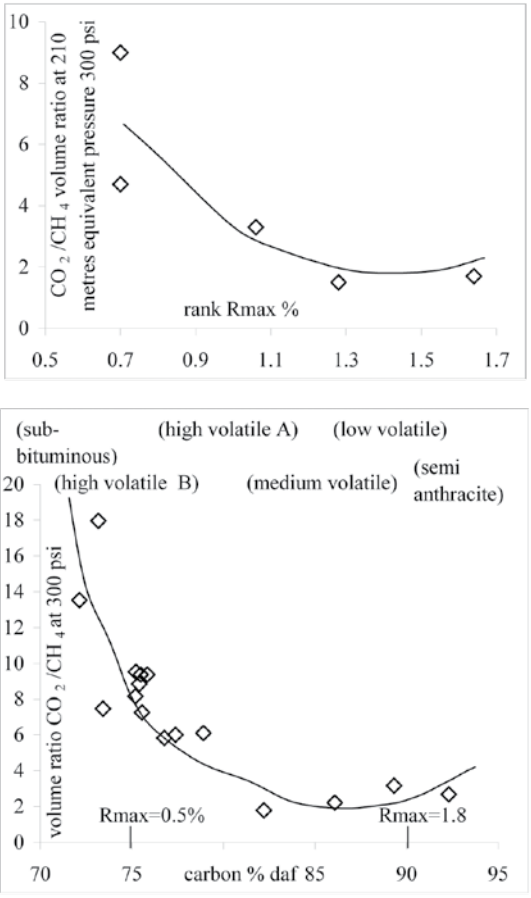

Figure 13. Plot of CO_2/CH_4 ratio (calculated at 210 m equivalent pressure) versus rank. Data from this study from Gluskoter *et al.* (2003).

This of course assumes that they are not already saturated with CO_2. Low-rank coals have better diffusivity and should maintain permeability and accommodate matrix swelling better than do higher-rank coals.

Macerals are not minerals and do not have defined crystal structures like minerals. However there are generalizations that hold about the different characteristics of macerals. Inert macerals have more mesoporosity and less microporosity than do reactive macerals (Harris and Yust, 1976; Gan *et al.,* 1972). At constant rank, the effect of petrography on methane adsorption has been studied by a number of authors (Ryan and Lane, 2002; Lamberson and Bustin, 1993). Either there is no correlation or adsorption ability tends to increase as the percentage of reactive macerals increases. These studies were done on medium- or low-volatile coals. In British Columbia, many of the Tertiary low-rank coals are composed, on a mineral-matter-free basis, of almost 100% reactive macerals, making it difficult (and less relevant) to study the effects of petrography on the adsorption characteristics of low-rank coals.

Studies of the maceral influence on the adsorption of CO_2 are more limited. Gluskoter *et al.* (2002) presented data that indicate no correlation between inert maceral content and adsorption of CO_2 for a range of 0% to 25% inerts in low-rank coals. In this study, a number of samples with a rank of 1.64% and varying petrography were analyzed (Table 5), as were two samples (rank 1.06%) with somewhat different petrography. These were actually the same sample screened to different sizes to provide a partial concentration of vitrinite. The Gething Formation samples with Rmax of 1.64% (Figure 14) are plotted on a total reactives versus gas plot, with the CO_2 gas contents plotted as gas contents at 210 m (300 psi) or as Langmuir volumes. The data indicate a weak negative correlation of gas content with increasing reactives content. This is the reverse of the situation for samples of the same coal analyzed for CH_4 adsorption (Figure 15). One of the Gething samples (Table 5) has distinctly

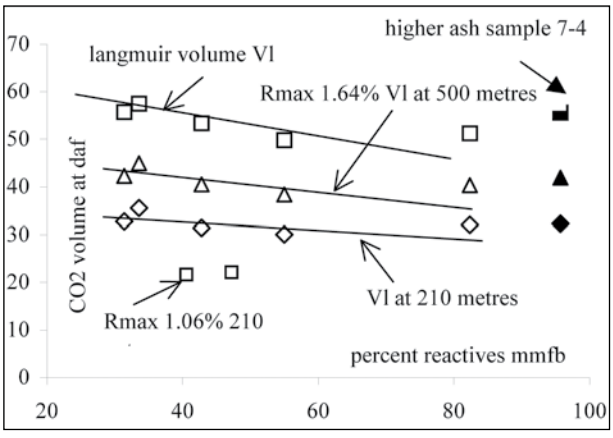

Figure 14. Plot of CO_2 adsorption at different depth versus reactive content for the Gething Formation samples.

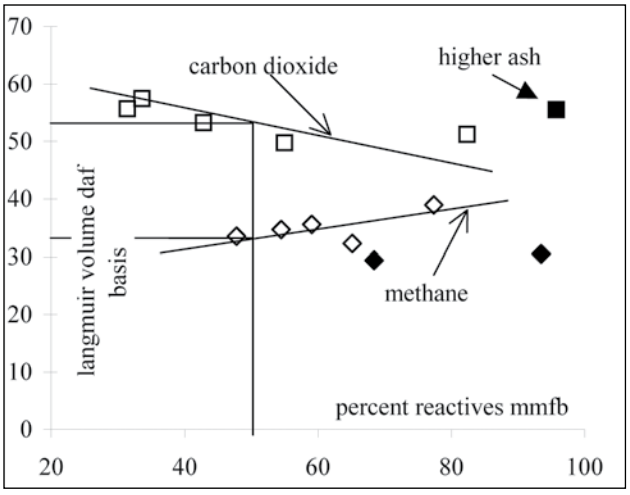

Figure 15. Plot CH_4 and CO_2 adsorption versus content for Gething Formatio samples. CH_4 data are from Ryan and Lane (2002).

higher ash than the other samples, and it is highlighted in the plot (Figure 14). It appears that the effect of petrography on CO_2 and CH_4 adsorption is different for high-rank coals. The CO_2/CH_4 ratio increases as the inert maceral content increases. This means that some of the Jurassic-Cretaceous coals of BC, which are characterized by moderately high inert maceral contents, may have improved ability to sequester CO_2. At lower ranks it appears that CO_2 adsorption does not vary much with maceral content, as indicated by the two samples (rank 1.06%) also plotted into Figure 14 and by the Gluskoter data for sub-bituminous coals.

Pure gas isotherms illustrate the ultimate replacement potential of CO_2 for CH_4. Unfortunately, they give no hints as to how to achieve this. The extended Langmuir equation predicts the ratio of adsorbed gases based on the mole ratio of gases in the free phase (Figure 16). For example, if the mole ratio of CO_2 in the gas phase is 0.5, then the mole

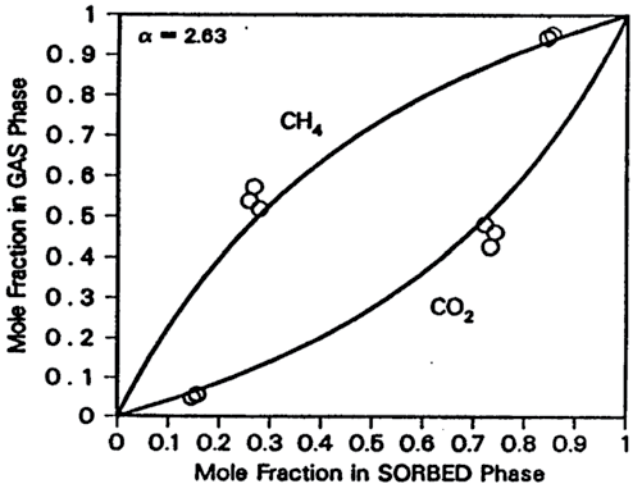

Figure 16. CO_2/CH_4 mole fraction in gas and adsorbed phase; data from Arri *et al.* (1992).

ratio in the adsorbed phase will be 0.7, and this requires a mole ratio of 0.3 CH_4 in the adsorbed phase and 0.45 in the gas phase. Figure 16 is coal- and temperature-specific but it does indicate trends as predicted by the extended Langmuir equation. Arri *et al.* (1992) found that the CO_2 data had, at best, a moderate fit to curves predicted by the extended Langmuir equation. Crosdale (1999) analyzed the composition of adsorbed gas for increasing pressure steps for a gas phase of 52.9% CO_2 and 47.1% CH_4. The results do not conform to the extended Langmuir equation. The amount of CO_2 adsorbed was, in agreement with a pore-filling model, influenced by the faster diffusion of the smaller CH_4 molecule. The CH_4 molecule was able to diffuse into the coal faster than the CO_2 molecule and block or occupy adsorption sites. During desorption, as pressure drops, CH_4 desorbs faster, leaving an increased concentration of adsorbed CO_2. Based on Crosdale's work, increasing the pressure of CO_2 in coal not desorbed of CH_4 may not release as much CH_4 or adsorb as much CO_2 as is predicted by the extended Langmuir equation. If the coal is undersaturated with CH_4, then it should be possible to predict CO_2 adsorption based on a CO_2 isotherm. The mechanics of getting the CO_2 to permeate coal depends on permeability, and the adsorbtion of CO_2 on coal depends on matrix swelling. If the coal seam has limited permeability, then CO_2 flooding and adsorption may not be possible.

Some of the early studies on CO_2 adsorption were interested in the potential of using CO_2 for enhanced coalbed methane recovery (ECBMR). In this case, a coal with low CO_2 selectivity is better than one with a high CO_2/CH_4 selectivity ratio. In all cases for ECBMR, it is important that the recovered gas does not have a high CO_2 component, as this adds to the costs of upgrading the gas to pipeline quality. In many situations ECBMR may not be practical because of low permeability and high concentration of CO_2 in the recovered gas. The results of the Allison CO_2 injection project of Burlington are somewhat inconclusive; injection of CO_2 certainly increased water production, in part probably because CO_2 went into solution in the water, decreasing its viscosity. In low-rank coals this may have the effect of drying the coals, which would then increase their adsorption ability. In an ECBMR situation, this may mean production of water and temporary sequestration of CO_2 and minimal release of CH_4. When water re-enters the seam, adsorption ability may decrease, causing CO_2 to be released.

INFLUENCE OF TEMPERATURE ON CO_2 ADSORPTION

Any temperature increase below the critical temperature decreases the ability of samples to adsorb CO_2. This effect has to be paired with a geothermal and pressure gradient to attempt to construct real adsorption versus depth tracts. In this study, two samples were analyzed at 25°C and 30°C (Table 6, Figure 17). The Langmuir pressures increase as the temperature increases.

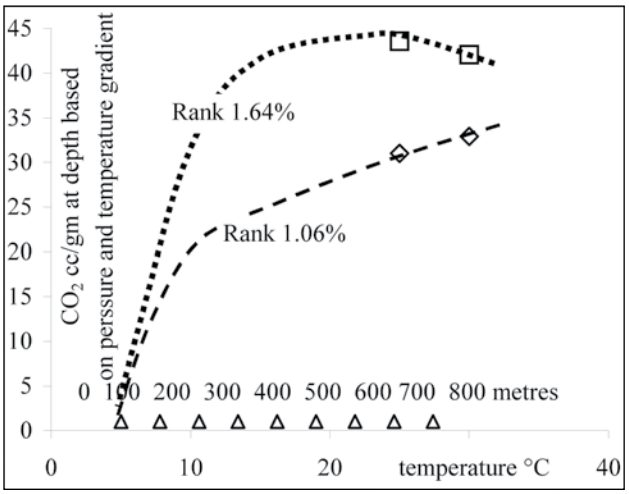

Figure 17. Plot of CO_2 adsorption at different temperatures. Data volumes calculated based on a normal hydrostatic gradient and a geothermal gradient of 28°C/km with surface temperature of 5°C.

The same effect is seen for CH_4 isotherms; however, the CO_2 Langmuir volumes do not consistently decrease as temperature increases. When the CO_2 gas contents are calculated at the depth and pressure that correspond to the temperature of the isotherm, the adsorption for the high-rank coals decreases as depth increases, and for the low-rank coals, the adsorption increases with depth (Figure 17). This is in a depth window of about 700 to 800 m. Higher-rank coals have lower Langmuir pressures, indicating curves that are steeper at the origin than are curves for low-rank coals. This, combined with the effect of increasing temperature, means that for low-rank coals, the adsorption still tends to increase with depth and temperature, whereas for high-rank coals, the adsorption decreases as depth and temperature increase.

It is very important to construct adsorption versus depth tracts for different rank coals for the depth range that corresponds to temperatures below the critical temperature. The implication of Figure 17 is that it might be better to sequester CO_2 in lower-rank coals at depth than to sequester it in higher-rank coals.

SEQUESTERING CO_2 IN BRITISH COLUMBIA COALS

One of the most understated facts about sequestering CO_2 in coal is that it can only happen by first displacing the CH_4 already adsorbed by the coal. The coal may or may not be saturated with adsorbed CH_4, but it will certainly have

some that will be released when the CO_2 is adsorbed. On a weight basis, the amount of CO_2 adsorbed is between 5 and 30 times the amount of CH_4 desorbed, calculated at a depth of 210 m (Table 8). The ratio of CO_2/CH_4 decreases as pressure (depth) increases, though the situation is more complicated when the effect of increasing temperature is factored in. This sounds very favourable in terms of sequestering CO_2; unfortunately the CH_4 released is about 20 times more powerful as a greenhouse gas. Consequently, unless CO_2 sequestration is paired with CH_4 recovery, there is likely to be, over the long term, a net increase in the release of greenhouse gases.

TABLE 8. THE RATIO OF CO_2/CH_4 ADSORBED ON COALS OF DIFFERENT RANKS.

Rank	Rmax%	volume ratio	wt ratio	CO_2 scf/t daf at 300psi =213 m depth	CO_2 cc/g	CH_4 cc/g
Gluskoter						
lignite		9.4	25.9	800	25.0	2.7
sub bit		7.6	20.9	900	28.1	3.7
high vol		5	13.8	700	21.8	4.4
medium vol		2.4	6.6	600	18.7	7.8
low vol		2	5.5	800	25.0	12.5
Semi anth		2.6	7.2	1000	31.2	12.0
this paper						
Low vol	1.64	1.7	4.7	998	31.2	18.3
medium vol	1.28	1.5	4.1	550	17.2	11.4
High vol A	1.06	3.3	9.1	685	21.4	6.5
High vol B	0.7	4.7	12.9	527	16.4	3.5
High vol B	0.7	9	24.8	611	19.1	2.1

Data calculated at a pressure of 300 psi, equivalent to a depth of 210 m.

Many coals are undersaturated with respect to CH_4 and CO_2. In these cases, CO_2 injected will initially be adsorbed without any release of CH_4. The coal matrix will expand, decreasing permeability and making it even more difficult for CO_2 to infuse coal and for CH_4 to escape. In situations where the coal is partially desorbed of CH_4 because of production, the pressure is reduced and there will be some matrix shrinkage, which may improve permeability. In this case, CO_2 should be able to permeate coal and be adsorbed; however, because the coal is undersaturated with respect to CH_4, there may not be an immediate release of additional CH_4 as the pressure increases and the composition of the gas phase becomes more CO_2 rich.

One of the best ways of locally sequestering CO_2 is to inject it into abandoned or mature CBM wells. It is possible to use the CBM at site to generate electricity either by burning it or by using a fuel cell. If a relatively pure stream of CO_2 is derived from these processes, then it can be injected back into the CBM well to be adsorbed on undersaturated coal or to replace CH_4 on saturated coal. As an added advantage, the gas may be hot, which would increase the release of CH_4. It is interesting to compare the amount of CO_2 produced by oxidizing or burning the CH_4 produced from a well with the amount of CO_2 that coal in the well could adsorb (Table 9). As an example, CO_2 and CH_4 isotherms for a medium-volatile coal are used (Bustin, 2001). The two isotherms run at 25°C indicate the actual adsorption conditions at a depth where the temperature is 25°C (assumed to be 300 m). The adsorption amounts are therefore high for depths greater than 300 m and low for depths shallower than 300 m. However, the data do illustrate trends. The CO_2 derived from oxidizing the CH_4 produced from one tonne of coal can be adsorbed onto about 0.5 tonnes. But based on estimating the matrix shrinkage caused by desorption of CH_4 and expansion caused by adsorption of CO_2, there will be about a 2% volume increase in the tonne of coal. These estimates are made assuming densities of the adsorbed gases and may change considerably, but it is probably valid to assume that there will be a matrix expansion.

Sequestration of CO_2 is simpler if a pure stream of CO_2 is obtained. Natural gas processing plants can produce relatively pure streams of CO_2. Power plants and coal gasification produce mixtures of N_2, CO_2, and other gases. However, a pure stream of CO_2 can be obtained by trapping CO_2, using CaO to produce $CaCO_3$, and then liming the $CaCO_3$ in a separate reactor. The process can be self-sustaining in terms of $CaCO_3$ or may require inputs of fresh $CaCO_3$, in which case sequestration may require a location where coal and limestone are both available. The locations of the coal deposits in BC and brief descriptions of their size and CBM potential can be found in Ryan (2003).

British Columbia releases about 63.5 million tonnes equivalent of CO_2 annually (Environment Canada, 2001). If this is assumed all to be CO_2, it is possible to estimate the amount of coal that would be required to sequester it all (Table 10), and the amount is in the range of 100 to 200 billion tonnes. This amount of coal is similar to the total amount of coal in the province above a depth of 2000 m (estimated to be about 250 billion tonnes). Sequestering CO_2 in coal will only be applicable for very specific point sources.

Sequestering CO_2 in coal is often discussed in the context of coal-fired power plants. Spath *et al.* (1999) studied greenhouse gas emissions resulting from all aspects of generating electricity from coal. A present-day 360 MW power plant burns about 1.4 million tonnes of coal per year. About 100 to 200 million tonnes of coal are required to sequester the CO_2 produced (Table 11). It is probably unrealistic to envisage the CO_2 produced from a power plant being sequestered in the same coal resource that is providing coal to the power plant.

TABLE 9. COMPARISON OF THE AMOUNTS OF CH_4 AND CO_2 ADSORBED ONTO A MEDIUM-VOLATILE COAL OVER A RANGE OF DEPTHS.

		CH_4	CO_2	SG coal				1.2
	SG liquid estimated	0.466	0.6	CO_2 from burning 1 tonne coal				
	density of gas g/m^3	714.3	1964				2567	Kg
	mole wt	16	44				cc/g to scf/t	32.04
	psi	1000	800	600	400	300	200	100
	depth metres	704	563	422	282	211	141	70
CH_4	scf/t	340	323	300	260	228	184	120
CH_4	cc/g	10.6	10.1	9.4	8.1	7.1	5.7	3.7
CH_4	wt kg /tonne	7.6	7.2	6.7	5.8	5.1	4.1	2.7
CH_4	moles	0.5	0.5	0.4	0.4	0.3	0.3	0.2
CO_2	scf/t	604.0	587.0	560.0	510.0	467.0	400.0	283.0
CO_2	cc/g	18.9	18.3	17.5	15.9	14.6	12.5	8.8
CO_2	wt kg /tonne	37.0	36.0	34.3	31.3	28.6	24.5	17.3
CO_2	moles	0.8	0.8	0.8	0.7	0.7	0.6	0.4
CO_2/CH_4 volume ratio		1.8	1.8	1.9	2.0	2.0	2.2	2.4
CO_2/CH_4 wieght ratio		4.9	5.0	5.1	5.4	5.6	6.0	6.5
CO_2/CH_4 mole ratio		1.8	1.8	1.9	2.0	2.0	2.2	2.4
wt kg CO_2 from burning CH_4		20.8	19.8	18.4	15.9	14.0	11.3	7.4
m^3 vol of resultant CO_2		10.6	10.1	9.4	8.1	7.1	5.7	3.7
tonnes coal required to sequester		0.56	0.55	0.54	0.51	0.49	0.46	0.42
liquid vol m^3/t of adsorbed CH_4		0.016	0.015	0.014	0.012	0.011	0.009	0.006
liquid vol m^3/t adsorbed CO_2		0.062	0.060	0.057	0.052	0.048	0.041	0.029
% vol increase if all CH_4 desorbed and replaced by CO_2		5.453	5.343	5.144	4.76	4.417	3.848	2.781
liquid volume m^3/t of CO2 resultant from burning CH4		0.035	0.033	0.031	0.027	0.023	0.019	0.012
% volume change if CO2 adsorbed onto 1 tonne coal		2.2	2.1	2.0	1.7	1.5	1.2	0.8

Data is approximate in part because isotherms do not recognize the change of temperature with depth.

TABLE 10. THE AMOUNT OF COAL REQUIRED TO SEQUESTER THE CO_2 PRODUCED IN BRITISH COLUMBIA IN ONE YEAR.

British Columbia CO_2 equivalent emissions (million tonnes per year (1999))			63.8	estimated assuming all greenhouse gas CO_2				
CO_2 produced (billion cubic metres per year)			32.5					
depth (metres)	704	563	422	282	211	141	70	
CO_2 adsorption cubic metres/tonne billion tonnes of coal to sequester	18.9	18.3	17.5	15.9	14.6	12.5	8.8	
CO_2 produced in 1 year	91	94	98	108	118	137	194	

Estimated using 1999 data.

TABLE 11. THE AMOUNT OF COAL REQUIRED TO SEQUESTER THE CO_2 PRODUCED BY A 360 MW POWER PLANT.

coal fired power plant MW	360						
efficiency %	32						
coal consumption/yr million tonnes	1.413						
% carbon	65						
CO_2 produced million tonnes	3.37						
CO_2 produced million cubic metres	1715						
depth metres	704	563	422	282	211	141	70
adsorption cubic metres/tonne	18.9	18.3	17.5	15.9	14.6	12.5	8.8
million tonnes of coal to sequester CO_2	91	94	98	108	118	137	194
ratio coal needed for sequestering versus coal burnt	64	66	69	76	83	97	137

Data from Spath *et al.* (1999).

One of the few places where it might be possible to sequester the CO_2 generated by a power plant adjacent to the plant is in the Hat Creek area in south-central BC. This deposit was explored by BC Hydro as a possible site for a large power plant, and the area contains a large resource of lignite to sub-bituminous coal, which is estimated to be between 10 and 30 billion tonnes. Data from Gluskoter *et al.* (2003) indicate that sub-bituminous and lignite coals can adsorb about 10 cm^3/g CO_2 at intermediate depths (300 m). When this is compared to the amount of carbon in the coal, it is apparent that, for a tonne of coal burnt, the amount of CO_2 produced is less than for high-rank coals and can be sequestered in fewer tonnes of in situ coal. At Hat Creek, coal delivered to a power plant would be less than 30% carbon and would require less than 100 tonnes in situ to sequester the CO_2 produced from 1 tonne burned. Because of the size of the Hat Creek resource, a power plant using 10 million tonnes per year for 25 years would require about 25 billion tonnes to sequester the CO_2 generated. The sequestering of CO_2 may also result in the recovery of CH_4, which can be used in the power plant or sold as natural gas.

Isotopic studies of the C^{13}/C^{12} isotopic ratios of CBM indicate that the gas is often a mixture of biogenic and thermogenic methane. Biogenic methane may originate from early coalification or during uplift of the coal-bearing formation. Generation of biogenic methane requires a consortium of bacteria and a series of biochemical reactions that in part require H_2 and CO_2. This raises the possibility that injection of CO_2, if associated with bacteria or nutrients, may stimulate generation of biogenic methane at the same time that CO_2 is sequestered (Budwill, 2003). The best candidates for synchronous CO_2 sequestration and generation of biogenic methane are low-rank coals at shallow depth. Deposits such as Coal River or Tuya River, as well as the much larger Hat Creek deposit, could be candidates.

CONCLUSIONS

The connection is made: climate change is at least in part related to increasing concentration of CO_2 in the atmosphere, and we are responsible for the most recent increase. The incentive to limit fossil fuel use or sequester the CO_2 produced by fossil fuel use is here and will not go away.

Sequestration of CO_2 in coal seams requires a clear understanding of the CO_2 phase diagram and the implications for the maximum depth of sequestration. The maximum depth varies based on combinations of geothermal and pressure gradients but is generally in the range of 500 to 900 m. Below this depth and in part above it, CO_2 goes into solution in coal and causes an increase in plasticity and swelling (Larson, 2004).

It is essential to understand the CO_2 and CH_4 adsorption behaviour in coals of different ranks and for different combinations of temperature and pressure. The mole ratio of CO_2/CH_4 adsorption varies from over 10 for low-rank coals to under 2 for medium- and high-rank coals. The CO_2 adsorption is moderately high for low-rank coals, decreases for medium-rank coals, and then increases substantially for high-rank coals. The interaction of adsorption and selectivity of CO_2 and CH_4 means that for maximum CO_2 sequestration with minimum production of CH_4, one should use lignite, whereas for maximum sequestration of CO_2 with maximum production of CH_4, one should use a high-rank coal.

Sequestration of CO_2 without collection of the released CH_4 may result in a net increase in the emission of greenhouse gases over time.

Actual sequestration of CO_2 and release of CH_4 is predicted by binary gas isotherms and may not obey the extended Langmuir equation. It will also be influenced by permeability, matrix swelling, and initial saturation.

Conditions of sequestration of CO_2 in coal may best be applied to small point sources; for example, where CBM is being burned on site to produce electricity.

Most discussions of CO_2 sequestration do not consider the implications of an impure gas stream composed of CO_2 and N_2. Addition of N_2 to the gas decreases the adsorption of CO_2.

ACKNOWLEDGEMENTS

Marc Bustin performed the isotherm measurements. Bob Lane, the regional geologist at Prince George, found time to collect the samples of the Gething Formation.

REFERENCES

Arri, L.E., Yee, D., Morgan, W.D. and Jeansonne, M.W. (1992): Modeling coalbed methane production with binary gas sorption; *Society of Petroleum Engineers*, Paper SPE 24363, pages 459-472.

Bachu, S., and Stewart, S. (2002): Geological sequestration of anthropogenic carbon dioxide in the Western Canadian Sedimentary Basin: suitability analysis; *Journal of Canadian Petroleum Technology*, Volume 41, pages 32-40.

Budwill, K. (2003) Microbial methanogenesis and its role in enhancing coalbed methane recovery; *CSEG Recorder*, November 2003, pages 41-46.

Bustin, R.M. (2001): Geology and engineering aspects of coalbed methane; Course by *CBM Solutions*, Calgary Alberta, April 25, 2001.

Bustin, R.M. and Clarkson, C.R. (1999): Free gas storage in matrix porosity: a potentially significant coalbed resource in low rank coals; *International Coalbed Methane Symposium*, Tuscaloosa, Alabama 1999; pages 197-214.

Crosdale, P.J. (1999): Mixed methane / carbon dioxide sorption by coal: new evidence in support of pore filling models; *International Coalbed Methane Symposium*, Tuscaloosa Alabama, pages 359-366.

Dawson, F.M. Marchioni, D.L. Anderson, T.C. and McDougall, W.J. (2000): An assessment of coalbed methane exploration projects in Canada; *Geological Survey of Canada*, Bulletin 549.

Environment Canada (2001): Canada's greenhouse gas inventory, 1990-1999.

Ettinger, I., Eremin, B., Zimakov, B. and Yanovskaya, M. (1966): Natural factors influencing coal sorption properties 111 comparative sorption of carbon dioxide and methane on coals; *Fuel*, Volume 45 pages 351-361.

Gan, H., Nandie, S.P, and Walker, P.L. (1972): Nature of porosity in American coals; *Fuel,* Volume 51, pages 272-277.

Gluskoter, H., Mastalerz, M. and Stanton, R. (202) The potential for carbon dioxide sequestration in coal beds: new evidence from methane and carbon dioxide adsorption analysis for coals from lignite to anthracite; Abstract 25, *Geological Association of America*, Annual Meeting, April 2002.

Grieve, D.A. (1993): Geology and Rank Distribution of the Elk Valley Coalfield, Southeastern British Columbia; *B.C. Ministry of Energy, Mines and Petroleum Resources,* Bulletin 82, pages 1-188.

Harris, L.A., Yust, C.S. (1976): Transmission electron microscopy of coal; *Fuel*, Volume55, page 233.

Hughes, D. (2003): Assessment of CO_2 storage capacity of deep coal seams in the vicinity of large CO_2 point sources in central Alberta and Nova Scotia; In press.

Jarrell, P. M., Fox, C. E. Stein M. H, and Webb, S. L (2002): Practical aspects of CO2 flooding; *Society of Petroleum Engineers,* Monograph 22, 220 pages.

Kalkreuth, W. and McMechan, M. (1988): Burial history and thermal maturation, Rocky Mountains foothills and foreland east central British Columbia and adjacent Alberta; Bulletin, *American Association of Petroleum Geologists*, Volume 72, pages 1395-1410.

Kalkreuth, W., Langenberg, W. and McMechan, M. (1989): Regional coalification pattern of Lower Cretaceous coal bearing strata, Rocky Mountain Foothills and Foreland, Canada - Implications for future exploration; *International Journal of Coal Geology*, Volume 13, pages 261-302.

Karst, R. and White, G.V. (1979): Coal rank distribution within the Bluesky-Gething stratigraphic horizon of Northeast B.C.; *Ministry of Energy Mines and Petroleum Geology*, Paper 80-1, pages 103-107.

Khan, M.R., and Jenkins, R.G. (1985): Thermoplastic properties of coal at elevated pressures: effects of gas atmospheres; *Proceedings International Conference on Coal Science,* Sydney.

Krooss, B.M., Gensterblum, Y., and Siemons, N. (2001): High-pressure methane and carbon dioxide adsorption on dry and moisture-equilibrated Carboniferous coals; *International Coalbed Methane Symposium*, Tuscaloosa Alabama, 2001, pages 177-191.

Lamberson, M.N., Bustin, R.M., and Kalkreuth, W.D. (1991): Lithotype maceral composition and variation as correlated with paleo-wetland environments; Gates Formation northeastern British Columbia, Canada; *International Journal of Coal Geology,* Volme18, pages 87-124.

Lamberson, M.N. and Bustin, R.M. (1993): Coalbed methane characteristics of the Gates Formation coals, northeastern British Columbia: effect of maceral composition; *American Association of Petroleum Geologists,* Bulletin, Volume 77, pages 2062-2076.

Larsen, J.W. (2004): The effects of dissolved CO2 on coal structure and properties; *International Journal of Coal Geology,* Volume 57, pages 63-70.

Leckie, D.A. (1983): Sedimentology of the Moosbar and Gates Formations (Lower Cretaceous); PhD Thesis, McMaster University.

Levine, J.R. (1993): Coalification: The evolution of coal as source rock and reservoir rock for oil and gas; Chapter 3, *American Association of Petroleum Geologists*; Studies in Geology Series, Number 38, pages 39-77.

Levy, J.H., Day, S.J., Killingley, J.S. (1997): Methane capacities of Bowen Basin coals related to coal properties; *Fuel,* Volume 76, pages 813-819.

Marchioni, D. and Kalkrueth, W. (1992): Vitrinite reflectance and thermal maturation in Cretaceous strata of the Peace River Arch region west-central Alberta and adjacent British Columbia; *Geological Survey of Canada*, Open File 2576.

Pashin, J.C., and McIntyre, M.R. (2003): Temperature-pressure conditions in coalbed methane reservoirs of the Black Warrior Basin: implications for carbon sequestration and enhanced coalbed methane recovery; *International Journal of Coal Geology,* Volume 54, pages 167-183.

Pruess, K., Xu, T., Apps, J. and Garcia, J. (2001): Numerical modeling of aquifer disposal of CO2; *Society of Petroleum Engineers,* SPE 66537, Exploration and Production Environmental Conference San Antonio Texas, February 2001.

Reucroft, C.F., and Sethurarman, A.R. (1987): Effect of pressure on carbon dioxide induced coals swelling; *Energy Fuels,* Volume 1, pages 72-75.

Righmire, C.T. (1984): Coalbed methane resource; *American Association of Petroleum Geologists;* Studies in Geology, Series 17, pages 1-14.

Ryan, B.D. (1992): An Equation for Estimation of Maximum Coalbed-Methane Resource Potential; *B.C. Ministry of Energy, Mines and Petroleum Resources,* Geological Fieldwork 1991, Paper 1992-1, pages 393-396.

Ryan, BD (1997): Coal quality variations in the Gething Formation northeastern British Columbia*; BC Ministry of Energy, Mines and Petroleum Resources,* Geological Fieldwork 1996, Paper 1997-1, pages 373-397.

Ryan, B.D. and Lane, R. (2002): Adsorption characteristics of coals from the Gething Formation northeast British Columbia; *B.C. Ministry of Energy and Mines,* Geological Fieldwork, Paper 2003-1.

Ryan, B.D. (2002): Pseudovitrinite: possible implications for gas saturation in coals and surrounding rocks*; B.C. Ministry of Energy and Mines,* Geological Fieldwork, Paper 2003-1.

Ryan, B.D. (2003): the CBM resource of some perspective areas of the Crowsnest Coalfield; In press *BC Ministry of Energy and Mines*.

Ryan, B.D. (2003): A summary of the coalbed methane potential in British Columbia; *CSEG Recorder*, November 2003, pages 32-40.

Spath, P.L., Mann, M/K., and Kerr, R.D. (1999): Life cycle assessment of coal-fired power production; *Nation Renewable Energy laboratory;* Contract Number DE AC36-98-GO10337.

ULTRAMAFIC ROCKS IN BRITISH COLUMBIA: DELINEATING TARGETS FOR MINERAL SEQUESTRATION OF CO_2

By D. A. Voormeij[1] and G. J. Simandl[1, 2]

KEYWORDS: CO_2 sequestration, ultramafic, mineral potential, serpentinite, dunite.

SUMMARY

British Columbia has favourable geology and excellent exploration potential to host the raw materials suitable for CO_2 mineral carbonation, one of the methods considered for lowering atmospheric greenhouse gas levels. British Columbia has been situated on the active, west-facing Pacific margin of continental North America for at least the last 530 million years and subjected to a subduction zone (accretionary) tectonic setting for the last 390 million years. Due to its tectonic history, BC contains numerous Alpine-type and several Alaskan-type complexes, both types rich in Mg-silicates. Dunite zones within these complexes are currently considered as the most promising sources of raw materials for the mineral sequestration process, since they contain the most Mg by weight, the component necessary for binding with CO_2 to form stable carbonates. In addition, stockpiles containing short-fibre chrysotile mined from serpentine-rich zones in ultramafic complexes may provide a source of starting material, thereby simultaneously disposing of CO_2 as well as other potentially hazardous materials. British Columbia's ultramafic rocks were studied previously as possible hosts of base metals, precious metals, and gemstones. This study draws relevant information from that research and utilizes the database originally designed to evaluate mineral potential for the province. From this database, a map depicting dunite- and serpentinite-bearing ultramafic rocks has been produced. Several targets have been selected, relying on preliminary data, including mineralogy, geochemistry, potential size of the resource, accessibility, and proximity to major CO_2 point sources. These include the dunite zone of the Alaskan-type Tulameen Complex near Princeton and the Cassiar chrysotile tailings in northern BC. These targets are the subject of current detailed research.

INTRODUCTION

A number of carbon dioxide (CO_2) sequestration methods, including geological storage, ocean storage, and mineral sequestration, have been proposed worldwide, and methods conceivably applicable to BC were listed and reviewed by Voormeij and Simandl (2003a). Mineral carbonation is considered to be the only method that truly disposes of CO_2 on a geological time-scale and with minimum risk of leakage (Lackner *et al*., 1997; O'Connor *et al*., 2000). Although Ca-silicates (e.g., wollastonite) may also have potential for mineral carbonation (Wu *et al*., 2001; Kakizawa *et al*., 2001), Mg-silicates are more common in high concentrations and as large deposits (Goff and Lackner, 1998). Mg-silicates also contain more reactive material per tonne than do Ca-silicates (Lackner *et al.,* 1997). The mineral carbonation concept is based on the natural weathering process of Mg-olivine (forsterite) and serpentine, which carbonate by the following reactions:

$$\underset{\text{[olivine]}}{Mg_2SiO_4} + 2CO_2 \rightarrow \underset{\text{[magnesite]}}{2MgCO_3} + \underset{\text{[silica]}}{SiO_2} \quad (1)$$

$$\underset{\text{[serpentine]}}{Mg_3SiO_3(OH)_4} + 3CO_2 \rightarrow \underset{\text{[magnesite]}}{3MgCO_3} + \underset{\text{[silica]}}{2SiO_2} + H_2O \quad (2)$$

This process is thermodynamically favoured in near-surface environments, and its products are stable on a geological time scale. The concept was first proposed by Seifritz (1990) and considered in more details by Lackner *et al.* (1997), O'Connor *et al*. (1999; 2000), and Kohlmann and Zevenhoeven (2001; 2002).

The mineral carbonation process, as considered in this paper, is envisioned in an industrial setting (ex situ). Geographical location, proximity to infrastructure, and the size of dunite and serpentinite resources and their physical and chemical properties are some of the important factors determining the potential viability of mineral sequestration in BC. Ideal sites should be located close to both the Mg-silicate deposit and a major CO_2 emission point source to minimize transportation costs of the CO_2 and raw materials. Geographic distribution of major stationary CO_2 point sources in BC has been completed (Voormeij and Simandl, 2003b). In order to match sinks to these point sources, areas with the potential to host raw material for mineral CO_2 sequestration need to be identified. Dunite zones of ultramafic complexes are preferred over the serpentinite zones, since they contain the most magnesium by weight. Serpentinite zones are more common and for this reason are also considered as candidates. Detailed methodology proposed for systematic evaluation of the ultramafic materials for use in mineral carbonation is outside of the scope of this study and is covered by Voormeij and Simandl (in preparation).

[1] *University of Victoria, voormeij@uvic.ca*
[2] *British Columbia Geological Survey Branch, george.simandl@gems2.gov.bc.ca*

ULTRAMAFIC ROCKS

Petrology and Mineralogy

Serpentine and forsteritic olivine are common silicates with high magnesium contents. There are three principal forms of serpentine: lizardite, antigorite, and chrysotile (Deer, Howie and Zussman, 1978), all with the approximate composition $Mg_3Si_2O_5(OH)_4$. The most abundant is lizardite, whereas the fibrous chrysotile is relatively rare. The latter is perhaps best known since it had many industrial applications, including fireproof insulation, specialty paints, brake pads, and gaskets. (Virta and Mann, 1994). It has also been used extensively in construction materials such as cements and tiles. However, the use of chrysotile was severely curtailed due to health hazards associated with its use (Hamel, 1998), and is banned in several European countries.

Olivine exists as a solid solution series between the Mg_2SiO_4 (forsterite) and Fe_2SiO_4 (fayalite) end members. The monomineralic rock of olivine is called dunite (Figure 1). Forsteritic olivine is currently the favoured mineral for the carbonation process because it does not require the energy-intensive pretreatment that serpentine needs (Lackner *et al*., 1997; O'Connor *et al*., 2000). However, research into optimization of energy used in the pretreatment of serpentine is ongoing (McKelvy *et al.*, 2002; O'Connor *et al*., 2000). Furthermore, serpentine-rich rocks are more widespread than those rich in olivine. Thus both have to be considered. Some selected chrysotile-bearing stockpile sites are also investigated because, in addition to sequestering CO_2, the mineral carbonation method may also aid in the disposal of unwanted asbestos waste (Huot *et al*., 2003).

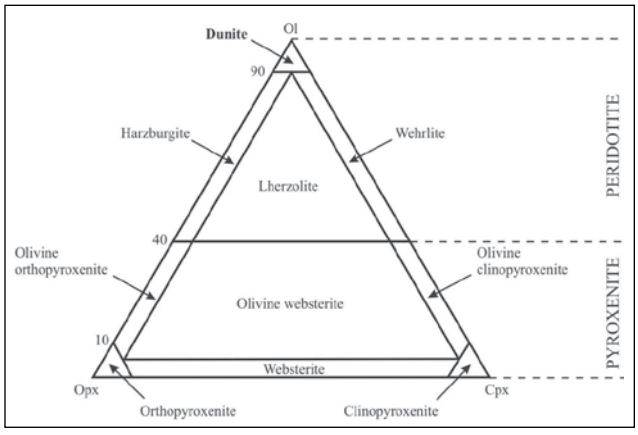

Figure 1. IUGS classification scheme for ultramafic rocks (after Le Maitre, 1989). Ol-olivine; Opx-orthopyroxene; Cpx-clinopyroxene. The general term "peridotite" is used when the olivine content is 40%–100%, whereas "pyroxenite" refers to an olivine content of 0%–40%. For example, "dunite" is a peridotite containing 90%–100% olivine.

ULTRAMAFIC COMPLEXES

Ultramafic complexes can be divided into three major categories: Alpine, Alaskan, and layered intrusive types. Their geographic distribution is restricted by tectonic setting, which also indirectly influences the physical and chemical characteristics of dunite and serpentinite rocks within these complexes. These characteristics include relative position of the dunite and serpentinite bodies, structural control, variation in mineralogy, and mineral composition. Table 1 lists well-documented examples of these categories and describes their geological setting.

Alpine-Type Complexes

Alpine-type ultramafics are the most voluminous and widespread of all ultramafic bodies (Coleman, 1977) and are interpreted as forming the basal part of an ophiolitic suite (Dewey, 1976 and Moores, 1982; 2002). A complete ophiolite sequence, tectonically emplaced over crystalline basement (Figure 2), consists of (from bottom to top) tectonic mélange, metamorphic sole, deformed mantle tectonite, cumulate peridotite (alternately layered olivine and pyroxene), cumulate gabbros grading upwards into massive gabbros and plagiogranites, overlain and partially intruded by sheeted dike swarms, followed by pillow basalts, capped by deep-sea and/or pelagic or, in some cases, volcaniclastic turbidites, all overlain by shallow-water sediments. This sequence is thought to represent an analogue for oceanic crust formed at fast-spreading centres, as exemplified by the Juan de Fuca Ridge situated off the coast of BC.

Dunitic rocks of ophiolitic sequences are divided into two broad categories based upon their texture and petrography: tectonite and cumulate. Dunites within the tectonite section generally occur as lenses within harzburgite or lherzolite, ranging from one metre to hundreds of metres in size. In most cases, the tectonite is gradational into the cumulate sequence, where forsteritic olivine is the dominant cumulate phase (Coleman, 1977; Moores, 2002). Podiform chromitite is commonly associated with the tectonite zone; stratiform or thin chromitite accumulations are typical of the cumulate zone (Coleman, 1977). During the serpentinization of the alpine peridotites, fibrous chrysotile veins and stockworks may be formed. Where chrysotile-filled fractures constituted 3% to 10% of the rock and formed long fibres of high quality, it was economically mined (Hora, 1999).

Alaskan-Type Complexes

Alaskan-type complexes (also called Alaskan-Ural, Uralian, and concentric or zoned complexes) are mafic and ultramafic intrusions. Their type locations are in a narrow,

TABLE 1. CHARACTERISTICS OF THE THREE MAIN TYPES OF ULTRAMAFIC COMPLEXES CONTAINING SIGNIFICANT DEPOSITS OF DUNITE AND/OR SERPENTINITE.

Geological Setting	Complex Type	Description	Distribution of dunite and/or serpentinite zones	Examples
Syn-orogenic ultramafic bodies	***Alpine-Type***	Tectonically emplaced ultramafic complex that makes up the basal section of an ophiolite (ocean-crust) sequence	Mantle tectonite section contains pods of dunite. Cumulate section contains layers of dunite. Dunite variably serpentinized. Tectonic melange is typically rich in serpentinite.	Nahlin UMF Complex (BC); Cache Creek UMF complex (BC); Shulaps UMF Complex (BC)
	Alaskan-Type	Podiform intrusions of mafic to ultramafic magmas into accreted island arcs.	Concentrically zoned. Successive zones of wehrlite, clinopyroxenite and orthopyroxenite around a dunite core. Dunite variably serpentinized, increasing outwards from core.	Duke Island (Alaska); Polaris (BC); Tulameen (BC); Turnagain (BC)
Intracratonic	***Layered Intrusion-Type***	Large, often funnel-shaped sill-like intrusions. Layering formed partly as a result of fractional crystallization of the primary melt	Laterally extensive, alternating layers of dunite/peridotite and pyroxenite.	Muskox (NWT), Bushveld (RSA), Great Dyke (Zimbabwe), Stillwater (MT), Windemurra (AUS)

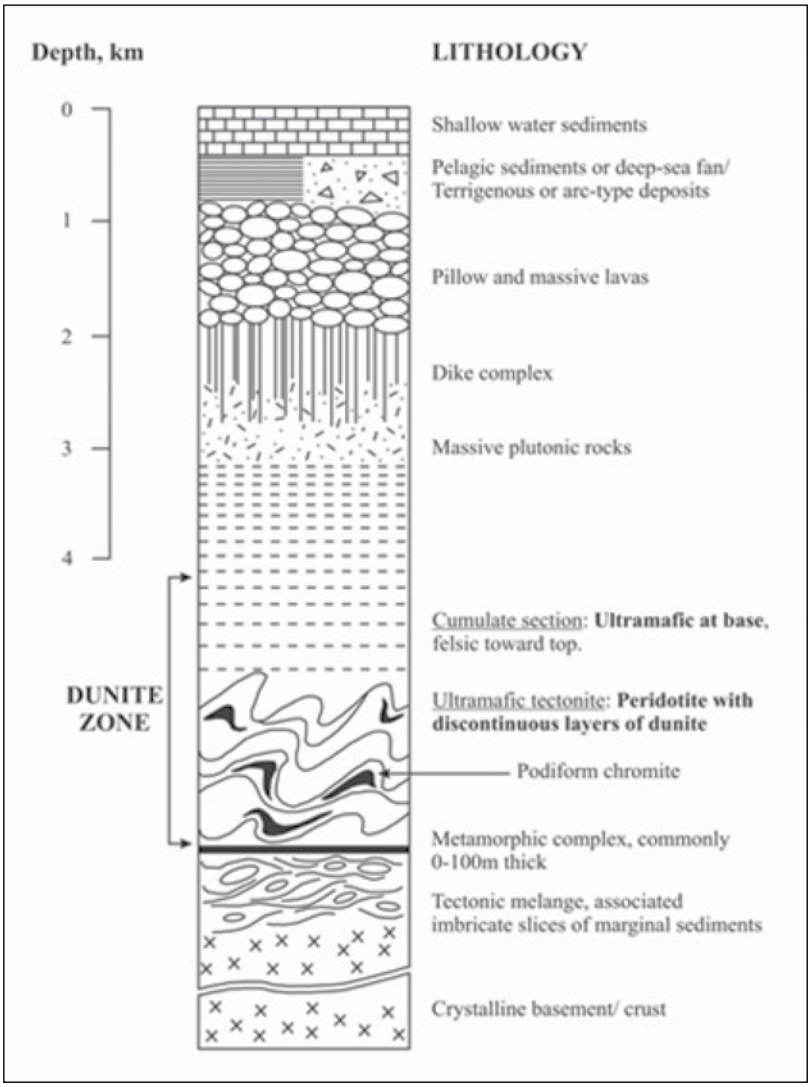

Figure 2. Cross section of a "complete" ophiolite complex. Few ophiolite complexes contain all of these units; most contain only part(s) of the entire complex (source: Moores, 2002).

north-trending belt, 600 km long, in southeastern Alaska (Irvine, 1967).Similar ultramafic bodies are found in belts along the central Ural Mountains of Russia (Irvine, 1987) and through the interior of BC (Findlay, 1963; Irvine, 1976; Clark, 1980; Nixon, 1990). Idealized Alaskan-type complexes are characterized by the crude zonation of successive wehrlite, clinopyroxenite, and hornblende-rich lithologies around a dunite core (Irvine, 1987). In many of the well-documented examples, any one of these zones may be missing or discontinuous (Nixon, 1990). Massive dunite cores consiting primarily of forsteritic olivine (Irvine, 1987) may be exposed over large areas, and in many cases dunite is well preserved.

Layered-Intrusive Complexes

Layered mafic-ultramafic intrusions are either sill-like (e.g., Stillwater) or funnel shaped (e.g., Skaergaard and Great Dyke). They are typically intruded into rifted cratons and may be associated with tholeitic flood basalt provinces. A good example of this is the Muskox intrusion, which is intimately associated with Coppermine River basalts (Baragar, 1969; Kerans, 1983).

As magma crystallizes and differentiates, cyclically layered sequences form. An ideal cycle consists of basal dunite followed upward by a harzburgite and an uppermost orthopyroxene layer (Naslund and McBirney, 1996). These cyclic units vary in thickness. For example, in the Bushveld Complex they are present on a millimetre scale (Eales and Cawthorn, 1996), at Great Dyke on a centimetre scale (Naslund and McBirney, 1996), and at Muskox intrusion on a metre scale (Irvine and Smith, 1967). Olivine composition in a typical layered ultramafic intrusion trends upwards in succession from forsterite-rich olivine towards fayalitic olivine (Table 2).

TABLE 2. OLIVINE COMPOSITION CHANGES FROM MG-RICH (FORSTERITE) TO FE-RICH (FAYALITE) FROM LOWER TO UPPER ZONES WITHIN LAYERED INTRUSIVE COMPLEXES.

Name, locality	Olivine composition in lower zone	Olivine composition in upper zone	References
Bjerkreim-Sokndal, Norway	Fo77-74	Fo50-19	Wilson *et al.* (1996)
Bushveld, RSA	Fo85-88	Fo63-35	Eales and Cawthorn (1996)
Great Dyke, Zimbabwe	Fo92	Fo91-87	Wilson (1996)
Skaergaard, Greenland	Fo74-68	Fo10-5	McBirney (1996)
Windimurra, Australia	Fo90-50	Fo35	Mathison and Ahmat (1996)

The layering is commonly laterally continuous for hundreds of square kilometres (Eales and Cawthorn, 1996), and the ultramafic sequence can be up to several kilometres in thickness. For example, the Windimurra Complex has a 0.5 km thick ultramafic section (Mathison and Ahmat, 1996), the Muskox intrusion has ultramafic layers that total 1.5 km in thickness (Irvine and Smith, 1967), and the Great Dyke has an ultramafic sequence several kilometres in thickness (Wilson, 1996).

TECTONIC SETTING OF BC

Since the breakup of the Rodinia supercontinent, BC has been located on a continent-ocean boundary for at least 530 million years (Monger, 1997). As a result of subduction-related activity, which started approximately 390 Ma, the Canadian Cordillera is commonly described as an orogenic collage made up of intra-oceanic arc and subduction complexes accreted to the craton margin and of arcs emplaced in and on the accreted bodies. The Canadian Cordillera has been subdivided into terranes (Figure 4), each consisting of characteristic assemblages (Monger and Berg, 1984).

Assemblages within the Slide Mountain, Cache Creek, and Bridge River Terranes (Figure 4) are of oceanic affinity, representing the deformed sequences of ocean basins that closed in the Mesozoic during the accretion of offshore island arcs to the North American craton. The Slide Mountain Terrane is composed of ultramafic rocks, gabbro, pillow basalt, and chert, which formed in a back-arc ocean basin (Figure 5). The ultramafic rocks in the Cache Creek and Bridge River Terranes are associated with a mélange of marine sediments with blocks, lenses, and slivers of ophiolitic origin, often in a serpentine matrix, representing an accretionary/subduction complex (Figure 5). These oceanic-affiliated terranes contain numerous Alpine-type complexes (Evenchick *et al*., 1986). The Stikinia and Quesnellia Terranes are composed of arc-related volcanic and sedimentary rocks and coeval intrusions (Evenchick *et al*., 1986). BC's Alaskan-type complexes are found in these terranes (Figure 5) and represent the high-level magma chambers of Late Triassic to Middle Jurassic arc volcanoes (Nixon, 1990). There are no large layered intrusive ultramafic complexes known in BC, as they are believed to be restricted to an intra-cratonic tectonic setting.

ULTRAMAFIC ROCKS IN BC

Depicted in Figure 6 is the geographic distribution of ultramafic rocks in BC, with emphasis on those Alpine- and Alaskan-type complexes that contain known dunite and/or serpentinite zones. This map was derived from the database developed for a mineral potential assessment of BC (Kilby, 1994) and was originally introduced in a BC Geological Survey Branch Geofile (Voormeij and Simandl, 2004).

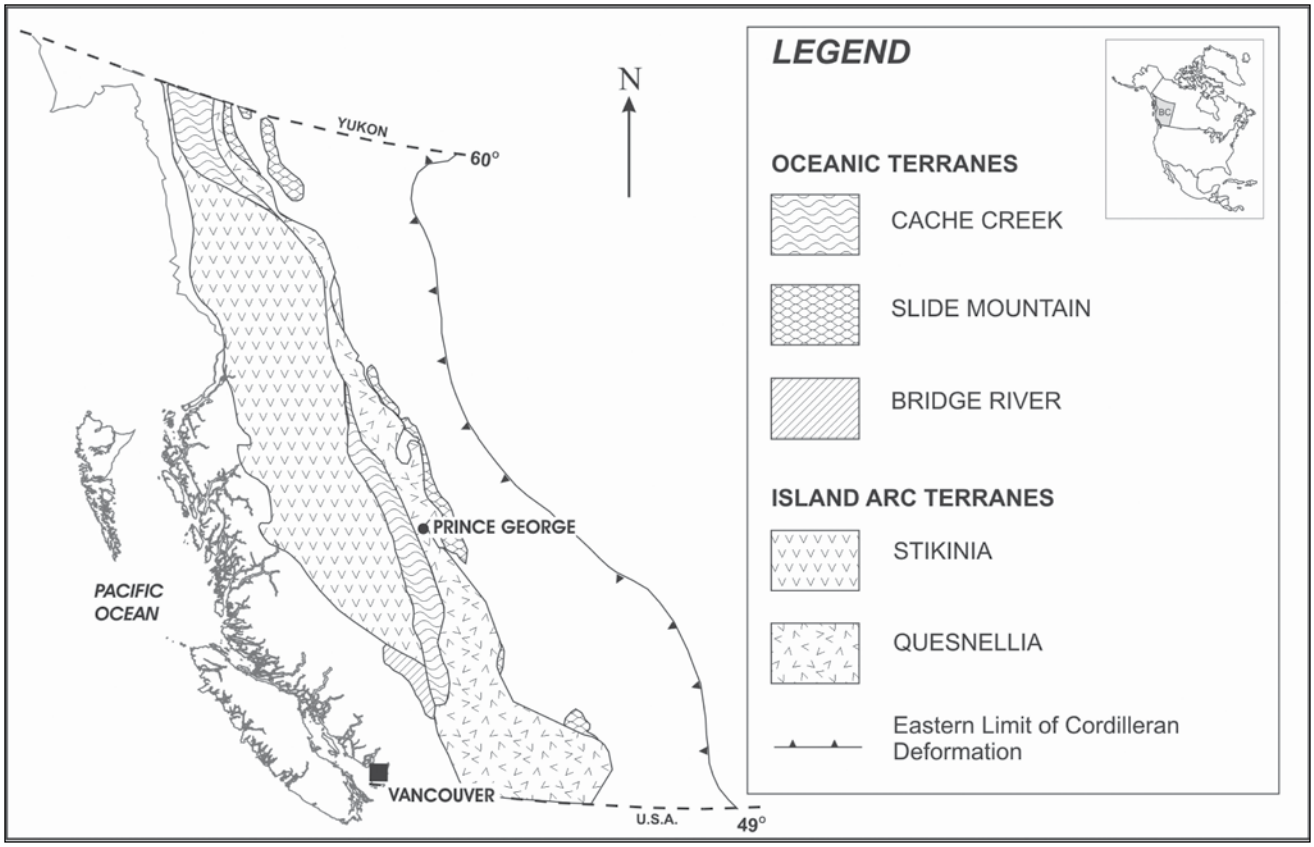

Figure 4. Distribution of major ultramafic-bearing terranes in British Columbia (based on Gabrielse et al., 1991). The Alpine-type ultramafic complexes are confined primarily to the Cache Creek, Slide Mountain, and Bridge River oceanic-affiliated terranes, whereas the Alaskan-type ultramafic bodies are associated with the Stikinia and Quesnellia island-arc terranes.

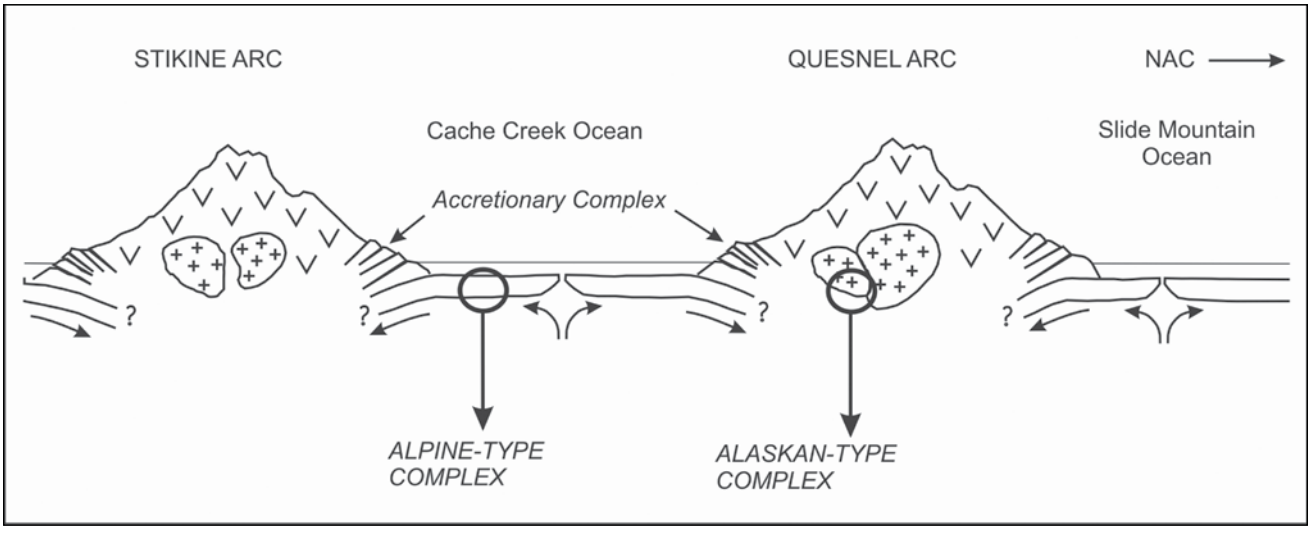

Figure 5. Simplified diagram depicting the different tectonic settings for the oceanic-affiliated, subduction-related, and island arc terranes in British Columbia and the origin of their ultramafic complexes (based on Monger and Journeay, 1994). NAC = North American Continent.

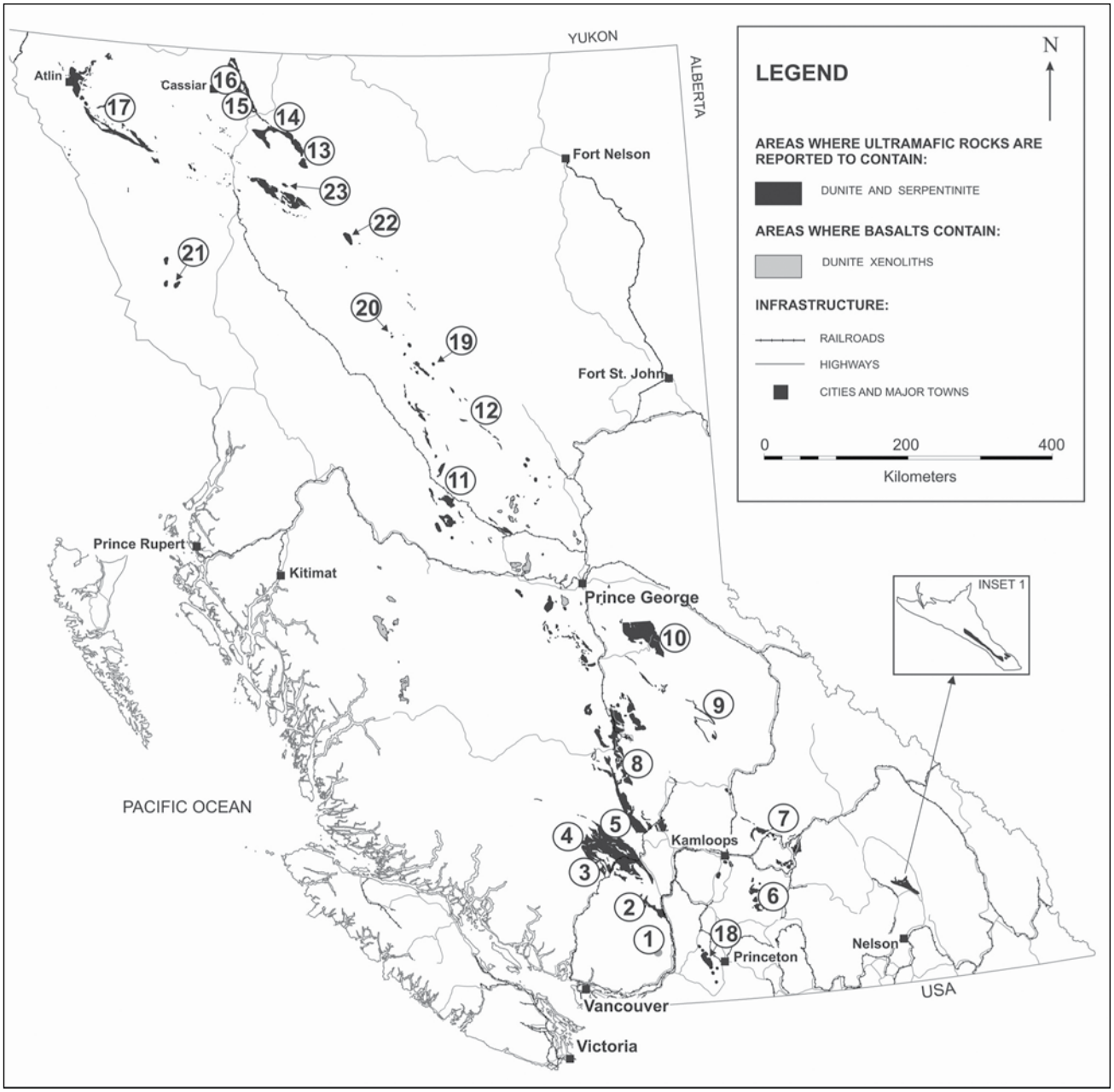

Figure 6. Distribution of dunite and serpentinite-bearing rocks in BC. Alpine-type ultramafic complexes include: 1. Cogburn Emory Zone, 2. Coquihalla Serpentine Belt, 3. Bralorne-East Liza, 4. Bridge River Complex, 5. Shulaps, 6. Chapperon Group, 7. Mount Ida Assemblage, 8. Southern Cache Creek Complex, 9. Crooked Amphibolite, 10. Antler Formation, 11. Central Cache Creek Complex, 12. Manson Lake Complex, 13. Blue Dome Fault Zone, 14. Sylvester Allochthon, 15. Cassiar and McDame, 16. Zus Mountain, 17. Northern Cache Creek Complex (includes Atlin and Nahlin Complexes). Alaskan-type ultramafic complexes include: 18. Tulameen, 19. Polaris, 20. Wrede, 21. Hickman, 22. Lunar Creek, 23. Turnagain.

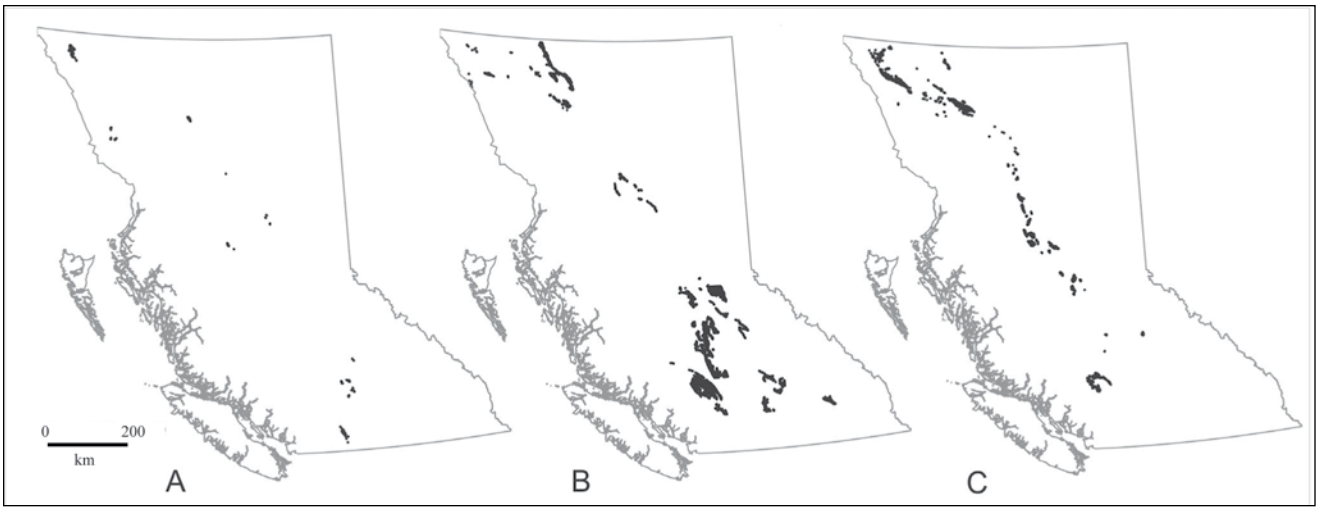

Figure 7. Separating out the dunite and serpentinite zones associated with ultramafic rocks: A. Areas where ultramafic rocks are reported to contain dunite only. B. Serpentinite only. C. Dunite and serpentinite are reported together.

The compiled geology used in Figure 6 has been captured in digital form at a scale of 1:250 000 by means of BC Geological Survey Branch Open File series releases (Massey, 1994; Schiarizza *et al*., 1994; Höy *et al*., 1994; MacIntyre *et al*., 1994; Bellefontaine and Alldrick, 1994; MacIntyre *et al*., 1995; Bellefontaine *et al*., 1995; Mihalynuk *et al*., 1996; Schiarizza and Church., 1996). From this electronic database, units containing the words "dunite" and "serpent-" were extracted, thereby assembling a digital file of zones that contain the words "dunite", "serpentinite", "serpentinized", or "serpentine" in their original description. Figure 6 shows the resulting zones.

Extraction of areas that contain the terms "dunite" and "serpent-" from the database does not discriminate between minor and major amounts of dunite and/or serpentinite present. Thus, most of the zones are overestimates of actual area underlain by dunites and/or serpentinites. For example, Figure 6 shows a zone in southeastern BC, approximately 120 km north of Nelson. This area appears approximately 100 km long by 50 km wide on the map. However, a more detailed map (Figure 6, Inset 1) shows the presence of serpentine-magnesite-talc related rocks only a few kilometres across (source: Read and Wheeler, 1977). Although the approach used to construct Figure 6 results in overestimating the areas underlain by ultramafic rocks, it is a preferred preliminary approach because large portions of BC have not been mapped in detail and may contain more ultramafic rocks than expected. Several potential dunite and serpentinite tracts shown on this map are abruptly terminated along straight lines that correspond to map boundaries. This happens where a geological unit extends across two or more 1:250 000 map sheet areas. This unit may have the same name on several of the mapsheets, but ultramafic rocks are not present in all of them.

Our approach also delineated areas that contain ultramafic xenoliths. For example, numerous zones within central BC correlate to spinel peridotite xenoliths described by Canil *et al.* (1987), many of which are hosted in the alkali basalts typical of the Chilcotin Group plateau-lavas (Dostal *et al*., 1996). The olivine-rich xenoliths are not significant as a potential source of raw material for the ex situ mineral carbonation process. However, recent studies have shown the mineral-trapping potential of injected CO_2 into deep saline aquifers located within thick sequences of flood basalt provinces (O'Connor *et al*., 2003). For this reason, the distribution of BC's flood basalts that contain olivine xenocrysts and dunite xenoliths is included in Figure 6.

Ultramafic rocks containing dunite zones but not serpentinite (Figure 7a) are not common. These zones are mostly restricted to Alaskan-type complexes. In contrast, ultramafic rocks containing serpentine but not dunite are relatively abundant (Figure 7b). As expected from the distribution of ultramafic rocks in Alpine-type complexes, dunite and serpentinite are commonly associated (Figure 7c).

Alpine-Type Complexes in BC

Most of BC's Alpine-type complexes are located within the Cache Creek, Slide Mountain and Bridge River Terranes. The Cache Creek Terrane forms a long narrow tract that extends within the Intermontane belt from southern BC to central Yukon Territory (Figure 4). The larger complexes of the Cache Creek Terrane include the Southern Cache Creek Ultramafic Assemblage in southwestern BC and the Nahlin Ultramafic Complex near Atlin, northwestern BC (Figure 6). The Slide Mountain Terrane forms a narrow, discontinuous belt extending 2000 km from southeastern BC to northwestern Yukon Territory (Figure 4). Alpine-type ultramafics are located in the Antler Formation in central BC, the Redfern and Crooked Amphibolite in east-central BC, and the Sylvester allochthon in north-central BC (Figure 6).

The Cassiar and McDame asbestos deposits are located in Sylvester serpentinites (Figure 6). Zus Mountain, located in the Sylvester allochthon, is known to contain intact oceanic upper mantle and ultramafic cumulate material (Nelson and Bradford, 1993). Bridge River is a small terrane, situated near latitude 52°N, just west of the Cache Creek Terrane. The Bridge River Complex, with the associated Shulaps and Bralorne-East Liza complexes (Figure 6), the Coquihalla Serpentine Belt, and the Cogburn body are probably the southern extent of the Cache Creek Terrane (Schiarizza *et al.,* 1997).

Alaskan-Type Complexes in BC

In BC, Alaskan-type complexes are found in the Stikinia and Quesnellia Terranes. However, only those with a recognized dunite zone are discussed, and their geographical distribution is given in Figure 6. Table 3 gives the major Alaskan-type complexes for BC that contain known dunite cores. Stikinia is the largest terrane in the Canadian Cordillera; it extends more than 1700 km from eastern Alaska to south-central BC (Figure 4). The Hickman Complex is an Alaskan-type ultramafic within Stikinia. The Lunar Creek Complex is located on the boundary between Quesnellia and Stikinia Terranes (Figure 6). Quesnellia forms an orogen-parallel belt that extends from south-central BC into the Yukon Territories (Figure 4). Complexes of the Alaskan type that are located in this terrane include the Tulameen (Figure 3), Polaris, Wrede, and Turnagain complexes. Tulameen is the largest Alaskan-type body in BC (Table 3).

Economic Potential of Ultramafic Rocks in BC

Up to now, BC's ultramafic complexes were primarily of interest to economic geologists in terms of associated metals, traditional industrial mineral deposits, and gemstones. These complexes are known to host Cyprus-type massive sulphides (Höy, 1995), Au-quartz veins (Ash and Alldrick, 1996), silica-carbonate mercury deposits (Ash, 1996a), podiform chromite (Ash, 1996b), stratiform chromite (Nixon *et al*., 1997), talc and magnesite (Simandl and Ogden, 1999), chrysotile asbestos (Hora, 1999), nephrite jade (Simandl *et al*., 2000), vermiculite (Simandl *et al*., 1999a), emeralds (Simandl *et al*., 1999b), and corundum-group gemstones (Simandl and Paradis, 1999). Also, they are known to host platinum-group elements (Rublee, 1986; Evenchick *et al*., 1986; Nixon, 1990; Nixon, 1996; Nixon *et al*., 1997), Ti and Fe oxide deposits (Gross *et al*., 1999), and nickel (Hancock, 1990). Olivine may be used as a foundry and blasting sand (White, 1987) as well as a raw material in the manufacture of refractories (Henning, 1994). In the past, most of the complexes were assessed with these commodities in mind; however, should mineral sequestration of CO_2 emissions become a reality, then these complexes will also become essential as sources of high-magnesia silicates. The synergy between the development of some of the traditional metal, industrial mineral, and gemstone commodities and magnesium silicates for CO_2 sequestration may be possible.

TABLE 3. SURFACE AREA OF DUNITE ZONES IN ALASKAN-TYPE COMPLEXES. ARC-RELATED TECTONOSTRATIGRAPHIC TERRANES WITHIN WHICH THESE COMPLEXES ARE LOCATED: QN = QUESNELLIA; ST = STIKINIA.

Complex Name	Terrane	Aerial Extent of Complex	Surface Area of Dunite zone	References
Hickman	ST	~11 km^2	< 1 km^2	Nixon *et al*. (1997)
Lunar Creek	QN	~45 km^2	~ 1.5 km^2	Nixon *et al*. (1997)
Polaris	QN	~50 km^2	~8-9 km^2	Nixon *et al.* (1997)
Tulameen	QN	~ 60 km^2	~ 6 km^2	Findlay (1963); Nixon *et al.* (1997)
Turnagain	QN	~25 km^2	~ 5 km^2	Clark (1980); Gabrielse
Wrede	QN	~10 km^2	~ 5km^2	Hammack *et al.* (1990)

Targets for Mineral Sequestration of CO2

Figure 6 also marks two specific areas considered for detailed study as part of the M.Sc. thesis of the senior author: the Tulameen site and the Cassiar asbestos. The Tulameen site was chosen because it contains a well-exposed, large (6 km^2), relatively unserpentinized dunite body and is located within the vicinity of several major point sources of CO_2 (Voormeij and Simandl, 2003b). Cassiar asbestos tailings, currently owned by Cassiar Resources Inc., are investigated because the waste piles have potential as raw material for the mineral carbonation process, since the serpentine has already been milled and therefore may lower the sequestration costs. The site contains 5 457 000 tonnes of broken rock, 17 021 000 tonnes of tailings, and 48 millions of tonnes of in situ serpentine-rich rock (Budinski, 2000). The fibrous nature of this variety of serpentine, which is considered a health concern (Hamel, 1998), may be effectively destroyed during the mineral carbonation process.

CONCLUSIONS

Should the mineral carbonation process be considered as a form of sequestering CO_2 emissions in BC, an overview of locations of raw material within the vicinity of major CO_2 point sources is an important parameter in conceptual modeling. The distribution of ultramafic rocks in BC, with emphasis on those complexes containing dunite and/or serpentinite zones, is depicted in Figure 6. Based on this map, less than 3% of BC's surface is underlain by

ultramafic rocks containing dunite and/or serpentinite. Of this 3%, less than 1% corresponds to areas where dunite is reported without serpentinite, approximately 2% is related to areas where serpentinite occurs without dunite, and 1% of BC is underlain by ultramafic rocks where dunite and serpentinite are reported together. Because of the methodology used to construct the map, surface areas corresponding to ultramafic rocks are overestimated.

Due to the subduction-related tectonic setting, Alpine-type and Alaskan-type ultramafic complexes are more common along the western margin of North America than they are in, for example, areas located on the stable craton or passive margin. With this in mind, claims made by Goff et al. (1997) and Goff and Lackner (1998), in which they state that "abundant resources of Mg-rich peridotite [dunite] and serpentinite exist within the United states and many other countries", should be questioned, and follow-up is needed.

Ultramafic complexes may host a wide variety of economic minerals. Thus, the geographic distribution of dunites and serpentinites can be used as a metallotect in exploration for a variety of metallic, industrial mineral, and gemstone deposits. In a number of specific cases, serpentine- and olivine-bearing rocks contain chromite, Ni, Co, and platinum-group elements. If these commodities can be recovered at profit as a by-product of mineral sequestration, then costs of the CO_2 disposal may be substantially reduced.

ACKNOWLEDGEMENTS

Special thanks to Don McIntyre, who was essential in manipulating the British Columbia Mineral Potential database to produce Figure 6. Thanks to Derek Brown from New Ventures for his interest and financial support. Joanne Nelson and Graham Nixon read early versions of this manuscript and provided useful and constructive criticism.

REFERENCES

Ash, C. (1996a): Silica-Carbonate Hg; *In*: Selected British Columbia Mineral Deposit Profiles, Volume 2, Metallic Deposits, D.V. Lefebure and T. Höy (eds.), *British Columbia Ministry of Energy and Mines*, pages 75-76.

Ash, C. (1996b): Podiform Chromite; *In*: Selected British Columbia Mineral Deposit Profiles, Volume 2, Metallic Deposits, D.V. Lefebure and T. Höy (eds.), *British Columbia Ministry of Energy and Mines*, pages 109-111.

Ash, C. and Alldrick, D. (1996): Au-Quartz Veins; *In*: Selected British Columbia Mineral Deposit Profiles, Volume 2, Metallic Deposits, D.V. Lefebure and T. Höy (eds.), *British Columbia Ministry of Energy and Mines*, pages 53-56.

Baragar, W. R. A. (1969): The Geochemistry of Coppermine River asalts, *Geological Survey of Canada, Paper* 69-44, 43 pages.

Bellefontaine, K., Legun, A., Massey, N.W.D. and Desjardins, P. (1995): Mineral Potential Project, Digital Geological Compilation NEB.C. South Half, *Geological Survey Branch Open File* 1995-24.

Bellefontaine, K. and Alldrick, D. (1994): Midcoast Arcview Data, *Geological Survey Branch Open File* 1994-17.

Budinski, D. (2000): Chrysotile Resources at Cassiar Mine, *Orcan Consulting Report*, February 15th, 2000.

Canil, D., Brearly, M. and Scarfe, C.M. (1987): Petrology of Ultramafic Xenoliths from Rayfield River, Southcentral British Columbia, *Canadian Journal of Earth Sciences*, v. 24, pages 1679-1687.

Clark, T. (1980): Petrology of the Turnagain Ultramafic Complex, Northwestern British Columbia, *Canadian Journal of Earth Sciences*, v. 17, pages 744-757.

Coleman, R.G. (1977): Ophiolites, *Springer-Verlag*, New York: 229 pages.

Deer, W.A., Howie, R.A and Zussman, J. (1978): An Introduction to the Rock Forming Minerals, Longman Group Ltd., London, 528 pages.

Dewey, J.F. (1976): Ophiolite Obduction, *Tectonophysics,* v. 31, pages 93-120.

Dostal, J., Hamilton, T.S., Church, B.N. (1996): The Chilcotin Basalts, British Columbia (Canada): Geochemistry, Petrogenesis and Tectonic Significance; *Neues Jarhbuch Fur Mineralogie Abhandlungen*, v. 170, no. 2, pages 207-229 (GSC Cont.# 40495).

Eales, H.V. and Cawthorn, R.G. (1996): The Bushveld Complex, *In*: R.G. Cawthorn (ed.), Layered Intrusions, *Elsevier Science*, pages 181-229.

Evenchick, C.A., Friday, S.J. and Monger, J.W.H. (1986): Potential Hosts to Platinum Group Element Concentrations in the Canadian Cordillera, *Geological Survey of Canada, Open File 1433*.

Findlay, D.C. (1963): Petrology of the Tulameen Ultramafic Complex, Yale District, British Columbia. Unpublished Ph.D. Thesis, *Queens University*, 415 pages.

Gabrielse, H. (1998): Geology of Cry Lake and Dease Lake Map Areas, North-Central British Columbia, *Geological Survey of Canada, Bulletin* 504, 147 pages

Gabrielse, H., Monger, J.W.H., Wheeler, J.O. and Yorath, C.J. (1991): Morphogeological Belts, Tectonic Assemblages and Terranes, Chapter 2, Part A, of Geology of the Cordilleran Orogen in Canada, Geology of Canada, no. 4, *Geological Survey of Canada*, pages 15-28.

Goff, F. and Lackner, K.S. (1998): Carbon Dioxide Sequestering Using Ultramafic Rocks, *Environmental Geosciences*, 5, 3, pages 89-101.

Goff, F., Guthrie, G., Counce, D., Kluk, E., Bergfeld, D. and Snow, M. (1997): Preliminary Investigations on the Carbon Dioxide Sequestering Potential of Ultramafic Rocks, *Los Alamos National Laboratory*, LA-13328 MS, 22 pages.

Gross, G.A., Gower, C.F. and Lefebure, D.V. (1999): Magmatic Ti-Fe +/-V Oxide Deposits, *In*: Selected British Columbia Mineral Deposit Profiles, Volume 3, Industrial Minerals and Gemstones, G.J. Simandl, Z.D. Hora and D.V. Lefebure (eds.), *British Columbia Ministry of Energy and Mines*, pages 57-60.

Hamel, D. (1998): Utilization of Chrysotile Asbestos; Lessons from Experiences, In: Proceedings of the 33rd Forum on the Geology of Industrial Minerals, Canadian Institute of Mining and Metallurgy Special Volume 50, pages 121-129.

Hammack, J.L., Nixon, G.T., Wong, R.H. and Paterson, W.P.E. (1990): Geology and Noble Metal Geochemistry of the Wrede Creek Ultramafics Complex, North-Central British Columbia; Geological Fieldwork 1989, B.C. Ministry of Energy, Mines, and Petroleum Resources, Paper 1990-1, pages 405-416.

Hancock, K.D. (1990): Ultramafic Associated Chrome and Nickel Occurrences in British Columbia; B.C. Ministry of Energy, Mines and Petroleum Resources, Open File 1990- 27, 62 pages

Henning, R.J. (1994): Olivine and Dunite, In: Industrial minerals and Rocks, 6th Edition, D. D. Carr (ed.), 1196 pages

Hora, Z.D. (1999): Ultramafic-Hosted Chrysotile Asbestos, In: Selected British Columbia Mineral Deposit Profiles, Volume 3, Industrial Minerals and Gemstones, G.J. Simandl, Z.D. Hora and D.V. Lefebure (eds.), British Columbia Ministry of Energy and Mines, pages 61-64.

Höy, T. (1995): Cyprus Massive Sulphide Cu (Zn), In: Selected British Columbia Mineral Deposit Profiles, Volume 1, Metallics and Coal, D.V. Lefebure and G.E. Ray (eds.), British Columbia Ministry of Energy and Mines, pages 51-52.

Höy, T., Church, B.N., Legun, A., Glover, K., Gibson, G., Grant, B., Wheeler, J.O. and Dunne, K.P.E. (1994): Kootenay Area, Geological Survey Branch Open File 1994-8.

Huot, F., Beaudoin, G., Hebert, R., Constantine, M., Bonin, G. and Dipple, G.M. (2003): Evaluation of Southern Quebec Asbestos Residues for CO2 Sequestration by Mineral Carbonation; Preliminary Result, Abstract, GAC-MAC-SEG Conference, Vancouver, 2003.

Irvine, T.N. (1987): Layering and Related Structures in the Duke Island and Skaergaard Intrusions: Similarities, differences, and Origins, In: Origins of Igneous Layering, I. Parsons (ed.), D. Reidel Publishing Company, pages 185-243.

Irvine, T.N. (1976): Alaskan-type ultramafic-gabbroic bodies in the Aiken Lake, McConnel Creek, and Toodoggone map-areas, geological Survey of Canada Paper, 76-1A, pages 76-81.

Irvine, T.N. (1967): The Duke Island Ultramafic Complex, Southeastern Alaska: In: Ultramafic and Related Rocks, P.J. Wyllie (ed.); John Wiley & Sons, Inc., N.Y., pages 84-96.

Irvine, T.N. and Smith, C.H. (1967): The Ultramafic Rocks of the Muskox Intrusion, NWT, Canada: In: Ultramafic and Related Rocks, P.J. Wyllie (ed.); John Wiley & Sons,Inc., N.Y., pages 38-49.

Kakizawa, M., Yamasaki, A. and Yanagisawa, Y. (2001): A New CO2 Disposal Process Using Artificial Rock Weathering of Calcium Silicate Accelerated by Acetic Acid, Energy, v.26, pages 341-354.

Kerans, C. (1983): Timing and Emplacement of the Muskox Intrusion: Constraints from Coppermine Homocline Cover strata, Canadian Journal of Earth Sciences, 20, 5, pages 673-683.

Kilby, W.E. (1994): Mineral Potential Project-Overview, Geological Fieldwork, Paper 1995-1, pages 411-416.

Kohlmann, J., Zevenhoven, R. and Mukherjee, A.B. (2002): Carbon Dioxide Emission Control by Mineral Carbonation: The Option for Finland, Proceedings of the 6th European Conference on Industrial Furnaces and Boilers, Estoril Lisbon, Portugal.

Kohlmann, J. and Zevenhoven, R. (2001): The Removal of CO2 from Flue Gases Using Magnesium Silicates, in Finland, Proceedings of the 11th International Conference on Coal Science, San Francisco, California.

Lackner, K.S., Butt, D.P. and Wendt, C.H. (1997): Magnesite Disposal of Carbon Dioxide, Proceedings of the 22nd International Technical Conference on Coal Utilization & Fuel Systems, Clearwater Florida, pages 419-430.

MacIntyre, D., Legun, A., Bellefontaine, K. and Massey, N.W.D. (1995): Northeast B.C. Mineral Potential Project, Geological Survey Branch Open File 1995-6.

MacIntyre, D., Ash, C. and Britton, J. (1994): Nass-Skeena, Geological Survey Branch Open File 1994-14.

Le Maitre, R.W., Editor (1989): A Classification of Igneous Rocks and Glossary of Terms, Blackwell Scientific Publishing Company: 193 pages

Massey, N.W.D. (1994): Vancouver Island, Geological Survey Branch Open File 1994-6.

Mathison, C.I. and Ahmat, A.L. (1996): The Windimurra Complex, Western Australia, In: R.G. Cawthorn (ed.), Layered Intrusions, Elsevier Science, pages 485-509.

McBirney, A.R. (1996): the Skaergaard Intrusion, In: R.G. Cawthorn (ed.), Layered Intrusions, Elsevier Science, pages 147-179.

McKelvy, M.J., Chizmeshya, A.V.G., Bearat, H., Sharma, R. and Carpenter, R.W. (2002): Developing a Mechanistic Understanding of CO2 Minerals Sequestration Reaction Processes, Proceedings of the 26th International Technical Conference on Coal Utilization & Fuel Systems, Clearwater, Florida, 2001, 13 pages

Mihalynuk, M., Bellefontaine, K., Brown, D., Logan, J., Nelson, J., Legun, A. and Diakow, L. (1996): Digital Geology, NW British Columbia, Geological Survey Branch Open File 1996-11.

Monger, J.W.H. (1997): Plate Tectonics and Northern Cordillera Geology: An Unfinished Revolution, Geoscience Canada, 24, 4, pages 189-198.

Monger, J.W.H. and Journeay, J.M. (1994): Guide to the Geology and Tectonic Evolution of the Southern Coast Mountains, Geological Survey of Canada Open File 2490, 77 pages plus maps.

Monger, J.W.H. and Berg, H.C. (1984): Lithotectonic Terrane Map of Western Canada and Southeastern Alaska, In: Lithotectonic terrane maps of the North American Cordillera, Silberling, N.J. and Jones, D.L. (eds.), Open File Report - U.S. Geological Survey, pages B1-B31.

Moores, E.D. (2002): Pre-1 Ga (pre-Rodinian) Ophiolites: Their Tectonic and Environmental Implications, GSA Bulletin, v. 114, no. 1, pages 80-95.

Moores, E.D. (1982): Origin and Emplacement of Ophiolites, Review of Geophysics and Space Physics, v. 20, no. 4., pages 735-760.

Naslund, H.R., and McBirney A.R. (1996): Mechanisms of Formation of Igneous Layering, In: Cawthorn, R.G. (Ed.), Layered Intrusions, Elsevier, pages 1-43.

Nelson, J.L. and Bradford, J.A. (1993): Geology of the Midway-Cassiar Area, Northern British Columbia (104O, 104P), Geological Survey Branch, Bulletin 83, 94 pages

Nixon, G.T., Hammack, J.L., Ash, C.H., Cabri, L.J., Case, G., Connelly, J.N., Heaman, L.M., Laflamme, J.H.G., Nuttall, C., Paterson, W.P.E. and Wong, R.H. (1997): Geology and Platinum-Group-Element Mineralization of Alaskan-Type Ultramafic-Complexes in British Columbia, Geological Survey Branch, Bulletin 93, 142 pages

Nixon, G.T. (1996): Alaskan-Type Pt ±Os ±Rh ±Ir; In: Selected British Columbia Mineral Deposit Profiles, Volume 2, Metallic Deposits, D.V. Lefebure and T. Höy (eds.), British Columbia Ministry of Energy and Mines, pages 109-111.

Nixon, G.T. (1990): Geology and Precious Metal Potential of Mafic-Ultramafic Rocks in British Columbia: Current Progress, Geologic Fieldwork, 1989, Paper 1990-1, pages 353-358.

O'Connor, W.K., Rush, G.E., Dahlin, D.C., Reidel, S.P. and Johnson, V.G. (2003): Geological Sequestration of CO2 in the Columbia River Basalt Group, Proceedings for the 28th International Technical Conference on Coal Utilization &Fuel Systems**,** Clearwater, Florida, 12 pages

O'Connor, W.K., Dahlin, D.C., Nilsen, D.N., Walters, R.P. and Turner, P.C. (2000): Carbon Dioxide Sequestration by Direct Mineral Carbonation with Carbonic Acid, Proceedings of the 25th International Technical Conference on Coal Utilization & Fuel Systems, Coal Technology Association, Clearwater, Florida.

O'Connor, W.K., Dahlin, D.C., Turner, P.C. and Walters, R.P. (1999): Carbon Dioxide Sequestration by Ex-Situ Mineral Carbonation, Proceedings of the 2nd Dixy Lee Ray Memorial Symposium: Utilization of Fossil Fuel-Generated Carbon Dioxide in Agriculture and Industry, Washington, D.C.

Read, P.B. and Wheeler, J.O. (1977): Geology, Lardeau, West-half, Geological Survey of Canada, Open File 432, map scale 1:125,000.

Rublee, V.J. (1986): Occurrence and Distribution of Platinum-Group Elements in British Columbia, B.C. Ministry of Energy, Mines, and Petroleum Resources, Open File 1986-7,94 pages

Schiarizza, P., Gaba, R.G., Glover, J.K., Garver, J.I. and Umhoefer, P.J. (1997): Geology and Mineral Occurrences of the Taseko-Bridge River Area, Geological Survey Branch Bulletin 100, 292 pages

Schiarizza, P. and Church, N. (1996): (East Part) the Geology of the Thompson-Okanagan Mineral Assessment Region, Geological Survey Branch Open File 1996-20.

Schiarizza, P., Panteleyev, A., Gaba, R.G. and Glover, J.K. (1994): Cariboo-Chilcotin Area, Geological Survey Branch Open File 1994-7.

Seifritz, W. (1990): CO2 Disposal by Means of Silicates, Nature, 345, pages 486.

Simandl, G.J., Riveros, C.P. and Schiarizza, P. (2000): Nephrite (jade) deposits, Mount Ogden Area, Central British Columbia (NTS 093N 13W), Geological Survey Branch, Geological Fieldwork 1999, pages 339-347.

Simandl, G.J. and Ogden, D. (1999): Ultramafic-Hosted Talc-Magnesite, In: Selected British Columbia Mineral Deposit Profiles, Volume 3, Industrial Minerals and Gemstones, G.J. Simandl, Z.D. Hora and D.V. Lefebure (eds.), British Columbia Ministry of Energy and Mines, pages 65-68.

Simandl, G.J. and Paradis, S. (1999): Ultramafic-Related Corundum, In: Selected British Columbia Mineral Deposit Profiles, Volume 3, Industrial Minerals and Gemstones, G.J. Simandl, Z.D. Hora and D.V. Lefebure (eds.), British Columbia Ministry of Energy and Mines, pages 123-127.

Simandl, G.J. Birkett, T. and Paradis, S. (1999a): Vermiculite, In: Selected British Columbia Mineral Deposit Profiles, Volume 3, Industrial Minerals and Gemstones, G.J. Simandl, Z.D. Hora and D.V. Lefebure (eds.), British Columbia Ministry of Energy and Mines, pages 69-72

Simandl, G.J., Paradis, S. and Birkett, T. (1999b): Schist-Hosted Emeralds, In: Selected British Columbia Mineral Deposit Profiles, Volume 3, Industrial Minerals and Gemstones, G.J. Simandl, Z.D. Hora and D.V. Lefebure (eds.), British Columbia Ministry of Energy and Mines, pages 113-117.

Virta, R.L. and Mann, E.L. (1994): Asbestos, In: Donald D. Carr (ed.), Industrial Minerals and Rocks, 6th Edition, pages 97-124.

Voormeij, D.A. and Simandl, G.J. (in prep): CO2 sequestration Potential of the Tulameen Ultramafic Complex, British Columbia, Canada.

Voormeij, D.A. and Simandl, G.J. (2004): Ultramafic Rocks in British Columbia- Applications in CO2 Sequestration and Mineral Exploration, Geological Survey Branch, Geofile 2004-1.

Voormeij, D.A. and Simandl, G.J. (2003a): Geological and Mineral CO2 Sequestration Options for British Columbia: A Technical Review, Geological Fieldwork 2002, Paper 2003-1, pages 265-282.

Voormeij, D.A. and Simandl, G.J. (2003b): CO2 Sequestration Options for B.C.: Matching Sinks and Sources, Geological Survey Branch, Geofile 2003-11.

White, G.V. (1987): Olivine Potential in the Tulameen Ultramafic Complex: Preliminary Report, Geological Fieldwork 1986, Paper 1987-1, pages 303-307.

Wilson, A.H. (1996): The Great Dyke of Zimbabwe, In: R.G. Cawthorn (ed.), Layered Intrusions, Elsevier Science, pages 365-401.

Wilson, J.R., Robins, B., Nielsen, F.M., Duchesne, J.C. and Vander Auwera, J. (1996): the Bjerkreim-Sokndal Layered Intrusion, Southwest Norway, In: R.G. Cawthorn (ed.), Layered Intrusions, Elsevier Science, pages 231-255.

Wu, J.C.S., Sheen, J.D., Chen, S.Y. and Fan, Y.C. (2001): Feasibility of CO2 Fixation via Artificial Rock Weathering, Ind. Eng. Chem. Res., v. 40, pages 3902-3905.


BRITISH
COLUMBIA
The Best Place on Earth

SAND AND GRAVEL MAPPING IN NORTHEAST BRITISH COLUMBIA USING AIRBORNE ELECTROMAGNETIC SURVEYING METHODS

Melvyn E. Best
Bemex Consulting International
5288 Cordova Bay Road
Victoria, B.C. V8Y 2L4

Victor Levson
Resource Development and Geoscience Branch, BC Ministry of Energy and Mines,
6th Flr-1810 Blanshard St., Victoria, BC, Canada, V8W 9N3

Doug McConnell
Fugro Airborne Surveys
200, 517 10th Ave. S.W.

KEYWORDS: Sand and gravel deposits, airborne electromagnetic (EM), resistivity, geophysics, Kotcho area, northeast BC

INTRODUCTION

The Ministry of Energy and Mines recently initiated, as part of the provincial Oil and Gas Development Strategy, a regional geological assessment of aggregate resources in northeast British Columbia. The area identified for this project (Figure 1) was selected because subsurface data collected during seismic shot hole drilling in the region indicated that gravels were present under 1 to 2 m of overburden. Aggregate deposits are extremely rare in this area, with the closest known deposits occurring many tens of kilometres distant. The study area occurs along the Kotcho winter road, about 40 km east of the Sierra-Yoyo-Desan (SYD) Road.

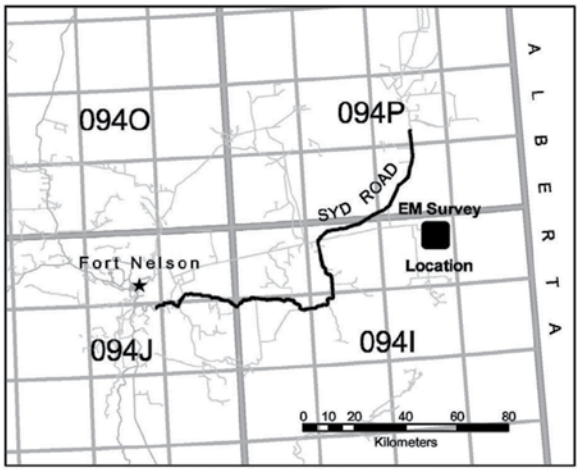

Figure 1. Map of the survey location relative to the Sierra-Yoyo-Desan (SYD) Road.

After initial identification of the area from the shot hole data, the Ministry of Energy and Mines contracted a geotechnical aggregate investigation in the region. The results of the study identified an area approximately 700 m long by 100 to 400 m wide that contained an estimated 410 000 m2 of sandy gravel (Dewer and Polysou, 2003). Excavations in the vicinity of the deposit showed gravels underlying silt-rich sediments. The buried sands and gravels were encountered in 10 test pits in an elongated, southwest-trending area, oblique to present surface stream channels. In the core of the deposit, the sands and gravels are at least 5 m thick, and in 6 of the test holes the base of the deposit was not encountered. Surprisingly, the water table was encountered in only 1 test hole at the south-easternmost edge of the deposit.

The gravel deposit occurs along a gentle south-easterly slope in an area with very little surface topography, and there is little or no geomorphic indication that subsurface gravels are present. The sands and gravels are overlain by silts and clays generally 1 to 2 m thick but locally up to 5 m thick. These sediments are interpreted to be glaciolacustrine in origin. Even though much of the area has been logged, and surface features are readily visible, air photographic interpretation alone would not have detected this deposit.

The present study was initiated to test the effectiveness of using airborne electromagnetic (EM) data for detecting such buried gravel deposits. The objectives of the EM study were threefold: 1) to determine whether the buried gravels could be detected remotely, 2) to attempt to trace the extent of the gravel deposit beyond the field tested boundaries, and 3) to locate any other aggregate sources in the area, either directly adjacent to the known deposit or within the general region. To accomplish these objectives, a detailed survey (Figure 1) with a 100 m line spacing was conducted directly over the known deposit, and a larger area (approximately 25 km2 in size—the total black area shown in Figure 1) was

covered with a 200 m line spacing (Cain, 2004).

Fugro Airborne Surveys was contracted to carry out a multi-frequency helicopter EM and magnetic survey using the RESOLVE™ EM system. The processed data include 5 apparent resistivity grids generated from the horizontal coplanar coils at frequencies of 380, 1400, 6200, 25 000 and 115 000 Hz. Fugro also generated apparent resistivity cross sections (differential resistivity) and resistivity inversion cross sections along several lines. The data set includes a series of magnetic grids as well (total field magnetic, vertical derivative, several high pass filters, with and without reduction to the pole; i.e., RTP).

This paper discusses the EM data sets and integrates them into a possible resistivity model of the subsurface within the survey area.

RESISTIVITY OF ROCKS AND GLACIAL SEDIMENTS

Approximate resistivity ranges for sedimentary rocks and glacial sediments are given in Figure 2. Note resitivity has units of ohm metres (ohm-m), and conductivity (which is the inverse of resistivity) has units of siemens per metre (S/m). In some instances these ranges could even be larger than those shown in Figure 2. The resistivity range for sandstone overlaps that of sand and gravel, and that of till overlaps both sandstone and sand and gravel.

The main factors that determine the resistivity of a rock or sediment are 1) porosity, 2) resistivity of pore fluid(s), and 3) percentage of conducting minerals (clays, graphite, sulphides) contained within the mineral grains. The influence of pore water on the resistivity of a rock or sediment can be determined from Archie's Law (Archie, 1942):

$$\rho_b = \rho_f \Phi^{-m} S_w^{\ 2} \qquad (1)$$

where ρ_b and ρ_f are the resistivity of the bulk material and of the fluid respectively, Φ is the porosity, and m is the cementation factor (usually between 1.5 and 2.0). The water saturation within the pores is S_w (assuming the other fluid in the pores is resistive; for example, oil or air). $S_w = 1$ when the pores are filled with 100% water.

Archie's Law implies that for a given pore fluid, the larger the porosity the larger the bulk resistivity. This equation does not take into account conducting mineral grains such as clay, graphite, and sulphides. Such conducting grains, if they are electrically connected, will lower the bulk resistivity of a rock or sediment from that predicted by Archie's Law.

When the conducting mineral grains are isolated from one another, no current will flow within the mineral grains. In this case the current will flow through the water in the pores, and the bulk resistivity is determined from Archie's Law. On the other hand, if there are continuous conducting pathways within the mineral grains, some of the current will flow within the pore water and some of the current will flow within the conducting mineral grains. The bulk resistivity of the material will therefore be less than that predicted by Archie's Law. Indeed, in the case of clay, the bulk resistivity can result almost entirely from conducting clay minerals rather than pore water.

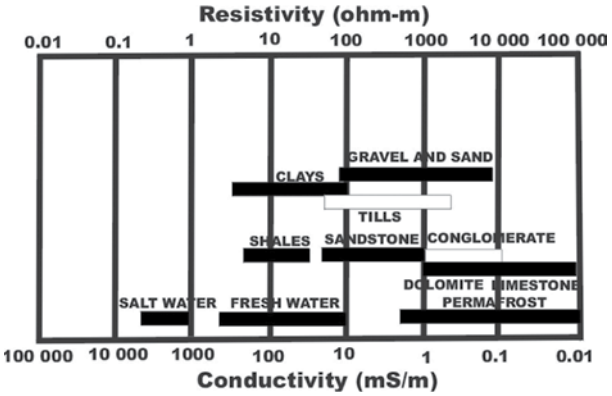

Figure 2. Resistivity ranges for rocks and glacial sediments (modified from Palacky and Stevens, 1990).

DESCRIPTION OF DATA

Resistivity Sections

Figures 3 and 4 are resistivity sections computed for lines 10110 to 10180. The upper diagram of each line was generated using apparent resistivity data from the horizontal coplanar configurations (differential resistivity). The estimated depth of the differential resistivity sections at each frequency and for a given position along a line is equal to the skin depth computed from the apparent resistivity value at that position. The lower section on each line is a layered earth inversion (in this case 4 layers) computed using the in-phase and quadrature data at all 5 frequencies.

The apparent resistivity is calculated from the normalized in-phase and quadrature values of the secondary magnetic field by assuming the earth is homogeneous with a resistivity equal to the apparent resistivity ρ_a. For a given frequency f and transmitter-receiver separation S, the apparent resistivity computed from the in-phase and quadrature values depends on the height above ground. As the height increases, the in-phase and quadrature values decrease in a predictable way, and hence the apparent resistivity will change accordingly.

The apparent resistivity is therefore considered to be an approximate measure of the average resistivity of the earth to a depth equal to the skin depth (δ).

$$\delta\ (\text{m}) = 503\ (\rho_a/f)^{1/2} \qquad (2)$$

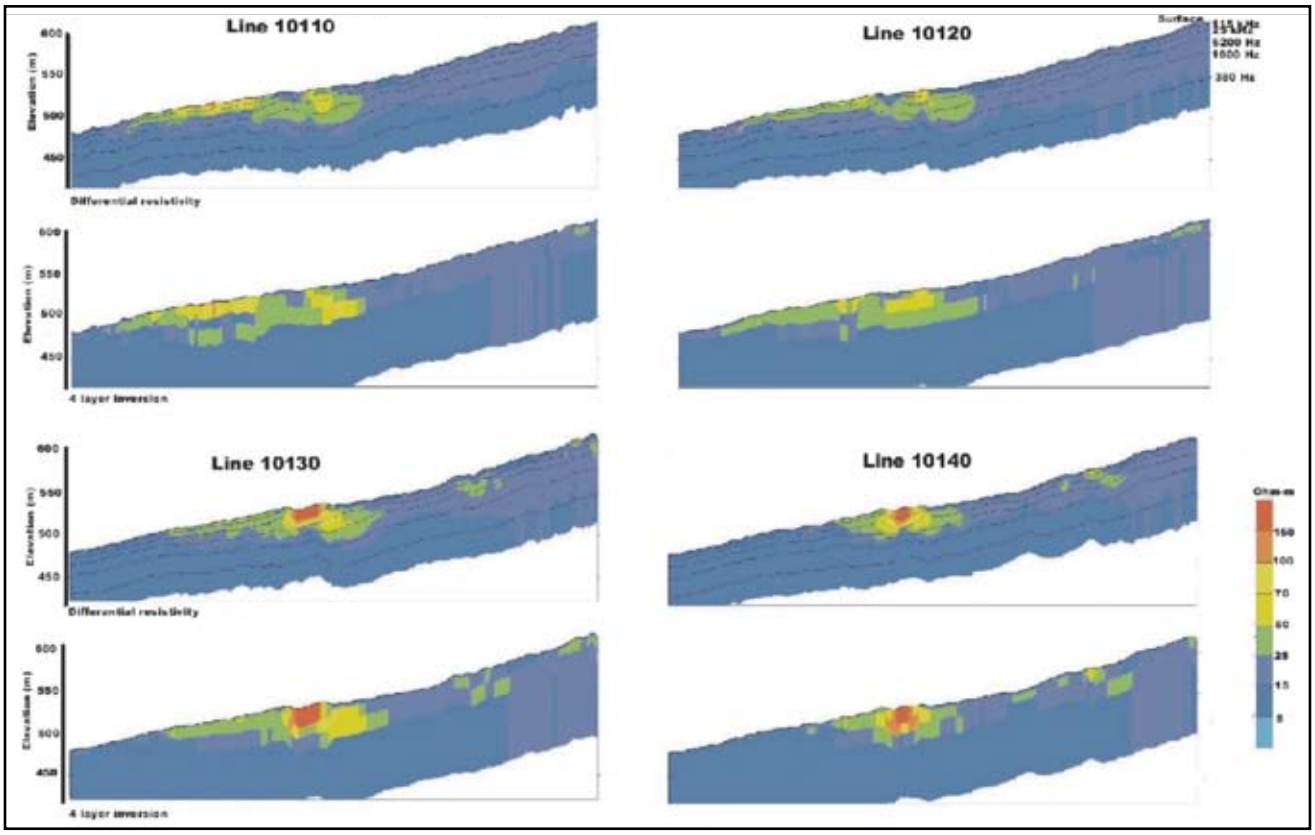

Figure 3. Resistivity cross sections for lines 10110 to 10140. The upper diagram of each line is the differential resistivity and the lower diagram is the 4-layer inversion as described in the text. North is to the right.

For a given resistivity, the skin depth decreases as the frequency increases. Consequently the highest frequency of 115 000 Hz represents the average resistivity at the shallow depths, while the lowest frequency of 380 Hz represents the average resistivity at the deepest depth the RESOLVE system can image.

The earth is generally not homogeneous but more complex. This is why the computed resistivity is called an apparent resistivty. As an example, consider a two-layer earth with the upper-layer resistivity equal to 100 ohm-m and the lower-layer resistivity equal to 5 ohm-m. The skin depth of the upper layer at 115 000 Hz and 380 Hz is 14.8 m and 258 m, respectively. If the upper layer is 20 m thick, then the apparent resistivity at 115 000 Hz will be close to the upper resistivity of 100 ohm-m and at 380 Hz would be approximately equal to the lower layer resistivity of 5 ohm-m. On the other hand, if the upper layer is only 5 m thick, the apparent resistivity at 115 000 Hz would be between 100 and 5 ohm-m—in other words, a weighted average of the upper and lower resistivities since the upper-layer skin depth is nearly 3 times the layer thickness. The apparent resistivity at 380 Hz would still be approximately equal to 5 ohm-m.

Notice the similarity between the upper and lower sections in Figures 3 and 4 for each of the lines, even though the upper resistivity section is computed assuming the earth is a homogeneous half-space at each frequency. This happens because the resistivity structure of the earth is either homogeneous (as observed on most of the lines) or is approximately two-layered with the upper layer more resistive.

Apparent Resistivity Maps

The upper resistivity in Figure 5 is the apparent resistivity calculated from the high-frequency (115 kHz) horizontal coplanar coils, and the lower map is the apparent resistivity calculated from the low-frequency coils (380 Hz). These maps illustrate the spatial variability of the average conductivity at shallow (115 kHz) and deep (380 Hz) depths.

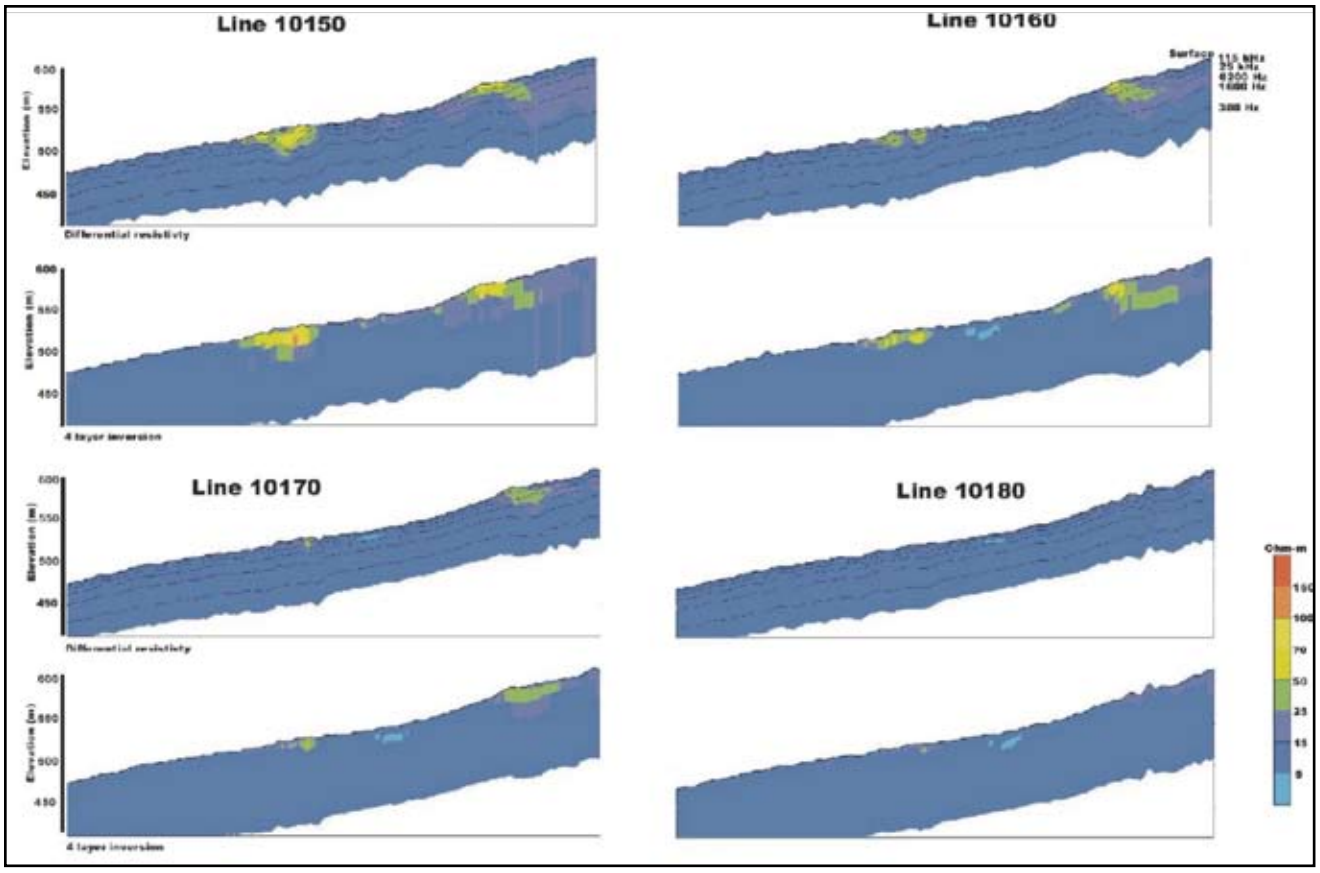

Figure 4. Resistivity cross sections from lines 10150 to 10180. The upper diagram of each line is the differential resistivity and the lower diagram is the 4-layer inversion as described in the text. North is to the right.

INTERPRETATION OF DATA

Apparent Resistivity Maps

As discussed, the 5 apparent resistivity maps represent resistivity values averaged over 5 different subsurface depths, depending on the frequency. These maps exhibit several interesting features worth noting (Figure 5). There is a resistivity high (Zone A) located in the northern part of the survey area between lines 10130 and 10180 that is prominent at frequencies between 115,000 and 6200 Hz. At lower frequencies the resistivity of this feature merges with the background resistivity values. This feature is related to the sand and gravel deposit outlined by trenching.

There is a resistive feature (Zone B) between lines 10060 and 10160 that starts near the southern boundary of the survey area and continues north to the middle of the survey. This resistive feature is most prominent on the 3 highest frequencies, similar to Zone A.

An approximately north-south boundary (with an east-west jog at approximately the midpoint of the survey) separates higher resistivity values to the west from lower resistivity values to the east. This boundary is located between lines 10180 and 10120 (Figure 5) and is visible on all 5 apparent resitivity maps. The eastern edges of Zones A and B are coincident with this boundary. It is not clear what this boundary represents geologically since it is observed on all 5 frequencies.

In addition to Zones A and B, there are 2 other resistive zones that can be seen on the higher frequencies (Figure 5). Zone C is along the northern boundary of the survey area between lines 10150 and 10110, and Zone D lies between lines 10240 and 10280. Both these features are more diffuse than Zones A and B, but the resistivity values are comparable.

Resistivity Sections

Resistivity sections between lines 10110 and 10180 provide information on the depth extent of Zones A and B (Figures 3 and 4). Zone A appears on lines 10130 to 10170, and zone B appears on lines 10110 to 10170. Zone C is most prominent on lines 10060 to 10100, although there is a hint of this resistive feature on lines 1010 and 10120. Zone D does not appear on any of these processed lines.

The background resistivity values (away from the resistivity features and at depth under the resistive features)

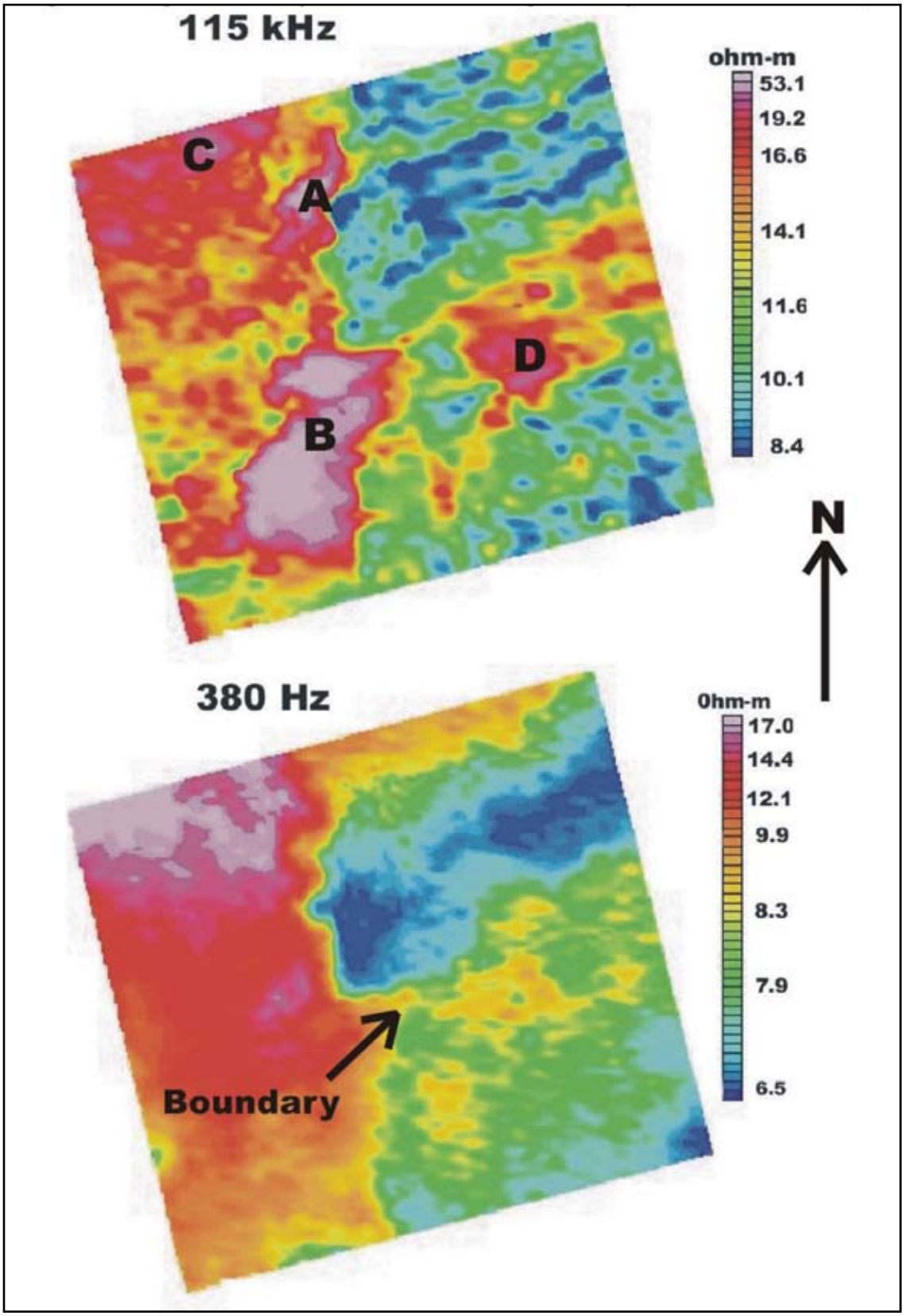

Figure 5. Apparent resistivity maps for frequencies of 115 kHz (upper diagram) and 380 Hz (lower diagram) . The 4 resistivity areas discussed in the text are labeled A to D in the upper diagram.

are low (less than 15 ohm-m) and most likely associated with shale or clay. The resistivity of the resistive features computed from the layered earth inversions generally have values greater than 50 ohm-m, although the outer fringes are somewhat less resistive (greater than 25 ohm-m). These values correspond either to sand and gravel or to sandstone. Sandstone bedrock is known to exist in the area, so there could be knobs of sandstone protruding through shale and/or till.

Once drilling or trenching confirms the presence of sand and gravel in any of these resistive features, we can assume that the entire area containing the resistive anomaly will most likely be composed of sand and gravel. The thicker regions of resistive Zones A and B are estimated to be between 25 and 35 m deep but do thin towards the edges. This is deeper than the trenching carried out to date. The depths from the resistivity cross sections can be used in conjunction with the apparent resistivity maps to estimate the total volume of sand and gravel in place.

RESULTS

On the high-frequency data reflecting the shallow geology, 4 main areas of high resistivity were identified in the survey. Zone A coincided remarkably well with the area of shallow buried gravels as mapped out by the field investigations. The northern and southern areas of Zone B are much larger and became the focus of recent reconnaissance-scale ground investigations. During these recent studies, both areas were found to contain sand and gravel. At least 4 m of sand and gravel under 1 to 2 m of overburden were encountered in test pits in the centre of these areas. Further work is required to outline these deposits in detail and to investigate the potential of Zones C and D. The results strongly indicate that high-resolution EM surveys can be an effective tool for mapping buried sand and gravel deposits.

SUMMARY AND CONCLUSIONS

Airborne EM was effective in mapping sand and gravel deposits in the Kotcho area of British Columbia. The areal extent of the known deposit (from seismic shot hole data and trenching) was mapped, and the total area containing sand and gravel was extended. The resistivity cross sections also provided an estimate of the depth of the sand and gravel deposit.

The survey outlined 2 other resistivity features as discussed above (Zones C and D). Unfortunately the resistivity range for sand and gravel overlaps the resistivity range for sandstone. Since sandstone may outcrop in this area, follow-up drilling or trenching is required to determine the material causing these anomalous resistivity features.

REFERENCES

Archie, G.E., 1942, The electrical resistivity log as an aid in determining some reservoir characteristics: *AIME*, 146, 54-67.

Cain, M.J. (2004): RESOLVE survey for the *British Columbia Geological Survey*; Fugro Airborne Surveys, Report 3091, 22 pages.

Dewer, D. and Polysou, N. (2003): Area 10 (Kotcho East) gravel investigation - Sierra-Yoyo-Desan Road area, North-eastern British Columbia; *Amec Earth and Environmental Limited,* Report No. KX04335, 13 pages.

Palacky, G.J., and Stevens, L.E., 1990, Mapping of Quaternary sediments in northeastern Ontario using ground electromagnetic methods: *Geophysics*, 55, 1595-1604.

HYDROCARBON SOURCE ROCK POTENTIAL AS DETERMINED BY ROCK-EVAL 6/TOC PYROLYSIS, NORTHEAST BRITISH COLUMBIA AND NORTHWEST ALBERTA

By A. Ibrahimbas[1] and C. Riediger[1,2]

KEYWORDS: Hydrocarbon source rocks, organic geochemistry, thermal maturity, petroleum systems.

ABSTRACT

The potential for conventional and/or unconventional hydrocarbon exploration requires the presence of organic-rich, thermally mature rock units containing oil- or gas-prone kerogen. This potential is poorly known in large parts of northeast BC and northern Alberta due to a paucity of organic geochemical studies.

Here, we investigate Lower Triassic to Lower Cretaceous potential source rocks within a large area of northeast BC and northwest Alberta (118° to 124°W and 57° to 58°N). Hydrocarbon source rock parameters, including type and amount of kerogen, and thermal maturity of these formations, are assessed by analyzing 74 core samples from 23 wells using Rock-Eval 6/TOC pyrolysis.

In general all units are immature in northwest Alberta, with increasing maturity to the west, where they become overmature. The Lower Triassic Montney Formation contains Type II kerogen with TOC (total organic carbon) values up to 4.2 wt.%, suggesting that this unit generated significant amounts of hydrocarbons where it is mature.

The base of the Doig Formation comprises a highly radioactive zone, the "Phosphate Zone", which contains Type II kerogen with TOC values up to 11 wt.%. This interval is an excellent hydrocarbon source rock.

The Upper Triassic Baldonnel and Pardonet Formations are late mature to overmature where sampled. The Baldonnel Formation contains up to 1.4 wt.% TOC, indicating only poor to fair source rock potential. The Pardonet Formation is overmature and contains residual TOC values up to 2.8 wt.%, which suggests this marine unit may have initially been a good source rock for hydrocarbons but is now spent.

The Lower Jurassic Gordondale Member comprises Type II kerogen with TOC values up to 10.45 wt.%, indicating that this unit is an excellent hydrocarbon source rock. The Lower Cretaceous Wilrich Shale is also of interest, as it has been suggested as a potential target for shale gas exploration. This unit is immature to mature within the study area. It contains Type III kerogen with TOC values up to 4.28 wt.%.

Future investigation will involve one-dimensional basin modeling in order to understand the amount and timing of hydrocarbon generation from these units with respect to timing of trap formation and accumulation of hydrocarbons.

INTRODUCTION

Hydrocarbon prospectivity in the Western Canada Sedimentary Basin (WCSB), or in any basin, hinges on the availability of oil- and/or gas-prone rock units that have generated and expelled hydrocarbons. Potential and proven hydrocarbon source rock intervals of Mesozoic age are known throughout much of the WCSB, with most available data from the Alberta portion of the basin (e.g., Creaney and Allan, 1990; Creaney et al., 1994). Results of the previous works are summarized in Table 1.

However, in the area of this study, bounded by 57° and 58°N latitude and 118° and 124°W longitude (Figure 1), there are few data available pertaining to hydrocarbon source rock potential. Furthermore, little is known of the thermal maturity of Paleozoic and Mesozoic strata in this area, and such information is critical for predicting what type of hydrocarbons, if any, may have been generated.

This paper reports the results of hydrocarbon source rock characterization of six formations of interest within the study area, namely, the Montney Formation, the "Phosphate Zone" at the base of the Doig Formation, the Baldonnel and the Pardonet Formations, the Gordondale Member (for discussion of the Gordondale, formerly Nordegg, terminology, see Asgar-Deen et al., in press), and Wilrich Formation (Figure 2). Samples were collected from cores in BC and Alberta and were analyzed by Rock-Eval 6/TOC pyrolysis.

Future investigation will involve one-dimensional quantitative basin modeling in order to understand the amount and timing of hydrocarbon generation relative to trap formation and the accumulation of hydrocarbons.

[1]*University of Calgary*
[2]*Corresponding author (e-mail: riediger@ucalgary.ca)*

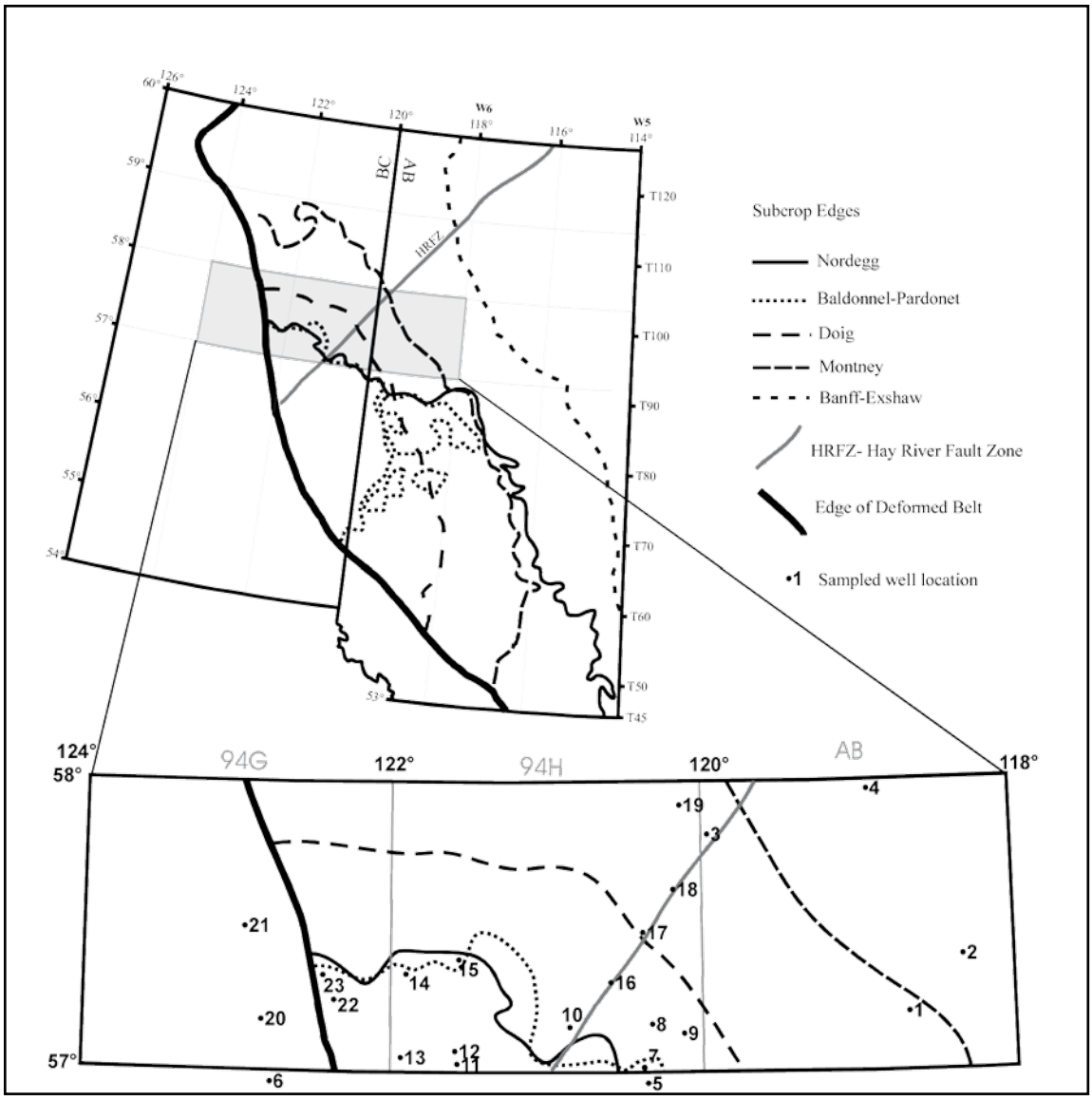

Figure 1. Map showing the study area, core sample locations, and the subcrop edges of the formations of interest (compiled from Richards et al., 1994; Edwards et al., 1994; Poulton et al., 1994).

STRATIGRAPHY

Devonian to Cretaceous stratigraphy in the study area is shown in Figure 2. Potential hydrocarbon source rock intervals are highlighted by shading. We use the new Gordondale Member terminology to refer to the organic-rich, fine-grained strata that are laterally equivalent to the Nordegg Member. These relationships are described by Asgar-Deen (2003) and Asgar-Deen et al. (in press).

Although the Devonian-Mississippian Exshaw Formation is a well-known and proven source rock for hydrocarbons, the lack of core through this zone precluded acquisition of samples during this study. However, Rock-Eval/TOC analyses of drill cuttings samples are planned.

Details of the stratigraphy shown in Figure 2 are not given here, but interested readers can find this information in the appropriate chapters of the Geological Atlas of the Western Canada Sedimentary Basin (Mossop and Shetson, 1994).

TABLE 1. PREVIOUS STUDIES OF ROCK-EVAL/TOC DATA SHOWING THE TOC'S AND THE KEROGEN TYPES OF THE UNITS OF INTEREST (*TOC VALUES WILL VARY, DEPENDING ON MATURITY)

Unit	*TOC range (average)(wt. %)	Kerogen Type	References
Wilrich	0.45-2.05 (1.4)	Type III	Faraj, 2003;Ibrahimbas, (Unpublished results)
Gordondale	0.55-28 (5)	Type I/IIS	Riediger et al., 1990b; Asgar-Deen, 2003; Faraj, 2003
Pardonet	0.26-6.5 (0.94)	Type II	Riediger, 1997; Carrelli, 2002
Baldonnel	0.14-2.08 (<1)	Type II	Riediger 1997; Carrelli 2002
Phosphate Zone	1.12-11 (3.6)	Type II	Riediger et al.,1990a; 1990b; Creaney and Allan, 1992; Faraj, 2003
Montney	0.8-4.7 (1.3)	Type II	Riediger et al., 1990a; 1990b; Hankel, 2001; Faraj, 2003

METHODOLOGY

For this study, 74 core samples were taken from 23 well locations (Figure 1). Samples were selected based on core availability within the zones of interest in the study area. Each sample was crushed to a fine powder prior to analysis. All samples were weighed to 100 mg and subjected to Rock-Eval 6/TOC analysis in order to determine the kerogen type, TOC content, and thermal maturity, which are the main parameters for characterizing a hydrocarbon source rock. Analyses were conducted at the Organic Geochemistry Labs of the Geological Survey of Canada (Calgary). Measured parameters include S1 (mg HC/g rock), S2 (mg HC/g rock), S3 (mg CO_2/g rock), Tmax (°C), and TOC (wt.%) (see Table 2). Several additional parameters, including HI (hydrogen index, S2/TOCx100), OI (oxygen index, S3/TOCx100), and PI (production index, S1/[S1+S2]) are calculated from these measured values and are shown in Table 2. Pyrolysis experiments were repeated for some samples at lower sample weight to ensure that the Rock-Eval/TOC detector was not overloaded by generated hydrocarbons during the original runs.

Details of the analytical procedure and discussion of Rock-Eval parameters are available in Espitalié et al. (1977), Peters (1986), and Snowdon et al. (1998). Peters (1986) and Peters and Cassa (1994) provide a summary of interpretive guidelines for Rock-Eval data.

RESULTS AND DISCUSSION

Rock-Eval 6/TOC results are summarized in Table 2. Of the 7 potential hydrocarbon source rocks shown in Figure 2, geochemical data from only the Montney, Phosphate Zone, Baldonnel/Pardonet, Gordondale, and Wilrich intervals are reported. As noted previously, no samples from the Exshaw Formation were collected for this study due to a lack of core through this zone.

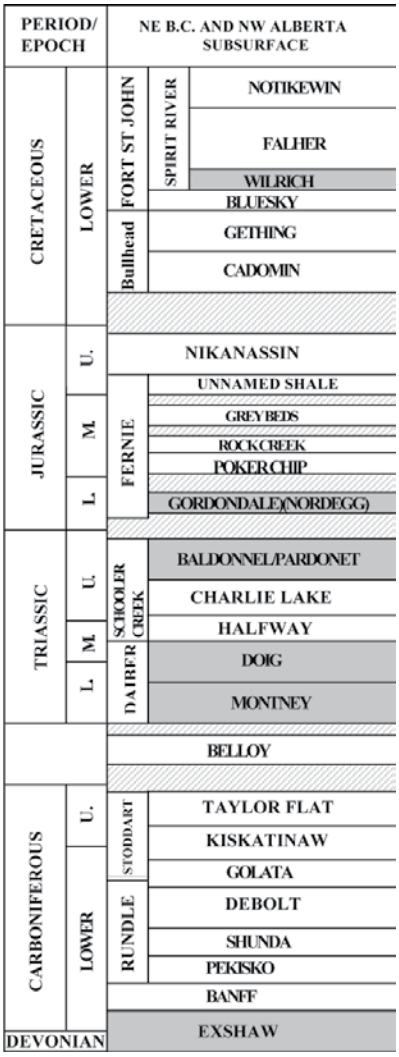

Figure 2. Stratigraphic chart of the study area (compiled from Richards et al., 1994; Henderson et al., 1994; Edwards et al., 1994; Poulton et al., 1994; Hayes et al., 1994). Potential source rocks are highlighted by shading.

However, geochemical data from well cuttings will be incorporated in the second phase of the study.

In this section, the thermal maturity and amount and type of organic matter are discussed. Interpretive guidelines from Peters (1986) and Peters and Cassa (1994) are used to evaluate the hydrocarbon source rock potential of each unit, and these guidelines are reproduced in Table 3. In Table 4, thermal maturity, TOC content, HI, and kerogen type are summarized for each unit.

Thermal Maturity

Rock-Eval Tmax data given in Table 2 are used to assess thermal maturity in the study area. Each unit is mapped individually in Figure 3 because variations in kerogen type affect the Tmax values (Peters, 1986). The overall maturity trend in the study area shows that the maturity of the units increases from east to west towards the Cordilleran deformation front. All units are thermally mature throughout the central part of the study area (Beatton River NTS map area 94H). Most of the studied units are immature in Alberta and are overmature in the Trutch map area (94G).

TOC Content, Kerogen Type, and Hydrocarbon Source Rock Potential

The ranges of TOC values for each unit are summarized in Table 4. Histograms showing the TOC variation for each unit with mean TOC values and standard deviations are also given in Figure 4. The plot of S2 against TOC for immature to early mature samples is used to determine the proportion of the inert carbon in the TOC measured by pyrolysis (Conford et al., 1998). During pyrolysis, only the labile kerogen will generate hydrocarbons to be recorded in S2 peak. Thus by discounting the proportion of inert carbon, it is possible to obtain a more accurate HI (S2/TOCx100) value from the slope of the best fitted lines of S2 versus TOC data (Figure 5). A bivariate plot of HI vs. OI (pseudo-Van Krevelen diagram) is also commonly used to assess the kerogen type (Figure 6).

In this section, information on TOC and kerogen type for each unit are used to evaluate the hydrocarbon source rock potential based on criteria outlined in Table 3.

The TOC values for the Montney Formation range from 0.51 to 4.18 wt.%, with a mean value of 2.01 wt.% (std. dev. = 1.24) (Figure 4). It contains 0.35 wt.% inert carbon (Figure 5), hence the proportion of organic carbon content that has the capacity to generate hydrocarbons ranges from 0.16 to 3.83 wt.%, with a mean value of 1.66 wt.%. The unit yields HI values of 43 to 450 mg HC/g TOC, which is typical for oil- and gas-prone Type II kerogen (Figure 6). Considering only the immature samples, adjusted HI_0 (original HI prior to maturation) is 571 mg HC/g TOC. These TOC and HI_0 values indicate good to very good source rock potential in the Montney Formation.

The "Phosphate Zone" has high TOC values ranging from 1.76 to 10.98 wt.% (Table 4), with a mean value of 6.14 wt.% (std. dev.=3.35) (Figure 4). The amount of the inert carbon in the "Phosphate Zone" is also high, with a value of 1.4 wt.% (Figure 5); therefore, the true organic carbon content of the unit is then between 0.4 and 9.6 wt.%. The unit comprises Type II oil- and gas-prone kerogen with HI values ranging from 189 to 489 mg HC/g TOC (263 to 645 mg HC/g TOC after discarding the effect of inert carbon [Figure 5]). The unit has excellent source rock potential.

The TOC values for Pardonet and Baldonnel Formations are fair to moderate. The samples are all overmature, and hence original kerogen type cannot be determined from geochemical data. However, these are marine carbonate units and thus likely contained Type II kerogen. This interpretation is also supported by the results of a previous study by Carrelli (2002) on these formations. The residual TOC values for Pardonet Formation range 0.97 to 2.79 wt.%, with a mean value of 1.73 wt.% (std. dev. = 0.60). Bordenave et al. (1993) suggested that overmature Type II source rocks would have lost 50% of their original TOC due to generation and expulsion of hydrocarbons. Hence, the original TOC values for Pardonet Formation were likely over 4 wt.%. The TOC values measured from the Baldonnel Formation range from 0.65 to 1.39 wt.%, which, by the same reasoning, were likely 1 to 2 wt.% originally. The Pardonet Formation had fair to good initial source rock potential, and the Baldonnel Formation had poor to fair initial source rock potential.

The Gordondale Member contains high TOC values ranging from 0.66 to 10.45 wt.% (mean = 5.71 wt.%, std. dev. = 2.66) (Figure 4). The unit yields HI values of 26 to 273 mg HC/g TOC and OI values of 3 to 23 mg CO_2/g TOC (Figure 6), and the high degree of maturity precludes a precise assessment of the organic matter type. Riediger et al. (1990b) and Asgar-Deen (2003) proposed this unit having Type I/IIS kerogen; therefore, the unit most likely comprises Type II kerogen, considering its marine origin. This interval has excellent source rock potential where mature.

The TOC values of the Wilrich Shale ranges from 1.08 to 4.28 wt.% (mean = 2.12 wt.%, std. dev. = 0.91) (Figure 4). After considering the approximately 0.5 wt.% inert carbon (Figure 5), it will contain 0.58 to 3.78 wt.% TOC with a mean value of 1.62 wt.%. The unit contains Type III, gas-prone kerogen, with HI values ranging from 138 to 393 mg HC/g TOC (Figure 6). The mean value of HI is 235 mg HC/g TOC after eliminating the effect of 0.5 wt.% inert carbon. The TOC and HI values indicate that the unit has good to very good source rock potential for gas generation.

TABLE 2. ROCK EVAL/TOC RESULTS FROM CORE SAMPLES IN THE STUDY AREA

(+REPEAT RUN AT LOWER SAMPLE WEIGHT)

Unit	Well #	Well ID	Depth (m)	Tmax (°C)	S1 (mg HC/ g rock	S2 (mgHC/ g rock)	S3 (mg CO_2/ g rock)	PI S1/ (S1+S2)	TOC (wt.%)	HI (mgHC/ g TOC)	OI (mgCO/ g TOC)
Wilrich	1	11-17-94-5W6	932.2	431	1.65	4.28	0.49	0.28	2.36	182	21
	2	7-25-96-4W6	827	428	1.06	3.15	0.38	0.25	1.96	161	19
	4	10-36-103-7W6	698.9	431	1.58	2.83	0.4	0.36	1.97	144	20
			704.8	429	0.59	4.8	0.44	0.11	3.16	153	14
	16	D-69-A/94-H-7	1100.5	441	0.22	2.69	0.16	0.08	1.83	148	9
			1103.1	442	0.3	2.84	0.16	0.10	1.83	156	9
	17	A-43-K/94-H-8	1194.5	438	0.14	1.49	0.27	0.09	1.08	139	25
			1196	438	0.27	2.84	0.26	0.09	1.47	194	18
	19	B-81-G/94-H-16	809.5	436	0.18	1.7	0.23	0.10	1.23	138	19
			811.4	437	1.06	16.8	0.18	0.06	4.28	393	4
Gordondale	5	A-58-K/94-A-16	1010.9	439	1.08	6.27	0.09	0.15	3.03	208	3
			1012.4	441	2.05	6.53	0.06	0.24	2.4	273	3
			1013.5	438	1	4.3	0.06	0.19	2.05	210	3
	11	A-43-A/94-H-4	1277.6	461	2.93	8.48	0.18	0.26	7.29	119	2
			1277.6	461	2.71	8.34	0.2	0.25	7.35	116	3
			1279.1	454	1.13	2.99	0.23	0.27	3.55	85	6
			1281.1	464	1.85	6.02	0.23	0.24	4.14	74	3
	12	D-93-A/94-H-4	1262.5	460	0.64	1.08	0.12	0.37	1.48	74	8
			1264.1	456	1.46	6.82	0.3	0.18	6.32	109	5
			1265.6	463	2.27	8.47	0.33	0.21	8.91	97	4
			1267.1	446	3.8	8.19	0.26	0.32	5.94	139	4
			1268.6	443	6.21	10.19	0.26	0.38	6.85	150	4
			1270.1	448	6.77	12.77	0.2	0.35	7.84	165	3
			1271.6	449	2.93	5.58	0.21	0.34	3.87	146	5
			1273.1	448	1.78	3.3	0.15	0.35	2.35	142	6
	13	D-65-D/94-H-4	1387.4	472	0.62	1.56	0.16	0.28	5.18	31	3
			1388.4	481	0.52	2.93	0.31	0.15	8.12	37	4
			1389.2	484	0.3	2.36	0.35	0.11	5.89	42	6
			1389.9	484	0.25	2.05	0.38	0.11	5.25	41	7
			1390.6	484	0.18	0.77	0.2	0.19	3.03	26	7
			1391.8	484	0.32	1.37	0.37	0.19	4.98	29	7
			1392.4	484	0.62	3.34	0.3	0.16	9.48	37	3
			1393	480	0.68	3.35	0.29	0.17	10.45	33	3
	14	A-5-E/94-H-6	1145.5	452	0.25	1.12	0.3	0.18	1.33	85	23
	15	B-54-H/94-H-5	1218.7	443	0.49	2.23	0.12	0.18	2.19	102	5
	22	C-86-C/94-G-8	1426.9	456	0.22	0.16	0.21	0.58	0.66	24	32
			1429.1	453	0.19	0.18	0.18	0.51	0.58	31	31
Pardonet	6	A-77-K/94-B-15	1050.4	480	0.27	0.84	0.15	0.24	1.73	51	9
			1055.8	461	0.36	0.42	0.19	0.46	1.83	23	10
			1059.3	471	0.21	0.39	0.17	0.35	1.16	34	15
			1061.8	468	0.33	0.34	0.21	0.49	1.34	26	16
	23	D-99-F/94-G-8	1316.6	468	0.65	1.44	0.15	0.31	2.29	64	7
			1317.6	464	0.53	0.92	0.11	0.37	0.97	96	11
			1319.1	466	0.73	1.6	0.15	0.31	2.79	58	5
Baldonnel	6	A-77-K/94-B-15	1065.1	472	0.14	0.24	0.16	0.37	0.86	29	19
	12	D-93-A/94-H-4	1274.1	452	0.52	0.56	0.13	0.48	0.98	57	13

TABLE 2. ROCK EVAL/TOC RESULTS (CONTINUED).

Unit	Well #	Well ID	Depth (m)	Tmax (°C)	S1 (mg HC/ g rock	S2 (mgHC/ g rock)	S3 (mg CO_2/ g rock)	PI (S1/ (S1+S2))	TOC (wt.%)	HI (mgHC/ g TOC)	OI (mgCO_2/ g TOC)
	22	C-86-C/94-G-8	1434.4	469	0.56	0.77	0.17	0.42	1.39	57	12
			1439.8	464	0.69	0.63	0.2	0.52	1.02	63	20
			1443.2	478	0.74	0.63	0.16	0.54	0.65	98	25
Phosphate Zone	8	A-78-F/94-H-1	1069.2	447	0.99	10.21	0.22	0.09	2.95	346	7
			1073.4	445	0.93	9.02	0.21	0.09	2.63	343	8
			1075	443	0.76	5.9	0.19	0.11	1.9	311	10
			1076.4	437	1.29	14.51	0.23	0.08	5.26	277	4
	9	D-48-H/94-H-1	1051.3	425	0.01	0.05	0.31	0.17	0.12	42	258
			1053.8	438	0.9	12.44	0.3	0.07	2.65	469	11
			1056	433	1.78	28.61	0.33	0.06	5.86	489	6
	10	D-72-E/94-H-2	1176.3	443	1.57	3.9	0.18	0.29	1.76	189	3
			1180.6	443	1.62	9.93	0.18	0.14	5.27	189	3
			*1180.6	441	1.59	9.79	0.21	0.14	5.02	196	4
			1182.9	442	1.64	15.9	0.2	0.09	7.73	207	3
			*1182.9	442	1.57	15.49	0.18	0.09	7.58	206	2
			1186.1	445	2.01	25.17	0.22	0.07	10.98	231	2
			*1186.1	445	2.08	24.62	0.21	0.08	10.79	230	2
			1187.4	444	2.14	25.68	0.18	0.08	10.95	236	2
			*1187.4	445	2.1	25.13	0.2	0.08	10.76	235	2
Montney	3	6-36-101-13W6	908.3	288	2.75	0.7	0.26	0.8	0.51	137	51
	7	D-13-D/94-H-1	1133.2	447	1.19	8.8	0.17	0.12	4.03	219	4
			1134.8	447	0.83	5.18	0.19	0.14	2.37	219	8
	18	D-45-G/94-H-9	905.8	431	0.8	4.8	0.23	0.14	1.23	390	19
			909.2	433	0.33	2.91	0.19	0.1	0.82	355	23
			914.5	439	0.41	9.09	0.26	0.04	2.02	450	13
			917.4	435	0.36	5.4	0.22	0.06	1.28	422	17
	20	D-88-F/94-G-2	2130.8	490	0.02	0.02	0.11	0.5	0.87	2	13
			2131.3	490	0	0.01	0.08	0	0.64	2	13
			2132.4	-40	0	0	0.15	0	0.4	0	38
			2133.1	500	0	0	0.1	0	0.43	0	23
	21	C-80-L/94-G-7	869.9	477	0.67	2.02	0.26	0.25	4.18	50	6
			873.4	466	0.48	0.69	0.18	0.41	1.63	43	11

TABLE 3. HYDROCARBON SOURCE ROCK EVALUATION PARAMETERS FOR ROCK-EVAL/TOC PYROLYSIS DATA (MODIFIED FROM PETERS, 1986). **(TABLE 3 (C) INCLUDES RANGES OF VITRINITE REFLECTANCE THAT ARE APPROXIMATELY EQUIVALENT TO ROCK-EVAL TMAX VALUES. VITRINITE REFLECTANCE DATA ARE NOT USED IN THIS STUDY)**

Petroleum Potential	Organic Matter		
	TOC	Rock-Eval Pyrolysis	
	(wt.%)	S1	S2
	0-0.5	0-0.5	0-2.5
	0.5-1	0.5-1	2.5-5
	1-2	1-2	5-10
	2-4	2-4	10-20
	>4	>4	>20

(A) Parameters for describing the petroleum potential of an immature source rock.

TABLE 3. HYDROCARBON SOURCE ROCK EVALUATION PARAMETERS (CONTINUED).

Kerogen Type	HI (mg HC/g TOC)	S2/S3
I	>600	>15
II	300-600	10-15
II/III	200-300	5-10
III	50-200	1-5
IV	<50	<1

(B) Parameters for describing kerogen type (quality) of an immature source rock.

Stage of Thermal Maturity for Oil	Maturation: Vitrinite Reflectance Ro (%)	Maturation: Rock-Eval Tmax (°C)
Immature	0.2-0.6	<435
Mature		
Early	0.6-0.65	435-445
Peak	0.65-0.9	445-450
Late	0.9-1.35	450-470
Postmature	>1.35	>470

(C) Parameters for describing the level of thermal maturation.

TABLE 4. SUMMARY OF ROCK-EVAL/TOC DATA FROM CORE SAMPLES (RAW DATA)

UNIT (number of samples)	DEPTH (m)	Tmax (°C) range	TOC (wt.%)	HI (mg HC/g TOC)	Kerogen Type	Source Rock Potential
WILRICH (10)	809.5-1196	428-442	1.08-4.28	138-393	Type III	Good to very good (gas only)
GORDONDALE (27)	1010.9-1429.1	438-484	0.66-10.45	26-273	Type II	Excellent (oil+gas)
PARDONET (7)	1050.4-1319.1	461-480	0.97-2.79	23-96	Type II	Fair to good (oil+gas)
BALDONNEL (5)	1065.1-1443.2	452-478	0.65-1.39	29-98	Type II	Poor to fair (oil+gas)
PHOSPHATE ZONE (12)	1051.3-1187.4	433-447	1.76-10.98	189-489	Type II	Excellent (oil+gas)
MONTNEY (13)	869.9-2133.1	431-500	0.51-4.18	43-450	Type II	Good to very good (oil+gas)

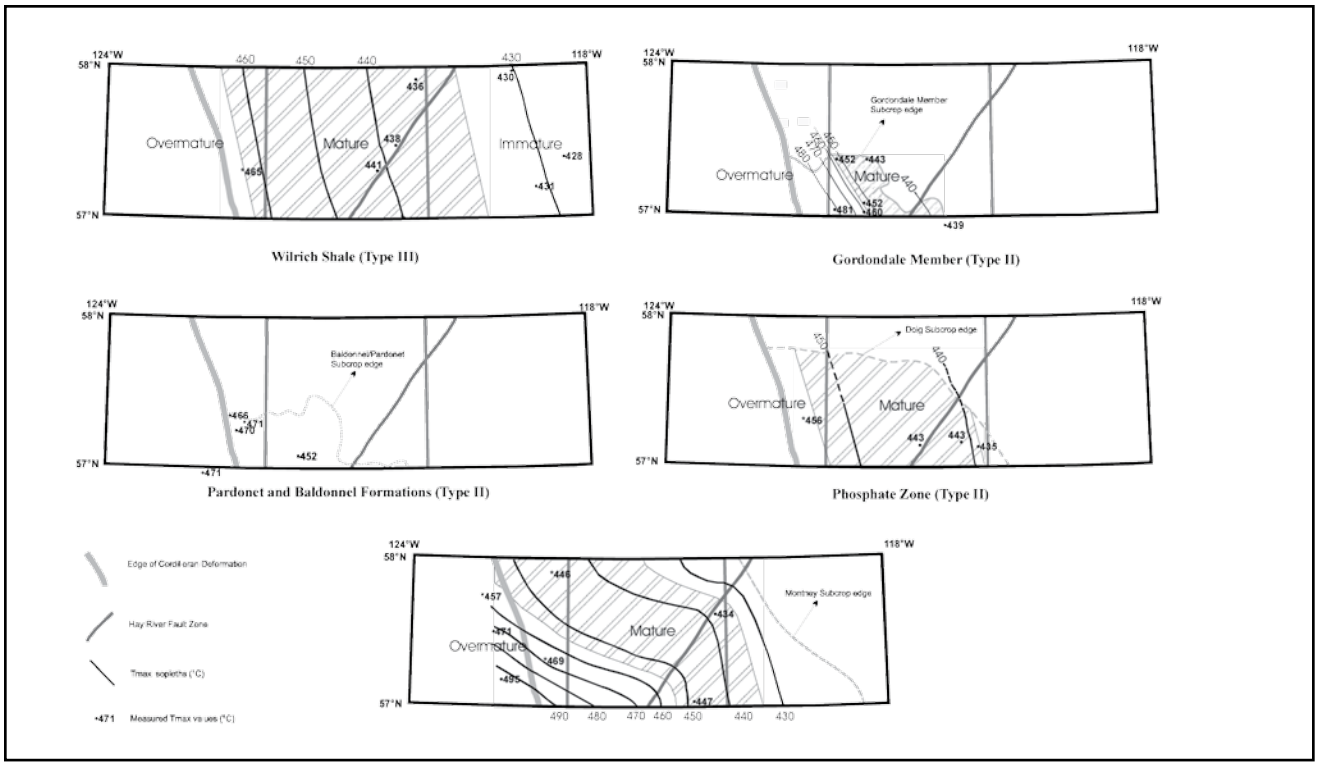

Figure 3. The thermal maturity distribution of each unit based on Rock-Eval Tmax values (ºC). * Tmax values from unpublished results (Dr. Larry Lane [GSC, Calgary], personal communication, 2003).

CONCLUSIONS

Six units of Early Triassic to Early Cretaceous age have been assessed for their hydrocarbon source potential in the study area. A total of 74 samples from 23 wells were analyzed by Rock-Eval 6/TOC pyrolysis.

The Montney Formation within the study area is thermally immature to overmature with increasing maturity from northeast to southwest. It contains Type II kerogen with TOC values up to 4.18 wt.%. This suggests that the Montney Formation may have generated significant amounts of hydrocarbons where it is mature in the BC part of the study area.

The highly radioactive "Phosphate Zone" at the base of the Doig Formation contains Type II kerogen with TOC values up to 10.98 wt.%. The maturity increases from east to west, and it is mature in the Beatton River map area (94H). The high TOC values suggest that this unit has excellent hydrocarbon source potential where mature.

The Baldonnel and Pardonet Formations are overmature in the west part of the study area where sampled. Both likely comprise Type II kerogen, although the high degree of maturity precludes a direct assessment of kerogen type. The Baldonnel Formation has TOC values up to 1.39 wt.%, suggesting that it had poor to fair initial source rock potential. The Pardonet Formation has TOC values up to 2.8 wt.%, which suggests that it had fair to good initial hydrocarbon generation potential when mature.

The Gordondale Member samples vary from peak mature to overmature. It contains Type II kerogen with TOC values up to 10.45 wt.%, suggesting that it is an excellent source rock where mature.

The Wilrich Shale contains Type III kerogen with TOC values up to 4.28 wt.%. Therefore, it has good to very good generation potential for gas. It is immature in the east part of the study area with increasing maturity to west.

The next step in this project is to apply one-dimensional basin modeling to understand the amount and timing of hydrocarbons generated from these units, which will then be correlated with the timing of trap formation and accumulation of the hydrocarbons in the study area.

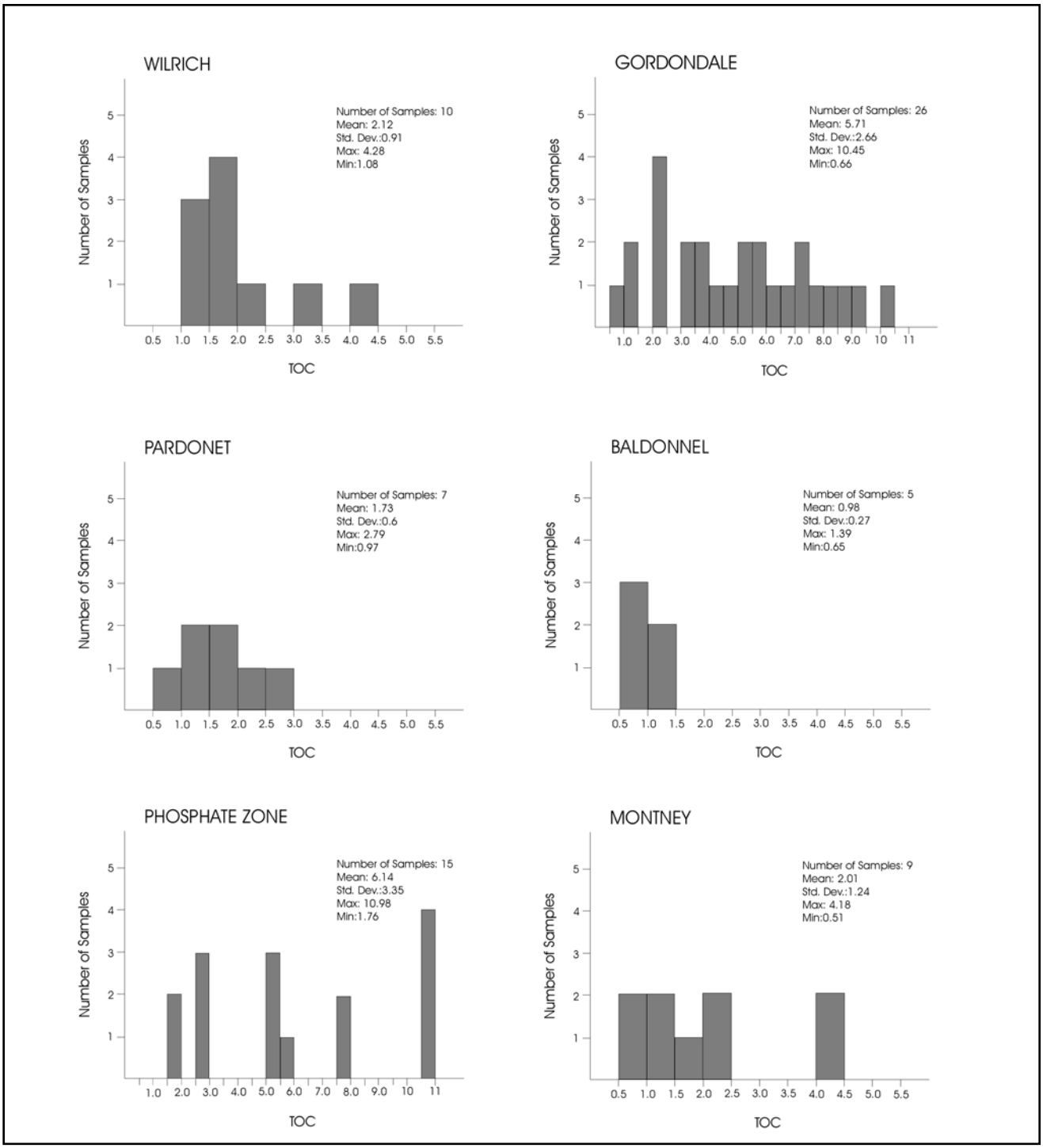

Figure 4. TOC histograms for the units with mean and standard deviation values. Note scale change for organically-richer units ("Phosphate Zone" and Gordondale Member).

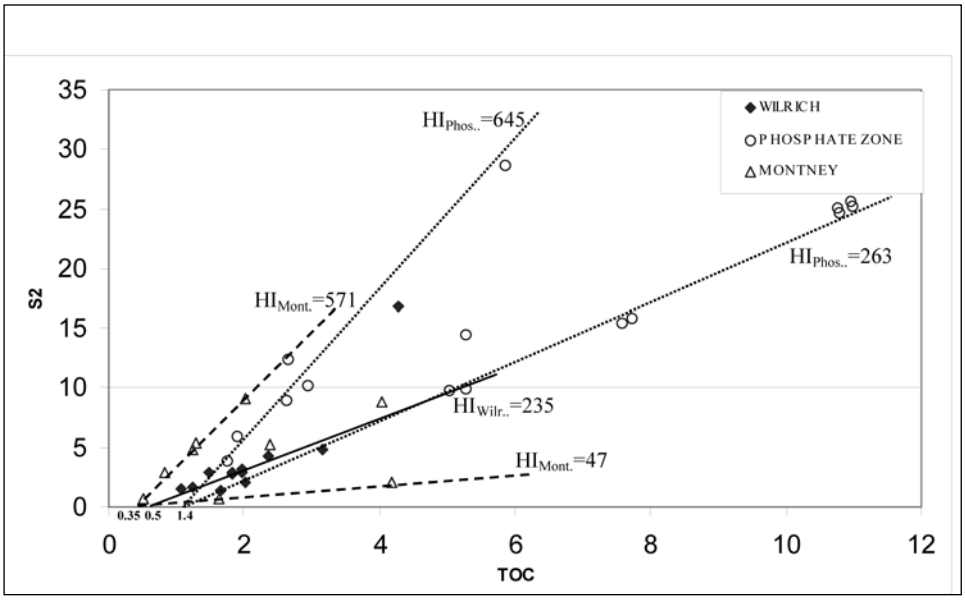

Figure 5. Rock-Eval pyrolysis S2 versus TOC, showing hydrogen index (HI) and inert carbon content of the units that have immature to early mature samples.

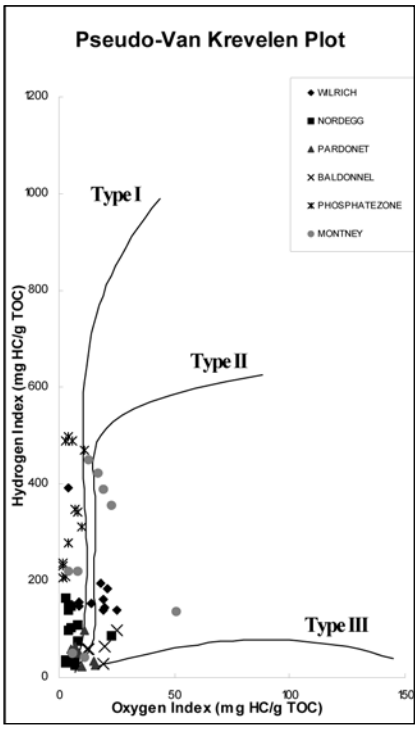

Figure 6. Pseudo-Van Krevelen diagram, showing Rock-Eval hydrogen index vs. oxygen index for the sampled units.

ACKNOWLEDGEMENTS

We wish to acknowledge Mark Hayes and Kevin Pederson of the BC Ministry of Energy and Mines and the BC Ministry of Energy and Mines Geology Facility-Core Lab in Charlie Lake for funding and logistical support for this project. Ross Stewart and the Organic Geochemistry Labs at GSC Calgary are gratefully acknowledged for providing the Rock-Eval VI/TOC pyrolysis data. Dr. Larry Lane is gratefully acknowledged for discussions of geology of the study area and access to his geochemical dataset.

REFERENCES

Asgar-Deen, M., 2003, Stratigraphy, Sedimentology and Paleogeography of the Lower Jurassic Nordegg Member (Gordondale Member), west-central Alberta, Canada. *Unpublished M.Sc. Thesis, Department of Geology and Geophysics, University of Calgary*, 206 pages.

Asgar-Deen, M., Hall, R., and Riediger, C.L., In press. The Gordondale Member: designation of a new member in the Fernie Formation to replace the informal "Nordegg Member" nomenclature of the subsurface of west-central Alberta. *Canadian Bulletin of Petroleum Geology.*

Bordenave, M.L., Espitalié, J., LePlat, P., Oudin, J.L., and Vandenbroucke, M., 1993. Screening techniques for source rock evaluation. Chapter II.2. In: *Applied Petroleum Geochemistry*. M.L. Bordenave (ed.). Éditions Technip, pages 217-278.Carrelli, G.G., 2002, Geology and source rock potential of the upper Triassic Baldonnel and Pardonet formations, northeastern British Columbia. *Unpublished MSc. Thesis, University of Calgary*, 2002, 335 pages. Cornford, C., Gardner, P., and Burgess, C, 1998, Geochemical truths in large data sets. I: Geochemical screening data. *Organic Geochemistry*, v.29, no.1-3, pages 519-530.

Creaney, S., and Allan, J., 1990, Hydrocarbon generation and migration in the Western Canada Sedimentary Basin. In: Classic Petroleum Provinces. J.Brooks (ed.) *Geological Society Special Publication*, No.50, pages 189-202.

Creaney, S., and Allan, J, 1992, Petroleum systems in the Foreland Basin of Western Canada. In: Foreland Basins and Foldbelts. R.W. Macqueen and D.A. Leckie (ed.). *American Association of Petroleum Geologists*, Memoir 55, pages 279-306.

Creaney, S., Allan, J., Cole, K., Brooks, P.W., Fowler, M.G., Osadetz, K.G., Snowdon, L.R., and Riediger C.L., 1994, Petroleum generation and migration in the Western Canada Sedimentary Basin. In: Geological Atlas of Western Canada Sedimentary Basin. G.D. Mossop and I. Shetsen (comps.), Calgary*, Canadian Society of Petroleum Geologists and Alberta Research Council*, pages 455-468.

Edwards, D.E., Barclay, J.E., Gibson, D.W., Kvill, G.E., Halton, E., 1994, Triassic strata of the Western Canada Sedimentary Basin. In: Geological Atlas of Western Canada Sedimentary Basin. G.D. Mossop and I. Shetsen (comps.), Calgary, *Canadian Society of Petroleum Geologists and Alberta Research Council*, pages 259-276.

Espitalié, J., Laporte, J.L., Madec, M., Marquis, F., Leplat, P., Paulet, J., and Boutefeu, A., 1977, Méthode rapide de caractérisation des roches de méres de leur potentiel pétrolier et de leur degré d'évolution. *Institut Francais Pétrolier Revue*, v.32, pages 23-42.

Faraj, B., 2003, Shale gas potential of selected formations from the WCSB of Western Canada. In: *5th Annual Unconventional Gas and Coalbed Methane Conference Proceedings*, 2003, Calgary.

Handerson, C.M., Richards, B.C., Barclay, J.E., 1994, Permian strata of the Western Canada Sedimentary Basin. In: Geological Atlas of Western Canada Sedimentary Basin. G.D. Mossop and I. Shetsen (comps.), Calgary, *Canadian Society of Petroleum Geologists and Alberta Research Council*, pages 251-258.

Hankel R., 2001, Source rock and oil geochemistry and conodont biostratigraphy of the Triassic Lower Montney Formation in the Peace River Arch area, west-central Alberta. *Unpublished MSc. Thesis, University of Calgary*, 2001, 61 pages. Fennell, J.W., 1994, Cretaceous Mannville Group of the Western Canada Sedimentary Basin. In: Geological Atlas of Western Canada Sedimentary Basin. G.D. Mossop and I. Shetsen (comps.), Calgary, Canadian Society of Petroleum *Society of Petroleum Geologists and Alberta Research Council*, pages 317-334.

Hayes, B.J.R., Cristopher, J.E., Rosenthal, L., Los, G., McKercher, B., Minken, D.F., Tremblay, Y.M., Ibrahimbas, A., (Unpublished data), Hydrocarbon source rock potential of the Wilrich Shale. *Unpublished data for the 701 Course Project, University of Calgary*, 2003, 50 pages.

Mossop G.D., and Shetsen, I., (compilers), 1994. Geological Atlas of Western Canada Sedimentary Basin. Calgary, *Canadian Society of Petroleum Geologists and Alberta Research Council*, 510 pages.

Peters, K.E., and Cassa, M.R., 1994, Applied Source Rock Geochemistry. In: The petroleum system- from source to trap; L.B. Magoon and W.G. Dow (ed.). *American Association of Petroleum Geologists*, Memoir 60, pages 93-117.

Peters, K.E., 1986, Guidelines for evaluating petroleum source rocks using programmed pyrolysis. *American Association of Petroleum Geologists Bulletin*, v.70, pages 318-329.

Poulton, T.P., Christopher, J.E., Hayes, B.J.R., Losert, J., Tittemore, J., Gilchrist, R.D., 1994, Jurassic and Lowermost Cretaceous strata of the Western Canada Sedimentary Basin. In: Geological Atlas of Western Canada Sedimentary Basin. G.D. Mossop and I. Shetsen (comps.), Calgary, *Canadian Society of Petroleum Geologists and Alberta Research Council*, pages 297-316.

Richards, B.C., Barclay, J.E., Bryan, D., Hartling, A., Henderson, C.M., Hinds, R.C., 1994, Carboniferous strata of the Western Canada Sedimentary Basin. In: Geological Atlas of Western Canada Sedimentary Basin. G.D. Mossop and I. Shetsen (comps.), Calgary, *Canadian Society of Petroleum Geologists and Alberta Research Council*, pages 221-250.

Riediger, C.L., 1997, Geochemistry of potential hydrocarbon source rocks of Triassic age in the Rocks Mountain Foothills of northeastern British Columbia and west-central Alberta. *Bulletin of Canadian Petroleum Geology*, v.45(4), pages 719-741.

Riediger, C.L., Fowler, M.G., Brooks, P.W., and Snowdon, L.R., 1990a, Triassic oils and potential Mesozoic source rocks, Peace River Arch area, Western Canada Basin. *Organic Geochemistry*, v.16, pages 295-305.

Riediger, C.L., Fowler, M.G., Snowdon, L.R., Goodarzi, F., and Brooks, P.W., 1990b, Source rock analysis of the Lower Jurassic "Nordegg Member" and oil-source rock correlations, northwestern Alberta and northeastern British Columbia. *Bulletin of Canadian Petroleum Geology*, v.38A, pages 236-249.

Snowdon, L.R., Fowler, M.G., and Riediger, C.L., 1998. Interpretation of organic geochemical data. *CSPG Short Course Notes*, November 5-6, 1998, Calgary, Alberta.

QUATERNARY GEOLOGY AND AGGREGATE POTENTIAL OF THE FORT NELSON AIRPORT AREA

T. Johnsen[1], T. Ferbey[1], V. M. Levson[1] and B. Kerr[1]

KEYWORDS: Surficial geology, aggregate, Sierra-Yoyo-Desan Road, Clarke Lake Bypass, Fort Nelson

INTRODUCTION

A key component of the British Columbia Oil and Gas Development Strategy (OGDS) is a comprehensive road infrastructure plan aimed at promoting better access to resources through improved infrastructure. The completion of road infrastructure improvements, such as the upgrade of Sierra-Yoyo-Desan (SYD) Resource Road and construction of Clarke Lake Bypass Road in the Fort Nelson area, northeast British Columbia (Fig. 1), are expected to promote longer drilling seasons, accelerate exploration and production programs, and increase industry and provincial government revenues. It has been estimated that 2 000 000 m^3 of aggregate material are needed for this initial road infrastructure improvement program. A study was conducted to evaluate existing local sources of aggregate material along SYD Road that could be used for this project (Thurber, 2000), and it was determined that existing aggregate reserves were largely depleted.

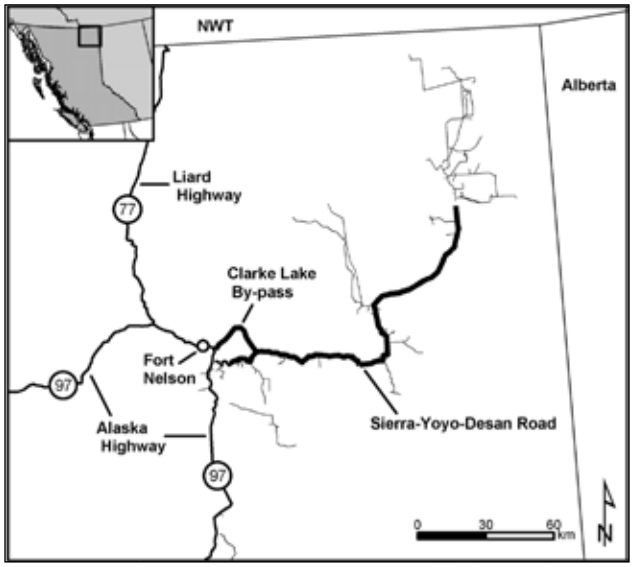

Figure 1: Location of Fort Nelson and major roadways in northeast British Columbia

To meet the aggregate needs for this initial improvement project and future resource and lease-road construction, a surficial mapping program was initiated to systematically explore for new, local aggregate sources in northeast British Columbia (see Levson *et al.*, this volume). Initial test-pit programs were conducted in spring 2003, with follow-up work and reconnaissance-scale fieldwork and preliminary aerial photograph mapping conducted during summer 2003. To date, four main aggregate resources have been identified within the SYD Road corridor, with a total resource of approximately 5 000 000 m^3 of granular material. This effort has also identified numerous other areas that are believed to have potential to host granular deposits but that require further work to sufficiently evaluate.

One such area is within the Fort Nelson airport area, approximately 8 km northeast of the Fort Nelson town site (Figs. 2, 3). This area is of particular interest due to its proximity to the Clarke Lake Bypass Road right-of-way. This report summarizes findings from detailed surficial mapping and test pitting conducted within Fort Nelson airport area.

PROJECT BACKGROUND

SYD Road is a high-grade, all-weather road located east of Fort Nelson and accessed from mile 293 of Alaska Highway. It extends 180 km to the east and northeast ending at the North Helmet airstrip in the Helmet District (Fig. 1). During the majority of summer and a good portion of winter, this resource road supports drilling, well tie-in, wellhead servicing, and well production activities in the area. As such, this road can experience high volumes of heavy oil-field service traffic, which has been increasing due to increased oil and gas exploration and production activities in the area. The volume of traffic on the SYD Road is greater than on the Alaska Highway. Current plans include upgrading and widening of the SYD Road to meet increased demands of this critical resource road. SYD Road provides access to resources that generate $200 to $300 million per year in direct revenue to the province.

As part of this infrastructure improvement project, a new 21 km road is to be constructed from Fort Nelson to the SYD, including a new two-lane bridge crossing of the Fort Nelson River—the Clarke Lake Bypass (Fig. 1). This will eliminate the need to use the narrow BC Rail train bridge and a set of switchbacks. This transportation project will improve safety and access, reduce travel time, and reduce maintenance costs of the road and of vehicles using the road.

[1]*British Columbia Ministry of Energy and Mines*

Finding aggregate deposits that are local can generate great savings. Aggregates account for 30% to 50% of road construction and maintenance costs in northeast BC. As well, costs of transportating aggregate can be prohibitive. For example, for the SYD project, rail transportation costs of aggregate from Fort St. John to Fort Nelson and truck transportation costs from Fort Nelson to the SYD are approximately $\$85/m^3$. Two million cubic metres of aggregate is needed for the 180 km SYD Road upgrade, totalling $170 million. If transportation costs were lowered by just $\$1/m^3$, a savings of $2 million could be generated. It is expected that if local sources of aggregate were found, total aggregate costs could be reduced significantly. Therefore to help minimize road construction costs, Quaternary geology and aggregate potential mapping was completed close to the Clarke Lake Bypass in the Fort Nelson airport area.

STUDY AREA

The study area includes part of the Fort Nelson airport area and is comprised of the area south and east of the main runway, down to the floodplain of Fort Nelson River below (Fig. 3). The study area is located within the Fort Nelson Lowland physiographic region, a flat to very gently rolling area with very little relief (Holland 1976).

The Fort Nelson airport area can be locally divided into three physiographic units: plain, valley side, and valley bottom (inset, Fig. 3). Fort Nelson airport is situated on a near-level plain above Muskwa Valley. This plain continues north and west but has been incised by McConachie Creek, which flows east into Fort Nelson River just north of airport property. This plain is moderately well drained, typically supporting stands of white spruce (*Picea glauca*) and rare lodgepole pine (*Pinus contorta* var. *latifolia*), but does have areas where black spruce (*Picea mariana*) bogs dominate. Closer to the valley sides, trembling aspen (*Populus tremuloides)* is common. Valley sides are steep and terraced; terrace flats are typically 25 to 150 m wide and up to 1000 m long. Terrace flats and risers support white spruce and trembling aspen stands almost exclusively and typically are well drained. The valley bottom setting is flat and moderately to poorly drained. Trembling aspen and balsam poplar (*Populus balsamifera ssp. balsamifera*) stands are more common here, with large blocks having been logged in recent years.

The Fort Nelson airport has had a long and complex land-use history. During the early 1940s it served as a base for the United States Army and Air Force for various staging and training exercises. As a result, much of the area, although now grown over with trees and vegetation, has been disturbed. Evidence of disturbance includes overgrown roads, building foundations, and excavations. These disturbances have made interpretation of aerial photographs and field observations challenging.

BEDROCK GEOLOGY

The Fort Nelson area is underlain by gently dipping marine shales and siltstones of the Lower Cretaceous Buckinghorse Formation of the Fort St. John Group (Okulitch *et al.*, 2002; Thompson, 1977). This formation has a minor component of sandstone. There are no bedrock exposures within the study area. Buckinghorse Formation rocks can however be seen in steep cutbanks south of the Fort Nelson airport area along Fort Nelson River.

Grading laterally and vertically from these rocks are coarser-grained sandstones and siltstones of the Lower Cretaceous Sikanni Formation. To the north of Fort Nelson and northwest of the Fort Nelson airport, Sikanni Formation rocks form a topographic high. Exposures of these rocks are common in road cuts north of town and in areas cleared for agricultural purposes. A similar topographic high is seen east of the airport property, across Fort Nelson River. In both cases these prominent topographic features rise approximately 150 m above the surrounding area.

This sequence of rocks is interpreted to be a transgressive/regressive cycle from marine shales into alluvial-deltaic sandstones, mudstones, conglomerates, and coal. This cycle is repeated three times in the stratigraphy and is attributed to orogenic activity within the Columbian Orogen (Stott, 1975; Thompson, 1977).

QUATERNARY HISTORY AND LANDFORMS

The last ice sheets to have covered northeastern British Columbia and adjacent Alberta have left a record of their presence in the existing landforms and surficial deposits: streamlined forms, meltwater channels, erratics and drift sheets, and traces of former ice-dammed lakes (Mathews 1980). Many of these landforms have been unmodified since the close of the Late Wisconsinan glaciation.

During deglaciation, 13 500 to 10 000 years before present, the Laurentide Ice Sheet retreated generally to the northeast (Mathews 1980). A series of ice-dammed and topographically dammed glacial lakes and meltwater channels developed. Within the Fort Nelson area, a number of meltwater channels and likely recessional moraines that have been mapped as part of this project record the retreat of the Laurentide Ice Sheet (Fig. 2). Moraines are arcuate-shaped in plan view, with northwest-southeast to north-south orientations and with their concave sides facing northeast to east. The recessional moraines are associated with a number of meltwater channels. A moderate-sized meltwater channel now occupied by Jackfish Creek (approximately 25 km south of Fort Nelson) occurs on the north-northeast edge of a topographic high (Fig. 2). Presumably the position of this meltwater channel was related to the presence of ice to

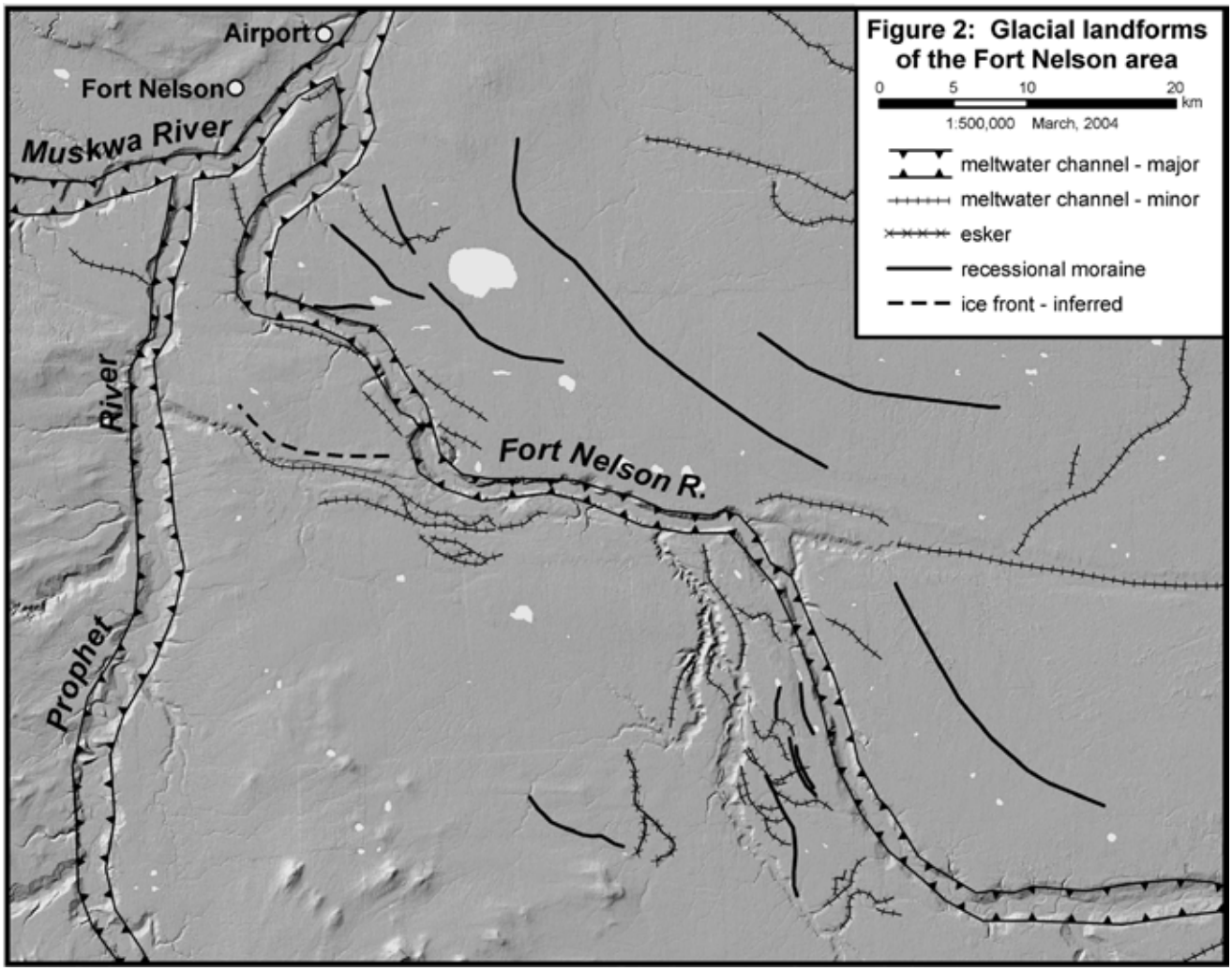

the north-northeast (mapped as an inferred ice front, Fig. 2), otherwise the channel would have developed at a lower elevation. Taken together these observations confirm the general northeast retreat of the Laurentide Ice Sheet within the Fort Nelson area and the importance of this pattern of retreat to the development of meltwater channels, some of which are being mined for aggregate.

The Fort Nelson airport area is located at the confluence of two major meltwater channels (each approximately 2 km wide and approximately 90 m deep) now occupied by the Muskwa and Fort Nelson Rivers (Mathews 1980; Fig. 2). These rivers are smaller in width and much more sinuous than the valleys they occupy. These channels once carried much larger volumes of water and sediment during deglaciation. These conditions led to the transport and deposition of gravel during deglaciation; consequently, there should be aggregate deposits associated with these meltwater systems, particularly at higher elevations within the valleys and on the adjacent plain. Aggregate deposits and landforms on the plain may also be associated with earlier stages of glaciation, when sediments were transported and deposited underneath (subglacial), within (englacial), or atop (supraglacial) former ice sheets. Shallow boreholes that were completed as part of an environmental baseline study for the Fort Nelson airport property indicate that drift thickness can be greater 7 m thick (Transport Canada 1998).

METHODS

Results from a previously conducted reconnaissance test-pit program by Atco Airports Ltd. indicated the occurrence of granular material on Fort Nelson airport property. This information stimulated interest in this area as a host to aggregate deposits. To further assess the area's potential to host such a deposit, British Columbia Ministry of Energy and Mines (MEM) personnel carried out detailed aerial photograph and field surveys.

MEM personnel made observations at 46 field stations, using hand augers and shovels. In areas of tree blowdown, natural exposures in tree-root wads were also utilized to determine subsurface sediment types. To characterize the study area and subsurface sediments, various data were collected: topographic position; dominant tree, shrub, and herb species; exposure height; unit thickness; and sediment texture, structure, and paleoflow. Black and white 1:10 000 and 1:40 000 scale aerial photographs were used throughout the various stages of this study.

Other data collected and compiled for this study included test-pit logs from the original test-pit program conducted by Atco Airports Ltd., subsurface borehole logs (Transport Canada 1998), and test-pit results from an investigation of Clarke Lake Bypass Road right-of-way (Thurber Engineering, unpublished). Following the methodology of Howes and Kenk (1997), detailed surficial geology mapping was completed using these data and 1:10 000 scale black and white aerial photographs.

A test-pitting program was initiated in December 2003 to assess the aggregate potential of the area. Using a Kobelco 220LC tracked excavator, 2 to 5 metre deep pits were excavated at 18 sites on Fort Nelson airport property. At each pit, sediments were described in detail and classified using both the Wentworth scale and the Modified Unified System of Soil Classification. Granular material was sampled from select sites for various laboratory analyses. Following procedures set by Cunningham (1990), sieve analyses, degradation tests (susceptibility of aggregates to mechanical breakdown), and sand equivalent tests (presence or absence of plastic fines) were completed on these samples.

RESULTS AND INTERPRETATION

Surficial geology

The results of surficial geology mapping are shown in Figure 3. Figure 4 summarizes test-pit log data and is classified as indicating either granular or non-granular material. Granular material of less than 1 metre thickness is mapped as non-granular. Granular sediments have grain sizes greater than and including fine sand (greater than 125 μm diameter, Wentworth scale).

The reader is referred to Howes and Kenk (1997) for detailed explanation of surficial geology map labels (Fig. 3). Due to the scale of mapping and the limited data, considerable variation in sediments may occur that is not reflected in the mapping. More confidence in interpretation is given to those polygons containing field data.

Four main types of deposits are found: fluvial (F), glaciofluvial (F^G), organic (O) and morainal (M). Secondary types include colluvium (C) and anthropogenic (A) deposits. Given the long land use history of the study area, many additional areas could be labelled as anthropogenic.

The valley-bottom physiographic area (inset, Fig. 3) includes active fluvial plains that contain flood channels, levees, and scroll bars. The Muskwa River is boxed between valley walls, causing the meander loops to appear boxed-shaped rather than gently looped-shaped in plan view. The area was visited during high water, when dramatic rates of bank erosion were observed. Surface sediments within the fluvial plain are dominantly silt and sand. The Muskwa River is transporting and depositing gravel today and likely did so in the past. Thus, gravel deposited from previous paths of the Muskwa River channel generally occurs beneath these finer-grained deposits. Buried gravels were locally observed along the modern cut banks of the Muskwa River.

The valley-side physiographic area (inset, Fig. 3) includes abandoned river terrace flats and terrace risers of the Muskwa River. These landforms were created during Muskwa River incision. The slopes of terrace risers vary considerably. Terrace flats vary in width from approximately 25 to 150 m. Gravel was observed at the bases of blown-down trees in the southwestern-most terrace flat, which indicates that when the Muskwa River was at this elevation it was transporting gravel. Elsewhere on the same terrace flat, two small swamps (Op) were observed in aerial photographs, suggesting that the sediments immediately underlying these swamps are fine-grained. It is unknown whether these fine-grained sediments are underlain by coarse-grained sediments. Fluvial terraces in the middle and northwest portion of the study area that are at a somewhat similar elevation may contain gravel and/or sand.

The terrace that is crossed by the Clarke Lake Bypass is composed of very fine-grained surficial sediments, likely overbank fines from the ancient Muskwa River. Swamps (Op) on this terrace further suggest that most of the feature is surfaced by fine-grained sediments. The slope above this terrace flat is composed dominantly of morainal material (till). Some of this material appears to have been reworked by mass wasting processes.

The plain physiographic area is an area of very low relief and contains glaciofluvial (F^G), organic (O), till (M), and anthropogenic (A) sediments. Deposits of glaciofluvial sediments are discontinuous and occur as elongate deposits rather than as continuous sheets. Portions of these deposits also have gentle elongate hill morphology, with hill crests aligned southwest-northeast. These observations suggest that these sediments were deposited by water flowing in conduits within glacial ice.

Glaciofluvial deposits are surrounded by organic sediments (bogs). Presumably these organic deposits are under-

Figure 3: Quaternary Geology, Fort Nelson Airport area
0 250 500 1,000 m
Projection: Albers Equal Area Conic (NAD83)
March 2004
Generalized Surficial Material
Organic
Fluvial
Glaciofluvial
Morainal (Till)
Anthropogenic
Roads
Streams
Fort Nelson River
Clarke Lake By-pass
Fort Nelson Airport
Nelson Main Line
Airport Drive
Muskwa River
zsFtm/zsMtm
Fta
szFp
gA'
Op
cdFtj
Ft
dM
Mj/dC'jh
cdFt
czFts-F
czFt
M-V
gsFt
Ftj
szFts-F
sgFtj
F-V
gFt
gF-V
F°
F° /A'
Hillshade map of area and local physiographic units
1 km
area of detail
Plain
Valley side
Valley bottom
N

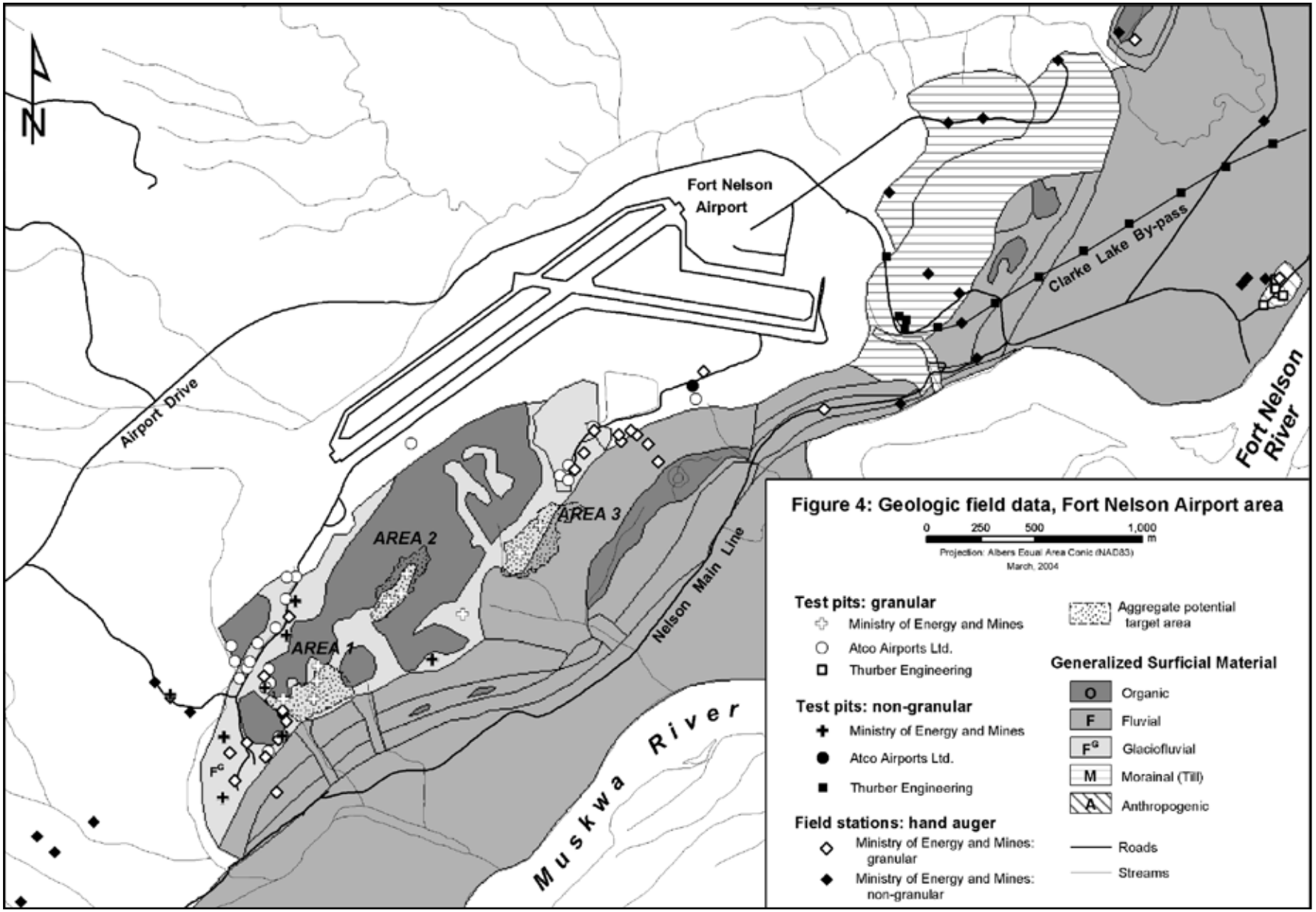
N
Fort Nelson Airport
Clarke Lake By-pass
Airport Drive
Fort Nelson River
AREA 1
AREA 2
AREA 3
Nelson Main Line
Muskwa River
Figure 4: Geologic field data, Fort Nelson Airport area
0 250 500 1,000 m
Projection: Albers Equal Area Conic (NAD83)
March, 2004
Test pits: granular
Ministry of Energy and Mines
Atco Airports Ltd.
Thurber Engineering
Test pits: non-granular
Ministry of Energy and Mines
Atco Airports Ltd.
Thurber Engineering
Field stations: hand auger
Ministry of Energy and Mines: granular
Ministry of Energy and Mines: non-granular
Aggregate potential target area
Generalized Surficial Material
O Organic
F Fluvial
F^G Glaciofluvial
M Morainal (Till)
A Anthropogenic
Roads
Streams

lain by till or thin beds of sand and gravel overlying till. Till is at the surface in the northeast portion of the study area; it is relatively clast rich and massive, with a silty clay matrix. Elsewhere till was observed to underlie glaciofluvial sediments (MEM test pits 3, 5, 8, 9, 11, 13, 15, 23, 53, 56, 57). Anthropogenic deposits are more common than indicated in Figures 3 and 4. Deposits of this type include piles of overburden, granular material, and buried garbage.

DISCUSSION ON GRANULAR DEPOSITS

Test pits were concentrated in the plain physiographic area because this area (i) has known gravel deposits and (ii) has numerous roads that provide relatively easy access for an excavator.

A total of 18 test pits were completed over 3 days (Fig. 4, Table 1). Seven samples were collected for analysis: gradation, degradation, and sand equivalent tests (Cunningham 1990). Based on test-pit data and lab analyses, three areas have been identified that may be of interest for mining granular material: Area 1 includes MEM test pits 11 and 12; Area 2 includes MEM test pits 20, 54 and 56; and Area 3 includes test pits 32 and 57 (Fig. 4).

Area 1

Test pits 11 and 12 in Area 1 lie above and northeast of an old pit face approximately 3 m high and 100 m long with a southeast aspect. Adjacent and southeast of this old pit face is evidence of an old clearing that was likely the site of previous aggregate mining. Area 1 had thicknesses of 2.6 m, more than 2.1 m, and 0.5 m of horizontally stratified gravel in test pits 11, 12, and 53, respectively (Table 1).

Results from degradation and sand equivalent tests indicate that material from test pit 11 meets Ministry of Transportation (MOT) specifications for all granular materials. Based on 4 gradation curves, the granular material in Area 1 is best suited for use as select granular sub-base (SGSB; Ministry of Transportation 2000). Due to disturbances related to land use history, it is difficult to estimate the volume of granular material in Area 1 (Fig. 4).

Area 2

This area is an elongate ridge of approximately 2 m relief, trending southwest-northeast and including test pits 20, 54, and 56. Test pit 20 contained more than 4.4 m of cross-bedded sandy gravel, test pit 54 contained 2.0 m of sandy gravel overlying 0.5 m sand and silt, and test pit 56 contained 1.3 m of sandy, pebbly gravel overlying till (Table 1). This landform is possibly an esker as (i) it has an elongate, hill morphology, (ii) it is composed of granular material, some of which is cross-bedded (approximately 30° dip), and (iii) it is located on the plain. Alternatively the ridge could be a fluvial bar related to high-elevation deposition from the Muskwa River during deglaciation. A number of pine trees, indicating a relatively dry site, occur at test pit 20. This is also the pit with the thickest gravels in the study area. The water table was not encountered.

Results from degradation and sand equivalent tests indicate that gravel from test pit 11 meets MOT specifications for all granular materials and appears best suited for use as SGSB. This classification is based on only two gradation curves, not the mean of four as required by provincial government standard (Ministry of Transportation 2000). Fracture count data (i.e., the number of fractured or naturally occurring angular clasts in specific grain-size fractions) is not required for classifying SGSB material as this material can be produced by direct excavation (i.e., pit-run). However, other MOT granular material classifications, such as high-fines granular surfacing aggregate (HFGSA) or 25 mm well-graded coarse base aggregate (WGCBA), require minimum 50% fracture count after processing. Fracture count tests were not conducted on Area 2 samples; it is therefore not known whether Area 2 sediments would meet the minimum fracture count requirement for these other granular material classifications.

A preliminary granular material volume estimate of 20 000 m^3 has been calculated. This volume was derived using the average thickness of gravels in the three test pits (2.3 m) and a conservative area estimate.

Area 3

Test pits 32 and 57 are located on a broad elongate ridge trending southwest-northeast. Sediments in test pit 32 and 57 are composed of more than 4.6 m and 2.0 m of cross-bedded fine sand, respectively (Table 1). As there was no gravel in these pits, degradation and sand equivalent tests were not completed. Based on one gradation curve, the granular material in Area 3 is not suitable for SGSB. Further testing and additional gradation results may therefore prove Area 3 sediments appropriate for use as SGSB material.

A highly preliminary granular material volume estimate of 50 000 m^3 has been calculated using a conservative area estimate and the average thickness (3.3 m) of granular material in two test pits.

EVALUATION OF MAPPING

Based on test-pit information, only minor changes were required to the surficial geology mapping. Many locations in the plain physiographic area were disturbed, indicating that anthropogenic activity was more common than

TABLE 1. SUMMARY OF MINISTRY OF ENERGY AND MINES TEST PIT DATA

Test Pit #	Depth (m)	Granular material (m) [1]	Description of granular material [2]	Overburden thickness (m)	Water table depth (m)	Sample collected
1	4.0	none	n/a	n/a	none	
3	4.0	0.3-0.8	sandy silty gravel (CL-GM)	0.3 soil	none	
5	3.5	0.6-1.6	pebble cobble gravel (GP)	0.6 soil and fine sand	none	
8	2.0	0-0.5	sandy gravel (GW)	none	none	
9	3.4	1-3.4	0.5 m silty sandy gravel (GP) underlain by 0.8 m pebble gravel (GP)	1.0 road fill and organics	2.3	yes
10	2.5	none	n/a	n/a	none	
11	3.0	0.2-2.8	pebbly cobble gravel (GM)	0.2 soil	2.5	yes
12	2.5	0.4->2.5	sandy gravel (GM)	0.4 soil	2.5	yes
13	2.0	0.5-1.0	silty sandy gravel (GM)	0.5 soil	none	
15	2.5	0.5-1	sandy gravel (GM)	0.5 soil	none	
20	4.5	0.1->4.5	sandy gravel (GM)	0.1 soil	~3.5	yes
23	2.8	0.2-4.5	silty fine sand (SM)	0.2 soil	none	
32	4.8	0.2->4.8	fine sand (SW)	0.2 soil	none	yes
53	2.8	1.8-2.3	silty sandy gravel (GM)	1.8 silt	2.3	yes
54	2.8	0.2-2.2	sandy gravel (GM)	0.2 soil	1.8	
55	2.0	0.4->2.0	gravelly coarse sand (SP)	0.4 soil	1.5	
56	2.0	0-1.3	sandy pebble gravel (GP)	none	none	yes
57	2.5	0.3-2.3	fine sand (SP-GM)	0.3 soil	none	

[1] Depth range

[2] Description after Wentworth grain size classification. Codes in brackets follow the Modified Unified Soil Classification System

is indicated in Figures 3 and 4. Historical activity included aggregate mining, as indicated above.

CONCLUSIONS

The Fort Nelson airport area is host to sediments deposited during and following the last glaciation. These sediments are of morainal, glaciofluvial, fluvial, organic, and anthropogenic origin. Reconnaissance test-pit results suggest that three areas on the Fort Nelson airport property have potential to host aggregate deposits. Detailed air photograph mapping, ground surveys, and a high density test-pit program are required to further assess the quality and volume of granular material present in these areas. As well, there may be other areas within the Fort Nelson airport area that warrant further aggregate potential investigations; for example, the area north of Area 3 and fluvial terrace flats on the valley side.

ACKNOWLEDGEMENTS

We gratefully acknowledge Northern Rockies Regional District and Atco Airports Ltd. for granting access and permission to conduct the test-pit program on the Fort Nelson airport property. Jim Ogilvie of Atco Airports Ltd. generously shared his knowledge of aggregate sightings and test-pit data. Field data was collected with the support of Sheila Jonnes, Jacqueline Blackwell, and Don McClenagan

REFERENCES

Cunningham, D., Editor. 1990. Manual of test procedures, soils and mineral aggregates. British Columbia Ministry of Transportation and Highways.

Howes, D.E. and Kenk, E. 1997. Terrain classification system for British Columbia (version 2): a system for the classification of surficial materials, landforms and geological processes of British Columbia. Ministry of Environment, Lands and Parks, Province of British Columbia, 101 p.

Holland, S.S. 1976. Landforms of British Columbia, a physiographic outline. Bulletin 48. British Columbia Department of Mines and Petroleum Resources. 138 p.

Mathews, W.H. 1980. Retreat of the last ice sheets in northeastern British Columbia and adjacent Alberta. Geological Survey, Bulletin 331. Geological Survey of Canada. 22 p.

Ministry of Transportation. 2000. Section 202 – granular surfacing, base and sub-bases, *In* Standard Specifications for Highway Construction, Volume 1, 586 p.

Stott, D.F. 1975. The Cretaceous system in northeastern British Columbia, *In* Caldwell, W.G.E. (ed.) The Cretaceous system in the Western Interior of North America – selected aspects. Geological Association of Canada, Special Paper 13: 441-467.

Thompson, R.I. 1977. Geology of Beatton River, Fontas River and Petitot River map-areas, northeastern British Columbia. Geological Survey of Canada, Paper 75-11, 8 p.

Transport Canada. 1998. Fort Nelson airport environmental baseline study: Volume 2. Completed by Beatty Franz and Associated Ltd.

QUATERNARY GEOLOGY AND AGGREGATE MAPPING IN NORTHEAST BRITISH COLUMBIA: APPLICATIONS FOR OIL AND GAS EXPLORATION AND DEVELOPMENT

By Victor M. Levson[1], Travis Ferbey[1], Ben Kerr[1], Timothy Johnsen[1], Jan Bednarski[2], Rod Smith[2], Jacqueline Blackwell[1] and Sheila Jonnes[1]

KEYWORDS: Quaternary geology, aggregate potential, shallow gas, Quaternary gas, diamonds, Northeast British Columbia

INTRODUCTION

Rapidly expanding oil and gas development in northeast British Columbia has resulted in a dramatic increase in the need for new geoscientific data in the region. In the field of Quaternary geology, there are two main applications of these data: 1) the identification of aggregate resources for petroleum development roads, and 2) the provision of a stratigraphic framework for the "Quaternary gas" exploration play. A third application of Quaternary geology studies in the region relates to the evaluation of diamond potential. This latter component was included in this study because of the increasingly important significance of diamonds in the mineral exploration sector in northern Canada and because of the associated potential for development of new economic activity in the region.

Quaternary geology studies were initiated in northeasternmost British Columbia (Figure 1) by the Ministry of Energy and Mines in 2002, primarily in response to the critical need for aggregate (sand and gravel) in the region. Access roads to new and rapidly developing gas fields require substantial volumes of aggregate for road construction, improvement, and maintenance. Current infrastructure developments in the region include a major upgrade of the Sierra-Yoyo-Desan (SYD) Road, the construction of a bypass route to the Clarke Lake Road, and a number of new petroleum development road proposals. The Quaternary geology mapping program is also intended to support future exploration and development within northeast British Columbia, including construction of the proposed Northern Link Road (between SYD and Rainbow Lake, Alberta, Figure 1).

Objectives

The main objectives of this study are to

- conduct regional geological inventories of aggregate resources in the vicinity of existing and planned resource roads in northeast British Columbia;
- conduct site-specific investigations to define sand and gravel reserves along the SYD Road, the Clarke Lake Bypass, and new petroleum development roads;
- investigate the natural gas reservoir potential of Quaternary/Tertiary paleovalleys; and
- conduct reconnaissance-scale investigations of diamond potential in the region.

Previous Studies

Few Quaternary geology studies have been conducted previously in the region northeast of Fort Nelson. They have mainly included a regional investigation of ice retreat during the last glaciation (Mathews, 1980) and an unpublished airphoto interpretation study of terrain features and potential aggregate deposits by Mollard (1984a,b). The soils of the Fort Nelson area were mapped by Valentine (1971). The bedrock geology of northeasternmost British Columbia was mapped by Thompson (1977) and Stott (1982).

Study area

The study area occurs within the boreal plains region of northeast British Columbia and includes the area between the Alberta border and the Alaska highway, extending north from Fort St. John to the Northwest Territories. The main areas of focus for the 2003 field season (Figure 1) were the Fontas River and Petitot River map areas (NTS 94 I and P, respectively) and the eastern half of the Fort Nelson map area (NTS 94 J). Results of some of the work conducted in the Fort Nelson area are provided elsewhere in this volume (see paper by Johnsen et al.)

[1]*British Columbia Ministry of Energy and Mines, Resource Development and Geoscience Branch, Victoria, British Columbia*
[2]*Geological Survey of Canada*

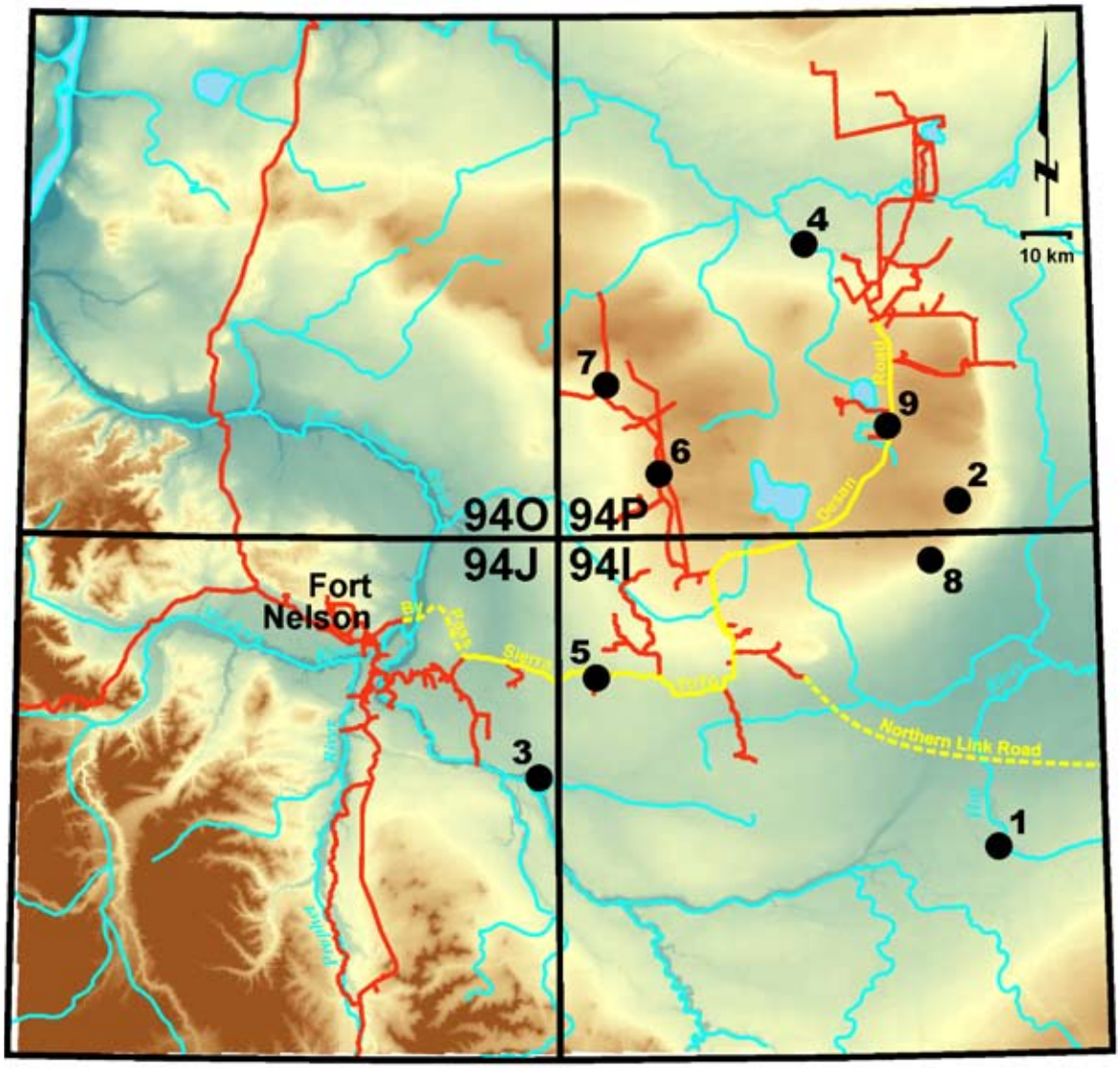

Figure 1. Location map of study area. Numbered sites are discussed in the text.

Low-relief topography and clay-rich soils dominate the study region, resulting in poor drainage and a shallow water table in most areas. Lakes, marshes, fens, and peat bogs with scattered black spruce are common. Areas that are elevated, even slightly, above the regional water table are largely forested, with the dominant tree species being aspen, pine, and white spruce.

PLEISTOCENE GEOLOGY

During the Pleistocene, glaciers advanced westward up the regional slope into northeast British Columbia and dammed rivers draining eastward off the Rocky Mountains. This resulted in the widespread deposition of glacial lake sediments over pre-existing Quaternary deposits and hence the dominance of clay-rich soils. In addition, the local bedrock is dominated by shales and other fine-textured rocks and, consequently, the derived glacial sediments are rich in clay. These fine-grained Pleistocene deposits are common at the surface and are one reason why shallow aggregate deposits are relatively rare in the region.

The dominant surficial materials in the study area are organic deposits and clay tills. Elevated areas that support a tree cover are invariably underlain by morainal deposits, whereas organic materials and glaciolacustrine sediments dominate lower, more poorly drained areas. Morainal landforms include low-relief till plains, rolling moraines, crevasse-fill ridges, flute ridges, recessional moraines, and interlobate moraines. Glaciofluvial landforms are relatively uncommon and include eskers, kames, fans, deltas, and terraces. The latter occur mainly within the Kimea Creek-Petitot River meltwater channel system.

During deglaciation, numerous meltwater channels were incised by streams generally flowing westward from the retreating Laurentide ice sheet. Sands and gravels were locally deposited in association with meltwater channels,

but many appear to be entirely erosional and may have formed subglacially. Some recently discovered aggregate deposits underlying stony diamicton along channel flanks are interpreted to be subglacial channel deposits overlain by meltout till (Figure 2). Although large surficial deposits of aggregate are rare, one exceptionally large glaciofluvial fan-delta (Figure 3; see Site 1, Figure 1 for location) was discovered on the east side of the Fontas River map area (NTS 94 I). This feature covers an area of approximately 100 km^2 and is likely the single largest sand and gravel deposit in northeast British Columbia. An indication of the enormous size of the fan is that it was first noticed on a satellite image. A measured section in the fan showed 7 m of well-rounded, quartzite-rich gravels overlain by 5 m of well-sorted sands. The thick sand cap has been largely removed in many areas by erosion of the Hay River, which dissects the fan. The best target areas for coarse aggregate are thus along lower terraces of the river where it cuts the fan. These sands and gravels overlie approximately 5 m of clay-rich diamicton interpreted to be basal till.

Dating of Pleistocene sediments in the area has been facilitated by the discovery of an interglacial peat underlying a thin till and oxidized sandy unit in the Spruce Road area (Site 2, Figure 1). The peat contains abundant plant matter, including many wood fragments, as well as numerous pelecypod and gastropod fossils. Radiocarbon analyses on two wood pieces yielded dates of more than 38 690 radiocarbon years before present (BP) (Beta 183832) and more than 40 590 radiocarbon years BP (Beta 183831). Another fragment of wood recovered from gravels stratigraphically underlying till in the Elleh Creek area (Site 3, Figure 1) was dated at 24 400±150 radiocarbon years BP (Beta 183598). Collectively, these dates and the associated stratigraphy provide new constraints on the Pleistocene history of the region and indicate that ice-free conditions probably existed from before 40 ka until after about 24 ka BP.

AGGREGATE STUDIES

Aggregate resources in northeast British Columbia are relatively rare outside of major river valleys. Existing deposits in many areas of active petroleum road development have been largely depleted (Thurber Engineering, 2001, 2002) while demand is increasing. The region northeast of Fort Nelson is an area of particularly active exploration and

Figure 2. Sands and gravels in the Nogah Road area, interpreted to be subglacial channel deposits, underlying thin, stony, meltout till. The gravels overlie thick, clay-rich, basal till at most locations.

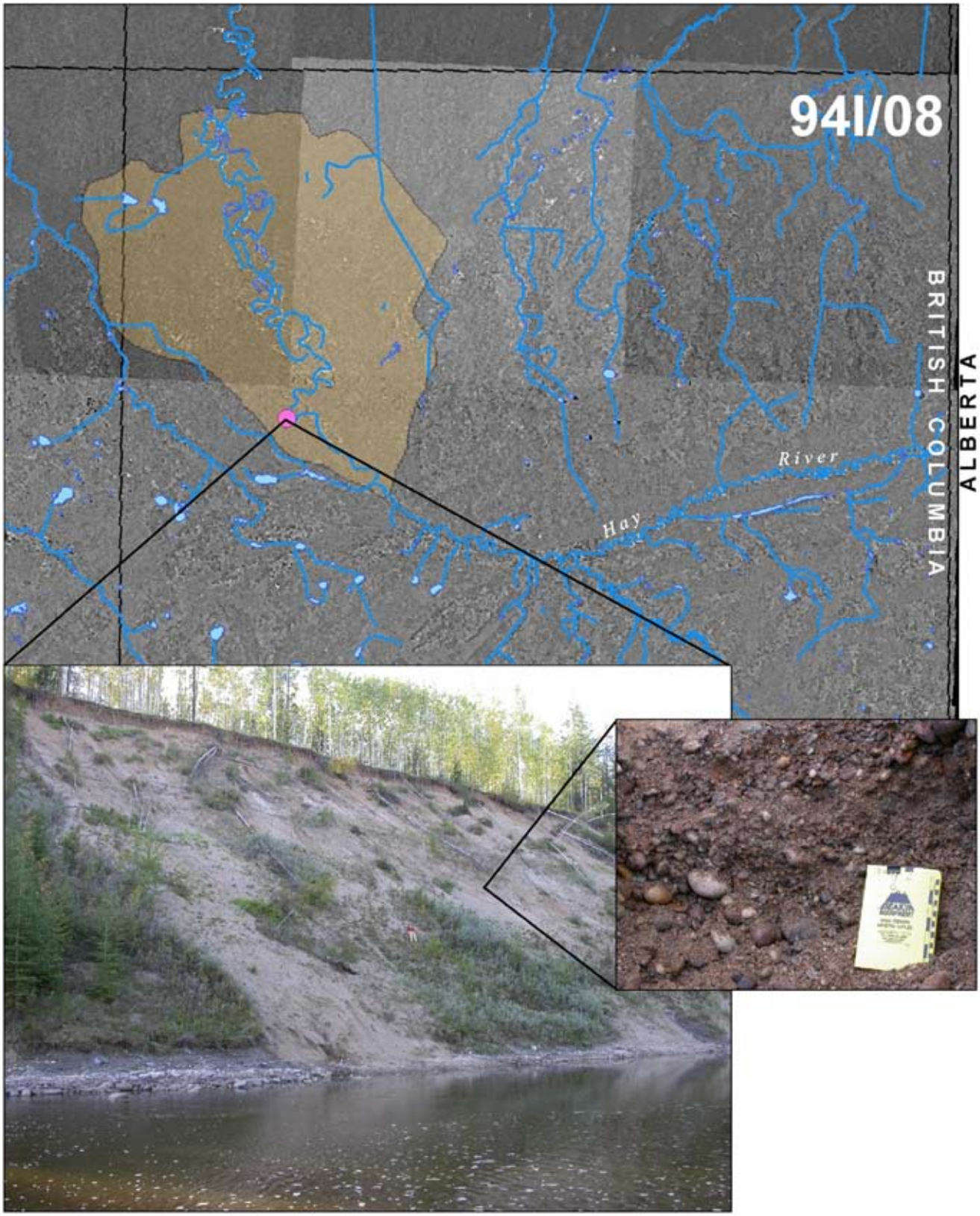

Figure 3. Large glaciofluvial fan-delta exposed along the Hay River. The orange polygon approximately delineates the extent of this fan. Inset photographs were taken at a section on Hay River where this fan-delta has been incised. Note person for scale.

development. For example, EnCana Corporation has described plans to drill about 100 new wells per year for the next several years on the Greater Sierra gas field, which is nearly 300 km long (Daily Oil Bulletin, June 2002). Road improvements in this area would reduce the requirement to impose road bans in the spring, allowing for an extended drilling season. The chronic shortage of aggregate has resulted in high prices and even the need for shipping of gravel into the region by train from Fort St. John.

To meet this need, a program was initiated as part of the British Columbia Oil and Gas Development Strategy (OGDS) to systematically explore for new, local aggregate sources in northeast British Columbia. The program includes both regional and site-specific aggregate evaluations. The identification of regional sand and gravel resources will provide the necessary information for developing a long-term strategy to ensure that roads in the region are capable of supporting the future demands of industry. Improved access and transportation cost savings to resource companies will also enhance viability of projects and encourage exploration investment, leading to new discoveries. The identification and evaluation of site-specific reserves will ensure an aggregate supply not only of adequate volume, but also of good quality. Sampling and laboratory testing will identify the areas of best aggregate quality for the various types of road improvement.

A key component of the OGDS is a comprehensive road infrastructure plan aimed at promoting better access to resources through improved infrastructure. The completion of road improvements, such as the upgrade of the SYD Road and construction of the Clarke Lake Bypass Road in the Fort Nelson area, is expected to promote longer drilling seasons, accelerate exploration and production programs, and increase industry and provincial revenues.

It has been estimated that the current upgrade of the SYD Road will require two million cubic metres of aggregate for the initial road infrastructure improvement program. However, a study completed by Thurber Engineering (2002) indicated that existing aggregate resources along the SYD Road were largely depleted. Four of the ten reserves investigated were completely depleted, and only three had more than 100 thousand m^3 of aggregate remaining. To meet this need, a program was initiated to systematically explore for new, local aggregate sources in the region.

Initial aggregate evaluations in the fall of 2002 focused on an airphoto study and brief field investigation of the SYD corridor (Blyth *et al.*, 2003). From this preliminary work, fourteen sites with aggregate potential were identified, including sites in the Kimea Creek (Figure 4), Hoffard Creek, Courvoisier Creek, Komie Road (Figure 5), Kotcho East (Figure 6), and Sahdoanah Creek areas (Sites 4 to 9, respectively, Figure 1).

As a follow-up to the airphoto study, ground investigations were conducted in the winter of 2003 at 9 sites (Dewar and Polysou, 2003a). A total of 458 test pits were excavated, and granular materials were encountered in 235 of these pits at 8 of the sites. Two additional areas, where bedrock was inferred to be shallow, were also investigated. Bedrock was encountered in all 15 test pits at the sites, although the quality of the rock appeared to be suitable only for general borrow material. Detailed investigations conducted at 4 sites included field sampling and laboratory testing (124 sieve analyses, 10 sand equivalent tests, and 10 degradation tests). Sieve tests were completed on an additional 47 samples from 3 other sites. The results of the sampling program and laboratory analyses are provided by Dewar and Polysou (2003b, c, d, e).

The 4 areas investigated in detail are referred to here as the Kimea, Kotcho East, Komie North, and Elleh sites. These sites have a total inferred resource of approximately 5 000 000 m^3 of granular material: Komie North (more than 300 000 m^3), Kimea (more than 3 000 000 m^3), Kotcho East (approximately 450 000 m^3) and Elleh (more than 1 000 000 m^3). The Kimea deposit is one of several prospective glaciofluvial terraces (Figure 4) within a large meltwater channel system extending along parts of Kimea Creek and Petitot River. The Komie North deposit is interpreted to be an ice-contact delta (Figure 5). The origin of the Kotcho East deposit (Figure 6) is enigmatic because it is entirely buried and has virtually no surface expression. It may be a raised delta or part of a proximal glaciofluvial stream deposit. The Elleh deposit is interpreted to consist mainly of advance-phase glaciofluvial deposits but also locally includes interglacial sands and gravels deeper in the deposit, where the 24 ka BP radiocarbon age was obtained. Late-glacial (retreat-phase) gravels, which stratigraphically overlie till, also occur in the area at the surface.

Electromagnetic Surveys

Subdued topography, extensive muskeg, and a general scarcity of glaciofluvial landforms make the use of traditional aggregate mapping techniques, such as aerial photograph interpretation, relatively ineffective for locating new deposits in many parts of the study area. In addition, sand and gravel deposits in the area are commonly blanketed by glaciolacustrine and glacial sediments. As a result, new subsurface investigations and geophysical techniques are being tested and used to identify these buried aggregate deposits. Data sources include down-hole geophysical logs, water-well logs, seismic shot hole data, and conductor pipe logs. Airborne aeromagnetic surveys, high-resolution electromagnetic (EM) surveys, light detection and ranging (LIDAR), and other remote sensing techniques are also being used in exploring for buried aggregate deposits. In this section we briefly report on the results of a high-resolution airborne EM survey of a buried gravel deposit in the Kotcho East area (NTS map area 93I/15).

Figure 4. Exposure of glaciofluvial terrace gravels in the Kimea Creek area. The deposit is within a large meltwater channel system extending along the Kimea Creek and Petitot River valleys. Note shovel in foreground for scale.

The survey was centred on a deposit originally discovered during a follow-up field investigation of buried gravels reported from seismic shot hole logs. Excavations in the vicinity of the reported occurrence show gravels underlying silt-rich sediments (Figure 6). The buried sands and gravels were encountered in 10 test pits in an elongated southwest-trending area, oblique to present surface stream channels. The sands and gravels occur along a gentle southeasterly slope with no obvious geomorphic indications of their presence. They are overlain by silts and clays generally 1 to 2 m thick but locally up to 5 m thick. These sediments are interpreted to be glaciolacustrine in origin. In the inferred core of the paleochannel, the sands and gravels are at least 5 m thick, and in 6 of the test holes the base of the channel was not encountered. Surprisingly, the water table was encountered in only one test hole at the southeasternmost edge of the deposit.

An airborne EM survey was conducted over this area to evaluate the utility of the method for mapping shallow gravel deposits, to attempt to trace the extent of the Kotcho East gravel deposit beyond the field-tested boundaries, and to identify any new gravel targets in the region. To accomplish these goals, a detailed survey with 100 m line spacing was flown over the Kotcho deposit and 200 m line spacing was flown over a larger area (about 25 km^2) around the known deposit. The survey employed the helicopter RESOLVE multicoil multifrequency EM system supplemented by two high-sensitivity cesium magnetometers and a GPS electronic navigation system. The EM system was located in a bird flown at an average height of 39 m above the ground. Apparent resistivity maps were produced from the 400, 1500, 6400, 25 000, and 115 000 Hz data.

Results (Figure 7) show that three main areas of high resistivity were identified in the survey on the high-frequency data, which best reflects the shallow geology. The northernmost area coincided remarkably well with the area of shallow buried gravels as mapped out by the field investigations. The southern two areas are much larger and will be the focus of future ground investigations. Preliminary testing indicates that these other areas of high resistivity are also sand and gravel deposits. The results of this work strongly indicate that high-resolution EM surveys can be an

Figure 5. Planar cross-bedded gravels exposed in the Komie North deposit, interpreted to be deltaic forset gravels.

effective tool for mapping buried sand and gravel deposits in the study region. A more detailed discussion of the results of this survey is provided elsewhere in this volume (see paper by Best *et al*.).

PALEOCHANNEL MAPPING

Reconstructions of the three-dimensional architecture of thick Quaternary sequences in northeast British Columbia and northwest Alberta have recently become of interest for several reasons. First, natural gas exploration companies have been investigating shallow gas targets in the region (see below). Secondly, rapidly expanding oil and gas infrastructure has depleted local surface aggregate supplies and created a critical need for identification of subsurface gravel deposits. Thirdly, shallow groundwater aquifers are used for agricultural purposes, as drinking water sources, and as possible discharge sites for waters extracted during coalbed methane operations. In addition, shallow aquifers are susceptible to contamination as development expands in the region. All of these applications have resulted in the need for an improved understanding of the Quaternary stratigraphy of the region. The main geological characteristic of shared importance to all these applications is the presence of relatively large bodies of granular sediment in a variety of paleochannel settings in the subsurface.

The depth and geometry of sand and gravel sequences of either glaciofluvial or interglacial origin in these paleovalleys is key to aquifer mapping and aggregate studies. Large, laterally continuous units can form significant aquifers at nearly any depth within the buried valleys; however, sand and gravel units must occur relatively close to surface and have a thin overburden to be of economic significance as aggregate resources. The greatest potential for shallow gravels is in smaller paleochannels that were tributary to the larger paleovalleys. Mapping these channel deposits is relatively difficult and often requires higher-resolution geophysics or dense borehole data.

Preliminary reconstruction of the bedrock topography—the first step in identification and mapping of paleochannels—has been completed using water-well logs and oil and gas well records (e.g., Figure 8). More detailed mapping of these buried features is being accomplished in

Figure 6. Test pit exposure of sands and gravels in the Kotcho East deposit buried by surficial silts. Test pit is approximately 1.5 m wide.

some areas by interpretation of geophysical data, including high-resolution aeromagnetics, resistivity surveys, seismic profiling, and ground-penetrating radar.

QUATERNARY/TERTIARY GAS

Interest in Quaternary gas was highlighted in the study region by development of the Sousa Quaternary gas field near High Level, Alberta. That field has successfully been producing gas since 1998 from paleochannel sediments underlying late Quaternary glacial deposits. The sands and gravels that form the reservoir are believed to be of early Quaternary age, although a Late Tertiary age is also possible. The cap for the gas is thick clay-rich glacial tills and glaciolacustrine sediments. Numerous wells have been drilled into Quaternary sediments and completed at depths of less than 300 m. One field in Alberta has yielded more than 4 billion cubic feet (bcf) of gas, with one well producing up to 4.4 million cubic feet per day (mmcf/d) (Canadian Discovery Digest, 2000).

Northeast British Columbia has a similar geological and glacial history to that of northwest Alberta, where these producing shallow gas fields have been developed, and, as such, the region has similar potential to host Quaternary gas. In order to identify potential paleochannel areas, the British Columbia Ministry of Energy and Mines is currently mapping the regional bedrock topography of NTS map areas 94 I (Figure 9) and 94 P. To date, about 1000 wireline-geophysical logs have been used to map the surface of the bedrock (Upper Cretaceous Dunvegan Formation conglomerates,

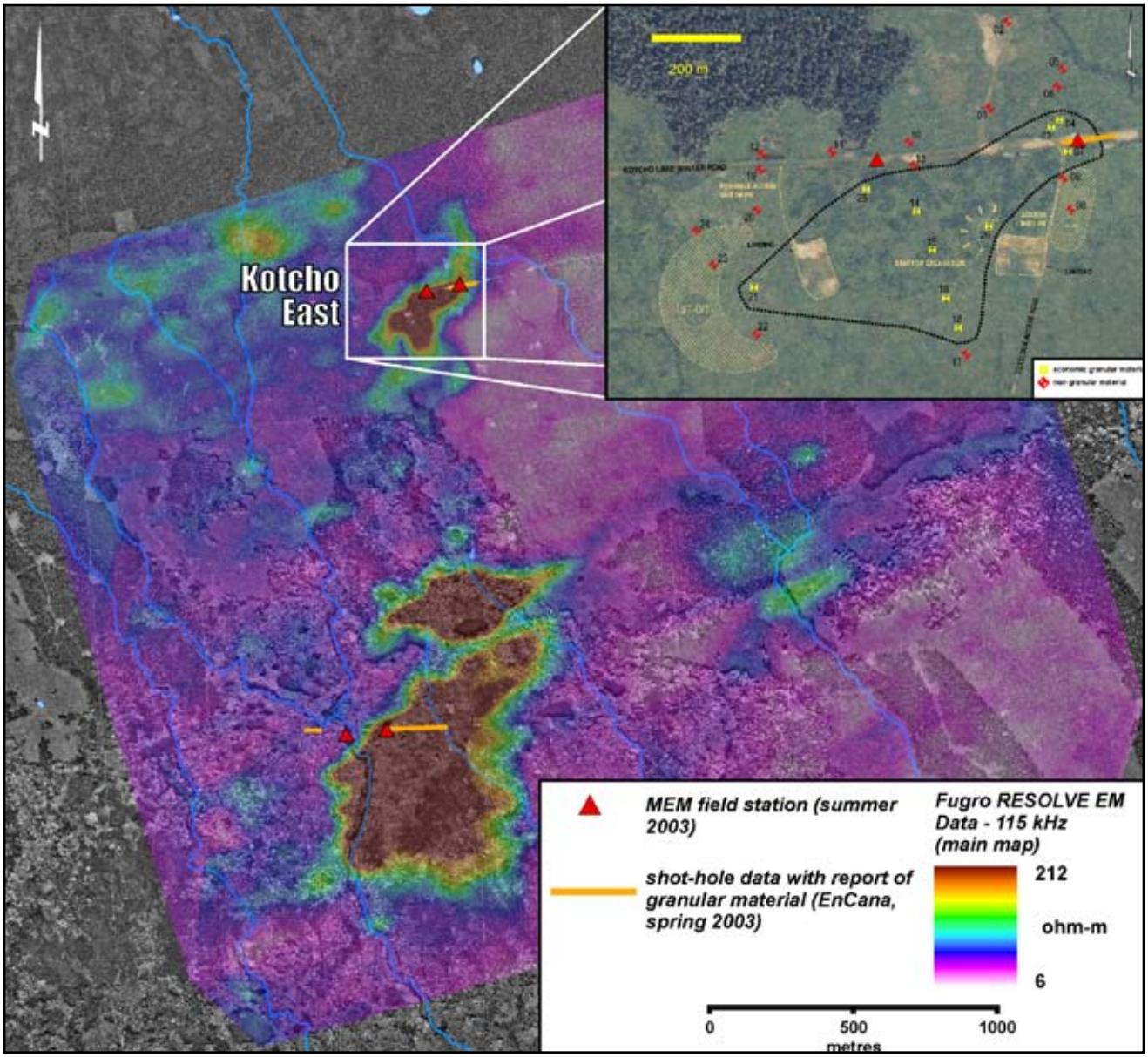

Figure 7. Results of an electromagnetic survey in the Kotcho East area. An area of high resistivity (in the north) corresponds closely with a known sand and gravel deposit (as determined by field investigations shown in the inset). Preliminary testing indicates that the large areas of high resistivity in the south are also sand and gravel deposits.

sandstones, and shales and Lower Cretaceous Fort St. John Group shales and sandstones). Where possible, lithologic and sedimentologic descriptions in nearby conductor pipe and water-well logs have been used to verify bedrock picks (Figure 8). Drift thickness in these map sheets varies from a few metres to as much as 280 m. Bedrock valleys and areas with granular material overlying bedrock indicate the presence of Late Tertiary to Pleistocene paleochannels that could be suitable targets for gas exploration.

Quaternary/Tertiary gas occurrences appear to be mainly in areas distant from deeply incised, large modern valleys. The reservoir sediments are buried by thick sequences of Middle to Late Pleistocene deposits of relatively low permeability. The westward advance of Laurentide glaciers up the regional slope in successive Quaternary glaciations effectively dammed eastward-draining rivers and deposited thick sequences of glaciolacustrine sediments and clay tills derived from local Mesozoic shales. Large paleovalleys in the Fort St. John area are up to a few hundred metres deep and a few kilometres wide and make significant exploration targets. Preliminary mapping indicates that a number of smaller buried paleovalleys in the Fontas River and Petitot River map areas are likely present (Figure 1). The proximity of these paleovalleys to producing Quaternary gas fields in Alberta as well as the similar geological setting suggest that this region has similar potential for new gas discoveries.

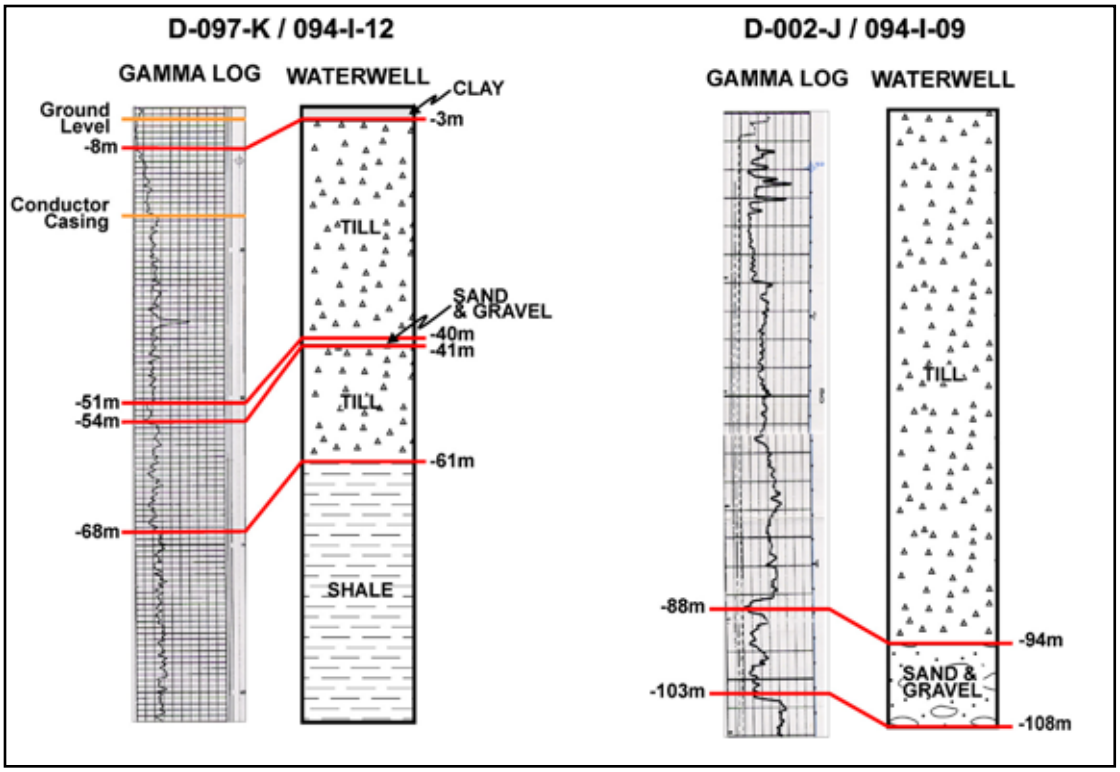

Figure 8. Examples of water-well logs and nearby oil and gas well geophysical logs used in the identification and mapping of Quaternary stratigraphy, subsurface aggregates, bedrock topography, and paleochannels.

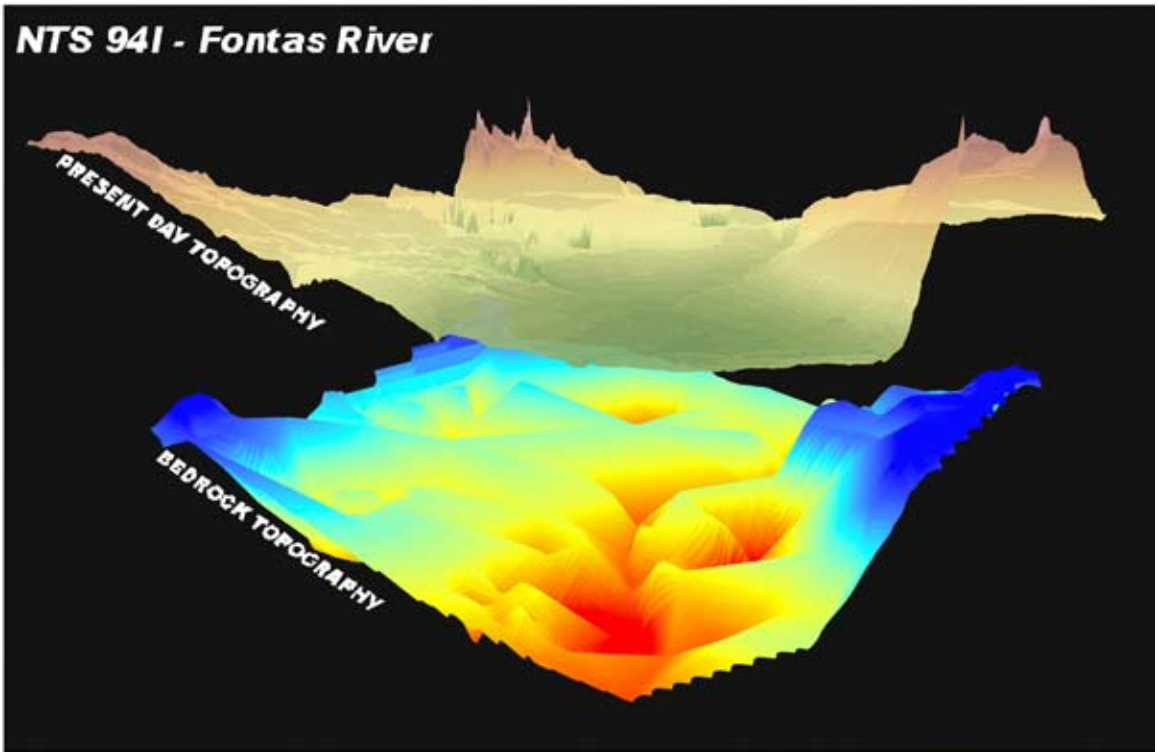

Figure 9. Preliminary reconstruction of the bedrock topography (lower panel) and surface relief (upper panel) of NTS map area 94 I based on data from about 400 wireline-geophysical logs. View is towards the southwest. Depth to bedrock varies from a few metres to as much as 280 m. Buried bedrock valleys are interpreted as Late Tertiary to Pleistocene paleochannels that are possible targets for gas exploration

DIAMOND POTENTIAL

A secondary component of recent Quaternary geoscience studies in northeast British Columbia involves the evaluation of the regional diamond potential. Sedimentary rocks in the area are underlain by Precambrian basement with possible Slave craton equivalents, but the diamond potential of the region is largely unknown. As part of the 2003 Quaternary geology program, reconnaissance sampling of glaciofluvial deposits was conducted. Glaciofluvial sediments were selected as a sampling medium because of their potential to reflect relatively large drainage areas compared to modern fluvial deposits. Bulk samples were collected and concentrates were produced in the laboratory using heavy liquids. Kimberlite indicator minerals have been detected at a number of sites. Microprobe analyses are in progress to evaluate possible sources for the indicator minerals.

CONCLUSIONS

Recent Quaternary geology investigations in the boreal plains in northeasternmost British Columbia have been initiated in response to the need for more information on the surficial geology of the region. The main demand has come from a rapidly expanding oil and gas road infrastructure and an accompanying critical need for the identification of aggregate deposits. Gravels close to surface with minimal overburden are preferred, but such deposits are relatively rare in northeast British Columbia. In addition, techniques commonly used for identifying gravel deposits, such as geomorphological mapping, are relatively ineffective in the region due to the widespread forest cover and subdued topography. Additionally, ground-based exploration techniques are too costly and time-consuming for covering vast areas of investigation such as the plains region of northeast British Columbia. As a consequence, Quaternary mapping programs in the region have focused on the collection of subsurface borehole and geophysical data as well as airborne aeromagnetic, high-resolution electromagnetic, and LIDAR survey data.

The result of this work has led to the discovery of several new aggregate occurrences in the region. To date, 4 main aggregate deposits have been investigated in detail within the study area, with a total resource of approximately 5 million m^3 of granular material. One of these deposits was completely buried and could not be detected by traditional airphoto mapping techniques. It was initially discovered from seismic shot hole data and was subsequently mapped using an airborne high-resolution electromagnetic survey. Several other occurrences have been investigated to various levels of detail. One of the most significant of these in terms of size is a large fan-delta in the Hay River that covers an area of approximately 100 km^2 and contains a maximum known thickness of 22 m of sand and gravel.

Mapping of buried channels in northeast British Columbia has recently become of interest because of the discovery of natural gas in Quaternary paleochannel sediments in northwest Alberta. Sands and gravels of probable Early Quaternary or Late Tertiary age form the reservoirs, which are capped by thick Pleistocene glaciolacustrine deposits and clay-rich tills that act as cap 'rocks'. Preliminary bedrock topography mapping in the study area suggests that paleochannels with gas potential are present. Finally, the discovery of kimberlite indicator minerals at several sites in the study area suggests that northeast British Columbia has diamond potential and that further diamond exploration in the region is warranted.

ACKNOWLEDGEMENTS

The authors would like to acknowledge John Pawlowicz, Mark Fenton, and Roger Paulen of the Alberta Geological Survey and Alain Plouffe of the Geological Survey of Canada, who provided many valuable ideas during the course of this work; their collaboration and contributions are greatly appreciated. The cooperation and advice of Tyson Pylypiw and Doug Anderson from Encana Corporation, Doug McConnnell of Fugro, and Doug Dewar of Amec are also greatly appreciated.

REFERENCES

Blyth, H., Levson, V. and Savinkoff, P. (2003): Sierra-Yoyo-Desan aggregate potential mapping; British Columbia Ministry of Energy and Mines, fourteen 1:50 000-scale map sheets.

Cain, M.J. (2004): RESOLVE survey for the British Columbia Geological Survey; *Fugro Airborne Surveys,* Report 3091, 22 pages.

Canadian Discovery Digest (2001): Sousa 111 2W6 Quaternary Gas; Exploration Review, Canadian Discovery Digest, January/ February 2001 Report, pages 25-39.

Dewer, D. and Polysou, N. (2003a): Project overview report: Sierra-Yoyo-Desan Road area gravel investigation, Northeastern British Columbia; *AMEC Earth and Environmental Limited*, Report No. KX04335-KX04395, 14 pages.

Dewer, D. and Polysou, N. (2003b): Field and laboratory work-Summary Report (Areas 1,2,3,4,5,5A,7,7A): Sierra-Yoyo-Desan Road gravel investigation, Northeastern British Columbia; *AMEC Earth and Environmental Limited,* Report No. KX04335-KX04395, 19 pages.

Dewer, D. and Polysou, N. (2003c): Area 8 (Komie North) gravel investigation - Sierra-Yoyo-Desan Road area, Northeastern British Columbia; *AMEC Earth and Environmental Limited,* Report No. KX04335, 19 pages.

Dewer, D. and Polysou, N. (2003d): Area 9 (Kimea) gravel investigation - Sierra-Yoyo-Desan Road area, Northeastern British Columbia; *AMEC Earth and Environmental Limited,* Report No. KX04335, 25 pages.

Dewer, D. and Polysou, N. (2003e): Area 10 (Kotcho East) gravel investigation - Sierra-Yoyo-Desan Road area, Northeastern British Columbia; *AMEC Earth and Environmental Limited,* Report No. KX04335, 13 pages.

Mathews, W.H. (1980): Retreat of the last ice sheets in Northeastern British Columbia and adjacent Alberta; *Geological Survey of Canada*, Bulletin 331, 22 pages.

Mollard, D.G. (1984a): Office airphoto study for the mapping of sand/gravel prospects in Kotcho Lake area, Northeastern British Columbia; *JD Mollard and Associates Ltd.*, 9 pages.

Mollard, D.G. (1984b): Terrain and surface geology map; Kotcho Area, British Columbia; *JD Mollard and Associates Ltd.*, 9 pages.

Stott, D.F. (1982): Lower Cretaceous Fort St. John Group and Upper Cretaceous Dunvegan Formation of the foothills and plains of Alberta, British Columbia, District of MacKenzie and Yukon Territory, Geological Survey of Canada, Bulletin 328, 124 pages.

Thompson, R.I. (1977): Geology of Beatton River, Fontas River and Petitot River map areas, Northeastern British Columbia; *Geological Survey of Canada*, Paper 75-11, 8pp.

Thurber Engineering (2001): Sierra-Yoyo-Desan Road gravel inventory; report to British Columbia Ministry of Energy and Mines, Oil and Gas Initiative Branch, 14 pages.

Thurber Engineering (2002): Sierra-Yoyo-Desan Road gravel inventory; supplementary report to British Columbia Ministry of Energy and Mines, Oil and Gas Initiative Branch, 9 pages.

Valentine, K.W.G. (1971): Soils of the Fort Nelson Area of British Columbia; *British Columbia Soil Survey, Canada Department of Agriculture,* Report No. 12, 60 pages.

A NOTE ON THE MARKET POTENTIAL OF LOW-VOLATILE BITUMINOUS COAL, WILLOW CREEK PROPERTY, NORTHEASTERN BRITISH COLUMBIA

By Barry Ryan[1], Ted Todoschuk[2] and Bob Lane[3]

KEYWORDS: Low-volatile coking coal, Willow Creek property, low-volatile pulverized coal injection (PCI), coke oven blends.

INTRODUCTION

The international coking coal market is very competitive and is segmented into many non-interchangeable coal products. Two products that are more in demand than many are low-volatile bituminous high-rank coking coal for blends into coke ovens and low-volatile bituminous coal for pulverization and injection into blast furnaces (pulverized coal injection or PCI coal). The Willow Creek property contains coal that may be suitable for these two markets. The higher-priced market is the low-volatile coking coal market, where up to 30% of this coal can be added into coal blends for coke ovens. This is a higher-priced market than the PCI market, and it is advantageous for mines if possible to switch from the low-volatile PCI market to the low-volatile coking coal market. Low-volatile coking coal is also in short supply as reserves in the US and other countries are running out. This note looks at the possible use of 7 Seam from the Willow Creek property in northeastern British Columbia as a low-volatile component in a standard coke oven blend. The Willow Creek property is located 40 km west of Chetwynd (Figure 1) and overlies seams in the Gething Formation.

THE WILLOW CREEK PROPERTY

There are two coal-bearing formations in the Peace River coalfield (Table 1). Coal from the younger Gates Formation was mined at the Quintette and Bullmoose mines (both now closed). There is active exploration of the formation in the Wolverine River area by Western Canadian Coal Corporation and Northern Energy and Mining Incorporated.

Coal from the older Gething Formation was mined briefly in the early 1900s but has not hosted any major coalmines. However, there is a long history of exploration in the formation, and coal was first reported in the formation by the explorer Alexander Mackenzie in 1793. The formation trends northwest across the Pine River about 40 km west of Chetwynd (Figure 1), and in this general area there have been a number of exploration projects. North of the Pine River, seams in the Gething Formation are generally medium-volatile in rank. South of the river in the Willow Creek area, rank increases and some seams are low-volatile bituminous. Further to the south, the rank of seams in the formation increases to semi-anthracite. The quality of seams in the Gething Formation has been discussed in a number of exploration reports and is summarized in Ryan (1997). Coal in the formation is characterized by low ash contents and variable inert maceral content. Sulphur and phosphorus contents are generally low, and rheology depends on rank and maceral content.

TABLE 1: GENERALIZED LOWER CRETACEOUS STRATIGRAPHY.

Pine River Area.			metres
Jurassic to lower Cretaceous	FORT ST JOHNS GROUP	CRUISER FORMATION marine shale	115
		GOODRICH FORMATION fine grained sandstone and shale	350
		HASLAR FORMATION marine shale	260
		BOULDER CREEK FORMATION sandstone and conglomerates	150
		HULCROSS FORMATION grey marine shale	100
		GATES FORMATION non marine sandstones and coal seams	110
		MOOSEBAR FORMATION marine shale	250
	BULLHEAD GROUP	GETHING FORMATION non marine sediments and coal	500
		CADOMIN FORMATION conglomerates	150

[1] *Resource Development and Geosciences Branch, B.C.Ministry of Energy and Mines, barry.ryan@gems4. gov.bc.ca*
[2] *Dofasco Canada*
[3] *Mines Branch, B.C. Ministry of Energy and Mines*

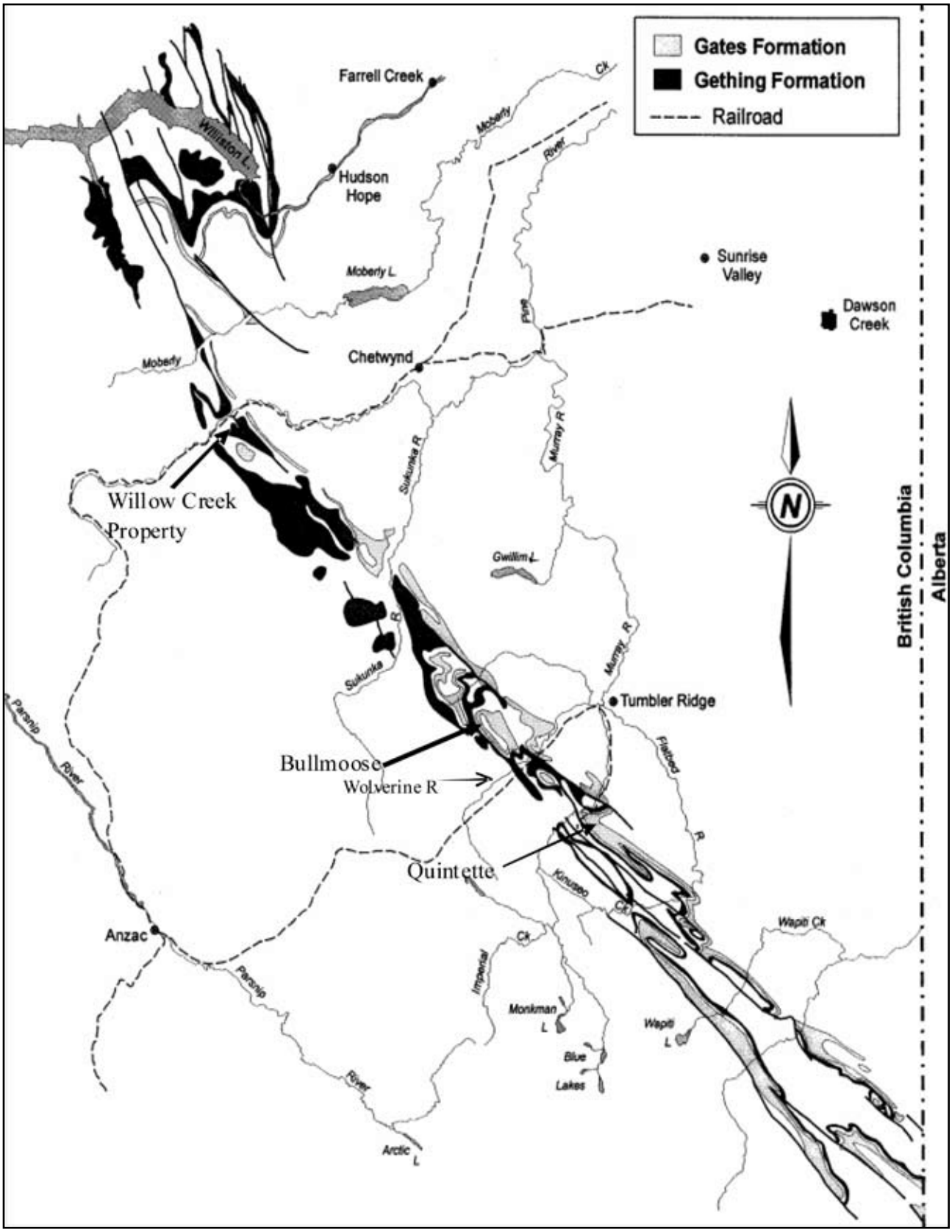

Figure 1. Location map for the Willow Creek property Pine Valley Coal Corporation, northeast British Columbia.

The area adjacent to and south of the Pine River has for some time been referred to as the Willow Creek property, which was explored in the early 1980s as a potential underground mine. Interest waned, and it was not till the mid 1990s that exploration was renewed with the intent of developing a small low strip-ratio open-pit mine. In 1993, Globaltex acquired control of the property and now has in place a British Columbia "Project Approval Certificate" and "Mine Permit". The company has continued development work in conjunction with a number of partners.

The operating company for the property is now called Pine Valley Mining Corporation, and they have conducted various mine feasibility studies that are based on mining the uppermost 9 seams in the Gething Formation (Table 2). These seams are numbered from 1 Seam near the top of the formation to 9 Seam, which occurs in the mid part of the formation at a depth stratigraphicaly about 300 m below 1 Seam. The rank of seams ranges from about 1.3% Rmax to 1.7% Rmax, with 6 and 7 Seams, which are thick, having ranks in the range of 1.6 to 1.67%. Raw-ash contents range from 15% to 7% and are generally low (Table 3). These seams, especially 7 Seam (which makes up a major part of the reserves), have the potential to be marketed as a low-volatile PCI coal or as a low-volatile blend coal in coke-oven blends.

The studies indicate that there are proven in-place reserves of about 15 million tonnes at an in-place strip ratio of about 3.6 to 1 bcm/t (bank cubic metre of overburden per tonne of coal). This is sufficient to justify an output level of some 900 000 to 1.5 million tonnes per year. In addition, there are identified resources in nearby areas that may significantly increase proven reserves and annual production in the future.

In the last few years, a number of raw coal bulk samples were excavated and coal shipped to Japan for test marketing. To date about 125 000 tonnes have been mined from an area referred to as the Peninsular Pit, where seams 6 and 7 outcrop. A rail spur capable of handling up to 25 coal cars and connected to the BC Rail Prince George line was constructed in the Pine Valley. At the moment, run-of-mine coal is screened and shipped raw. A 37 000 tonne test shipment was sold in 2001, and in 2002 a larger shipment of about 84 000 tonnes was shipped. Work performed to date suggests that up to 1.0 million tonnes of very low strip-ratio coal (estimated at 1.8:1) in the Peninsula Pit can be mined and sold on a raw coal basis without incurring material coal dilution or recovery problems.

The company's current plan is to start mining in this area and then move into more steeply dipping coal measures within the Willow Central and Willow North areas. Construction of a coal preparation plant is planned to coincide with the move to the Willow Central and Willow North areas.

7 SEAM COAL QUALITY AND SAMPLE COLLECTION

The carbonization sample was collected from the outcrop face of the small 7 Seam test pit (Peninsular Pit) in winter. The snow and cold made sampling and access difficult. Sufficient fist-sized or larger fragments of the seam were collected from parts of the seam ranging from hanging wall to footwall to fill a 45 gallon drum. The drum was shipped to Canmet carbonization laboratories at Bells Corners, Ontario. Pilot oven coking tests and related analyses were performed by Gransden and Price (2003), and the results are summarized in the next section. In addition, small grab samples of bright and dull bands were collected to check for oxidation.

The bright and dull samples were analysed for oxidation using the "Alkali Extraction" test that is now recognized by American Standards for Testing Materials (test D5263-93[2001]). The test measures the amount of humic acid developed as a result of natural weathering. The test is only applicable to mid-rank coals from high-volatile to low-volatile bituminous. Lower rank coals have humic acids that are naturally occurring at the rank, and high rank coals are resistant to this type of chemical action but can be damaged by other weathering processes. Because of the high rank of 7 Seam, bright samples, which are not representative of the whole seam, were analysed because these would be most sensitive to this type of weathering. Transmittance results (Table 4) range from 90% to 95%, indicating that the seam is not oxidized and there are marginal free swelling index (FSI) values, ranging from 1 to 1.5.

In the Willow Creek area, the raw-ash content for 7 Seam averages 5% and ranges from 1% to 39%, based on exploration drilling. The FSI values range from 0 to 3 and the variations appear to be related to varying inert maceral content and not ash content. This is based on a plot of ash versus FSI with the data coded based upon volatile matter (VM) dry mineral-matter-free (dmmf) values (Figure 2). Oxidation increases the volatile matter content (VM dmmfb) of samples; therefore, low FSI data points with high VM dmmf values are probably oxidized, whereas low FSI data points with low VM dmmf values probably represent samples with high inert maceral contents. It is clear in Figure 2 that samples with high VM dmmfb have, on average, higher FSI values than those with low VM dmmfb values.

Petrography on previous samples of 7 Seam (Table 5) indicates that 7 Seam contains from 40% to 60% vitrinite macerals, being mostly collodetrinite. It was not possible to do a petrographic analysis of the 7 Seam sample collected for the pilot coke-oven test before it was shipped to Canmet, because the sample was crushed by Canmet. Petrographic analyses of the carbonization sample by Canmet and the author indicate that the coal has a very low content of finely

TABLE 2. STRATIGRAPHIC SECTION, WILLOW CREEK AREA.

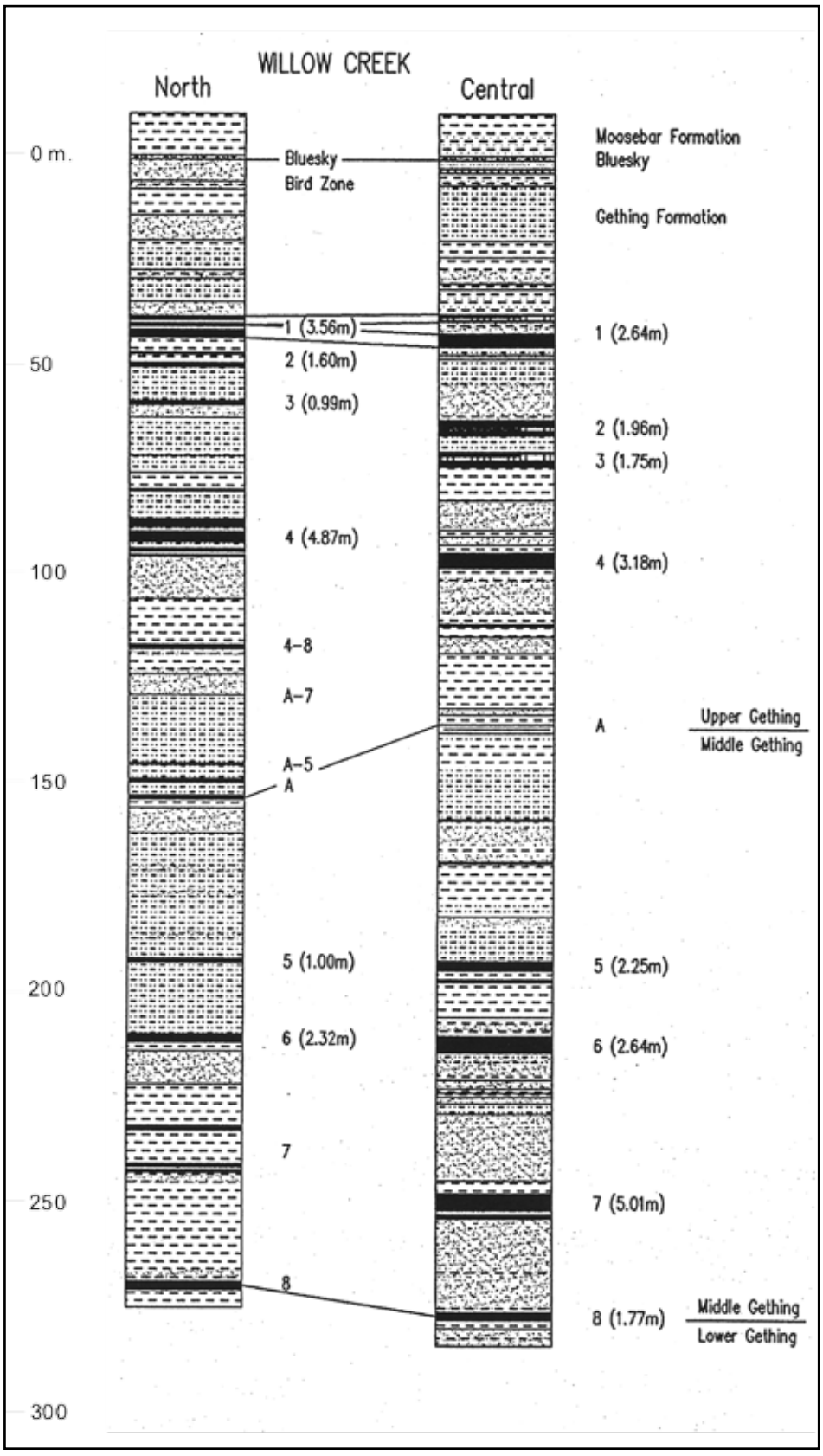

(P.C. KEVIN JAMES)

TABLE 3. AVERAGE QUALITY AND THICKNESS FOR SEAMS AT WILLOW CREEK.

Seam	metres from Moosbar	thickness north metres	thickness central metres	raw ash% DB	VM% DB	CV cals/g	Megajoules/kg	Sulphur%	FSI raw data	Rmax%
1	40	3.56	2.64	7.9	23.5	7870	32.95	0.5	4.5	1.28
2	55	1.6	1.96	14.5	23	7734	32.38	0.59	6	1.33
3	70	1	1.75	8.7	21.1	7729	32.36	0.43	2	1.34
4	100	4.87	3.18	10.1	20	7688	32.19	0.48	3	1.4
A	140	?	?	?	?	?	?	?	?	1.49
5	190	1	2.25	8.3	16.9	7898	33.07	0.7	1	?
6	210	2.32	2.64	7.3	16.3	7957	33.31	0.62	1	?
7	250	?	5.01	8	16.1	7897	33.06	0.65	1.5	1.67
8	280	?	1.77	?	?	?	?	?	?	?
9	?	?	?	?	?	?	?	?	?	?

TABLE 4. PROXIMATE ANALYSES FOR 7 SEAM AND "ALKALI EXTRACTION" TEST FOR SAMPLE OXIDATION.

		H_2O% AR	VM% DB	Ash% DB	FC% DB	FSI	Sulphur%	HGI	Alkali exctraction
WC 2002	8 bright	0.74	17.23	3.4	79.38	1.5			93.3
WC 2002	9 bright	0.7	17.14	3.48	79.38	1.5			91.7
WC 2002	10 bright	0.65	16.58	11.13	72.29	1.5			95
WC 2002	1 dull	0.56	14.47	3.09	82.44	1			90
bulk 1			15.31	4.73	79.96		0.53	70	
bulk 2			15.65	4.23	76.72		0.53		
product quality			16.4	4	79.6	1	0.55	70	
Canmet 7 seam			14.7	2.93	82.4	0.5	0.48		95.5

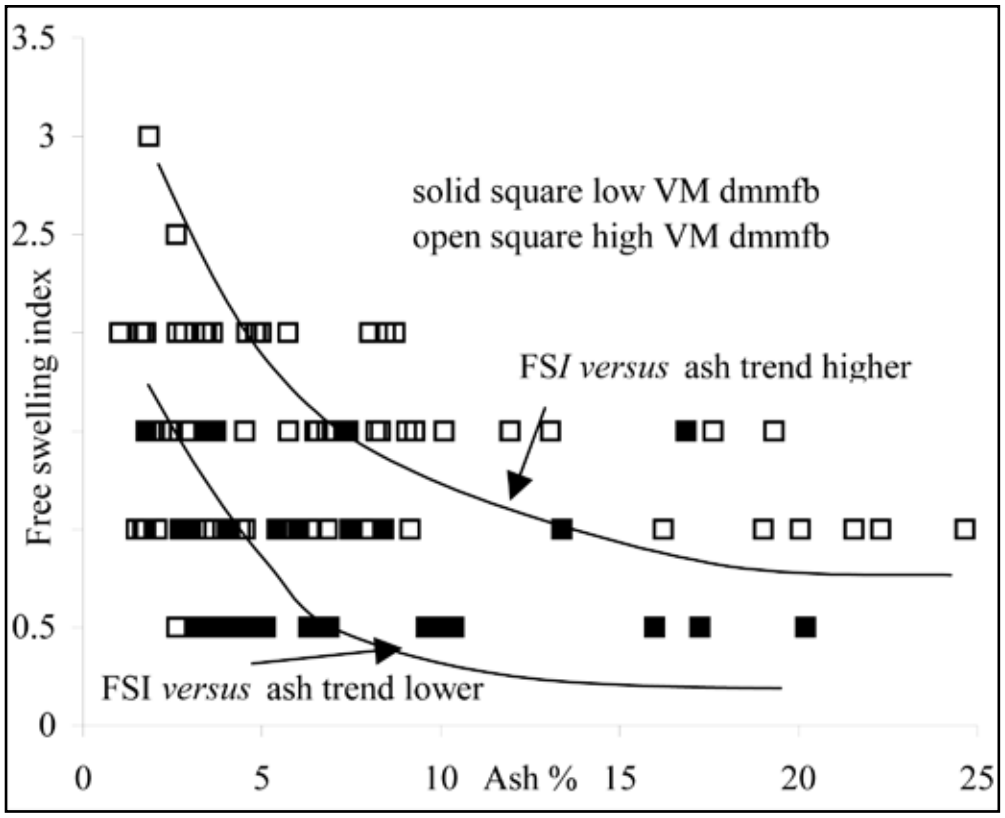

Figure 2. Ash versus FSI data for 7 Seam; from coal assessment report 690, British Columbia Ministry of Energy and Mines library.

TABLE 5. PETROGRAPHY OF 7 SEAM SAMPLES COLLECTED IN 2001.

						VOLUME PERCENTS						Petrography for samples 300 point count.							
Description	length cm	H2O% AR	VM% DB	Ash% DB	FC% DB	telinite	collotelinite	collodetrinite	vitrodetrinite	pseudovitrinite	total reactives	semifusinite	fusinite	inertodetrinite	macrinite	micrinite	total inerts	mineral matter	weight ash%
C	163	4.3	12.7	1.8	85.5	2	6	37	0	2	48	33	1	1	7	6	48	3	5.1
C	111	3.1	12.4	12.7	74.9	0	19	39	2	1	61	10	2	2	9	6	29	10	16.3
C	70	5.1	12.5	2.4	85.1	8	3	32	1	3	47	23	2	0	19	6	50	2	4.0
bright		2.7	14.9	1.7	83.4	2	12	50	1	15	80	8	0	2	6	1	17	1	2.3
dull		3.6	13.1	1.4	85.4	4	13	36	0	4	58	23	2	2	9	4	40	2	4.0
bright		6.7	14.8	13.2	72.1	24	21	34	1	0	81	1	1	2	1	0	5	13	20.5
dull		2.9	12.7	3.8	83.5	2	7	44	0	0	53	14	0	2	20	9	45	3	4.5

C=channel sample bright and dull are grab samples of lithotypes

dispersed mineral matter and a moderate to high content of inert organic material. The Canmet petrographic analysis, after the sample was crushed at Bells Corners, measured 76% semifusinite, which is partitioned as 50% reactive and 50% inert, providing a total reactive maceral content of 58.5% but with a very low percentage of vitrinite (Table 6). The petrographic analysis by the author identified more vitrinite macerals (mainly collodetrinite) with dispersed macrinite and inertodetrinite and less semifusinite. However the proportions of inert and reactive macerals are similar (54% by the author and 58.4% by Canmet). Identification of macerals is a somewhat interpretative process; Canmet appears to identify reactive semifusinite, whereas the author identifies it as high-reflecting collodetrinite. Previous petrographic analyses on channel samples and bright and dull grab samples indicate the range of petrography in the seam (Table 5).

TABLE 6. PETROGRAPHY OF THE 7 SEAM SAMPLES USED IN THE PILOT COKE-OVEN TEST AND PETROGRAPHY OF OTHER LOW-VOLATILE COALS USED IN COKE-OVEN BLENDS.

	7 seam			other low-volatile seams			
	PVCL	Ryan	NrCan ref 3	Jellinbah ref 1	Smoky River ref 2	US low vol from ref 1	US low vol range from-to from ref 2
vitrinite	28.5		15	79.3	61.8	79.3	
telinite		1					
collo telinite		10					
collo detrinite		41					
vitro detrinite		2					
reactive semifusinite	30	0	37.9		13		
total reactives	**58.5**	**54**	**52.9**	**79.3**	**74.8**	**79.3**	**79.8-66.7**
semifusinite	30	25	37.9	13.4	13	13.4	
micrinite	2.2	1	0.7		4.3		
macrinite	0	11	0				
fusinite	7.5	0	6.8		4		
inertodetrinite	0	6	0	4.6		4.6	
mineral matter	1.8	4	1.7	2.6	3.9	2.6	2.4-4.8
total inerts	**41.5**	**47**	**47.1**	**20.6**	**25.2**	**20.6**	**11.7-28.5**
Rmax	**1.68**	**1.64**	**1.68**	**1.7**	**1.62**	**1.7**	**1.54-1.72**
sulphur	0.5		0.48	0.83	0.42	0.83	
HGI	70			96		96	
VM dry			14.72	19.3	17.4	19.3	17.8-20.5
FSI			0.5	2	7	4.5	
Fluidity			0	0	2		58-455
total dilatation			0	7	10	46	15-79

1=Caldeira and Stainly (2002); 2=Fawcett and Dawson (1990)
3=Gransden and Price (2003)

Schapiro *et al.* (1961) introduced a way to predict cold coke strength using coal petrography. The method, which considers one-third of the inert macerals as reactive, is used extensively when pilot coke-oven test data are not available. Canmet considers 50% of the inert macerals to be reactive, based on studies of Cretaceous Western Canadian coals. However, these methods presuppose that petrography is the main influence and that other factors such as coking conditions and the way the different macerals are intermixed do not also play a major role in influencing cold coke strength. Coin *et al*. (1997) suggest that rank is the overriding factor and petrography is not very important in influencing cold coke strength. Pearson (1998) suggests that petrography can be useful in predicting cold coke strength but that the proportion of inert macerals that is reactive varies with rank (measured using random reflectance of vitrinite, Rrand) and vitrinite content. For 7 Seam the random reflectance cut-off that separates reactive from nonreactive inert macerals is 1.76%, based on the equation of Pearson (1998):

cut-off reflectance = Rrand*0.99+0.24

The reactive cut-off converges on the Rrand value as rank increases, and this means that there is a tendency to increase the proportion of inerts designated as reactive as rank increases. This is obviously important for high-rank coals with high inert maceral contents. One should be very careful in deciding if they have coking potential based only on an interpretation of petrography. A comparison of Australian Gondwana coals with western Canadian Cretaceous coals appears to indicate that the proportion of inert macerals that is reactive is also dependent on the origin of the coal (Figure 3; Pearson, 1998). In fact it appears that the reactive cut-off is higher at the same rank for Australian coals than it is for western Canadian coals. Diessel (1996) did not find a difference between inert material in Australian and US Carboniferous coals.

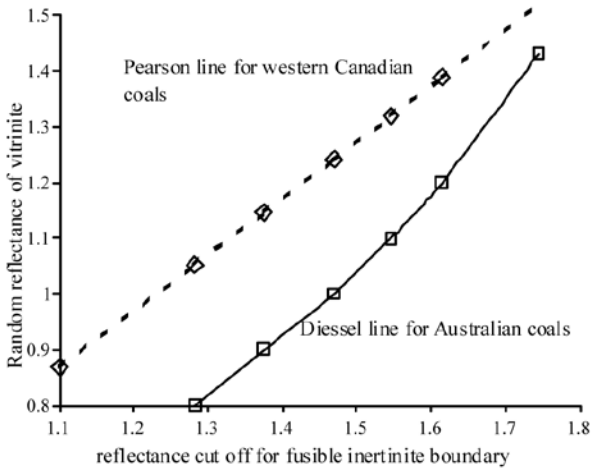

Figure 3. Relationship between reactive semifusinite and rank; Figure modified from Pearson (1998).

TABLE 7. ASH OXIDE ANALYSES FOR 7 SEAM AND OTHER SEAMS ON THE PROPERTY.

Sample	Ash %	SiO_2 %	TiO_2 %	Al_2O_3 %	Fe_2O_3 %	MgO %	CaO %	Na_2O %	K_2O %	P_20_5 %	Ba(4) %	B/A ratio
7 sm Pilot oven sample	2.4	63.00	0.95	23.29	2.48	0.33	1.10	1.97	1.12	1.70	0.65	0.08
7sm central P1	4.5	69.94	0.82	21.22	1.8	0.9	1.04	1	2.35	0.8		0.08
7 Seam data from Coal assessment report 690	5.48	24.65	13.99	0.71	35.68	2.97	7.07	2.1	0.48	2.13		1.23
	6.48	67.7	18.27	0.75	3.5	1.1	2.07	1.54	2.53	0.27		0.12
	6.31	69	20.85	1.41	0.79	0.35	0.95	1.16	1.81	1.57		0.06
Seam1	3.26	54.92	24.17	2.68	1.67	0.78	3.98	2.31	0.37	4.73		0.11
Seam 1	8.52	62.91	8.13	0.32	13.12	1.09	5.18	1.41	0.24	0.49		0.29
Seam 2	3.59	59.62	25.52	1.88	2.43	0.7	3.11	2.91	1.57	1.09		0.12
Seam 4	2.59	23.05	16.65	0.71	9.27	2.75	21.08	2.56	0.49	2.45		0.89
Seam 4	5.21	56.86	26.79	1.06	1.88	0.92	2.69	1.58	0.73	4.07		0.09
Seam 5	4.77	66.84	19.85	0.49	2.15	0.62	1.06	1.37	2.29	0.48		0.09
Seam 6	4.33	64.14	23.68	1.08	1.17	0.54	1.4	1.48	1.45	1.81		0.07
Seam 6	5.95	61.52	23.69	0.99	2.75	1	1.68	1.83	2.41	1.4		0.11

The ash chemistry of the 7 Seam sample was analysed, and previous analyses exist for seams on the property (Table 7), mainly from Coal Assessment Report 690, which is in the Ministry of Energy and Mines library. The data generally indicate a very basic ash with low base-to-acid ratio. Occasional samples have siderite in them, which increases the Fe2O3 concentration in the ash. All base elements are in low concentration, except for moderate concentrations of K and Na. Phosphorous contents are low and, based on an average ash content of 5%, represent a concentration about 0.03% phosphorous in the total sample. The low ash content of the samples will ensure that the effects of the base oxides will be negligible in any blend.

PILOT COKE-OVEN TEST RESULTS

The 45 gallon drum of 7 Seam sample was crushed at Bells Corners to 80% less than 3 mm. A split of the sample was returned to the author for petrographic and ash-oxide analysis. A second split was analysed for proximate and ultimate analysis and, in addition, rheology (Table 8 and 9). In order to test the applicability of using 7 Seam as a blend in coke ovens, it was necessary to obtain a suite of coals that make up a normal coke-oven blend, to coke the blend, and then to make up a new blend with 10% of 7 Seam replacing the low-volatile component in the standard blend before doing a second coke test.

Dofasco Inc. provided three coals, and these coals were mixed in the proportions 28% low-volatile (Rmax 1.7%), 35% high-volatile (Rmax 1%), and 37% medium-volatile (Rmax 1.08%) in preparation for a pilot coke-oven test on a standard coke-oven blend. A second blend was prepared in which the Dofacso coals contributed 18% low-volatile, 37% high-volatile, and 35% medium-volatile, with the balance being made up with 10% 7 Seam. Component seam proportions and proximate and ultimate analyses of the two blends are in Table 8. The addition of 10% 7 Seam decreased the ash and volatile content of the blend. The rheology data for the two blends (Table 9) indicate that the addition of 7 Seam has had no measurable effect on Gieseler plasticity but has had a detrimental affect on dilatation, which has decreased from 112% to 69%.

The pilot coke-oven tests and related analyses were performed by Gransden and Price (2003). The two blends were coked in the Canmet 18 inch oven, which takes a sample load of 350 kg of blended coal. The coal was charged at 3% moisture and 80% less than 3 mm. The coking conditions were those used for other pilot coke-oven tests and are contained in Table 10.

TABLE 8. BLEND PROPORTIONS AND PROXIMATE AND ULTIMATE ANALYSES OF THE TWO BLENDS AND 7 SEAM THAT WERE COKED IN THE PILOT OVEN BY CANMET.

	Base Blend	7Seam blend	7 Seam
Low-volatile Rmax 1.7%	28	18	
medium-volatile Rmax 1.08%	35	35	
high-volatile Rmax 0.99%	37	37	
7 Seam	0	10	100
Coal proximate analysis			
ash% db	6.43	6	2.93
Volatile matter db%	29.85	28.22	14.72
fixed carbon db%	63.72	65.78	82.35
Sulphur db%	0.89	0.83	0.48
Ultimate analysis			
Carbon	81.95	82.92	88.28
hydrogen	4.84	4.84	3.84
nitrogen	1.55	1.52	1.22
ash% db	6.43	6	2.93
Oxygen by dif	4.34	3.89	3.25
Coke proximate analysis			
ash% db	8.46	7.84	
Volatile matter db%	0.46	0.5	
fixed carbon db%	91.08	91.66	
Sulphur db%	0.71	0.65	

TABLE 9. RHEOLOGY OF THE TWO BLENDS AND OF 7 SEAM.

	Base Blend	7Seam blend	7 Seam
Low-volatile Rmax 1.7%	28	18	
medium-volatile Rmax 1.08%	35	35	
high-volatile Rmax 0.99%	37	37	
7 Seam	0	10	100
FSI	7.5	7	0.5
Gieseler Plasticity			
Initial softening temp °C	42	403	
Fusuion temp °C	415	416	
Max fluid temp °C	445	443	493
Final fluid temp °C	485	486	
Solidification temp °C	491	492	
melting range temp °C	83	83	
Max fluiditiy ddpm	2422	2547	0.1
Dilitation			
Softening temp °C	376	374	
Max contration temp °C	417	419	
Max dilatation temp °C	470	468	
Contraction	24	28	
Dilation	106	63	

The quality of the coke produced by the blend with 10% of 7 Seam was the same as or not as good as the standard blend on a number of counts. Coke strength after reaction and coke reactivity index were unchanged within the limits of the measurements (Table 9). However, cold coke strength decreased markedly. On the plus side, maximum wall pressure and maximum gas pressure both decreased. The ash and sulphur contents of the coke decreased.

The poor performance of 7 Seam in the blend is probably the result of a combination of the low percent of active reactives and the high rank. Coke textures (Table 11) confirm a noticeable decrease in the reactive components of the 7 Seam blend as coke inerts increase by about 6%. It was unfortunate that the petrographic composition could not be checked prior to coking. There is a distinct possibility that in other areas the seam will have higher reactives content or lower rank. It is also possible that either the upper or lower part of the seam has a higher reactive content and could be mined separately for a coke-oven blend market. Six Seam, which is about 30 m above 7 Seam, may provide a better candidate for blending.

TABLE 10. CARBONIZATION CONDITIONS AND RESULTS FOR THE TWO COKE TESTS.

	Base Blend	7Seam blend
Low-volatile Rmax 1.7%	28	18
medium-volatile Rmax 1.08%	35	35
high-volatile Rmax 0.99%	37	37
7 Seam	0	10
moisture %	2.6	2.4
Minus 3.35 mm %	81.2	81
ASTM bulk density Kg/m3	778	782
Oven bulk density Kg/m3	824	823
Coking time h:min	18:30	18:05
Final centre temp °C	1068	1064
Time to 900 °C	14:55	14:30
Time to 950 °C	15:30	15:05
Time to 1000 °C	16:05	15:50
Max wall pressure Kpa	7.7	5.0
Max gas pressure Kpa	14.8	3.4
Coke yield %	75.7	76.5
100 mm sieve %	0.0	0.8
75 mm sieve %	5.7	8.2
50 mm sieve %	43.6	42.2
37.5 mm sieve %	79.5	77.1
25 mm sieve %	92.7	91.9
19 mm sieve %	94.7	94.5
12.5 mm sieve %	95.7	95.8
Passsing 12.5 mm sieve %	4.3	4.2
Mean coke size	50.2	50.3
ASG	0.954	0.987
Stability	61.0	57.3
Hardness	67.0	65.2
I 10	19.3	20.7
I 20	78.5	77.0
I 40	49.4	42.6
CSR %	55.0	56.6
CRI %	30.7	28.8

TABLE 11. COKE TEXTURES FOR THE TWO BLENDS.

	Base Blend	7Seam blend
Low-volatile Rmax 1.7%	28	18
medium-volatile Rmax 1.08%	35	35
high-volatile Rmax 0.99%	37	37
7 Seam	0	10
isotropic	0.00	0.94
incipient	1.85	2.62
circular fine	41.08	37.83
circular medium	1.18	1.50
circular coarse	0.00	0.00
total circular	**44.11**	**41.95**
lenticular fine	20.54	18.35
lenticular medium	2.86	3.00
lenticular coarse	0.51	0.75
total lenticular	**23.91**	**22.10**
ribbon coarse	3.03	4.12
ribbon medium	3.70	2.62
ribbon fine	11.62	8.80
total ribbon	**18.35**	**15.54**
fusinite	0.17	0.37
semi-fusinite	3.37	10.67
unidentified inerts	10.10	7.68
altered vitrinite	0.00	0.00
green coke	0.00	0.00
depositional carbon	0.00	0.75
petroleum coke	0.00	0.00
breeze	0.00	0.00
total inerts	**13.64**	**19.48**
blend Rmax%	1.16	1.14
low vol	21.54	19.77
medium vol	27.39	26.98
high vol	51.07	53.26

MARKET OPPORTUNITIES FOR PCI AND LOW VOLATILE PCI

A large percent of the reserves in the Willow Creek area are derived from 6 and 7 Seams. The rank of these seams is low-volatile bituminous, and they have moderate and variable inert maceral content. On average, they do not exhibit good coking characteristics, and consequently coal on the property is considered suitable for thermal or pulverized coal injection (PCI) purposes. There are two important ratios to consider when discussing PCI. The first is the the PCI ratio (kg/t)—the amount of PCI coal used for each tonne of hot metal produced. The second is the coke replacement ratio—the ratio of weight of PCI coal for weight of coke; i.e., the reduction in coke requirement divided by the amount of PCI coal used.

The coke replacement ratio varies with the rank of coal used and ranges from about 0.6 for high-volatile low-rank coals to nearly 1 for low-volatile high-rank coals. The rate is in part related to the hydrogen content of the fuel. Hydrogen is an effective reductant but has a cooling effect in the raceway at the base of the blast furnace where it is injected. This limits the amount of hydrogen-rich fuels (natural gas) that can be injected. Higher coke replacement ratios are achieved with coal rather than oil and gas. The hydrogen content of coal decreases as rank increases, so the coke replacement ratio increases as rank increases (Figure 4). This has been pointed out by a number of authors (Hutny *et al*., 1991), and more recently by Stainlay (2003). There is, therefore, an expanding market for PCI coal and especially for high-rank low-volatile bituminous coal.

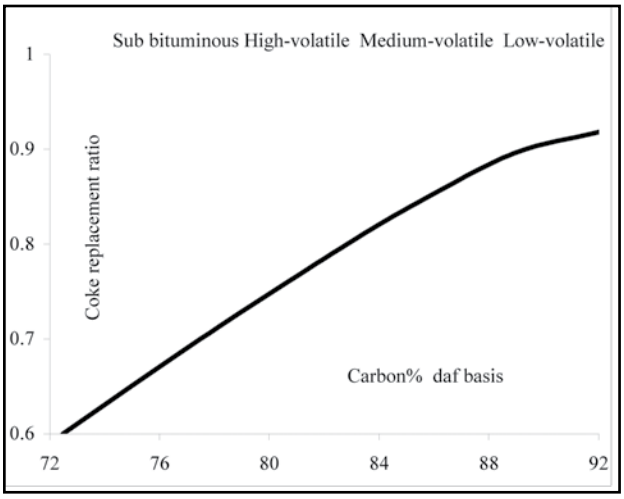

Figure 4. Coke replacement ratio versus coal rank.

It requires 1.2 to 1.5 tonnes of coal to make a tonne of coke, so if the coke replacement ratio is 0.75, the coal replacement ratio is at least 0.75 x 1.2; i.e., 1.0 or more. However, PCI coal sells for much less than coking coal. Prices vary but are often only 70% of the price of premium coking coal. Obviously there is the potential for considerable savings for the blast furnace operator. Based on the price variation, it is to the advantage of the operator to use low-volatile coals for PCI to save even more money.

The burning characteristics of high-rank low-volatile PCI coal in the blast furnace are different from low-rank high-volatile coals, but once the blast furnace is adapted there can be a considerable saving in requirement for higher-priced coking coal. At the moment the majority of blast furnaces have converted to PCI, and the global average injection rate is 96 kg/t. The present demand is about 31 million tonnes, and this is expected to grow to 42 million tonnes by 2010 (Stainlay, 2003). The increase in consumption will be caused by more conversions and an increase in the PCI rate from about 100 to maybe as high as 200 kg/t. This increase in PCI rate will in part be achieved by switching from high- to low-volatile PCI coals. The maximum PCI rate reported is from China, where a rate of about 280 kg/t was achieved using anthracite.

Traditionally, the main component of coking coal blends for coke ovens has been medium-volatile bituminous coals with good rheology and ash chemistry. As science and international coal trade developed, it was found that a mixture of coals would result in an optimum blend whose composition plotted in the optimum blend field of various diagrams (for example, the MOF diagram). As few single coals plotted in the field, most steel mills moved to at least a ternary blend of low-, medium-, and high-volatile coals. High-volatile coals add fluidity to the blend, and low-volatile coals improve coke yield at the expense of increasing coke-oven pressure. Low-volatile coals represent a balancing act between increasing rank and preservation of rheology, which is destroyed as rank increases. The three-component blend of coals for coke ovens has become the norm in recent years; however, reserves of low-volatile coal are becoming depleted, especially in the US (Kolijn and Khan, 2003). Steel mills looking to maintain a low-volatile component in their coke-oven blends will have limited opportunities in the future.

In Australia, the Jellinbah mine mines a low-volatile seam (Table 6), which is being marketed as a PCI product and as a possible blend component in coke ovens (Calderia and Stanlay, 2003). The coal is higher rank than 7 Seam but also has a much higher reactives content.

Low-volatile coals can be replaced in the coal blend with medium-volatile coals, especially if the amount of high-volatile coal is also reduced (Kolijn and Khan, 2003). This can maintain coke quality and coke yield because of the reduction in amounts of both low- and high-volatile coal and has the added advantage of reducing oven pressure.

REGIONAL AVAILABILITY OF LOW-VOLATILE COALS IN BRITISH COLUMBIA

The rank of coals in the Gething Formation was studied by a number of authors (Marchioni and Kalkreuth, 1992; Karst and White, 1979). The rank of the formation decreases to the northeast into the Western Canadian Sedimentary Basin and is generally medium-volatile bituminous along the trend of the Rocky Mountain Foothills. Within this trend, there are three areas where the rank is low-volatile bituminous (Figure 5; adapted from Marchioni and Kalkreuth, 1992). The northernmost underlies the subcrop area of the Willow Creek, Lossan, and Burnt River properties (Figure 5). To the south along the trend of the foothills, another area is east of the town of Tumbler Ridge and at depth within the Gething Formation. The third area is to the southeast in Alberta. The best opportunity for low-volatile mineable coal resources is in the area around Willow Creek and to the southeast.

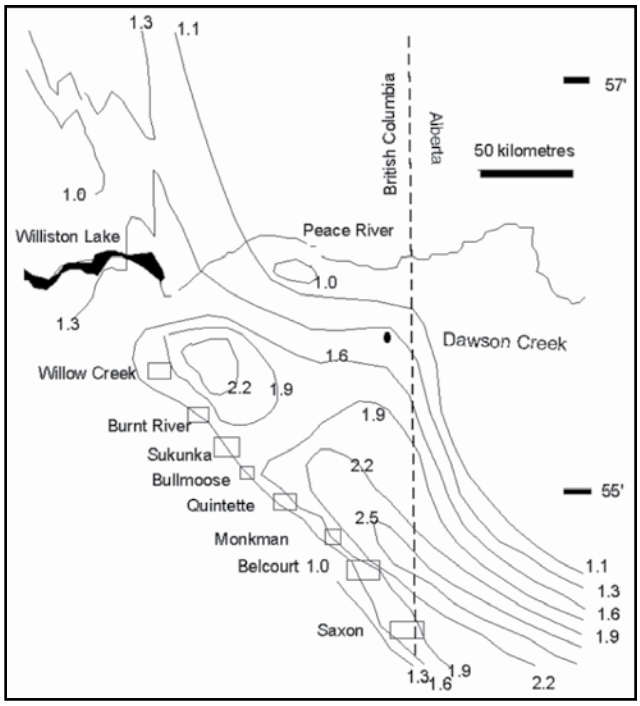

Figure 5. Reflectance isograds for the top of the Gething Formation; adapted from Machioni and Kalkreuth (1992).

The Mist Mountain coal section in Morrissey Ridge area in the southwest part of the Crowsnest coalfield (southeast British Columbia) contains low-volatile coal (Pearson and Grieve, 1985). Coal in the area was mined in the period from 1902 to 1906 in the Carbonado Mine. The coal was used as single component in beehive ovens but it did not make good coke, and this was in part the reason for the failure of the mine.

Outside British Columbia, the Smoky River mine (now closed) in Alberta exported a low-volatile coking coal (Table 6). The coal has a similar rank to 7 Seam but a higher reactive maceral content and much better FSI. The mine is expected to re-open as the Grande Cache mine in the near future.

CONCLUSIONS

The internationally traded coal market will remain very competitive in the long term, especially when China re-enters the coking coal and coke export markets in a big way. However, there are two brands of coking coal that are presently in demand and will probably remain in an under-supply situation. These are low-volatile coal for PCI and low-volatile coal for coke-oven blends. The latter commands a higher price. British Columbia has limited potential to take advantage of these markets. The best opportunities are at Willow Creek and possibly in other parts of the Gething Formation. There are also possibilities in the southeast corner of the Crowsnest coalfield in southeastern British Columbia.

This limited test did not indicate that 7 Seam from the Willow Creek property could be used in a coke-oven blend; however, it appears that the sample may not have been representative. When the mine is in production, sampling will be easier and channel samples may indicate better potential for samples to use in additional coke-oven tests.

ACKNOWLEDGEMENTS

Age and the expanding breadth of coal science, including coalbed methane, ensures that the senior author cannot pretend to be more than a generalist in his field. This short report has benefited considerably from conversations with John Gransden.

REFERENCES

Caldeira, J.G. and Stainly R.S. (2002): The challenge to use extremely low-volatile Australian weak coking coals in the production of good quality cokes; 2002 Iron making Conference Proceedings, pages 405-415.

Coin C.D.A., and Broome, A.J. (1997): Coke Quality Prediction from Pilot Scale Ovens and Plant Data, International Coal Conference, Calgary, September 1997, pages 325-333.

Diessel C.E.K. (1996): Inertinite; ACARP Report, Australian Coal Research Limited, Issue No2, July 1996.

Fawcett, D.A., and Dawson, R.F. (1990): Unique blending properties of Smoky River coal; American Institute of Mining Engineering, Iron Making Conference Detroit, March 1990, pages 110-108.

Gransden, J. and Price, J.T. (2003): Carbonization Project Report 7 Seam coal in a coke makers blend; Canmet Energy technology Centre, Job No. 3586R

Hutny, W.P., Lee, G.K. and Price, J.T. (1991): Fundamentals of coal combustion during injection into a blast furnace; Prog. Energy Combustion Sciences, Volume 17, pages 373-395.

Karst, R. and White, G.V. (1979): Coal Rank Distribution within the Bluesky-Gething Stratigraphic Horizon of Northeast B.C.; in Geological Fieldwork 1979, B.C. Ministry of Energy, Mines and Petroleum Resources, Paper 80-1, pages 103-107.

Kolijn, C. J. and Khan, M.A. (2003) Medium-volatile coal-The solution for coke oven blends with reduced low-volatile coal content; ACE Steel technology, July 2003, pages 42-49.

Marchioni, D. and Kalkreuth, W. (1992): Vitrinite reflectance and thermal maturity in Cretaceous strata of the Peace River Arch region west central Alberta and adjacent British Columbia; Geological Survey of Canada, Open file 2576.

Pearson, D. and Grieve, D.A. (1985): Rank variation, coalification pattern and coal quality in the Crowsnest Coalfield, British Columbia; Canadian Institute of Mining and Metallurgy, Bulletin, Volume 78, pages 39-46.

Pearson, D. (1998): Fusible inertinites in Coking Coals; 1998 (Toronto) ICSTI/ Iron making Conference Proceedings, pages 753-755.

Pine Valley Mining Corporation (2001): Willow Creek Project raw coal production study; Amendment to Permit C-153. British Columbia Ministry of Energy and Mines.

Ryan, B.D. (1997): Coal quality variations in the Gething Formation northeast British Columbia; British Columbia Ministry of Energy and Mines Geological Fieldwork 1996:1 pages 373-397.

Schapiro, N., Gray R.J., and Eusner, G.R. (1961): The use of coal petrography in coke making, J.Inst. Fuel. Volume. 37, 1961, pages 234-242.

Stainlay, R. (2003): PCI- current status and prospects for growth; Asia Steel International Conference, Jamshedpur, India - April 2003.

THE COALBED METHANE RESOURCE OF SOME PROSPECTIVE AREAS OF THE CROWSNEST COALFIELD

By Barry Ryan[1]

KEYWORDS: Coal rank, gas contents, coal thicknesses, Mist Mountain Formation

INTRODUCTION

The majority of literature refers to the extraction of coalbed methane (CBM) from coal. This is not scientifically correct as the gas extracted from coal is a mixture of methane, carbon dioxide, and other gases. The British Columbia government is adopting the term coalbed gas (CBG). The abbreviations CBM and CBG both refer to the commercial gas extracted from coal at depth. To avoid confusion with existing scientific literature, this paper uses the term CBM.

The Crowsnest coalfield is located between the Elk River and Michel Creek drainages and covers a total area of about 600 km^2. A major pipeline, which trends north-south through the coalfield (Figure 1), connects the Alberta gas fields with the US market. This pipeline has been expanded from the original 36-inch Trans Canada pipeline and is now twinned with a 48-inch Foothills pipeline following the same right-of-way. An 8-inch pipeline, which branches off the main line in the northeast corner of the coalfield, serves the towns of Sparwood and Elkford and some of the mines. A second 8-inch pipeline branches off at Morrissey and serves the town of Fernie. Title to the gas rights in the coalfield is in part with the crown and in part unassigned at this time. This paper summarizes existing mapping data, coal quality, and coal resource data. It also attempts to delineate the resource potential of areas where the crown has clear title; this means disregarding areas where various companies have at least freehold coal rights.

The Crowsnest coalfield has been mapped by a number of geologists. One of the earliest was Newmarch (1953), who provided a preliminary map of the coalfield and detailed geology of the Coal Creek area, which was compiled at a time when the mines in the creek were still operating. Price (1961) produced a regional map of the Crowsnest coalfield, which also provides strike and dip information. The area was mapped using orthophotos in the period 1977 to 1981 by a number of personnel from the British Columbia Ministry of Mines (Pearson *et al.,* 1977; Pearson and Grieve, 1978, 1980). These maps outline seam trends and provide structural information. Recently, a compilation of the mapping and construction of geological sections was completed by Johnson and Smith (1991). Other recent studies such as Dawson *et al.* (1998) have used these maps and accompanying sections. Monahan (2002), as part of an assessment of the oil and gas potential of the area, produced a revised map using existing mapping and well data.

The map from Johnson and Smith is reproduced here (Figure 1) with additional information, which includes approximate delineation of various land blocks, areas in which the Mist Mountain Formation is at least in part at a depth of less than 1000 m, and fold axial plunge data transferred from Price (1961). In addition, geological sections from Johnson and Smith (1991) are reproduced with some additional sections to give a spacing of 5 km for sections through the coalfield (Figure 2). The 1000 m depth line is shown on the sections.

There are a number of publications that deal with coal quality and surface and underground coal resources of the coalfield. A summary paper (Pearson and Grieve, 1985) discusses coal quality. Coal rank in the coalfield varies from high-volatile bituminous to low-volatile bituminous, with higher rank coals in the southwest part of the basin. There is also evidence that rank increases down dip into the core of the major syncline that crosses Morrissey Creek

Johnson and Smith (1991) were the first to estimate the CBM resource of the coalfield, and they calculated a value of 12 trillion cubic feet (Tcf). They used an average gas versus depth curve derived from data from the San Juan Basin. In 1990, a number of companies drilled stratigraphic test holes in the southern part of the coalfield (Dawson *et al*., 2000) (Figure 3). A best-fit curve to all desorption data (Figure 4) resulting from this drilling in the coalfield indicates a lower total resource for the coalfield of 6.7 Tcf.

To date, the only assessment that covers parts of the coalfield is that by Dawson et al. (1998), who assessed the CBM resource potential of the two Dominion Blocks (Block 73 in the north and Block 82 in the south; Figure 1). These blocks have a total area of 202 km2 (Block 73, 20.2 km2; Block 82, 182.1 km2). Dawson et al. (1998) considered gas contents to vary from 10.9 to 20.1 cm3/g (350 to 650 standard cubic feet per tonne [scf/t]). They estimated a total resource for the two blocks of 6.57 Tcf to a depth of 1000 m. The northern Block 73 having 0.65 Tcf (93% shallower than 1000 m) and Block 82 having 5.92 Tcf (62% shallower

[1] *Resource Development and Geosciences Branch, BC Ministry of Energy and Mines, barry.ryan@gems4.gov.bc.ca*

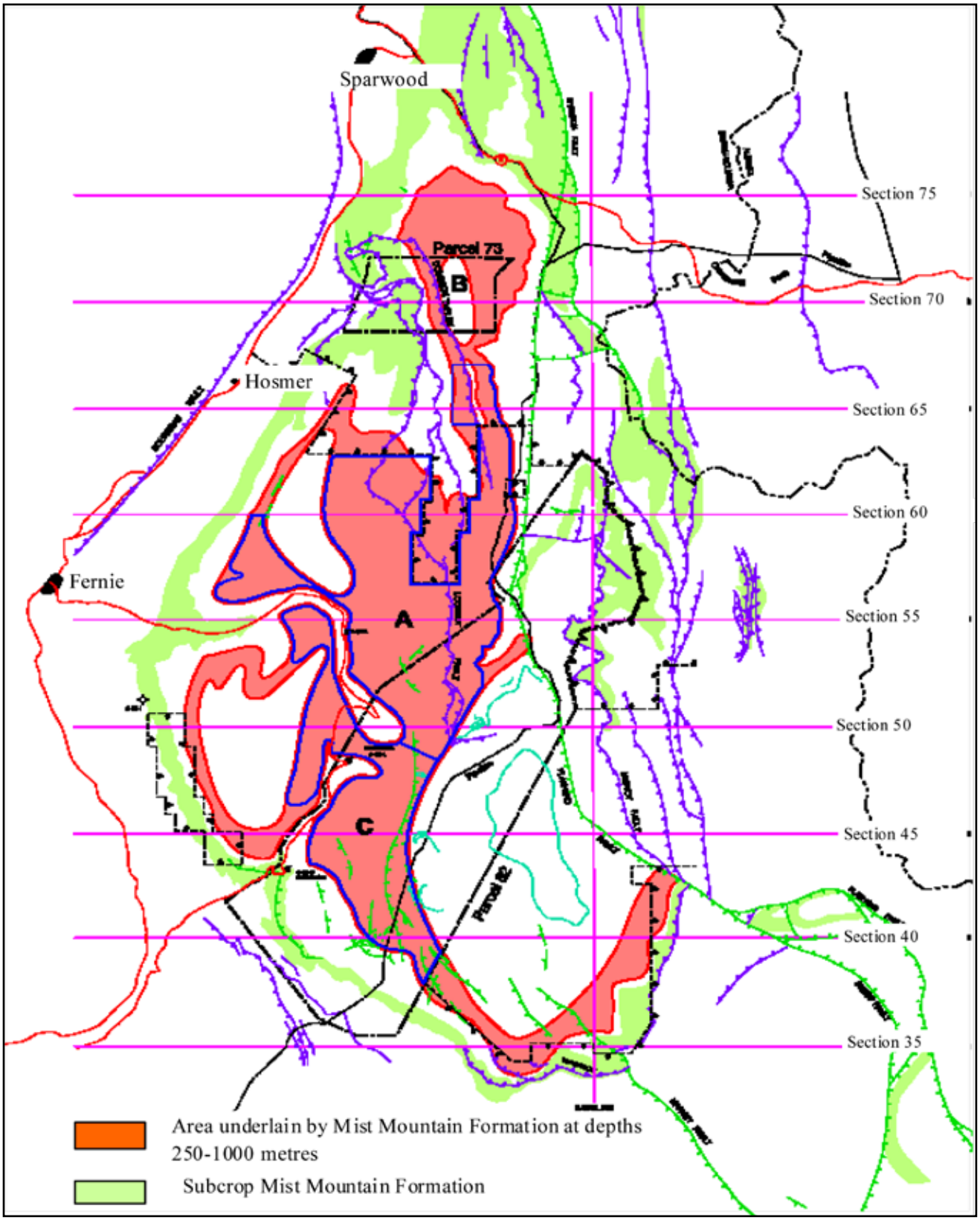

Figure 1. Outline of the Crowsnest coalfield. CBM resources of areas A, B, and C discussed in text.

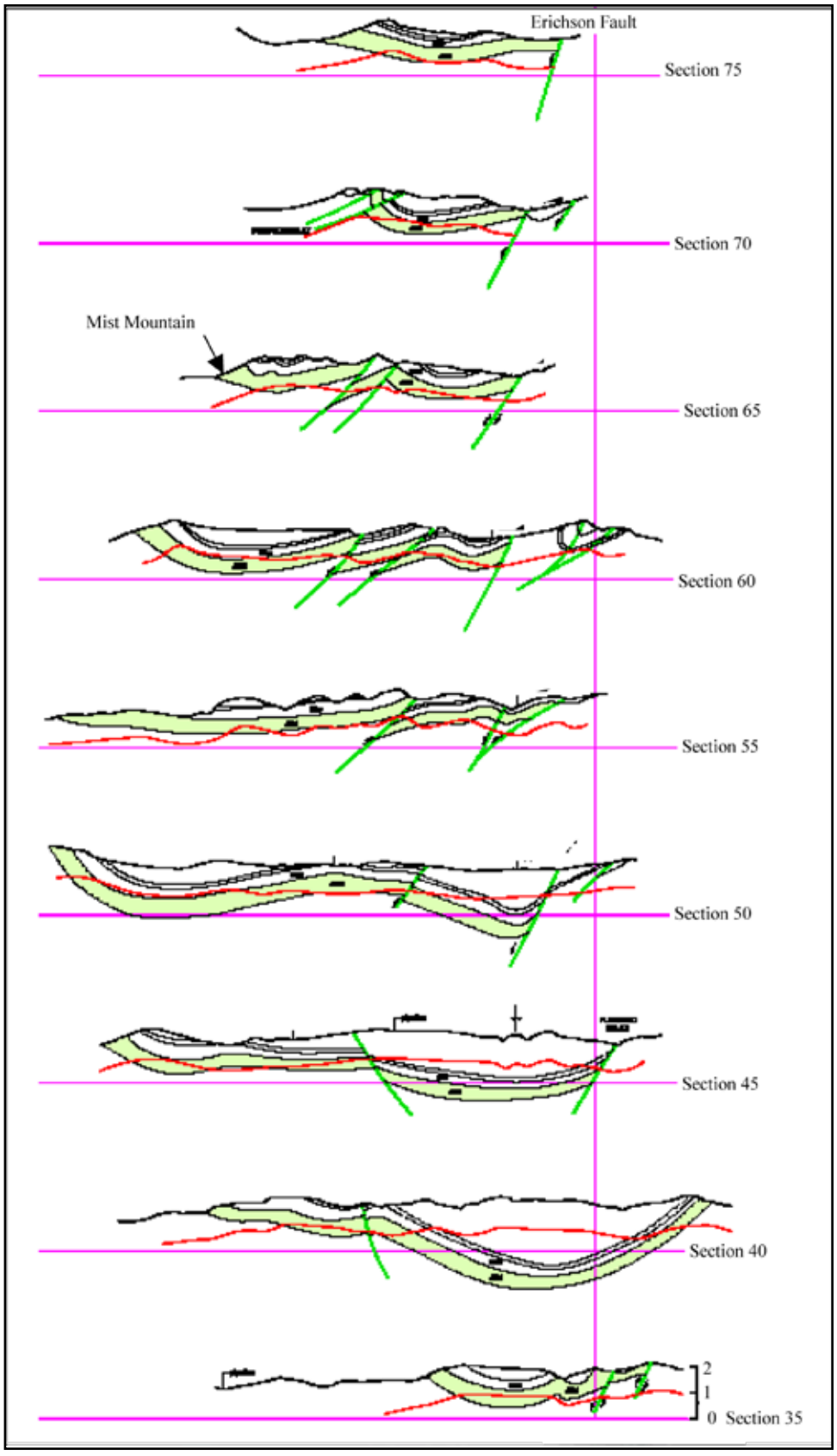

Figure 2. Schematic sections of Crowsnest coalfield.

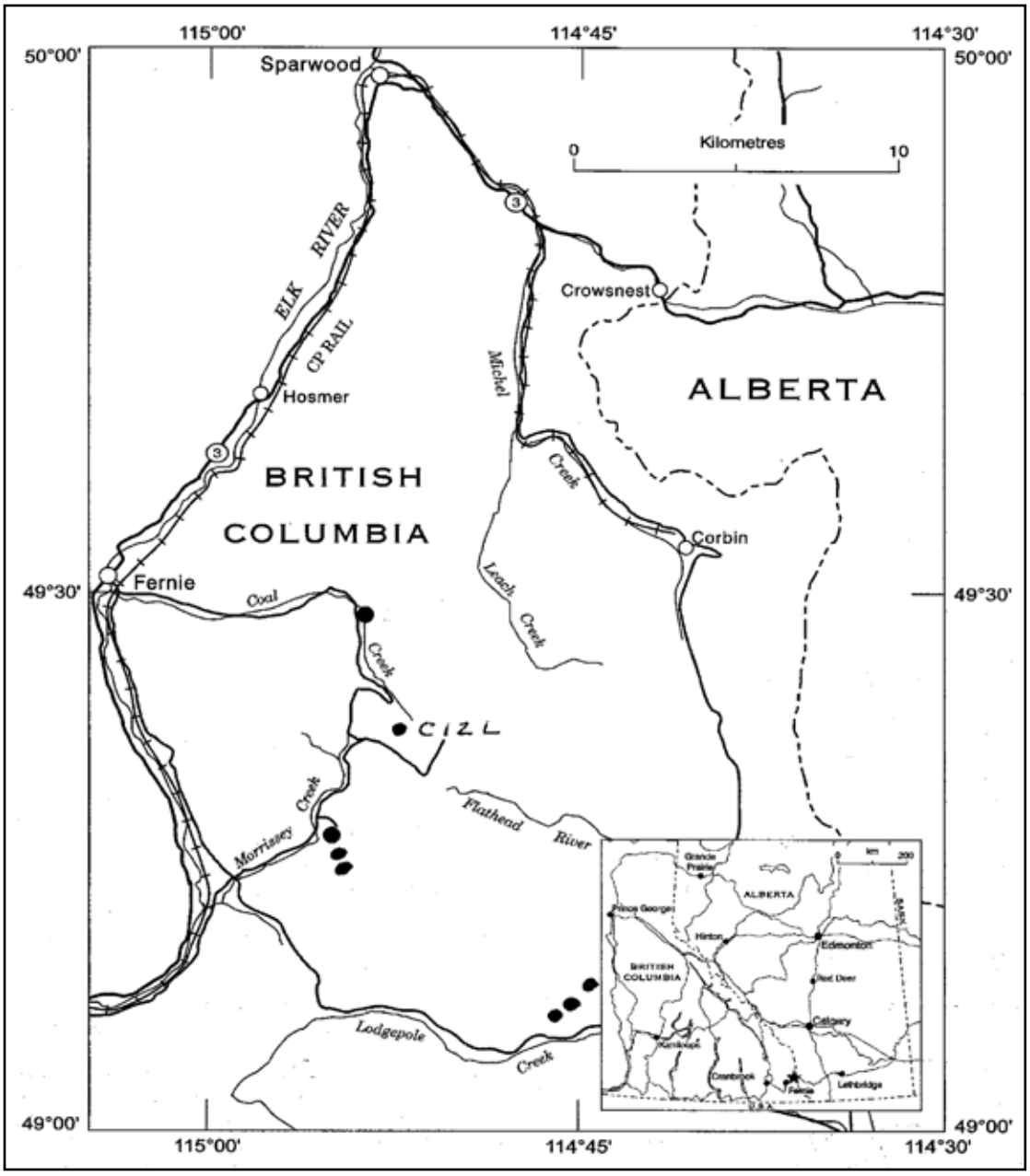

Figure 3. Location of stratigraphic test holes drilled in 1990; data from Dawson et al. (2000).

than 1000 m), providing a resource shallower than 1000 m of 4.28 Tcf. They used estimated gas contents of 16 and 18 cm^3/g applied to all seams (Table 1). The specific seam thickness and gas content values used by Dawson *et al.* (1998) seem to be high, based on available desorption data (Figure 4) and on cumulative coal thickness data for the Crowsnest coalfield as a whole (Table 2).

Dawson *et al.* (1998) used the seam designation applied to the northern part of the Crowsnest coalfield where the basal seam is number 10. Some papers (for example, Newmarch, 1953) designate the basal seam in the Crowsnest coalfield as 1 Seam and count up section. People checking literature on coal in southeast BC should make sure they know the specific seam designation being used in each paper.

STRATIGRAPHY

Any estimation of the depth to the Mist Mountain Formation requires at least some knowledge of the thickness of overlying formations and of the regional dips. In the Crowsnest coalfield, formations above the Mist Mountain include the Elk Formation and Blairmore Group (Figure 5), which includes the basal Cadomin Formation and overlying lower and middle Blairmore rocks. Most authors

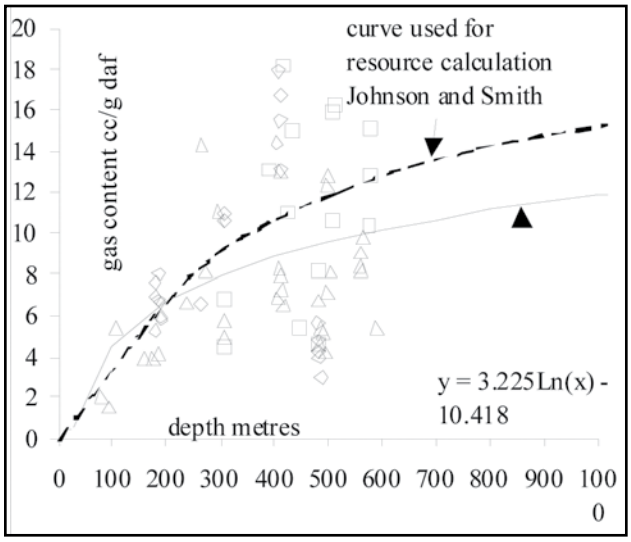

Figure 4. Desorption data for Crowsnest coalfield. Squares are for hole C12L, diamonds from Mobile Chevron holes, and triangles from Saskoil holes.

indicate that the Elk and Mist Mountain Formations thin to the east. Table 3 summarizes some of the thickness information available in a number of papers.

Newmarch (1953) indicates that the Kootenay Group, which includes the Elk and Mist Mountain Formations, varies in thickness along the western margin of the coalfield from 1097 m at Michel to 686 m at Hosmer and 625 m at Fernie. The Kootenay Group is described as 305 to 777 m thick (Crabb, 1957). It thins to the east in the Lewis Thrust block (Price 1964) and is 1076 m at Coal Creek, 488 m at Mt Taylor, and 396 m 12.1 km northeast from the mouth of Lodgepole Creek (Price, 1961).

The Mist Mountain Formation at Coal Creek is described as 645 m thick (Gibsons, 1985) or 629 m thick (Newmarch, 1953). Gibsons (1985) states that it is up to 625 m thick in southeast BC. Pearson and Grieve (1978) provide a number of Mist Mountain sections for the western and southern margins of the coalfield (Table 3) that range from 657 to 490 m in thickness. The overlying Elk Formation varies in thickness up to 488 m (Gibson, 1977; Jansa, 1972).

The Cadomin Formation forms the base of the Blairmore Group and ranges up to 170 m thick (White and Leckie, 2000). The formation is 137 to 168 m thick on the east side of the McEvoy syncline and 184 m thick at Coal Creek. The Blairmore group thins to the east and Crabb (1957) provides thicknesses of 700 m on the west and 300 m on the east. Price (1961) quotes thicknesses of 365 to 2000 m.

The Blairmore Group is overlain by the upper Cretaceous Crowsnest Formation (mainly alkaline volcanics), which is 40 to 100 m thick below the Lewis Thrust but does not occur within the thrust sheet.

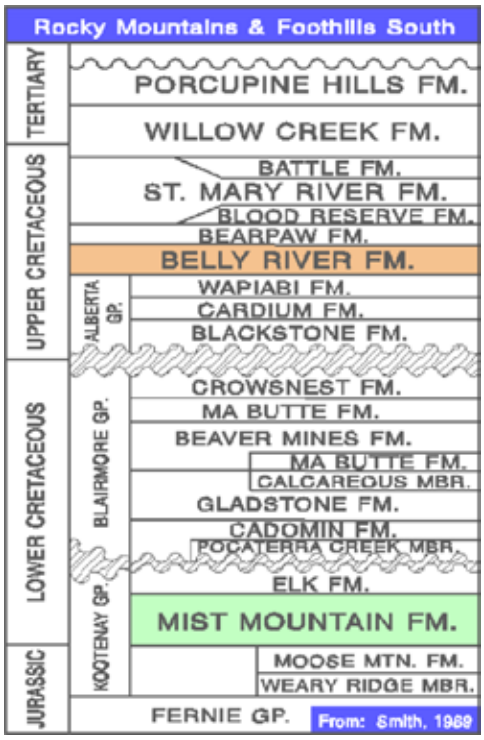

Figure 5: Statigraphic table from Smith (1989).

Outcrops of the Upper Cretaceous Alberta Group survive in the Crowsnest coalfield only in the core of the McEvoy syncline, where it is up to 229 m thick.

Stratigraphic thickness data is essential for estimating depth to the prospective seams in the Mist Mountain Formation. However, thicknesses need to be adjusted to take account of bed dips. As mentioned, strike and dip data are available on a number of published maps and are not reproduced in Figure 1. A simple nomograph (Figure 6), in conjunction with Table 3, provides estimates of drill depth to seams in the Mist Mountain Formation.

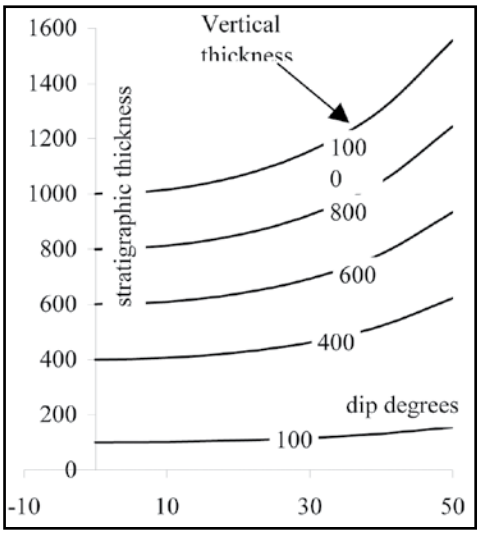

Figure 6. Nomograph of vertical thickness from dip and stratigraphic thickness.

TABLE 1. DOMINION BLOCKS CBM RESOURCE SUMMARY*

block 73

section	A-A	500-1000	metres	A-A	1000-1500		A-A	>1500	
	thick	gas	bcf	thick	gas	bcf	thick	gas	bcf
Elk	1.37	18	9.87	1.37	18	5.17			
1	2.07	18	16.09	2.07	18	7.1			
2U	2.44	18	15.82	2.44	18	7.37	2.44	18	3.84
2L	5.64	18	34.25	5.64	18	16.5	5.64	18	12.95
3	13.71	18	54.79	13.71	18	32.35	13.71	18	72.91
5U	7.32	18	28.79	7.32	18	15.89	7.32	18	41.23
5L	1.52	18	5.88	1.52	18	2.97	1.52	18	9.04
7U	3.66	18	13.13	3.66	18	3.45	3.66	18	27.29
7L	1.52	18	5.5	1.52	18	1.24	1.52	18	13.88
8U	3.5	18	14.87				3.5		27.64
8L	7.32	18	29.71				7.32		58.96
9	20.09	18	60.69				20.09		194.7
10U	3.05	18	8.83				3.05		30.23
10L	6.1	18	17.27				6.1		61.23
totals	79.31		315.49	39.25		92.04	75.87		553.9

Block 83

	Mt Taylor		A-A						
seam	250-500			500-1000			1000-1500		
	thick	gas	bcf	thick	gas	bcf	thick	gas	bcf
1	2.86	16.6	0	2.86	18	6.14	2.86	18	3.61
2	2.13	16.6	0	2.13	18	5.66	2.13	18	1.62
3	7.68	16.6	0	7.68	18	21.84	7.68	18	4.1
4	1	16.6	0.27	1	18	3.18			
5	10.61	16.6	6.19	10.61	18	30.63			
6	1.16	16.6	0.7	1.16	18	3			
7	5.39	16.6	3.11	5.39	18	12.13			
8	13.23	16.6	9.56	13.23	18	23.87			
9	5.79	16.6	4.37	5.79	18	7.66			
10	1.31	16.6	1.16	1.31	18	1.2			
B	2.47	16.6	2.32	2.47	18	1.74			
totals	53.63		27.68	53.63		117.05			9.33

	Mt Taylor		B-B						
seam	500-1000			1000-1500			>1500		
	thick	gas	bcf	thick	gas	bcf	thick	gas	bcf
1	2.86	18	23.47	2.86	18	13.75	2.86	18	6.34
2	2.13	18	16.31	2.13	18	9.34	2.13	18	3.29
3	7.68	18	25.83	7.68	18	33.28	7.68	18	7.48
4	1	18	5.25	1	18	4.26			
5	10.61	18	60.11	10.61	18	42.66			
6	1.16	18	8.57	1.16	18	3.51			
7	5.39	18	45.79	5.39	18	8.56			
8	13.23	18	121.93						
9	5.79	18	49.5						
10	1.31	18	10.24						
B	2.47	18	15.85						
totals	53.63		382.85	30.83		115.36	12.67		17.11

*from Dawson *et al.* (1998).

TABLE 1. CONTINUED

Block 83

	Lookout C-C								
seam	250-500			500-1000			1000-1500		
	thick	gas	bcf	thick	gas	bcf	thick	gas	bcf
1				33.8	18	116.67	33.8	18	63.37
2				5.2	18	27.67	5.2	18	3.41
3				12.2	18	72.98			
5	9	16	20.07	9	18	39.79			
6	4.8	16	14.17	4.8	18	18			
9	2.5	16	6.82	2.5	18	6.14			
10	1.8	16	4.97	1.8	18	3.63			
totals	18.1		46.03	69.3		284.88	39		66.78

	Lookout D-D					
seam	1000-1500			>1500		
	thick	gas	bcf	thick	gas	bcf
1				12.11	18	161.36
2				14.4	18	191.87
3	3.55	18	10.72	3.55	18	35.51
4	11.04	18	55.58	11.04	18	91.89
5	13.07	18	156.16	13.07	18	23.69
7	1	18	13.32			
9	1.7	18	22.65			
10	1	18	13.32			
totals	31.36		271.75			504.32
south extension	54.17	18	612.83	54.17	18	573.65
totals		total	884.58	54.17		1077.97

	Pipeline C-C		
seam	500-1000		
	thick	gas	bcf
1	33.8	18	1410.14
2	5.2	18	216.94
3	12.2	18	508.98
5	9	18	375.48
6	4.8	18	200.26
9	2.5	18	104.3
10	1.8	18	75.1
totals	69.3		2891.2

total <1000 metres 3.42 tcf
total 5.77 tcf

TABLE 2
CUMULATIVE COAL THICKNESSES FOR SECTIONS IN THE CROWSNEST COALFIELD.

seam	Fernie Ridge	Morrissey Ridge	Coal Creek	Hosmer Ridge	West Lodgepole	North Lodgepole	Mclatchie Creek	martin Ridge	Parcel 73
11	4.48	0.00	2.44						
10	2.44	2.32	2.44						
9	3.23	3.38	3.20						
8	6.22	2.19	1.37	1.52					
7	2.99	5.09	0.30	5.79	5.94			1.52	
6	2.77	2.41	0.76	10.67	2.65			6.00	6.10
5	7.25	3.72	5.49	1.83	8.08	6.40		5.43	1.50
4	3.41	4.15	3.81	2.13	6.89	5.79	7.62	2.20	
3	4.02	9.57	2.44	11.58	9.33	7.92	7.47	8.35	11.30
2	6.71	5.49	7.62	5.79				8.02	18.89
1	4.30	7.22	6.10	6.10	14.02	12.19	6.64		
			3.05						
			3.66						
total coal	**47.82**	**45.54**	**42.68**	**45.42**	**46.91**	**32.31**	**21.73**	**31.53**	**37.79**

note seam 11=B seam

TABLE 3
SUMMARY OF STRATIGRAPHIC THICKNESSES FOR JURA-CRETACEOUS UNITS.

location	thickness metres	
		Blairmore Group
Coal Creek	610	Lower Blairmore Price, R.A. (1961)
McEvoy Syncline	365-2000	Blairmore Price, R.A. (1961)
west	700	Blairmore Crabb, J. (1957)
east	305	Blairmore Crabb, J. (1957)
		Cadomin Formation
Coal Creek	185	Jansa, L. (1972)
Michel	731	Jansa, L. (1972)
Coal Creek	32	McLean, J. R. (1977)
		Kootenay Group
lodgepole	549	Price, R.A. (1961)
Mt Taylor	465	Price, R.A. (1964)
West	700	Crabb, J. (1957)
East	305	Crabb, J. (1957)
		Elk Formation
SE BC	up to 488	Gibson, D.W. (1977)
Michel	483	Jansa, L. (1972)
Coal Creek	519	Jansa, L. (1972)
		Mist Mountian Fomraion
Lodgepole	490	Pearson, D.E. and Grieve, D.A. (1978)
Flathead	604	Pearson, D.E. and Grieve, D.A. (1978)
Morrissey Creek	663	Pearson, D.E. and Grieve, D.A. (1978)
Morrissey Ridge	460	Pearson, D.E. and Grieve, D.A. (1978)
Coal Creek	616	Pearson, D.E. and Grieve, D.A. (1978)
Coal Creek	645	Gibson, D.W. (1985)
Coal Creek	617	Jansa, L. (1972)
Coal Creek	629	Newmarch, C.B. (1953)
Fernie Ridge	634	Pearson, D.E. and Grieve, D.A. (1978)
Hosmer	657	Pearson, D.E. and Grieve, D.A. (1978)
Sparwood Ridge	628	Pearson, D.E. and Grieve, D.A. (1978)
Michel	645	Jansa, L. (1972)

COAL SECTIONS

There has been very limited exploration in the centre of the coalfield where the Mist Mountain Formation does not outcrop; consequently; most of the information on seam thickness and cumulative coal thickness in the Mist Mountain Formation comes from mapping, exploration, and mining along the western and southern margin of the coalfield. There are a number of partial coal sections described for the purpose of estimating mineable reserves. It is probable that in many cases these sections do not document all coal in the formation, so that cumulative coal thicknesses probably represent minimum values. Data (Table 2 and Figure 7) indicate that cumulative coal thicknesses range from 40 to 50 m on the west and from 30 to 40 m on the east. Seams generally decrease in thickness up section, and the third or second seam from the base is usually the thickest.

COAL RANK AND MACERAL DATA

Coal rank varies from high-volatile bituminous to low-volatile bituminous, increasing down dip to the east and along strike to the south (Pearson and Grieve, 1985). There is also evidence that rank increases down dip into the core of the major syncline that crosses Morrissey Creek. If rank increases down dip into major synclines, then upward migration of biogenic methane may saturate up-dip lower-rank coal within a seam, leaving the deeper, higher-rank parts of a seam undersaturated. Obviously production from a shallow saturated seam with lower gas content is more economic than production from a deeper undersaturated seam with higher gas content. Rank gradients (ΔRmax/100 m) range from 0.01 to 0.12 (Figure 8).

Adsorption characteristics of seams are controlled by environmental factors (depth and temperature) and physical properties such as rank and maceral content. Jura-Cretaceous coals in southeast BC differ from many coals now producing CBM in that they have high and variable contents of organic inert macerals on a mineral-matter-free-basis (mmfb). These are grouped under the name inerts and include in part the macerals, fusinite, semifusinite, inertodetrinite, and macrinite. Various subvarieties of the vitrinite maceral make up the rest of the seam on a mineral-matter-free basis. The inert macerals, when compared to the vitrinite macerals, are characterized by lower adsorption ability, higher diffusivity and greater strength. The inert maceral content of seams (mmfb) varies and tends to increase down section with rank (Figure 9), though it is usually the second or third seam above the base of the section that contains the highest inert maceral content. There is also a tendency for the upper parts of seams to be vitrinite-rich. The lower parts of seams with higher inertinite content will have better diffusivity and may be less sheared.

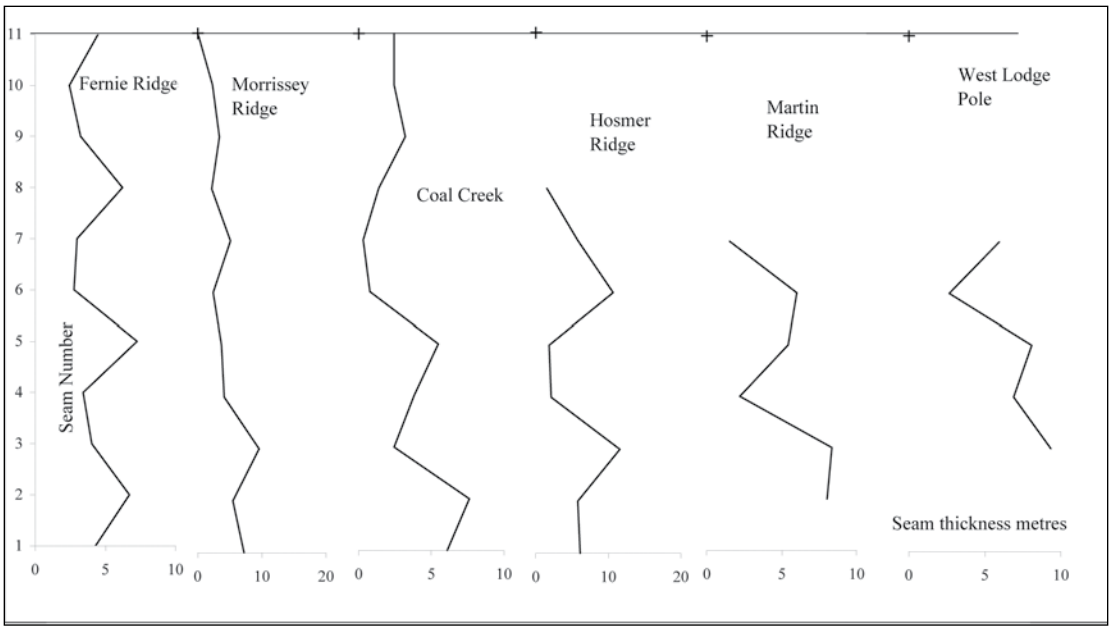

Figure 7. Plot of seam thicknesses by seam number.

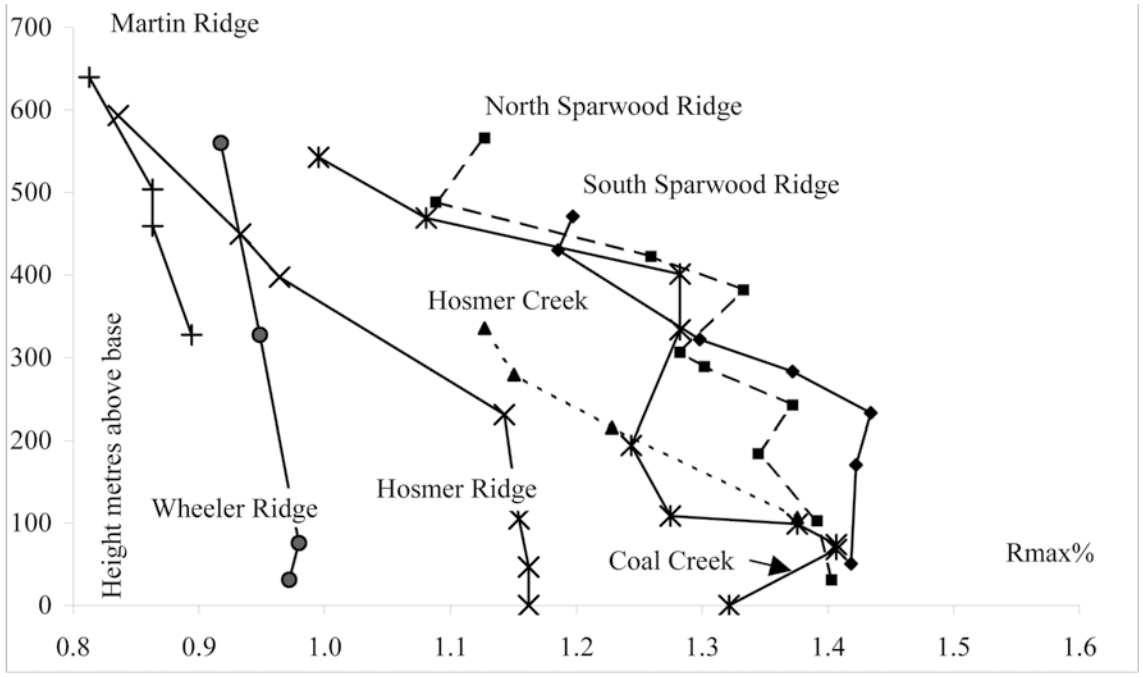

Figure 8. Rank gradients in the Crowsnest coalfield.

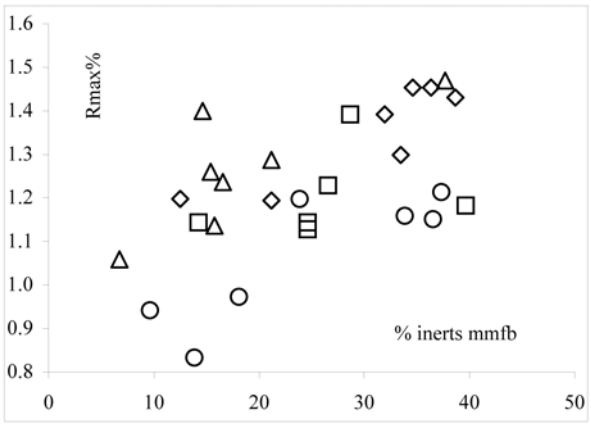

circle=Hosmer Ridge triangle =Sparwood North
square=Hosmer Creek diamonds=Sparwwod South

Figure 9. Variation in inerts content (mmfb) with rank.

CBM RESOURCE AREA

Experience in moderately deformed coals indicates that, except in unusual structural environments, reasonable permeability (greater than 2 mD) does not extend below about 1000 m. Areas where at least the top of the Mist Mountain Formation is less than 1000 m from surface are outlined on the map derived from Johnson and Smith (Figure 1) and in the accompanying sections (Figure 2).

The eastern margin of the Crowsnest coalfield is in part defined by the Erickson/Flathead normal fault system, which, by down-dropping the Kootenay Group on the west by 1000 to 3000 m, has preserved the coalfield. A simplified structural model of the coalfield is represented by two thrust blocks, each containing a north-trending syncline. The Sparwood syncline (Dawson *et al*., 1998) in the north and the McEvoy syncline in the south (Price, 1961) are the dominant structures in the block below the Lookout/Dominion thrust and above the Erickson/Flathead normal fault. Above the Lookout/Dominion thrust, the tight Hosmer syncline (Dawson *et al*., 1998) is cut off by a thrust north of Hosmer. To the south the syncline opens up, has very flat limbs, and merges with the flat limb of the McEvoy syncline.

Within these two synclinal trends, there are obviously areas where seams are too shallow to contain gas. This depth depends on topography and groundwater flow patterns. Ideally, groundwater flow should be down dip and away from seam outcrop. Generally, seams below 200 m and not intersected close to valley walls or above valley floor should contain gas; consequently, areas where Mist Mountain Formation seams are within 200 to 1000 m of surface are most prospective for CBM. There is insufficient structural control to accurately delineate the 200 m depth to the Mist Mountain Formation. As a conservative approximation, the formation is assumed to be at a depth greater than 200 m wherever it was overlain by the full thickness of the Elk Formation, which varies in thickness up to 488 m (Gibson, 1977). This line is easy to mark on Figure 1 and, with data from the sections (Figure 2), helps to delineate the area prospective for CBM. Figure 1 also locates the two Dominion Blocks (73 and 82) and areas where companies have freehold coal rights. Data are derived from standard 1:50 000 topographic maps and Grieve and Kilby (1989).

It appears that potential exists in three areas where the crown has gas rights. These areas are

a) the headwaters of Bray and Martin Creeks.

b) Dominion Block 73.

c) west of Dominion Block 82 and the southwest part of the block.

Area A

The main area where the BC government has the gas rights covers the headwaters of Bray and Martin Creeks, north of Coal Creek (Figure 1). The area includes parts of Block 82 and skirts the freehold blocks in the centre of the coalfield. The area is about 93 km^2. The area overlies the west limb of the Coal Creek syncline, which is traced north from the headwaters of Coal Creek. In the north it plunges to the southwest at 10° to 30° (Armstrong *et al*., 1976), with dips on the limbs increasing to the north. In the south, the syncline plunges to the north (Price 1961). The Dominion thrust progressively cuts off the east limb of the syncline and it is not present in Dominion Block 73.

The west limb of the syncline is steep and overridden by a number of thrusts. There are probably more thrusts than are mapped, and they will tend to seal seams so that up-dip migration of gas to the west will be limited and water movement in seams will probably be along the up-plunge direction of the syncline, either to the north or south. Steeply dipping seams below thrusts probably initially developed west-dipping shear surfaces that, as the seam is rotated, become near horizontal. A vertical hole drilled into these seams will intersect an extended apparent thickness of coal with near-horizontal fractures. Fracing of these seams at shallow depth will open up the fractures in directions extending along strike to the north and south. Drainage areas may extend along strike and not up and down dip. Holes may access structural traps below west-dipping thrusts. Also, as hydrostatic pressure is decreased, the effective lithostatic pressure will be somewhat reduced because of the increased amount of low-density coal in the vertical column.

Mining occurred from 1908 to 1914 west of an area near Hosmer Creek. Portals were driven through the Fernie Formation into the Mist Mountain Formation, which contains at least 10 seams, and the basal Number 1 Seam was mined for a time. The Mist Mountain Formation is

described as 762 m thick with 79 m of coal (Armstrong, *et al.,* 1976); however, these may be apparent rather than true thicknesses, based on thicknesses quoted elsewhere (Tables 2 and 3), which indicate true cumulative coal thicknesses ranging from 45 m at Hosmer to 31 m on Martin Ridge. The rank at Hosmer Creek ranges from 0.95% to 1.19%, with a gradient of 0.12 ΔRmax per 100 m and to the east on Martin Ridge from 0.83% to 0.91% (gradient 0.03 ΔRmax per 100 m). To the north in Dominion Block 73, rank of the basal seam is 1.16% (Grieve and Kilby, 1989). In the past, there was a lot of exploration and mining to the south in the Coal and Morrissey Creeks and adjacent areas. In these areas, the Mist Mountain section contains between 45 and 48 m of coal dispersed in about 11 seams.

Gulf Canada drilled a 590 m stratigraphic test hole (hole C12L, Dawson *et al*., 2000) (Figure 3) south of the area at the head waters of Martin and Coal Creeks. The hole intersected 24.4 m of coal in the top 280 m of the Mist Mountain Formation. It was drilled west of a major thrust into an area where the Mist Mountain Formation is flat dipping. Gas contents indicate that coals are undersaturated, but gas contents were higher than they were in holes drilled by other companies further to the south. Data for coals near the bottom of the hole indicate that coals are close to saturated. These seams are in the mid part of the Mist Mountain Formation section. The lowermost coal was the thickest, and this may correspond to Seam 5 in the Morrissey and Fernie Ridge sections, in which case the coal remaining lower in the section would be between 18 and 24 m cumulative thickness, providing a possible total cumulative thickness between 42 and 48 m.

No detailed estimates of the coal resources in Area A (delineated in Figure 1) exist. However, mining studies estimate a coal resource on Hosmer Ridge of about 700 million tonnes to 760 m. Alternatively, the resource can be estimated by utilizing the area of 93 km^2 and a cumulative coal thickness of 45 m; this provides an estimated coal resource of 5200 million tonnes.

The average gas content of the Gulf Canada hole is about 10 cm^3/g on an as-received basis. This is probably a low average value to use for resource estimates; however, the value of 18 cm^3/g used by Dawson *et al.* (1998) may be high. Using the lower gas content of 10 cm^3/g provides an estimated in-place resource of about 1.6 Tcf.

Area B

The Dominion Block 73 covers an area of 20.23 km^2. Dawson *et al.* (1998) calculated a CBM potential resource of 0.32 Tcf to 1000 m (Table 1). They provide a 750 m thick stratigraphic section of Mist Mountain that appears to contain over 70 m of cumulative coal. Grieve and Kilby (1989) identified a section of 480 m, which excludes seams number 1 and 2 and contains 37.8 m of coal up to and including 3 Seam. The basal seam has a rank of 1.16%, but ranks appear to increase down dip and definitely increase to the south.

Structurally, most of Block 73 is in a thrust block below the Dominion/Lookout thrust and east of area A. The structural style is similar to that of area A, being a syncline with steep-dipping west limb and shallow east limb. Opportunities for thrust-generated traps in the steep-dipping west limb exist. The syncline is along the trend of the McEvoy syncline to the south and Sparwood syncline to the north. The Sparwood syncline trends across Michel Creek to the north, where it becomes the Elk syncline in the Elkview coal mine north of Highway 3 at the north end of the Crowsnest coalfield.

The coal potential was analyzed by Grieve and Kilby (1989), who used seams with a cumulative thickness of 37.8 m in their study. The thickness of coal available for CBM resource calculations is probably between this thickness and that used by Dawson *et al.* (1998). They provide a total coal resource in the block of about 1 billion tonnes, which agrees with the estimate provided by Latour (1970). The tonnage estimated to be shallower than 1000 m is 550 million tonnes. Dawson *et al.* (1998) used an average gas content of 18 cm^3/g for all coal deeper than 250 m and calculated a gas resource of 0.32 Tcf. Using a lower gas content of 10 cm^3/g (320 scf/t), this resource decreases to 0.18 Tcf.

Area C

In the south, the southern extension of the Hosmer syncline is ill-defined, and dips west of Morrissey Ridge are flat. There is an extensive area where the Mist Mountain Formation is flat dipping and, at least in part, shallower than 1000 m. There are also some areas where the formation on the west limb of the McEvoy syncline is shallower than 1000 m. In this area, the offset on the Lookout/Dominion thrust reverses, and it is shown on sections in the south as a normal fault (Figures 1 and 2). If this interpretation is correct, then the southern area west of the fault should have experienced extension at the time of faulting and may still have better permeability on cleats.

Most of Area C is within Block 82 with some of the area on the southwestern margin of the block. The total area is about 51 km^2. Block 82 has a CBM resource potential of 3.42 Tcf to 1000 m (Dawson *et al,* 1998), and most of this is in the Pipeline area (Table 1) in the southwest, where the pipeline crosses the area trending north through the coal field. The centre and northern part of the block is underlain by the McEvoy syncline, which is cored by the Blairmore Formation and younger rocks. Based on the presence of these formations and their thicknesses, the Mist Mountain Formation is over 1000 m deep in the core of the syncline.

In the southwest of Block 82, there is an area where the east limb of the southern extension of Coal Creek syncline is flat and partially within the 1000 m depth window. Small changes in the structural interpretation could change the resource assessment significantly.

Saskoil (Dawson *et al.,* 2000) drilled two holes in 1991 in the Lodgepole Creek area. The holes were drilled near the subcrop in different parts of the Mist Mountain Formation. By combining the data from the holes, it appears that in the area, the full Mist Mountain section is 500 m thick and contains a cumulative coal thickness of 63 m. To the west, the cumulative coal in the section at Coal Creek is 42.7 m and at Morrissey Ridge is 45.5 m.

The rank of coal to the west under Fernie and Morrissey Ridges ranges from low-volatile bituminous to high-volatile bituminous (Figure 8). The vitrinite reflectance values are 1.45% for the basal seam at Morrissey Creek, decreasing to 1.38% at Coal Creek. However, rank appears to increase down dip to the east into the syncline (Pearson and Grieve, 1978).

Gas contents of samples from the holes drilled by Saskoil were low but are probably not representative of contents further to the northeast. For the purposes of calculation, an assumed gas content of 10 cm^3/g (320 scf/t) is used. This is considerably lower than the value used by Dawson *et al.* (1998), but is approximately the average gas content for samples from hole C12 L drilled by Gulf (Figure 3).

Based on an area of 51 km^2, 50 m cumulative coal, and a gas content of 10 cm^3/g, the CBM resource is 1 Tcf.

ESTIMATED RESOURCE AVAILABLE ON CROWN LANDS

The total resource estimated in the three areas is 2.78 Tcf (Table 4). This is an estimate of the gas resource available in all the coal in the section to a depth of 1000 m. It is derived using a conservative gas content value but assumes that all the area outlined is underlain by the full coal section, and this is probably an optimistic assumption. Other than the order of magnitude size of the 2.78 Tcf resource and the general areas to which it is assigned, not too much significance should be attached to its value. Companies interested in fine-tuning estimates of the resource potential in the coalfield should use the process and references outlined in this paper as a guide and complete their own assessment. In terms of the available reserve, this will depend on the presence of permeability and on the number of seams in the section that can be economically drained of gas.

COAL QUALITY AND IMPLICATIONS FOR CBM PRODUCTION

If higher-rank coals are to achieve gas saturation or near gas saturation at present depths, then it is probable that a large component of the gas will be biogenic. One should therefore consider the conditions that favour generation and retention of biogenic gas, which is generated on coal surfaces and then penetrates the microporosity to be adsorbed. Excessive water movement will limit the ability of biogenic gas to migrate into coal microporosity and to be adsorbed. Some seams in the Crowsnest coalfield are sheared, which increases surface area available for bacteria but limits the ability of a seam to maintain permeability when hydrostatic pressure is decreased. In situations where biogenic gas is generated down dip within a syncline limb, introduction of hot CO_2 could initiate up-dip movement of water, CO_2 in solution, and methane without any decrease in hydrostatic pressure. Hot CO_2 would be readily available from a coal-fired power plant.

Coal petrography varies, and seams lower in the section contain more inertinite on a mineral-matter-free basis. However, it is often the third seam above the Moose Mountain Member that contains the most inertinite (Pearson and Grieve, 1978). The inertinite content of seams varies from hanging wall to footwall, with the lower parts of seams having consistently higher inertinite contents (Pearson and Grieve, 1985). As a maceral group, inertinite is stronger than vitrinite and resists shearing better. It has lower adsorption abilities and higher diffusivities. These properties may be advantageous for CBM recovery. In thick seams that are initially undersaturated, but in which biogenic methane is being generated in the microfractures of the coal, inert macerals will reach re-saturation sooner because of lower demands and better diffusivity of methane from microfractures into the micropores. A seam may therefore be partitioned with the lower inertinite-rich part being satu-

TABLE 4. CBM RESOURCES WHERE THE CROWN HAS GAS RIGHTS.

	Reference	gas content cc/g	tonnage billion tonnes	total gas tcf
Area A	south of Dominion Block 73	10	2.2	0.7
Area B	Dominion Block 73	10	560	0.18
Area C	part of Dominion Block 82 and area to west	10	6.55	2.1
		total	**568.75**	**2.98**

rated at a moderate gas content and the upper vitrinite-rich part being undersaturated, possibly with the same gas content. Completion in the whole seam may result in no gas reaching surface, because gas released from one part of the seam may be adsorbed by another part. Completion in the inertinite-rich lower part of the seam may result in immediate gas production. The higher diffusivity and strength of the inertinite should help it maintain fracture opening and permeability despite the fact that there is probably less matrix shrinkage to aid permeability.

In the Elk Formation, there are some thin coal seams, which are generally less than 1 m thick and are characterized by high liptinite contents. They are often referred to as needle coals because of their structure, which derives from a high algae content. They tend to be better developed near the Mist Mountain contact. Coals of this type generate large quantities of thermogenic methane at ranks of 0.6% to 1.0%. The liptinite macerals are not very microporous, so that they have lower adsorption abilities than other macerals. However, the maceral is less brittle than vitrinite and tends to withstand deformation better. In areas where the Mist Mountain is below prospective depths, the overlying Elk Formation, which contains a higher sand content than the Mist Mountain Formation, may well contain free gas in sandstones and adsorbed gas in thin coal seams.

HISTORICAL DATA

In 1939, the Minister of Mines Report states that in the Coal Creek Number 1 Colliery "a considerable amount of methane is given off this amounting to an average of 1250,000 cubic feet in 24 hours". Elsewhere in the report, it states that ventilation was 74 300 cubic feet per minute. The numbers suggest that the methane content in the mine air was upwards of 1%. McCulloch *et al.* (1975) indicate that there is an approximate empirical relationship between the amount of methane per tonne released for a mature mine and the in-place gas content of the coal (Figure 10). The relation predicts that the in-place gas content (cm^3/g) is one-seventh the gas emission per tonne of mined coal. In 1939, coal production in the East Kootenays was about 500 000 tonnes, and production from the Number 1 East Colliery, Coal Creek, was 124 616 tons (Newmarch, 1953). If this tonnage is assigned to the Number 1 mine, and it operated for 300 days in the year, then the predicted gas content is over 13 cm^3/g. The Number 1 seam (lowest in the section) was reported to be the gassiest seam mined. There are a number of reports indicating that the coal from the Coal Creek Collieries was gassy and dusty.

The Carbonado Colliery (6.5 km up Morrissey Creek from the Elk River), which opened in 1902, is described as being very gassy and prone to outbursts. It was closed in 1909 after a number of severe gas outbursts. Other reports indicate that seams low in the section were very fractured and produced a lot of fine coal.

There are very limited public data on CO_2 concentrations in coals in the Crowsnest coalfield. A report (Rice, 1918) provides some analyses. In 1916, five

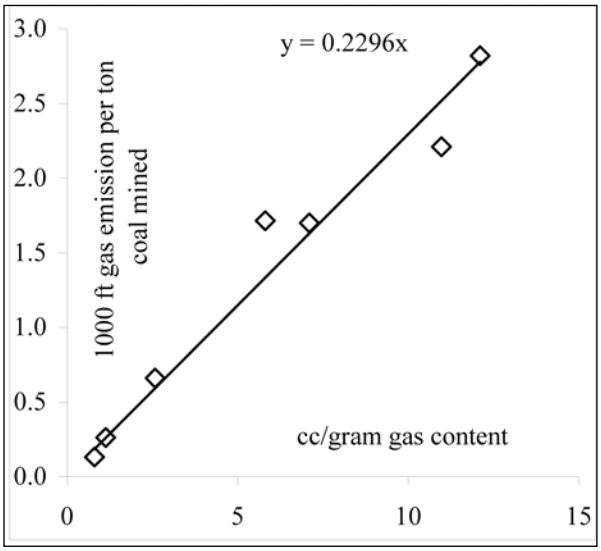

Figure 10. Relationship of gas released in underground mine and adsorbed gas content plot; derived from McCulloch *et al*. (1975).

samples were collected from the working face in the underground Coal Creek Colliery and placed into sealed jars (Table 5). When the gas was analyzed, it was apparent that all had leaked; however, the CO_2 content may be estimated from the $CO_2/(CH_4+CO_2)$ ratio, and it appears that, except for one sample, CO_2 contents were probably less than 5% (data are reported as cm^3 per 100 g, equivalent to mole fractions). Based on the trace of the Bourgeau thrust relative to the outcrop of the basin (Monahan, 2002), it appears that seams in the Mist Mountain Formation in the Crowsnest may not have been as close to carbonates in the overlying Bourgeau thrust plate as seams in the Elk Valley coalfield were and may therefore have lower CO_2 concentrations.

TABLE 5
ESTIMATED GAS COMPOSITION.

sample	CH_4	CO_2	O_2	N_2	$CO_2/(CO_2+CH_4)$
17	64.1	1.4	1	33.5	2.1
18	24.6	0.9	4.4	70.1	3.5
19	27	1.2	3.2	68.6	4.3
20	15.8	0.4	1.2	82.6	2.5
21	0.3	1.6	20	78.1	84.2

Data from Rice (1918). Composition of gas in coal samples, volume percent. Samples from working faces of Coal Creek Colliery (1916), Coal Creek, Crowsnest coalfield.

COAL DEFORMATION AND IMPLICATIONS FOR CBM PRODUCTION

The Crowsnest coalfield is folded into a series of north-trending anticlines and synclines, which generally have steep-dipping west limbs and shallower-dipping east limbs. Folds open to the south, indicating less east-west compression of the coalfield in that direction. They are contained in a number of north-trending blocks defined by thrusts and normal faults. On the east, the major fault system is composed of the Erickson and Flathead normal faults, and on the west, it is the Lookout/Dominion thrust system. The folds reverse plunge through the basin, with the McEvoy syncline in the south forming a distinct basin, and the Coal Creek syncline forming a basin under Fernie Ridge. The map of Price (1961) indicates a number of plunge reversals for folds; it is not clear whether these are related to a later phase of cross folding or are controlled by changes in stratigraphic thickness. Obviously if they are related to a later stage of cross folding, then this could cause extension and improved permeability in areas where the cores of synclines or anticlines form culminations.

The Crowsnest coalfield forms part of the Lewis Thrust sheet, which in southeastern BC was transported between 140 and 200 km at a rate of about 1.5 cm per year (Osadetz *et al*., 2003). Movement took place in the period from 74 to 59 Ma, as is indicated by profound cooling in the thrust block at about 75 Ma (Osadetz *et al*., 2003). This movement is documented by analyzing the displacement on the thrust plane; however, there was also probably bedding plane slip within the thrust sheet, which would, over the estimated 7 km thickness of the sheet, (Osadetz *et al.,* 2003) account for more displacement.

Some of this additional displacement is hidden in the Fernie Formation, in that rocks below the Fernie Formation are more folded than are the overlying Kootenay Group and fold geometries are offset (Price 1961). Additional displacement almost certainly occurred along coal seams. Bedding plane movement along seams will increase coal fragmentation, and its amount will not be related to the degree of any subsequent folding. If the coal was maturing through high-volatile bituminous rank at the time of thrust displacement, it would be very susceptible to bedding-plane slip.

In-seam shearing related to Lewis Thrust movement and not to folding produces fine coal and inhibits the formation of cleats or destroys those that have formed. It plays a key role in limiting permeability and causing production problems. It is therefore important to consider what factors might limit the amount of shearing in seams. Some examples of seams that may resist shearing are:

- Thinner seams
- Seams rich in inert macerals or liptinite
- Seams that attain high rank before thrusting started
- Seams with higher ash content
- Seams with clay-poor hanging walls and footwalls.

There have been a number of studies of coal seam deformation in the northern part of the Crowsnest coalfield. Norris (1965) studied A Seam in underground A-North mine at the north end of the coalfield. This seam is approximately 420 m above the basal Balmer or 10 Seam in the Mist Mountain Formation. He describes the seam as being highly sheared, with abundant shear surfaces and intrastratal folds. Joints tended to strike north or northwest with evidence of early minor extension faults cut off by renewed bedding-plane slip. He does not directly discuss cleats or the degree of shearing in the seam, but the impression is left that the seam is highly sheared and fragmented.

Bustin (1982) studied the lowest seam in the Mist Mountain Formation in a number of underground coal mines (Balmer North, Five Panel, and Six Panel) at the north end of the Crowsnest coalfield. In the Balmer North mine, the best-developed cleats formed acute angles to bedding, striking northwest and dipping shallowly to the southeast. Cleat surfaces were polished and striated. Other cleat sets were measured but did not have a consistent orientation through the mine. Cleats in the Five and Six Panel mines are more consistent with a set striking north to northwest with a steep dip to the west. These cleats are subperpendicular to bedding and trend parallel to the regional fold axis. All fractures and most cleats in the seam appear to have a tectonic influence, with surfaces polished and often showing evidence of shearing. However, their orientations are not easily related to a regional stress field. Thrusting probably started with differential movement between the roof and floor (Norris, 1965) that disrupted earlier extension faults. As seam thickening and thrusting progressed, exogenetic fractures with fold axis-parallel trends and variable dips to the west developed in the coal.

SUMMARY

The Crowsnest coalfield is an area of 600 km^2 underlain by the Jura-Cretaceous Mist Mountain Formation, which contains from 30 to 60 cumulative metres of high-volatile to low-volatile bituminous coal. The combination of area and cumulative coal guarantees a large resource of coalbed methane, which has been estimated at 12 Tcf. However, outlining a resource is a far cry from defining a reserve. The coalfield forms part of the Lewis Thrust sheet and has therefore had a protracted deformational history, which started with thrusting followed by folding in the late Cretaceous and continued with extension on north-trending major faults in the Tertiary. The thrusting caused shearing within some seams that is unrelated to the amount of subsequent folding. This has probably limited permeability and generated fine coal that will make production more difficult.

Successful production will probably rely on understanding the interplay between deformation coal quality and location in specific structures. With these caveats in mind, the more prospective area is where the Mist Mountain Formation is in the depth window of approximately 200 to 1000 m. The Crown has clear title to the CBM in part of this area (Figure 1), and it is within this sub-area that a more detailed assessment of the CBM resources has been made. The value of about 3 Tcf defines the size of a box within which, hopefully, reserves can be located.

A number of ideas relating structure, coal quality, and CBM are proposed that may help explorationists zero in on areas where reserves are located.

ACKNOWLEDGEMENTS

Bob Morris was kind enough to read the manuscript and correct some of the more obvious errors in the original draft.

REFERENCES

Armstrong, W.M., Fyles, J.T., Guelke, C.B., MacGregor, E.R., Peel, A.L., Thompson, A.R. and Warren, L.H. (1976) Coal in British Columbia, A technical Appraisal*; Coal task Force,* Report of the Technical Committee.

Bustin, R.M. (1982): Geological factors affecting roof conditions in some underground coal mines in the southeastern Canadian Rocky Mountains; *Geological Survey of Canada,* Paper 80-34.

Crabb, J. (1957): a summary of the geology of the Crowsnest coalfields and adjacent areas; *Alberta Society of Petroleum Geology* 7th annual field conference Guide book

Dawson, F.M. Marchioni, D.L. Anderson, T.C. and McDougall, W.J. (2000): An assessment of coalbed methane exploration projects in Canada; *Geological Survey of Canada,* Bulletin 549.

Dawson, F.M., Lawrence, G.F. and Anderson, T.C. (1998): Coalbed methane resource assessment of the Dominion coal blocks southeast British Columbia; *Geological Survey of Canada,* Open File 3549.

Gibson, D.W. (1977): Sedimentary facies in the Jura-Cretaceous Kootenay Formation, Crowsnest Pass area southwestern Alberta and southeastern British Columbia, Bulletin of the *Canadian Petroleum Geology*, Volume 25, pages 767-789.

Grieve, D.A. and Kilby, W.E. (1989): Geology and coal resources of the Dominion coal block southeastern *British Columbia; Ministry of Energy and Mines,* paper 1989-4.

Jansa, L. (1972): Depositional history of the coal-bearing Upper Jurassic-Lower Cretaceous Kootenay Formation Southern Rocky Mountains, Canada*; Geological Society of America,* Bulletin, Volume 83, pages 3199-3222.

Johnson, D.G.S. and Smith, L.A. (1991): Coalbed Methane in southeastern British Columbia; *British Columbia Ministry of Energy and Mines, Petroleum Geology Branch,* Special paper 1991-1.

Latour, B.A. (1970): Coal deposits of the dominion government coal block Fernie area British Columbia*; Department of Energy Mines and Resource, Geological Survey of Canada,* Report.

McLean, J,R. (1977): The Cadomin Formation Stratigraphy, sedimentology and tectonic implications; Bulletin of the *Canadian Petroleum Geology*, Volume 25, pages 792-827.

McCulloch, C.M., Levine, J.R. Kissell, F.N., and Deul, M. (1975): Measuring the methane content of bituminous coals; United States department of the *Interior Bureau of Mines* report 8043.

Monahan, P. (2002): The Geology and oil and gas potential of the Fernie-Elk Valley Area, southeastern *British Columbia, Ministry of Energy and Mines.*

Newmarch, C.B. (1953): Geology of the Crowsnest Coal Basin; *British Columbia Department of Mines*, Bulletin Number 33.

Norris, D.K. (1965): Structural analysis of part of the north A-North Coal Mine Michel, British Columbia; Geological Survey of Canada, Paper 64-24.

Osadetz, K.G., Kohn, B.P. Kohn, Feinstein, S. and R. A. Price (2003): Aspects of foreland belt thermal and geological history in southern Canadian Cordillera from fission-track data, *Petroleum Geology Special Paper 2002-2*

Pearson, D.E. and Grieve, D.A. (1977): Coal Investigations, Crowsnest coalfield; *BC Ministry of Energy and Mines* pages 47-54.

Pearson, D.E. and Grieve, D.A. (1978): Petrographic evaluation of the Crowsnest Coalfield; *Canadian Institute of Mining and Metallurgy,* Annual General meeting Vancouver 1978.

Pearson, D.E. and Grieve, D.A. (1978): Preliminary geological map of the Crowsnest Coalfield, west part*; BC Ministry of Energy and Mines*, Preliminary Map 27.

Pearson, D.E., Gigliotti, F.B. Ollerenshaw, N.C., and Grieve, D.A. (1977): Preliminary map of the Crowsnest coalfield northwest part; *BC Ministry of Energy and Mines,* Preliminary Map 24.

Pearson, D.E. and Grieve, D.A (1980): Coal measures of the Crowsnest coalfield; *BC Ministry of Energy and Mines*, Preliminary Map 42.

Pearson, D.E. and Grieve, D.A (1985): Rank variation, coalification pattern and coal quality in the Crowsnest Coalfield, British Columbia; *Canadian Institute of Mining and Metallurgy* Bulletin, Volume 78, pages 39-46.

Price, R.A. (1961): Fernie map area east half Alberta and British Columbia 82G E1/2; *Geological Survey of Canada,* Paper 61-24.

Price, R.A. (1964): Flathead map area British Columbia and Alberta; Memoir 336.

Rice, G.S. (1918): Bumps and outbursts of gas in the mines of the Crowsnest Pass Coalfield, British Columbia Department of Mines, Bulletin Number 2.

Smith, G.G. (1989): Coal resources of Canada; *Geological Survey of Canada,* Paper 89-4.

White, J.M. and Leckie, D.A. (2000): the Cadomin and Dalhousie formations of SW Alberta and SE British Columbia; age sedimentology and tectonic implications; *Canadian Society of Exploration Geologists* Conference 2000, abstract.

INTERIOR BASINS STRATEGY

By M. Hayes, F. Ferri and S. Morii

Resource Development and Geoscience Branch, B.C. Ministry of Energy and Mines,
6th Flr-1810 Blanshard St., Victoria, BC, Canada, V8W 9N3

KEYWORDS: oil, gas, hydrocarbons, Intermontane, Interior Basins, Nechako, Bowser, Whitehorse Trough.

INTRODUCTION

The government of British Columbia, through the Ministry of Energy and Mines, has a Service Plan goal of achieving a 17% increase in natural gas production and a 31% increase in the number of wells drilled over the next three fiscal years. (*B.C. Ministry of Energy And Mines*: Service Plan [2004/5–2006/7]). One of the key Ministry strategies developed to realize this goal involves improving knowledge of the province's petroleum geology in order to identify new energy development opportunities within British Columbia. The aim of this strategy is to realize B.C.'s ultimate hydrocarbon potential within its relatively under-explored portion of the Western Canada Sedimentary Basin (WCSB) and see development of commercial oil and gas production within its interior and offshore basins. The achievement of these goals will benefit all British Columbians through increases in oil and gas royalties and tenure disposition fees and the creation of new employment opportunities.

The Resource Development and Geoscience Branch is mandated to identify, quantify, and promote the hydrocarbon potential of onshore regions of British Columbia. In addition, the branch undertakes community relations initiatives, including those with First Nations, in areas of hydrocarbon potential.

In onshore regions outside of the WCSB, oil and gas potential occurs primarily within Mesozoic and Cenozoic clastic sediments of the Interior Basins. The main areas include, from north to south, the Whitehorse Trough, the Bowser and Sustut Basins, and the Nechako Basin (Figure 1). In addition, there are several small Tertiary basins (e.g., Hat Creek) and the onshore portions of the Georgia Basin. Although some of these areas have seen limited subsurface exploration (e.g., Bowser and Nechako Basins), they remain 'frontier basins' because of infrastructure challenges and lack of extensive geological information.

Recent publications on the oil and gas resource potential of the intermontane basins suggests upwards of 18.8 trillion cubic feet (tcf; 5.3 x 10^{11} m^3) of gas and 7.6 billion barrels (bb; 1.2 x 10^9 m^3) of oil (Hannigan *et al*., 1994; 1995; 2001). In light of this, the B.C. Ministry of Energy and Mines has undertaken several initiatives to better quantify this potential resource and attract industry investment.

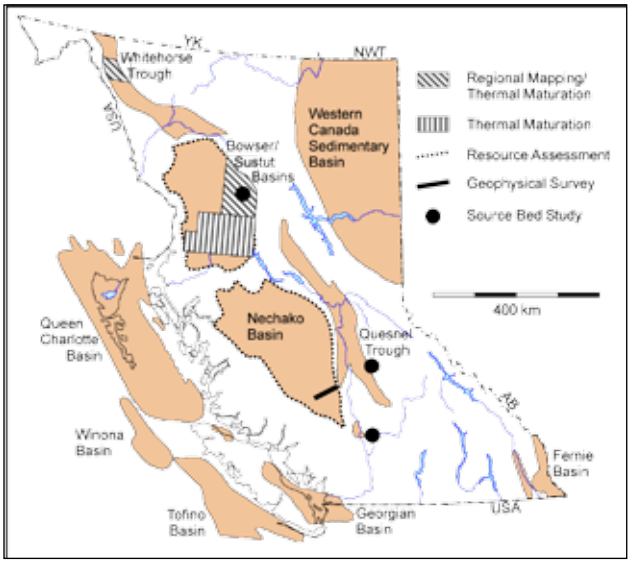

Figure 1. Map of British Columbia showing the outline of its major petroleum basins and location of projects within the Intermontane Basins funded entirely, or in part, by the Resource Development and Geoscience Branch of the B.C. Ministry of Energy and Mines.

NEW INITIATIVES

The Resource Development and Geoscience Branch (RDGB) has initiated or supported several projects within these areas, leading to the capture of new energy-related geoscience information. Projects have started in the Whitehorse Trough and Bowser-Sustut and Nechako Basins.

Whitehorse Trough

In central Whitehorse Trough, English *et al.* (2003, 2004), through a grant to the University of Victoria and in conjunction with the RDGB, have gathered baseline thermal maturation and source rock potential data as part of a more regional mapping program. These new Rock-Eval data have been released as two open file reports (Fowler, 2003, 2004).

Nechako Area and Quesnel Trough

In 2002, the RDGB commissioned Petrel Robertson Ltd. to produce a report on the petroleum exploration potential of the Nechako-Chilcotin area (Hayes, 2002). This paper summarizes current information about surface and subsurface geology and outlines several areas of varying hydrocarbon potential.

Subsequent to this, RDGB entered into a working agreement with the Geological Survey of Canada for a new petroleum resource assessment of the Nechako Basin. This is an ongoing project and has produced several milestone products, including Rock-Eval and total organic content (TOC) analysis of subsurface samples from all interior wells (Osadetz *et al.*, 2003) and new strip logs of all interior wells, incorporating digital well logs and qualitative porosity and permeability descriptions (Thornsteinsson *et al*., in press). In addition, a new heat-flow model is being generated, which, together with new and current information, will be integrated into a new resource assessment.

The lack of a recognized source horizon was one of the shortcomings listed by Hayes (2002) for the Nechako Basin, and this is generally the case for all Interior basins. Ferri (2004) addresses, in part, this issue through sampling of organic-rich Jurassic and Cretaceous sediments within the Quesnel Trough and within the Bowser and Sustut Basins.

The RDGB also acquired new high-resolution gravity and magnetic data along a 30 km transect immediately west of Williams Lake (Figure 1; *see* Best, 2004). The purpose of this survey was to validate the presence of a gravity low delineated by data obtained by Canadian Hunter Exploration Ltd. in the early 1980s (Salt, 1980). One interpretation is that this gravity low represents a thick sequence of sediments, possibly of Tertiary age.

Bowser-Sustut Basins

The Bowser and Sustut Basins potentially represent the largest petroleum exploration target area within the Intermontane region (Figure 1). This area has received renewed interest in the last few years as a result of new thermal maturation data indicating that large portions of these basins are within the oil and gas window (Evenchick *et al.*, 2002). Prior to this, much of the area, particularly the Bowser Basin, was considered to be over-mature with respect to oil and in the upper end of the gas window (Hannigan *et. al.*, 1995). This new data suggests the potential for hydrocarbon resources beyond those described in the report by Hannigan *et al.* (1995).

In light of this new information, the B.C. Ministry of Energy and Mines embarked on a program to better quantify potential resources through the acquisition of new geoscience information. Part of this strategy involved collaborative research with the Geological Survey of Canada, leading to a new resource assessment of the basins. An uplift history of the northern two-thirds of the Bowser and Sustut Basins is being modeled, based on apatite fission track analysis from several localities within the basins (O'Sullivan *et al.*, 2004). Sampling during acquisition of data points for this study led to the discovery of oil staining in several samples, analysis of which suggests the presence of two petroleum systems (Osadetz *et al.*, 2003). Further examination of catalogued surface and subsurface samples and core recognized more oil staining (Osadetz *et al.*, 2004; Evenchick *et al.*, 2004). These occurrences also confirmed the new thermal model generated for these areas.

These new data, together with the impetus from the British Columbia government for more energy-related information in the area, led the Canadian government to initiate a multi-year, multi-million dollar program to better define the geology and energy resources of the Bowser and Sustut Basins ("Integrated Petroleum Resource Potential and Geoscience Studies of the Bowser and Sustut Basins"; *see* Evenchick *et al.*, 2004). The province is a partner in this new project, which runs from 2003 to 2007.

REFERENCES

Best, M. (2004): Gravity and Magnetic Survey, Nechako Basin Study, Acquisition and Processing Phase; B.C. Ministry of Energy and Mines; Petroleum Geology Open File 2004-1.

English, J.M., Mihalynuk, M.G., Johnston, S.T., Orchard, M.J., Fowler, M. and L.J. Leonard (2003): Atlin TGI, Part VI: Early to Middle Jurassic Sedimentation, Deformation and a Preliminary Assessment of Hydrocarbon Potential, Central Whitehorse Trough and Northern Cache Creek Terrane; in Geological Fieldwork 2002, B.C. Ministry of Energy and Mines, Paper 2003-1, pages 187-201.

English, J.M., Fowler, M., Johnston, S.T., Mihalynuk, M.G. and Wight, K.L. (2004): Thermal Maturity in the Central Whitehorse Trough, Northwest British Columbia; Resource Development and Geoscience Branch, B.C. Ministry of Energy and Mines, Summary of Activities 2004, this volume.

Evenchick, C.A., Hayes, M.C., Buddell, K.A. and Osadetz, K.G. (2002): Vitrinite and Bitumen Reflectance Data and Preliminary Organic Maturity Model for the Northern two thirds of the Bowser and Sustut basins, North-central British Columbia; B.C. Ministry of Energy and Mines, Petroleum Geology Open File 2002-1.

Evenchick, C.A., Ferri, F., Mustard, P.S., McMechan, M., Osadetz, K.G., Stasiuk, L., Wilson, N.S.F, Enkin, R.J., Hadlari, T. and McNicoll, V.J. (2004): Recent Results and Activities of the Integrated Petroleum Resource Potential and Geoscience Studies of the Bowser and Sustut Basins Project, British Columbia; in Current Research, Geological Survey of Canada, 2003-A13, 11 pages.

Ferri, F. (2004): Potential Source Rock Characterization, Intermontane Basins, British Columbia; Resource Development and Geoscience Branch, B.C. Ministry of Energy and Mines, Summary of Activities 2004, this volume.

Fowler, M. (2003): Atlin TGI - Rock EVAL VII Program Pyrolysis Results from Whitehorse Trough; B.C. Ministry of Energy and Mines, Geofile 2003-1.

Fowler, M. (2004): Rock-Eval VI analysis of samples from the central Whitehorse Trough by the Geological Survey of Canada, Calgary in partnership with the B.C. Ministry of Energy and Mines; B.C. Ministry of Energy and Mines, Petroleum Geology Open File 2004-2.

Hannigan, P., Lee, P.J., Osadetz, K.G., Dietrich, J.R. and Olsen-Heise, K. (1994): Oil and Gas Resource Potential of the Nechako-Chilcotin Area of British Columbia; B.C. Ministry of Energy and Mines, Geofile 2001-6.

Hannigan, P., Lee, P.J., and Osadetz, K. (1995): Oil and Gas Resource Potential of the Bowser-Whitehorse area of British Columbia; B.C. Ministry of Energy and Mines, Geofile 2001-5.

Hannigan, P., Dietrich, J.R., Lee, P.J. and Osadetz, K.G. (2000): Hydrocarbon Resources of Pacific Margin Basins; in Canadian Society of Exploration Geophysicists, Annual Meeting, Program and Abstracts.

Hannigan, P., Dietrich, J.R., Lee, P.J. and Osadetz, K.G. (2001): Petroleum Resource Potential of Sedimentary Basins on the Pacific Margin of Canada; Geological Survey of Canada, Bulletin 564, 72 pages.

Hayes, B. (2002): Petroleum Exploration Potential of the Nechako Basin, British Columbia; B.C. Ministry of Energy and Mines, Petroleum Geology Special Paper 2002-3.

O'Sullivan, P.B., Donelick, R.A., Osadetz, K.G., Evenchick, C.A. and Ferri, F. (2004): Apatite Fission Track Data for Northern Two Thirds of the Bowser Basin; B.C. Ministry of Energy and Mines, Petroleum Geology Open File 2004-3.

Osadetz, K.G., Evenchick, C.A., Ferri, F., Stasiuk, L., Obermajer, D.M. and Wilson, N.S F. (2003): Molecular composition of Crude Oil Stains from Bowser Basins in Geological Fieldwork 2002, B.C. Ministry of Energy and Mines, Paper 2003-1, pages 257-264.

Osadetz, K.G., Jiang, C., Evenchick, C.A., Ferri, F., Stasiuk, L.D., Wilson, N.S.F. and Hayes, M. (2004): Sterane compositional traits of Bowser and Sustut basin crude oils: Indications for three effective petroleum systems; Resource Development and Geoscience Branch, B.C. Ministry of Energy and Mines, Summary of Activities 2004, this volume.

Salt, W.T. (1980): Gravity Survey of the Big Creek Area; B.C. Ministry of Energy and Mines, Geological and Geophysical Report 2393.

Thornsteinsson, E.T., Osadetz, K.G., Ferri, F. and Hayes, M. (in press): Stratigraphy and Lithology of Petroleum Wells within the Bowser Basin and Nechako area; B.C. Ministry of Energy and Mines, Petroleum Geology Open File 2004-4.

QUALITATIVE INTERPRETATION OF POTENTIAL FIELD PROFILES: SOUTHERN NECHAKO BASIN

By Melvyn E. Best

Bemex Consulting International
5288 Cordova Bay Road

KEYWORDS: potential fields, gravity, magnetics, Nechako Basin, petroleum exploration, Big Creek-Riske Creek gravity/magnetic profile

INTRODUCTION

The Nechako Basin (Figure 1) is one of several interior basins within British Columbia. Although the potential for economic quantities of hydrocarbons exists within the basin (Hannigan et. al., 1994), only limited exploration has been carried out. Quaternary surficial sediments and Tertiary volcanic outcrop cover large areas of the basin, limiting surface geological mapping and potentially creating problems in acquiring seismic data. In addition, volcanic rocks within the sedimentary section can cause seismic acquisition and processing problems. The presence of these volcanic rocks also complicates the interpretation of seismic and magnetic data.

Several companies explored for oil and gas within the Nechako Basin prior to 1980, but no commercial quantities were found. In the early 1980s Canadian Hunter Exploration carried out an exploration program consisting of a regional gravity survey, a limited number of two-dimensional seismic lines, and the drilling of several wells (Robertson, 2002). As no economic accumulations of hydrocarbons were encountered during drilling, they abandoned the play. No additional exploration activity has been conducted since that time.

As part of the BC government's initiative for economic development within British Columbia, Bemex Consulting International was awarded a contract to carry out ground gravity and magnetic surveys in the southern Nechako Basin. The purpose of the survey is to promote the basin's potential and to illustrate how integrated potential field data can provide constraints on basin structure, sediment thickness, and volcanic structures within the sedimentary section. An approximate east-west profile was selected for this survey based on the regional gravity data collected by Canadian Hunter. Data collected along this profile included gravity, total field magnetic and the vertical gradient of the total field. Elevations and UTM coordinates were acquired along the profile as well.

This report describes the data acquisition and processing steps for the ground geophysical survey and presents a preliminary qualitative interpretation of these profiles.

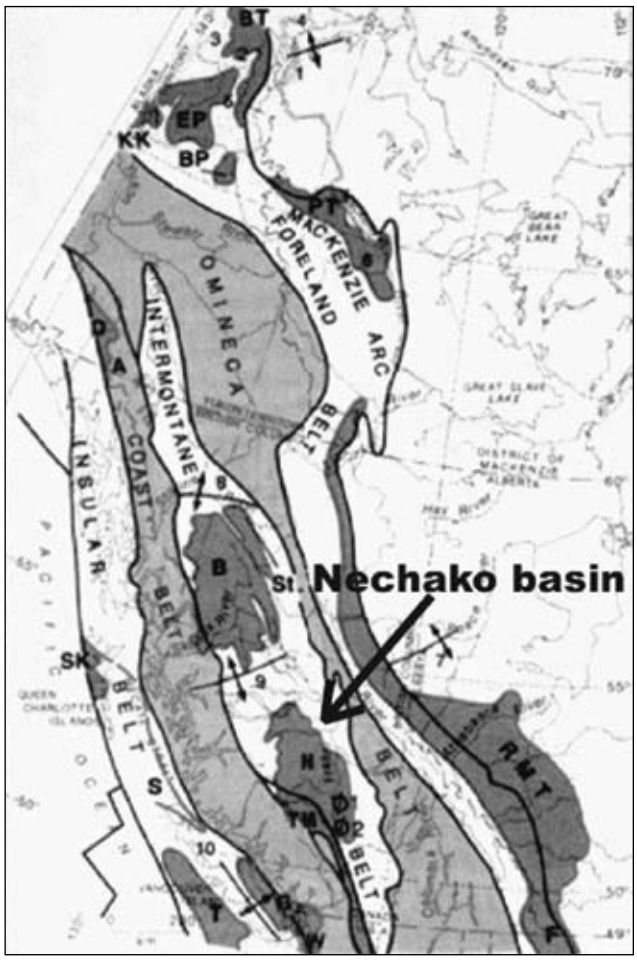

Figure 1. Morphological Belts of the Canadian Cordillera, showing the position of the Nechako Basin and related tectonic elements (from Yorath, 1991). Note: B = Bowser Basin, N = Nechako Basin.

ACQUISITION AND PROCESSING

Ground gravity and magnetic data were collected along a 33 km profile at approximately 330 m and 165 m spacing, respectively. The data were collected along the road that connects Riske Creek and Big Creek (Figure 2). The loca-

tion of the profile was chosen to cross a significant gravity low centred near Big Creek that was observed on the Canadian Hunter regional gravity survey.

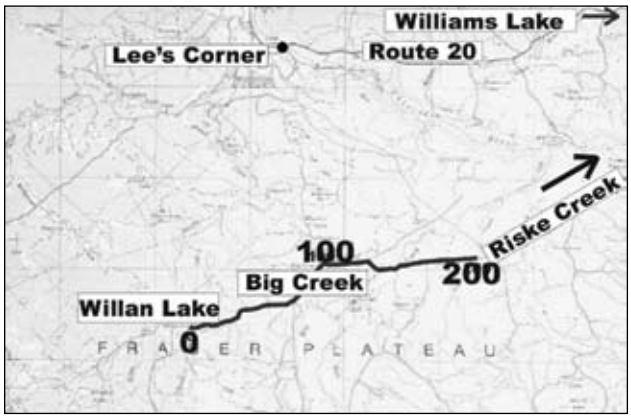

Figure 2. Location of profile along Big Creek–Riske Creek Road (from NTS 92O). The profile goes from station 0 in the west near Willan Lake to station 200 in the east.

A Lacoste-Romberg gravity meter was used to measure the relative change in gravity between each station. Measurements at several stations were repeated approximately 4 hours apart to correct for instrument and tidal drift. Relative elevations were measured at each gravity station using a laser level. These relative elevations were then tied to a known elevation above sea level near station 122. UTM coordinates (NAD 83) were obtained from BC Terrain Resource Information Mapping (TRIM) maps at a scale of 1:50 000.

A GEM rover gradiometer was used to measure the magnetic field and the vertical gradient of the magnetic field at each gravity station and approximately midway between each gravity station. A second GEM magnetometer was used as a base station. Several base stations were located along the profile, depending on where the roving survey was being conducted that day.

Processing of the gravity data consisted of drift corrections, latitude corrections, free-air elevation corrections, and Bouguer elevation corrections. (A Bouguer density of 2350 kg/m3 (2.35 g/cc) was determined from tests carried out over areas with significant topographic relief. The density is consistent with the density used for the Canadian Hunter survey). Terrain corrections up to and including ring D (Hammer, 1939) were also computed. The overall accuracy of the gravity data is estimated to be ±0.60 mGal or better.

The total magnetic field data were corrected for diurnal variations using the base station readings. No other corrections were applied to the total magnetic field data and the vertical gradient of the total magnetic field data.

Plots of the corrected gravity data, elevation above sea level, and corrected magnetic field data are given in Figure 3. More details on data acquisition and processing can be found in Best (2004).

REGIONAL SETTING

The Nechako Basin is a Mesozoic forearc basin (Yorath, 1991) located in the Intermontane Belt of the southern Canadian Cordillera (Figure 1). Spatially, the Nechako Basin is bounded by the Skeena Arch to the north, the Fraser River Fault System to the east, and the Coast Mountain plutons to the west (Figure 1).

The tectonic history of the Nechako Basin is complex. Its structural geology is poorly understood, due largely to extensive Quaternary sediments covering the surface and large areas of Tertiary volcanic outcrop. Outcrops of deformed Mesozoic sediments are present,but isolated within the basin proper. More continuous outcrop occurs along the western flank (Petrel Robertson, 2002).

The Nechako Basin sediments were derived from bordering uplifts related to contraction during terrane accretion (Gabrielse et al.., 1991). The Takla and Hazelton Groups, comprising volcanic and sedimentary strata, were deposited during Triassic and Early-Middle Jurassic time. The formation of the Skeena Arch (Yorath, 1991) during the Middle Jurassic (?) segregated the Nechako Basin from the Bowser Basin to the north.

In Middle Jurassic to Early Cretaceous time, the Intermontane and Insular super-terranes were accreted to each other and to North America. (Gabrielse and Yorath, 1991). Sedimentation from the resulting uplifts was shed both west into the Nechako Basin and other intermontane basins and east into the Rocky Mountain Fold Belt. Transpressional tectonics dominated until the Eocene, at which time there was a change to a regime of dextral transtension (Price, 1994) and an episode of associated magmatism.

Deformation styles in the Nechako Basin were affected by both lithological contrasts and tectonics. Deformation of Stikine and Cache Creek rocks can be related to early Mesozoic accretionary prisms and subduction zones. Structures related to the early Mesozoic include folds and (northwest-trending) thrust faults, which verge either east or west, depending on position in the Intermontane Belt (Gabrielse, 1991; Price, 1994). Major transcurrent faults (related to Eocene extension) cut and bound the basin.

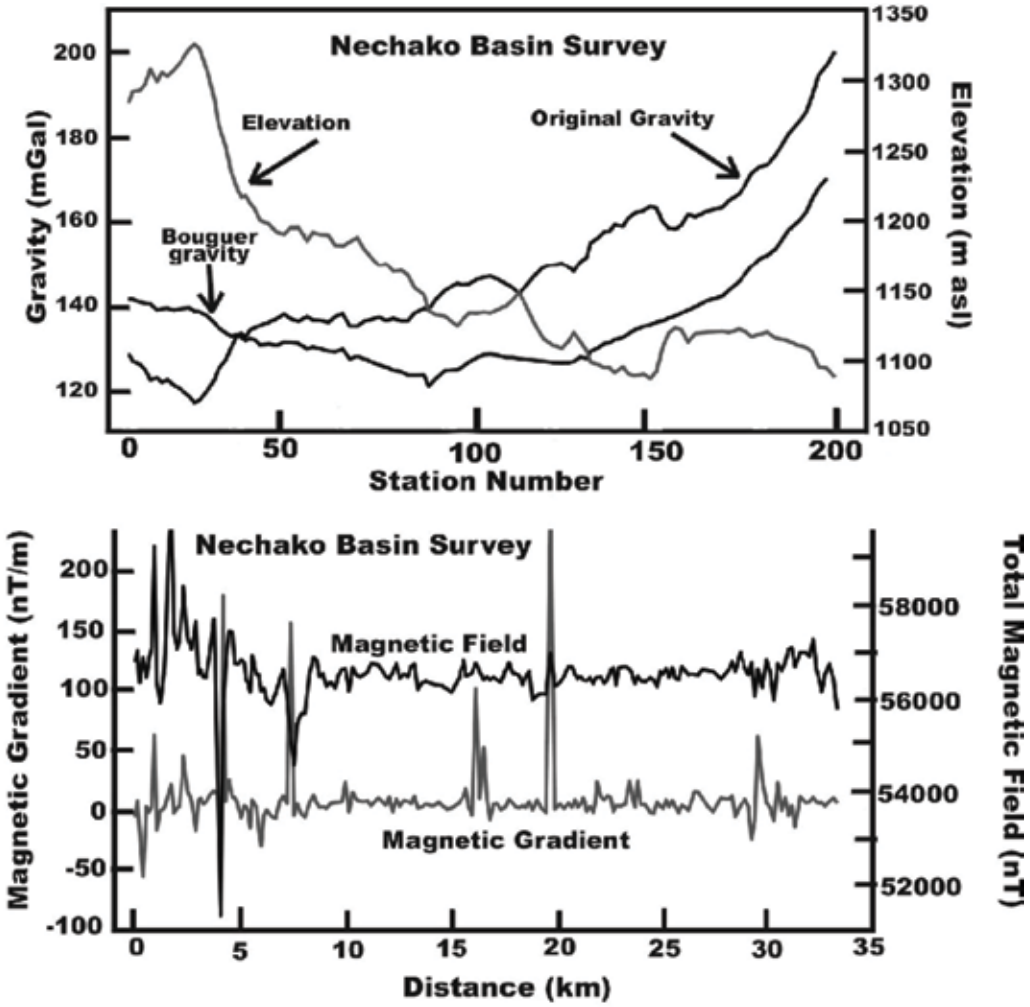

Figure 3. Elevation above sea level, corrected gravity, and corrected magnetic data versus distance (km) from station zero. Station number is shown on the upper diagram with station zero at the western end of the Big Creek–Riske Creek profile.

PRELIMINARY INTERPRETATION OF GRAVITY AND MAGNETIC PROFILES

The final processed gravity and magnetic data are shown in Figure 3. The gravity profile confirms the presence of a low near Big Creek with a magnitude comparable to that of the low on the regional Canadian Hunter gravity map (Petrel Robertson, 2002). This feature has an approximate width of 20 to 25 km.

A plot of a linear regional gravity trend passing through stations 0 and 200 of the final gravity data is provided in Figure 4(a). Although a linear regional trend may not be the best choice, it is as good a choice as any for this single profile. Figure 4(b) is the residual gravity data after the linear regional trend has been subtracted from the gravity data.

There are several features worth noting along the gravity profile in Figure 4(b). A gravity low centred near 14.5 km has a width of approximately 800 m and a magnitude of 3 to 4 mGal. This feature may be related to a paleochannel associated with Big Creek since the profile is closest to the creek at this location. A broader low with a magnitude of 3 to 4 mGal centred around 21 km has a width of approximately 3 to 4 km. Neither of these local lows appears to be associated with elevation changes (Figure 3).

The gravity low that crosses the entire profile has a magnitude of approximately 35 mGal. Negative gravity anomalies are caused by material of higher density surrounding lower density rocks centred over the negative anomaly. There are an infinite number of models that can fit the gravity data.

One tempting model is to assume a fault-related grabben filled with low-density sedimentary rocks. Figure 5 is an example of such a density model that fits the general shape of the residual gravity anomaly. In this case it is a 3 to 4 km thick, low-density body (0.3 g/cc lower than the surrounding rock) centred over the gravity low. The top of the body in this case is only a few hundred metres below the surface.

Unfortunately a change in volcanic rock type (density) could also cause such a gravity low. Without additional information we cannot be sure of the model.

The total magnetic field data and vertical gradient are also shown in Figure 3. The average value of the total magnetic field is approximately 57 500 nT between stations 0 and 36 (0 and 6 km). There are large variations within the magnetic field (from 52 000 to 60 000 nT) along this same segment of the profile. These large magnetic field values are associated with higher elevation and are likely related to shallow basalt flows. This may explain, at least in part, the tendency towards higher gravity values in that region.

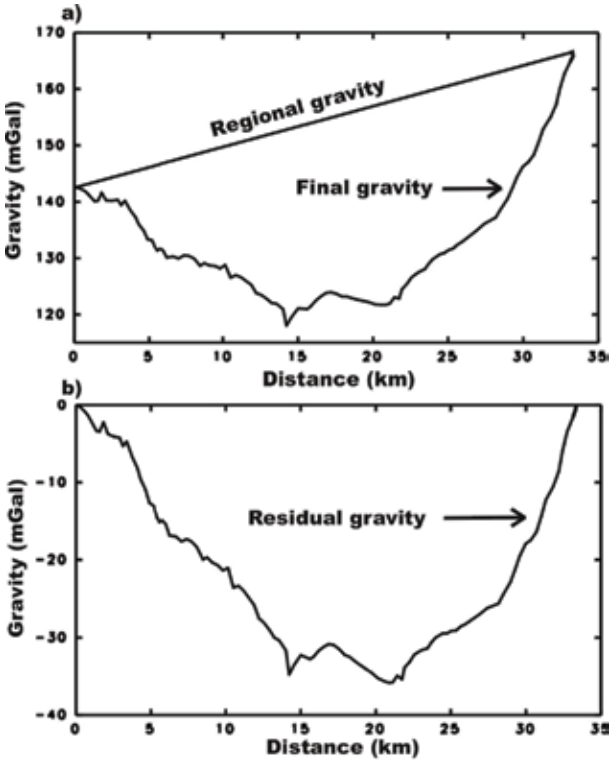

Figure 4. Regional residual gravity separation. a) Bouguer gravity and linear regional gravity. b) Residual gravity (regional minus Bouguer).

The rest of the profile has an average total field value closer to 56 500 nT, with less variation in the magnetic field magnitude. The magnetic features from station 36 to the end of the line at station 200 are therefore likely deeper than the magnetic features between station 0 and station 36. The deeper magnetic features are coincident with the gravity low, which perhaps indicates that sediments may exist above the magnetic basement in this area.

RECOMMENDATIONS FOR FURTHER INTERPRETATION

The qualitative description of the gravity and magnetic profiles presented above is quite limited. However, if the gravity and magnetic profiles are studied in conjunction with regional potential field data, a more detailed interpretation can be provided.

Consequently we recommend integrating the above profiles with regional potential field data (GSC regional aeromagnetic data and the Canadian Hunter regional gravity data) to carry out a preliminary interpretation of the southern portion of the Neshkoro basin, particularly in the vicinity of the regional gravity low.

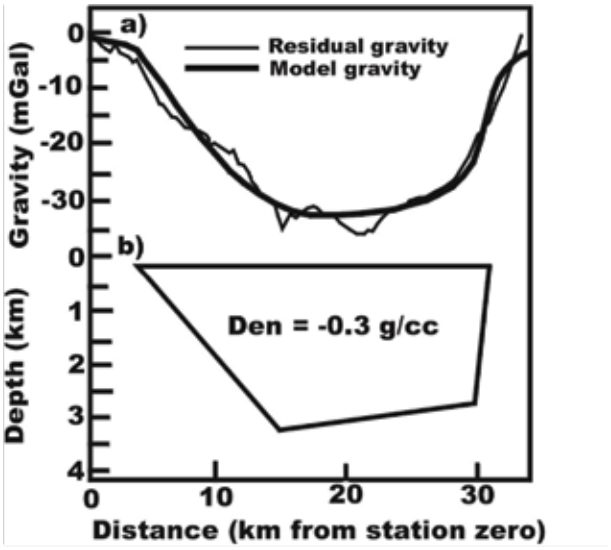

Figure 5. Example of two-dimensional gravity modelling. a) Model versus residual gravity data. b) Depth model assuming a density contrast between the host rock and gravity anomaly of −0.3 g/cc.

In addition to the regional potential field data, the interpretation should incorporate geological information as well as all available well and seismic data. One or more of the Canadian Hunter seismic lines that cross or are close to the regional gravity low should be incorporated into the interpretation (they should be reprocessed first, if the digital data is available). The seismic and well data can be used to provide depth constraints for the quantitative interpretation of the gravity and magnetic data.

REFERENCES

Best, M.E., 2004, Gravity and Magnetic survey, Nechako basin study, acquisition and processing phase: Petroleum Geology Open File 2004-1, British Columbia Ministry of Energy and Mines.

Gabrielse, H., 1991, Structural styles : Chapter 2 in Geology of the Cordilleran Orogen of Canada: H. Gabrielse and C.J. Yorath (ed.): Geological Survey of Canada, no. 4, p. 329-371 (also Geological Society of America, The Geology of North America, v. G-2).

Gabrielse3, H., and Yorath, C.J., 1991, Tectonic synthesis: Chapter18 in Geology of the Cordilleran Orogen of Canada: H. Gabrielse and C.J. Yorath (ed.): Geological Survey of Canada, no. 4, p. 329-371 (also Geological Society of America, The Geology of North America, v. G-2).

Gabrielse, H., Monger, J.W.H., Wheeler, J.O., and Yorath, C.J., 1991, Part A, Morphological belts, tectonic assemblages, and terranes: in Geology of the Cordilleran Orogen of Canada: H. Gabrielse and C.J. Yorath (ed.): Geological Survey of Canada, no. 4, p. 329-371 (also Geological Society of America, The Geology of North America, v. G-2).

Hammer, S., 1939, Terrain corrections for gravimeter stations: Geophysics, 4, 184.

Hannigan, P., Lee, P.J., Osadetz, K.G., Dietrich, J.R., and Olsen-Heise, K., 1994, Oil and gas resource potential of the Nechako-Chilcoten area of British Columbia: Report, Petroleum Resource Subdivision, Geological Survey of Canada.

Robertson, P., 2002, Petroleum exploration potential of the Nechako basin, British Columbia: Petroleum Geology Special Paper 2002-3, British Columbia Ministry of Energy and Mines.

Price. R.A., 1994, Cordilleran tectonics in the evolution of the western Canada sedimentary basin: Chapter 2 in Geolgocial Atlas of the Western Canada Sedimentary Basin, Mossop, G., and Shetsin, I. (eds.), Alberta Research Council and the Canadian Society of Petroleum Geologists, Calgary.

Yorath, C.J., 1991, Upper Jurassic to Paleogene assemblages: Chapter 9 in Geology of the Cordilleran Orogen of Canada: H. Gabrielse and C.J. Yorath (ed.): Geological Survey of Canada, no. 4, p. 329-371 (also Geological Society of America, The Geology of North America, v. G-2).

THERMAL MATURITY IN THE CENTRAL WHITEHORSE TROUGH, NORTHWEST BRITISH COLUMBIA

By J.M. English[1], M. Fowler[2], S.T. Johnston[1], M.G. Mihalynuk[3] and K.L. Wight[1]

KEYWORDS: Whitehorse Trough, Laberge Group, Sinwa Formation, Atlin Lake, Tulsequah, regional geology, organic maturation, programmed pyrolysis, vitrinite reflectance.

INTRODUCTION

The Whitehorse Trough is an early Mesozoic marine sedimentary basin that extends from southern Yukon to Dease Lake in British Columbia. Early studies recognised the potential of the low-grade sedimentary rocks of the Whitehorse Trough to host hydrocarbon accumulations (e.g., Gilmore, 1985; Hannigan et al., 1995; National Energy Board, 2001). These assessments were based on data from samples collected in southern Yukon (Gilmore, 1985; National Energy Board, 2001), and indicate that the region is gas-prone. It is not known if potential hydrocarbon traps were filled and preserved, as none have been drilled. Structural complexity decreases and metamorphic grade is lower in the British Columbia portion of the Whitehorse Trough. On the basis of flat-lying Eocene volcanic rocks of the Sloko Group, no widespread deformation postdates Early Eocene time (Mihalynuk, 1999). Undeformed Middle Jurassic plutons that intrude structures within the Whitehorse Trough in British Columbia constrain deformation to between about 174 and 172 Ma (the age of youngest deformed strata and oldest cross-cutting plutons, respectively; e.g., Mihalynuk et al., 1999; Mihalynuk et al., in press). Such a simple deformation history limits the possibility of post-generation hydrocarbon escape. Previous assessments of source rock potential in British Columbia were based on extrapolation of data from the Yukon portion of the Whitehorse Trough. The objective of this paper is to determine the level of organic maturation and the source rock potential in this portion of the Whitehorse Trough.

GEOLOGICAL BACKGROUND

The Whitehorse Trough is an elongate arc-marginal sedimentary basin and is believed to represent submarine-fan deposition in a forearc basin that received detritus from the Upper Triassic Stuhini and Lower Jurassic Hazelton magmatic arcs to the west and southwest during Upper Triassic to Middle Jurassic time (e.g., Tempelman-Kluit, 1979; Dickie and Hein, 1995; Hart et al., 1995; Johannson et al., 1997; Figure 1); the Stuhini Group is known as the Lewes River Group in Yukon (Wheeler, 1961). The Whitehorse Trough is juxtaposed along the Nahlin Fault with oceanic crustal rocks to the northeast, including thick platformal carbonate and argillaceous chert successions of the northern Cache Creek Terrane. The Laberge Group of the Whitehorse Trough ranges in age from Lower Sinemurian to Middle Bajocian; proximal conglomeratic strata onlap onto Upper Triassic volcanic and carbonate rocks of the Stuhini Group to the south and southwest (e.g., Souther, 1971; Monger et al., 1991). Whitehorse Trough strata within the study area include carbonate rocks of the Upper Triassic Sinwa Formation and interbedded sandstone, siltstone, and argillite of the Lower Jurassic Inklin Formation.

Contraction of the Whitehorse Trough occurred in the Middle Jurassic when the Cache Creek Terrane was emplaced over it during an accretionary event (e.g., Thorstad and Gabrielse, 1986; Mihalynuk, 1999). The timing of this deformational event is constrained by the age of the youngest blueschist in the Cache Creek Terrane (French Range, approximately 174 Ma: Mihalynuk et al., in press) and the age of the oldest post-deformational stitching intrusions (approximately 172 Ma: Mihalynuk et al., 1992; Mihalynuk et al., 2003; Bath, 2003). A Middle Jurassic southwest-vergent fold and thrust belt is developed in the Whitehorse Trough that includes the regional-scale King Salmon Thrust. During this deformation, the Cache Creek Terrane was thrust westward over the Whitehorse Trough and the Stikine arc. During Bajocian time, chert-pebble conglomerates derived from the Cache Creek Terrane were deposited across the Whitehorse Trough and the more southerly Middle-Upper Jurassic Bowser Basin (Ricketts et al., 1992; Mihalynuk et al., in press).

THERMAL MATURITY IN THE CENTRAL WHITEHORSE TROUGH

Systematic sample collection for programmed pyrolysis was undertaken in the central Whitehorse Trough in order to assess the level of organic maturation and source rock potential of this basin. Programmed pyrolysis of whole rock using the Rock-Eval 6 system provides information on the type, maturity, and quantity of associated organic matter (Behar et al., 2001; Lafargue,

[1] *University of Victoria*
[2] *Geological Survey of Canada (Calgary)*
[3] *B.C. Ministry of Energy and Mines*

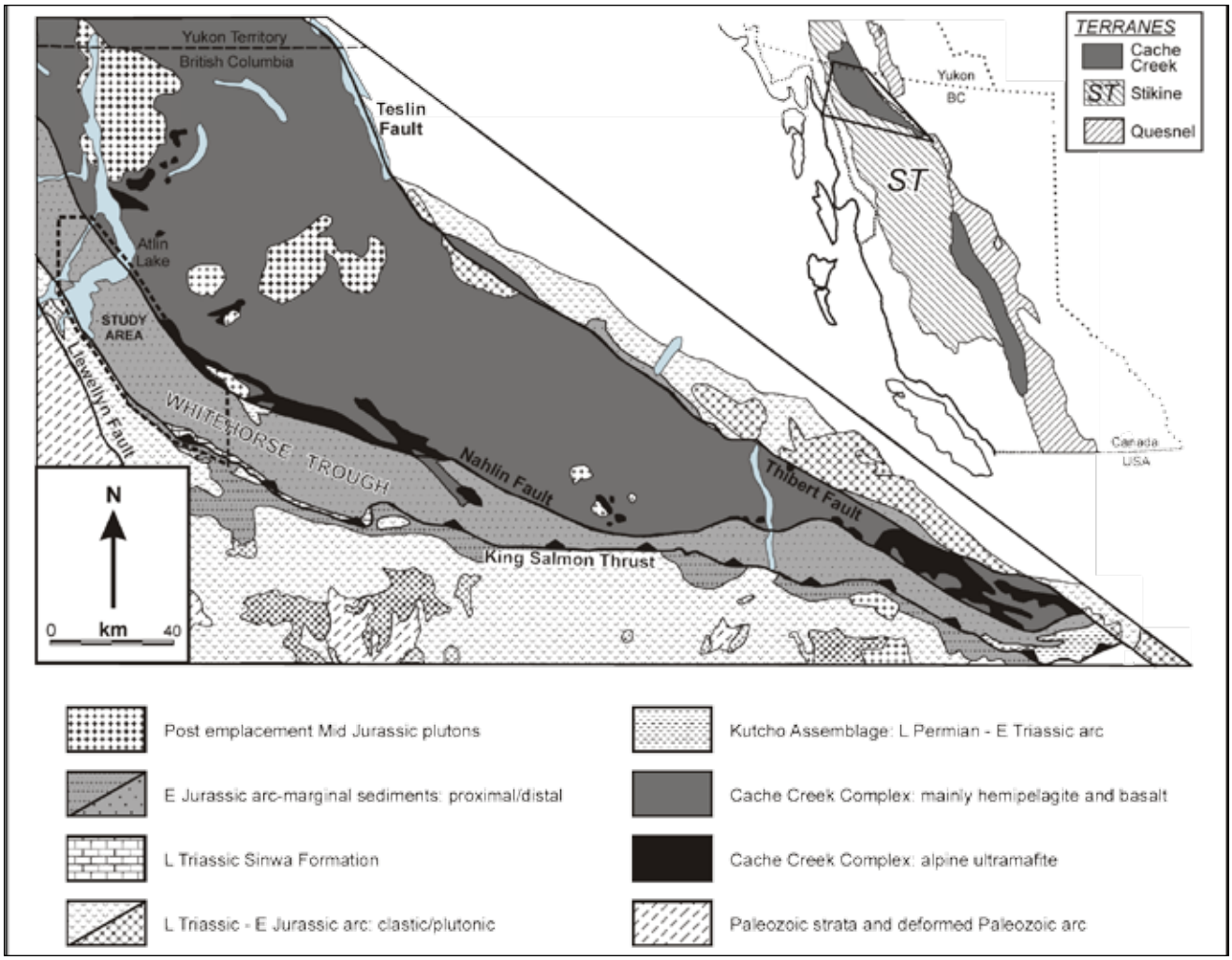

Figure 1. Map of British Columbia showing the distribution of the primary components of the Intermontane Belt in the northern Canadian Cordillera (top right) and a regional geologic map (main). This geology map does not include post-Middle Jurassic rock units. The central Whitehorse Trough study area is outlined by a dashed box.

et al., 1998). Aliquots of sediment samples were dried and powdered for Rock-Eval/TOC analysis at the Geological Survey of Canada, Calgary (GSCC). A Vinci Technologies Rock-Eval 6 instrument was used. Duplicate analyses of samples were carried out to test reproducibility of data. Each sample of about 100 mg of finely ground source rock is put in a furnace at 300°C, raised to 850°C, and then allowed to cool. The hydrocarbons liberated during heating are analysed by a flame ionisation detector, which separates the components into two parameters (Figure 2). The first peak, denoted S1 (mg $_{HC}$/g rock), indicates 'free bitumen' already in the sample. The second peak, denoted S_2 (mg HC/g rock), results from thermal breakdown of kerogen. The Rock-Eval 6 S_3 parameter (mgCO2/g or mg CO/g rock) represents the oxygen-bearing compounds released at the same time as the S_1 peak added to that obtained between 300° and 400°, as measured by an infrared cell. The temperature corresponding to the maximum of the S_2 peak (T_{max}) is an indicator of source rock maturity, although this value is only reliable when S_2 is greater than 0.2 (Peters, 1986) and is also affected by organic matter type. An indication of source rock richness is given by the sum of the first two peaks ($S_1 + S_2$). Other parameters determined include the

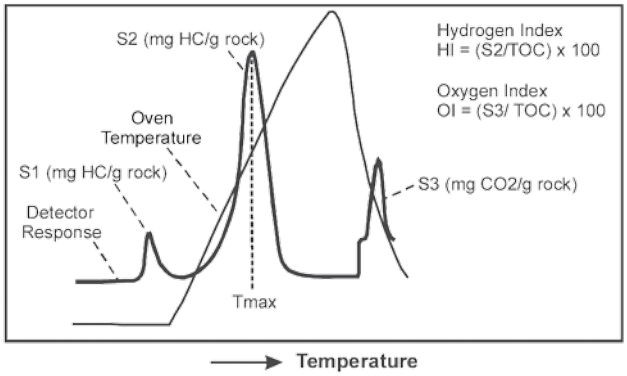

Figure 2. Schematic pyrogram illustrating the liberation of hydrocarbon during heating of the rock sample. Determined parameters include S_1, S_2, S_3, T_{max}, and the hydrogen and oxygen indices.

hydrogen index (S_2/TOC) and the oxygen index (S_3/TOC); these parameters are used to determine the type of organic matter present in a low maturity potential source rock.

The complete Rock-Eval pyrolysis dataset may be obtained at the British Columbia Geological Survey (BCGS) website (Fowler, 2004). Source rocks with total organic carbon (TOC) contents of 0% to 0.5%, 0.5% to 1%, 1% to 2%, and greater than 2% are considered poor, fair, good, and very good, respectively (Peters, 1986). Using this classification, most samples, including all samples from the Sinwa Formation, are classified as poor to fair source rocks, with 22% classified as good, and 8% classified as very good (Figure 3). The good and very good source rocks within the Inklin Formation appear to occur dominantly in Pliensbachian successions.

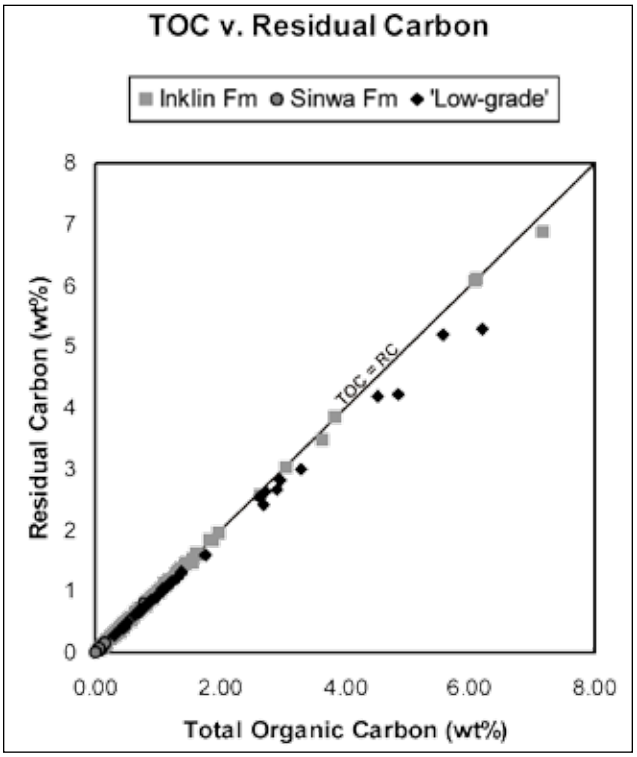

Figure 3. Plot of total organic carbon (TOC) versus residual carbon for samples from the central Whitehorse Trough. 'Low-grade' samples form a subset of the Inklin Formation samples, for which S_2 > 0.2 and T_{max} < 480°C.

However, most authors now believe that a TOC content of greater than 1% and likely a minimum of 2% is needed for the generation and expulsion of liquid hydrocarbons (Hunt, 1996; Meyer and Nederlof, 1984; Peters and Moldowan, 1993; Thomas and Clouse, 1990). Thus, few of the Whitehorse Trough samples are likely to have been oil-prone source rocks. TOC is almost equal to residual carbon in the majority of samples (Figure 3), indicating that there is little generative potential left in these rocks. Therefore, depending on organic matter type in these samples originally, they may have had much higher initial TOC contents. Consequently, samples presently having a TOC content of at least 1% could have been hydrocarbon source rocks assuming they originally contain oil-prone Type I or II organic matter.

The organic matter type in a source rock can be determined by plotting hydrogen index against the oxygen index (Espitalié et al., 1977; Figure 4). None of the potential source rocks sampled in the central Whitehorse Trough are oil prone; the majority are inert (low hydrogen index) due to the lack of generative potential, while the rest are gas prone (Figure 4). The lack of generative potential is mostly a function of high thermal maturity. From a spatial standpoint, samples that are gas prone and have generative potential are from the northeastern flank of the central Whitehorse Trough. This belt of rock is interpreted to represent the structurally and stratigraphically highest units within the Laberge Group in this region and is interpreted to continue northeast beneath the structurally overlying Cache Creek Terrane.

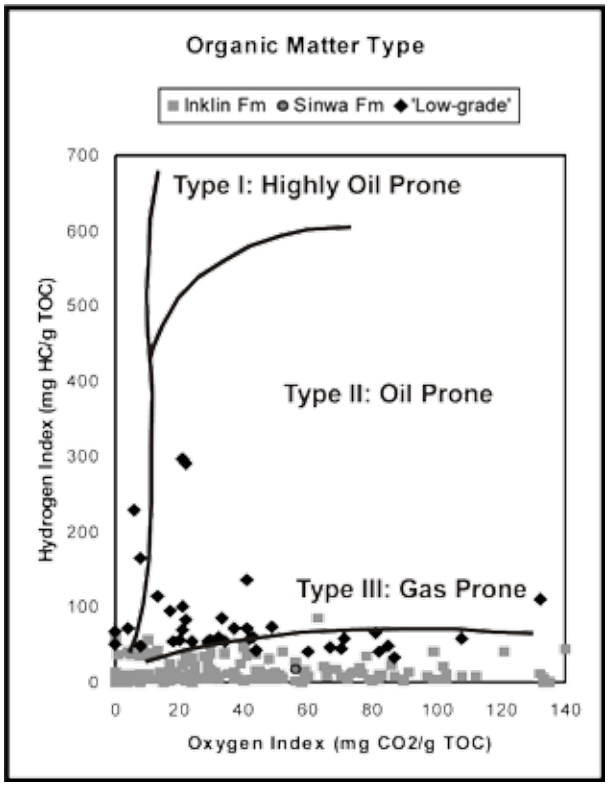

Figure 4. Plot of hydrogen index versus oxygen index for samples from the central Whitehorse Trough. 'Low-grade' samples form a subset of the Inklin Formation samples, for which S_2 > 0.2 and T_{max} < 480°C. The organic matter type in a source rock can be determined from this plot (Espitalié et al., 1977).

Tmax can be used as an indicator of thermal maturation as long as S_2 is greater than 0.2. Unfortunately, for the majority of samples, this qualifier rules out the interpretation of the pyrolysis data for maturation purposes. Once again, qualifying samples tend to come from the northeastern flank of the Whitehorse Trough, and these samples are within the oil and gas windows (Figure 5). Although T_{max} values of samples with S_2 less than 0.2 must be viewed cautiously, it can be graphically shown that most samples from the southwestern flank of the Whitehorse Trough are overmature (Figure 5). Distribution of mature and overmature areas of the central Whitehorse Trough can been seen by contouring Tmax values (Figure 6) and is consistent with limited available vitrinite reflectance data (Table 1).

The vitrinite reflectance values suggest that potential source rocks along the northeastern flank of the central Whitehorse Trough are almost immature. If these vitrinite reflectance data are accurate, this may imply that there was little hydrocarbon potential in the basin even originally, as these 'low maturity' samples have low hydrogen index values. Higher levels of organic maturation along the southwestern flank of the central Whitehorse Trough may reflect increased structural burial of these strata or contact metamorphism during Eocene magmatism.

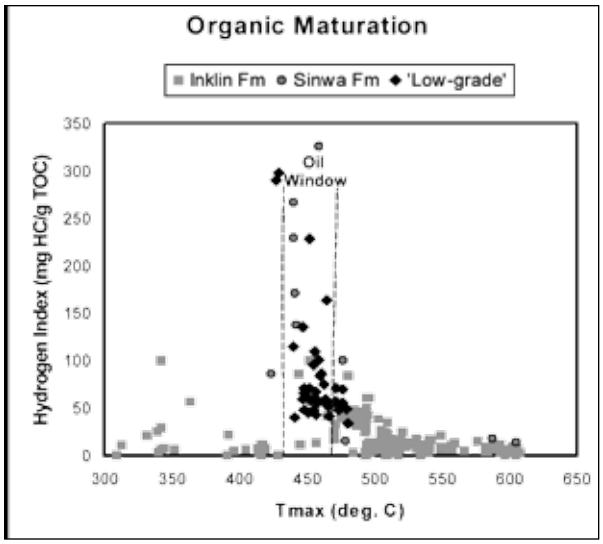

Figure 5. Plot of hydrogen index versus T_{max} for samples from the central Whitehorse Trough. 'Low-grade' samples form a subset of the Inklin Formation samples, for which S_2 > 0.2 and T_{max} < 480°C. Due to low S_2 values, T_{max} values for the majority of other Inklin Formation samples are suspect and are dominantly overmature.

TABLE 1. VITRINITE REFLECTANCE DATA FROM THE ATLIN AREA, NW BRITISH COLUMBIA.

Sample Number	Age	NAD	Easting	Northing	$R_o$max
GGAJ-92-59-2T	Late Pliensbachian	27	571625	6578475	0.6
GGAJ-92-56-T	Early Pliensbachian	27	568200	6576600	0.85
GGAJ-92-184-T	Early Pliensbachian	27	568575	6575975	0.85
GGAJ-92-119-T	Late Sinemurian	27	566725	6559450	1.45
GGAJ-92-177-T	Early Sinemurian	27	562950	6576175	1.54
GGAJ-92-45-T	Early? Sinemurian	27	566300	6574850	1.62
ABA02-13-1	na	83	602818	6543186	1.45
FCO02-1-2c	na	83	605002	6540947	2.36
JEN02-5-7	na	83	588036	6557555	0.85
JEN02-6-2a	na	83	588883	6557054	0.98
JEN02-19-9e	na	83	590287	6547881	1.87
LLE02-10-7	na	83	586892	6546875	1.79
MMI02-6-1-1	na	83	588017	6552900	1.07
MMI02-7-5-2	na	83	588090	6551600	1.65
MMI02-19-4-6	na	83	593505	6549108	2.05
MMI02-20-6	na	83	593040	6546960	1.79
ORO02-6-1c	na	83	589770	6555472	0.92
STJ02-3-3a	na	83	591257	6553403	1.05

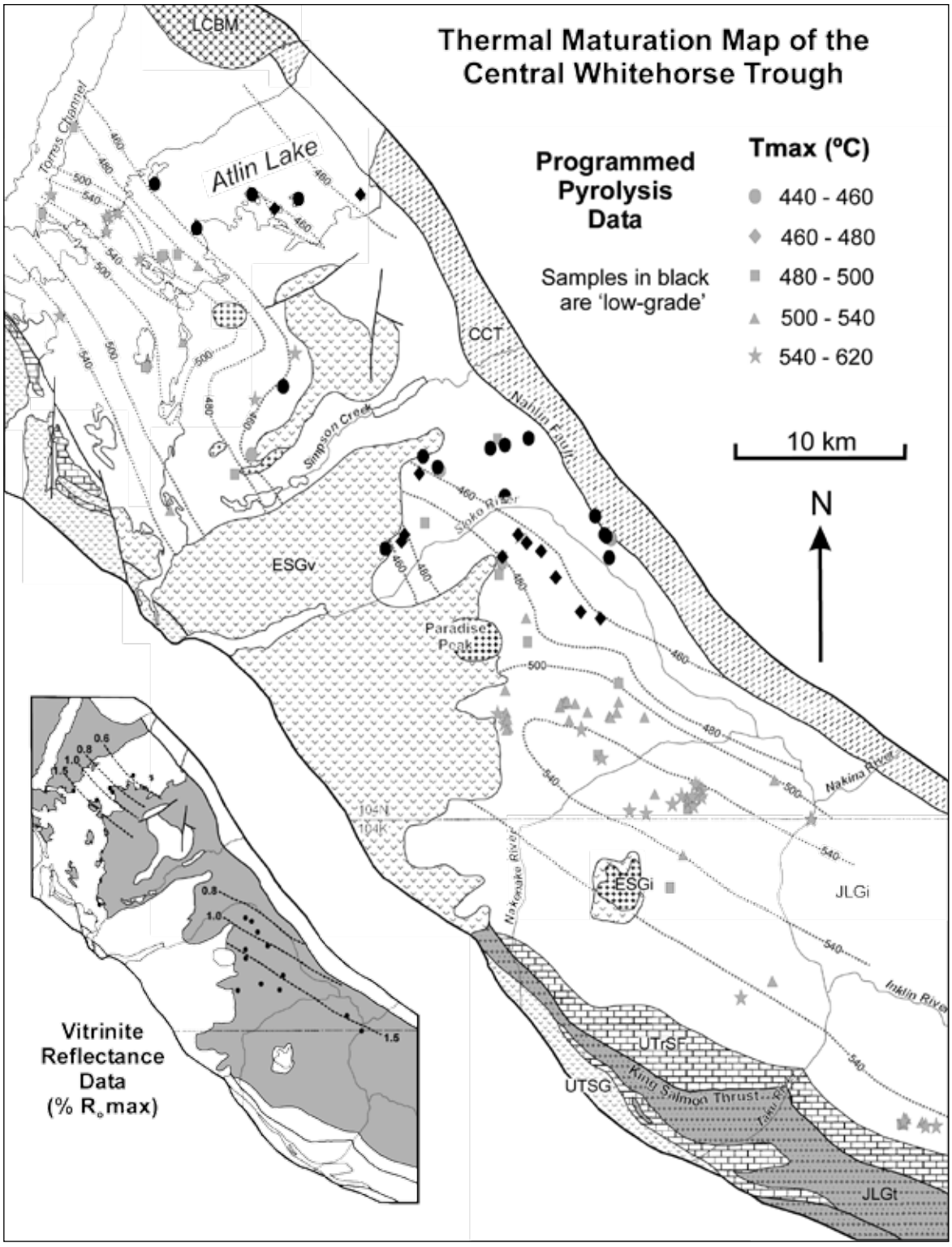

Figure 6. Contoured thermal maturation map for the central Whitehorse Trough based on T_{max} values. Note: T_{max} values are poorly constrained for relatively 'high-grade' samples due to the low (< 0.2) S_2 values; despite this, all samples with S_2 values > 0.03 were plotted as a crude representation of maturation levels in the region. Vitrinite reflectance data shown in Table 1. Abbreviations: CCT – Cache Creek Terrane; ESGi – Eocene Sloko Group intrusions; ESGv – Eocene Sloko Group volcanics; JLGi – Jurassic Laberge Group Inklin Formation; JLGt – Jurassic Laberge Group Takwahoni Formation; LCBM – Late Cretaceous Birch Mountain pluton; UTrSF – Upper Triassic Sinwa Formation; UTSG – Upper Triassic Stuhini Group.

SUMMARY

The Whitehorse Trough is an early Mesozoic marine sedimentary basin that extends from southern Yukon to Dease Lake in British Columbia. Strata within the central Whitehorse Trough include carbonate rocks of the Upper Triassic Sinwa Formation and interbedded sandstone, siltstone, and argillite of the Lower Jurassic Inklin Formation. Programmed pyrolysis data indicate that potential source rocks in the Inklin Formation are gas prone and are within the oil and gas windows along the northeastern flank of the central Whitehorse Trough.

ACKNOWLEDGEMENTS

This research was funded by a University of Victoria Fellowship to J. English, an NSERC Discovery Grant to S.T. Johnston, an NSERC Undergraduate Student Research Award to K. Wight, and by the Geological Survey of Canada and the British Columbia Ministry of Energy and Mines. Thanks to the rest of the bedrock geology mappers who worked in the Whitehorse Trough as part of this project: Fabrice Cordey, Lucinda Leonard, Adam Bath, Lee Ferreira, Jacqueline Blackwell, Fionnuala Devine, and Oliver Roenitz. Thanks to Lucinda Leonard for assistance in drafting figures. Thanks also to Norm Graham at Discovery Helicopters for logistical assistance. Figure 6 was prepared with the GMT software (Wessel and Smith, 1995).

REFERENCES

Bath, A. (2003): Atlin TGI, Part IV: Middle Jurassic granitic plutons within the Cache Creek terrane and their aureoles: Implications for terrane emplacement and deformation; in Geological Fieldwork 2002: B.C. Ministry of Energy and Mines, Paper 2003-1, pages 51-55.

Behar, F., Beaumont, V. and Penteado, H. L. D. B. (2001): Rock-Eval 6 Technology: Performances and Developments; Oil & Gas Science and Technology, Volume 56, pages 111-134.

Dickie, J. R. and Hein, F. J. (1995): Conglomeratic fan deltas and submarine fans of the Jurassic Laberge Grup, Whitehorse Trough, Yukon Territory, Canada: fore-arc sedimentation and unroofing of a volcanic island arc complex; Sedimentary Geology, Volume 98, pages 263-292.

Espitalié, J., Madec, M., Tissot, B., Mennig, J. J. and Leplat, P. (1977): Source rock characterisation method for petroleum exploration; Proceedings of the 9th Annual Offshore Technology Conference, Volume 4, pages 439-448.

Fowler, M. (2004): Rock-Eval VI analysis of samples from the central Whitehorse Trough; Energy-Resource Development and Geoscience Branch, B.C. Ministry of Energy and Mines, Petroleum Geology Open File 2004-2.

Gabrielse, H. (1998): Geology of Cry Lake and Dease Lake map areas, north-central British Columbia; Geological Survey of Canada, Bulletin 504, 147 pages.

Gilmore, R. G. (1985): Whitehorse field party; unpublished report; Petro-Canada, 16 pages.

Hannigan, P., Lee, P. J. and Osadetz, K. G. (1995): Oil and gas potential of the Bowser - Whitehorse area of British Columbia; unpublished report; *Institute of Sedimentary and Petroleum Geology*, 47 pages plus appendices.

Hart, C. J. R., Dickie, J. R., Ghosh, D. K. and Armstrong, R. L. (1995): Provenance constraints for Whitehorse Trough conglomerate: U-Pb zircon dates and initial Sr ratios of granitic clasts in Jurassic Laberge Group, Yukon Territory; in Jurassic magmatism and tectonics of the North American Cordillera, Miller, D. M. and Busby, C., Boulder, Colorado, Geological Society of America, Special Paper 299, pages 47-63.

Hunt, J. M. (1996): Petroleum Geochemistry and Geology; W.H. Freeman and Company, New York, 743 pages.

Johannson, G. G., Smith, P. L. and Gordey, S. P. (1997): Early Jurassic evolution of the northern Stikinian arc: evidence from the Laberge Group, northwestern British Columbia; *Canadian Journal of Earth Sciences*, Volume 34, pages 1030-1057.

Lafargue, E., Marquis, F. and Pillot, D. (1998): Rock-Eval 6 applications in hydrocarbon exploration, production and soils contamination studies; *Oil & Gas Science and Technology*, Volume 53, pages 421-437.

Meyer, B. L. and Nederlof, M. H. (1984): Identification of source rocks on wire-line logs by density/resistivity and sonic transit time/resistivity crossplots; *American Association of Petroleum Geologists Bulletin*, Volume 68, pages 121-129.

Mihalynuk, M. G. (1999): Geology and mineral resources of the Tagish Lake area (NTS 104M/8, 9, 10E, 15 and 104N/12W) northwestern British Columbia; *B.C. Ministry of Energy, Mines and Petroleum Resources*, Bulletin 105, 217 pages.

Mihalynuk, M. G., Erdmer, P., Ghent, E. D., Archibald, D. A., Friedman, R. M., Cordey, F., Johannson, G. G. and Beanish, J. (1999): Age constraints for emplacement of the northern Cache Creek terrane and implications of blueschist metamorphism; *in* Geological Fieldwork 1998, *B.C. Ministry of Energy, Mines and Petroleum Resources*, Paper 1999-1, pages 127-141.

Mihalynuk, M. G., Erdmer, P., Ghent, E. D., Cordey, F., Archibald, D., Friedman, R. M. and Johannson, G. G. (in press): Subduction to obduction of coherent French Range blueschist - In less than 2.5 Myrs?; *Geological Society of America Bulletin*.

Mihalynuk, M. G., Johnston, S. T., English, J. M., Cordey, F., Villeneuve, M. E., Rui, L. and Orchard, M. J. (2003): Atlin TGI, Part II: Regional geology and mineralization of the Nakina area (NTS 104N/2W and 3); *in* Geological Fieldwork 2002, *B.C. Ministry of Energy and Mines*, Paper 2003-1, pages 9-37.

Mihalynuk, M. G., Smith, M. T., Gabites, J. E., Runkle, D. and Lefebure, D. (1992): Age of emplacement and basement character of the Cache Creek terrane as constrained by new isotopic and geochemical data; *Canadian Journal of Earth Sciences*, Volume 29, pages 2463-2477.

Monger, J. W. H., Wheeler, J. O., Tipper, H. W., Gabrielse, H., Harms, T., Struik, L. C., Campbell, R. B., Dodds, C. J., Gehrels, G. E. and O'Brien, J. (1991): Upper Devonian to Middle Jurassic assemblages - Part B. Cordilleran terranes; *in* Geology of the Cordilleran Orogen in Canada, The Geology of North America, Gabrielse, H. and Yorath, C. J., Denver, Colorado, *Geological Society of America*, pages 281-327.

National Energy Board (2001): Petroleum resource assessment of the Whitehorse Trough, Yukon Territory, Canada; *Yukon Energy Resources Branch*, 50 pages.

Peters, K. E. (1986): Guidelines for evaluating petroleum source rock using programmed pyrolysis; *The American Association of Petroleum Geologists Bulletin*, Volume 70, pages 318-329.

Peters, K. E. and Moldowan, J. M. (1993): The Biomarker Guide; Prentice-Hall, Eaglewood Cliffs, New Jersey, 363 pages.

Ricketts, B. D., Evenchick, C. A., Anderson, R. G. and Murphy, D. C. (1992): Bowser basin, northern British Columbia : Constraints on the timing of initial subsidence and Stikinia - North America terrane interactions; Geology, Volume 20, pages 1119-1122.

Souther, J. G. (1971): Geology and mineral deposits of Tulsequah map-area, British Columbia; Geological Survey of Canada, Memoir 362, 84 pages.

Tempelman-Kluit, D. J. (1979): Transported cataclasite, ophiolite and granodiorite in Yukon : evidence of arc-continent collision; Geological Survey of Canada, Paper 79-14, 27 pages.

Thomas, M. M. and Clouse, J. A. (1990): Primary migration by diffusion through kerogen: II. Hydrocarbon diffusivities in kerogen; Geochimica et Cosmochimica Acta, Volume 54, pages 2781-2792.

Thorstad, L. E. and Gabrielse, H. (1986): The Upper Triassic Kutcho Formation, Cassiar Mountains, north-central British Columbia; Geological Survey of Canada, Paper 86-16, 53 pages.

Wessel, P. and Smith, W. H. F. (1995): New version of the Generic Mapping Tools released; Eos, Volume F359.

Wheeler, J. O. (1961): Whitehorse map-area, Yukon Territory (105D); Geological Survey of Canada, Memoir 312, 156 pages.

PETROLEUM SOURCE ROCK POTENTIAL OF LOWER TO MIDDLE JURASSIC CLASTICS, INTERMONTANE BASINS, BRITISH COLUMBIA

Filippo Ferri
Resource Development and Geoscience Branch, BC Ministry of Energy and Mines,
6th Flr-1810 Blanshard St., Victoria, BC, Canada, V8W 9N3

Kirk Osadetz
Geological Survey of Canada: Calgary, 3303 33 St. NW, Calgary, AB, Canada, T2L 2A7

Carol Evenchick
Geological Survey of Canada: Pacific, 101-605 Robson St. Vancouver, BC, Canada, V6B 5J3

KEYWORDS: petroleum source rocks, petroleum, crude oil, natural gas, Bowser Basin, Quesnel Trough, Nechako Basin, Sustut Basin, Intermontane, Interior Basins, Canadian Cordillera, Jurassic

INTRODUCTION

The presence of suitable petroleum source rocks is a necessary condition for the presence of an effective total petroleum system, which constrains the petroleum potential of under-explored basins such as those within the Intermontane region of British Columbia (Curiale, 1994). Hayes (2002), in his report on the crude oil and natural gas potential of the Nechako Basin of British Columbia, indicated that a major issue for the basin was the lack of recognition of a good petroleum source rock horizon. This perception is applicable to all the Intermontane basins due to the limited amount of crude oil and natural gas exploration activity and a subsequent lack of relevant information.

This paper summarizes some of our current understanding of Early and Middle Jurassic stratigraphy within parts of the Intermontane region of the Canadian Cordillera that may have petroleum source rock potential. It also provides an update on the activities undertaken by the Resource Development and Geoscience Branch (RDGB) of the British Columbia Ministry of Energy and Mines to address the issue through recognition and basic characterization of potential source bed horizons within the Intermontane region. This is part of a much larger collaborative program, which began in 2001, between the Geological Survey of Canada (GSC) and the RDGB to look at energy-related aspects of the Intermontane Basins. The RDGB is also collaborating with the GSC on a new, multiyear initiative, which started in 2003, entitled "Integrated Petroleum Resource Potential and Geoscience Studies of the Bowser and Sustut Basins".

Subsurface characterization of potential Cretaceous and Tertiary petroleum source rocks within the Nechako area has been documented by Hunt (1992) and Hunt and Bustin (1997). Osadetz et al. (2003) obtained Rock-Eval pyrolytic and total organic content (TOC) data for well cuttings from all bore holes within the Nechako and Bowser Basins. Evenchick et al. (2003) reported bleeding crude oil from paleomagnetic coring operations in fine-grained clastics that may be either migrated petroleum or residual crude oil stains in potential petroleum source rocks. The purpose of the present study was to sample potential source-bed horizons of Early and Middle Jurassic age in areas where subsurface data is lacking. In addition, the following brief summary on the extent of potential source-bed horizons of this age within certain parts of the Canadian Cordillera indicates these units are potentially regionally distributed.

The author, as part of the regional mapping program examining Bowser Lake and Sustut Group rocks within the western portion of the McConnell Creek map area (NTS 094D; see Evenchick et al., 2003), sampled potential petroleum source rock horizons in this area (Figures 1 and 2). In addition, one week was spent examining possible source beds on the east side of the Nechako area within the Quesnel Trough (Figures 1, 3, and 4). Twenty-five samples were collected in the McConnell Creek area, and 12 samples were taken from the Quesnel Trough. Further sampling is planned in both regions during the 2004 field season.

Current research in the Bowser Basin has recognized crude oil staining in surface and subsurface samples of the Bowser and Sustut Groups (Osadetz *et al.,* 2004, 2003; Evenchick *et al.*, 2003). The data suggest the presence of at least 3 source-bed horizons, one of Jurassic to Cretaceous age, another within carbonate sequences of Paleozoic age, and a third of fresh-water origin. Data in this paper, in part, reviews sampling undertaken in the field in an attempt to locate the stratigraphic horizons responsible for the staining.

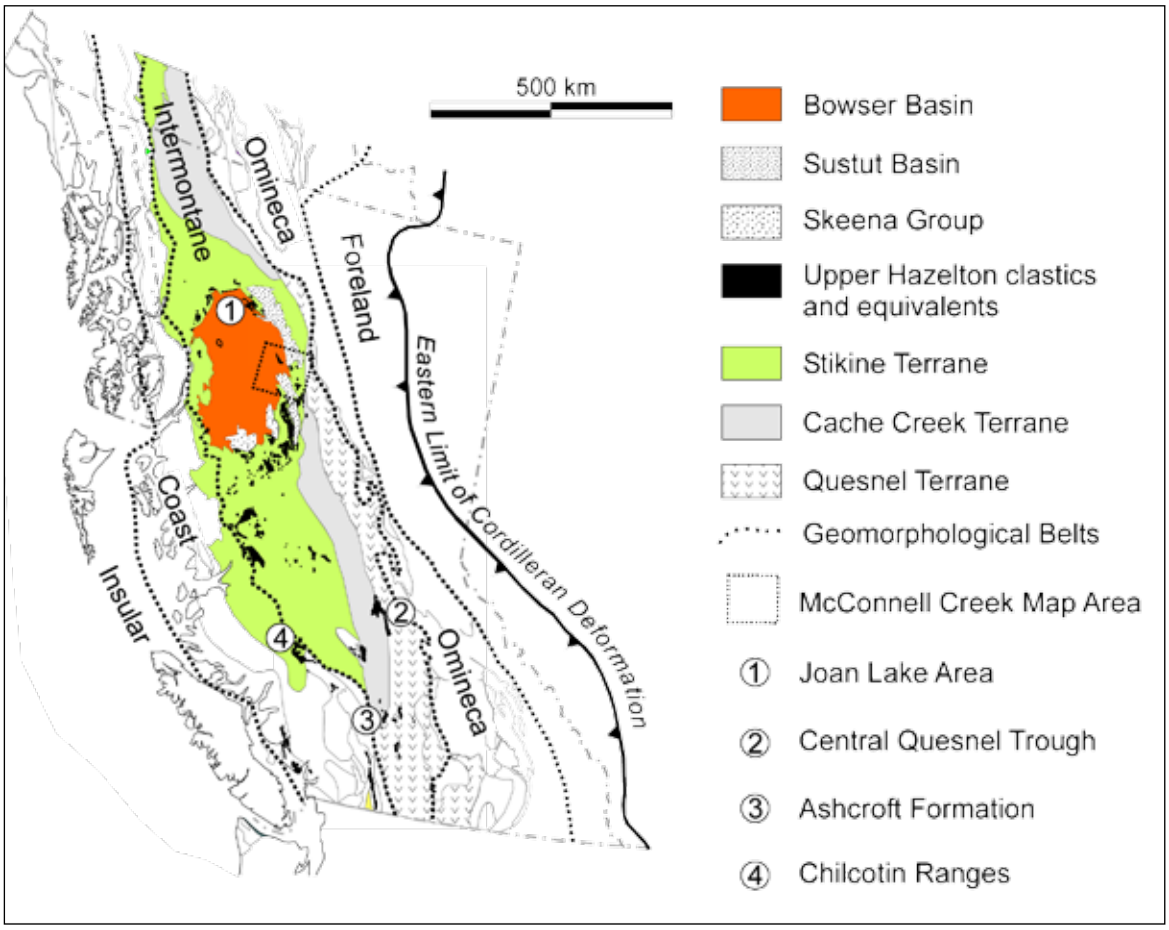

Figure 1. Geomorphological belts of the Canadian Cordillera together with selected terranes and locations of areas mentioned in text or shown in subsequent diagrams. The regional distribution of Early to Middle Jurassic clastics is also indicated. Base map modified from Osadetz et al., 2003.

In Bowser-Sustut and Quesnel Trough areas, the focus of sampling was within black carbonaceous sequences of Early to Middle Jurassic age, which are believed to underlie coarser clastic units of the basins. This stratigraphic interval encompasses the Toarcian-Aalenian time period, which on a worldwide scale is inferred to record an interval of anoxic water conditions resulting in enhanced preservation of accumulated organic material (Jenkyns, 1988).

Worldwide oceanic anoxic events are documented at several stratigraphic levels within Jurassic and Cretaceous sedimentary rocks. In addition to the Toarcian, these include intervals within the Aptian-Albian, Cenomanian-Turonian, and Santonian ages (Jenkyns, 1980, 1988). Most of these time periods are well represented within the Western Canada Sedimentary Basin and have contributed a large proportion of the petroleum within known pools (e.g., First and Second White Speckled Shale, Base of Fish Scales zone, and Fernie Formation; see Creaney et al., 1994).

BOWSER AND SUSTUT BASINS

The Bowser and Sustut Basins are overlap assemblages deposited on an allochthonous terrane of the Canadian Cordillera. Located in north-central British Columbia, they are found within the northern part of the Intermontane Belt and sit on Devonian to Jurassic rocks of Stikinia (Figure 1).

There are 3 main successions within these basins: the Middle Jurassic to mid-Cretaceous Bowser Lake Group, the Lower to mid-Cretaceous Skeena Group, and the mid- to Upper Cretaceous Sustut Group. Bowser Lake strata represent a southwestward-prograding delta to distal submarine fan sequence and contain marine to nonmarine sediments (Evenchick et al., 2001). Skeena rocks, located along the southern part of Bowser Basin, are inferred to have been deposited in marine to nonmarine deltaic environments, but their relationship to Bowser Lake stratigraphy is uncertain (Tipper and Richards, 1976). The Sustut Group is inferred to have been deposited in fluvial to lacustrine environments (Eisbacher, 1974) that existed in a foreland basin east of deforming Bowser Lake strata (Evenchick and Thorkelson, in press).

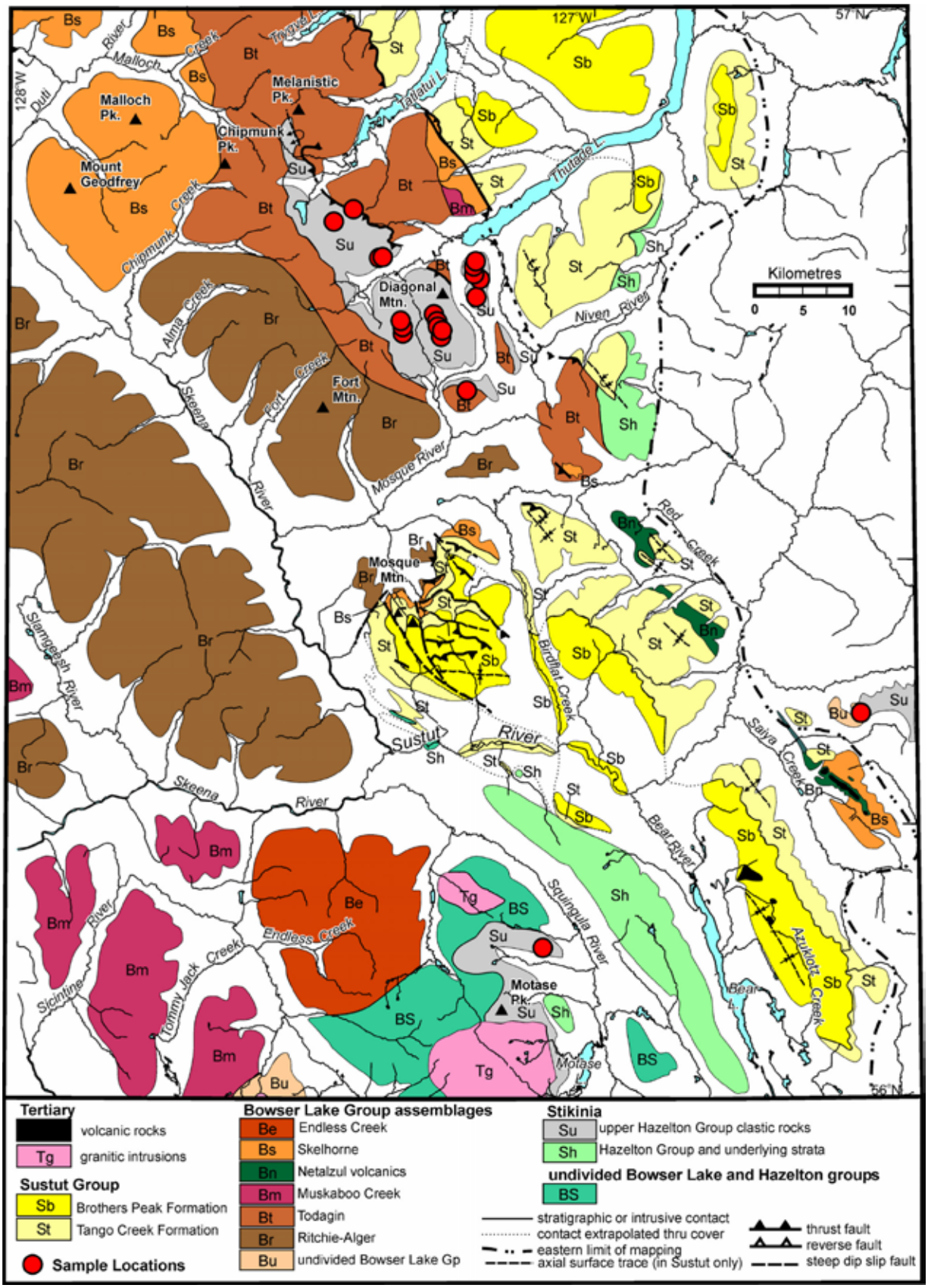

Figure 2. Generalized geology of the McConnell Creek map area, showing sample locations. Modified from Evenchick et al., 2003.

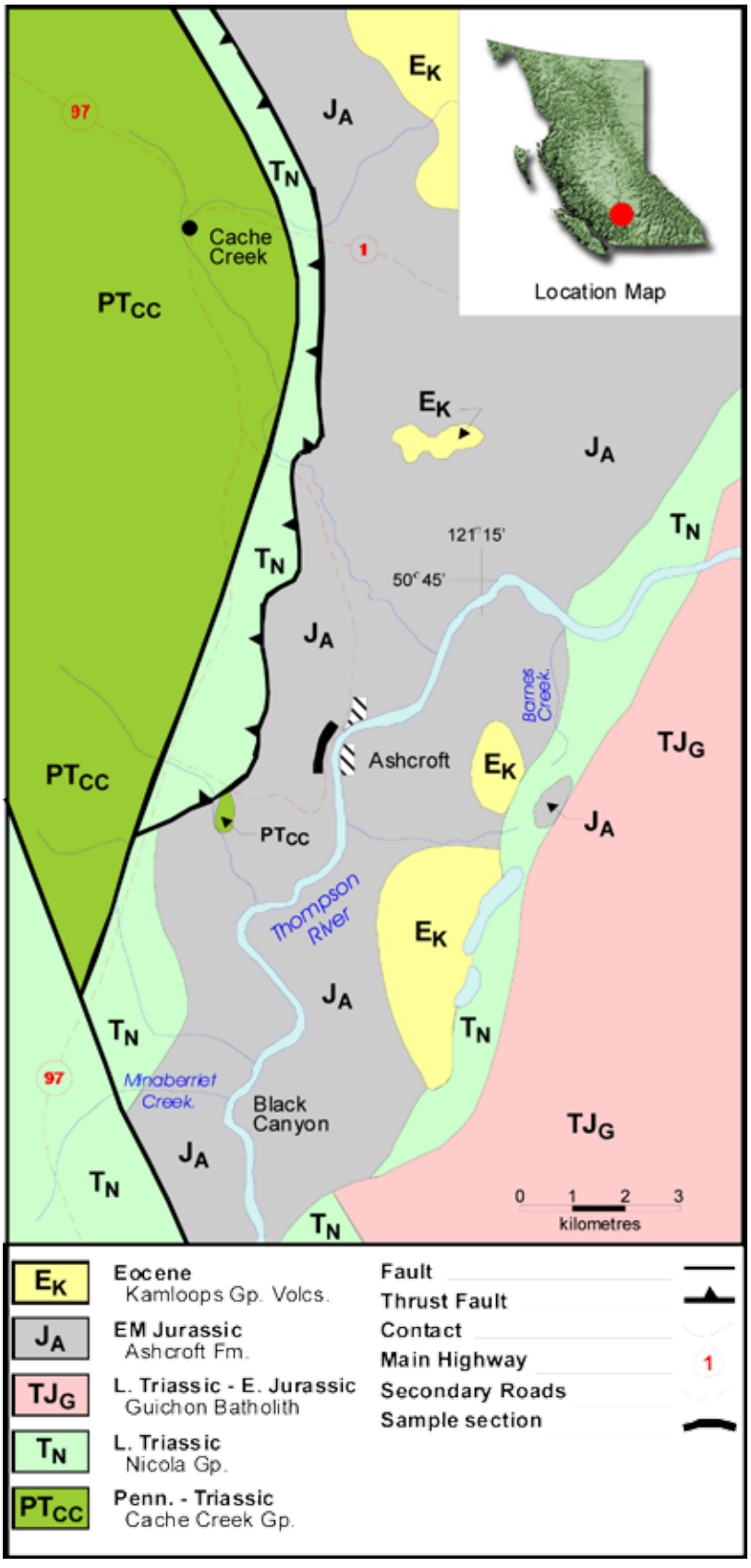

Figure 3. Generalized geology map of the Ashcroft area, showing extent of Ashcroft Formation and sample locations. Modified from Travers, 1978.

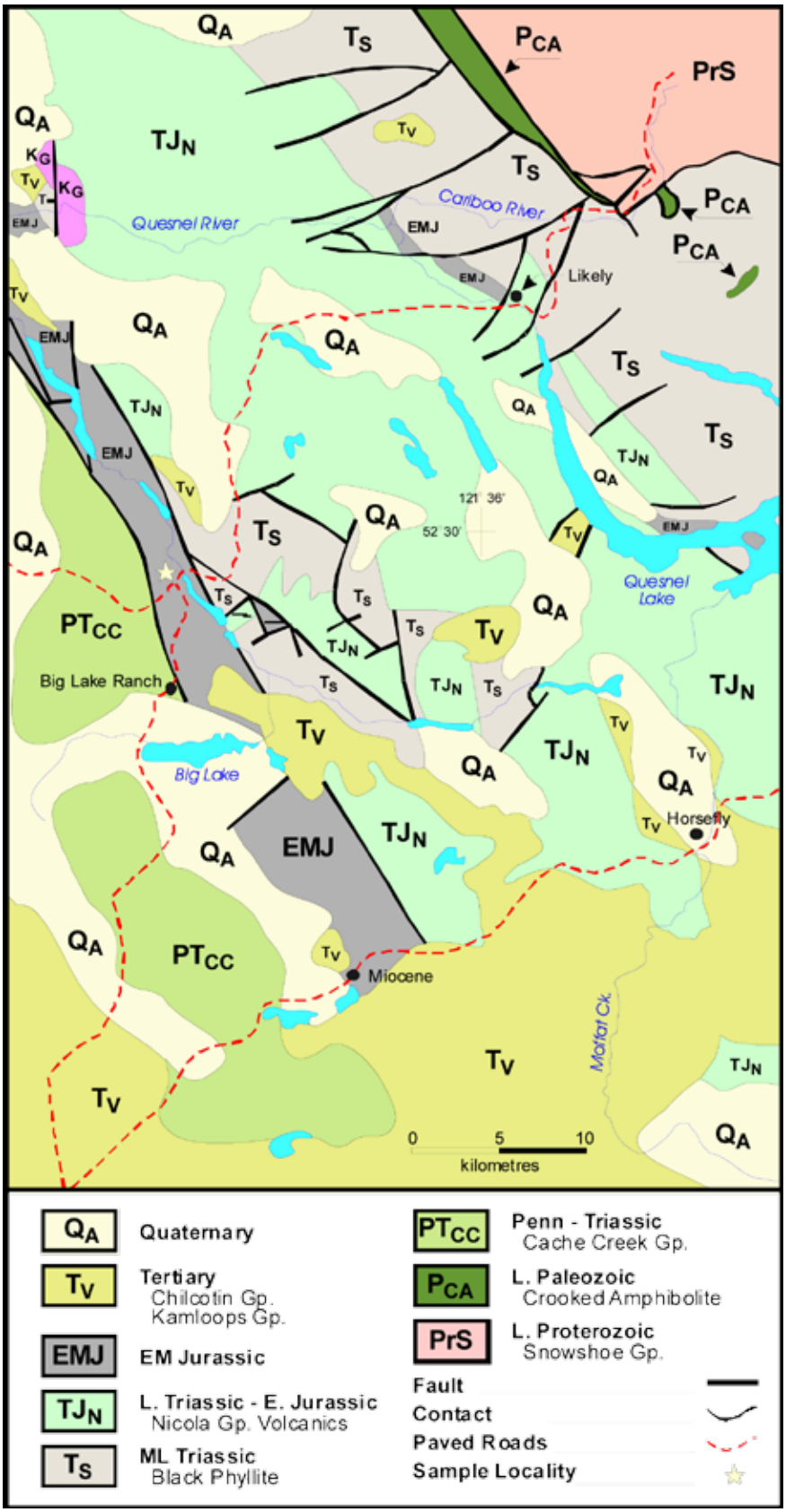

Figure 4. Generalized geology of Quesnel Terrane west of Quesnel Lake, showing sample location and distribution of Early to Middle Jurassic clastics.

Bowser, Skeena, Sustut, and underlying Stikinia rocks are deformed into dominantly northwest-trending fold and thrust structures comprising the Skeena Fold Belt (Evenchick, 1991). Evenchick (1991) demonstrated that this thin-skinned structural belt of mid-Cretaceous age contains a well-developed triangle zone at its northeastern margin within Sustut strata.

Potential Source Beds

In the area of the Bowser and Sustut Basins, black organic-rich shales have been recognized within the Lower to Middle Jurassic sediments of the upper Hazelton Group (Thomson et al., 1986). In addition, slope and submarine fan facies of the Bowser Lake Group contain abundant sections of black shale that may have elevated organic contents.

Effective Mesozoic and Paleozoic petroleum source rocks are postulated based on analysis of crude oil stains from surface and subsurface samples of Bowser and Sustut lithologies (Evenchick *et al.*, 2003; Osadetz *et al.*, 2003, 2004). Indirect confirmation of a Paleozoic source horizon is indicated by crude oil staining in cored paleomagnetic samples taken from Permian and Triassic sequences (Evenchick *et al.*, 2003). Stikine Assemblage strata contain black carbonaceous sequences of Devonian-Mississippian age (Logan *et al.*, 2000) similar in composition to other time-equivalent sequences throughout Cordilleran terranes and within the miogeocline (e.g., Exshaw and Bakken Formations).

HAZELTON GROUP

Strata of the Bowser Lake Group overlie fine-grained clastic sedimentary rocks of the upper Hazelton Group (Figure 2). This latter succession is dominantly a volcanic sequence of broadly Early to Middle Jurassic age (Tipper and Richards, 1976). Although upper Hazelton clastics are well developed below the Bowser Lake Group, these rocks locally grade into dominantly volcanic sequences.

Terminology of the Hazelton Group varies along the basin margins. In the northwestern part of the basin, upper clastics are termed the Spatsizi Formation (Evenchick and Thorkelson, in press) whereas further west, in the Eskay Creek and Forrest Kerr areas, this horizon contains 3 facies with varying proportions of volcanic rocks and is referred to as the Salmon River Formation (Anderson, 1993; Logan et al., 2000). In southern Bowser Basin, Tipper and Richards (1976) subdivided upper Hazelton clastics into the Nilkitkwa and Smithers Formations.

Upper Hazelton Group clastic rocks span Early Pliensbachian to Bajocian-Bathonian times in the northern Bowser Basin (Thomson, et al., 1986; Evenchick et al., 2001). Volcanic rocks become increasingly voluminous northward in Spatsizi River map area (Thomson et al., 1986). There, upper Hazelton Group rocks have been formally assigned to the Spatsizi Formation (Evenchick and Thorkelson, in press). In the Joan Lake area of this map region, Thomson et al. (1986) initially assigned these rocks to group status and defined the Joan, Wolf Den, Melisson, Abou, and Quock Formations. Although subdivision of this horizon is possible in the Joan Lake area, Evenchick and Thorkelson (ibid.) suggested this succession be lowered to formation status (and the constituent formations to members) because it was difficult to recognize all units on a regional scale, and strata in similar stratigraphic positions around the Bowser Basin are formations in the Hazelton Group.

In the Joan Lake area, Upper Pliensbachian to Middle Toarcian Wolf Den and Aalenian Abou Members are dominanted by black to dark grey shales which, together with their faunal assemblages, suggest anoxic water conditions (Thomson et al., 1986). The Bajocian Quock Member, with its distinctive sections of interlayered black siliceous carbonaceous siltstone, shale, and light-coloured ash tuff ("pyjama beds"), are also inferred to have been deposited in anaerobic conditions. Thomson et al. (ibid.) describe parts of these lithologies as containing up to 20% organic material. The authors speculated this horizon would have acted as an excellent petroleum source rock and noted its well-placed stratigraphic position at the base of the Bowser Lake sequence.

Although the members of the Spatsizi Formation in the Joan Lake area may represent a restrictive facies of the upper Hazelton Group, the overall basinal, anoxic conditions (as inferred for upper Hazelton clastics around the margins of the Bowser Basin and within structural windows or culminations) suggests that these organic-rich lithologies may underlie much of the basin (Thomson et al., 1986).

MCCONNELL CREEK MAP AREA (094D)

The author spent approximately 5 weeks in the western and central parts of the McConnell Creek map area as part of a provincial-federal cooperative regional mapping program (Evenchick et al., 2003). During this time, sections of the upper Hazelton Group were examined and sampled in the Diagonal Mountain and Motasse Peak areas for characterization of organic content. In addition, parts of the lower Bowser Lake Group together with black siltstone or shales in the Ritchie-Alger and Todagin assemblages were also sampled.

Upper Hazelton rocks in this area have been previously described by Tipper and Richards (1976), Jeletzky (1976), Evenchick and Porter (1993), Jakobs (1993), and Evenchick et al. (2003). The largest area covered by these rocks in the western McConnell Creek map sheet is roughly centred on Diagonal Mountain. The total thickness of the

upper Hazelton Group is difficult to determine as the base is not exposed; however, the exposed section is conservatively in the order of 300 m thick. The dominant lithology is variably cleaved, rusty- to orange-weathering, blocky, dark grey to black siliceous siltstones and shales with variable proportions of thin bedded white to pinkish tuff (Photo 1). These tuffaceous lithologies comprise the typical Toarcian to Bajocian sections of the upper Hazelton Group seen around the Bowser Basin and are informally referred to as the "pyjama beds". The amount of tuff is variable within sections exposed in the Diagonal Mountain area, but is usually less than 30% of the section where present. Tuff varies from less than 1 mm to 10 cm thick and, although usually homogenous, can display graded bedding or ripple marks. Parts of the sequence are composed almost entirely of dark grey to black, platy siltstone or shale. Some sections are blue-grey in colour and quite carbonaceous.

Minor lithologies include light grey- to grey-weathering calcareous siltstone exhibiting a dark grey-brown colour on fresh surface and brown to grey-brown weathering, grey micritic to clastic limestone up to 30 cm thick, which forms lenses up to several metres in length. Sections of this sequence are rusty-weathering and contain several percent authigenic (or detrital?) pyrite. Pyrite is best developed within tuffaceous sections, although it is also present in siliceous siltstone. The anoxic conditions inferred for this sequence, together with the abundance of pyrite, suggests the potential to host sedimentary exhalative mineral deposits.

The contact between the upper Hazelton clastics and overlying Bowser Lake Group is transitional (Evenchick et al., 2003; Jakobs, 1993). Interbedded tuff is lost up-section, and the siliceous nature of the siltstone disappears, resulting in well-cleaved, rusty- to brown-weathering shales and slate up to 20 m thick. The first thin beds of chert(?) sandstone are observed at the top of this lithology, together with the first indications of bioturbation in shale and siltstone. Sandstone becomes more abundant up-section and the percentage of rusty-weathering horizons decreases. The contact has been placed at the top of the rusty-weathering section, occurring some 100 m above the first sandstone horizon and approximately 15 m below the base of the first chert-pebble conglomerate typical of the Bowser Lake Group (Evenchick et al., 2003).

The present interpretation of the upper contact for the Hazelton Group would make it as young as late Bathonian (*see* Evenchick *et al.*, 2001; 2003). Evenchick *et al.* (2003) argue that, considering the Oxfordian ages for the Bowser Lake Group in the area, the age of this contact may be younger and within the Callovian. The oldest ages for the Hazelton Group in the Diagonal Mountain area are Toarcian (Evenchick *et al.*, 2001). Palfy *et al.* (2000) reported an age of 167.2 +10.5 –0.4 Ma for tuff sampled from "pyjama beds" approximately 4.5 km south-southeast of Diagonal Mountain.

Photo 1. Typical interlayered tuff and dark grey to black siliceous siltstone of the "pyjama beds", upper Hazelton Group clastics, McConnell Creek map area.

Lithologies at Diagonal Mountain are similar to those of the Quock Member (Thomson et al., 1986). Based on fossil ages (Evenchick et al., 2001), sections at Diagonal Mountain would also be equivalent age to units of the Abou, Melisson, and Wolf Den Members. The lack of shallower-water lithologies at Diagonal Mountain (represented by the Melisson Member) suggests that this unit was either removed below the Late Toarcian unconformity or that it was not deposited. Descriptions of the Wolf Den, Abou, and Quock Members are entirely consistent with lithologies observed at Diagonal Mountain, although they are not distributed in a simple stratigraphy that can be mapped.

At Motasse Peak, the Hazelton Group also contains the striped, interlayered siltstone and tuff as described in the Diagonal Mountain area. Tuff is also lost up-section, resulting in rusty-weathering siltstone and shale. The recognition of the upper contact is difficult because of the thick section of rusty-weathering siltstones and shales together with a lack of coarse clastic lithologies typical of the basal Bowser Lake Group. There is no definite break in the rusty nature of the siltstone lithologies. This may be due to the presence of nearby Tertiary intrusions, in conjunction with structural complication.

Ritchie-Alger and Todagin assemblages represent coeval slope and submarine fan assemblages, respectively, of Late Jurassic to Early Cretaceous age. These units have an abundance of dark grey and black fine-grained lithologies that may have accumulated abundant organic matter. The Todagin assemblage contains dark grey- and black-weathering siltstone and shale, which are not as dominant within the Ritchie-Alger. These units also are inferred to have been deposited in turbiditic deposits and higher-energy sequences of chert sandstone and conglomerate, which are more voluminous in the Ritchie-Alger assemblage than they are in the Todagin (Evenchick et al., 2001; 2003).

Siltstone units are typically orange-brown to dark grey-weathering and massive to thickly bedded. They can display poor cleavage, but are typically blocky- to crumbly-weathering. They commonly contain thin orange-brown weathering laminae, which are commonly bioturbated. Nodules or discontinuous horizons of orange-weathering grey limestone up to several tens of centimeters thick are also present within sections of the siltstone. Several horizons (up to 5 m thick) of rusty-weathering black siltstone were also observed in these units.

QUESNEL TROUGH

The senior author spent several days sampling sections of organic-rich shale within parts of the Quesnel Trough. These localities are described by Macauley (1984) as potential oil shale horizons based on descriptions of earlier workers. These sections are within Lower to Middle Jurassic fine clastic rocks, similar in composition to the upper Hazelton Group, and include the Ashcroft Formation in the south and an unnamed sequence near the town of Likely. Both units overlie Triassic to Jurassic arc sequences of the Quesnel Terrane and are considered part of the overlap succession.

Ashcroft Formation

The Ashcroft Formation is well exposed in the area of Ashcroft and comprises approximately 1200 to 1600 m of carbonaceous shale, siltstone, and minor sandstone and conglomerate (Travers, 1978; Duffell and McTaggart, 1952). Exposures east of Ashcroft are believed to be nonmarine in origin (McMillan, 1974; Monger, 1982). Conglomerate, although a minor constituent, is distinctive by its polymict nature, containing clasts derived from ancestral North America and the Cache Creek and Quesnel Terranes (Travers, 1978; Duffell and McTaggart, 1952). The unit rests unconformably on the volcanics of Quesnellia and possibly the Cache Creek Terrane (Travers, 1978; Monger, 1982).

The age of the Ashcroft Formation is broadly Early to Middle Jurassic, and a compilation of fossil localities show this succession to be possibly Sinemurian to Callovian in age (Monger and Lear, 1989; Travers, 1978). Fossils collected near the base of the unit are possibly Sinemurian in age (Travers, 1978, Frebold and Tipper, 1969) and range up to Bajocian at the same locality (Monger and Lear, 1989). Along the eastern, nonmarine part of the sequence, fossil data suggest an unconformity between Pliensbachian and Callovian lithologies (Travers, 1978). Travers (1978) inferred that the western succession of Ashcroft strata were deposited during an interval of continuous sedimentation between Sinemurian and Callovian time, based on the lack of regolith and channel conglomerate associated with the unconformity in eastern sections. This may be true; however, no fossils of Toarcian or Bathonian age have been recovered from this area, which could indicate non-deposition, erosion, or lack of data.

McMillan (1974) describes up to 10 m of fetid, dark grey crystalline limestone in the Barnes Creek area, which he believed to be of bioclastic origin. In other sections along the creek, fetid limestone occurs as clasts within conglomerate deposited above a regolith. Associated shales, as elsewhere in the Ashcroft Formation, are black and carbonaceous. The section here contains Callovian fossils.

Duffel and McTaggart (1952) describe thick sections of black carbonaceous shale, which contain Callovian age fossils, in Black Canyon and near the mouth of Minaberriet Creek. This may have been the locality of the suspected oil shale. Recently, similar carbonaceous sequences were sampled along the highway into Ashcroft. Further sampling is planned for this area during 2004.

The Ashcroft Formation was sampled near the town of Ashcroft, where the unit is well exposed in road and railway cuts (Figure 3). Travers (1978) shows this sequence as being an overturned panel along the footwall of a thrust carrying the Nicola Group. No fossil data is available at this locality, although fossil collections to the south, along strike, are Pliensbachian or Sinemurian and Bajocian (Monger and Lear, 1989).

At this locality, the Ashcroft Formation consists of platy and blocky, rusty-weathering, dark grey to black siliceous siltstone. Cleavage is well developed locally but is commonly a spaced parting. Non-siliceous siltstone units typically exhibit blue-grey weathering and yellow salt residue. Discontinuous light-coloured bands were observed (tuffaceous?) and locally contained authigenic pyrite crystals. Some horizons are quite coarse and texturally approach a sandstone. Interbedded with these typical siliceous siltstone sequences are sections of black, crumbly, sooty (carbonaceous) siltstone and shale ranging from 5 to 10 m thick. These graphitic horizons locally contain 2 to 5 cm thick beds of pale to medium grey micritic limestone. The entire section at this locality is at least 100 m thick. Both lithologies were sampled at several points along the section. Results of organic petrographic and anhydrous pyrolysis analysis of these samples will be reported subsequently.

Central Quesnel Trough

Oil shales were described southwest of Likely in the early part of the 20th century (Robertson, 1904, 1905; Ells, 1925; Macauley, 1984). Analysis of these rocks demonstrated that they contain appreciable amounts of kerogen, and one report indicated a potential value of 25 litres/tonne for producible liquid petroleum (see Macauley, 1984). Macauley (ibid.) suggested that, based on descriptions and local geology, the unit that was sampled was probably part of the Lower to Middle Jurassic clastic succession overlying arc sequences of Quesnellia (Figure 4).

These Lower to Middle Jurassic sediments are considered overlap assemblages as they contain coarse clastics in their upper parts with cobbles derived from Cache Creek and Quesnel Terrane and ancestral North American sources, indicating that they formed after amalgamation of these terranes. This succession is also shown to overlap both Cache Creek and Quesnel Terrane rocks northwest and southeast of Likely (Tipper, 1978).

Panteleyev et al. (1996) detailed the geology and metallogenic nature of central Quesnel Terrane. Units described by these authors that could have been the source of the early samples include the fine-grained Pliensbachian to Aalenian siltstones and shales (Units 5 and 6). The older Upper Triassic "Black Phyllite", although composed of dark fine-grained clastics, is generally of too high a metamorphic grade (greenschist and higher) to contain any residual kerogen.

These Pliensbachian to Aalenian sediments contain sections of thin-bedded dark grey to grey calcareous siltstone, siltstone, and sandstone in the lower part. Polymictic conglomerate occurs in the top of the sequence and can also be interbedded with the finer lithologies. A Pliensbachian to possibly Toarcian age is suggested for the lower fine-grained unit, whereas Aalenian ammonites were extracted from interbedded fine-grained lithologies within the upper conglomeratic sequence (Panteleyev et al., 1996; Poulton and Tipper, 1991). The thickness of these sections is not reported, although structural sections, based on the geology of Panteleyev et al. (1996), would suggest several hundred metres.

Numerous sections were visited in 2003, based on mapping by Panteleyev et al. (1996), but due to the recessive nature of the units and limited time available, only one exposure was found on a road cut along the main highway, near Beaver Lake. This exposure consists of black sooty siltstone and dark grey to black calcareous siltstone. Both lithologies appear to be quite organic rich. The entire section at this locality was some 10 m thick. Results of organic petrographic and anhydrous pyrolysis analyses of these samples will be reported subsequently.

REGIONAL IMPLICATIONS

Sampling of Lower to Middle Jurassic organic-rich horizons within the Stikine and Quesnel terranes has shown these lithologies to be quite similar, not only in age but in overall composition. Both sequences were deposited after underlying terranes coalesced and amalgamated to ancestral North America, suggesting that sedimentary basins may have been contiguous.

Deep-water, fine-grained sediments of Early to Middle Jurassic age (Toarcian to Bajocian) appear to be widespread within the Canadian Cordillera and overlie many of the allochthonous terranes (Monger et al., 1991; Poulton and Tipper, 1991). These units are characterized by dark shales and siltstones interbedded with varying amounts of volcanics and coarser clastics. They are found within northern and central Stikine Terrane (Tipper and Richards, 1976), along the Chilcotin Ranges underlying rocks of the Tyaughton Trough (Umhoefer and Tipper, 1998; Figure 1) and eastward within the Quesnel Terrane (Panteleyev et al., 1996). Clearly the deeper-water conditions leading to the deposition of these sediments were extensive in the Canadian Cordillera, although punctuated by several volcanic episodes. The present configuration of these depocentres is a result of dextral strike-slip motion since the Cretaceous along major terrane-bounding faults (Gabrielse, 1991).

Lower to Middle Jurassic black shales within both

northern Stikine Terrane and Quesnellia are inferred to have been deposited in anaerobic depositional conditions. This time period brackets a major worldwide anoxic event (Jenkyns, 1988), which suggests that many of these sedimentary sequences within the Canadian Cordillera were also deposited in these environments. These low-oxygen conditions are conducive to the preservation of organic matter. To the east, within the Western Canada Sedimentary Basin, shale, siltstone, and carbonate of the Fernie Group were deposited during the same time period and are inferred to have been deposited under similar conditions. These rocks have proven to be one of the major petroleum source horizons within this basin.

The wide geographic distribution of Lower and Middle Jurassic fine-grained sediments suggests these units underlie coarser, clastic successions of the Interior Basins. Furthermore, the implied anoxic depositional environment recorded by these Lower and Middle Jurassic clastics suggests that these successions, under the right conditions, could have been sources of petroleum that migrated into overlying clastics.

ACKNOWLEDGEMENTS

The senior author would like to thank Chris Slater, Angelique Magee, Jamel Joseph, and Gareth Smith for excellent field assistance within the McConnell Creek map area. Our stay in this area was made much more comfortable by the hospitality of Arleyene and Dennis Farnworth of Steelehead Valhalla Lodge. Many thanks to Tom Brooks, Daryll Adzich, Ryan Hines, and Craig Kendell of Canadian Helicopters for dependable and safe flying.

REFERENCES

Anderson, R.G. (1993): A Mesozoic Stratigraphic and Plutonic Framework for northwestern Stikinia (Iskut River area), northwestern British Columbia, Canada; *in* G. Dunne and K. McDougall, (*eds*.), Mesozoic Paleogeography of the Western United States--II, S*ociety of Economic Palaeontologists and Mineralogists*, Pacific Section, Volume 71, pages 477-494.

Creaney, S., Allan, J., Cole, K.S., Fowler, M.G., Brooks, P.W., Osadetz, K.G., Macqueen, R.W., Snowdon, L.R., Riediger, C. (1994): Petroleum Generation and Migration in the Western Canada Sedimentary Basin; *in* Geological Atlas of the Western Canada Sedimentary Basin. G.D. Mossop and I. Shetsen (*comp*.), Calgary, Canadian Society of Petroleum Geologists and Alberta Research Council, pages 455-468.

Curiale, J.A. 1994. Correlation of Oils and Source Rocks - A Conceptual and Historical Prospective; *in*: Magoon, L.B., Dow, W.G. (*Editors.*), The Petroleum system-from Source to Trap. American Association of Petroleum Geologists, Memoir 60, pages 251-260.

Duffell, S. and McTaggart, K.C. (1952): Ashcroft Map-area, British Columbia; *Geological Survey of Canada*, Memoir 262, 122 pages.

Eisbacher, G.H. (1974): Sedimentary History and Tectonic Evolution of the Sustut and Sifton Basins, North-central British Columbia; *Geological Survey of Canada*, Paper 73-31, 57 pages.

Ells, S.C. (1925): Oil Shales of Canada; *in* Shale Oil, R.H. McKee (*ed.*), *American Chemical Society*, Monograph Series No. 25, The Chemical Catalog Company Inc., New York, pages 57-58.

Evenchick, C.A. (1991): Geometry, Evolution and Tectonic Framework of the Skeena Fold Belt, North-central British Columbia; *Tectonics*, Volume 10, pages 527-546.

Evenchick, C.A. and Thorkelson, D.J. (in press):Geology of the Spatsizi River Map Area, North-central British Columbia; *Geological Survey of Canada*, Bulletin 577.

Evenchick, C.A. and Proter, J.S. (1993): Geology of West McConnell Creek Map Area, British Columbia; *in* Current Research, Part A, *Geological Survey of Canada*, Paper 93-1A, pages 47-55.

Evenchick, C.A., Poulton, T.P., Tipper, H.W. and Braidek, I., (2001): Fossils and Facies of the Northern Two-thirds of the Bowser Basin, British Columbia; *Geological Survey of Canada*, Open File 3956.

Evenchick, C.A., Ferri, F., Mustard, P.S., McMechan, M., Osadetz, K.G., Stasiuk, L., Wilson, N.S.F, Enkin, R.J., Hadlari, T. and McNicoll, V.J. (2003): Recent Results and Activities of the Integrated Petroleum Resource Potential and Geoscience Studies of the Bowser and Sustut Basins Project, British Columbia; *in* Current Research, *Geological Survey of Canada*, 2003-A13, 11 pages.

Frebold, H. and Tipper, H.W. (1969): Lower Jurassic Rocks and Fauna near Ashcroft, British Columbia and Their Relation to Some Granitic Plutons (92-I); *Geological Survey of Canada*, Paper 69-23, 20 pages.

Gabrielse, H. (1991): Structural Styles, Chapter 17 *in* Geology of the Cordilleran Orogen in Canada, H. Gabrielse and C.J. Yorath (*ed.*.); *Geological Survey of Canada*, Geology of Canada, No. 4, pages 571-675.

Hayes, B. (2002): Petroleum Exploration Potential of the Nechako Basin, British Columbia; *B.C. Ministry of Energy and Mines*, Petroleum Geology Special Paper 2002-3.

Hunt, J.A. (1992): Stratigraphy, Maturation and Source Rock Potential of Cretaceous Strata in the Chilcotin-Nechako Region of British Columbia; *University of British Columbia*, Masters Thesis, 448 pages.

Hunt, J.A. and Bustin, R.M. (1997): Thermal Maturation and Source Rock Potential of Cretaceous Strata in the Chilcotin-Nechako Region, South-Central British Columbia; *Bulletin of Canadian Petroleum Geology*, Volume 45, pages 239-248.

Jakobs, G. (1993): Jurassic Stratigraphy of the Diagonal Mountain Area, McConnell Creek Map Area, North-Central British Columbia; *in* Report of Activities, Part A; *Geological Survey of Canada*, Paper 93-1, pages 43-46.

Jeletzky, O.L. (1976): Preliminary Report on Stratigraphy and Depositional History of Middle to Upper Jurassic Strata in McConnell Creek Map Area, (94D West Half), British Columbia *in* Report of Activities, Part A, *Geological Survey of Canada*, Paper 76-1A, pages 63-67.

Jenkyns, H.C. (1980): Cretaceous Anoxic Events: from Continents to Oceans; *Journal of the Geological Society of London*, Volume 137, pages 171-188.

Jenkyns, H.C. (1988): The Early Toarcian (Jurassic) Anoxic Event: Stratigraphic, Sedimentary and Geochemical Evidence; *American Journal of Science*, Volume 288, pages 101-151.

Logan, J.M., Drobe, J.R. and McClelland, W.C. (2000): Geology of the Forrest Kerr-Mess Creek Area, Northwestern British Columbia; *B.C. Ministry of Energy and Mines*; Bulletin 104, 164 pages.

Macauley, G. (1984): Geology of the Oil Shale Deposits of Canada; *Geological Survey of Canada*, Paper 81-25, 65 pages.

McMillan, W.J. (1974): Stratigraphic Section from the Jurassic Ashcroft Formation and Triassic Nicola Group Contiguous to the Guichon Creek Batholith; *in* Geological Fieldwork, *Geological Department of Mines and Petroleum Resources*; pages 27-34.

Monger, J.W.H. (1982): Geology of the Ashcroft Map Area, Southwestern British Columbia; *in* Current Research, Part A, Paper 82-1, pages 293-297.

Monger, J.W.H. and Lear, S. (1989): Geology, Ashcroft, British Columbia, *Geological Survey of Canada*, Preliminary Map 42-1989.

Monger, J.W.H., Wheeler, J.O., Tipper, H.W., Gabrielse, H., Harms, T., Struik, L.C., Campbell, R.B., Dodds, C.J., Gehrels, G.E. and O'Brien, J. (1991): Part B. Cordilleran Terranes *in* Upper Devonian to Middle Jurassic Assemblages, Chapter 8 of Geology of the Cordilleran Orogen in Canada, H. Gabrielse and C.J. Yorath (*ed.*); *Geological Survey of Canada*, Geology of Canada, No. 4, pages 281-327.

Osadetz, K.G., Snowdon, L.R., and Obermajer, M. (2003): ROCK-EVAL/TOC results from 11 Northern British Columbia boreholes. *Geological Survey of Canada*, Open File 1550 and *B.C. Ministry of Energy and Mines*, Petroleum Geology Open File 2003-1.

Osadetz, K.G., Evenchick, C.A., Ferri, F., Stasiuk, L., Obermajer, D.M. and Wilson, N.S F. (2003): Molecular composition of Crude Oil Stains from Bowser Basins *in* Geological Fieldwork 2002, *B.C. Ministry of Energy and Mines*, Paper 2003-1, pages 257-264.

Osadetz, K.G., Jiang, C., Evenchick, C. A., Ferri, F., Stasiuk, L. D., Wilson, N. S. F. and Hayes, M. (2004): Sterane Compositional Traits of Bowser and Sustut Basin Crude Oils: Indications for Three Effective Petroleum Systems; *Resource Development and Geoscience Branch, BC Ministry of Energy and Mines,* Summary of Activities 2004.

Pálfy, J., Mortensen, J.K., Smith, P.L., Friedman, R.M., McNicoll, V. and Villeneuve, M. (2000): New U-Pb Zircon Ages Integrated with Ammonite Biochronology from the Jurassic of the Canadian Cordillera; *Canadian Journal of Earth Sciences*; Volume 37, pages 549-567.

Panteleyev, A, Bailey, D.G., Bloodgood, M.A. and Hancock, K.D. (1996): Geology and Mineral Deposits of the Quesnel River-Horsefly Map Area, Central Quesnel Trough, British Columbia; *Ministry of Employment and Investment*, Bulletin 97, 156 pages.

Poulton, T.P. and Tipper, H.W. (1991): Aalenian Ammonites and Strata of Western Canada; *Geological Survey of Canada*, Bulletin 411, 71 pages.

Robertson, J. (1904): Progress of Mining – Oil Shales; *British Columbia Department of Mines*, Annual Report, 1903, page 24.

Robertson, J. (1905): Progress of Mining – Oil Shales; *British Columbia Department of Mines*, Annual Report, 1904, pages 23-24.

Thomson, R.C., Smith, P.L. and Tipper, H.W. (1986): Lower to Middle Jurassic (Pliensbachian to Bajocian) Stratigraphy of the Northern Spatsizi Area, North-central British Columbia; *Canadian Journal of Earth Science,* Volume 23, pages 1963-1973.

Tipper, H.W. (1978): Northeastern Part of Quesnel (93B) Map-Area, British Columbia, *in* Current Research, Part A, *Geological Survey of Canada*, Paper 78-1, pages 67-68.

Tipper, H.W. and Richards, T.A. (1976): Jurassic Stratigraphy and History of North-central British Columbia; *Geological Survey of Canada*, Bulletin 270, 73 pages.

Travers, W.B. (1978): Overturned Nicola and Ashcroft Strata and Their Relation to the Cache Creek Group, Southwestern Intermontane Belt, British Columbia; *Canadian Journal of Earth Science*, Volume 15, pages 99-116.

Umhoefer, P.J. and Tipper, H.W. (1998): Stratigraphy, Depositional Environment, and Tectonic Setting of the Upper Triassic to Middle Jurassic Rocks of the Chilcotin Ranges, Southwestern British Columbia; *Geological Survey of Canada*, Bulletin 519, 58 pages.

STERANE COMPOSITIONAL TRAITS OF BOWSER AND SUSTUT BASIN CRUDE OILS: INDICATIONS FOR THREE EFFECTIVE PETROLEUM SYSTEMS

By K.G. Osadetz[1], C. Jiang[2] ,C. A. Evenchick[3], F. Ferri[4], L. D. Stasiuk[1], N. S. F. Wilson[1] and M. Hayes[4]

KEYWORDS: Crude oil, natural gas, petroleum stains, seepages, Bowser-Sustut Basins, organic geochemistry, solvent extracts, biomarkers, steranes, terpanes, gas chromatography-mass spectrometry.

ABSTRACT

Crude oils extracted from Bowser Lake and Sustut Groups have distinctive compositions that are inferred to be indicative of at least three effective petroleum systems that have generated, expelled, and accumulated crude oil. Compositional differences among the three effective petroleum systems are illustrated by compositional variations of steranes, complicated molecules that have retained structural similarities to their inferred biological precursor, cholesterol. Oil stains occur widely, both geographically and stratigraphically. One compositional oil family is inferred to be derived from Stikine Assemblage, the sub-Hazelton succession. This petroleum is derived from pre-Jurassic marine carbonate source rocks deposited in hypersaline to mesohaline environments. A second compositional oil family is derived from Mesozoic open-marine source rocks that are inferred to be within the upper Hazelton or lower Bowser Lake Group, as the lowest stratigraphic occurrence of these oils lies in marine-slope deposits of the Bowser clastic wedge. A third oil family, which is inferred to be derived from lacustrine Mesozoic source rocks, occurs in northern Bowser and Sustut Basins, where it is probably derived from thick, often coaly, nonmarine Bowser Lake successions. The occurrence and composition of these crude oils expand the petroleum prospectivity of the Bowser and Sustut Basins by reducing petroleum system risks and indicating a possible petroleum system for Hazelton Group, which is now attributed petroleum potential.

INTRODUCTION

This report results from work performed as part of the project "Integrated Petroleum Resource Potential and Geoscience Studies of the Bowser and Sustut Basins", a collaborative research project of the BC Ministry of Energy and Mines (Oil and Gas Emerging Opportunities and Geoscience Branch) and the Geological Survey of Canada (Evenchick *et al.*, 2003). The current multiyear project is multidisciplinary in scope and broad in geographic coverage, including the length and breadth of both the Bowser and Sustut Basins. Primary activities include geological framework and energy resource studies and petroleum resource assessment.

Previous petroleum assessment work of the region identified substantial petroleum potential while recognising that there are several poorly understood but significant risks (Hannigan *et al.*, 1995). That study showed that there were significant play-level risks associated with the inferred petroleum potential of the Bowser Basin. More recent GSC/BCMEM research resulted in a profound shift in perceptions of organic and thermal maturity patterns in the Bowser and Sustut Basins (Evenchick *et al.*, 2002). The first regional organic maturity dataset illustrates that large areas, including the lowest stratigraphic levels of the Bowser Basin, have sufficiently low organic maturity levels to be favourable for the formation and preservation of crude oil. This fundamentally changed previous views that considered the high thermal maturity of some of the stratigraphically highest coals as a negative indication for hydrocarbon potential in all stratigraphic levels and all the geographic regions of the basins. The recent discovery of petroleum seepages and stains within the basin (Osadetz *et al.*, 2003a) provides information that eliminates play-level risks associated with petroleum system function and reservoir occurrence. The results presented herein indicate that there are at least three operational petroleum systems, each with sources and crude oils of different molecular composition and stratigraphic characteristics operating in Bowser and Sustut Basins. The results are consistent with the revised observations and models of thermal maturity and history. Integration of these data, models, and interpretations will increase the robustness of petroleum resource assessments in this potential frontier petroleum province.

[1]*Geological Survey of Canada: Calgary, 3303 33 St. NW, Calgary, AB, Canada, T2L 2A7*
[2]*Humble Geochemical Services Division, 218 Higgins Street, Humble, Texas 77338 U.S.A.*
[3]*Geological Survey of Canada: Pacific, 101-605 Robson St. Vancouver, BC, Canada, V6B 5J3;*
[4]*Resource Development and Geoscience Branch, BC Ministry of Energy and Mines, PO Box 9323, 6th Floor, 1810 Blanshard St., Victoria, BC, Canada, V8W 9N3*

REGIONAL GEOLOGICAL OVERVIEW

The Bowser and Sustut Basins are located in north-central British Columbia (Figure 1) in the Intermontane Belt of the Canadian Cordillera, a region of sedimentary diagenesis or low metamorphic grade (mainly greenschist facies) relative to the adjacent Omineca and Coast metamorphic and plutonic belts. They overlie Devonian to early Middle Jurassic strata of the allochthonous terrane Stikinia.

The basins comprise 3 stratigraphic successions with overlapping ages. The Bowser Lake Group is the lowest, ranging from upper Middle Jurassic to mid-Cretaceous. It constitutes a major clastic depositional wedge that includes strata deposited in distal submarine fan, slope, shallow-marine shelf, deltaic, fluvial, and lacustrine environments (e.g., Tipper and Richards, 1976; Evenchick *et al.*, 2001). It was deposited directly on Stikinia, a volcanic arc that includes Jurassic upper Hazelton Group clastic successions. The Lower to mid-Cretaceous Skeena Group occurs south of the Bowser Lake Group, with uncertain stratigraphic relationships. Skeena Group strata were deposited in marine and nonmarine environments and are intercalated with volcanic successions (Tipper and Richards, 1976). The mid- to Upper Cretaceous Sustut Group, a fluvial and lacustrine foreland basin succession, unconformably onlaps the Hazelton and Bowser Lake Groups that are deformed in older Skeena Fold Belt structures. The Skeena Fold Belt subsequently involved and deformed the Sustut Group (Eisbacher, 1974; Figure 2).

All 3 successions and underlying Stikinia are deformed in the Skeena Fold Belt, a thin-skinned contractional fold and thrust belt of Cretaceous and possibly early Tertiary age (Evenchick 1991). Northeast-vergent open to closed folds of about 100 to 1000 m wavelengths are the dominant structures at exposed levels, but larger wavelength folds often outlined by anticlinoria and synclinoria in Bowser Lake Group are associated with structural culminations and depressions inferred to be controlled by the involvement of Stikine Assemblage volcanic and clastic strata. The fold hinges trend northwest dominantly, but domains of northeast fold hinge trends occur in western Skeena Fold Belt (ibid.). Hinterland-verging thrusts in the vicinity of the boundary between Bowser Basin and Sustut Basin (Evenchick and Thorkelson, in press) define a triangle zone (Gordy *et al.*, 1977), similar to major productive and prospective structures in many thrust and fold belts (MacKay *et al.*, 1996).

CRUDE OIL OCCURRENCE

New field work and the analysis of existing samples have identified, extracted, and characterized 20 crude oil occurrences from locations in Bowser and Sustut Basins (Table 1, Figure 2). Numerous additional indications of crude oil staining and petroleum fluid inclusions occur within the Bowser and Sustut Basins, but only 20 samples (Table 1) are characterized here. Petroleum occurrences include:

1. Tsatia Mountain (NAD 27, UTM Zone V E442468 N6380068), a breeched oil field in Muskaboo Creek Assemblage Bowser Lake Group (GSC Extract X9693 and X9694; Osadetz *et al.*, 2003);
2. Sandstone in the roof of the triangle zone north of Cold Fish Lake (NAD 27, UTM Zone V E511100 N6396070), Tango Creek Formation, Sustut Group (GSC Extract 9746);
3. Footwall of the Crescent Fault near the confluence of Buckinghorse Creek and Spatsizi River (NAD 27, UTM Zone V E525670 N6366320), Eaglenest (deltaic) Assemblage of the Bowser Lake Group (GSC Extract X9731);
4. Amoco Ritchie well a-3-J/104-A-6, one of the only 2 petroleum exploration wells in the basin, shows extensive oil stains, which were extracted from samples at depths of 644.8 m, 1321.9 m, 1439.7 m, and 2055.8 m (2115.7', 4337.0', 4723.4', and 6745.0') (GSC Extracts X9742-X9745);
5. Twelve diverse samples from the northern Bowser and Sustut Basins (between 57.4284° N to 57.7803°N and 127.7689° W to 130.0625° W; GSC Extracts X9790 to X9801);
6. New field examples of rocks, potentially stained with crude oil, that were identified during sample drilling for paleomagnetic samples (Evenchick *et al.*, 2003). Oil films were present in the circulating fluid during paleomagnetic sampling of all Stikinia rocks sampled at Oweegee Dome. Oil films were present in a large number of lithologies through this antiformal culmination, including limestone, volcanic flows, volcaniclastic turbidites and conglomerates in Hazelton Group and lower units, as well as from Bowser Lake Group sandstone at Mount Ritchie (Figure 2, ibid.). These samples remain to be extracted and characterized, but they might reasonably be expected to resemble oil samples from the Ritchie wells;
7. Confirmed flammable natural gas seeps of biogenic methane into Tatogga Lake (Osadetz *et al.*, 2003), which will be reported elsewhere (Evenchick *et al.*, in prep).

All these indications demonstrate that petroleum (both crude oil and natural gas) occurs in Bowser and Sustut Basins. The existing resource assessment suggests that significant petroleum resources and large pool sizes can be expected (Hannigan *et al.*, 1995), but only exploratory drilling will confirm the existence of a significant undiscovered petroleum resource.

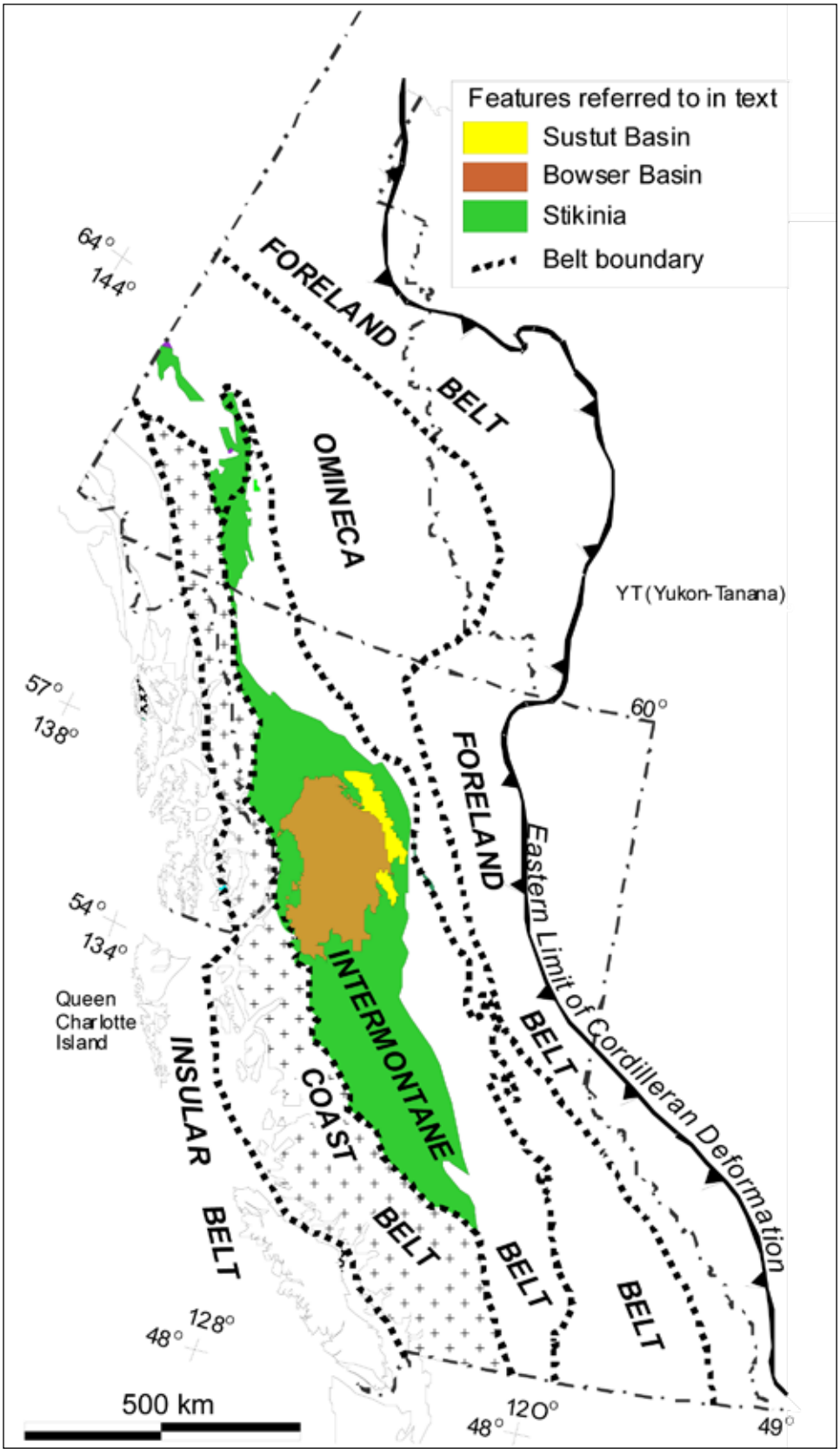

Figure 1. Location of the Bowser and Sustut Basins on a base map showing the morphogeological belts of the Canadian Cordillera.

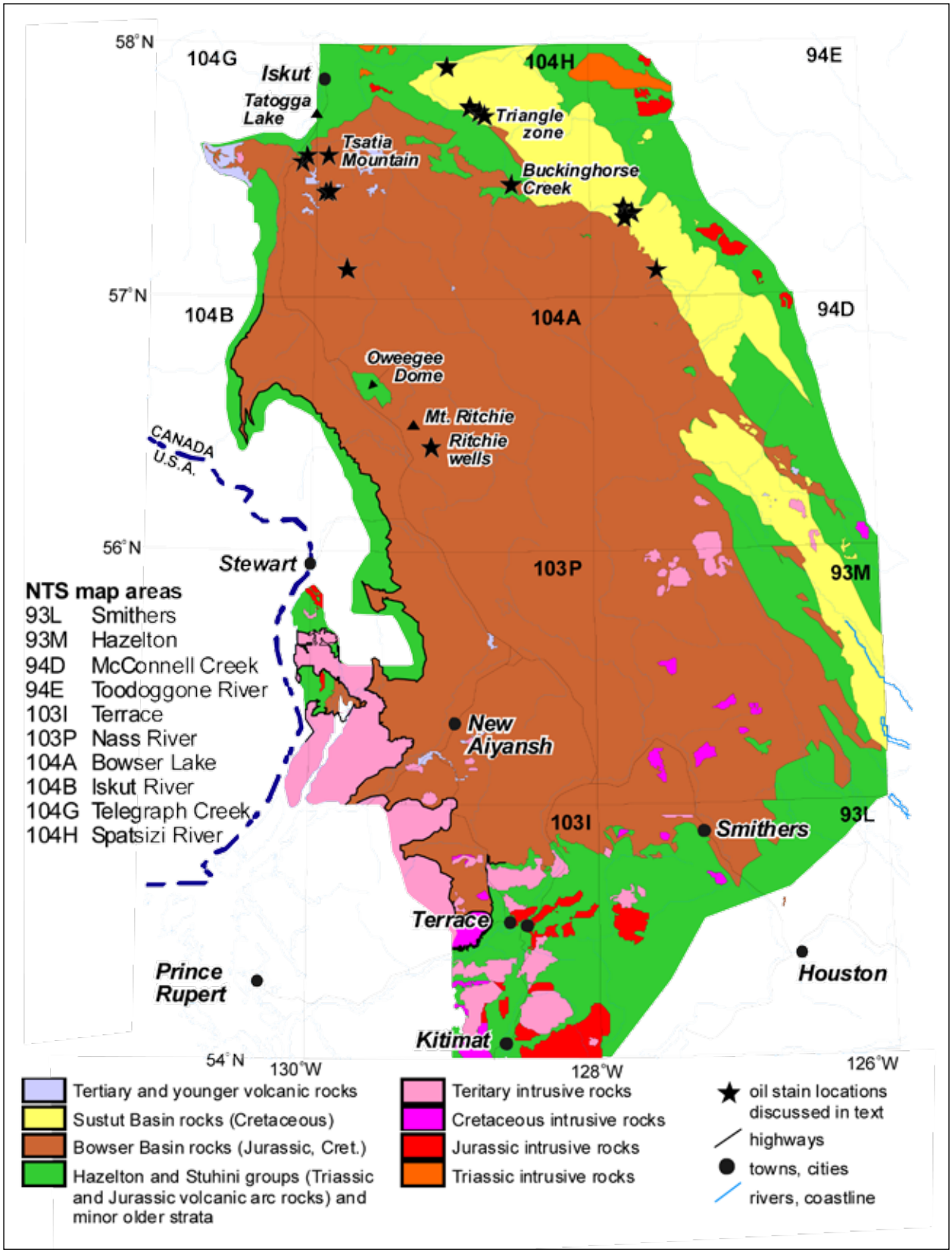

Figure 2. The locations of select crude oil samples discussed in text shown on a regional map of the Bowser and Sustut Basins. The locations of all samples are listed in Table 1.

TABLE 1. CRUDE OIL STAIN AND FLUID INCLUSION SAMPLE LOCATIONS.

Extract #	Latitude (°N)	Longitude (°W)	Depth	Map Unit
X9693	57.5613	129.9616	outcrop	Bowser Lake Gp; Muskaboo Creek Assemblage
X9694	57.5613	129.9616	outcrop	Bowser Lake Gp; Muskaboo Creek Assemblage
X9731	57.4408	128.5724	outcrop	Bowser Lake Gp; Eaglenest Assemblage
X9742	56.4188	129.1531	644.8 m	Bowser Lake Group
X9743	56.4188	129.1531	1321.9 m	Bowser Lake Group
X9744	56.4188	129.1531	1439.6 m	Bowser Lake Group
X9745	56.4188	129.1531	2055.8 m	Bowser Lake Group
X9746	57.5613	129.9616	outcrop	Sustut Group; Tango Creek Fm.
X9790	57.9247	129.1408	outcrop	Sustut Group; Tango Creek Fm.
X9791	57.5559	130.0481	outcrop	Bowser Lake Gp; Todagin Assemblage
X9792	57.1124	129.7686	outcrop	Bowser Lake Gp; Todagin Assemblage
X9793	57.4284	129.9309	outcrop	Bowser Lake Gp; Skelhorne Assemblage
X9794	57.4322	129.8974	outcrop	Bowser Lake Gp; Skelhorne Assemblage
X9795	57.3179	127.7667	outcrop	Sustut Group; Tango Creek Fm.
X9796	57.3137	127.7329	outcrop	Sustut Group; Tango Creek Fm.
X9797	57.1170	127.5309	outcrop	Bowser Lake Gp; Eaglenest Assemblage
X9798	57.7310	128.7963	outcrop	Sustut Group; Brothers Peak Fm.
X9799	57.7803	128.8793	outcrop	Sustut Group; Brothers Peak Fm.
X9800	57.5460	130.0625	outcrop	Bowser Lake Gp; Skelhorne Assemblage
X9801	57.3060	127.7689	outcrop	Sustut Group; Tango Creek Fm.

PETROLEUM CHARACTERIZATION USING MOLECULAR COMPOSITIONAL TRAITS

Crude oil compositional characteristics reflect kerogen paleoecology, depositional environments, diagenesis, and maturity. Differential expulsion, migration, and post-accumulation effects (processes like catagenesis, biodegradation, and water washing) can also affect crude oil composition (Peters and Moldowan, 1993; Waples and Machihara, 1990; Seifert and Moldowan, 1986, 1981, 1978); therefore, it is important to distinguish source characteristics from migration and post-accumulation effects before inferring depositional and diagenetic characteristics directly from crude oils. Extracts studied herein exhibit three distinguishable and distinctive compositional associations, or family groups, defined by persistent compositional characteristics that are exhibited by a variety of fractions and compounds, but which are especially well-illustrated by steranes, the focus of this discussion.

Phytolic acid side-chains from chlorophyll molecules indicate a particular phototrophism. The acyclic isoprenoid compounds pristane (Pr) and phytane (Ph), which are ubiquitous compounds in crude oils, are commonly derived from these side chains of chlorophyll molecules, although other sources for these compounds exist (Figure 3; Volkman and Maxwell, 1986). Low Pr/Ph ratios are commonly inferred to indicate water column anoxia, especially when accompanied by even-odd n-alkane predominance (Welte and Waples, 1973). High Pr/Ph ratios are commonly interpreted as indicative of oxic water columns (Volkman and Maxwell, 1986).

Steranes, both regular and rearranged, are common biological markers in oils. Acid clays in the depositional environment can control early diagenetic reactions that result in sterane rearrangement via unsaturated intermedi-

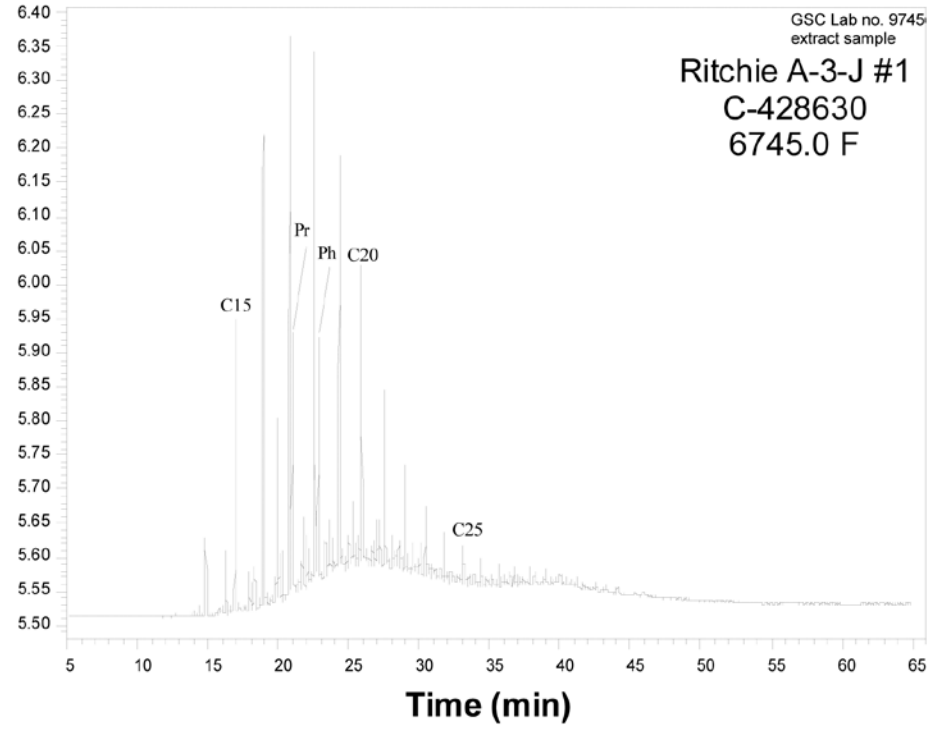

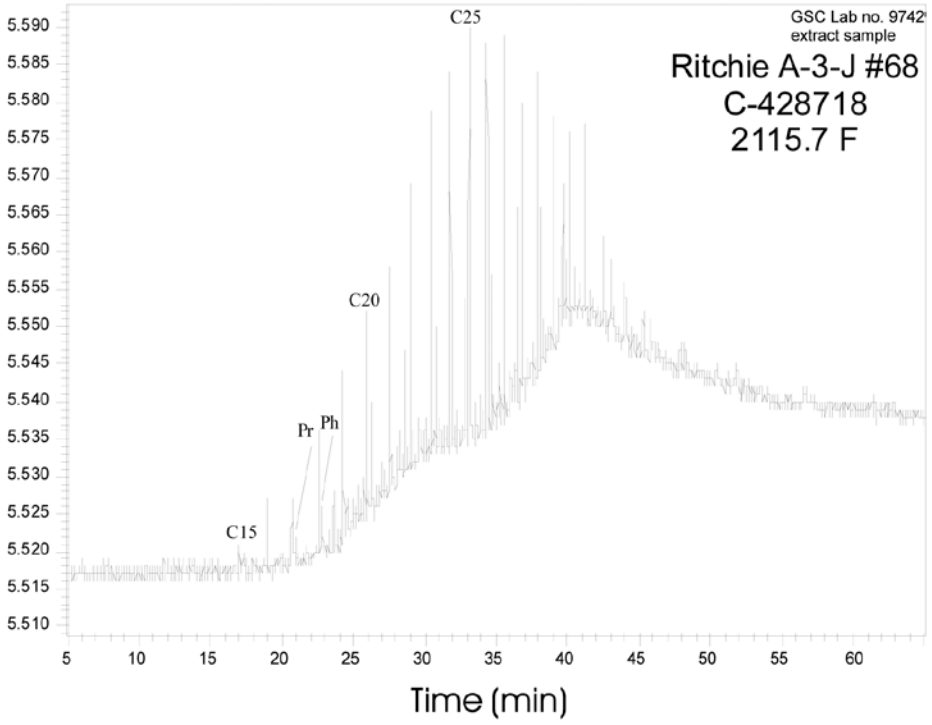

Figure 3. Illustrative saturate fraction gas chromatograms (SFGC) of two solvent extract samples from the Ritchie A-3-J well at 2055.8 m (6745.0', top) and 644.8 m (2115.7', bottom) (Figure 2). All figures show detector response (y axis) as a function of time since injection on the chromatographic column (x axis). The obvious SFGC compositional differences between these two samples are interpreted as due primarily to biodegradation of the shallower crude oil sample by aerobic bacteria.

ates to produce diasteranes (Figure 4; Sieskind et al, 1979; Rubinstein et al., 1975). Low relative diasterane abundances, like those in some carbonate-sourced petroleum systems, are generally interpreted to indicate a clay-starved depositional environment (i.e., a "carbonate" source rock), although many "carbonate" source rocks have ratios of diasterane to regular sterane like those attributed to "clastic" source rocks (Osadetz et al., 1992). A biological source of diasteranes is unlikely, but the association of anomalously high diasteranes in carbonate rocks with evaporitic depositional environments suggests a relationship (Clark and Philp, 1989).

Strongly reducing depositional environments are required to preserve organic matter and form kerogen in sedimentary petroleum source rocks. Since strongly reducing conditions can persist below the sediment-water interface, even in the absence of water column anoxia, euxinic sediments do not directly indicate water column environmental conditions. However, some biological compounds of source rock kerogen, notably phytoloic acid side-chains of chlorophyll and bactirohopane-tetrol, are commonly inferred to be affected by reduction and oxidation reactions in the water column prior to, or at the earliest stages of, their incorporation into the sediment (Peters and Moldowan, 1993). Peters and Moldowan (1991) suggest that C32 to C34 hopane prominences could result from either redox reactions controlled by the depositional environment or from precursor molecules other than bacteriohopane-tetrol. The first alternative is preferred because C34 hopane and C35 hopane prominence commonly follows source rock depositional environment and paleoecology (Osadetz et al., 1992). This results in a water column chemistry indicator that is preserved in compounds that are a common trace component of crude oils (Figure 5; Peters and Moldowan, 1991). The higher the carbon number of predominant extended hopanes, the stronger and more persistant the water column anoxia.

RESULTS

Select gross and molecular compositional results of the 20 samples examined appear in Table 2. All subsequent illustrations of gas chromatograms and mass chromatograms show detector response (y axis) as a function of time since injection on the chromatographic column (*x* axis).

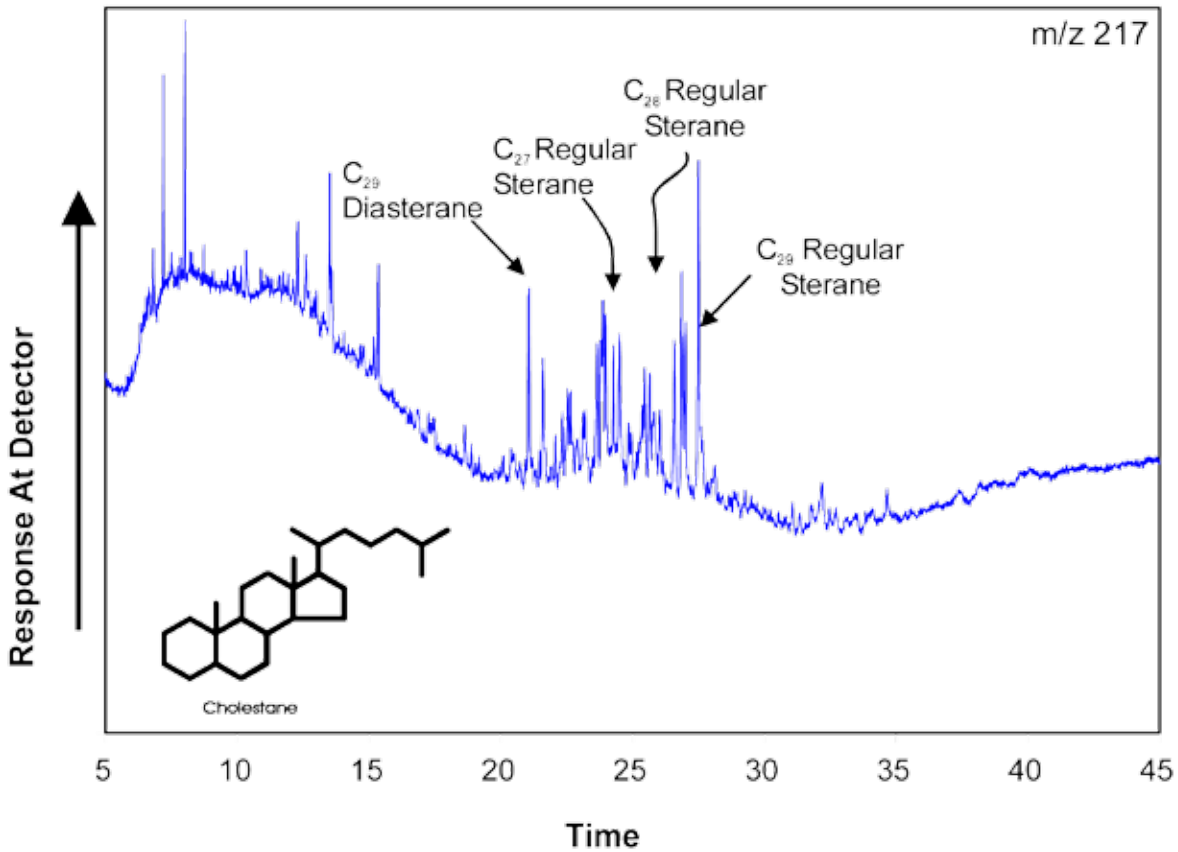

Figure 4. An example m/z 217 mass chromatogram showing the relative abundance of both regular and rearranged steranes (or diasteranes) in solvent extract sample X9693, from a sample of Muskaboo Creek Assemblage bioclastic sandstone at Tsatia Mountain.

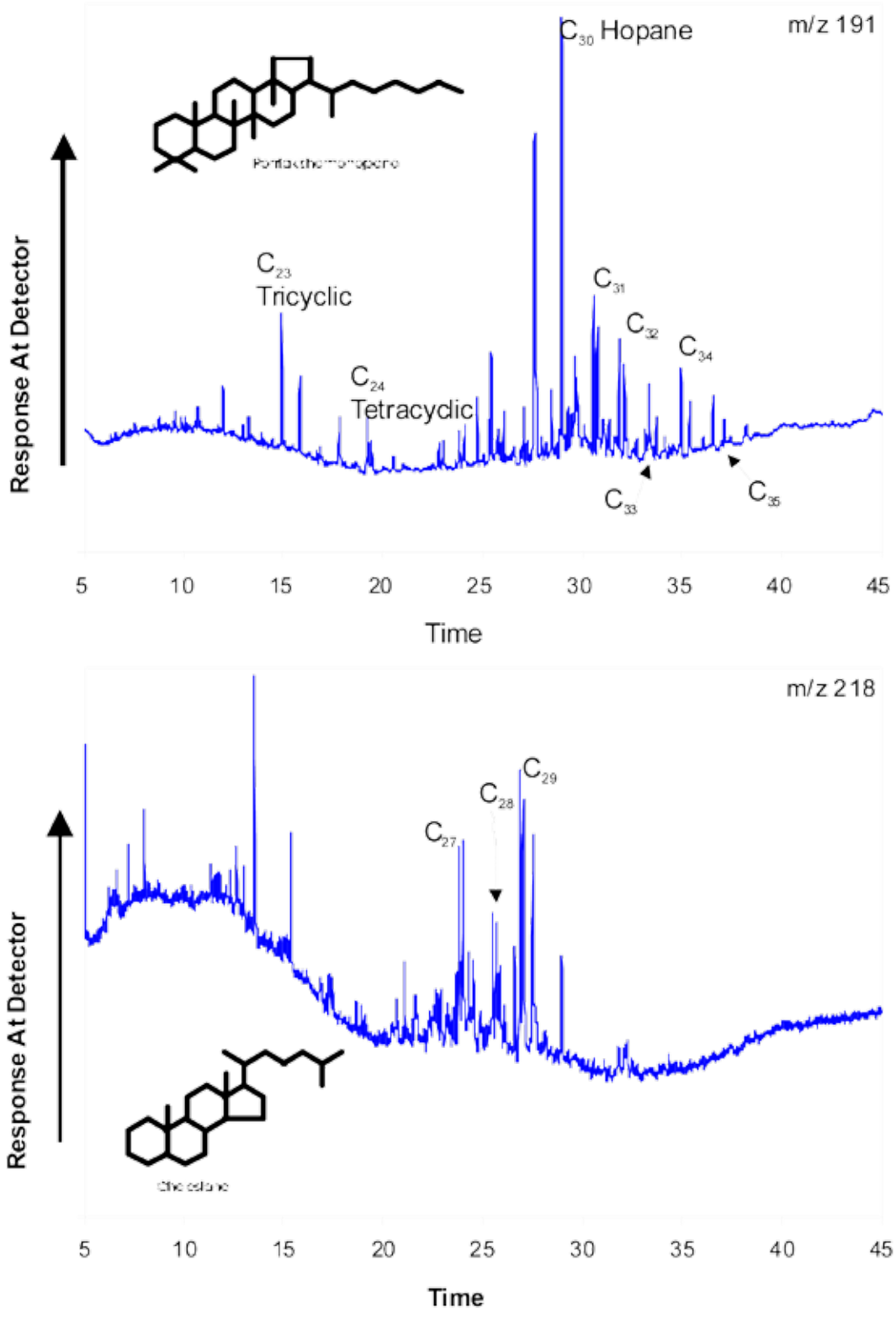

Figure 5. An example m/z 191 (terpanes, top) and 218 (regular steranes, bottom) mass chromatogram in solvent extract sample X9693, from Muskaboo Creek Assemblage bioclastic sandstone at Tsatia Mountain.

Compounds are identified by both standard elution order and by full scan triple sector GCMS operating in MS-MS mode. All samples have been characterized optically or petrographically as being stains or petroleum fluid inclusions. The low hydrocarbon yields and low HC% values are due to the small recoverable volumes (Table 2). This is expected, considering the exposure of both outcrops and old well cuttings to processes of dissipation and alteration resulting from their exposure to the elements, especially in light of the inferred low densities and expected volatility of the hydrocarbons (Osadetz *et al.*, 2002).

SELECT CRUDE OIL MOLECULAR COMPOSITIONAL TRAITS

Molecular compositional differences among the samples are diverse, but they can be characterized by consideration of select compound variations. The observed variations are interpreted using standard techniques and previous studies to distinguish variations due to the alteration (specifically biodegradation) so that other variations due primarily to source can be isolated and interpreted. The variation of biological marker compounds (like steranes and terpanes) within the sample set are observed and interpreted to be unaffected by alteration, allowing interpretation of compositional variations attributed to source rock age (regular steranes, Grantham and Wakefield, 1988), lithology (diasteranes/regular steranes, Seiskind *et al.*, 1979; hopane prominence, Osadetz *et al.*, 1992), and depositional environment (Peters and Moldowan, 1991) that form the basis of compositional family and petroleum system definition.

Figure 3 illustrates the range of saturate fraction gas chromatogram (SFGC) compositions observed in the samples. Both samples are from the Ritchie A-3-J well at 2055.8 m (6745.0'; Figure 3, top) and 644.8 m (2115.7'; Figure 3, bottom; Figure 2) and both have similar biological marker compositions. Solvent extract X9745 (top) exhibits a normal crude oil response dominated by normal alkanes derived from cell wall phospholipids and the irregular isoprenoid, most noticeably pristane (Pr) and phytane (Ph). The low amplitude baseline hump defines the envelope of a complicated mixture of co-eluting compounds. Solvent extract X9742 (bottom) exhibits a biodegraded crude oil response dominated by normal alkanes that are paired, for samples with longer elution times than nC_{20}, with a homologous series of alkylcyclohexanes and methylalkylcyclohexanes that were identified by GC-MS-MS experiments not discussed herein. Sample X9742 also exhibits a high amplitude baseline hump of more complicated co-eluting compounds. Note especially the relative change between the two samples in response of the hump to compounds eluting prior to and after nC_{20}. The sterane compositions of these two samples are essentially similar (Table 2, Figures 4, 5, 6), illustrating that the composition of the lower molecular weight saturate fraction has been altered by the preferential removal of normal alkanes. Such compositional variations are commonly inferred to be indicative of biodegradation (Peters and Moldowan, 1993; Osadetz *et al.*, 1992).

The sample set compositional variation can be illustrated using a few key compounds. The most illustrative variations are shown by the regular and rearranged steranes (Figure 4). An example m/z 217 mass chromatogram showing the relative abundance of regular and rearranged

TABLE 2. SELECT GROSS AND MOLECULAR COMPOSITIONAL RESULTS FROM BOWSER BASIN CRUDE OILS.

Sample No.	TOC (%)	(ppm of rock)	Extract (% of TOC)	HC (%)	R+A (%)	Sat/Aro	Pr/Ph	C_{29} St Dia/Reg	% C_{27}	% C_{28}	% C_{29}	C_{27}/C_{29}	C_{28}/C_{29}
X9693	BD	2385	N/A	10.8	85.0	1.0	N/A	0.22	26	21	53	0.49	0.40
X9694	BD	22500	N/A	8.9	80.0	1.0	N/A	0.26	32	19	48	0.67	0.39
X9731	BD	N/A	N/A	N/A	N/A	N/A	N/A	0.76	42	26	31	1.35	0.83
X9742	BD	5500	N/A	4.6	87.7	0.3	N/A	0.54	30	29	40	0.76	0.73
X9743	0.10	396	40	7.9	86.8	2.0	N/A	0.56	25	33	42	0.59	0.80
X9744	0.01	771	771	10.7	57.1	0.8	0.44	0.64	22	33	44	0.50	0.75
X9745	5.05	579	1	27.3	58.2	0.6	1.11	0.55	26	34	40	0.66	0.86
X9746	0.05	1179	236	5.4	75.0	4.0	0.69	0.52	30	29	41	0.73	0.71
X9790	4.69	4442	9	4.7	90.6	0.1	1.29	0.57	16	18	66	0.24	0.28
X9791	0.88	1897	22	3.6	86.4	1.0	0.86	0.65	41	27	31	1.32	0.87
X9792	0.74	2857	39	3.9	85.0	0.4	0.67	0.76	41	27	32	1.28	0.86
X9793	1.07	4080	38	4.9	73.5	0.3	0.97	0.61	40	27	33	1.22	0.83
X9794	19.15	9238	5	6.2	90.2	0.7	1.67	0.38	21	24	55	0.38	0.43
X9795	8.07	8600	11	7.4	84.5	0.2	4.49	0.27	7	19	73	0.10	0.26
X9796	3.26	6657	20	8.2	82.0	0.4	2.59	0.32	16	22	62	0.26	0.35
X9797	43.28	29875	7	15.7	83.7	0.2	4.56	0.23	5	25	70	0.07	0.35
X9798	0.78	4903	63	2.0	89.5	0.5	0.7	0.54	36	26	37	0.97	0.71
X9799	0.53	3448	65	12.0	81.5	0.3	0.56	0.37	25	30	46	0.53	0.64
X9800	0.52	1832	35	8.1	84.3	0.9	1.04	0.77	38	27	35	1.10	0.77
X9801	3.19	3701	12	10.2	86.3	0.3	1.87	0.19	9	19	72	0.13	0.27

steranes (or diasteranes) in solvent extract sample X9693 is from Muskaboo Creek Assemblage at Tsatia Mountain. Steranes are derived from cholestane-like molecules that act as common cell wall rigidifiers in eukaryotic organisms. The presence of diasteranes is an indicator of depositional environment and source rock lithology (Sieskind et al, 1979; Rubinstein et al., 1975).

Two important groups of biological marker are the terpanes (m/z 191; Figure 5, top) and regular steranes (m/z 218; Figure 5, bottom). Their occurrence is also illustrated by mass chromatograms from solvent extract sample X9693, from Muskaboo Creek Assemblage at Tsatia Mountain. The m/z 191 mass chromatogram illustrates terpanes, which are primarily derived from bacteriohopanetetrol, a cell wall rigidifier in prokaryotic organisms (Peters and Moldown, 1993). The ratio of similar carbon number hopanes in the homologous group of compounds that occurs to the right of the C_{30} hopane peak as annotated double peaks is controlled by physical conditions of the depositional environment (Peters and Moldowan, 1991). This sample shows that C_{34} hopanes are prominent, due to the accumulation of the source rock in an environment where anhydrite of gypsum was accumulating (Osadetz *et al.*, 1992). The m/z 218 mass chromatogram illustrates regular steranes that were probably derived primarily from cholesterol. The ratio of C_{28} to C_{29} steranes is known to increase with geological age in marine depositional environments, due to biochemical evolution in the marine biosphere (Grantham and Wakefield, 1998). The observed ratio of C_{28}/C_{29} steranes, combined with the standard interpretation of the m/z 191 mass chromatogram, indicates that the source rock of this oil stain is a sub-Hazelton Group carbonate deposited in submarine hypersaline to mesohaline environments and probably occuring in the underlying Stikine succession.

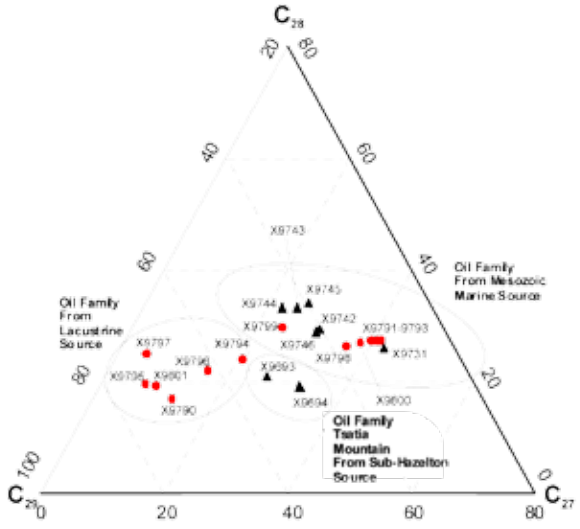

Figure 6. A ternary diagram illustrating compositional variations and affinities of all 20 solvent extract samples using the relative abundance of C_{27}-C_{28}-C_{29} regular steranes (Table 2). The three oil families are identified.

A ternary diagram shows the variations and affinities of all 20 samples using the relative abundance of C27-C28-C29 regular steranes (Figure 6, Table 2). The biodegradation of some oils (Figure 3) does not affect regular sterane compositions, such that observed variations can be attributed primarily to source rock compositional differences. This figure illustrates the presence of the three oil families identified. One, composed of two extracts from Tsatia Mountain (X9693, X9694), is inferred using terpane and sterane compositional characteristics to be derived from a carbonate source in the underlying Stikine succession, as discussed above. Using similar standard interpretations (Peters and Moldowan, 1993), we interpret the steranes and terpanes of the other samples. The second compositional family includes samples from the Amoco Ritchie a-3-J/104-A-6 well at depths of 644.8 m, 1321.9 m, 1439.7 m, and 2055.8 m (2115.7', 4337.0', 4723.4', and 6745.0') (GSC Extracts X9742-X9745), the Tango Creek Formation sample from the Triangle zone (GSC Extract X9746), the Eaglenest assemblage sample from Buckinghorse Creek (GSC Extract X9731), as well as six samples from other locations in the northern Bowser Basin region (GSC Extracts X9791-93 and X9798-80, Table 1) that have compositional characteristics that suggest derivation from a Mesozoic open-marine source rock. This potential source facies probably lies in the upper Hazelton or lower Bowser Lake Groups, as the lowest stratigraphic occurrence of these oils lies in slope and shelf facies of the Bowser Lake Group. A third oil family composed of 6 samples from the group of 12 diverse samples from northern Bowser Basin (GSC Extracts X9790, X9794-97 and X9801) is distinguished by having lower C27 regular steranes and generally higher C29 regular steranes compared to all other samples. This oil compositional family is inferred to have a nonmarine, possibly lacustrine, source in Bowser Lake or Sustut Groups (Peters and Moldowan, 1993). The transitional positions of samples X9794 and X9796 do not preclude the possibility that they could be mixtures of the two oil families inferred to have Mesozoic source rocks. This is possible, since the geographic ranges of the two end-member compositions of the Mesozoic marine and nonmarine source oils overlap; however, other evidence presented below suggests that mixing is not important.

A cross plot of the ratio C29 diasteranes to regular steranes and ratio of regular C28 steranes to C29 steranes (Figure 7) shows additional compositional variations within families using variation of diasteranes/regular steranes (Sieskind et al, 1979; Rubinstein et al., 1975). Those oils inferred to have a nonmarine Mesozoic source have an overlapping range of diaterane/regular sterane ratios to those inferred to have Mesozoic marine sources; however, the range of nonmarine source oil compositions is illustrated by X9790, which is one of the samples that is most different from the oils inferred to have marine Mesozoic sources. Therefore, it is unlikely that the samples X9794 and X9796 are mixtures of any significant proportion. A cross plot of the ratio

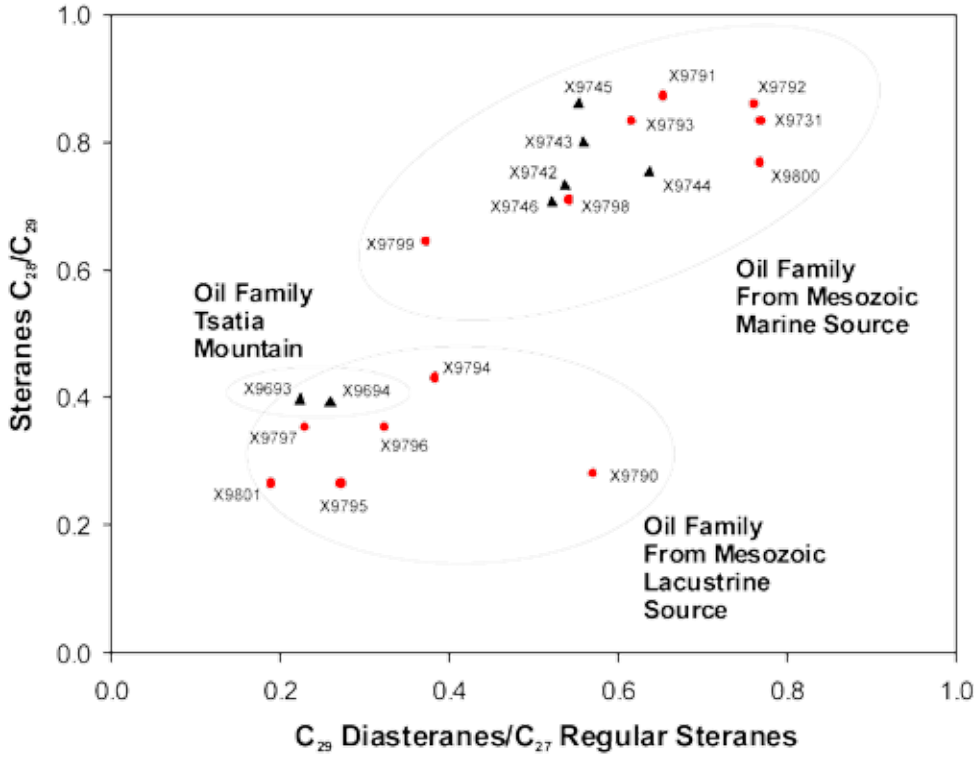

Figure 7. A cross plot of the ratios C_{29} diasteranes to C_{27} regular steranes and ratio of regular C_{28} steranes to C_{29} steranes showing that the compositional variations within families, as typified by the variation of diasteranes/regular steranes.

C29 diasteranes to regular steranes and the ratio of pristane to phytane from the SFGC illustrates that the compositional distinction between the two interpreted Mesozoic oil families is also reflected by other compositional traits (Figure 8). Insufficient pristane and phytane were observed in the oils inferred to be sourced from the Stikine Assemblage strata (X9693; X9694) to allow their characterization using pristane and phytane; however, they are distinguished from most Mesozoic sourced oils by their generally higher saturate to aromatic hydrocarbon ratio (Table 2).

DISCUSSION

The interpretation that biodegradation has altered the composition of some crude oils at or near the surface is important but not surprising. The Amoco Ritchie a-3-J/104-A-6 well has a porous interval containing a resistive fluid that is either "by-passed petroleum pay" or fresh water. The nature of the wireline-log resistivity anomaly is not diagnostic. Some crude oil extracts from this well are clearly biodegraded (Figure 3) as a result of aerobic bacterial degradation that implies a connection with oxygenated (probably fresh and meteoric) water, which, like hydrocarbons, is electrically resistive. In the same well, Koch (1973) reported other petroleum shows, including both dry and wet gas in cuttings samples at depths less than 792 m (2600') where the gas detector indicated more than 40 units, compared to background readings of 10 to 20 units. Therefore, the nature of the resistivity anomaly in the well remains unresolved. Regardless, the combined observations are important since the wireline logs indicate the presence of porous zones in some of the deepest strata in Bowser Lake Group, while the oil stains indicate an effective petroleum system in the same region. The results are consistent with the revised thermal maturity model (Evenchick *et al.*, 2002).

The analysis of the molecular composition of these oil stains and seepages has identified at least three distinct compositional crude oil families. One oil family is inferred to be derived from carbonate source rocks in underlying Stikinia. The second and third oil families, one of which has the characteristics of a marine source, and the other of which has compositional characteristics of a nonmarine or lacustrine source, are inferred to be derived from Jurassic or younger sources in the Hazelton-Bowser-Sustut successions. The source rocks of these petroleum systems have not been identified explicitly, nor have the oils been correlated to solvent extracts from potential source rocks, although potential source rock intervals have been identified in a variety of stratigraphic positions (Evenchick et al., 2002; Osadetz et al., 2003b). However, the significant number of petroleum stains and their association with structures that could be traps for petroleum (as at the Ritchie well, Tsatia Mountain, and in the roof of the triangle zone) all point

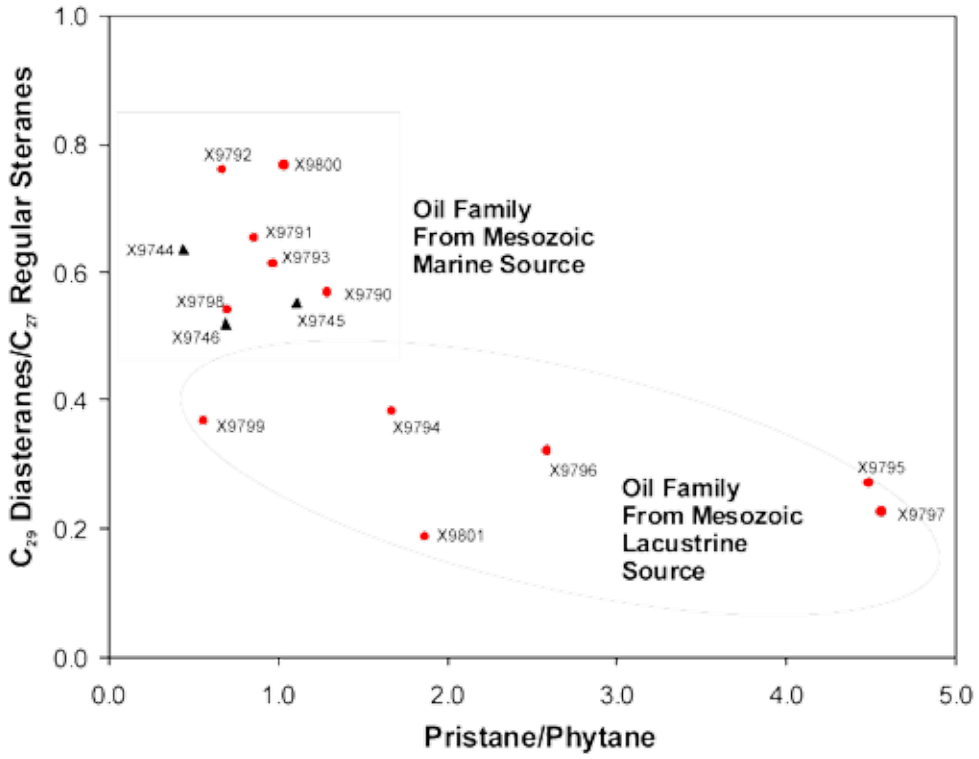

Figure 8: A cross plot of the ratio C_{29} diasteranes to C_{27} regular steranes and ratio of pristane (Pr) and phytane (Ph) from the saturate fraction gas chromatogram (SFGC) that illustrates how compositional distinctions between the two Mesozoic oil families is reflected by additional compositional traits.

toward a complete removal of play-level risks for both petroleum system and reservoir. This suggests that a revised petroleum assessment would be even more encouraging than the existing one (Hannigan et al., 1995).

CONCLUSIONS

Oil stains occur widely, both geographically and stratigraphically, with only the northern half of these basins being investigated. Twenty crude oil stains and petroleum fluid inclusions have been extracted from Bowser Lake and Sustut Group rocks, and their compositions have been characterized. The molecular compositions of these samples are interpreted to show that there are at least three compositionally distinct oil families representative of three effective petroleum systems in Bowser and Sustut Basins.

Molecular compositional differences can be characterized by sterane compositional variations using standard techniques and previous studies, once the effects of alteration (specifically biodegradation) are discounted. One compositional oil family is inferred derived from the sub-Hazelton succession. A second compositional oil family derived from normal Mesozoic marine source rocks is inferred derived from the upper Hazelton or lower Bowser Lake Groups. A third oil family derived from lacustrine Mesozoic source rocks is inferred to occur in the Bowser Lake Group.

The occurrence and composition of these crude oils expand the petroleum prospectivity of Bowser Basin by reducing petroleum system risks and indicating a possible petroleum system for Hazelton Group. The preservation of crude oils is also a strong confirmation of the revised thermal maturity model for the basin (Evenchick et al., 2002). Existing petroleum resource assessments (Hannigan et al., 1995) do not attribute petroleum potential to sub-Bowser successions, indicating a need for revision.

ACKNOWLEDGEMENTS

We thank Sneh Achal, Rachel Robinson, and Marina Milovic for their technical assistance in the production of the data employed here. GSC colleagues Mark Obermajer, Maowen Li, and David Ritcey provided helpful discussions and technical assistance in the preparation of this paper. This is Geological Survey of Canada contribution #2003313.

APPENDIX 1: ANALYTICAL PROCEDURES

Anhydrous Pyrolysis

Rock-Eval/TOC is a useful screen for recognizing sources and stained lithologies. Rock samples suspected or identified as having crude oil stains or petroleum fluid inclusions were pyrolyzed using Rock-Eval/TOC (Table 2) to determine total organic carbon content (Table 2; Espitalie et al., 1985; Peters, 1986; Tissot and Welte, 1978, p. 443-447). The Rock-Eval/TOC analysis gives five parameters: S1, S2, S3, TOC, and Tmax. The S1 parameter measures free or adsorbed hydrocarbons volatilized at moderate temperatures (300° C). S2 measures the hydrocarbons liberated during a ramped heating (300° C to 550° C at 25oC/min.). The S3 parameter measures organic CO_2 generated from the kerogen during rapid heating (300° C to 390° C at 25° C/min.). Milligrams of product per gram of rock sample, the equivalent to kilograms per tonne, is the measure of all these parameters. Total Organic Carbon (TOC) is measured and reported in weight percent. Tmax, the temperature corresponding to the S2 peak maximum temperature, is measured in oC.

Rock-Eval/TOC parameters have significance only above threshold TOC, S1, and S2 values. If TOC is less than about 0.3%, then all parameters have questionable significance and the experiment suggests no potential. Oxygen index (OI = S3/TOC), has questionable significance if TOC is less than about 0.5%. OI values greater than 150 mg/g TOC can result from either low TOC determination or from a mineral matrix CO_2 contribution during pyrolysis. Both Tmax and production index (PI = S1/[S1+S2]) have questionable significance if S1 and S2 values are less than about 0.2. Results can be affected by mineral matrix effects; these either retain generated compounds, generally lowering the S1 or S2 peaks while increasing Tmax, or liberate inorganic CO_2 and increase S3 and OI. Mineral matrix effects are important if TOC, S1, and S2 are low—an effect not significant in this study.

Solvent Extract Gross Composition

The amount and composition of solvent extractable bituminous material, including crude oil stains and petroleum fluid inclusions, was obtained by extracting the bitumen from the rock sample using the Soxhlet technique (Table 2). Solvent extracts were fractionated using packed column chromatography, following a method effectively similar to that published by Snowdon (1978). The resulting gross composition can be used to identify crude oil stains or to characterize source rock richness and maturity. Normalized solvent extract hydrocarbon (HC) yield, quoted in milligrams of extract per gram of organic carbon (mg/g TOC), is a richness indicator. HC yields of less than 30 mg/g TOC suggest no source rock potential. Those between 30 and 50 mg/g TOC suggest marginal potential. HC yields between 50 and 80 mg/g TOC show good potential. Greater values indicate excellent potential. Hydrocarbon percentage criteria for maturity are commonly independent of OM type and lithology. Stained samples are those with more than 55% HCs, and lower values are characteristic of petroleum source rocks if sufficient material is available, which is not the case for this study. Less than 20% HCs characterizes thermally immature sources; 25% to less than 45% HCs is the interval of marginal maturity; higher values occur during the the main HC generation stage.

Solvent Extract Molecular Composition

The extractable bitumen was de-asphalted by adding an excess of pentane (40 volumes) and then fractionating using open-column liquid chromatography. Saturate hydrocarbons were analysed using gas chromatography (GC) and gas chromatography-mass spectrometry (GCMS). A Varian 3700 FID gas chromatograph was used with a 30 m DB-1 column coated with OV-1 and helium as the mobile phase. The temperature was programmed from 50° C to 280° C at a rate of 4° C/min and then held for 30 min at the final temperature. The eluting compounds were detected and quantitatively determined using a hydrogen flame ionization detector. The resulting saturate fraction chromatograms (SFGC) were integrated using Turbochrom software. GCMS was performed in both single ion monitoring and full scan modes on both saturate and aromatic hydrocarbon fractions of solvent extracts, although only select saturate fraction compositional characteristics obtained from single ion monitoring experiments are reported here. Single ion monitoring GCMS experiments were performed on a VG 70SQ mass spectrometer with a HP gas chromatograph attached directly to the ion source (30 m DB-5 fused silica column used for GC separation), or under similar analytical conditions. The temperature, initially held at 100° C for 2 min, was programmed at 40° C/min to 180° C and at 4° C/min to 320° C, then held for 15 min at 320° C. The mass spectrometer was operated with a 70 eV ionization voltage, 300 mA filament emission current and interface temperature of 280° C. Terpane and sterane ratios reported herein were calculated using m/z 191 and m/z 217 and m/z 218 mass chromatograms.

REFERENCES

Clark, J. P., and Philp, R. P. (1989): Geochemical characterization of evaporite and carbonate depositional environments and correlation of associated crude oils in the Black Creek Basin, Alberta. *Bulletin of Canadian Petroleum Geology*, v. 37, no. 4., pages 401-416.

Eisbacher, G.H.(1974): Sedimentary history and tectonic evolution of the Sustut and Sifton basins, north-central British Columbia; *Geological Survey of Canada*, Paper 73-31, 57 pages.

Espitalie, J., Deroo, G. and Marquis, F. (1985): Rock Eval Pyrolysis and Its Applications. Preprint; Institut Francais du Petrole, Geologie No. 27299, 72 p. English translation of, La pyrolyse Rock-Eval et ses applications, Premiere, Deuxieme et Troisieme Parties, in *Revue de l'Institut Francais du Petrole,* v. 40, p. 563-579 and 755-784; v. 41, pages 73-89.

Evenchick, C.A. (1991): Geometry, evolution, and tectonic framework of the Skeena Fold Belt, north-central British Columbia; *Tectonics*, v. 10, page 527-546.

Evenchick, C.A., Poulton, T.P., Tipper, H.W., and Braidek, I. (2001): Fossils and facies of the northern two-thirds of the Bowser Basin, northern British Columbia; *Geological Survey of Canada,* Open File 3956.

Evenchick, C.A., Ferri, F., Mustard, P.S., McMechan, M., Osadetz, K. G., Enkin, R., Hadlari, T., and McNicoll, V. J. (2003): Recent results and activities of the Integrated Petroleum Resource Potential and Geoscience Studies of the Bowser and Sustut Basins project; in *Current Research, Geological Survey of Canada, A-13*, 11 pages.

Evenchick, C.A., Hayes, M.C., Buddell, K.A., and Osadetz, K.G. (2002): Vitrinite reflectance data and preliminary organic maturity model for the northern two thirds of the Bowser and Sustut basins, north-central British Columbia. Geological Survey of Canada, Open File 4343 and *B.C. Ministry of Energy and Mines*, Petroleum Geology Open File 2002-1.

Evenchick, C.A., Osadetz, K.G., Ferri, F., Mayr, B., and Snowdon, L. R., (in prep.): A Natural Seepage of Biogenic Methane in the Intermontane Belt (Bowser Basin) of the Canadian Cordillera. *Bulletin of Canadian Petroleum Geology,* v. XX, no. X., p. XXX-XXX.

Evenchick, C.A. and Thorkelson, D.J. (in press): Geology of the Spatsizi River map area, north-central British Columbia, *Geological Survey of Canada Bulletin* 577.

Gordy., P.L., Frey, F.R., and Norris, D.K. (1977): Geological guide for the C.S.P.G. 1977 Waterton - Glacier Park Field Conference. - *Candian Society of Petroleum Geologists*, Calgary.Grantham, P. J., and Wakefield, L. L.(1988): Variations in the sterane carbon number distributions of marine source rock derived crude oils through geological time, *Organic Geochemistry*, v. 12, no. 1, pages 61-73.

Hannigan P. K., Lee, P. J. and Osadetz, K. G. (1995): Oil and gas resource potential of the Bowser-Whitehorse area of British Columbia, *Report to BCEMR,* March 1995, 72 pages.

Koch, N. G. (1973): Central Cordilleran Region; in R. G. McCrossan ed., The Future Petroleum Provinces of Canada - Their Geology and Potential, *Canadian Society of Petroleum Geologists*, Memoir 1, pages 37-71.

MacKay, P. A., Varsek, J. L., Kubli, T. E., Dechesne, R. G., Newson, A. C., Reid, J. P. (1996): Triangle Zones and Tectonic Wedges. *Bulletin of Canadian Petroleum Geology,* v.44, No.2, pages. I-1-I-5.

Osadetz, K.G., Evenchick, C. A. , Ferri, F. , Stasiuk, L. D., and Wilson, N. S. F. (2003a): Indications for effective petroleum systems in Bowser and Sustut basins, north-central British Columbia. *in* Geological fieldwork, 2002; *B.C. Ministry of Energy and Mines*, Paper 2003-1, pages 257-264.

Osadetz, K.G., Snowdon, L.R., and Obermajer, M. (2003b): ROCK-EVAL/TOC results from 11 Northern British Columbia boreholes. *Geological Survey of Canada*, Open File 1550 and *B.C. Ministry of Energy and Mines*, Petroleum Geology Open File 2003-1 (CD-ROM).

Osadetz, K. G., Brooks, P. W., and Snowdon, L. R. (1992): Oil families and their sources in Canadian Williston Basin (southeastern Saskatchewan and southwestern Manitoba). *Bulletin of Canadian Petroleum Geology*, 40, pages 254-273.

Peters, K. E. (1986): Guidelines for evaluating petroleum source rock using programmed pyrolysis. *American Association of Petroleum Geologists*, Bulletin, v. 70/3, p. 318-329.

Peters, K. E., and Moldowan, J. M. (1993): *The Biomarker Guide,* Prentic-Hall, Englewood Cliffs, N. J., 363 pages.

Peters, K. E., and Moldowan, J. M. (1991): Effects of source, thermal maturity, and biodegradation on the distribution and isomerization of homohpanes in petroleum. *Organic Geochemistry*, v. 17, no. 1, pages 47-61.

Rubinstein, I., Sieskind, O., and Albercht, P. (1975): Rearranged sterenes in a shale: occurrence of simulated formation. *Journal of the Chemical Society*, Perkin Transactions I, pages 1833-1835.

Seifert, W. K., and Moldowan, M. J. (1986): Use of biological markers in petroleum exploration; in R. B. Johns (ed.), Biological Markers in the Sedimentary Record. Amsterdam: Elsevier, pages 261-290.

Seifert, W. K., and Moldowan, J. M. (1981): Paleoreconstruction of biological markers. *Geochimica et Cosmochimica Acta,* v. 45, pages 783-794.

Seifert, W. K., and Moldowan, J. M. (1978): Applications of steranes, terpanes and monoaromatics to the maturation, migration and source of crude oils. *Geochimica et Cosmochimica Acta,* v. 42, pages 77-95.

Sieskind, O., Joly, G., and Alberecht, P. (1979): Simulation of the geochemical transformation of sterols: superacid effect of clay minera. *Geochimica et Cosmochimica Acta,* V. 43, pages 1675-1679.

Snowdon, L. R. (1978): Organic geochemistry of the Upper Cretaceous/Tertiary delta complexes of the Beaufort Mackenzie Sedimentary Basin. *Geological Survey of Canada,* Bulletin 291.

Tipper, H.W. and Richards, T.A. (1976): Jurassic stratigraphy and history of north-central British Columbia*; Geological Survey of Canada,* Bulletin 270, 73 pages.

Tissot, B. P., and Welte, D. H. (1978): Petroleum formation and occurrence; Springer-Verlag, Berlin, 538 pages.

Volkman, J. K., and Maxwell, J. R. (1986): Acyclic isoprenoids as biological markers; in R. B. Johns (ed.), Biological Mrakers in the Sedimentary Record. Methods in Geochemistry and Geophysics, 24, Amsterdam: Elsevier, pages 1-42.

Waples, D. W., and Machihara, T. (1990): Application of sterane and triterpane biomarkers in petroleum exploration. *Bulletin of Canadian Petroleum Geology*, v. 38, pages 357-380.

Welte, D. H., and Waples, D. W. (1973): Uber die Bevorzugung geradzahliger n-Alkane in *Sedimentgesteinen. Naturwissenschaften,* v. 60, pages 516-517.

STRUCTURAL RELATIONSHIP BETWEEN THE LABERGE GROUP AND SINWA FORMATION ON COPPER ISLAND, SOUTHERN ATLIN LAKE, NORTHWEST BRITISH COLUMBIA

by Kara L. Wight, Joseph M. English and Stephen T. Johnston

University of Victoria

KEYWORDS: king salmon thrust, whitehorse trough, llewellyn fault, atlin lake, copper island fault

INTRODUCTION

The Whitehorse Trough is an elongate Mesozoic arc-marginal volcano-sedimentary basin that extends from central Yukon to Dease Lake in northwest British Columbia (Figure 1). The Whitehorse Trough contains volcaniclastic and carbonate strata of the Upper Triassic Stuhini Group and siliciclastic strata of the Lower to Middle Jurassic Laberge Group (Figure 2). Major structures within the southern Whitehorse Trough include the Llewellyn and Nahlin Faults and the southwest-vergent King Salmon Thrust.

The King Salmon Thrust carries the Upper Triassic Sinwa Formation (Stuhini Group) and Lower Jurassic Inklin Formation (Laberge Group) in its hanging wall over top of more proximal facies of the Laberge Group to the southwest (Souther, 1971; Figure 1). Regional mapping suggests that the King Salmon Thrust extends northwards into the southern Atlin Lake region (e.g., Wheeler and McFeely, 1991). The major structure in the Atlin Lake region is, however, the Llewellyn Fault (Wheeler and McFeely, 1991), a steep north-northwest-trending strike-slip fault of largely Triassic to Cretaceous age (Mihalynuk, 1999). The fault that marks the southwest limit of the Laberge Group in the southern Atlin Lake region (herein called the Copper Island Fault) has previously been interpreted to be the northern extension of the King Salmon Thrust. Both the King Salmon Thrust and the Copper Island Fault trend northwest. The main goal of this paper is to determine whether the Copper Island Fault in the southern Atlin Lake region is an extension of the King Salmon Thrust or whether it is a separate and possibly younger structure. To address this question, a detailed geological mapping program was undertaken on Copper Island in southern Atlin Lake. Mapping focused on determining the nature of the Copper Island Fault and its relationship to other regional structures and on documenting the structure and stratigraphy of adjacent strata of the Laberge Group.

The goals of this paper are to (1) describe the stratigraphy and structure of Copper Island, (2) construct and discuss the structural cross sections for Copper Island, and (3) establish whether the Copper Island Fault is a northern continuation of the King Salmon Thrust (as previously assumed) or a separate entity.

GEOLOGICAL BACKGROUND

Early Mesozoic arc-marginal volcano-sedimentary rocks of the Whitehorse Trough include conglomerate, siltstone, sandstone, and greywacke that were deposited in a deep-marine setting of submarine fans and conglomeratic fan deltas (e.g., Dickie and Hein, 1995; Johannson et al., 1997). Laberge Group sediments were derived from the unroofing of the Stikine magmatic arc and Yukon-Tanana Terrane to the west and southwest (Dickie and Hein, 1995; Johnston et al., 1996; Johannson et al., 1997) and are divisible into a distal sandstone facies in the northeast (Inklin Formation) and a proximal conglomeratic facies in the southwest (Souther, 1971; Monger et al., 1991).

The marine Inklin Formation consists of a roughly 3 km thick succession of interbedded greywacke, shale, and siltstone with minor conglomerate (Johannson et al., 1994), interpreted as the distal facies of coalescing submarine fans and conglomeratic fan deltas (Dickie and Hein, 1995). In the southern Atlin Lake area, the Inklin Formation ranges in age from Early Sinemurian to Late Pliensbachian (Johannson et al., 1997). In the southern Whitehorse Trough, the conglomeratic facies of the Laberge Group onlaps the Upper Triassic volcanic and carbonate rocks of the Stuhini Group (Souther, 1971). In the southern Atlin area, the distal Laberge Group facies are faulted against the Stuhini Group strata by the Copper Island Fault, and the proximal conglomeratic facies of the Laberge Group are missing.

The Whitehorse Trough was tectonically shortened during the Middle Jurassic as a result of a collisional event that involved the westward emplacement of the Cache Creek Terrane over the Whitehorse Trough and Stikine Terrane (Mihalynuk, 1999). Structures of the central Whitehorse Trough are dominated by southwest-vergent folds and thrusts (English et al., 2003). The age of the fold and thrust belt development is constrained as mainly Middle Jurassic on the basis of biostratigraphy (Tipper, 1978) and between 174 and 172 Ma based on isotopic cooling age determinations (Mihalynuk et al., in press).

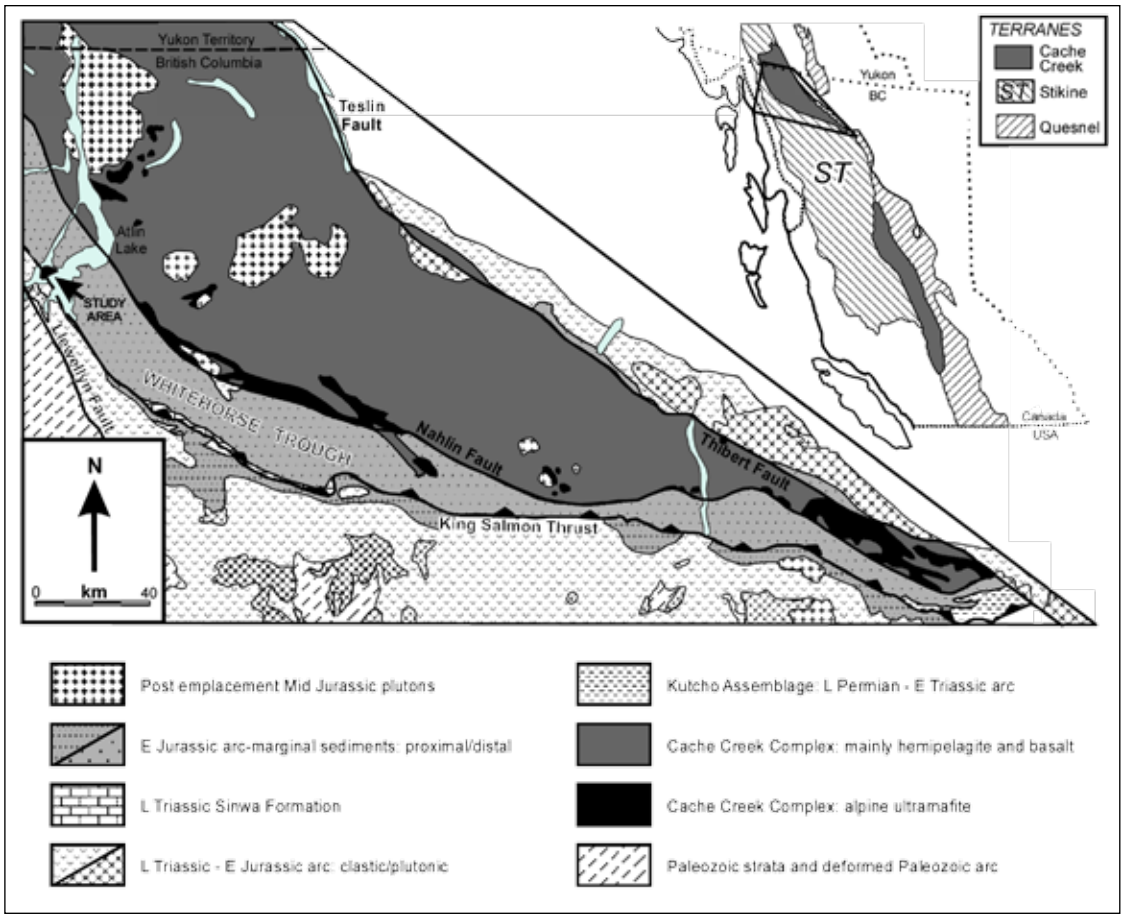

Figure 1. Location of Copper Island study area in southern Atlin Lake.

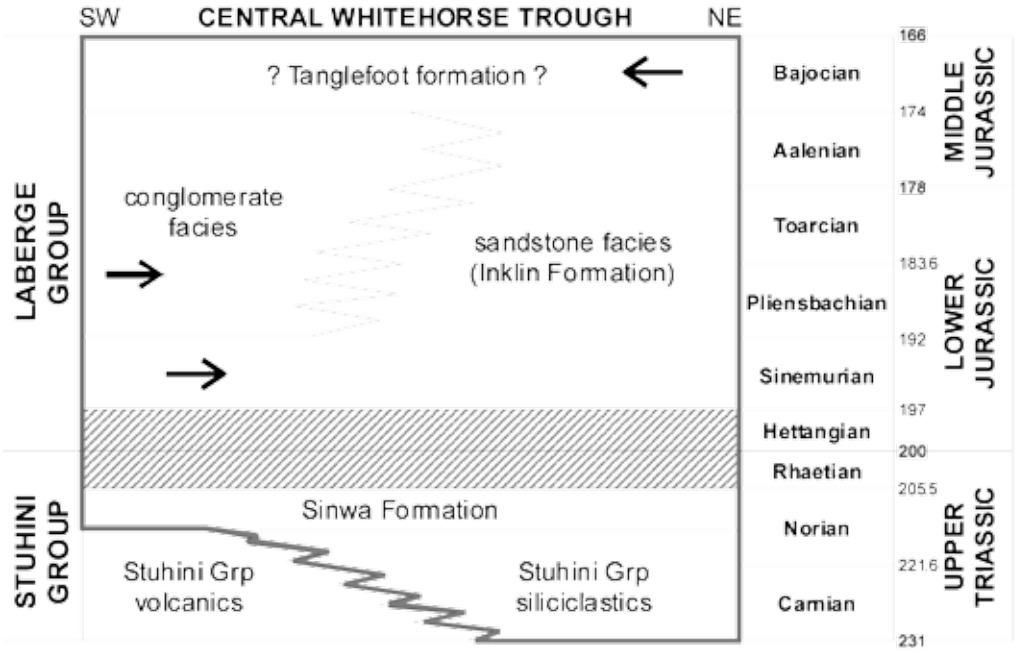

Figure 2. Stratigraphy of Laberge Group within the Whitehorse Trough. Arrows indicate paleoflow direction. Tanglefoot Formation is a chert and pebble conglomerate from the Cache Creek Terrane in Yukon (source: English et al., in review).

Two major thrust faults that developed during collision are the King Salmon Thrust and the Nahlin Fault. The Nahlin Fault bounds the northeast limit of the Whitehorse Trough at the surface (Aitken, 1959) and carries Cache Creek Terrane in its hanging wall. In the southern Whitehorse Trough, the King Salmon Thrust carries the Upper Triassic Sinwa Formation and Lower Jurassic Inklin Formation in its hanging wall over more conglomeratic facies of the Laberge Group in its footwall. The King Salmon Thrust occurs near the base of the Sinwa Formation, and subsidiary thrust faults splay from and mimic the trend and vergence of this major structure (English et al., 2003).

The northern extent of the King Salmon Thrust is, however, uncertain. In the area southeast of Atlin Lake, Early Eocene Sloko Group volcanic rocks conceal the northern continuation of the King Salmon Thrust (Aitken, 1959; Mihalynuk, 1999). A similarly positioned fault, the Copper Island Fault, occurs on the northwest side of the exposed Sloko Group through Atlin Lake and was previously interpreted as the King Salmon Thrust. The Copper Island Fault can be distinguished from the King Salmon Thrust based on its geometry and relationship to adjacent rocks. This fault may instead represent a splay of the Llewellyn Fault. The possibility that the Copper Island Fault is a strike-slip splay was investigated.

STUDY AREA

The structure and stratigraphy of the Laberge Group on Copper Island in southern Atlin Lake were used to evaluate the Copper Island Fault. The study area covers a 30 km2 region straddling the Copper Island Fault. This fault, which separates the Sinwa Formation and Inklin Formation, was mapped from the southwest shore of Atlin Lake, across Second Narrows and Copper Island, to the western shore of Torres Channel (Figure 3). At its western extent, the Copper Island Fault is plugged by a Late Cretaceous intrusion in the vicinity of Cathedral Mountain (Mihalynuk, 1999).

STRATIGRAPHY

The study area is underlain by volcanic, volcaniclastic, and carbonate strata of the Upper Triassic Stuhini Group and Lower Jurassic Inklin Formation (Figures 2 and 3). Volcanic rocks of the Stuhini Group are a minor component of the area and outcrop on the southwest corner of Copper Island.

The Norian Sinwa Formation of the Stuhini Group consists of light to dark grey massive to bedded limestone. Fossiliferous undulating light grey beds are 0.2 to 5 cm thick and interbedded with 0.25 to 2 cm thick beds of dark grey limestone. Some of these shallow marine carbonates have an extensive lattice of calcite veining and a marbled appearance near the contact zone with the Laberge Group. Some samples were fetid. In the Second Narrows region, limestone is intercalated with Late Triassic volcaniclastic strata and pyroclastic rocks of the Stuhini Group (Mihalynuk, 1999). The fault zone extending across Second Narrows marks the unexposed contact between the Sinwa Formation limestone and the Laberge Group.

Early to Late Pliensbachian greywacke, siltstone, argillite, sandstone, and minor conglomerate are characteristic of the Inklin Formation within the Laberge Group. The most common sediments on Copper Island consisted of medium grey to dark grey-green massive to graded wacke beds (more than 15% matrix) that range from 1.5 to 100 m thick, with the thickest beds exposed on the northwest shore of Copper Island. Two to three metre thick beds of these lithic wackes are commonly interbedded with argillite, siltstone and sandstones. Flame structures and convoluted and planar contacts mark the boundaries between beds. The greywacke consists of angular, poorly sorted medium to coarse sand in a 15% to 70% mud matrix. Clasts include lithic clasts (predominantly volcanic rock), feldspar, quartz, biotite, and less than 15% mafic minerals. Most beds were right way up; however, bedding of greywacke and siltstone is overturned in the central portion of Copper Island. Veins of calcite are found in the vicinity of fault zones, and orange weathering is common.

Within the Inklin Formation, there is a siliciclastic unit of medium- to coarse-grained quartz-rich wacke and sandstone that occurs as 100+ m thick beds, coarsens upwards, and displays dark orange weathering. Rip-up clasts (approximately 20 by 40 cm) and lenses of siltstone commonly are contained within the sandstone.

The 1 to 10+ m thick siltstone occurs as black to medium rusty brown 0.5 to 3 cm laminations. The bedding varies from undulating and convoluted to planar. The siltstone is subordinate within wacke-dominant sequences and is commonly interbedded with coarser orange-brown fine-grained sandstone. Bioturbation, orange weathering, and lenses of sandstone are common.

Pebble to cobble conglomerate occurs as one minor 20 m thick bed on southeast Copper Island. The clasts are dominantly rounded to subrounded volcanics, greywacke, and shale. This unit was not found outcropping in any other portion of the island. The absence of the conglomeratic facies of the Laberge Group in the southern Atlin area is different from the stratigraphy found in the footwall of the King Salmon Thrust in the Taku River area, where coarse conglomeratic facies of the Laberge Group are dominant (Souther, 1971).

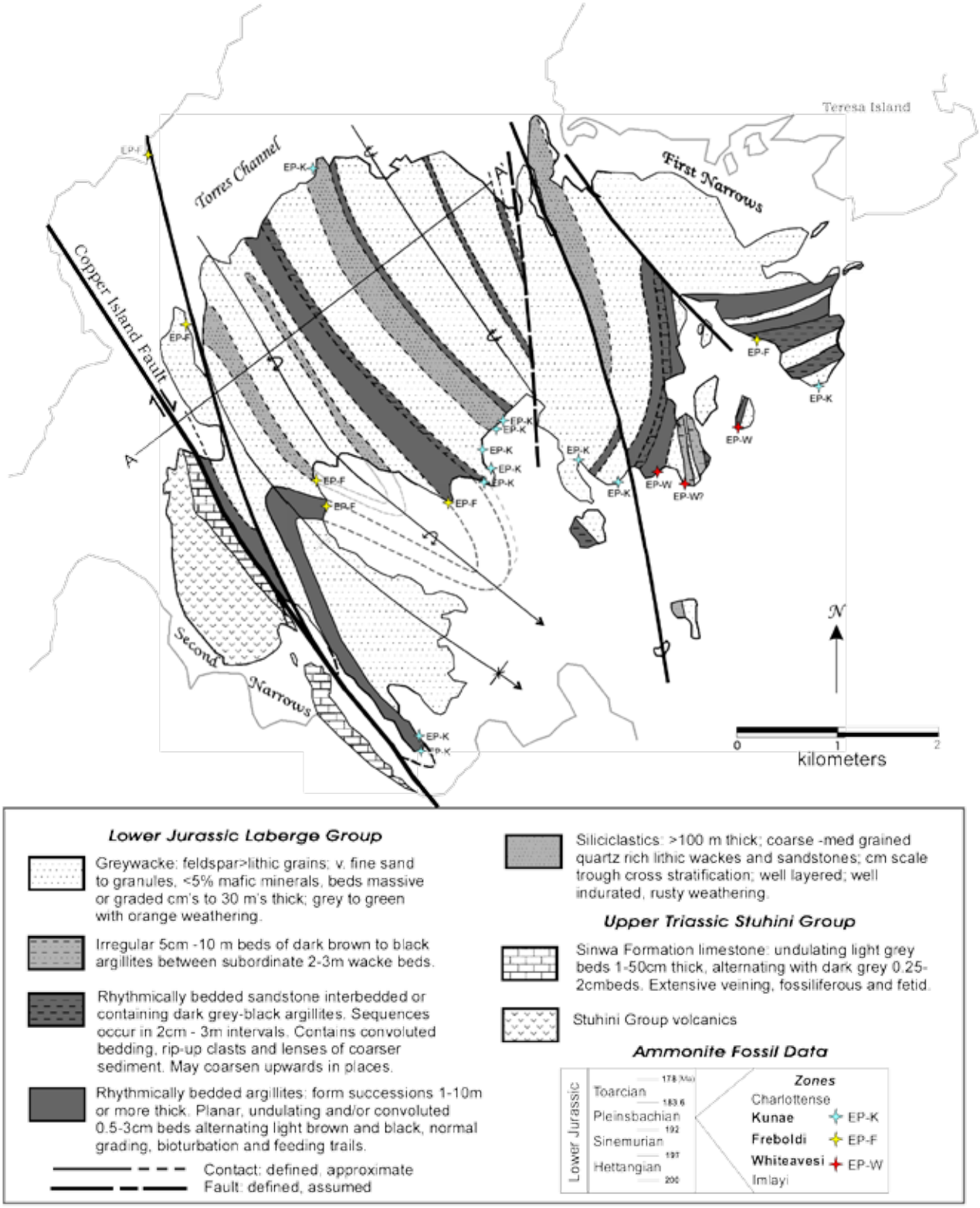

Figure 3. Bedrock geology map of Copper Island.

STRUCTURE

Copper Island is characterised by northwest-southeast trending folds and faults. One shallowly southeast-plunging syncline occurs on southwest Copper Island adjacent to the Copper Island Fault. An overturned anticline in central Copper Island shallowly plunges to the southeast (Figure 4 and 5). Minor folds perpendicular to the Copper Island Fault occur along the ridge top northeast of Second Narrows. A tight minor antiform on a centrally located island off the southeast shore of Copper Island could not be followed onto Copper Island.

The Copper Island Fault separates the Sinwa Formation to the southwest from the younger Inklin Formation to the northeast. Laberge Group siltstone adjacent to the fault contains Late Pliensbachian (Kunae Zone) ammonites (Johannson et al., 1997), and previous dating of the Sinwa Formation concludes the age to be Norian (Upper Triassic) (Souther, 1971).

Bedding attitude is variable adjacent to the Copper Island Fault. The Sinwa Formation limestone dips from subvertical to shallow in multiple orientations (e.g., 138/79; 260/60; 356/011). The Inklin strata are moderately shallow and dip inconsistently (e.g., 018/23; 226/40; 233/52; 336/54). Variability in bedding may be due to local deformation along the Copper Island Fault. The Copper Island Fault is a subvertical structure trending northwest through Second Narrows and Copper Island (Figure 3 and 5). The linear fault zone is 175 to 200 m wide and crosscuts different-aged bedding of adjacent strata. Extensively fractured rocks and slickenfibre lineations that shallowly plunge to the southeast (17°→148° and 18°→126°) are observed in the Copper Island Fault zone. The shallow orientation of the slickenfibres may indicate a largely translational motion on the Copper Island Fault.

Additional post Mid-Jurassic linear faults divide the northeast portion of Copper Island and crosscut Laberge Group bedding and the northwest-trending folds. The rocks in these faulted areas are shattered or gouged, and the faults form linear features on air photographs and commonly have intrusions along the margins of the fault zone. Intrusions often are in or directly next to narrow linear bays that formed along the fault zones. The younger faults variably cut across the folds formed in the Mid-Jurassic (Tipper, 1978; Mihalynuk, in press). Several other faults cut across Copper Island on the eastern shore, variably trending 270° to 330°. Variable orientations and the number of faults added much complexity to structural interpretation of the east portion of Copper Island. In detail, thick beds may disappear over short distances and are thought to be interrupted by a fault rather than pinched out stratigraphically.

Subvertical strike-slip faults are common in the southern Atlin Lake area and are exposed along Atlin Lake on Bastion and Griffith Islands (English et al., in review). Additionally, the subvertical Llewellyn Fault trends northwest across Llewellyn Inlet. Mihalynuk (1999) documented abundant vertical to subvertical northeast-trending faults of sinistral and dextral motion with less than 10 m offset in the Tagish Lake Area. Regionally, the subvertical Copper Island Fault continues to separate the Upper Triassic Stuhini Group and the Lower Jurassic Laberge Group to the northwest and merges with the Llewellyn Fault near Tagish Lake (based on bedrock geology map of Mihalynuk, 1999). Therefore, the Copper Island Fault represents a splay on the Llewellyn strike slip system rather than a continuation of the King Salmon Thrust.

DISCUSSION

The Copper Island Fault is commonly interpreted as an extension of the King Salmon Thrust (Wheeler and McFeely, 1991); however, these two faults may be independent structures.

In the central portion of the Whitehorse Trough near the Taku River, the Sinwa and Inklin Formations occur northeast of and in the hanging wall of the King Salmon Thrust and are carried over younger Lower Jurassic conglomeratic facies of the Laberge Group to the west (Souther, 1971). The Copper Island Fault, however, juxtaposes older, Upper Triassic Sinwa Formation limestones to the southwest, against younger, Late Pliensbachian Laberge Group strata to the northeast; Sinemurian and Early Pliensbachian strata are absent across the fault. The cutting out and structural thinning of the stratigraphic section and the juxtaposition of younger rocks to the northeast against older rocks to the southwest is the opposite of what would be expected if the Copper Island Fault were a west-verging thrust fault.

Arguably, the history of the King Salmon Thrust is similar to the history of the Nahlin Fault. The Nahlin Fault bounds the northeast margin of the Whitehorse Trough (Figure 1) and originated as a thrust fault during emplacement of the Cache Creek Terrane (Mihalynuk, 1999). As the Nahlin Fault extends into Atlin Lake area, the structure becomes vertical and displays dextral wrench displacement, perhaps due to reactivation between about 55 and 46 Ma (Mihalynuk et al., 2003). Thus, the Copper Island Fault could represent younger strike-slip motion on a northern continuation of the King Salmon Thrust; however, this remains problematic because the age relation of stratigraphy across Copper Island Fault differs from that of the King Salmon Thrust.

The steep nature of the Copper Island Fault, the variable bedding adjacent to the structure, the shallowly plunging slickenfibres, and the crosscutting of beds all suggest a translational strike-slip motion for the Copper Island Fault. In addition, the well-developed fold and thrust belt characteristic of the southern Whitehorse Trough is not seen in

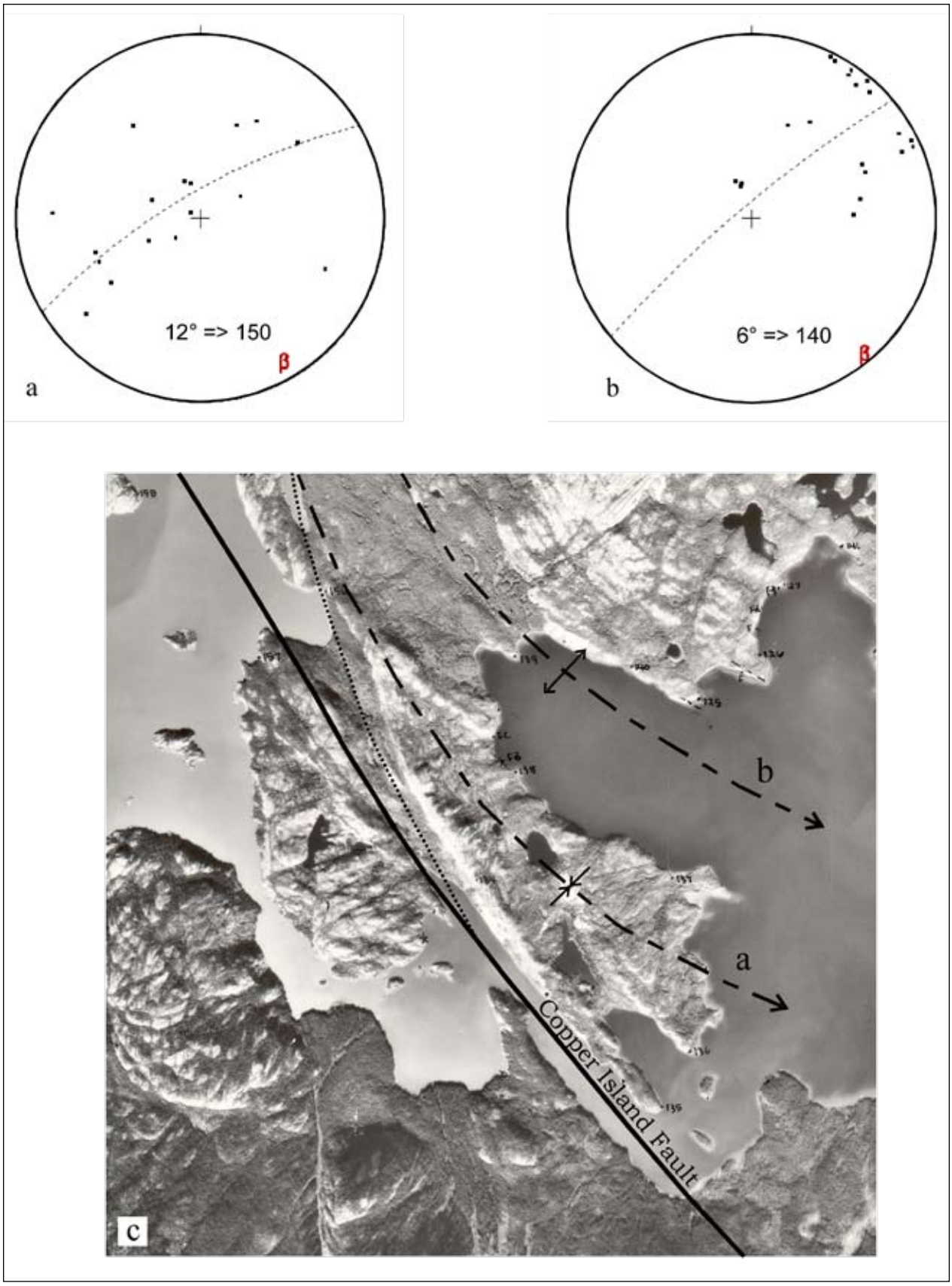

Figure 4. Syncline (a) and overturned anticline (b) plunging shallowly towards the southeast located northeast of Copper Island Fault. Compare to air photo (c) which shows the plunging nature of syncline (a) (source: BC5624 059).

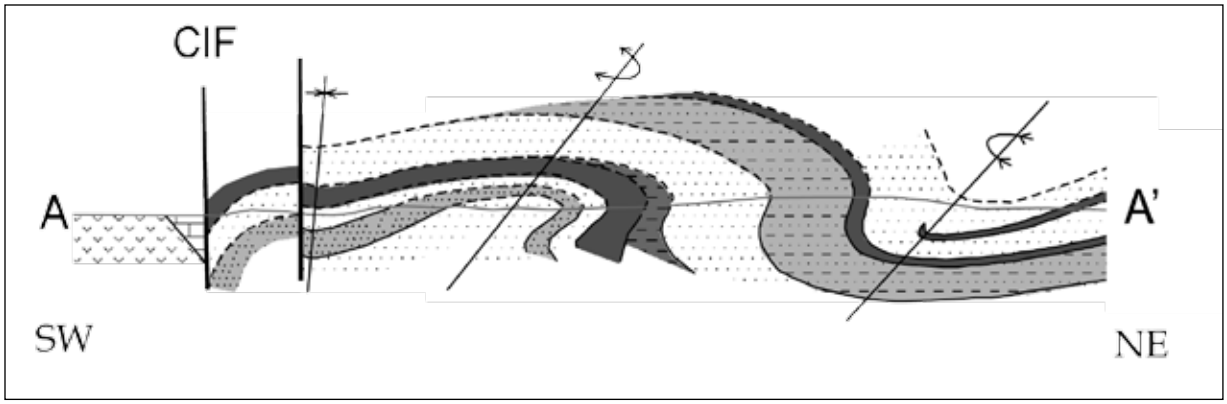

Figure 5. Cross section of western Copper Island. Central folds are overturned and have undergone further deformation perpendicular to fold axis. Note the vertical-subvertical Copper Island Fault in the SW and fault splay slightly NE of the CIF. See Figure 3 for section line and legend.

southern Atlin Lake (English et al., in review), and local and regional faults in the area are dominantly strike-slip in nature (e.g., Llewellyn Fault, Figure 1). Given that the subvertical Copper Island Fault can be traced to the northwest, continuing to separate the Stuhini Group and the Laberge Group until it merges with the Llewellyn Fault near Tagish Lake, the Copper Island Fault represents a splay of the Triassic to Cretaceous Llewellyn strike-slip system rather than a northern continuation of the King Salmon Thrust.

IMPLICATIONS FOR HYDROCARBONS

In the Taku River area, the Sinwa Formation carbonates extend to depth beneath the Laberge Group in the hanging wall of the shallow-angle King Salmon Thrust and may be a potential source rock for hydrocarbon accumulations. However, this relationship is not as clear in the southern Atlin Lake and Copper Island areas. The steep angle fault separating the Sinwa Formation from the Laberge Group may have developed during strike-slip motion, and the extent of the Sinwa Formation, and concomitant source rock potential, in the subsurface beneath the Laberge Group in the Atlin Lake area remains unconstrained (Figure 5).

CONCLUSIONS

In the southern Atlin Lake region, the subvertical Copper Island Fault separates the Upper Triassic Sinwa Formation from Late Pliensbachian sediments of the Inklin Formation. The Copper Island Fault has previously been interpreted to represent the northwestern continuation of the King Salmon Thrust. The geometry and stratigraphic relationship across the fault suggest that the Copper Island Fault is a separate and younger feature from the King Salmon Thrust and is probably characterised by strike-slip displacement. The King Salmon Thrust carries the Sinwa and Inklin Formations in its hanging wall and places them above the proximal conglomerate facies of the Laberge Group. These conglomerates are not exposed in the Atlin Lake area, and the subvertical Copper Island Fault does not display an older-over-younger relationship. Moreover, the basal Sinemurian strata of the Inklin Formation are missing across the fault. The Copper Island Fault can be traced to the northwest until it merges with the Llewellyn Fault; therefore, the Copper Island Fault represents a splay of the Llewellyn strike-slip system rather than a northern continuation of the King Salmon Thrust.

REFERENCES

Aitken, J. D. (1959): Atlin map-area, British Columbia; *Geological Survey of Canada*, Memoir 307, 89 pages.

Dickie, J. R. and Hein, F. J. (1995): Conglomeratic fan deltas and submarine fans of the Jurassic Laberge Group, Whitehorse Trough, Yukon Territory, Canada: fore-arc sedimentation and unroofing of a volcanic island arc complex; *Sedimentary Geology*, Volume 98, pages 263-292.

English, J. M., Johannson, G. G., Johnston, S. T., Mihalynuk, M. G., Fowler, M. and Wight, K. L. (in review): Structure, stratigraphy and hydrocarbon potential of the central Whitehorse Trough, northern Canadian Cordillera; *Bulletin of Canadian Petroleum Geology*.

English, J. M., Mihalynuk, M. G., Johnston, S. T., Orchard, M. J., Fowler, M. and Leonard, L. J. (2003): Atlin TGI, Part VI: Early to Middle Jurassic sedimentation, deformation and a preliminary assessment of hydrocarbon potential, central Whitehorse Trough and northern Cache Creek terrane; *in* Geological Fieldwork 2002; *B.C. Ministry of Energy and Mines*, Paper 2003-1, pages 187-201.

Johannson, G. G. (1994): Provenance constraints on Early Jurassic evolution of the northern Stikinian arc: Laberge Group, Whitehorse Trough, northwestern British Columbia; M.Sc. thesis; *University of British Columbia*, 297 pages.

Johannson, G. G., Smith, P. L. and Gordey, S. P. (1997): Early Jurassic evolution of the northern Stikinian arc: evidence from the Laberge Group, northwestern British Columbia; *Canadian Journal of Earth Sciences*, Volume 34, pages 1030-1057.

Mihalynuk, M. G. (1999): Geology and mineral resources of the Tagish Lake area (NTS 104M/8, 9, 10E, 15 and 104N/12W) northwestern British Columbia; *B.C. Ministry of Energy, Mines and Petroleum Resources*, Bulletin 105, 217 pages.

Mihalynuk, M. G., Erdmer, P., Ghent, E. D., Cordey, F., Archibald, D., Friedman, R. M. and Johannson, G. G. (in press): Subduction to obduction of coherent French Range blueschist - In less than 2.5 Myrs?; *Geological Society of America Bulletin*.

Mihalynuk, M. G., Johnston, S. T., English, J. M., Cordey, F., Villeneuve, M. E., Rui, L. and Orchard, M. J. (2003): Atlin TGI, Part II: Regional geology and mineralization of the Nakina area (NTS 104N/2W and 3); *in* Geological Fieldwork 2002, *B.C. Ministry of Energy and Mines*, Paper 2003-1, pages 9-37.

Monger, J. W. H., Wheeler, J. O., Tipper, H. W., Gabrielse, H., Harms, T., Struik, L. C., Campbell, R. B., Dodds, C. J., Gehrels, G. E. and O'Brien, J. (1991): Upper Devonian to Middle Jurassic assemblages - Part B. Cordilleran terranes; *in* Geology of the Cordilleran Orogen in Canada, The Geology of North America, Gabrielse, H. and Yorath, C. J., Denver, Colorado, *Geological Society of America*, pages 281-327.

Souther, J. G. (1971): Geology and mineral deposits of Tulsequah map-area, British Columbia; *Geological Survey of Canada*, Memoir 362, 84 pages.

Tipper, H. W. and Richards, T. A. (1976): Jurassic stratigraphy and history of north-central British Columbia; *in* Current Research Part A, *Geological Survey of Canada*, Paper 78-1a, pages 25-27.

Wheeler, J. O. and McFeely, P. (1991): Tectonic assemblage map of the Canadian Cordillera and adjacent portions of the United States of America; *Geological Survey of Canada,* Open File 1712A.

UNIQUE ASPECTS OF BRITISH COLUMBIA COALBED METHANE GEOLOGY: INFLUENCES ON PRODUCEABILITY

By Barry Ryan[1]

KEYWORDS: Elk Valley, Crowsnest and Peace River coalfields; gas composition; Lewis Thrust; deformation history.

INTRODUCTION

The majority of literature refers to the extraction of coalbed methane (CBM) from coal, which is not scientifically correct as the gas extracted from coal is a mixture of methane, carbon dioxide, and other gases. The British Columbia government is adopting the term coalbed gas (CBG). The abbreviations CBM and CBG both refer to the commercial gas extracted from coal at depth. To avoid confusion with existing scientific literature, this paper uses the term CBM.

Based on the amount of public data available, British Columbia is still in the grassroots stage of CBM exploration. In the last few years, companies have drilled a number of holes in southeast, northeast, and central British Columbia. Most of the drilling was done as part of experimental schemes, which provide a three-year confidentiality period, and consequently most of the information is still confidential. This paper therefore relies in part on coal rather than CBM data and on speculation as input for a discussion of influences of CBM geology on produceability. Under this general topic a number of observations or ideas are developed; they are related only in that they may all help in delineating prospective CBM areas.

Most of the coalfields in British Columbia have experienced some level of deformation. It is very important to understand the timing of coal maturation relative to deformation. In the simplest context, one should know whether structural traps were formed before or after generation of thermogenic methane. In the southeast of the province, the Elk Valley and Crowsnest coalfields (Figure 1) form part of the Lewis Thrust sheet, and this somewhat unique macrotectonic environment should be considered when assessing the CBM characteristics of the coalfields. This leads to a provisional comparison of the structural setting between the Peace River in the northeast and the southeastern coalfields. Finally, one of the most important aspects of CBM produceability is the recent tectonic history of coalfields and how it may improve permeability and interrelate with coal properties.

COMMENTS ON THE TIMING OF DEFORMATION AND COAL MATURATION

Coal, more than any other rock, changes during maturation. The main change is shrinkage, at first associated with loss of water, then with loss of carbon dioxide, and finally with loss of methane. There are a number of experimental ways of determining mass lost during maturation, but it can also be estimated from standard analyses of coals of different ranks. In the latter case, it is assumed that the fixed carbon component of a proximate analysis remains constant and that coal shrinkage is caused by loss of water and volatile matter. This is obviously only an approximation of what happens as coal rank increases; however, it enables a useful plot to be developed (Figure 2), which indicates that most of the water loss and coal shrinkage occur in the rank range defined by mean maximum vitrinite reflectance (Rmax) values of 0.4% to 0.7% (also represented by the transition from sub-bituminous to high-volatile bituminous). A second period of rapid shrinkage corresponds to the expulsion of thermogenic methane at a rank of about Rmax = 0.9%.

During the two periods of rapid shrinkage (Figure 2), seams are expelling water and volatile matter and may become overpressured. Under these conditions, especially during the first period, seams are most susceptible to bedding-parallel slip and thrusting. If deformation starts when seams are in the rank window Rmax = 0.4% to 0.7%, then pervasive deformation may well be localized in seams, in part because of overpressuring. Seams will be extensively sheared and may not develop cleats, or pre-existing cleats may be destroyed. Methane generated as rank continues to increase may have structural traps available, but permeability in seams may be low. On the other hand, if deformation occurs when the coal has reached higher ranks, then it is less likely to be as pervasive within seams, and pre-existing cleats may survive. Methane generated prior to development of structural traps may be lost as it is expelled with increasing rank.

The two periods of matrix shrinkage indicated in Figure 2 may correspond to cleat development. The earlier one is caused in part by compaction and loss of surface water, with some loss of CO_2 from the coal matrix. This shrinkage

[1] *Resource Development and Geosciences Branch, B.C. Ministry of Energy and Mines, barry.ryan@gems4.gov.bc.ca*

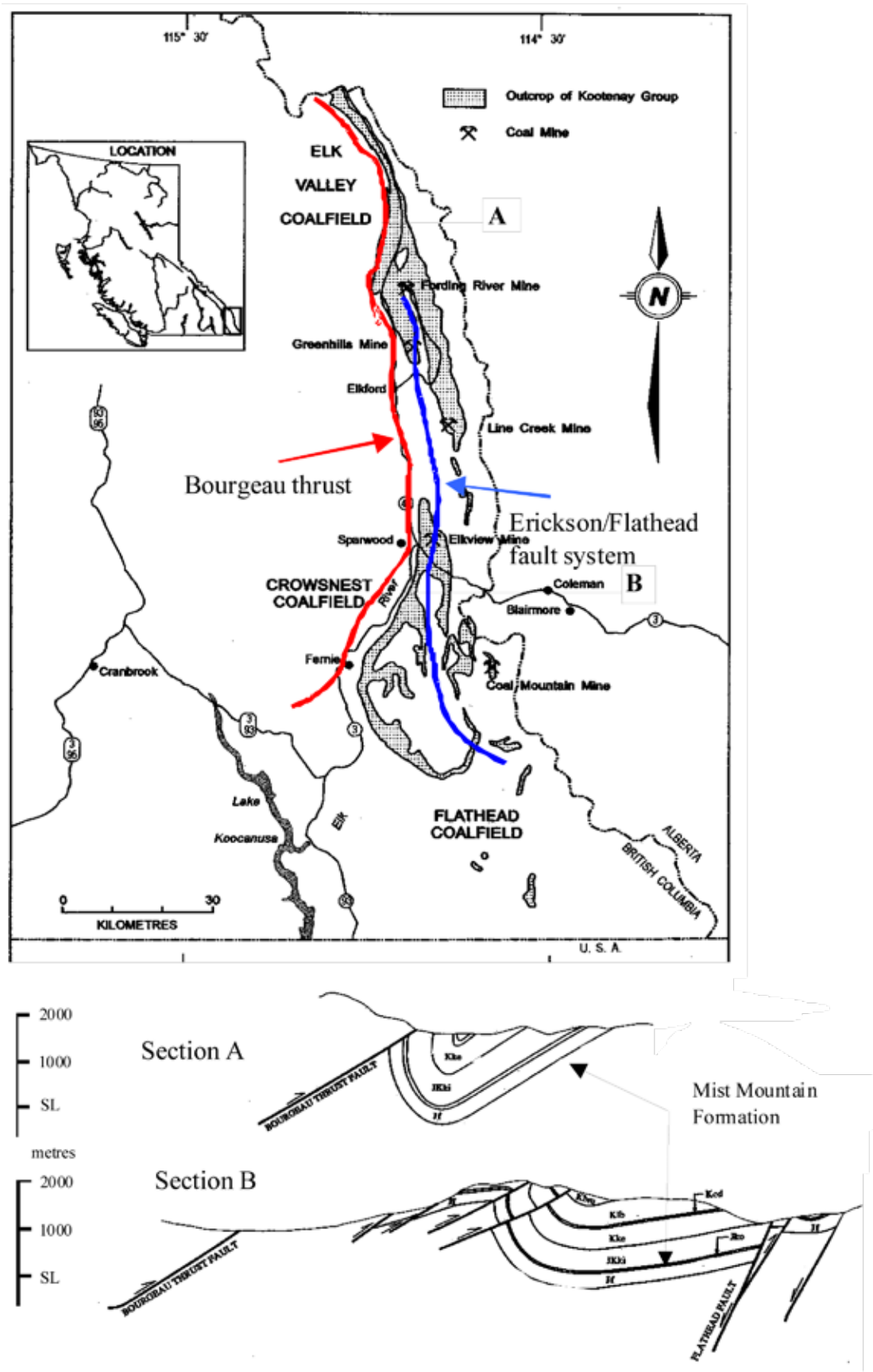

Figure 1. Structural setting of the Elk Valley and Crowsnest coalfields.

probably forms widely spaced cleats, because coal at this rank still contains, in part, a vegetation structure that will hinder the formation of closely spaced cleats. At increased rank (about Rmax = 0.9%), the coal goes through another period of rapid contraction that is caused by loss of methane from vitrinite. At this time, closely spaced cleats may form in vitrain-rich bands.

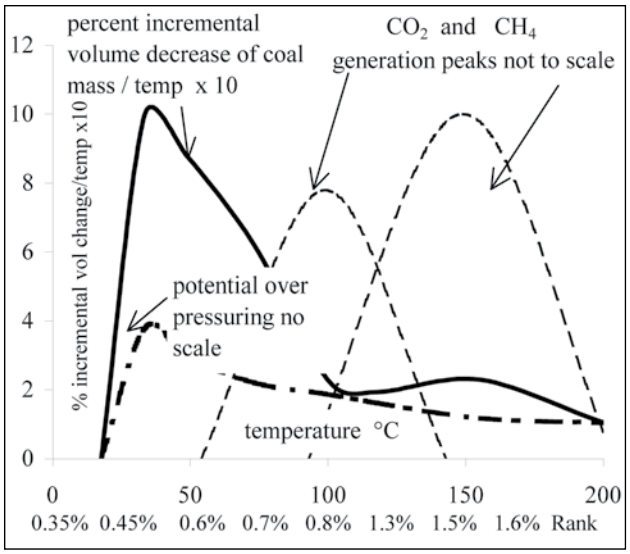

Figure 2. Matrix shrinkage and potential over-pressure as estimated from proximate analyses.

Face cleats exist in Powder River Basin coals, which have ranks of about Rmax = 0.4%. Generally, face cleats form parallel to the direction of regional compression and perpendicular to the basin axis. In that they are probably forming at fairly shallow depth (represented by a rank of about 0.4% to 0.7%), it is easy for the fold-axis-normal direction to become extensional, especially because of coal shrinkage. The regional nature of these fractures is probably accentuated because they offer pathways for water expelled from coal to escape upwards within seams to basin margins. Butt cleats that may form later during methane generation will generally be constrained to form at 90° to bedding and face cleats. These are surfaces of no or low cohesion, and therefore principle compressive stress directions must be perpendicular to them.

The spacing of face cleats decreases as rank increases up to a rank of low-volatile bituminous or semi-anthracite and then may increase (Law, 1993). If cleat development and spacing is related to the two periods of maximum shrinkage, then there should be a relationship between the plot provided by Law (1993) (Figure 3, this paper) and Figure 2. The curve in Figure 3 can be represented by a number of model points (open diamonds) that allow for the calculation of the change of cleat frequency versus rank or temperature. It is apparent that the maximum rate of change in cleat frequency is at low rank or temperature and tends to conform to the maximum period of coal shrinkage.

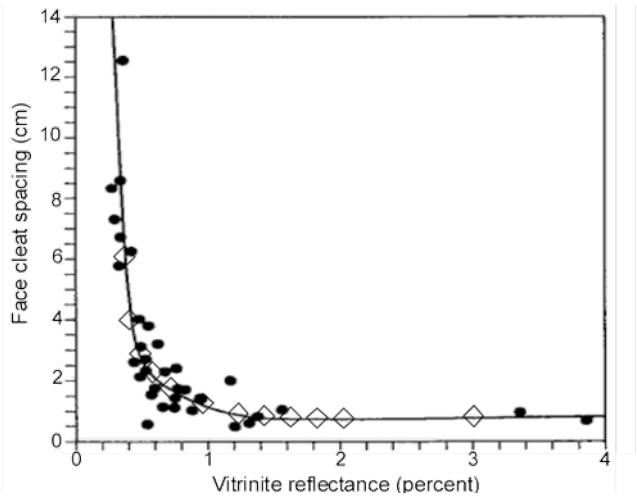

Figure 3. Spacing of face cleats versus rank (from Law, 1993); open diamonds are model points.

The generation of thermogenic methane can start at ranks as low as 0.5% in liptinite-rich coals. The gas is rich in heavier hydrocarbons, i.e., wet gas (Scott, 2001). The main stage of thermogenic methane generation starts at a rank of about 0.8% (Figure 4, from Scott, 2001), and the gas becomes progressively drier (dryness defined as C1/[C2+C3]) as rank increases. However, it will generally have lower ratios than does biogenic gas, which has high C1/(C2+C3) ratios. Coals rich in inert macerals may generate fairly dry gas (high C1/[C2+C3] ratio).

In deformed seams in British Columbia, it is important to differentiate between the effects of regional deformation (thrust faults) and local (in-seam) deformation. Regional deformation that precedes local folding probably occurs when coal rank is low, and its intensity will not vary based on location in folds. Shear joints associated with the early thrusting may not intersect bedding along fold-axis directions of later folding, and they will not vary their relative orientation with respect to bedding, depending on which limb they occur on. The simplistic geometry of shear joints related to regional shearing and local flexural flow folding is illustrated in Figures 5 and 6.

The data are plotted into lower-hemisphere stereonets as poles to bedding and poles to shear joints. It is useful to note that in the stereonets, the pole to shear joints migrates away from the pole to bedding in the direction of shearing to form an acute angle between the two poles. The orientation of shear joints related to thrusting should be regionally consistent, whereas those related to folds will change orientation depending on which limb they are on. Limited data from southeast BC indicate that the shear joints at the Greenhills coal mine on the west limb of the syncline are related to the flexural slip associated with the syncline. In other mines, the relationship is less obvious. The shear joints are, however, rotated such that they appear to be related to folds trending more to the northwest or thrusting from the southwest. (Figure 7). Face cleats appear to strike normal

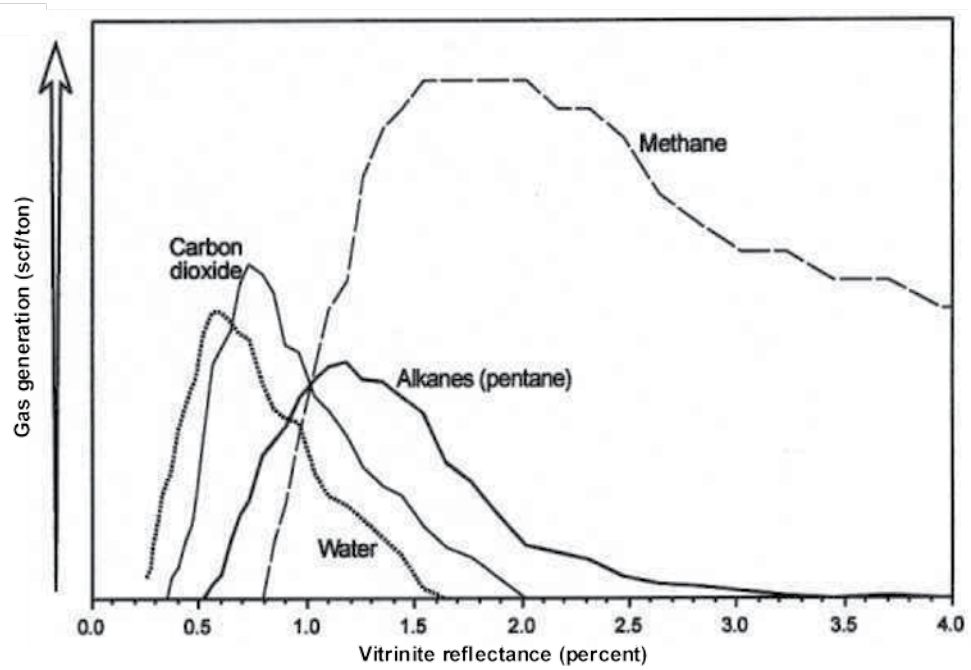

Figure 4. Generation of gases; diagram from Scott (2001).

to this early folding (or parallel to the thrusting) rather than normal to the later fold-axis direction.

In the Peace River coalfield (Figure 8), shear joints indicate northeastward thrusting or the prevalent northwest-trending folds. The properties indicated in Figure 8 are located in Figure 9. Face cleats are generally normal to the fold-axis direction, except in the north in the Gething Formation, where some trend parallel to the fold-axis direction. These cleats may in fact be axial planar features related to folding of the coal that occurred after it reached moderate rank. In the area, coal in the Gething Formation is inertinite-rich and consequently would not have shrunk as much during early coalification. Inert-rich coals that are characteristic of some Cretaceous British Columbia and Permian Australian coals may not form face cleats during early coalification and may contain fractures formed during later tectonic activity. These fractures may or may not be of extensional origin.

STRUCTURAL AND CBM HISTORY OF THE ELK VALLEY AND CROWSNEST COALFIELDS IN THE LEWIS THRUST SHEET

The Elk Valley and Crowsnest coalfields have had a complex tectonic history, in part because they are contained in the Lewis Thrust sheet (Figure 1). This unique tectonic setting, in conjunction with the Cretaceous to Early Tertiary deformation history, may be significant in terms of the produceability of the CBM resource of the coalfields.

Coal in the coalfields is contained in the Mist Mountain Formation of the Kootenay Group (Table 1), which was deposited into the miogeosyncline developed on the eastern edge of the Purcell Arch. Sediment was derived from the west as the Columbian Orogeny uplifted rocks. The Kootenay Group is separated from the overlying Blairmore Group by a disconformity that separates the Elk Formation from the overlying Cadomin conglomerate. To the north and east, there was considerable erosion associated with this unconformity, which in the Elk Valley and Crowsnest coalfields appears to be more of a disconformity.

The Mist Mountain Formation, which is Lower Cretaceous to Upper Jurassic (about 152 to 140 Ma; Mossop and Shetsen, 1994), is up to 625 m thick in southeast British Columbia (Gibson, 1985). The overlying Elk Formation varies in thickness up to 488 m (present thickness; Gibson, 1977). It is unlikely, therefore, that the coal seams in the Mist Mountain Formation were buried by much more than 1000 m at the time of the pre-Blairmore erosional event. Erosion and associated uplift probably did not have any lasting effect on gas contents of seams in the formation.

The gas contents of coals in Carboniferous rocks in the Ruhr area of Germany reflect the effects of a post-Carboniferous unconformity. Samples from just below the unconformity are close to saturated, whereas deeper coals are undersaturated. This is the opposite of what might be expected, based on degassing of the coal during erosion and uplift related to the unconformity. Freudenberg et al. (1996) suggest that shallower coals were recharged with biogenic methane generated using both CO_2 introduced during uplift and hydrogen from the coals. Seams deeper in the section are undersaturated because they were hotter, did not

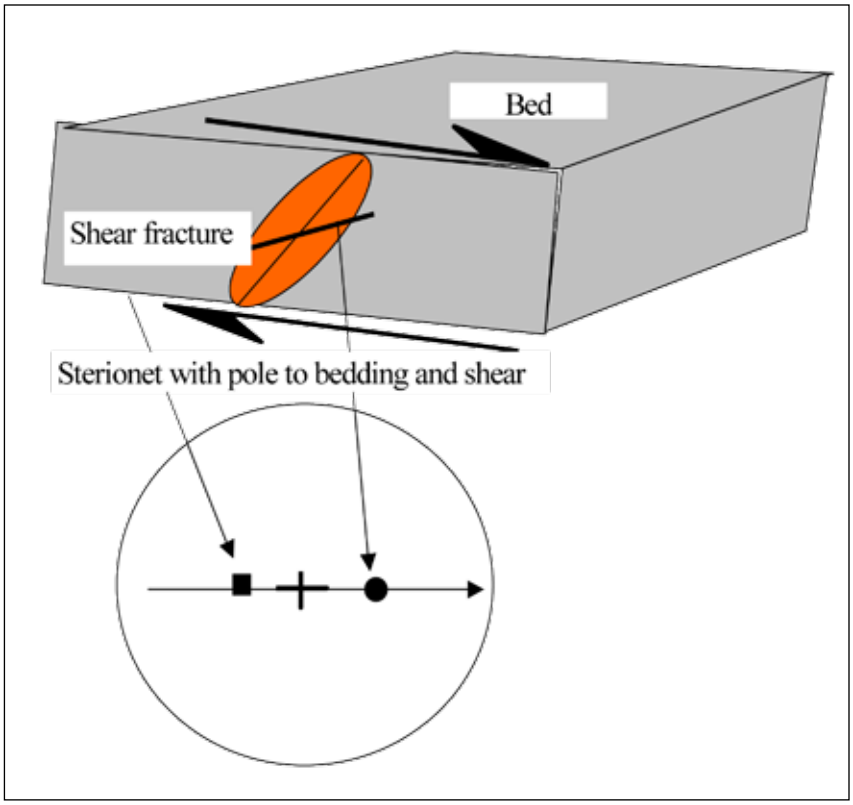

Figure 5. Orientation of shear joints in a thrust.

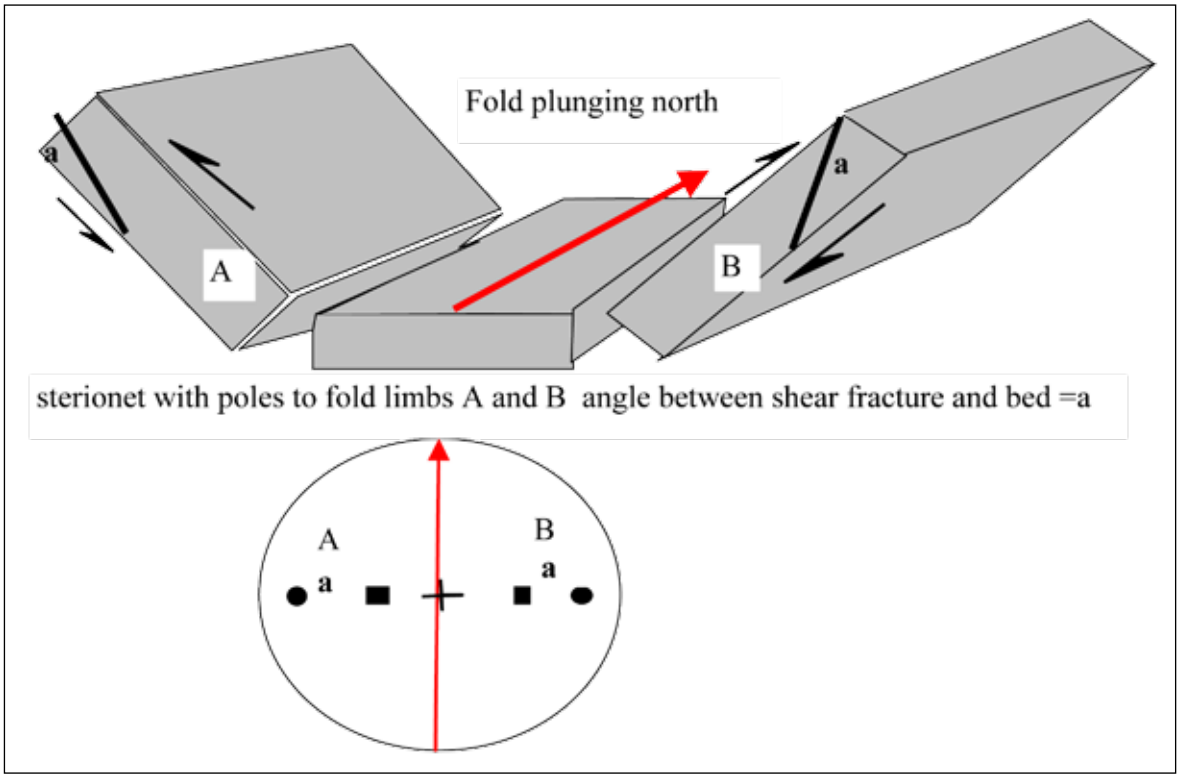

Figure 6. Orientation of shear joints in flexural flow fold.

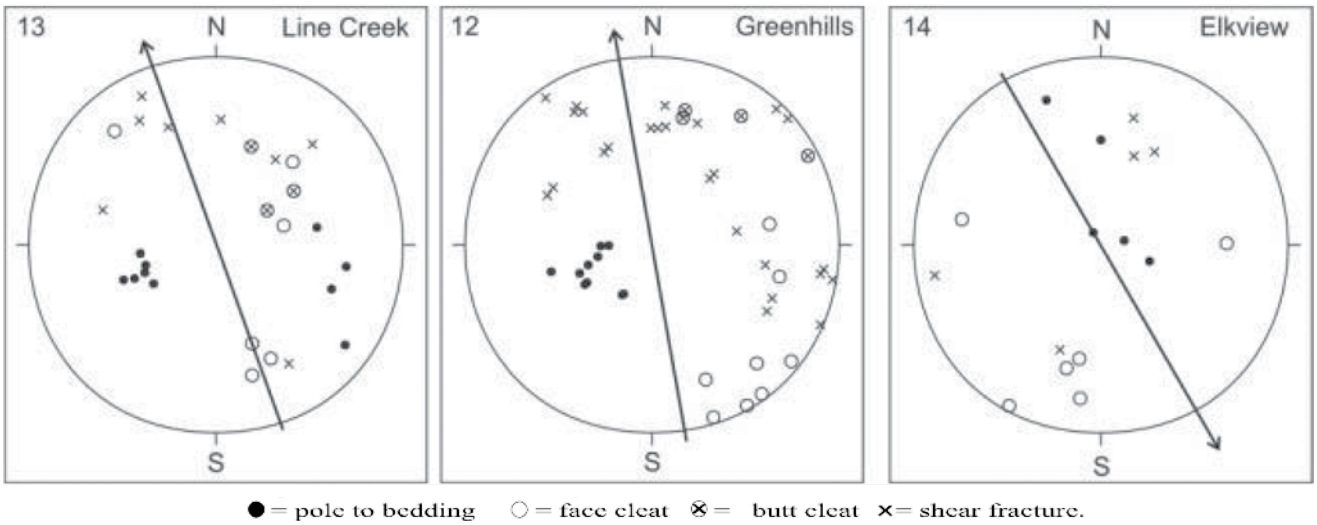

Figure 7. Sterionet of shear joints and cleats in southeast coalfields.

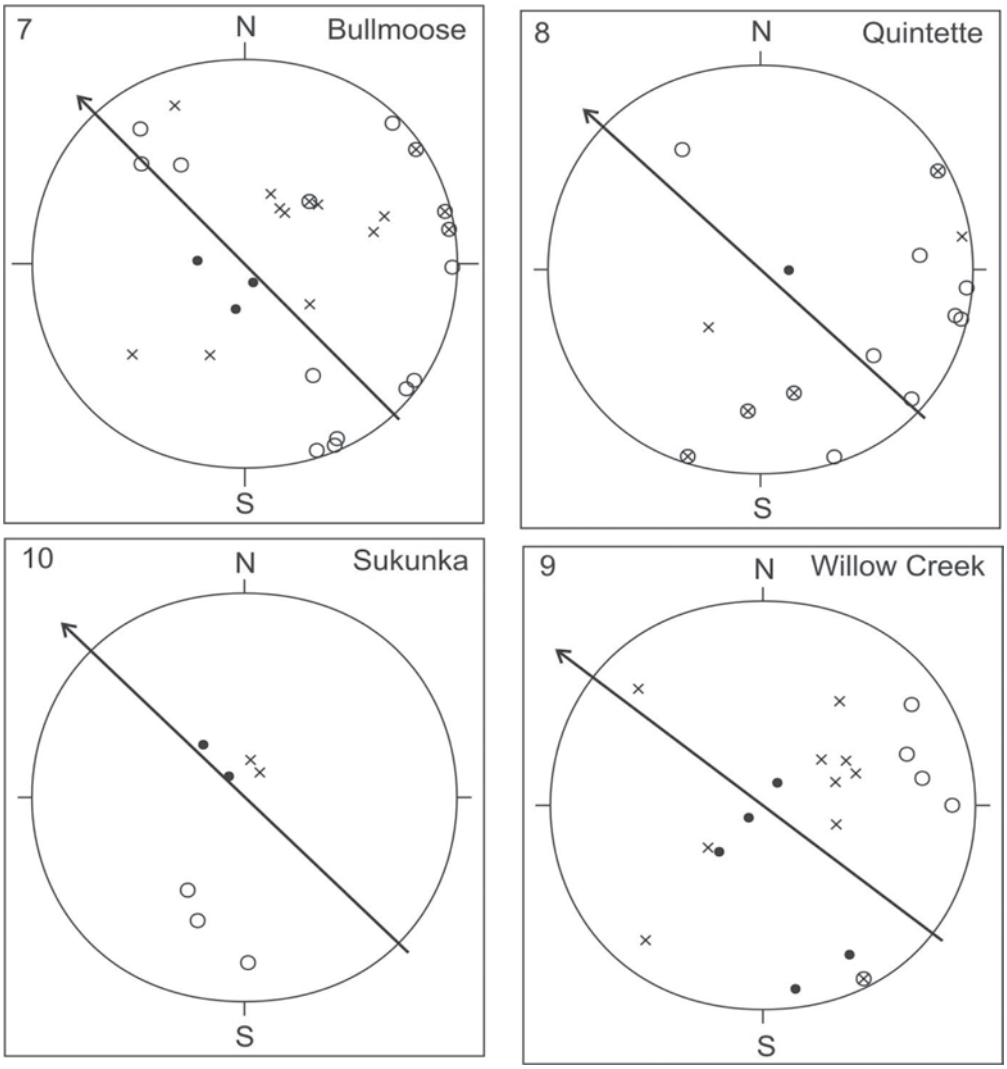

Figure 8. Sterionet of shear joints and cleats in northeast coalfields.

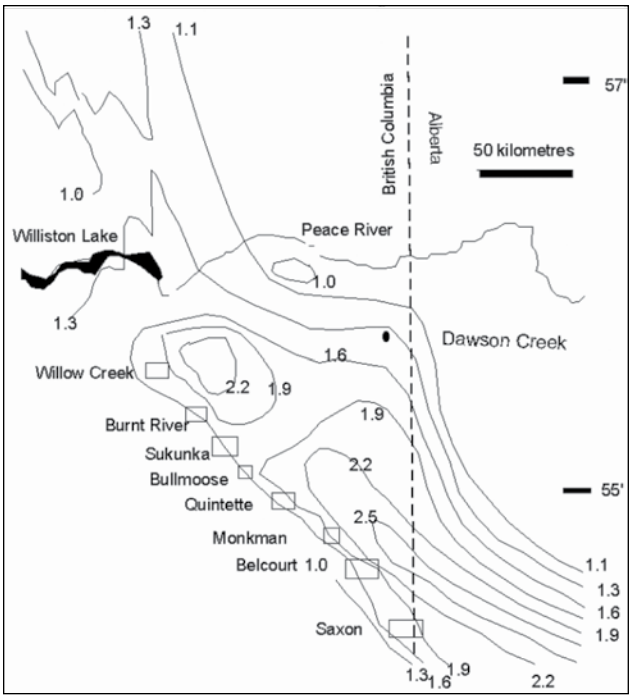

Figure 9. Reflectnace isograds for the top of the Gething Formation adapted from Machioni and Kalkreuth, (1992).

have access to CO_2, and retained a thermogenic imprint. As discussed later, it does appear that coals lower in the Mist Mountain section are undersaturated, but the explanation above cannot be used because the depth of burial of Mist Mountain coals at the time of the Cadomin unconformity was too shallow, and subsequent increase in rank would have generated sufficient methane to remove any imprint of the unconformity.

The Cadomin Formation, which is up to 170 m thick (White and Leckie, 2000), forms the base of the Lower Cretaceous Blairmore Group. It was probably deposited from about 140 to 125 Ma, based on palynology data discussed by White and Leckie (2000). There is therefore not a major time difference between the deposition of the Elk and Cadomin Formations. The Blairmore Group, which was deposited disconformably on top of the Kootenay Group, spans the time 140 to 95 Ma, and therefore deposition predates formation of the Lewis Thrust, which was active from 74 to 59 Ma (Sears, 2001). The thickness of the group ranges from 365 to 2000 m (Price, 1961). It is overlain by the Upper Cretaceous Crowsnest Formation (mainly alkaline volcanics), which is 40 to 100 m thick below the Lewis Thrust but does not occur within the thrust sheet. The formation is dated at 95 Ma using K-Ar data (Follinsbee et al., 1957), and its deposition therefore predates formation of the Lewis Thrust. Outcrops of the Upper Cretaceous Alberta Group survive in the Crowsnest coalfield in the core of the McEvoy syncline, where it is up to 230 m thick.

Prior to thrust development in the period 74 to 59 Ma, seams in the Mist Mountain Formation were probably covered by over 3000 m of rock comprised of the cumulative thickness of the Elk Formation, Blairmore Group, Crowsnest Formation, and Alberta Group. This is supposing that additional thrusts were not stacked on top of the Lewis Thrust sheet. At a depth of 3000 to 4000 m and based on normal geothermal gradients, seams in the upper part of the Mist Mountain Formation would have achieved a rank of high-volatile bituminous represented by Rmax values in the range of 0.6% to 0.8%. Seams lower in the section would have achieved higher rank. Thus at the time when Cordilleran orogenic forces to the west initiated development of the Lewis Thrust, some seams in the Mist Mountain were possibly overpressured with CO_2-laden water and in an ideal condition to participate in thrusting on all scales. Pearson and Grieves (1986) document evidence for post-folding coal maturation in the southwest corner of the Crowsnest coalfield.

The Lewis Thrust carried a thick slab, which probably consisted of over 6000 m (Price, 1962) of Paleozoic and Mesozoic rocks, eastward over rocks as young as Mesozoic. Osadetz et al. (2003) estimate the thickness at over 7 km. Movement took place during the period from 74 to 59 Ma at a rate of about 1.5 cm/yr in the Crowsnest Pass area, based on an estimated cumulative offset of between 140 and 200 km. Initiation of movement is indicated by profound cooling in the thrust block at about 75 Ma (Osadetz et al., 2003).

Thrust movement resulted in an increase in topography. It also fractured the cold and brittle thrust sheet, increasing permeability and allowing cold fluids to reach greater depths (Price et. al., 2001). This refrigeration of the thrust sheet delayed increase in rank and reduced the risk of gas loss because the decrease in temperature increased the adsorption ability of seams. However, at the time that this was occurring, the Bourgeau Thrust (Figure 1) was emplacing Paleozoic carbonates over the Lewis Thrust, and it was easy for fluids containing thermogenic CO_2 contained in the Paleozoic limestones to move downwards into the Lewis Thrust block. At the time of emplacement of the Bourgeau Thrust over the Lewis Thrust block, folds in the Lewis Thrust block would probably be largely formed and, to some extent, depth below the overlying Paleozoic limestones would in part be controlled by stratigraphy and in part by position in folds. This may explain the high CO_2 concentrations seen in some of the upper seams in the Elk Valley (Figure 10) (data from holes drilled by Norcen in 1990; Dawson et al., 2000). There is, therefore, reason to suspect that the CO_2 is thermogenic, though this cannot be confirmed without isotope data.

There are very limited public data on CO_2 concentrations in coals of the Crowsnest coalfield. A report by Rice (1918) provides some analyses. In 1916, 5 samples were collected from the working face in the underground Coal Creek Colliery and placed into sealed jars (Table 2). When

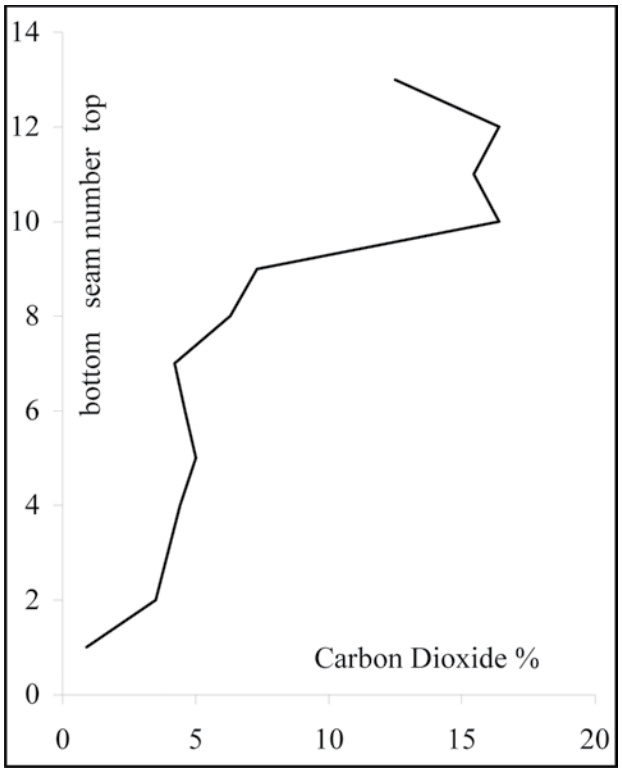

Figure 10. Elk Valley coalfield, carbon dioxide contents by seam Norcen 1990 holes Elk Valley, (Dawson et al., 2000).

the gas was analyzed, it was apparent that all had leaked; however, the CO_2 content is estimated from the CO_2/(CH_4+CO_2) ratio and it appears that, except for one sample, CO_2 contents were probably less than 5% (data are reported as cm^3 per 100 g, equivalent to mole fractions). Based on the trace of the Bourgeau Thrust relative to the outcrop of the basin (Johnson and Smith, 1991; Monahan, 2002), it appears that seams in the Mist Mountain Formation in the Crowsnest coalfield may not have been as close to the limestones in the overlying Bourgeau thrust plate or as close to the Crowsnest Volcanics as were seams in the Elk Valley coalfield; the Mist Mountain Formation may therefore have lower CO_2 concentrations.

There are no public isotope data for the methane in the Elk Valley or Crowsnest coalfields; however, some compositional data provide hints as to the origin of the gas. The ratio C1/(C2+C3) is an indication of the thermogenic component of methane; ratios less than 100 tend to indicate thermogenic methane, while ratios greater than 100 indicate biogenic methane (Wiese and Kvenvolden, 1993). This is complicated by the fact that biogenic activity can crack heavier hydrocarbons in thermogenic methane, increasing the C1/(C2+C3) ratio, and that at high ranks there may be secondary cracking of condensates to methane, which also will increase the ratio. Also, inert-rich coals probably will generate gas with higher C1/(C1+C2) ratios. These processes are illustrated in Figure 11 from Warwick *et al.* (2002).

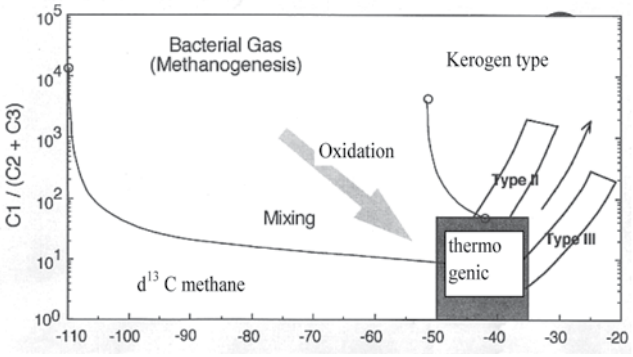

Figure 11. Isotope and gas composition diagram from Warwick et al., (2000).

In the Elk Valley, CO_2 increases as the ratio C1/(C2+C3) decreases in holes drilled by Norcen in 1990 (Figure 12) and increases for seams higher in the section (Figure 10). This tends to confirm a thermogenic origin for the CO_2. It also appears that seams lower in the section may have a biogenic imprint (high C1/[C2+C3] ratios) (Figure 13). The C1/(C2+C3) ratio varies during desorption, and it is not clear at what stage of desorption the Norcen gas samples were collected. However, gas composition data (Figure 14) collected from the hole drilled by Suncor into the Alexander syncline in the Elk Valley is for a single desorbing sample and indicates the extent that CO_2 concentrations and C1/(C2+C3) ratios can change during the desorption experiment. It is apparent that the range over which these values change within a single canister cannot explain the range in values seen in Figures 12 and 13.

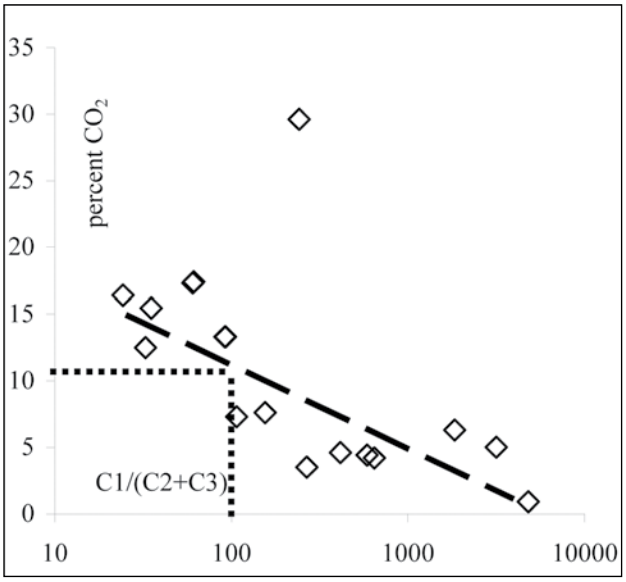

Figure 12. Elk Valley CO2 versus C1/(C2+C3) ratio for Norcen 1990 holes, Elk Valley (Dawson et al., 2000).

The very high C1/(C2+C3) ratios seen in the lower seams may indicate the presence of biogenic methane, but it is difficult to envisage a process that introduces biogenic methane into the lower seams but not into the upper seams.

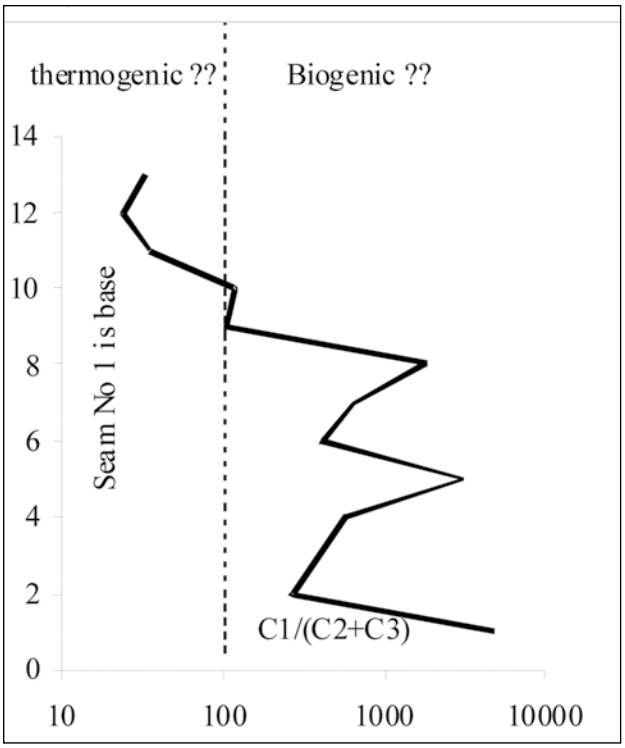

Figure 13. C1/(C2+C3) ratios versus seam number; Norcen 1990 holes, Elk Valley (Dawson et al., 2000).

Alternatively, the high ratios may indicate gas generated from liptinite-poor and inertinite-rich seams, in which case there should be a close correlation between coal seam petrography and C1/(C2+C3) ratios. Grieve (1993) provides petrographic analyses of coals at Weary Ridge in the north end of the Elk Valley coalfield close to the Norcen holes, and similar data are available for the southern end of the coalfield (Figure 15). In both cases it is clear that there is considerable variation in vitrinite content in the lower seams, and although the third seam above the base of the Mist Mountain Formation usually has a high inertinite content, other seams have variable and not necessarily low vitrinite contents. There is no clear correlation of high C1/(C2+C3) ratios with low vitrinite content. It is unlikely that petrography alone can explain the high C1/(C2+C3) ratios.

Often the degree of undersaturation of a single seam increases with depth (Figure 16). In part, the apparent near-saturation of seams higher in the section may be because they contain a mixture of CH_4 and CO_2 and the total gas contents are being compared to CH_4 isotherms. In general, partial degassing of a seam should decrease the C1/(C2+C3) ratio of the remaining gas. The high ratios are characteristic of seams irrespective of the depth at which they were sampled. The rank in the northern end of the Elk Valley coalfield is higher than it is to the south, and Rmax values range from 1.0% to over 1.6% (Grieve, 1993). It is possible that at the higher ranks, thermal cracking of the heavier hydrocarbons has increased the C1/(C2+C3) ratio.

After emplacement of the Lewis Thrust and before removal of the overlying Bourgeau Thrust sheet, Laramide heating may have been responsible for increasing the rank of Mist Mountain coals. Symons *et al.* (1999) discuss evidence for a Late Cetaceous to Tertiary Laramide heating and dolomitization event. This heating event must have ended prior to normal movement on the Flathead Fault at about 46 Ma. Evidence for post-deformation maturation is recorded in the Crowsnest coalfield by Pearson and Grieve (1985) and is evidenced in some deep drill holes (Bustin and England, 1989).

This second heating event may have affected seams low in the section more than it affected seams higher in the section. Previously generated wet gas was expelled upwards, and the increased rank was responsible for generating more gas with a much higher C1/(C2+C3) ratio. Because this event occurred after folding within the Lewis Thrust, it was possible for gas to move upwards within a single seam until the decrease in temperature allowed it to be re-adsorbed. It is important to remember that the heavier hydrocarbons have different adsorption characteristics than methane does and will be preferentially adsorbed, whereas some of the methane may escape the system. This could explain lower C1/(C2+C3) ratios for seams higher in the section or at shallower depth.

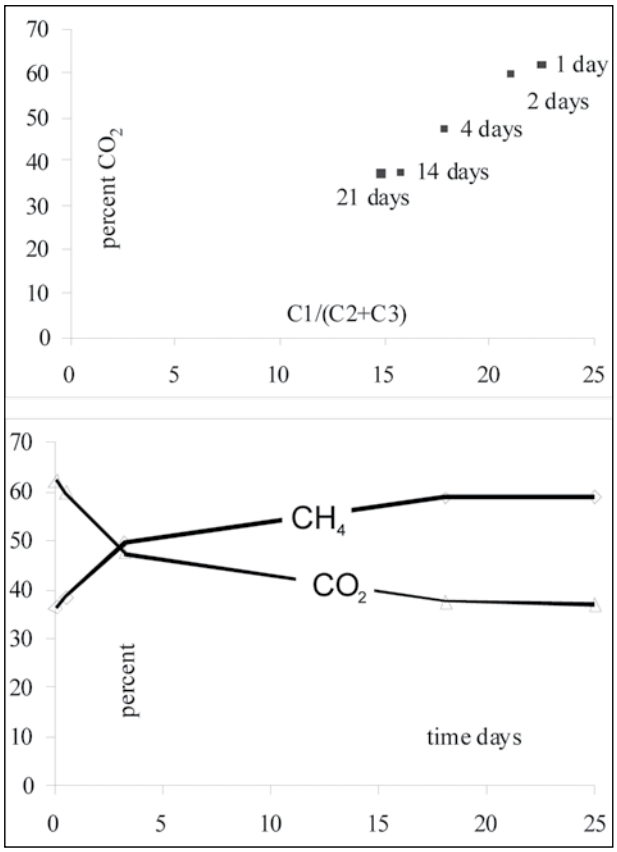

Figure 14. Data set of C1/(C2+C3) data from a single canister; numbers are days after canister sealed. Suncor data, Elk Valley coalfield (Dawson et al., 2000).

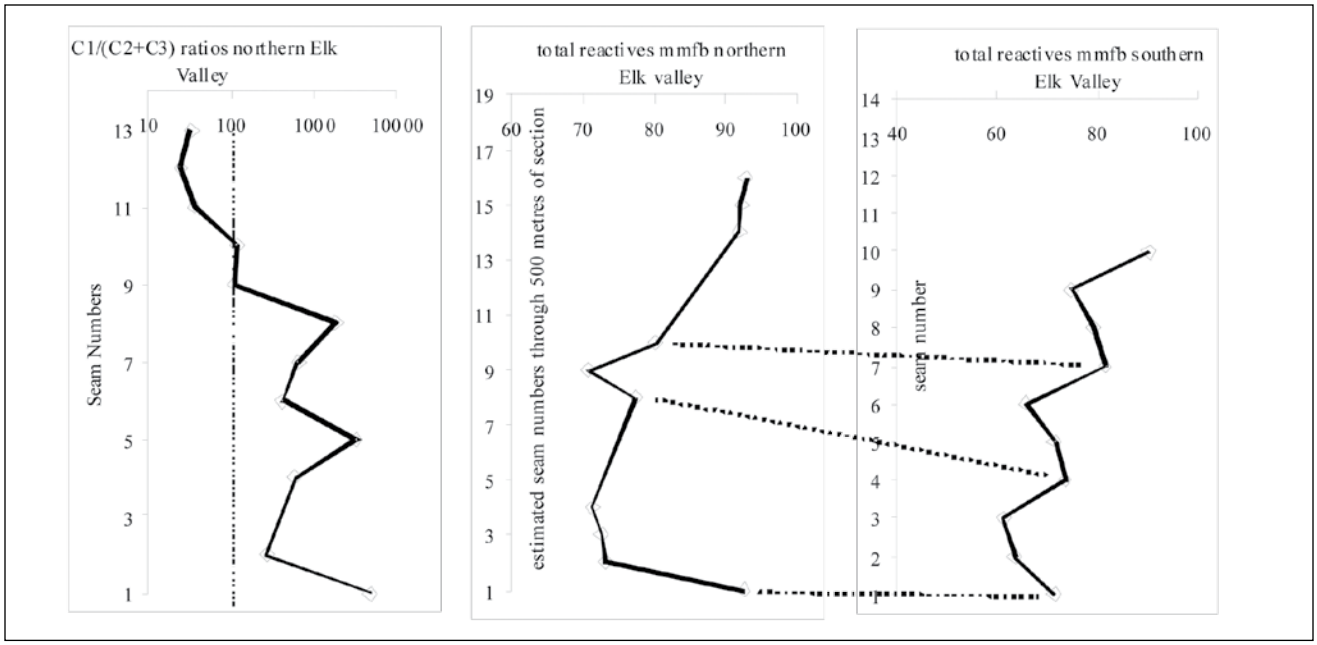

Figure 15. Petrographic variations in the Elk Valley, and C1/(C2+C3) ratios. Petrographic data from Grieve (1993). Inert-rich seams should correlate with higher C1/(C2+C3) ratios.

The increase in rank of seams at depth or lower in the section was accompanied by matrix shrinkage that temporarily improved permeability, allowing gas expelled because of increased temperature to move upwards either through the stratigraphy or along seams. The duration of the heating event was limited by the rapid unroofing of the Lewis Thrust sheet.

Any post-thrusting and post-folding maturation of coals in the Elk and Crowsnest coalfields could mean that gas expelled from coals undergoing increased maturation would have the opportunity to move into existing structural traps. There should be a clear distinction between structures that act as traps for upward-migrating thermogenic methane from those that might act as traps for biogenic gas moved in conjunction with ground water.

The onset of deformation when coal is at a rank range of 0.5% to 0.8% probably has detrimental effects on cleat development and seam permeability. The linkage results in the extensive shearing within seams and tends to destroy cleats or make their development unnecessary in terms of the coal's response to dehydration and devolatilization.

Present data indicate that permeability of seams in the Elk Valley and Crowsnest coalfields is low (Dawson et al., 2000), and it therefore becomes very important to identify areas of recent stress relief. The Erickson and Flathead fault system may be part of the same failed thrust system, in which the upper plates slipped back. If this is the case, then part of the plate may be in extension, and this would improve permeability within seams. Movement on the Lewis Thrust increases to the north across the US border, implying a clockwise rotation of the thrust sheet; this is consistent with the development of right-lateral strike-slip motion on a number of major faults. Stress environments around these faults may indicate areas of extension.

COMPARISONS BETWEEN NORTHEAST AND SOUTHEAST BRITISH COLUMBIA COALFIELDS

Coal-bearing rocks of interest to CBM exploration in the Peace River coalfield are contained in the Gething and Gates Formations (Table 3). These formations cover the age span of about 110 to 100 Ma. (Mossop and Shetsen, 1994). They overlie the Cadomin Formation and make up the second major Cordilleran-derived clastic wedge of the foreland basin. They record the first basin-wide sedimentation (Mossop and Shetsen, 1994, Chapter 17) and indicate the northeastward movement of the centre of deposition of the foreland basin. Initiation of thrusting at the craton edge caused it to subside, providing accommodation in the foredeep for the huge volume of sediments shed from the up-thrusted sheets. This thrusting predates the Lewis Thrust in the Elk Valley.

Deformation in the Peace River coalfield started later than it did in the southeast coalfields. Coalification generally preceded thrusting and folding (Kalkreuth et al., 1989), and the Gething and Gates Formations reached their maximum burial depth about 75 Ma in the west and 50 Ma to the east. This timing of maturation relative to deformation is important because it means that, in the Peace River coalfield, seams largely matured in the absence of thrusting

and therefore may have escaped a lot of in-seam shearing. In general, seams in the northeast have better cleat development than do seams in the Mist Mountain Formation. However, gas generated during coalification did not have the opportunity to be contained in structural traps. At this stage, only stratigraphic traps were effective for containing thermogenic methane expelled from seams. Later, thrusting and folding caused extensive deformation in seams in some areas but not in others.

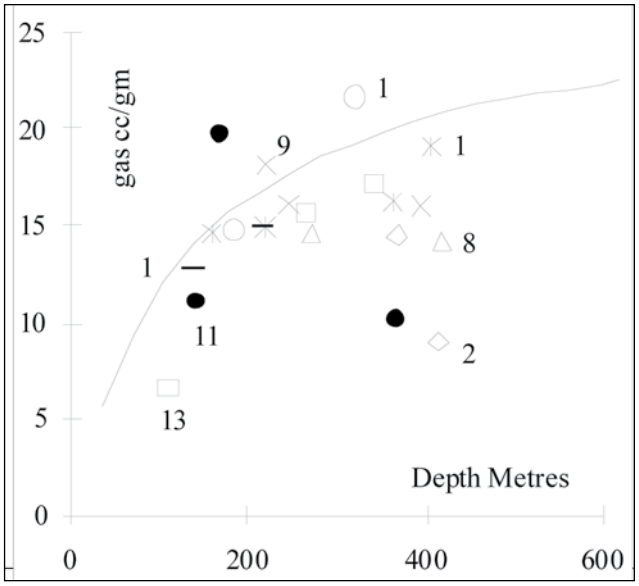

Figure 16. Desorption data from Norcen holes, 1990, Elk Valley (Dawson et al., 2000).

There are limited public desorption data available for seams in the Peace River coalfield. Data from the Gates Formation (Phillips holes drilled in 1996, Dawson *et al*., 2000) indicate that seams are nearly saturated. Also, the gas has a clear thermogenic fingerprint, based on C1/(C2+C3) ratios (Figure 17). The CO_2 concentrations are less than they are in the Norcen holes in the Elk Valley and increase as the C1/(C2+C3) ratio decreases and as depth increases. It appears that the CO_2 is of deep and thermogenic origin. Thrusting in the Peace River coalfield has not emplaced Paleozoic limestones over Cretaceous coal-bearing rocks, and there are no extrusive or intrusive magmatic rocks in the sequence, therefore access to thermogenic carbon dioxide is probably via deep faults.

There is probably semiquantative information that can be gleaned from the desorption curves. Airey (1968) modeled the shape of the desorption curve and indicated that his constant "to", which is the time to 63.2% of total desorbed gas, is strongly dependent on the degree of fracturing of the coal; this is confirmed by the work of Harris et al. (1996). Work by Gamson et al. (1996) indicates that desorption time is also dependent on coal petrology, with dull lithotypes desorbing faster. Data for Mist Mountain Formation coals indicate that they generally have desorption times (63.2% of total desorbed gas) less than 30 hours (Dawson, 1993; Feng et al., 1981). However, desorption times for Gates Formation coals from the Phillips drill program in the Peace River coalfield (Dawson et al., 2000) average over 70 hours. On a regional scale, desorption times may indicate the degree of microfracturing of coals and of pervasive deformation. On the local scale, they may correlate with a combination of petrography and fracture size. As a caution, desorption times can also be influenced by the way the desorption experiment is conducted.

In the northeast, variation in rank must be explained

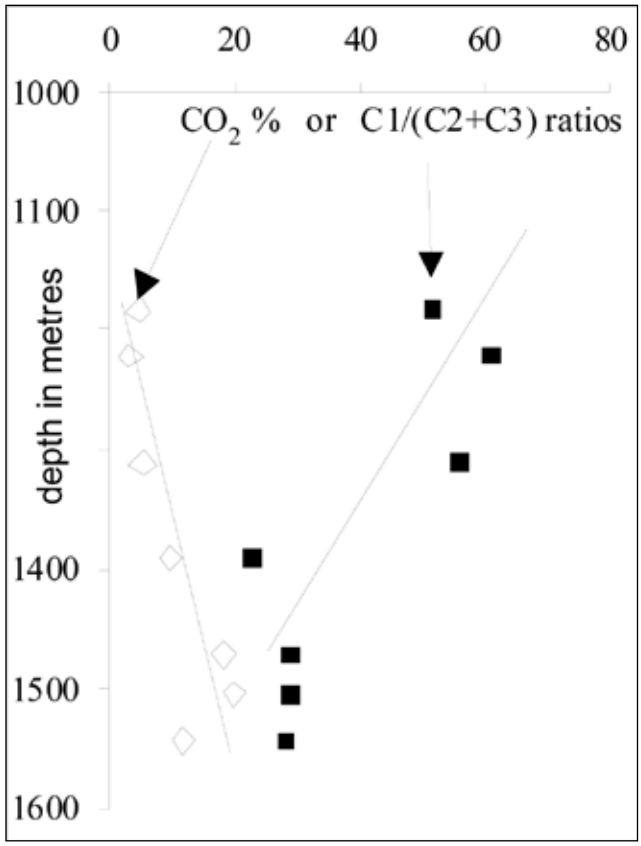

Figure 17. C1/(C2+C3) ratios for Gates Formation coals, Phillips exploration project, 1996 (Dawson et al., 2000).

by variation in stratigraphic thickness or by variation in upward heat flow, because coalification preceded deformation. There are a number of enclosed areas of high rank apparent in the Gething Formation (Marchioni and Kalkreuth, 1992) (Figure 9), and, depending on their origin, they could have implications for CBM exploration. One that is very conspicuous is located between the Willow Creek and Burnt River properties (Figure 9) and is responsible for locally increasing the rank of seams in the Gething Formation to semi-anthracite. If convective movement of fluids causes rank increase, then methane could be swept out of seams and CO_2 introduced. On the other hand if it is caused by increased burial, then there is more chance that seams will retain methane and less chance of CO2 introduction.

Convective movement of fluids should be evident by mineralization on cleat surfaces. Spears and Caswell (1986) provide estimates of the temperature of deposition for a number of diagenetic minerals found on cleats. Calcite and ankerite are deposited in the temperature range 100°C to 130°C, which corresponds to a rank of high-volatile bituminous. This represents the final expulsion of diagenetic water from seams. At this time, cleats have already formed and may be mineralized. For higher-rank coals, preservation of calcite on cleats indicates that hotter fluids associated with the higher rank did not remove calcite. The rank of the Gething and Gates Formation coals is generally higher than high-volatile bituminous, and there is calcite on face cleats in Gates coals and indications of calcite on cleats in Gething coals.

Coal ash generally has CaO contents less than 4%; higher contents often indicate the presence of carbonates on cleats, especially if a plot of ash versus CaO% indicates that CaO concentrations increase as ash contents decrease. In fact, in the absence of other data, ash chemistry data (available from existing coal studies) can provide information on the possible prevalence of carbonate on cleats. Calcite is present on cleats in the lowest seam of the Comox Formation in the Quinsam area (Ryan, 1994), whereas calcite is absent on cleats in seams from the lower part of the Mist Mountain Formation but does occur on some seams in the upper part of the formation. These cleat facies are easily separable on a CaO versus ash plot (Figure 18).

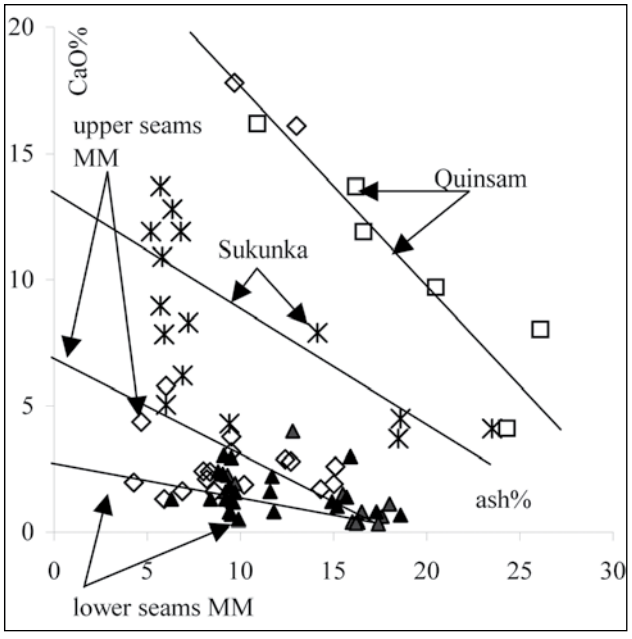

Figure 18. CaO% versus ash% for seams from the Mist Mountain, Gething, and Comox Formations.

The limited amount of CaO analysis data available for Gates and Gething coals indicates that there is probably some calcite on cleats in Gething coals from south of Willow Creek to Sukunka River and in Gates coals from Bullmoose to Belcourt. The area of high rank in the Gething Formation centred on Highhat Mountain (Marchioni and Kalkreuth, 1992) does not appear to be an area where there is unusually high or low CaO in the ash. Two analyses from the Burnt River property, which is at the centre of the area, are both under 3% CaO. A late thermal event would be expected to introduce CaO and CO_2 into the system, on one hand leaving calcite on cleats and the other replacing CO_2 with CH_4 in coal. A high-temperature thermal event may introduce CO_2 and remove CH_4 from the coal and CaO from cleats. A more detailed study of ash chemistry may lead to a better indication of whether to expect increased CO_2 in high-rank areas of the Gething Formation

THE INTERPLAY OF COAL CHARACTERISTICS AND RECENT TECTONICS

Coal preparation involves the removal of rock from the coal to reduce the ash concentration to acceptable levels for the customer. Coal is less dense than rock, and this property is used to advantage in wash plants, as is the fact that coal is generally less wettable than rock. The hydrophobicity of coal is used for cleaning fine coal by froth floatation. The wettability of coal varies with rank, largely because as rank increases, different oils and gases are expelled. This is referred to as the oil window (Dow, 1977) and is defined by Rmax values in the range of 0.5% to 1.35%. The hydrophobicity of coal attains a maximum value in the middle of the rank spectrum at ranks ranging from Rmax = 1% to 1.6% and is measured by contact angle of fluid on the coal surface (Osborne, 1988) (Figure 19).

Obviously the exact placement of the oil window depends on the petrography of samples. Samples with high liptinite contents will generate oil at lower ranks. The generation of oil at medium rank probably affects the adsorption and surface properties of coal, as discussed by Levine (1993). The most obvious effect on surface properties is that of capillary action (or wetting) as measured by contact angle. Another way of estimating the wettability of coal is to measure the difference between equilibrium moisture and air-dried moisture. This difference is probably a good measure of surface moisture, and the value also is at a minimum for the range of ranks 0.9% to 1.5% (Figure 20). The shift to higher ranks of the surface effects from the oil window probably indicates that it is the heavier oils that have the most effect on surface wetting.

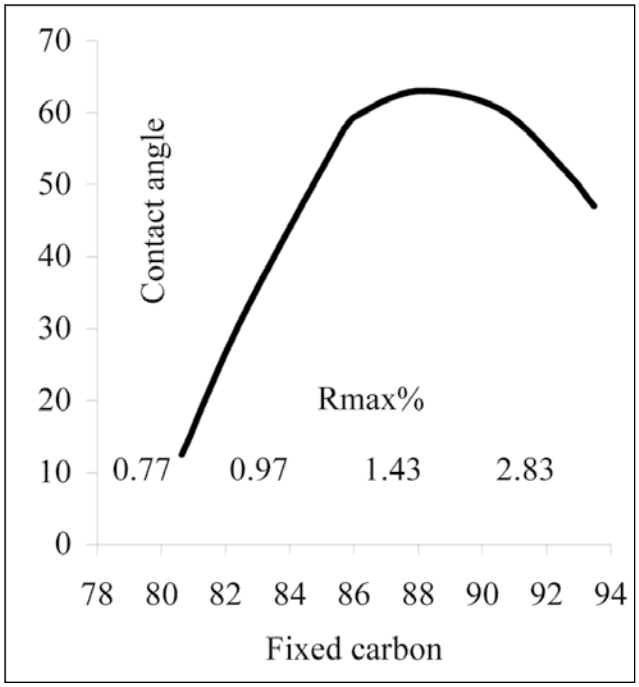

Figure 19. Contact angles of fluids on the surface of coals of different rank (Osborne, 1988).

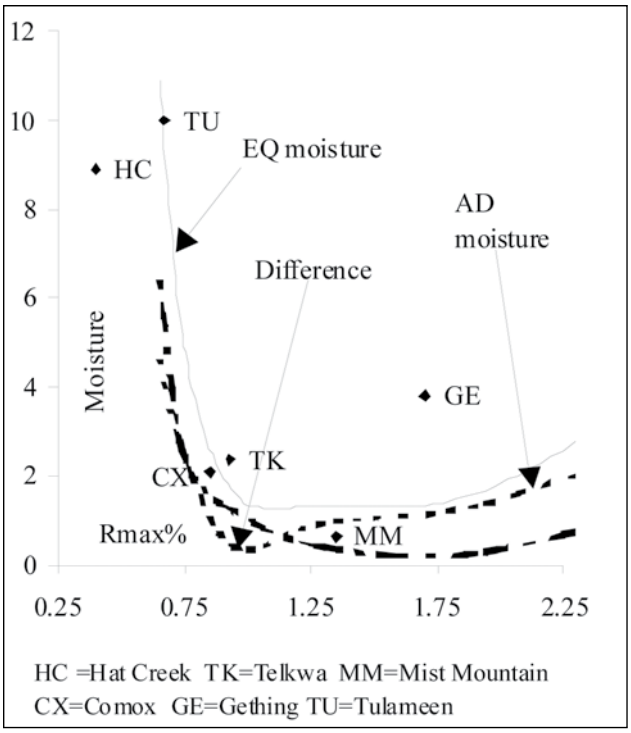

Figure 20. Contact angles of fluids on the surface of coals of different rank (Osborne, 1988).

The minimum wettability identifies coals that will have longer diffusion times but will have better relative permeability for gas because of lower water saturation on cleats than high- or low-rank coals will have. High- or low-rank coals with high wettability will have higher water saturation on cleat surfaces than will mid-rank coals and, under set conditions, will have lower relative permeability. This is because cleat surfaces of mid-rank coals can be dewatered to lower saturation values, and the relative permeability of gas approaches more closely the maximum permeability for a single fluid in the cleat system. Obviously coals in the mid-rank window may have reduced adsorption ability (Levine 1993), but cleats may contain little water and they may produce gas with minimal extraction of water.

Even with low wettability on cleat surfaces, over time cleats will probably become water-saturated. The ideal situation is one where cleats are opened up fairly recently. This would cause a decrease of pressure and desorption of gas into the cleats. Under these conditions, a seam would be saturated because the adsorbed gas would be in contact with a free gas phase. The seam may be under-pressured and gas contents may be low, but gas will be produced quickly with little water production. Obviously this requires the combination of recent stress relief, an opening of cleats (but not too much), and the correct rank window for the coal.

There are a number of areas where Tertiary stress fields are oriented such as to open cleats. However, much of Canada has the advantage of another regional event that could help open cleats. The country is undergoing isostatic rebound as a result of the removal of the continental ice sheet. Uplift amounts are in the order of tens of metres. The rapid removal of overburden pressure and resultant decompression of the more compressible units (coal) results in extension in a vertical direction and contraction in a horizontal direction. This will open cleats, and for coals with low wettability, water may not have had time to penetrate all cleat surfaces because uplift is relatively recent.

CONCLUSIONS

British Columbia contains a very large coal resource available for CBM exploration. However, much of this resource is in areas of fairly complex geology. Learning how to overcome the challenges resulting from the geology by exploration can be expensive. Sometimes, making better use of existing databases can reduce the cost.

The relative timing of deformation and the time at which the coal is the most susceptible (based on rank) to deformation is important. It affects the degree to which cleats form or are preserved in seams. Early deformation occurring when the rank is high-volatile bituminous may result in pervasive shearing of coal seams and limited development of cleats. Deformation that occurs later, after coal maturation has progressed, may cause more limited damage to cleat systems.

The orientation of cleats and fractures can help in understanding the sequence of deformation and coalification. The main problem for the geologist may be remembering long-passed structural geology courses.

Coalfields in southeast British Columbia occupy the Lewis Thrust sheet and are partially over-ridden by the Bourgeau Thrust sheet. Coal may have attained maximum rank after thrusting and consequently may have experienced in-seam deformation related to the Lewis Thrust. Thrusting also may be responsible in part for the introduction of thermogenic(?) CO_2.

In the Peace River coalfield, deformation post-dated most of the coalification, and consequently the degree of in-seam deformation is variable and in places seams retain good cleating. Rank in the Peace River coalfield is more variable than it is in the southeast. This may indicate fluid movement that could be associated with lower gas contents and introduction of CO_2. However, ash chemistry data collected from existing exploration projects do not indicate extensive fluid movement but do indicate that some cleat systems are mineralized with calcite.

After all this, it may seem that there are more problems than challenges in British Columbia. However, we may have at least one possible advantage that our neighbours to the south do not have. Isostatic rebound may be responsible for strain within seams that has opened cleats and improved permeability. This, in conjunction with high-volatile coals that resist wetting, may provide low-pressure gas-saturated systems at moderate depth.

REFERENCES

Airey, E.M. (1968): Gas emission from broken coal: an experimental and theoretical investigation*; International Journal of Rock Mechanics and Mineral Science* Volume 5, pages 475-494.

Bustin, R.M. and England, T.D.J. (1989): Timing of orogenic maturation (coalification) relative to thrust faulting in the southeastern Canadian Cordillera; *International Journal of Coal Geology*, Volume 13, pages 327-339.

Dawson, F.M. (1993): Joint venture project Fording Coal Limited; *Geological Survey of Canada,* Summary Report.

Dawson, F.M. Marchioni, D.L. Anderson, T.C. and McDougall, W.J. (200): An assessment of coalbed methane exploration projects in Canada; *Geological Survey of Canada,* Bulletin 549.

Dow, W.G. (1977): Kerogen studies and geological interpretations; *Journal of Geochemical Exploration*, Volume 7, pages 79-99.

Feng, K.K., Cheng, K.C. and Augsten, R. (1981): Methane desorption of Fording coal from Greenhills multiple seams; CANMET, Energy Research Program, Mining Research Laboratories Division report ERP/MRL 81-67(J).

Freudenberg, U. Lou, S. Schlurer, R Schutz, K and Thomas, K. (1966):Mina factors controlling coalbed methane distribution in the Ruhr district, Germany; Coalbed Methane and Coal Geology, *Geological Society*, Special Publication Number 10, pages 67-88.

Follinsbee, R.E., Ritchie, W.D. and Stansberry, G.F. (1957): The Crowsnest volcanics and Cretaceous geochronology, in 7th Annual Field Conference *Alberta Society of Petroleum Geologists,* pages 20-26.

Gamson, P., Beamish, B., and Johnson, D (1996): Coal microstructure and secondary mineralization: their effect on methane recovery; Coalbed Methane Geology, *Geological Societ,y* Special Publication Number 109, pages 165-179.

Gibson, D.W. (1985): Sedimentary facies in the Jura-Cretaceous Kootenay Formation, Crowsnest Pass area, southwestern Alberta and southeastern British Columbia; *Bulletin of Canadian Petroleum Geology*, Volume 25, pages 767-791.

Gibson, D.W. (1985): Stratigraphy, sedimentology and depositional environments of the coal-bearing Jurassic-Cretaceous Kootenay Group, Alberta and British Columbia; *Geological Survey of Canada*, Bulletin 357.

Grieve, D.A. (1993): Geology and rank distribution of the Elk Valley coalfield southeastern *British Columbia Ministry of Energy and Mines,* Bulletin 82.

Harris, I.H., Davies, A.G., Gayer, R.A. and Williams, K. (1996): Enhanced methane desorption characteristics from South Wales anthracites affected by tectonically induced fracture sets; Coalbed Methane Geology, *Geological Society*, Special Publication Number 109, pages 181-196.

Johnson, D.G.S. and Smith, L.A. (191):Coalbed Methane in southeastern British Columbia; *British Columbia Ministry of Energy and Mines, Petroleum Geology Branch*, Special Paper 1991-1.

Kalkreuth, W. Langenberg, W and McMechan, M. (1989): Regional coalification pattern of Lower Cretaceous coal-bearing strata, Rocky Mountain Foothills and foreland, Canada – implications for future exploration; *International Journal of Coal Geology*, Volume 123, pages 261-302.

Law, B.E. (1993): The Relationship Between Coal Rank and Cleat Spacing; Implications for the Prediction of Permeability in Coal; in Proceedings of the 1993 *International Coalbed Methane Symposium*, May 17-21 1993 Birmingham, Alabama, Volume 2, pages 435-442.

Levine, J.R. (1993): Coalification: The evolution of coal as source rock and reservoir rock for oil and gas; in Hydrocarbons from Coal; *American Association of Petroleum Geologists*, Series number 38, Chapter 3, pages 39-77.

Marchioni, D and Kalkreuth, W. (1992): Vitrinite reflectance and thermal maturation in Cretaceous strata of the Peace River Ach Region: West-central Alberta and adjacent British Columbia; *Geological Survey of Canada,* Open File 2576.

Monahan, P. (2002): The Geology and oil and gas potential of the Fernie-Elk Valley Area, southeastern *British Columbia Ministry of Energy and Mine,* Petroleum Geology Special Paper 2002-2.

Mossop, G.D. and Shetsen, I. (1994): Geological Atlas of the Western Canada Sedimentary Basin; Alberta Geological Survey.

Osadetz, K.G., Kohn, B.P. , Feinstein, S. and. Price, R. A. (2003): Aspects of foreland belt thermal and geological history in southern Canadian Cordillera from fission-track data.

Osborne, D.G. (1988): Coal Preparation technology; *Graham Trotman limited;* page 420.

Pearson, D.E., and Grieve, D.A. (1985): Rank variation coalification pattern and coal quality in the Crowsnest Coalfield, British Columbia; *Canadian Institute of Mining and Metallurgy,* Bulletin, Volume 78, pages 39-46.

Price, R.A. (1957): Flathead Map area, British Columbia and Alberta*; Geological Survey of Canada*, Memoir 336.

Price, R.A. (1961): Fernie map area east half, Alberta and British Columbia 82G E1/2; *Geological Survey of Canada*, Paper 61-24.

Price, R.A.,Kohn, B.P. and Feinstein, S. (2001): Deep refrigeration of a thrust and fold belt because of enhanced syntectonic penetration of meteoric water: the Lewis thrust sheet, southern Canadian Rocky Mountains; *Earth System Global Meeting* June 24-28 2001 Edinburgh International Conference Centre.

Rice, S.G. (1918): Bumps and gas outbursts of gas in mines of Crowsnest Pass Coalfield; *British Columbia Department of Mines*, Bulletin Number 2.

Ryan, B.D. (1994): Calcite in Coal from the Quinsam Coal Mine, British Columbia, Canada, Origin, Distribution and Effects on Coal Utilization; in Geological fieldwork 1994, Grant, B. and Newell, J.M., Editors, *B.C. Ministry of Energy, Mines and Petroleum Resources*, Paper 1995-1, pages 245-256.

Scott, A.R. (2001): A Coalbed methane producibility and exploration model: defining exploration fairways; 2001 *International Coalbed Methane Symposium*, Tuscaloosa, Short Course #1, chapter 5.

Sears, J.W. (2001): Emplacement and denudation history of the Lewis-Eldorado-Hoadley Thrust slab in the northern Montana Cordillera USA: Implications for steady-state orogenic processes; *American Journal of Science,* Volume 301, pages 359-373

Spears, D.A. and Caswell, S.A. (1986): Mineral matter in coals: cleat minerals and their origin in some coals from English Midlands; *International Journal of Coal Geology*, Volume 6, pages 107-125.

Symons, D.T.A., Enkin, R.J. and Cioppa, M.T. (1999): Paleomagnetism in the Western Canada Sedimentary Basin :Dating fluid flow and deformation events; *Bulletin of Canadian Petroleum Geology*, Volume 47, pages 534-547.

Warwick, P.D. Barker, C.E. and SanFilipo, J.R. (2002): Preliminary evaluation of coalbed methane potential of the Gulf Coastal Plain USA and Mexico; *Rocky Mountain Association of Geologists*, Coalbed Methane of North America II, pages 99-107.

White, J.M. and Leckie, D.A. (2000): The Cadomin and Dalhousie formations of SW Alberta and SE British Columbia; age sedimentology and tectonic implications; *Canadian Society of Exploration Geologists,* Conference 2000, abstract.

Wiese, K. and Kvenvolden, K.A. (1993): Introduction to Microbial and thermal methane*; US Geological Survey* Professional Paper 1570, pages 13-20.

THE POTENTIAL FOR CO_2 SEQUESTRATION IN BRITISH COLUMBIA COAL SEAMS

By Barry Ryan[1] and Dave Richardson[2]

KEYWORDS: Carbon dioxide phase diagram, coal macerals, carbon dioxide isotherms, coal rank.

INTRODUCTION

Most people accept that climate change resulting from human activity is a reality. The details of the causes and progress are much in dispute, but there is general consensus that increase in the concentration of carbon dioxide (CO_2) in the atmosphere is one of the causes. The amount of carbon dioxide released when any fossil fuel is burned is dependent on the ratio of carbon to hydrogen in the fuel. This ratio is a maximum for coal and a minimum for natural gas (mainly methane, CH_4), with oil having an intermediate ratio. The amount of CO_2 produced per unit of heat (in this case 10^6 BTU) for the various fossil fuels (Table 1) is a maximum for coal, but it is not zero for natural gas. The true impact of using the various fossil fuels requires an analysis of the efficiency of turning them into more useful forms of energy (often electricity or, in the case of oil, momentum). Natural gas and conventional oil reserves will be substantially depleted in the next 50 years, leaving coal as the most readily available fossil fuel. Technology that uses the energy from coal while minimizing or eliminating the release of CO_2 to the environment will become critically important; this involves sequestering CO_2 as a gas, liquid, or solid or in the adsorbed state on coal.

TABLE 1. CARBON DIOXIDE PRODUCED BY BURNING VARIOUS FOSSIL FUELS.

	oil	gas	coal
unit	barrel	cubic M	tonne
cost $US	30	5$/1000scf	25
exchange rate	0.76	0.76	0.76
cost US$ per unit	30.00	0.177	25.00
cost can$ per unit	39.47	0.23	32.89
wt of unit in kg	136.40	0.7142	1000
heat GJ per unit	6.12	0.0373	29.30
heat kcals per unit	1462007	8899	6999477
btu 10^6 per unit	5.801	0.035	27.771
kcals/kg	10719	12460	6999
GJ/tonne	44.87	52.16	29.30
cost GJ $can	6.45	6.24	1.12
cost Kcal 10^6 $can	27.0	19.8	4.7
cost btu 10^6 $can	6.81	6.58	1.18
CO2 emissions in kg from one million BTU			
coal	92.4		
oil	77.6		
gas	56.1		
Note Assumptions are made concerning heat value of each fuel and carbon content. Numbers are only approximate			

In recent years there has been a lot of discussion on the possibility of sequestering CO_2 in coal seams or using CO_2 to aid in the recovery of coalbed methane (CH_4). The basis of both these ideas is the fact that CO_2 is more strongly adsorbed onto coal surfaces than is CH_4. Once adsorbed, if temperature and pressure conditions do not change, then the CO_2 is permanently sequestered. There are of course two concerns: firstly, pressure and temperature conditions must not change, and secondly and more importantly, there are limited pressure and temperature ranges over which CO_2 is a gas. At higher temperatures and pressures, CO_2 becomes a supercritical fluid, and under these conditions it is not clear whether it is adsorbed by coal, occupies the pore spaces (acting like a fluid with very low viscosity), or infuses into the coal matrix. Under these conditions it is probably not realistic to talk of sequestering the CO_2, because it might be mobile.

Studies have looked at the potential to sequester CO_2 in a number of areas. Pashin et al. (2003) studied the Black Warrior Basin; Bachu and Stewart (2002) and Hughes (in press) have studied the potential for CO_2 sequestration in the Western Canadian Sedimentary Basin. These studies involve analysis of the coal basins and measurement of CO_2 isotherms from representative coal seams. This report is an initial study of the CO_2 sequestration potential for coals in British Columbia. BC ranks fourth of the provinces in Canada in total greenhouse gas emissions but ranks eighth in terms of tonnes of CO_2 per person per year (Figure 1). The province does not generate electricity by burning coal, so that the more obvious point sources of anthropogenic CO2 emissions are less readily identifiable in the province. In fact the largest sources of CO_2 emissions are commercial and private transportation (Table 2); the easiest way for the province to reduce CO_2 emissions may be to improve the efficiency of fuel consumption in diesel and gasoline engines. Smaller point sources may be located close to coal deposits and it may be possible to sequester in coal seams some of the CO_2 that they generate. Ideal candidates may be cement plants and natural gas processing plants, because they produce relatively pure streams of CO_2.

[1]*Resource Development and Geosciences Branch, B.C. Ministry of Energy and Mines*
[2]*Oil & Gas Titles, B.C. Ministry of Energy and Mines*

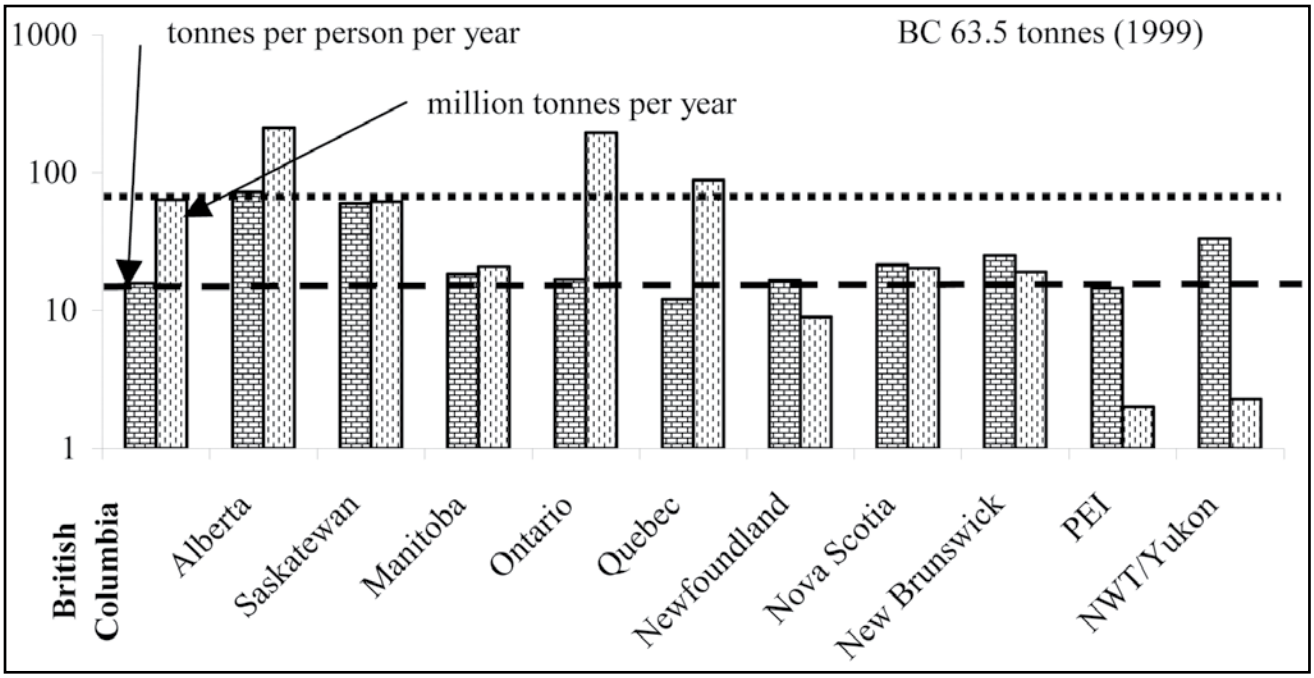

Figure 1. Total CO_2 emissions and CO_2 emissions per person for the provinces.

Data from Environment Canada 2000; Canada Greenhouse gas inventory 1990-1999.

The predominance of literature refers to the extraction of coalbed methane (CBM) from coal; this is not scientifically correct as the gas extracted from coal is a mixture of methane, carbon dioxide, and other gases. The British Columbia government is adopting the term coalbed gas (CBG). The abbreviations CBM and CBG both refer to the commercial gas extracted from coal at depth. To avoid confusion with existing scientific literature, this paper uses the term CBM.

TABLE 2. CO_2 EMISSIONS BY SOURCE IN BC FOR 1999.

			kg CO_2 equivalent
Energy	industry combustion		12.7
	transportation		26.1
	non-commercial combustion		7.95
	fugative	coal mines	0.5
		oil and gas	5.4
Industry process			2.9
Agriculture			2.6
Waste			4.9
Forestry			0.8
		total	63.85

Data from Environment Canada 2001,
Canada Greenhouse gas inventory 1990-1999.

SAMPLES AND SAMPLE LOCATIONS

Samples for this study were collected from a number of formations and from a single seam to provide some indication of the variation of CO_2 adsorption with changes in rank, maceral content, and temperature. A number of samples were collected from the Gething Formation in northeast BC at the same location as samples collected for a previous study of CH_4 adsorption characteristics (Ryan and Lane, 2002). Also in the northeast, two samples were collected from the Gates Formation at the Bullmoose Mine, which is now closed. In southeast British Columbia, one sample was collected from the Mist Mountain Formation. Two samples were collected from the Quinsam Coal mine on Vancouver Island. Tertiary coal deposits were represented by a drill core sample from the Princeton Basin.

The Gates and the Gething Formations, which are both Lower Cretaceous in age, are the two major coal-bearing formations in the Peace River coalfield in northeast BC. The formations outcrop extensively throughout the coalfield (Figure 2). Coal seams of economic interest in the Gates Formation occur exclusively south of the Sukunka River (Figure 2), and in the Gething Formation, mainly north of the Sukunka River.

The Gething Formation overlies the Cadomin Formation (Table 3), therefore it is slightly younger than the Mist Mountain Formation, which underlies the Cadomin in the southeast BC coalfields (Table 4). The Gething Formation samples were collected from the Willow Creek property, located on the south side of the Pine River about 40 km

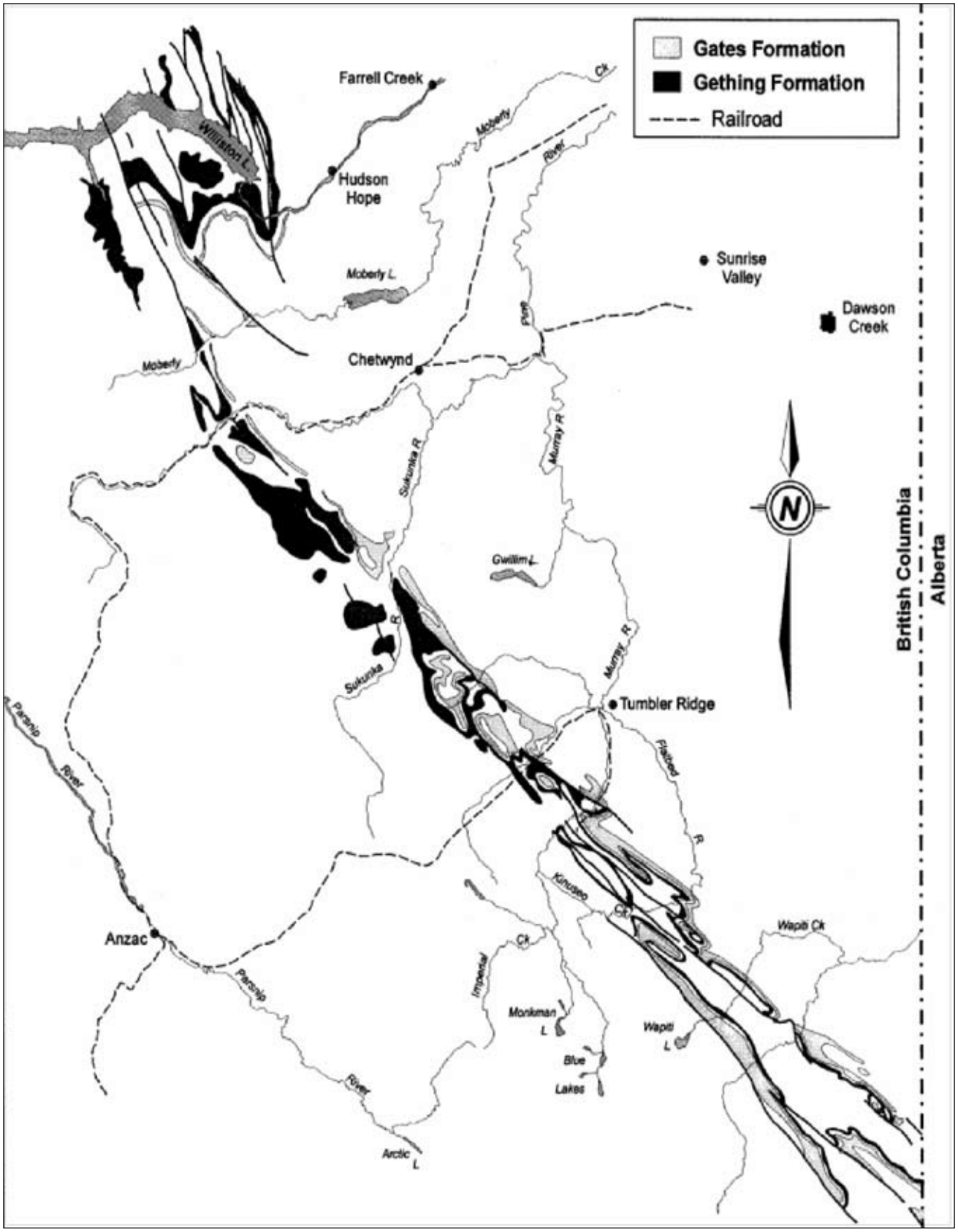

Figure 2. Outcrop pattern of the Gething and Gates Formations in the Peace River coalfield.

TABLE 3. GENERALIZED LOWER CRETACEOUS STRATIGRAPHY.

Pine River Area.			metres
Jurassic to lower Cretaceous	FORT ST JOHNS GROUP	CRUISER FORMATION marine shale	115
		GOODRICH FORMATION fine grained sandstone and shale	350
		HASLAR FORMATION marine shale	260
		BOULDER CREEK FORMATION sandstone and conglomerates	150
		HULCROSS FORMATION grey marine shale	100
		GATES FORMATION non marine sandstones and coal seams	110
		MOOSEBAR FORMATION marine shale	250
	BULLHEAD GROUP	GETHING FORMATION non marine sediments and coal	500
		CADOMIN FORMATION conglomerates	150

west of Chetwynd (Figure 2). The Pine Valley Mining Corporation plans to initiate mining in the formation at Willow Creek and has excavated a test pit. In this area, the Gething Formation has eight coal seams ranging in thickness from 1 to over 5 m and numbered from 1 downwards from the top of the formation. Six samples were collected from Seam 7-0 (Figure 3). The samples were collected from various locations in the seam, with the intention of representing a wide range of maceral composition. Samples were collected in the same area as the samples used in a previous methane adsorption study (Ryan and Lane, 2002).

The younger Gates Formation is separated from the older Gething Formation by the marine Moosebar Formation (Table 3). The formation hosts two major coalmines, both now closed. Western Canadian Coal Corporation proposes to renew mining in the formation. There are some CH_4 adsorption data available for the formation (Lamberson and Bustin, 1993) but no published CO_2 isotherm data. Samples of Gates Formation coal (B Seam) were collected from the Bullmoose Mine and from the Western Canadian Coal Corporation property (J Seam). Coal in the Gates Formation is generally restricted to 4 zones that are numbered from A counting up section to D. However, convention at the Quintette Mine and properties in the vicinity is to number the basal seam as K and with letters decreasing up section. Consequently B Seam at Bullmoose and J Seam in the Quintette area occupy similar stratigraphic levels in the Gates Formation.

The Mist Mountain Formation of Upper Jurassic to Lower Cretaceous age (Table 4) outcrops extensively in the Elk Valley and Crowsnest coalfields. The coal geology of the Elk Valley coalfield is summarized by Grieve (1993) and, to a lesser extent, Ryan (2003) has summarized the CBM potential of the Crowsnest coalfield. Both these publications list many other useful references. EnCana has drilled 17 CBM holes in the Elk Valley coalfield and at the moment is operating two pilots. As a consequence there exists a lot of CH_4 and CO_2 isotherm data, which are not yet public. Dawson *et al.* (2000) have summarized public data available for the two coalfields. In this study, Dave Endicott and Pat Gilmar (Elkview coal mine) provided a sample of the basal seam (10 Seam) from the Mist Mountain Formation.

On Vancouver Island, Upper Cretaceous coals occur in the older Comox Formation in the Comox Coal Basin and in the younger Protection and Extension Formations in the Nanaimo Coal Basin. There are four seams in the Comox Formation; unfortunately, some papers number the seams from 1 at the base, counting up to 4 at the top, and some papers start at 4 at the base, counting down to 1 at the top. The Quinsam mine extracts coal from two seams in the Comox Formation, the basal (1 Seam) and the third seam up section (3 Seam). Steve Gardner (chief geologist, Quinsam coal mine) provided samples of 1 Seam and 3 Seam.

There are a number of Tertiary coal basins in British Columbia; however, it is difficult to get fresh samples. John Hodgins of Connaught Energy provided a drill core sample from the Princeton Coal Basin. Four coal zones are contained in the Allenby Formation; the sample was collected from the lowest zone, designated as the Black-Jack, Princeton, or Blue Flame zone.

TABLE 4. GENERALIZED JURASSIC-CRETACEOUS STRATIGRAPHY, EAST KOOTENAYS .

LOWER CRETACEOUS	CADOMIN FORMATION		
JURASSIC AND CRETACEOUS	KOOTENAY GROUP	ELK FORMATION minor coal	
		MIST MOUNTAIN FORMATION coal seams	
		MORRISSEY FORMATION	MOOSE MOUNTAIN MEMBER
			WEARY RIDGE MEMBER
JURASSIC	FERNIE FORMATION	PASSAGE BEDS	

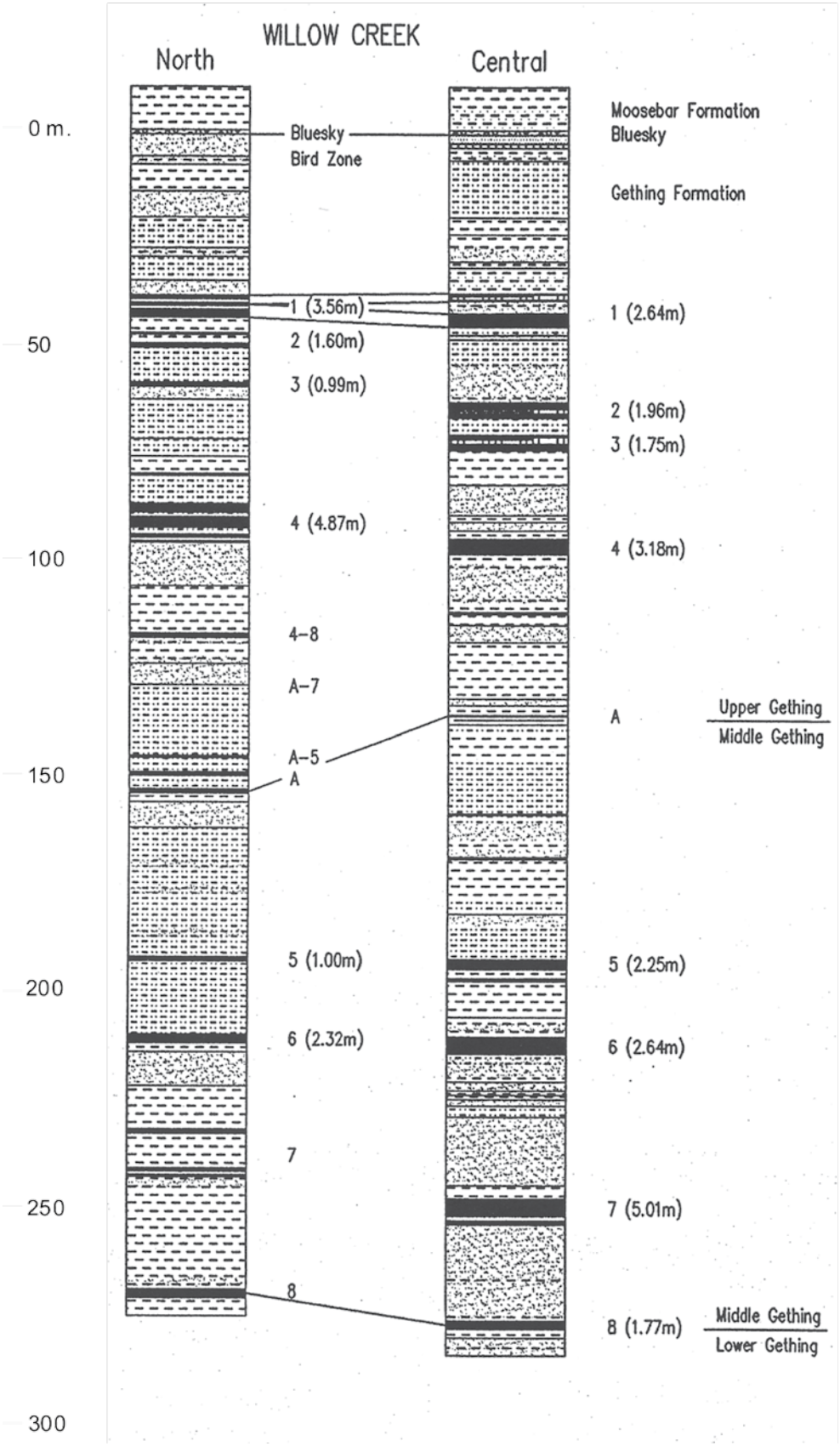

Figure 3. Stratigraphic section of the Gething Formation at the Willow Creek property (P.C. Kevin James).

SAMPLE PETROGRAPHY AND RANK

Karst and White (1979), Kalkreuth and McMechan (1988), Kalkreuth et al. (1989), and Marchioni and Kalkreuth (1992) have all discussed coal rank in the Gething Formation. Rank varies from semianthracite to high-volatile bituminous. Along the outcrop belt in the foothills, the rank is high, in places reaching semianthracite. To the north and east it decreases to high-volatile bituminous. There is some evidence that outcrops at the western outcrop edge of the formation have lower ranks. Rank was established prior to deformation and variations are related to changes in the thickness of the collective Gething and post-Gething sedimentary package (Leckie, 1983).

The rank at Willow Creek, where the samples were collected, ranges from medium- to low-volatile bituminous. The rank of the 7-Seam samples is low-volatile bituminous; Rmax = 1.64% (Table 5). Ryan (1997) and Ryan and Lane (2002) discuss the petrography of Gething Formation coal. Coal from the formation is characterized by variable reactives content and often low ash concentrations, which make it ideal for providing samples for studies investigating the influence of maceral content on adsorption of various gases. Reactive maceral contents range from approximately 80% to less than 50%. Samples (Table 5) have a high collodetrinte content, which contains fragments of non-structured inert macerals such as macrinite and inertodetrinite. Structured macerals, such as semifusinite and fusinite, are less common. Generally, compared to coals from the Mist Mountain Formation, there is less fusinite and semifusinite and consequently less preserved cell structure; this limits the possible content of dispersed mineral matter, which often fills cell lumen in these macerals. Some of the collotelinite contains the eye-shaped slits characteristic of pseudovitrinite, the origin of which is discussed by Ryan (2002).

The petrography of the three Gates Formation samples (Table 5) is similar to that of the Gething Formation samples, though the rank is lower (1.06% and 1.23%). The samples contain liptinite that is not present in the Gething samples, but they do contain pseudovitrinite that appears to be characteristic of most samples from the two formations collected from surface and at depth in drill holes. Lamberson et al. (1991) emphasize the importance of fires in forming inertinite in Gates coals. There is no obvious explanation for the variable and sometimes high content of inertinite in Gething coals. Gething coal swamps may have experienced more episodes of drying and a greater frequency of forest fires than did Gates swamps.

Grieve (1993) and others have studied the petrography of seams from the Mist Mountain. Rank varies from high-

TABLE 5. PETROGRAPHY AND MEAN MAXIMUM REFLECTANCE OF SAMPLES ANALYZED FOR CO_2 ISOTHERMS.

Data as volume percent	telinite	collo telinite	collo detrinite	vitro detrinite	liptinite	pseudo Vitrinite	semi fusinite	fusinite	macrinite	micrinite	inerto detrinite	mineral matter	Rmax %	total reactives	total inerts	TR mmfb
			Gething Formation													
7 seam -7	0	43	38	0	0	0	8	0	5	0	5	2	1.64	81	17	82
-2	0	37	52	0	0	0	1	0	0	0	3	6	1.64	90	4	96
-4	0	5	26	0	0	0	41	0	10	1	11	6	1.64	32	63	34
-3	0	3	28	0	0	0	34	0	17	1	14	2	1.64	31	67	31
-8	0	5	37	0	0	0	27	1	14	0	14	3	1.64	42	56	43
-5	0	14	39	0	0	0	35	0	3	0	5	3	1.64	53	44	55
			Gates Formation													
B seam fine	2	10	31	0	3	0	24	0	12	0	14	4	1.06	45	51	47
B seam coarse	0	3	32	0	3	0	30	0	10	0	16	5	1.06	39	57	41
J seam	0	26	26	1	0	0	18	0	5	0	8	16	1.23	53	31	63
			Mist Mountain Formation													
10 seam	0	20	25	1	0	0	26	0	6	0	8	13	1.28	46	41	53
			Comox Formation													
Quinsam 1 seam	5	18	47	0	5	1	9	0	2	0	6	9	0.68	75	17	82
Quinsam 3 seam	6	21	44	1	4	1	10	0	2	0	6	5	0.71	78	18	81
			Allenby													
Black-jack zone	1	21	57	0	7	0	0	0	0	0	0	14	0.70	85	0	100

volatile bituminous to low-volatile bituminous. Generally, seams are characterized by variable and higher inert maceral contents than are Carboniferous coals and are similar to Permian coals from Australia. They are similar in many aspects to coals in the Gething and Gates Formations, though they tend to contain more semifusinite and less macrinite than these formations. One of the more conspicuous differences is the near absence of pseudovitrinite.

The Upper Cretaceous coals on Vancouver Island are generally sub-bituminous to high-volatile A bituminous in rank. They are characterized by high vitrinite contents with moderate contents of liptinite and minor amounts of semifusinite. Psuedovitrinite is present but not common. They are less deformed than the coals in the Rocky Mountain foothills and often well cleated, though sometimes the seams low in the section have carbonate coating on cleat surfaces.

There are a number of Tertiary coal deposits varying in size from Hat Creek, which could contain 30 billion tonnes of lignite and higher-rank coals, to Coal River, which may contain about 100 million tonnes of lignite. Coal rank varies from lignite at Coal River to medium-volatile bituminous at Seaton, near the town of Smithers. Most of the Tertiary coals are sub-bituminous to high-volatile C bituminous. Coals in the Princeton Basin are sub-bituminous (Rmax = 0.7%; Table 5) and characterized by a very high percentage of vitrinite, with minor amounts of liptinite. Mineral matter is finely dispersed in the vitrinite.

SAMPLE DATA

Fifteen samples were submitted for CO_2 isotherm analysis (Table 6). The ash contents of the samples range from 1% to 20% and are generally low. Moisture contents are in the range of 2.5% to 12% and generally decrease as rank increases. The exception is the J-Seam sample, which was collected from an exploration outcrop and probably contains some oxidation. Most of the samples were analyzed at 25°C, but two were also run at 30°C. The Langmuir volumes (dry ash-free [daf] basis) range from 34 to 58 cm^3/g, though these values should not be taken as representative of the samples' adsorption ability, because at pressures over about 7.4 MPa, CO_2 is not a gas. Langmuir pressures for samples analyzed at 25°C range from 1.1 to 2.6 MPa, with a tendency to decrease as coal rank increases. The Langmuir pressures increase as temperatures of the isotherms increase.

CARBON DIOXIDE PHASE DIAGRAM AND CO_2 ADSORPTION POTENTIAL

The CO_2 phase diagram is well documented in terms of the boundaries between liquid, solid, and gas fields (Figure 4). However, the boundary between the gas and supercritical fluid fields at high temperatures and moderate pressures is less well defined and is probably represented by a zone. It is therefore difficult to determine the maximum depth at which coal can sequester CO_2 by adsorption in conditions where there is a high geothermal gradient. Figure 4 assumes that the supercritical fluid is separated from gas by a horizontal line, implying no temperature sensitivity; in fact the line should probably have a negative slope.

The vertical axis of Figure 4 is pressure, and consequently, to plot a depth tract for a stratigraphic section onto the figure one must have both temperature and pressure gradients. Once this is done, the point at which the depth tract crosses the gas-liquid or gas-critical fluid phase lines can be determined. The pressure at this point is then converted to a depth, based on the pressure gradient, and this is the maximum depth for CO_2 sequestration by adsorption on coal. By selecting a number of geothermal and pressure gradient pairs, it is possible to construct a diagram (Figure

TABLE 6. CO_2 ISOTHERM ANALYSIS RESULTS.

	as received		dry ash free						
	AR Lang Vol (cc/g)	AR Lang Pres (Mpa)	DAF Lang Vol(cc/g)	DAF Lang Pres (Mpa)	temperature (°C)	Ash (%)	as received moisture (%)	SG	Rmax
Gething									
7 seam -7	45.56	1.34	48.49	1.34	30	2.7	3.31	1.339	1.64
-7	48.15	1.23	51.25	1.23	25	2.7	3.31	1.345	1.64
-2	50.54	1.48	55.59	1.48	25	6.2	2.83	1.382	1.64
-4	54.66	1.27	57.49	1.27	25	1.1	3.85	1.338	1.64
-3	50.02	1.44	53.33	1.44	25	2.5	3.69	1.369	1.64
-8	51.95	1.44	55.69	1.44	25	2.9	3.88	1.369	1.64
-5	47.31	1.35	49.81	1.35	25	1.3	3.76	1.359	1.64
Gates									
B seam fine	31.14	1.15	34.45	1.15	25	6.9	2.74	1.370	1.06
B seam coarse	31.60	1.28	35.09	1.28	25	7.5	2.48	1.407	1.06
J seam	23.58	2.45	34.28	2.45	25	20.4	10.77	1.528	1.23
Mist Mountain									
10 seam	28.17	2.04	35.28	2.04	25	17.8	2.37	1.468	1.28
Comox									
Quinsam 1 seam	41.80	4.27	48.99	4.27	30	8.4	6.28	1.466	0.68
Quinsam 1 seam	31.40	1.32	36.80	1.32	25	8.4	6.28	1.444	0.68
Quinsam 3 seam	40.35	2.61	47.12	2.61	25	8.5	5.92	1.375	0.71
Allenby									
Black-jack zone	44.44	4.65	55.98	4.65	25	8.5	12.15	1.351	0.7

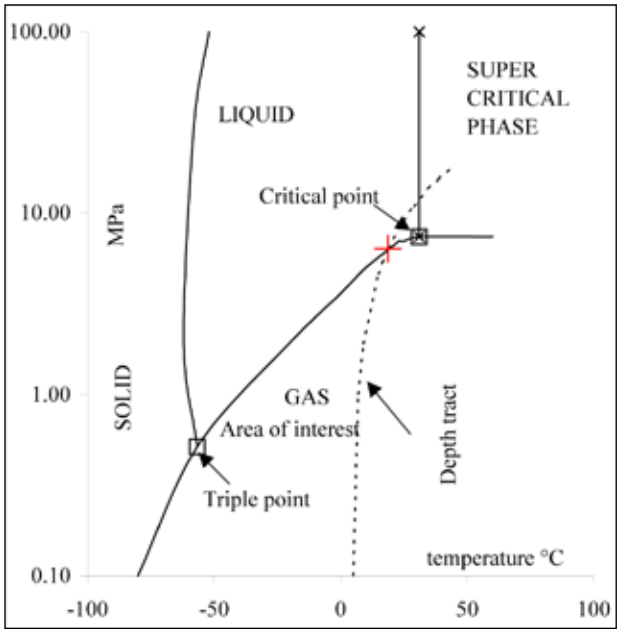

Figure 4. Carbon dioxide phase diagram.

5) in which the *x* axis is the pressure gradient and the *y* axis is the geothermal gradient and the contour lines represent the approximate maximum depths for sequestration by adsorption.

The area probably occupied by pressure and temperature gradients in BC coal basins is plotted into Figure 5, based on geothermal gradients for various coalfields in BC (Table 7). Generally, temperature data are available for holes drilled for oil and gas exploration. Often this is bottom hole temperature, so that an average temperature gradient is calculated assuming that the single temperature value is representative. Temperature gradients range from 18°C/km to 36°C/km; this compares to gradients in the Black Warrior Basin that range from 11°C/km to 22°C/km (Pashin and McIntyre, 2003). Pressure gradient information is not readily available from drill holes. If there is a normal hydrostatic gradient, the pressure gradient varies slightly based on the salinity of the water and will increase from 0.009818 MPa/m for fresh water to 0.00984 MPa/m for water with 3000 mg/L total dissolved solids. In a lot of sedimentary basins, normal hydrostatic gradients do not apply. Gradients in parts of the Western Canadian Sedimentary Basin are as low as 0.005 MPa/m. In the Black Warrior Basin, gradients range from normal (.00984 MPa/m to as low as 0.004 MPa/m and lower [Pashin and McIntyre, 2003]). In areas of complex structure such as northeast British Columbia, there can be considerable overpressuring, and hydrostatic pressure gradients can approach lithostatic gradients of 0.2 MPa/m or more.

The maximum depth of sequestration is estimated using the contour lines in Figure 5. The effect of the temperature gradient is minimal for low pressure gradients, though it increases as pressure gradients increase. The depth tract depends on the interrelationship of geothermal and pressure gradients, and the depth at which CO2 becomes supercritical or liquid can vary from about 400 m to over 1000 m. At shallow depths, conditions are defined by a low geothermal gradient matched to a high pressure gradient. At maximum depths, conditions are defined by a high geothermal gradient and low pressure gradient. These conditions may allow for adsorption of CO2 at greater depth, but the increased temperature will greatly reduce the ability of coal to adsorb any gas. The window for potential CO2 sequestration is probably below 200 m and above a depth defined in part by the CO2 phase diagram.

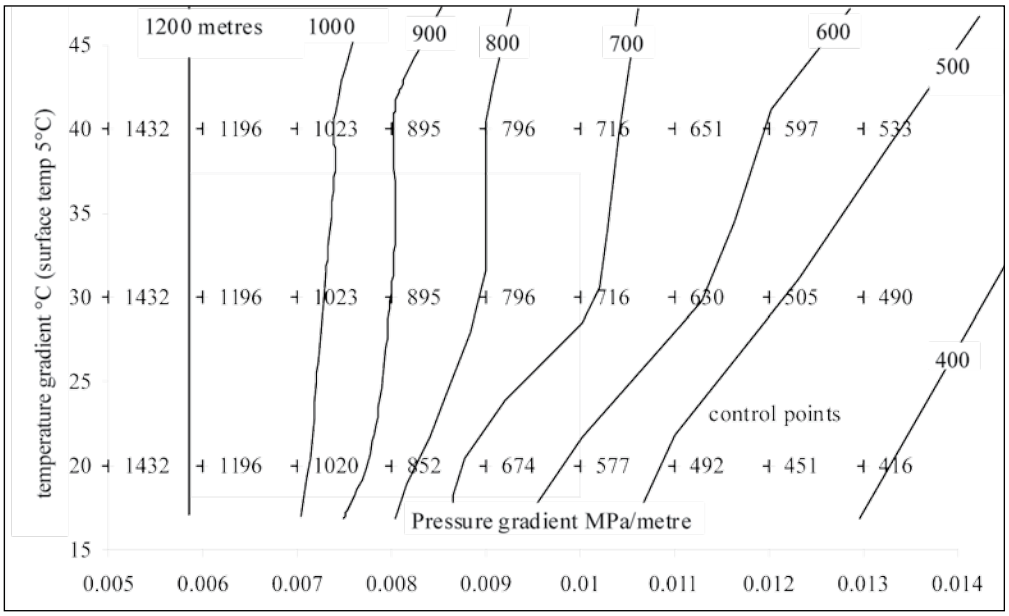

Figure 5. Diagram illustrating the approximate relationship between temperature and pressure gradients and the depth to the liquid or critical fluid fields for carbon dioxide.

TABLE 7. TEMPERATURE GRADIENTS IN COAL BASINS IN BRITISH COLUMBIA.

Region	local area	Surface temperature	gradient C /Km
SW BC	Comox	7	20.8
SW BC	Naniamo	7	27.5
SW BC	Naniamo	7	28.3
SW BC	Naniamo	7	23.3
SW BC	Naniamo	7	22.1
SE BC	Crowsnest area	8	25.4
SE BC	Crowsnest area	8	20.5
SE BC	Crowsnest area	8	18
SE BC	Elk Valley	8	23.6
SE BC	Elk Valley	8	36.2
NE BC	Bullmoose area	4	23.1
NE BC	Bullmoose area	4	30.2
NE BC	Bullmoose area	4	31.5
NE BC	Grizzly area	5	26
NE BC	Grizzly area	5	25.7
NE BC	Willow Creek	5	25.6
NE BC	Hudson Hope	5	30
NE BC	Hudson Hope	5	28.6
NE BC	Hudson Hope	5	36.4
NE BC	Hudson Hope	5	22.8

CARBON DIOXIDE AS A FREE GAS OR IN SOLUTION IN WATER OR AS A SUPER-CRITICAL FLUID

When CO_2 is injected into seams, some of the CO_2 goes into solution in the water associated with the coal. Water associated with coal occurs in three forms, defined in different ways and given different names. In simple terms, the three forms may be referred to as free and mobile water in fractures, surface water loosely bound to coal surfaces, and structural water, which forms part of the coal structure. Surface water is the difference between equilibrium moisture and inherent moisture. The amount of surface water depends on rank (Figure 6) and on the amount of porosity. The amount of CO_2 that can be held in solution in water therefore depends on rank, porosity, and temperature and pressure conditions. The solubility of CO_2 in water increases with pressure but decreases with temperature. There are numerous sources of data describing CO_2 solubility; unfortunately, there are as many combinations of units as there are

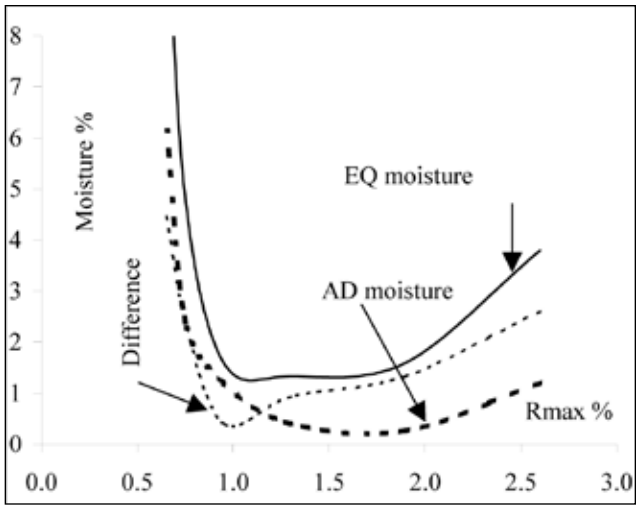

Figure 6. Air-dried, equilibrium, and free water versus rank

examples of CO_2 solubility plots. The plots (Figure 7) are adapted from Jarrell (2002) and Rightmire (1984). Based on the interplay of geothermal and temperature gradients, the amount of CO_2 held in solution ranges from about 25 to 35 m^3 gas in solution in 1 m^3 water. The actual amount held in 1 tonne of coal depends on rank and water-filled porosity. For low-rank coals, the amount of CO_2 in solution can range up to 8 cm^3/g, and for higher-rank coals probably is not more than 1 cm^3/g.

Below the critical point, CO_2 is contained in the coal by adsorption, in part by solution in the interstitial water and as free gas. The amount of CO_2 held in a free-gas phase can be estimated from the ideal gas law and ranges up to about 8 cm^3/g for 15% gas-filled porosity at a depth less than that equivalent to the critical point (Figure 8). Obviously the amount held by adsorption is much greater than that held in solution or as free gas for all ranks of coal.

The density of CO_2 gas as it approaches critical conditions is about 0.15 g/cm^3. Once CO_2 enters the supercritical phase, the density increases rapidly to about 0.7 g/cm^3 (Figure 9) and maintains this value as pressure and temperature increase as predicted by normal hydrostatic and geothermal gradients. Density tends to stay in a narrow range above the critical point because of the opposing effects of increasing pressure and increasing temperature. The rapid change in density as conditions approach the critical point makes it very difficult to determine the adsorption characteristics of CO_2 at temperatures approaching critical conditions.

GENERAL COMMENTS REGARDING ADSORPTION OF CO_2 ON COAL

As pressure increases, CO_2 becomes a liquid or a supercritical fluid as indicated by the CO_2 phase diagram (Figure 4). The diagram indicates the limited pressure-temperature

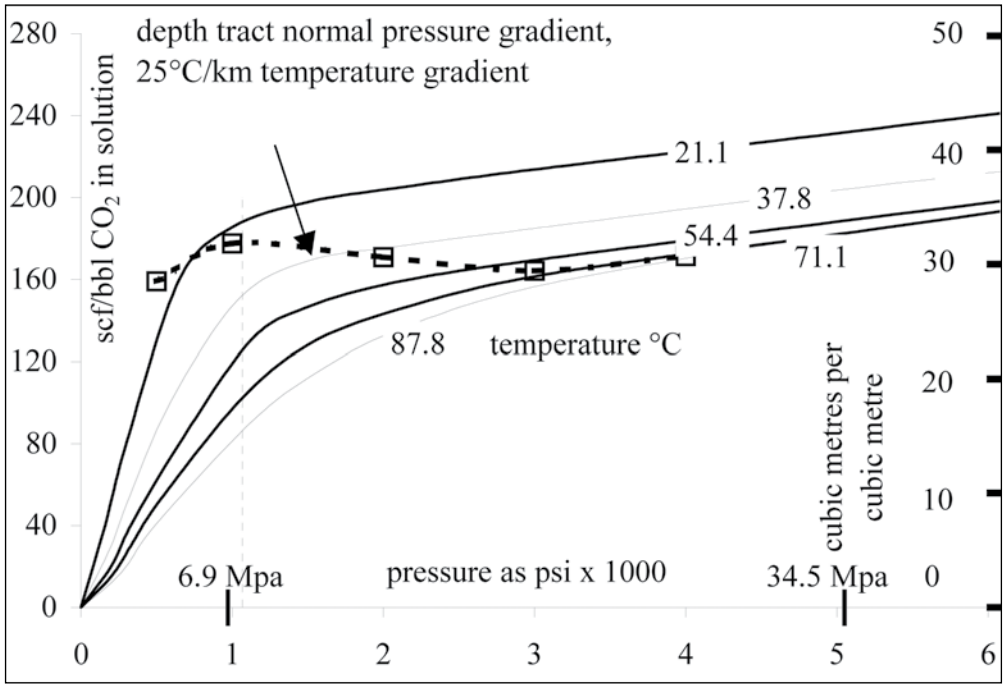

Figure 7. Plots of CO_2 solubility versus depth and temperature; data from Jarell et al. (2002) and Rightmire (1984).

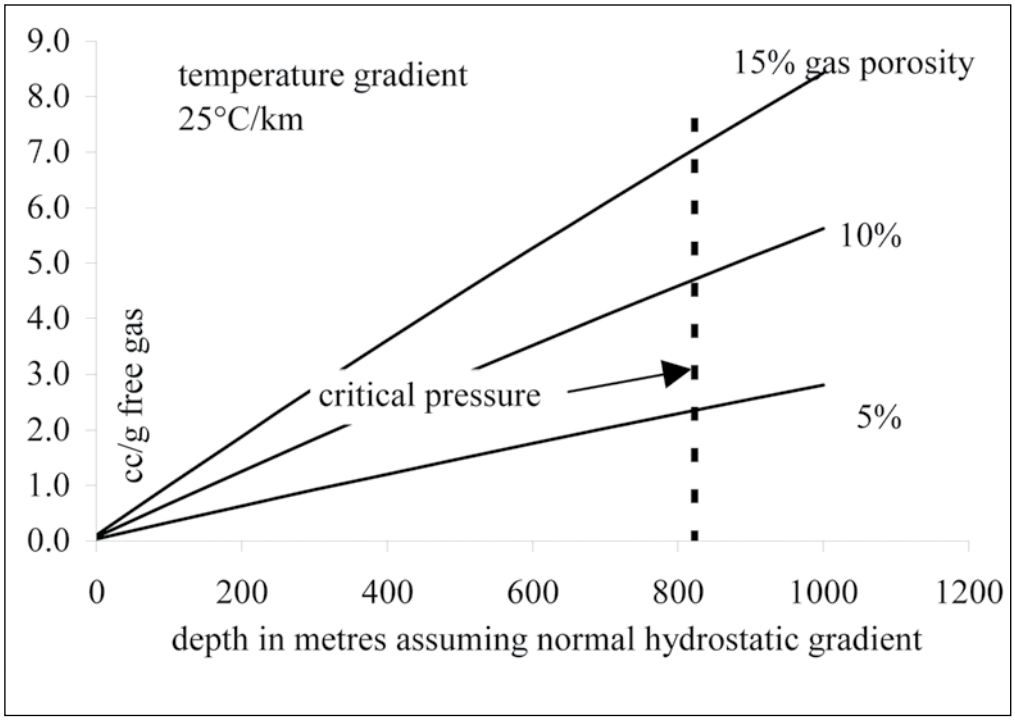

Figure 8. Potential free gas based on porosity assuming a normal hydrostatic gradient and a geothermal gradient of 25°C.

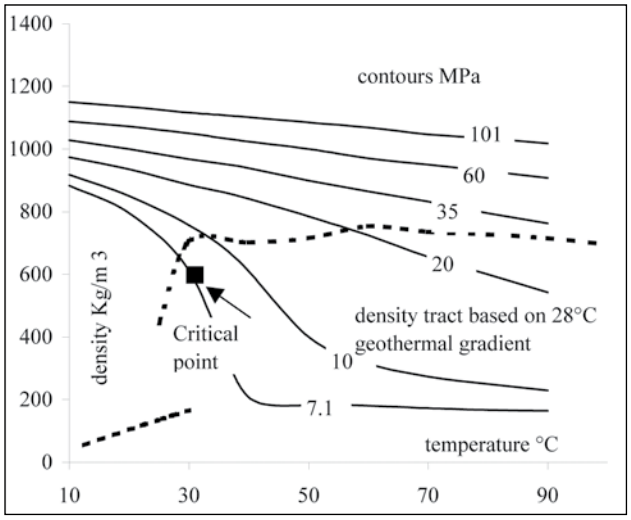

Figure 9. Density of CO_2 as a gas and in the supercritical phase; plots adapted from Bachu and Stewart (2002) and Pruess *et al.* (2001).

field in which CO_2 is a gas and therefore, based on pressure and temperature gradients, defines the depth range through which CO_2 can be sequestered by adsorption. The diagram is for pure CO_2; the addition of other gases will change the field boundaries, probably increasing the size of the gas field in terms of pressure. This is important because it may not always be cost effective to obtain a pure CO_2 gas for injection.

It is not reasonable to consider the Langmuir volume (adsorbed volume at infinite pressure) as a measure of the CO_2 adsorption ability of a sample, because CO_2 becomes a supercritical fluid at quite low pressures. It is therefore best to compare the adsorption of CO_2 at a fixed depth and not at infinite pressure. In this study isotherms were run at 25°C and 30°C, temperatures typically seen at depths of 600 to 900 m in sedimentary basins in BC. The temperature at which isotherms are run combined with temperature and pressure gradients in an area combine to provide the specific depth at which the isotherm is predicting real gas contents. Adsorption data from a number of isotherms should be compared based on calculated gas contents at this depth.

Some of the earliest investigations of the CO_2 adsorption capacity of coal were conducted by Ettinger *et al.* (1966). They recognized the stronger adsorption of CO_2 than of CH_4 onto coal and suggested that the relative adsorption of gases such as H_2S, CO_2, CH_4, N_2, and H_2O is related to their liquefaction temperature. They also pointed out that there is an increased danger of mine outbursts when coals contain a higher proportion of adsorbed CO_2. Levy *et al.* (1997) documented the difference in Langmuir volumes for nitrogen, methane, and carbon dioxide for isotherms measured on moist coal at 30°C. Working with Bowen Basin coals covering a rank range of high-volatile bituminous to low-volatile bituminous, Levy *et al.* (1997) found that the CO_2/CH_4 molar ratio for adsorbed gases decreased consistently from 1.82 to 1.37 as rank increased. They suggest that the greater adsorption of CO_2 is probably related to the increased polar nature of the molecule compared to CH_4 (Levy *et al.,* 1997).

Krooss *et al.* (2001) studied the adsorption behaviour of CO_2 at high pressures and temperatures, in part above the critical point. They discussed the difficulty of interpreting experimental results above the critical point. The density of the adsorbed phase and of the phase occupying the void in the canister are both difficult to determine. They assumed a density of 1.028 g/cm^3 for the adsorbed CO_2. In addition, the coal probably swells, which makes it even harder to correct for the component of CO_2 that is not adsorbed. Adsorption experiments do not generally confine the coal, because it is loosely packed as fine grains, and therefore they do not model the competing effects of matrix swelling and adsorption that occur in nature. In general, the results of Krooss *et al.* (2001) conform to Langmuir adsorption below the critical point, but above pressures of about 6 MPa (similar to the critical point pressure 7.47 MPa), results are inconsistent with normal adsorption. Even after data are corrected for the assumed volume of the adsorbed phase using a density of 1.028 g/cm^3, adsorption is negative. This probably indicates swelling of the coal and use of an overly large void space in the canister to correct for the non-adsorbed CO_2 phase. As Krooss *et al.* (2001) state, it is difficult to interpret the results above the critical point and even more difficult to predict what they might mean for a seam at depth.

Larsen (2004) documented the solution of CO_2 in coal over a wide range of pressure and temperature conditions extending below the critical point. Solution of CO_2 causes coal to expand but also increases the plasticity of coal. These two effects are potentially devastating to the permeability needed to inject CO_2 into coal. The amount of CO_2 dissolved in coal increases as pressure increases and as rank decreases. At pressures equivalent to depths of 150 to 200 m, about half the CO_2 contained in medium- or low-rank coals is in solution (Reucroft and Sethurarman, 1987). The softening temperature of coal appears to decrease to about 31ºC at the critical pressure (Figure 10), implying that the coal becomes a plastic solid above critical conditions of temperature and pressure.

The stronger adsorption of CO_2 affects the relative rate of desorption of CO_2 relative to CH_4, and the CO_2 content of produced gases generally increases over time. The effect is predicted by the extended Langmuir equation (Arri *et al*., 1992).

INFLUENCE OF RANK AND PETROGRAPHY ON CO_2 ADSORPTION

Adsorption of methane tends to increase as rank increases, initially rapidly and then more slowly at high ranks, though the relationship of adsorption to rank for medium-

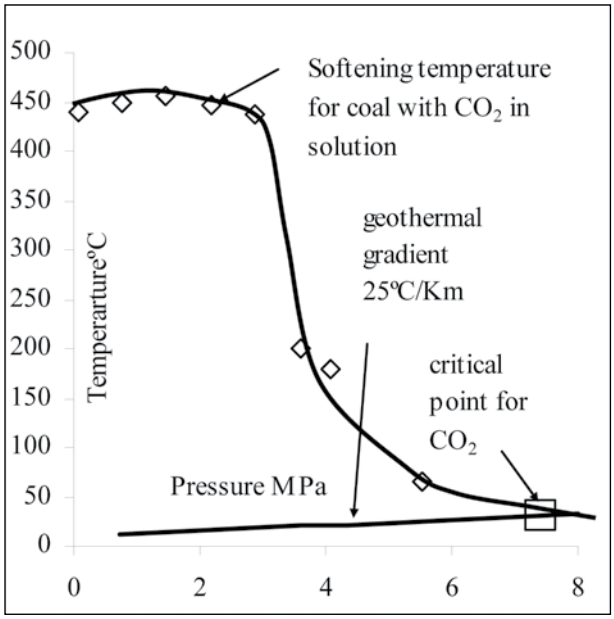

Figure 10. Softening temperature of Lower Kittanning coal (89.6% C, dry ash-free) at increasing pressure; plot adapted from Khan and Jenkins (1985) in Larsen (2004).

volatile coals is less well defined. For example, coals from the Bowen Basin (Levy *et al*., 1997) have higher adsorption capacities than coals of similar rank from the US (Levy *et al.,* 1997). Some of the variation may be caused by variable maceral content in the samples. Despite the fact that many diagrams (Ryan, 1992) imply a consistent relationship between rank and adsorption ability for CH_4, the reality is much more complicated.

Carbon dioxide adsorption capacity has a weak correlation with rank, increasing at high rank, but there are indications that adsorption is higher for lignite and sub-bituminous coals than it is for bituminous coals. This is hinted at in the data from Gluskoter *et al.* (2003) and from data in this study (Figure 11). Volume data from Gluskoter *et al.* are plotted at 300 psi and as standard cubic feet per ton (scf/t, dry ash-free [daf] basis) so that data from this study (Figure 11) are recalculated to the same pressure. Gluskoter *et al.* (2003) do not specifically identify rank by reflectance so that some assumptions are made in incorporating their data into Figure 11. However, it is obvious that both data sets imply higher adsorption for low- and high-rank coals than for medium-rank coals. The present data set was generated at 25°C. The temperature of the Gluskoter *et al.* data set is not stated.

The adsorption behaviour of CO_2 at low rank is different from that of CH_4, and this probably relates both to the distribution of micro-, meso-, and macroporosity by rank and to the stronger polarity of the CO_2 molecule compared to the CH_4 molecule. Rightmire (1984), Bustin and Clarkson (1999), and Levine (1993) have all summarized the distribution of porosity in coal (Figure 12). Total po-

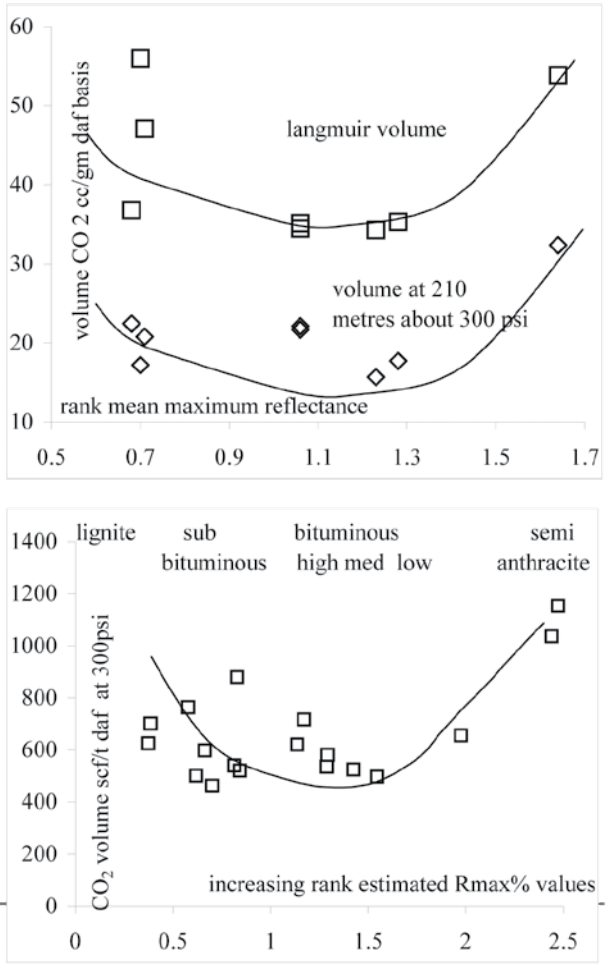

Figure 11. Carbon dioxide adsorption versus rank. Data from this study and from Gluskoter et al. (2002).

rosity is a minimum for medium-volatile rank coals, and macroporosity decreases as rank increases. At low ranks, the increased mesoporosity allows CO_2 to adsorb, possibly as a volume filling in meso-sized pores, whereas CH_4 with lower polarity forms layer adsorption in micropores. The selectivity of CO_2 over CH_4 is high, and the amount of CO_2 adsorbed high, despite low rank. As rank increases, the amount of mesoporosity decreases, CO_2 adsorption decreases, and CH_4 adsorption increases. Consequently the selectivity for CO_2 decreases. At high rank, the increase in microporosity causes increases in the adsorption of both CO_2 and CH_4 without a major increase in the selectivity for CO_2. Determining the effective porosity distribution in coals is difficult because experiments are often not done on moisture-equilibrated coal at in situ pressures. Also, the structure of low-rank coals is less predictable than that of higher-rank coals, and this results in a wider variation of porosity distribution. It is therefore hard to predict the CO_2 and CH_4 adsorption characteristics of low-rank coals.

The selectivity of CO_2 versus CH_4 of coals decreases as rank increases but may increase again at high ranks. Data

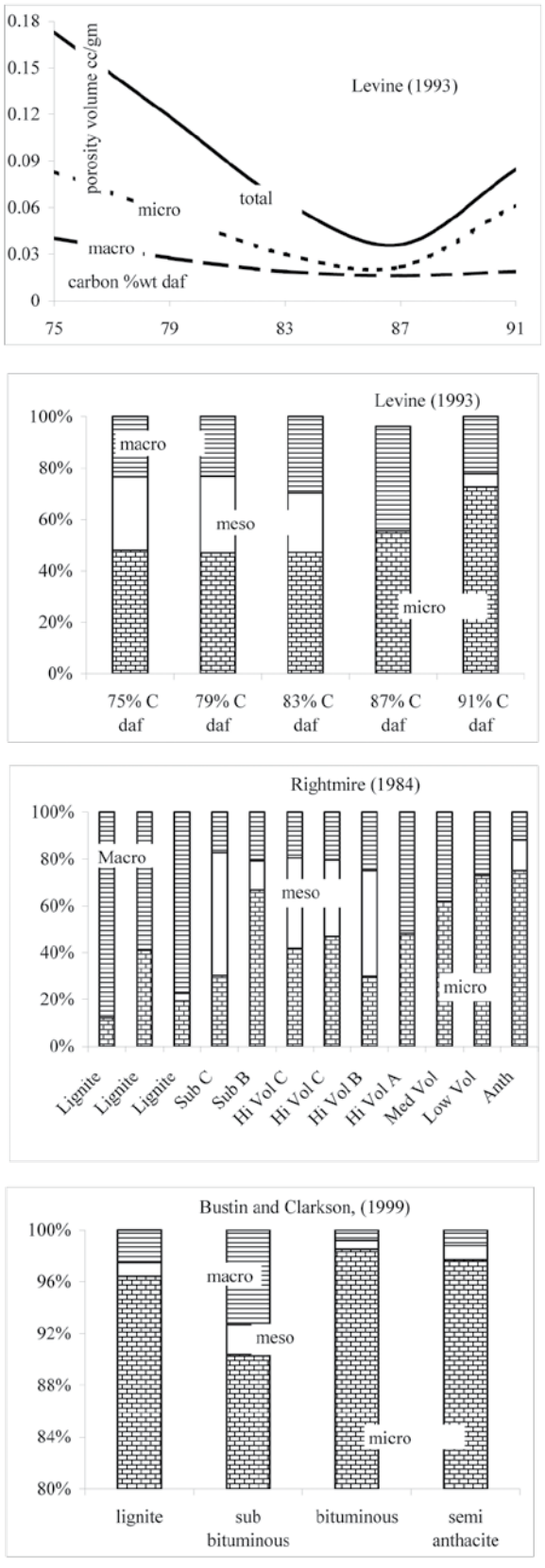

Figure 12. Distribution of porosity in coal data; adapted from Rightmire (1984), Bustin and Clarkson (1999), and Levine (1993).

from this study include only CO_2 isotherms, but in most cases CH_4 isotherms exist for the coals from previous studies, so that it is possible to construct an approximate plot of CO_2/CH_4 ratio versus rank (Figure 13). Ratios in Figure 13 are calculated at a pressure of 300 psi to conform to the data from Gluskoter *et al.* (2003), which is also reproduced in Figure 13. The ratio is very high (approaching 20) for low-rank coals and then decreases to a range of 1.5 to 2 for medium-rank coals. It might increase slightly in high-rank coals. For coals of all ranks, the volume ratio of CO_2/CH_4 decreases as pressure increases (Gluskoter *et al.,* 2003) and probably also as temperature increases.

It is important to recognize the difference between molecule-for-molecule replacement and weight-for-weight replacement when comparing the adsorption capacity of CO_2 and CH_4. If there is a one-for-one molecule replacement, then 2.75 g of CO_2 will replace 1 g of CH_4 (the ratio of the molecular weights). In terms of greenhouses gases, one is interested in sequestering a weight of CO_2, not a volume. The increased selectivity and adsorption of low-rank coals may make them better candidates for CO_2 sequestration than higher-rank coals.

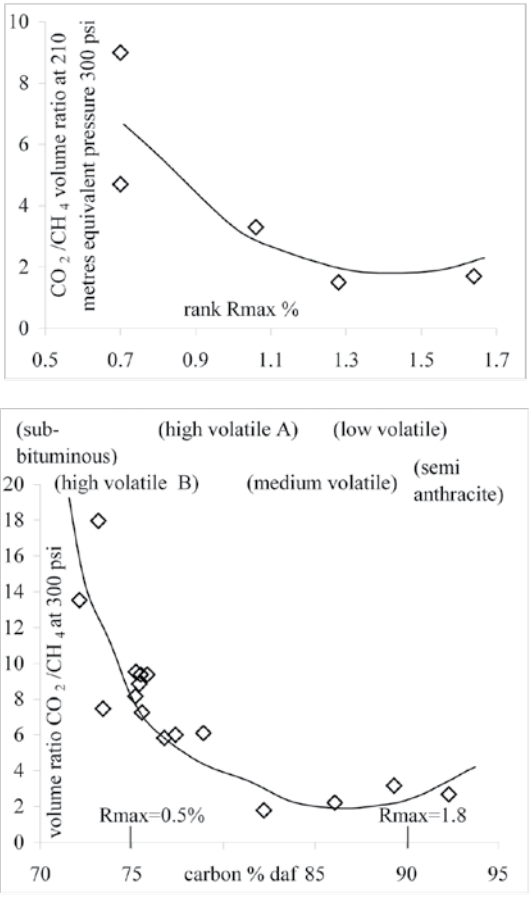

Figure 13. Plot of CO_2/CH_4 ratio (calculated at 210 m equivalent pressure) versus rank. Data from this study from Gluskoter *et al.* (2003).

This of course assumes that they are not already saturated with CO_2. Low-rank coals have better diffusivity and should maintain permeability and accommodate matrix swelling better than do higher-rank coals.

Macerals are not minerals and do not have defined crystal structures like minerals. However there are generalizations that hold about the different characteristics of macerals. Inert macerals have more mesoporosity and less microporosity than do reactive macerals (Harris and Yust, 1976; Gan *et al.,* 1972). At constant rank, the effect of petrography on methane adsorption has been studied by a number of authors (Ryan and Lane, 2002; Lamberson and Bustin, 1993). Either there is no correlation or adsorption ability tends to increase as the percentage of reactive macerals increases. These studies were done on medium- or low-volatile coals. In British Columbia, many of the Tertiary low-rank coals are composed, on a mineral-matter-free basis, of almost 100% reactive macerals, making it difficult (and less relevant) to study the effects of petrography on the adsorption characteristics of low-rank coals.

Studies of the maceral influence on the adsorption of CO_2 are more limited. Gluskoter *et al.* (2002) presented data that indicate no correlation between inert maceral content and adsorption of CO_2 for a range of 0% to 25% inerts in low-rank coals. In this study, a number of samples with a rank of 1.64% and varying petrography were analyzed (Table 5), as were two samples (rank 1.06%) with somewhat different petrography. These were actually the same sample screened to different sizes to provide a partial concentration of vitrinite. The Gething Formation samples with Rmax of 1.64% (Figure 14) are plotted on a total reactives versus gas plot, with the CO_2 gas contents plotted as gas contents at 210 m (300 psi) or as Langmuir volumes. The data indicate a weak negative correlation of gas content with increasing reactives content. This is the reverse of the situation for samples of the same coal analyzed for CH_4 adsorption (Figure 15). One of the Gething samples (Table 5) has distinctly

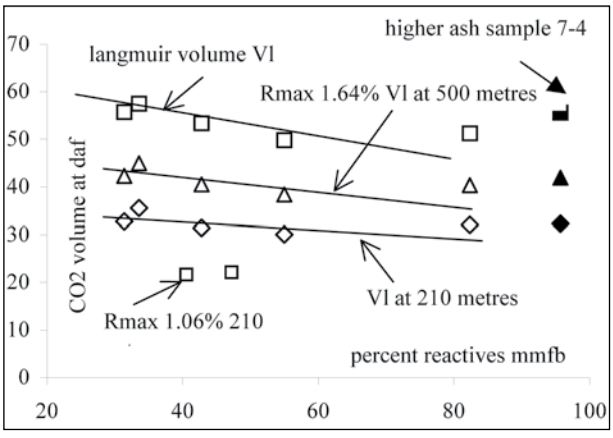

Figure 14. Plot of CO_2 adsorption at different depth versus reactive content for the Gething Formation samples.

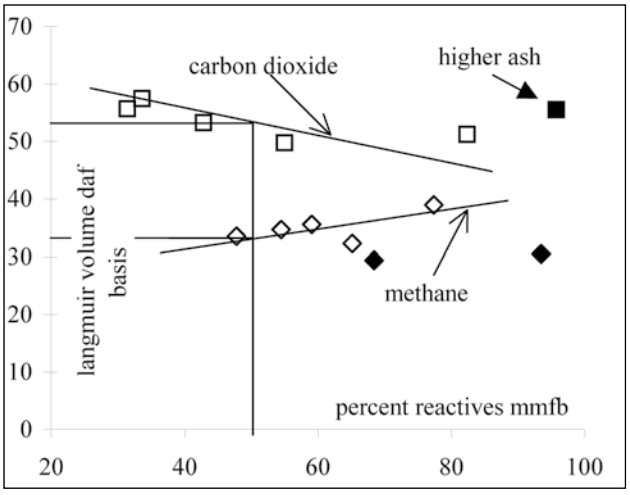

Figure 15. Plot CH_4 and CO_2 adsorption versus content for Gething Formatio samples. CH_4 data are from Ryan and Lane (2002).

higher ash than the other samples, and it is highlighted in the plot (Figure 14). It appears that the effect of petrography on CO_2 and CH_4 adsorption is different for high-rank coals. The CO_2/CH_4 ratio increases as the inert maceral content increases. This means that some of the Jurassic-Cretaceous coals of BC, which are characterized by moderately high inert maceral contents, may have improved ability to sequester CO_2. At lower ranks it appears that CO_2 adsorption does not vary much with maceral content, as indicated by the two samples (rank 1.06%) also plotted into Figure 14 and by the Gluskoter data for sub-bituminous coals.

Pure gas isotherms illustrate the ultimate replacement potential of CO_2 for CH_4. Unfortunately, they give no hints as to how to achieve this. The extended Langmuir equation predicts the ratio of adsorbed gases based on the mole ratio of gases in the free phase (Figure 16). For example, if the mole ratio of CO_2 in the gas phase is 0.5, then the mole

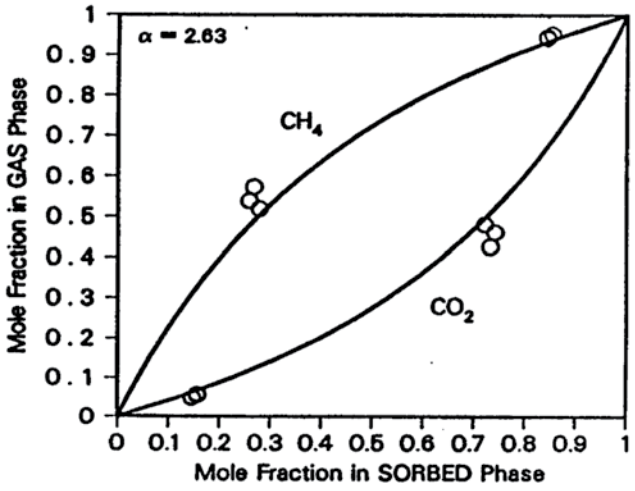

Figure 16. CO_2/CH_4 mole fraction in gas and adsorbed phase; data from Arri *et al.* (1992).

ratio in the adsorbed phase will be 0.7, and this requires a mole ratio of 0.3 CH_4 in the adsorbed phase and 0.45 in the gas phase. Figure 16 is coal- and temperature-specific but it does indicate trends as predicted by the extended Langmuir equation. Arri *et al.* (1992) found that the CO_2 data had, at best, a moderate fit to curves predicted by the extended Langmuir equation. Crosdale (1999) analyzed the composition of adsorbed gas for increasing pressure steps for a gas phase of 52.9% CO_2 and 47.1% CH_4. The results do not conform to the extended Langmuir equation. The amount of CO_2 adsorbed was, in agreement with a pore-filling model, influenced by the faster diffusion of the smaller CH_4 molecule. The CH_4 molecule was able to diffuse into the coal faster than the CO_2 molecule and block or occupy adsorption sites. During desorption, as pressure drops, CH_4 desorbs faster, leaving an increased concentration of adsorbed CO_2. Based on Crosdale's work, increasing the pressure of CO_2 in coal not desorbed of CH_4 may not release as much CH_4 or adsorb as much CO_2 as is predicted by the extended Langmuir equation. If the coal is undersaturated with CH_4, then it should be possible to predict CO_2 adsorption based on a CO_2 isotherm. The mechanics of getting the CO_2 to permeate coal depends on permeability, and the adsorbtion of CO_2 on coal depends on matrix swelling. If the coal seam has limited permeability, then CO_2 flooding and adsorption may not be possible.

Some of the early studies on CO_2 adsorption were interested in the potential of using CO_2 for enhanced coalbed methane recovery (ECBMR). In this case, a coal with low CO_2 selectivity is better than one with a high CO_2/CH_4 selectivity ratio. In all cases for ECBMR, it is important that the recovered gas does not have a high CO_2 component, as this adds to the costs of upgrading the gas to pipeline quality. In many situations ECBMR may not be practical because of low permeability and high concentration of CO_2 in the recovered gas. The results of the Allison CO_2 injection project of Burlington are somewhat inconclusive; injection of CO_2 certainly increased water production, in part probably because CO_2 went into solution in the water, decreasing its viscosity. In low-rank coals this may have the effect of drying the coals, which would then increase their adsorption ability. In an ECBMR situation, this may mean production of water and temporary sequestration of CO_2 and minimal release of CH_4. When water re-enters the seam, adsorption ability may decrease, causing CO_2 to be released.

INFLUENCE OF TEMPERATURE ON CO_2 ADSORPTION

Any temperature increase below the critical temperature decreases the ability of samples to adsorb CO_2. This effect has to be paired with a geothermal and pressure gradient to attempt to construct real adsorption versus depth tracts. In this study, two samples were analyzed at 25°C and 30°C (Table 6, Figure 17). The Langmuir pressures increase as the temperature increases.

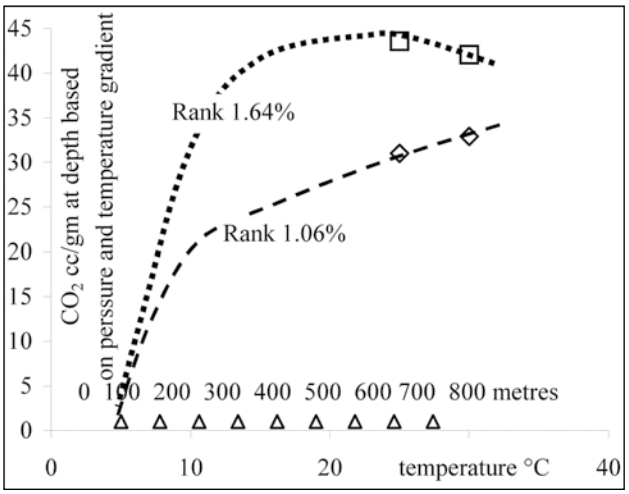

Figure 17. Plot of CO_2 adsorption at different temperatures. Data volumes calculated based on a normal hydrostatic gradient and a geothermal gradient of 28°C/km with surface temperature of 5°C.

The same effect is seen for CH_4 isotherms; however, the CO_2 Langmuir volumes do not consistently decrease as temperature increases. When the CO_2 gas contents are calculated at the depth and pressure that correspond to the temperature of the isotherm, the adsorption for the high-rank coals decreases as depth increases, and for the low-rank coals, the adsorption increases with depth (Figure 17). This is in a depth window of about 700 to 800 m. Higher-rank coals have lower Langmuir pressures, indicating curves that are steeper at the origin than are curves for low-rank coals. This, combined with the effect of increasing temperature, means that for low-rank coals, the adsorption still tends to increase with depth and temperature, whereas for high-rank coals, the adsorption decreases as depth and temperature increase.

It is very important to construct adsorption versus depth tracts for different rank coals for the depth range that corresponds to temperatures below the critical temperature. The implication of Figure 17 is that it might be better to sequester CO_2 in lower-rank coals at depth than to sequester it in higher-rank coals.

SEQUESTERING CO_2 IN BRITISH COLUMBIA COALS

One of the most understated facts about sequestering CO_2 in coal is that it can only happen by first displacing the CH_4 already adsorbed by the coal. The coal may or may not be saturated with adsorbed CH_4, but it will certainly have

some that will be released when the CO_2 is adsorbed. On a weight basis, the amount of CO_2 adsorbed is between 5 and 30 times the amount of CH_4 desorbed, calculated at a depth of 210 m (Table 8). The ratio of CO_2/CH_4 decreases as pressure (depth) increases, though the situation is more complicated when the effect of increasing temperature is factored in. This sounds very favourable in terms of sequestering CO_2; unfortunately the CH_4 released is about 20 times more powerful as a greenhouse gas. Consequently, unless CO_2 sequestration is paired with CH_4 recovery, there is likely to be, over the long term, a net increase in the release of greenhouse gases.

TABLE 8. THE RATIO OF CO_2/CH_4 ADSORBED ON COALS OF DIFFERENT RANKS.

Rank	Rmax%	volume ratio	wt ratio	CO_2 scf/t daf at 300psi =213 m depth	CO_2 cc/g	CH_4 cc/g
Gluskoter						
lignite		9.4	25.9	800	25.0	2.7
sub bit		7.6	20.9	900	28.1	3.7
high vol		5	13.8	700	21.8	4.4
medium vol		2.4	6.6	600	18.7	7.8
low vol		2	5.5	800	25.0	12.5
Semi anth		2.6	7.2	1000	31.2	12.0
this paper						
Low vol	1.64	1.7	4.7	998	31.2	18.3
medium vol	1.28	1.5	4.1	550	17.2	11.4
High vol A	1.06	3.3	9.1	685	21.4	6.5
High vol B	0.7	4.7	12.9	527	16.4	3.5
High vol B	0.7	9	24.8	611	19.1	2.1

Data calculated at a pressure of 300 psi, equivalent to a depth of 210 m.

Many coals are undersaturated with respect to CH_4 and CO_2. In these cases, CO_2 injected will initially be adsorbed without any release of CH_4. The coal matrix will expand, decreasing permeability and making it even more difficult for CO_2 to infuse coal and for CH_4 to escape. In situations where the coal is partially desorbed of CH_4 because of production, the pressure is reduced and there will be some matrix shrinkage, which may improve permeability. In this case, CO_2 should be able to permeate coal and be adsorbed; however, because the coal is undersaturated with respect to CH_4, there may not be an immediate release of additional CH_4 as the pressure increases and the composition of the gas phase becomes more CO_2 rich.

One of the best ways of locally sequestering CO_2 is to inject it into abandoned or mature CBM wells. It is possible to use the CBM at site to generate electricity either by burning it or by using a fuel cell. If a relatively pure stream of CO_2 is derived from these processes, then it can be injected back into the CBM well to be adsorbed on undersaturated coal or to replace CH_4 on saturated coal. As an added advantage, the gas may be hot, which would increase the release of CH_4. It is interesting to compare the amount of CO_2 produced by oxidizing or burning the CH_4 produced from a well with the amount of CO_2 that coal in the well could adsorb (Table 9). As an example, CO_2 and CH_4 isotherms for a medium-volatile coal are used (Bustin, 2001). The two isotherms run at 25°C indicate the actual adsorption conditions at a depth where the temperature is 25°C (assumed to be 300 m). The adsorption amounts are therefore high for depths greater than 300 m and low for depths shallower than 300 m. However, the data do illustrate trends. The CO_2 derived from oxidizing the CH_4 produced from one tonne of coal can be adsorbed onto about 0.5 tonnes. But based on estimating the matrix shrinkage caused by desorption of CH_4 and expansion caused by adsorption of CO_2, there will be about a 2% volume increase in the tonne of coal. These estimates are made assuming densities of the adsorbed gases and may change considerably, but it is probably valid to assume that there will be a matrix expansion.

Sequestration of CO_2 is simpler if a pure stream of CO_2 is obtained. Natural gas processing plants can produce relatively pure streams of CO_2. Power plants and coal gasification produce mixtures of N_2, CO_2, and other gases. However, a pure stream of CO_2 can be obtained by trapping CO_2, using CaO to produce $CaCO_3$, and then liming the $CaCO_3$ in a separate reactor. The process can be self-sustaining in terms of $CaCO_3$ or may require inputs of fresh $CaCO_3$, in which case sequestration may require a location where coal and limestone are both available. The locations of the coal deposits in BC and brief descriptions of their size and CBM potential can be found in Ryan (2003).

British Columbia releases about 63.5 million tonnes equivalent of CO_2 annually (Environment Canada, 2001). If this is assumed all to be CO_2, it is possible to estimate the amount of coal that would be required to sequester it all (Table 10), and the amount is in the range of 100 to 200 billion tonnes. This amount of coal is similar to the total amount of coal in the province above a depth of 2000 m (estimated to be about 250 billion tonnes). Sequestering CO_2 in coal will only be applicable for very specific point sources.

Sequestering CO_2 in coal is often discussed in the context of coal-fired power plants. Spath *et al.* (1999) studied greenhouse gas emissions resulting from all aspects of generating electricity from coal. A present-day 360 MW power plant burns about 1.4 million tonnes of coal per year. About 100 to 200 million tonnes of coal are required to sequester the CO_2 produced (Table 11). It is probably unrealistic to envisage the CO_2 produced from a power plant being sequestered in the same coal resource that is providing coal to the power plant.

TABLE 9. COMPARISON OF THE AMOUNTS OF CH_4 AND CO_2 ADSORBED ONTO A MEDIUM-VOLATILE COAL OVER A RANGE OF DEPTHS.

		CH_4	CO_2	SG coal				1.2
	SG liquid estimated	0.466	0.6	CO_2 from burning 1 tonne coal				
	density of gas g/m^3	714.3	1964				2567	Kg
	mole wt	16	44				cc/g to scf/t	32.04
	psi	1000	800	600	400	300	200	100
	depth metres	704	563	422	282	211	141	70
CH_4	scf/t	340	323	300	260	228	184	120
CH_4	cc/g	10.6	10.1	9.4	8.1	7.1	5.7	3.7
CH_4	wt kg /tonne	7.6	7.2	6.7	5.8	5.1	4.1	2.7
CH_4	moles	0.5	0.5	0.4	0.4	0.3	0.3	0.2
CO_2	scf/t	604.0	587.0	560.0	510.0	467.0	400.0	283.0
CO_2	cc/g	18.9	18.3	17.5	15.9	14.6	12.5	8.8
CO_2	wt kg /tonne	37.0	36.0	34.3	31.3	28.6	24.5	17.3
CO_2	moles	0.8	0.8	0.8	0.7	0.7	0.6	0.4
CO_2/CH_4 volume ratio		1.8	1.8	1.9	2.0	2.0	2.2	2.4
CO_2/CH_4 wieght ratio		4.9	5.0	5.1	5.4	5.6	6.0	6.5
CO_2/CH_4 mole ratio		1.8	1.8	1.9	2.0	2.0	2.2	2.4
wt kg CO_2 from burning CH_4		20.8	19.8	18.4	15.9	14.0	11.3	7.4
m^3 vol of resultant CO_2		10.6	10.1	9.4	8.1	7.1	5.7	3.7
tonnes coal required to sequester		0.56	0.55	0.54	0.51	0.49	0.46	0.42
liquid vol m^3/t of adsorbed CH_4		0.016	0.015	0.014	0.012	0.011	0.009	0.006
liquid vol m^3/t adsorbed CO_2		0.062	0.060	0.057	0.052	0.048	0.041	0.029
% vol increase if all CH_4 desorbed and replaced by CO_2		5.453	5.343	5.144	4.76	4.417	3.848	2.781
liquid volume m^3/t of CO2 resultant from burning CH4		0.035	0.033	0.031	0.027	0.023	0.019	0.012
% volume change if CO2 adsorbed onto 1 tonne coal		2.2	2.1	2.0	1.7	1.5	1.2	0.8

Data is approximate in part because isotherms do not recognize the change of temperature with depth.

TABLE 10. THE AMOUNT OF COAL REQUIRED TO SEQUESTER THE CO_2 PRODUCED IN BRITISH COLUMBIA IN ONE YEAR.

British Columbia CO_2 equivalent emissions (million tonnes per year (1999))			63.8	estimated assuming all greenhouse gas CO_2				
CO_2 produced (billion cubic metres per year)			32.5					
depth (metres)	704	563	422	282	211	141	70	
CO_2 adsorption cubic metres/tonne billion tonnes of coal to sequester	18.9	18.3	17.5	15.9	14.6	12.5	8.8	
CO_2 produced in 1 year	91	94	98	108	118	137	194	

Estimated using 1999 data.

TABLE 11. THE AMOUNT OF COAL REQUIRED TO SEQUESTER THE CO_2 PRODUCED BY A 360 MW POWER PLANT.

coal fired power plant MW	360						
efficiency %	32						
coal consumption/yr million tonnes	1.413						
% carbon	65						
CO_2 produced million tonnes	3.37						
CO_2 produced million cubic metres	1715						
depth metres	704	563	422	282	211	141	70
adsorption cubic metres/tonne	18.9	18.3	17.5	15.9	14.6	12.5	8.8
million tonnes of coal to sequester CO_2	91	94	98	108	118	137	194
ratio coal needed for sequestering versus coal burnt	64	66	69	76	83	97	137

Data from Spath *et al.* (1999).

One of the few places where it might be possible to sequester the CO_2 generated by a power plant adjacent to the plant is in the Hat Creek area in south-central BC. This deposit was explored by BC Hydro as a possible site for a large power plant, and the area contains a large resource of lignite to sub-bituminous coal, which is estimated to be between 10 and 30 billion tonnes. Data from Gluskoter *et al.* (2003) indicate that sub-bituminous and lignite coals can adsorb about 10 cm^3/g CO_2 at intermediate depths (300 m). When this is compared to the amount of carbon in the coal, it is apparent that, for a tonne of coal burnt, the amount of CO_2 produced is less than for high-rank coals and can be sequestered in fewer tonnes of in situ coal. At Hat Creek, coal delivered to a power plant would be less than 30% carbon and would require less than 100 tonnes in situ to sequester the CO_2 produced from 1 tonne burned. Because of the size of the Hat Creek resource, a power plant using 10 million tonnes per year for 25 years would require about 25 billion tonnes to sequester the CO_2 generated. The sequestering of CO_2 may also result in the recovery of CH_4, which can be used in the power plant or sold as natural gas.

Isotopic studies of the C^{13}/C^{12} isotopic ratios of CBM indicate that the gas is often a mixture of biogenic and thermogenic methane. Biogenic methane may originate from early coalification or during uplift of the coal-bearing formation. Generation of biogenic methane requires a consortium of bacteria and a series of biochemical reactions that in part require H_2 and CO_2. This raises the possibility that injection of CO_2, if associated with bacteria or nutrients, may stimulate generation of biogenic methane at the same time that CO_2 is sequestered (Budwill, 2003). The best candidates for synchronous CO_2 sequestration and generation of biogenic methane are low-rank coals at shallow depth. Deposits such as Coal River or Tuya River, as well as the much larger Hat Creek deposit, could be candidates.

CONCLUSIONS

The connection is made: climate change is at least in part related to increasing concentration of CO_2 in the atmosphere, and we are responsible for the most recent increase. The incentive to limit fossil fuel use or sequester the CO_2 produced by fossil fuel use is here and will not go away.

Sequestration of CO_2 in coal seams requires a clear understanding of the CO_2 phase diagram and the implications for the maximum depth of sequestration. The maximum depth varies based on combinations of geothermal and pressure gradients but is generally in the range of 500 to 900 m. Below this depth and in part above it, CO_2 goes into solution in coal and causes an increase in plasticity and swelling (Larson, 2004).

It is essential to understand the CO_2 and CH_4 adsorption behaviour in coals of different ranks and for different combinations of temperature and pressure. The mole ratio of CO_2/CH_4 adsorption varies from over 10 for low-rank coals to under 2 for medium- and high-rank coals. The CO_2 adsorption is moderately high for low-rank coals, decreases for medium-rank coals, and then increases substantially for high-rank coals. The interaction of adsorption and selectivity of CO_2 and CH_4 means that for maximum CO_2 sequestration with minimum production of CH_4, one should use lignite, whereas for maximum sequestration of CO_2 with maximum production of CH_4, one should use a high-rank coal.

Sequestration of CO_2 without collection of the released CH_4 may result in a net increase in the emission of greenhouse gases over time.

Actual sequestration of CO_2 and release of CH_4 is predicted by binary gas isotherms and may not obey the extended Langmuir equation. It will also be influenced by permeability, matrix swelling, and initial saturation.

Conditions of sequestration of CO_2 in coal may best be applied to small point sources; for example, where CBM is being burned on site to produce electricity.

Most discussions of CO_2 sequestration do not consider the implications of an impure gas stream composed of CO_2 and N_2. Addition of N_2 to the gas decreases the adsorption of CO_2.

ACKNOWLEDGEMENTS

Marc Bustin performed the isotherm measurements. Bob Lane, the regional geologist at Prince George, found time to collect the samples of the Gething Formation.

REFERENCES

Arri, L.E., Yee, D., Morgan, W.D. and Jeansonne, M.W. (1992): Modeling coalbed methane production with binary gas sorption; *Society of Petroleum Engineers*, Paper SPE 24363, pages 459-472.

Bachu, S., and Stewart, S. (2002): Geological sequestration of anthropogenic carbon dioxide in the Western Canadian Sedimentary Basin: suitability analysis; *Journal of Canadian Petroleum Technology*, Volume 41, pages 32-40.

Budwill, K. (2003) Microbial methanogenesis and its role in enhancing coalbed methane recovery; *CSEG Recorder*, November 2003, pages 41-46.

Bustin, R.M. (2001): Geology and engineering aspects of coalbed methane; Course by *CBM Solutions*, Calgary Alberta, April 25, 2001.

Bustin, R.M. and Clarkson, C.R. (1999): Free gas storage in matrix porosity: a potentially significant coalbed resource in low rank coals; *International Coalbed Methane Symposium*, Tuscaloosa, Alabama 1999; pages 197-214.

Crosdale, P.J. (1999): Mixed methane / carbon dioxide sorption by coal: new evidence in support of pore filling models; *International Coalbed Methane Symposium*, Tuscaloosa Alabama, pages 359-366.

Dawson, F.M. Marchioni, D.L. Anderson, T.C. and McDougall, W.J. (2000): An assessment of coalbed methane exploration projects in Canada; *Geological Survey of Canada*, Bulletin 549.

Environment Canada (2001): Canada's greenhouse gas inventory, 1990-1999.

Ettinger, I., Eremin, B., Zimakov, B. and Yanovskaya, M. (1966): Natural factors influencing coal sorption properties 111 comparative sorption of carbon dioxide and methane on coals; *Fuel*, Volume 45 pages 351-361.

Gan, H., Nandie, S.P, and Walker, P.L. (1972): Nature of porosity in American coals; *Fuel,* Volume 51, pages 272-277.

Gluskoter, H., Mastalerz, M. and Stanton, R. (202) The potential for carbon dioxide sequestration in coal beds: new evidence from methane and carbon dioxide adsorption analysis for coals from lignite to anthracite; Abstract 25, *Geological Association of America*, Annual Meeting, April 2002.

Grieve, D.A. (1993): Geology and Rank Distribution of the Elk Valley Coalfield, Southeastern British Columbia; *B.C. Ministry of Energy, Mines and Petroleum Resources,* Bulletin 82, pages 1-188.

Harris, L.A., Yust, C.S. (1976): Transmission electron microscopy of coal; *Fuel*, Volume55, page 233.

Hughes, D. (2003): Assessment of CO_2 storage capacity of deep coal seams in the vicinity of large CO_2 point sources in central Alberta and Nova Scotia; In press.

Jarrell, P. M., Fox, C. E. Stein M. H, and Webb, S. L (2002): Practical aspects of CO2 flooding; *Society of Petroleum Engineers,* Monograph 22, 220 pages.

Kalkreuth, W. and McMechan, M. (1988): Burial history and thermal maturation, Rocky Mountains foothills and foreland east central British Columbia and adjacent Alberta; Bulletin, *American Association of Petroleum Geologists*, Volume 72, pages 1395-1410.

Kalkreuth, W., Langenberg, W. and McMechan, M. (1989): Regional coalification pattern of Lower Cretaceous coal bearing strata, Rocky Mountain Foothills and Foreland, Canada - Implications for future exploration; *International Journal of Coal Geology*, Volume 13, pages 261-302.

Karst, R. and White, G.V. (1979): Coal rank distribution within the Bluesky-Gething stratigraphic horizon of Northeast B.C.; *Ministry of Energy Mines and Petroleum Geology*, Paper 80-1, pages 103-107.

Khan, M.R., and Jenkins, R.G. (1985): Thermoplastic properties of coal at elevated pressures: effects of gas atmospheres; *Proceedings International Conference on Coal Science,* Sydney.

Krooss, B.M., Gensterblum, Y., and Siemons, N. (2001): High-pressure methane and carbon dioxide adsorption on dry and moisture-equilibrated Carboniferous coals; *International Coalbed Methane Symposium*, Tuscaloosa Alabama, 2001, pages 177-191.

Lamberson, M.N., Bustin, R.M., and Kalkreuth, W.D. (1991): Lithotype maceral composition and variation as correlated with paleo-wetland environments; Gates Formation northeastern British Columbia, Canada; *International Journal of Coal Geology,* Volme18, pages 87-124.

Lamberson, M.N. and Bustin, R.M. (1993): Coalbed methane characteristics of the Gates Formation coals, northeastern British Columbia: effect of maceral composition; *American Association of Petroleum Geologists,* Bulletin, Volume 77, pages 2062-2076.

Larsen, J.W. (2004): The effects of dissolved CO2 on coal structure and properties; *International Journal of Coal Geology,* Volume 57, pages 63-70.

Leckie, D.A. (1983): Sedimentology of the Moosbar and Gates Formations (Lower Cretaceous); PhD Thesis, McMaster University.

Levine, J.R. (1993): Coalification: The evolution of coal as source rock and reservoir rock for oil and gas; Chapter 3, *American Association of Petroleum Geologists*; Studies in Geology Series, Number 38, pages 39-77.

Levy, J.H., Day, S.J., Killingley, J.S. (1997): Methane capacities of Bowen Basin coals related to coal properties; *Fuel,* Volume 76, pages 813-819.

Marchioni, D. and Kalkrueth, W. (1992): Vitrinite reflectance and thermal maturation in Cretaceous strata of the Peace River Arch region west-central Alberta and adjacent British Columbia; *Geological Survey of Canada*, Open File 2576.

Pashin, J.C., and McIntyre, M.R. (2003): Temperature-pressure conditions in coalbed methane reservoirs of the Black Warrior Basin: implications for carbon sequestration and enhanced coalbed methane recovery; *International Journal of Coal Geology,* Volume 54, pages 167-183.

Pruess, K., Xu, T., Apps, J. and Garcia, J. (2001): Numerical modeling of aquifer disposal of CO2; *Society of Petroleum Engineers,* SPE 66537, Exploration and Production Environmental Conference San Antonio Texas, February 2001.

Reucroft, C.F., and Sethurarman, A.R. (1987): Effect of pressure on carbon dioxide induced coals swelling; *Energy Fuels,* Volume 1, pages 72-75.

Righmire, C.T. (1984): Coalbed methane resource; *American Association of Petroleum Geologists;* Studies in Geology, Series 17, pages 1-14.

Ryan, B.D. (1992): An Equation for Estimation of Maximum Coalbed-Methane Resource Potential; *B.C. Ministry of Energy, Mines and Petroleum Resources,* Geological Fieldwork 1991, Paper 1992-1, pages 393-396.

Ryan, BD (1997): Coal quality variations in the Gething Formation northeastern British Columbia*; BC Ministry of Energy, Mines and Petroleum Resources,* Geological Fieldwork 1996, Paper 1997-1, pages 373-397.

Ryan, B.D. and Lane, R. (2002): Adsorption characteristics of coals from the Gething Formation northeast British Columbia; *B.C. Ministry of Energy and Mines,* Geological Fieldwork, Paper 2003-1.

Ryan, B.D. (2002): Pseudovitrinite: possible implications for gas saturation in coals and surrounding rocks*; B.C. Ministry of Energy and Mines,* Geological Fieldwork, Paper 2003-1.

Ryan, B.D. (2003): the CBM resource of some perspective areas of the Crowsnest Coalfield; In press *BC Ministry of Energy and Mines*.

Ryan, B.D. (2003): A summary of the coalbed methane potential in British Columbia; *CSEG Recorder*, November 2003, pages 32-40.

Spath, P.L., Mann, M/K., and Kerr, R.D. (1999): Life cycle assessment of coal-fired power production; *Nation Renewable Energy laboratory;* Contract Number DE AC36-98-GO10337.

ULTRAMAFIC ROCKS IN BRITISH COLUMBIA: DELINEATING TARGETS FOR MINERAL SEQUESTRATION OF CO_2

By D. A. Voormeij[1] and G. J. Simandl[1, 2]

KEYWORDS: CO_2 sequestration, ultramafic, mineral potential, serpentinite, dunite.

SUMMARY

British Columbia has favourable geology and excellent exploration potential to host the raw materials suitable for CO_2 mineral carbonation, one of the methods considered for lowering atmospheric greenhouse gas levels. British Columbia has been situated on the active, west-facing Pacific margin of continental North America for at least the last 530 million years and subjected to a subduction zone (accretionary) tectonic setting for the last 390 million years. Due to its tectonic history, BC contains numerous Alpine-type and several Alaskan-type complexes, both types rich in Mg-silicates. Dunite zones within these complexes are currently considered as the most promising sources of raw materials for the mineral sequestration process, since they contain the most Mg by weight, the component necessary for binding with CO_2 to form stable carbonates. In addition, stockpiles containing short-fibre chrysotile mined from serpentine-rich zones in ultramafic complexes may provide a source of starting material, thereby simultaneously disposing of CO_2 as well as other potentially hazardous materials. British Columbia's ultramafic rocks were studied previously as possible hosts of base metals, precious metals, and gemstones. This study draws relevant information from that research and utilizes the database originally designed to evaluate mineral potential for the province. From this database, a map depicting dunite- and serpentinite-bearing ultramafic rocks has been produced. Several targets have been selected, relying on preliminary data, including mineralogy, geochemistry, potential size of the resource, accessibility, and proximity to major CO_2 point sources. These include the dunite zone of the Alaskan-type Tulameen Complex near Princeton and the Cassiar chrysotile tailings in northern BC. These targets are the subject of current detailed research.

INTRODUCTION

A number of carbon dioxide (CO_2) sequestration methods, including geological storage, ocean storage, and mineral sequestration, have been proposed worldwide, and methods conceivably applicable to BC were listed and reviewed by Voormeij and Simandl (2003a). Mineral carbonation is considered to be the only method that truly disposes of CO_2 on a geological time-scale and with minimum risk of leakage (Lackner *et al*., 1997; O'Connor *et al*., 2000). Although Ca-silicates (e.g., wollastonite) may also have potential for mineral carbonation (Wu *et al*., 2001; Kakizawa *et al*., 2001), Mg-silicates are more common in high concentrations and as large deposits (Goff and Lackner, 1998). Mg-silicates also contain more reactive material per tonne than do Ca-silicates (Lackner *et al.,* 1997). The mineral carbonation concept is based on the natural weathering process of Mg-olivine (forsterite) and serpentine, which carbonate by the following reactions:

$$\underset{\text{[olivine]}}{Mg_2SiO_4} + 2CO_2 \rightarrow \underset{\text{[magnesite]}}{2MgCO_3} + \underset{\text{[silica]}}{SiO_2} \quad (1)$$

$$\underset{\text{[serpentine]}}{Mg_3SiO_3(OH)_4} + 3CO_2 \rightarrow \underset{\text{[magnesite]}}{3MgCO_3} + \underset{\text{[silica]}}{2SiO_2} + H_2O \quad (2)$$

This process is thermodynamically favoured in near-surface environments, and its products are stable on a geological time scale. The concept was first proposed by Seifritz (1990) and considered in more details by Lackner *et al.* (1997), O'Connor *et al*. (1999; 2000), and Kohlmann and Zevenhoeven (2001; 2002).

The mineral carbonation process, as considered in this paper, is envisioned in an industrial setting (ex situ). Geographical location, proximity to infrastructure, and the size of dunite and serpentinite resources and their physical and chemical properties are some of the important factors determining the potential viability of mineral sequestration in BC. Ideal sites should be located close to both the Mg-silicate deposit and a major CO_2 emission point source to minimize transportation costs of the CO_2 and raw materials. Geographic distribution of major stationary CO_2 point sources in BC has been completed (Voormeij and Simandl, 2003b). In order to match sinks to these point sources, areas with the potential to host raw material for mineral CO_2 sequestration need to be identified. Dunite zones of ultramafic complexes are preferred over the serpentinite zones, since they contain the most magnesium by weight. Serpentinite zones are more common and for this reason are also considered as candidates. Detailed methodology proposed for systematic evaluation of the ultramafic materials for use in mineral carbonation is outside of the scope of this study and is covered by Voormeij and Simandl (in preparation).

[1] *University of Victoria, voormeij@uvic.ca*
[2] *British Columbia Geological Survey Branch, george.simandl@gems2.gov.bc.ca*

ULTRAMAFIC ROCKS

Petrology and Mineralogy

Serpentine and forsteritic olivine are common silicates with high magnesium contents. There are three principal forms of serpentine: lizardite, antigorite, and chrysotile (Deer, Howie and Zussman, 1978), all with the approximate composition $Mg_3Si_2O_5(OH)_4$. The most abundant is lizardite, whereas the fibrous chrysotile is relatively rare. The latter is perhaps best known since it had many industrial applications, including fireproof insulation, specialty paints, brake pads, and gaskets. (Virta and Mann, 1994). It has also been used extensively in construction materials such as cements and tiles. However, the use of chrysotile was severely curtailed due to health hazards associated with its use (Hamel, 1998), and is banned in several European countries.

Olivine exists as a solid solution series between the Mg_2SiO_4 (forsterite) and Fe_2SiO_4 (fayalite) end members. The monomineralic rock of olivine is called dunite (Figure 1). Forsteritic olivine is currently the favoured mineral for the carbonation process because it does not require the energy-intensive pretreatment that serpentine needs (Lackner *et al*., 1997; O'Connor *et al*., 2000). However, research into optimization of energy used in the pretreatment of serpentine is ongoing (McKelvy *et al.*, 2002; O'Connor *et al*., 2000). Furthermore, serpentine-rich rocks are more widespread than those rich in olivine. Thus both have to be considered. Some selected chrysotile-bearing stockpile sites are also investigated because, in addition to sequestering CO_2, the mineral carbonation method may also aid in the disposal of unwanted asbestos waste (Huot *et al*., 2003).

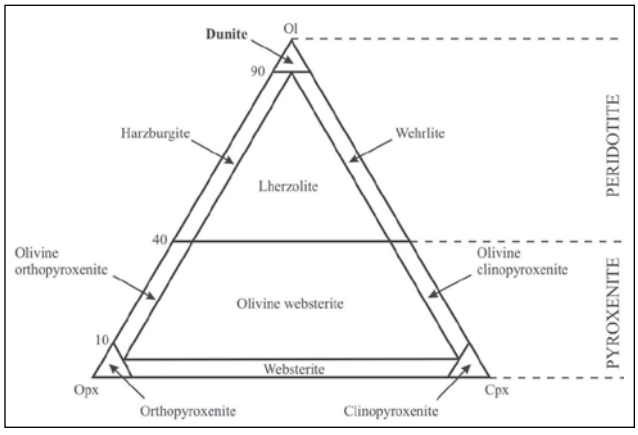

Figure 1. IUGS classification scheme for ultramafic rocks (after Le Maitre, 1989). Ol-olivine; Opx-orthopyroxene; Cpx-clinopyroxene. The general term "peridotite" is used when the olivine content is 40%–100%, whereas "pyroxenite" refers to an olivine content of 0%–40%. For example, "dunite" is a peridotite containing 90%–100% olivine.

ULTRAMAFIC COMPLEXES

Ultramafic complexes can be divided into three major categories: Alpine, Alaskan, and layered intrusive types. Their geographic distribution is restricted by tectonic setting, which also indirectly influences the physical and chemical characteristics of dunite and serpentinite rocks within these complexes. These characteristics include relative position of the dunite and serpentinite bodies, structural control, variation in mineralogy, and mineral composition. Table 1 lists well-documented examples of these categories and describes their geological setting.

Alpine-Type Complexes

Alpine-type ultramafics are the most voluminous and widespread of all ultramafic bodies (Coleman, 1977) and are interpreted as forming the basal part of an ophiolitic suite (Dewey, 1976 and Moores, 1982; 2002). A complete ophiolite sequence, tectonically emplaced over crystalline basement (Figure 2), consists of (from bottom to top) tectonic mélange, metamorphic sole, deformed mantle tectonite, cumulate peridotite (alternately layered olivine and pyroxene), cumulate gabbros grading upwards into massive gabbros and plagiogranites, overlain and partially intruded by sheeted dike swarms, followed by pillow basalts, capped by deep-sea and/or pelagic or, in some cases, volcaniclastic turbidites, all overlain by shallow-water sediments. This sequence is thought to represent an analogue for oceanic crust formed at fast-spreading centres, as exemplified by the Juan de Fuca Ridge situated off the coast of BC.

Dunitic rocks of ophiolitic sequences are divided into two broad categories based upon their texture and petrography: tectonite and cumulate. Dunites within the tectonite section generally occur as lenses within harzburgite or lherzolite, ranging from one metre to hundreds of metres in size. In most cases, the tectonite is gradational into the cumulate sequence, where forsteritic olivine is the dominant cumulate phase (Coleman, 1977; Moores, 2002). Podiform chromitite is commonly associated with the tectonite zone; stratiform or thin chromitite accumulations are typical of the cumulate zone (Coleman, 1977). During the serpentinization of the alpine peridotites, fibrous chrysotile veins and stockworks may be formed. Where chrysotile-filled fractures constituted 3% to 10% of the rock and formed long fibres of high quality, it was economically mined (Hora, 1999).

Alaskan-Type Complexes

Alaskan-type complexes (also called Alaskan-Ural, Uralian, and concentric or zoned complexes) are mafic and ultramafic intrusions. Their type locations are in a narrow,

TABLE 1. CHARACTERISTICS OF THE THREE MAIN TYPES OF ULTRAMAFIC COMPLEXES CONTAINING SIGNIFICANT DEPOSITS OF DUNITE AND/OR SERPENTINITE.

Geological Setting	Complex Type	Description	Distribution of dunite and/or serpentinite zones	Examples
Syn-orogenic ultramafic bodies	***Alpine-Type***	Tectonically emplaced ultramafic complex that makes up the basal section of an ophiolite (ocean-crust) sequence	Mantle tectonite section contains pods of dunite. Cumulate section contains layers of dunite. Dunite variably serpentinized. Tectonic melange is typically rich in serpentinite.	Nahlin UMF Complex (BC); Cache Creek UMF complex (BC); Shulaps UMF Complex (BC)
	Alaskan-Type	Podiform intrusions of mafic to ultramafic magmas into accreted island arcs.	Concentrically zoned. Successive zones of wehrlite, clinopyroxenite and orthopyroxenite around a dunite core. Dunite variably serpentinized, increasing outwards from core.	Duke Island (Alaska); Polaris (BC); Tulameen (BC); Turnagain (BC)
Intracratonic	***Layered Intrusion-Type***	Large, often funnel-shaped sill-like intrusions. Layering formed partly as a result of fractional crystallization of the primary melt	Laterally extensive, alternating layers of dunite/peridotite and pyroxenite.	Muskox (NWT), Bushveld (RSA), Great Dyke (Zimbabwe), Stillwater (MT), Windemurra (AUS)

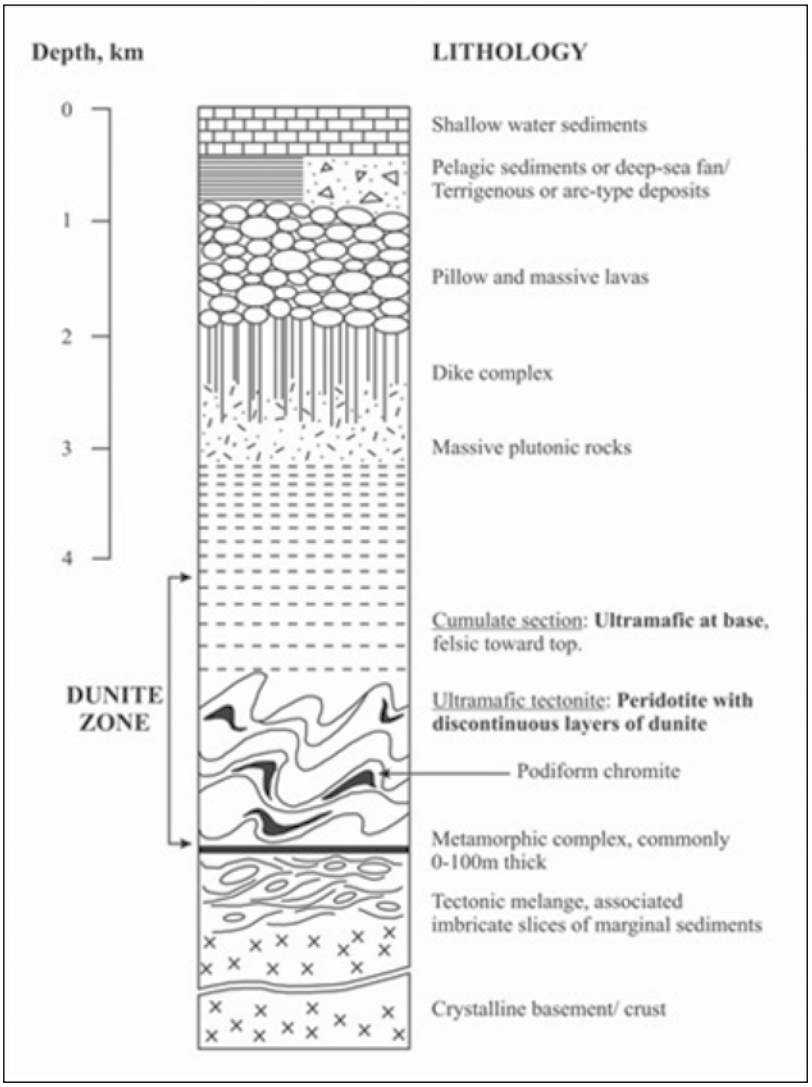

Figure 2. Cross section of a "complete" ophiolite complex. Few ophiolite complexes contain all of these units; most contain only part(s) of the entire complex (source: Moores, 2002).

north-trending belt, 600 km long, in southeastern Alaska (Irvine, 1967).Similar ultramafic bodies are found in belts along the central Ural Mountains of Russia (Irvine, 1987) and through the interior of BC (Findlay, 1963; Irvine, 1976; Clark, 1980; Nixon, 1990). Idealized Alaskan-type complexes are characterized by the crude zonation of successive wehrlite, clinopyroxenite, and hornblende-rich lithologies around a dunite core (Irvine, 1987). In many of the well-documented examples, any one of these zones may be missing or discontinuous (Nixon, 1990). Massive dunite cores consiting primarily of forsteritic olivine (Irvine, 1987) may be exposed over large areas, and in many cases dunite is well preserved.

Layered-Intrusive Complexes

Layered mafic-ultramafic intrusions are either sill-like (e.g., Stillwater) or funnel shaped (e.g., Skaergaard and Great Dyke). They are typically intruded into rifted cratons and may be associated with tholeitic flood basalt provinces. A good example of this is the Muskox intrusion, which is intimately associated with Coppermine River basalts (Baragar, 1969; Kerans, 1983).

As magma crystallizes and differentiates, cyclically layered sequences form. An ideal cycle consists of basal dunite followed upward by a harzburgite and an uppermost orthopyroxene layer (Naslund and McBirney, 1996). These cyclic units vary in thickness. For example, in the Bushveld Complex they are present on a millimetre scale (Eales and Cawthorn, 1996), at Great Dyke on a centimetre scale (Naslund and McBirney, 1996), and at Muskox intrusion on a metre scale (Irvine and Smith, 1967). Olivine composition in a typical layered ultramafic intrusion trends upwards in succession from forsterite-rich olivine towards fayalitic olivine (Table 2).

TABLE 2. OLIVINE COMPOSITION CHANGES FROM MG-RICH (FORSTERITE) TO FE-RICH (FAYALITE) FROM LOWER TO UPPER ZONES WITHIN LAYERED INTRUSIVE COMPLEXES.

Name, locality	Olivine composition in lower zone	Olivine composition in upper zone	References
Bjerkreim-Sokndal, Norway	Fo77-74	Fo50-19	Wilson *et al.* (1996)
Bushveld, RSA	Fo85-88	Fo63-35	Eales and Cawthorn (1996)
Great Dyke, Zimbabwe	Fo92	Fo91-87	Wilson (1996)
Skaergaard, Greenland	Fo74-68	Fo10-5	McBirney (1996)
Windimurra, Australia	Fo90-50	Fo35	Mathison and Ahmat (1996)

The layering is commonly laterally continuous for hundreds of square kilometres (Eales and Cawthorn, 1996), and the ultramafic sequence can be up to several kilometres in thickness. For example, the Windimurra Complex has a 0.5 km thick ultramafic section (Mathison and Ahmat, 1996), the Muskox intrusion has ultramafic layers that total 1.5 km in thickness (Irvine and Smith, 1967), and the Great Dyke has an ultramafic sequence several kilometres in thickness (Wilson, 1996).

TECTONIC SETTING OF BC

Since the breakup of the Rodinia supercontinent, BC has been located on a continent-ocean boundary for at least 530 million years (Monger, 1997). As a result of subduction-related activity, which started approximately 390 Ma, the Canadian Cordillera is commonly described as an orogenic collage made up of intra-oceanic arc and subduction complexes accreted to the craton margin and of arcs emplaced in and on the accreted bodies. The Canadian Cordillera has been subdivided into terranes (Figure 4), each consisting of characteristic assemblages (Monger and Berg, 1984).

Assemblages within the Slide Mountain, Cache Creek, and Bridge River Terranes (Figure 4) are of oceanic affinity, representing the deformed sequences of ocean basins that closed in the Mesozoic during the accretion of offshore island arcs to the North American craton. The Slide Mountain Terrane is composed of ultramafic rocks, gabbro, pillow basalt, and chert, which formed in a back-arc ocean basin (Figure 5). The ultramafic rocks in the Cache Creek and Bridge River Terranes are associated with a mélange of marine sediments with blocks, lenses, and slivers of ophiolitic origin, often in a serpentine matrix, representing an accretionary/subduction complex (Figure 5). These oceanic-affiliated terranes contain numerous Alpine-type complexes (Evenchick *et al*., 1986). The Stikinia and Quesnellia Terranes are composed of arc-related volcanic and sedimentary rocks and coeval intrusions (Evenchick *et al*., 1986). BC's Alaskan-type complexes are found in these terranes (Figure 5) and represent the high-level magma chambers of Late Triassic to Middle Jurassic arc volcanoes (Nixon, 1990). There are no large layered intrusive ultramafic complexes known in BC, as they are believed to be restricted to an intra-cratonic tectonic setting.

ULTRAMAFIC ROCKS IN BC

Depicted in Figure 6 is the geographic distribution of ultramafic rocks in BC, with emphasis on those Alpine- and Alaskan-type complexes that contain known dunite and/or serpentinite zones. This map was derived from the database developed for a mineral potential assessment of BC (Kilby, 1994) and was originally introduced in a BC Geological Survey Branch Geofile (Voormeij and Simandl, 2004).

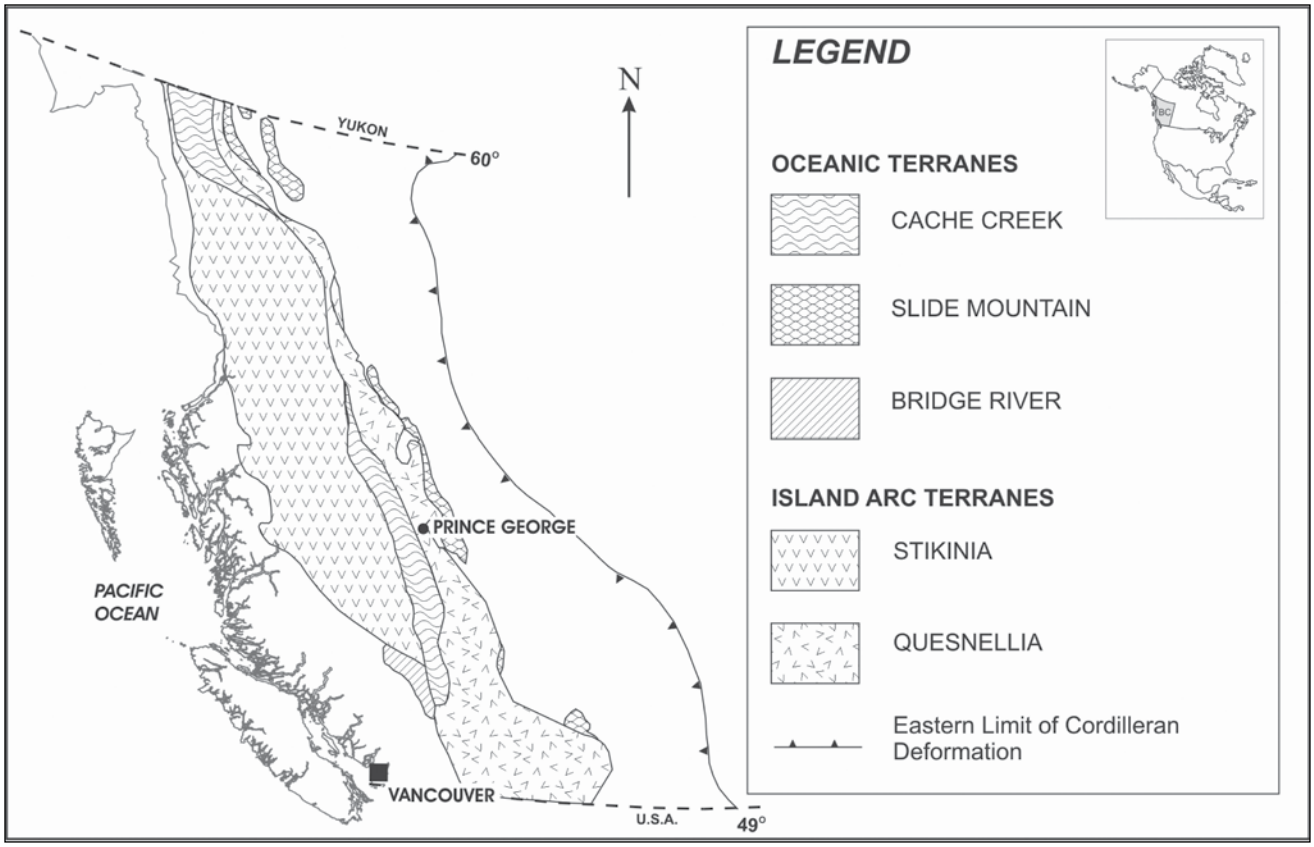

Figure 4. Distribution of major ultramafic-bearing terranes in British Columbia (based on Gabrielse et al., 1991). The Alpine-type ultramafic complexes are confined primarily to the Cache Creek, Slide Mountain, and Bridge River oceanic-affiliated terranes, whereas the Alaskan-type ultramafic bodies are associated with the Stikinia and Quesnellia island-arc terranes.

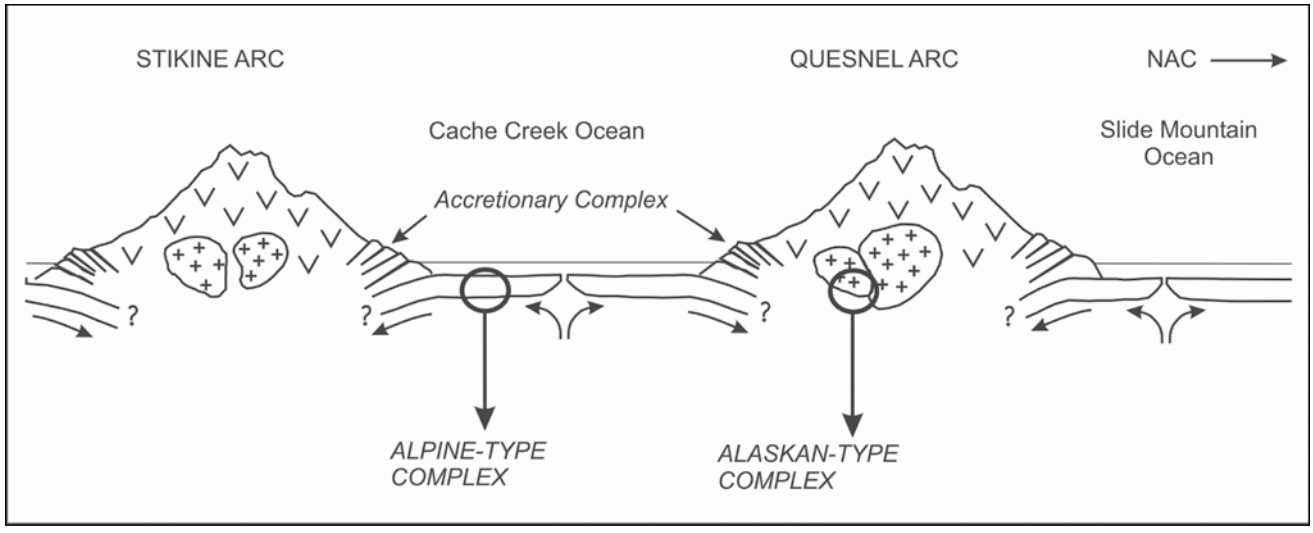

Figure 5. Simplified diagram depicting the different tectonic settings for the oceanic-affiliated, subduction-related, and island arc terranes in British Columbia and the origin of their ultramafic complexes (based on Monger and Journeay, 1994). NAC = North American Continent.

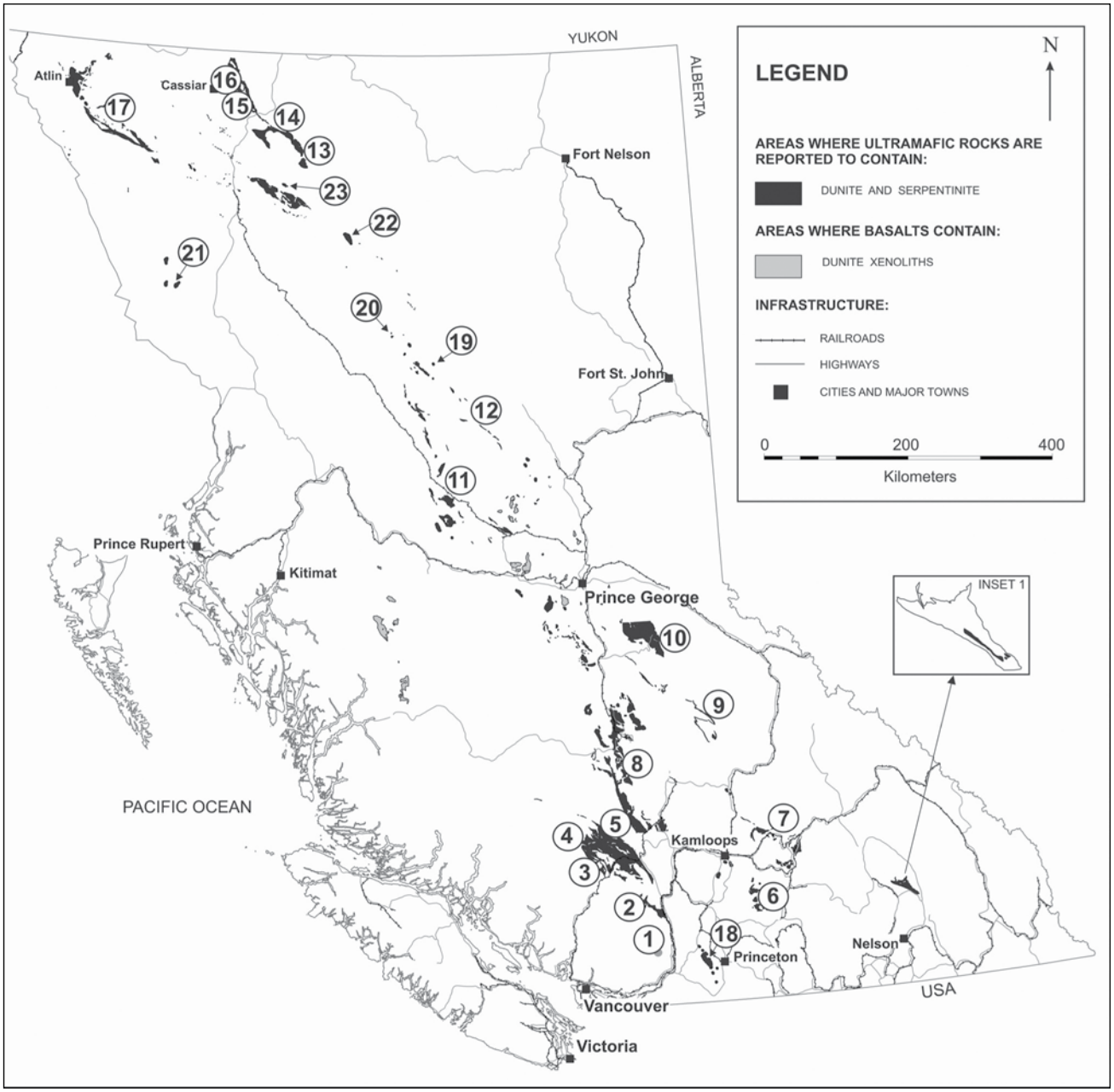

Figure 6. Distribution of dunite and serpentinite-bearing rocks in BC. Alpine-type ultramafic complexes include: 1. Cogburn Emory Zone, 2. Coquihalla Serpentine Belt, 3. Bralorne-East Liza, 4. Bridge River Complex, 5. Shulaps, 6. Chapperon Group, 7. Mount Ida Assemblage, 8. Southern Cache Creek Complex, 9. Crooked Amphibolite, 10. Antler Formation, 11. Central Cache Creek Complex, 12. Manson Lake Complex, 13. Blue Dome Fault Zone, 14. Sylvester Allochthon, 15. Cassiar and McDame, 16. Zus Mountain, 17. Northern Cache Creek Complex (includes Atlin and Nahlin Complexes). Alaskan-type ultramafic complexes include: 18. Tulameen, 19. Polaris, 20. Wrede, 21. Hickman, 22. Lunar Creek, 23. Turnagain.

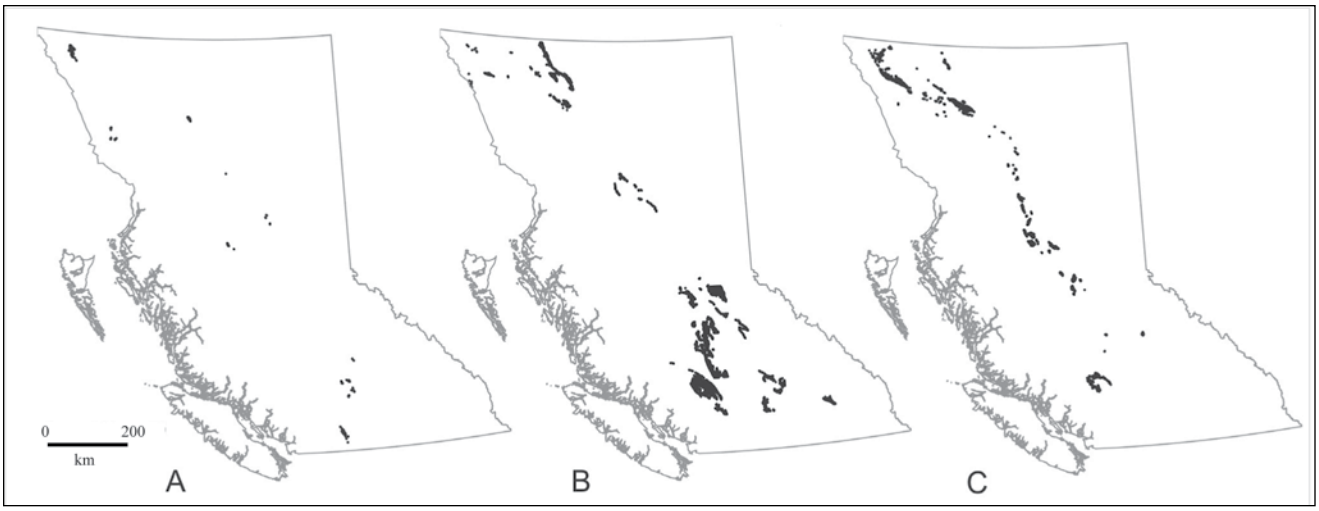

Figure 7. Separating out the dunite and serpentinite zones associated with ultramafic rocks: A. Areas where ultramafic rocks are reported to contain dunite only. B. Serpentinite only. C. Dunite and serpentinite are reported together.

The compiled geology used in Figure 6 has been captured in digital form at a scale of 1:250 000 by means of BC Geological Survey Branch Open File series releases (Massey, 1994; Schiarizza *et al*., 1994; Höy *et al*., 1994; MacIntyre *et al*., 1994; Bellefontaine and Alldrick, 1994; MacIntyre *et al*., 1995; Bellefontaine *et al*., 1995; Mihalynuk *et al*., 1996; Schiarizza and Church., 1996). From this electronic database, units containing the words "dunite" and "serpent-" were extracted, thereby assembling a digital file of zones that contain the words "dunite", "serpentinite", "serpentinized", or "serpentine" in their original description. Figure 6 shows the resulting zones.

Extraction of areas that contain the terms "dunite" and "serpent-" from the database does not discriminate between minor and major amounts of dunite and/or serpentinite present. Thus, most of the zones are overestimates of actual area underlain by dunites and/or serpentinites. For example, Figure 6 shows a zone in southeastern BC, approximately 120 km north of Nelson. This area appears approximately 100 km long by 50 km wide on the map. However, a more detailed map (Figure 6, Inset 1) shows the presence of serpentine-magnesite-talc related rocks only a few kilometres across (source: Read and Wheeler, 1977). Although the approach used to construct Figure 6 results in overestimating the areas underlain by ultramafic rocks, it is a preferred preliminary approach because large portions of BC have not been mapped in detail and may contain more ultramafic rocks than expected. Several potential dunite and serpentinite tracts shown on this map are abruptly terminated along straight lines that correspond to map boundaries. This happens where a geological unit extends across two or more 1:250 000 map sheet areas. This unit may have the same name on several of the mapsheets, but ultramafic rocks are not present in all of them.

Our approach also delineated areas that contain ultramafic xenoliths. For example, numerous zones within central BC correlate to spinel peridotite xenoliths described by Canil *et al.* (1987), many of which are hosted in the alkali basalts typical of the Chilcotin Group plateau-lavas (Dostal *et al*., 1996). The olivine-rich xenoliths are not significant as a potential source of raw material for the ex situ mineral carbonation process. However, recent studies have shown the mineral-trapping potential of injected CO_2 into deep saline aquifers located within thick sequences of flood basalt provinces (O'Connor *et al*., 2003). For this reason, the distribution of BC's flood basalts that contain olivine xenocrysts and dunite xenoliths is included in Figure 6.

Ultramafic rocks containing dunite zones but not serpentinite (Figure 7a) are not common. These zones are mostly restricted to Alaskan-type complexes. In contrast, ultramafic rocks containing serpentine but not dunite are relatively abundant (Figure 7b). As expected from the distribution of ultramafic rocks in Alpine-type complexes, dunite and serpentinite are commonly associated (Figure 7c).

Alpine-Type Complexes in BC

Most of BC's Alpine-type complexes are located within the Cache Creek, Slide Mountain and Bridge River Terranes. The Cache Creek Terrane forms a long narrow tract that extends within the Intermontane belt from southern BC to central Yukon Territory (Figure 4). The larger complexes of the Cache Creek Terrane include the Southern Cache Creek Ultramafic Assemblage in southwestern BC and the Nahlin Ultramafic Complex near Atlin, northwestern BC (Figure 6). The Slide Mountain Terrane forms a narrow, discontinuous belt extending 2000 km from southeastern BC to northwestern Yukon Territory (Figure 4). Alpine-type ultramafics are located in the Antler Formation in central BC, the Redfern and Crooked Amphibolite in east-central BC, and the Sylvester allochthon in north-central BC (Figure 6).

The Cassiar and McDame asbestos deposits are located in Sylvester serpentinites (Figure 6). Zus Mountain, located in the Sylvester allochthon, is known to contain intact oceanic upper mantle and ultramafic cumulate material (Nelson and Bradford, 1993). Bridge River is a small terrane, situated near latitude 52°N, just west of the Cache Creek Terrane. The Bridge River Complex, with the associated Shulaps and Bralorne-East Liza complexes (Figure 6), the Coquihalla Serpentine Belt, and the Cogburn body are probably the southern extent of the Cache Creek Terrane (Schiarizza *et al.,* 1997).

Alaskan-Type Complexes in BC

In BC, Alaskan-type complexes are found in the Stikinia and Quesnellia Terranes. However, only those with a recognized dunite zone are discussed, and their geographical distribution is given in Figure 6. Table 3 gives the major Alaskan-type complexes for BC that contain known dunite cores. Stikinia is the largest terrane in the Canadian Cordillera; it extends more than 1700 km from eastern Alaska to south-central BC (Figure 4). The Hickman Complex is an Alaskan-type ultramafic within Stikinia. The Lunar Creek Complex is located on the boundary between Quesnellia and Stikinia Terranes (Figure 6). Quesnellia forms an orogen-parallel belt that extends from south-central BC into the Yukon Territories (Figure 4). Complexes of the Alaskan type that are located in this terrane include the Tulameen (Figure 3), Polaris, Wrede, and Turnagain complexes. Tulameen is the largest Alaskan-type body in BC (Table 3).

Economic Potential of Ultramafic Rocks in BC

Up to now, BC's ultramafic complexes were primarily of interest to economic geologists in terms of associated metals, traditional industrial mineral deposits, and gemstones. These complexes are known to host Cyprus-type massive sulphides (Höy, 1995), Au-quartz veins (Ash and Alldrick, 1996), silica-carbonate mercury deposits (Ash, 1996a), podiform chromite (Ash, 1996b), stratiform chromite (Nixon *et al*., 1997), talc and magnesite (Simandl and Ogden, 1999), chrysotile asbestos (Hora, 1999), nephrite jade (Simandl *et al*., 2000), vermiculite (Simandl *et al*., 1999a), emeralds (Simandl *et al*., 1999b), and corundum-group gemstones (Simandl and Paradis, 1999). Also, they are known to host platinum-group elements (Rublee, 1986; Evenchick *et al*., 1986; Nixon, 1990; Nixon, 1996; Nixon *et al*., 1997), Ti and Fe oxide deposits (Gross *et al*., 1999), and nickel (Hancock, 1990). Olivine may be used as a foundry and blasting sand (White, 1987) as well as a raw material in the manufacture of refractories (Henning, 1994). In the past, most of the complexes were assessed with these commodities in mind; however, should mineral sequestration of CO_2 emissions become a reality, then these complexes will also become essential as sources of high-magnesia silicates. The synergy between the development of some of the traditional metal, industrial mineral, and gemstone commodities and magnesium silicates for CO_2 sequestration may be possible.

TABLE 3. SURFACE AREA OF DUNITE ZONES IN ALASKAN-TYPE COMPLEXES. ARC-RELATED TECTONOSTRATIGRAPHIC TERRANES WITHIN WHICH THESE COMPLEXES ARE LOCATED: QN = QUESNELLIA; ST = STIKINIA.

Complex Name	Terrane	Aerial Extent of Complex	Surface Area of Dunite zone	References
Hickman	ST	~11 km^2	< 1 km^2	Nixon *et al*. (1997)
Lunar Creek	QN	~45 km^2	~ 1.5 km^2	Nixon *et al*. (1997)
Polaris	QN	~50 km^2	~8-9 km^2	Nixon *et al.* (1997)
Tulameen	QN	~ 60 km^2	~ 6 km^2	Findlay (1963); Nixon *et al.* (1997)
Turnagain	QN	~25 km^2	~ 5 km^2	Clark (1980); Gabrielse
Wrede	QN	~10 km^2	~ 5km^2	Hammack *et al.* (1990)

Targets for Mineral Sequestration of CO2

Figure 6 also marks two specific areas considered for detailed study as part of the M.Sc. thesis of the senior author: the Tulameen site and the Cassiar asbestos. The Tulameen site was chosen because it contains a well-exposed, large (6 km^2), relatively unserpentinized dunite body and is located within the vicinity of several major point sources of CO_2 (Voormeij and Simandl, 2003b). Cassiar asbestos tailings, currently owned by Cassiar Resources Inc., are investigated because the waste piles have potential as raw material for the mineral carbonation process, since the serpentine has already been milled and therefore may lower the sequestration costs. The site contains 5 457 000 tonnes of broken rock, 17 021 000 tonnes of tailings, and 48 millions of tonnes of in situ serpentine-rich rock (Budinski, 2000). The fibrous nature of this variety of serpentine, which is considered a health concern (Hamel, 1998), may be effectively destroyed during the mineral carbonation process.

CONCLUSIONS

Should the mineral carbonation process be considered as a form of sequestering CO_2 emissions in BC, an overview of locations of raw material within the vicinity of major CO_2 point sources is an important parameter in conceptual modeling. The distribution of ultramafic rocks in BC, with emphasis on those complexes containing dunite and/or serpentinite zones, is depicted in Figure 6. Based on this map, less than 3% of BC's surface is underlain by

ultramafic rocks containing dunite and/or serpentinite. Of this 3%, less than 1% corresponds to areas where dunite is reported without serpentinite, approximately 2% is related to areas where serpentinite occurs without dunite, and 1% of BC is underlain by ultramafic rocks where dunite and serpentinite are reported together. Because of the methodology used to construct the map, surface areas corresponding to ultramafic rocks are overestimated.

Due to the subduction-related tectonic setting, Alpine-type and Alaskan-type ultramafic complexes are more common along the western margin of North America than they are in, for example, areas located on the stable craton or passive margin. With this in mind, claims made by Goff et al. (1997) and Goff and Lackner (1998), in which they state that "abundant resources of Mg-rich peridotite [dunite] and serpentinite exist within the United states and many other countries", should be questioned, and follow-up is needed.

Ultramafic complexes may host a wide variety of economic minerals. Thus, the geographic distribution of dunites and serpentinites can be used as a metallotect in exploration for a variety of metallic, industrial mineral, and gemstone deposits. In a number of specific cases, serpentine- and olivine-bearing rocks contain chromite, Ni, Co, and platinum-group elements. If these commodities can be recovered at profit as a by-product of mineral sequestration, then costs of the CO_2 disposal may be substantially reduced.

ACKNOWLEDGEMENTS

Special thanks to Don McIntyre, who was essential in manipulating the British Columbia Mineral Potential database to produce Figure 6. Thanks to Derek Brown from New Ventures for his interest and financial support. Joanne Nelson and Graham Nixon read early versions of this manuscript and provided useful and constructive criticism.

REFERENCES

Ash, C. (1996a): Silica-Carbonate Hg; *In*: Selected British Columbia Mineral Deposit Profiles, Volume 2, Metallic Deposits, D.V. Lefebure and T. Höy (eds.), *British Columbia Ministry of Energy and Mines*, pages 75-76.

Ash, C. (1996b): Podiform Chromite; *In*: Selected British Columbia Mineral Deposit Profiles, Volume 2, Metallic Deposits, D.V. Lefebure and T. Höy (eds.), *British Columbia Ministry of Energy and Mines*, pages 109-111.

Ash, C. and Alldrick, D. (1996): Au-Quartz Veins; *In*: Selected British Columbia Mineral Deposit Profiles, Volume 2, Metallic Deposits, D.V. Lefebure and T. Höy (eds.), *British Columbia Ministry of Energy and Mines*, pages 53-56.

Baragar, W. R. A. (1969): The Geochemistry of Coppermine River asalts, *Geological Survey of Canada, Paper* 69-44, 43 pages.

Bellefontaine, K., Legun, A., Massey, N.W.D. and Desjardins, P. (1995): Mineral Potential Project, Digital Geological Compilation NEB.C. South Half, *Geological Survey Branch Open File* 1995-24.

Bellefontaine, K. and Alldrick, D. (1994): Midcoast Arcview Data, *Geological Survey Branch Open File* 1994-17.

Budinski, D. (2000): Chrysotile Resources at Cassiar Mine, *Orcan Consulting Report*, February 15th, 2000.

Canil, D., Brearly, M. and Scarfe, C.M. (1987): Petrology of Ultramafic Xenoliths from Rayfield River, Southcentral British Columbia, *Canadian Journal of Earth Sciences*, v. 24, pages 1679-1687.

Clark, T. (1980): Petrology of the Turnagain Ultramafic Complex, Northwestern British Columbia, *Canadian Journal of Earth Sciences*, v. 17, pages 744-757.

Coleman, R.G. (1977): Ophiolites, *Springer-Verlag*, New York: 229 pages.

Deer, W.A., Howie, R.A and Zussman, J. (1978): An Introduction to the Rock Forming Minerals, Longman Group Ltd., London, 528 pages.

Dewey, J.F. (1976): Ophiolite Obduction, *Tectonophysics,* v. 31, pages 93-120.

Dostal, J., Hamilton, T.S., Church, B.N. (1996): The Chilcotin Basalts, British Columbia (Canada): Geochemistry, Petrogenesis and Tectonic Significance; *Neues Jarhbuch Fur Mineralogie Abhandlungen*, v. 170, no. 2, pages 207-229 (GSC Cont.# 40495).

Eales, H.V. and Cawthorn, R.G. (1996): The Bushveld Complex, *In*: R.G. Cawthorn (ed.), Layered Intrusions, *Elsevier Science*, pages 181-229.

Evenchick, C.A., Friday, S.J. and Monger, J.W.H. (1986): Potential Hosts to Platinum Group Element Concentrations in the Canadian Cordillera, *Geological Survey of Canada, Open File 1433*.

Findlay, D.C. (1963): Petrology of the Tulameen Ultramafic Complex, Yale District, British Columbia. Unpublished Ph.D. Thesis, *Queens University*, 415 pages.

Gabrielse, H. (1998): Geology of Cry Lake and Dease Lake Map Areas, North-Central British Columbia, *Geological Survey of Canada, Bulletin* 504, 147 pages

Gabrielse, H., Monger, J.W.H., Wheeler, J.O. and Yorath, C.J. (1991): Morphogeological Belts, Tectonic Assemblages and Terranes, Chapter 2, Part A, of Geology of the Cordilleran Orogen in Canada, Geology of Canada, no. 4, *Geological Survey of Canada*, pages 15-28.

Goff, F. and Lackner, K.S. (1998): Carbon Dioxide Sequestering Using Ultramafic Rocks, *Environmental Geosciences*, 5, 3, pages 89-101.

Goff, F., Guthrie, G., Counce, D., Kluk, E., Bergfeld, D. and Snow, M. (1997): Preliminary Investigations on the Carbon Dioxide Sequestering Potential of Ultramafic Rocks, *Los Alamos National Laboratory*, LA-13328 MS, 22 pages.

Gross, G.A., Gower, C.F. and Lefebure, D.V. (1999): Magmatic Ti-Fe +/-V Oxide Deposits, *In*: Selected British Columbia Mineral Deposit Profiles, Volume 3, Industrial Minerals and Gemstones, G.J. Simandl, Z.D. Hora and D.V. Lefebure (eds.), *British Columbia Ministry of Energy and Mines*, pages 57-60.

Hamel, D. (1998): Utilization of Chrysotile Asbestos; Lessons from Experiences, In: Proceedings of the 33rd Forum on the Geology of Industrial Minerals, Canadian Institute of Mining and Metallurgy Special Volume 50, pages 121-129.

Hammack, J.L., Nixon, G.T., Wong, R.H. and Paterson, W.P.E. (1990): Geology and Noble Metal Geochemistry of the Wrede Creek Ultramafics Complex, North-Central British Columbia; Geological Fieldwork 1989, B.C. Ministry of Energy, Mines, and Petroleum Resources, Paper 1990-1, pages 405-416.

Hancock, K.D. (1990): Ultramafic Associated Chrome and Nickel Occurrences in British Columbia; B.C. Ministry of Energy, Mines and Petroleum Resources, Open File 1990- 27, 62 pages

Henning, R.J. (1994): Olivine and Dunite, In: Industrial minerals and Rocks, 6th Edition, D. D. Carr (ed.), 1196 pages

Hora, Z.D. (1999): Ultramafic-Hosted Chrysotile Asbestos, In: Selected British Columbia Mineral Deposit Profiles, Volume 3, Industrial Minerals and Gemstones, G.J. Simandl, Z.D. Hora and D.V. Lefebure (eds.), British Columbia Ministry of Energy and Mines, pages 61-64.

Höy, T. (1995): Cyprus Massive Sulphide Cu (Zn), In: Selected British Columbia Mineral Deposit Profiles, Volume 1, Metallics and Coal, D.V. Lefebure and G.E. Ray (eds.), British Columbia Ministry of Energy and Mines, pages 51-52.

Höy, T., Church, B.N., Legun, A., Glover, K., Gibson, G., Grant, B., Wheeler, J.O. and Dunne, K.P.E. (1994): Kootenay Area, Geological Survey Branch Open File 1994-8.

Huot, F., Beaudoin, G., Hebert, R., Constantine, M., Bonin, G. and Dipple, G.M. (2003): Evaluation of Southern Quebec Asbestos Residues for CO2 Sequestration by Mineral Carbonation; Preliminary Result, Abstract, GAC-MAC-SEG Conference, Vancouver, 2003.

Irvine, T.N. (1987): Layering and Related Structures in the Duke Island and Skaergaard Intrusions: Similarities, differences, and Origins, In: Origins of Igneous Layering, I. Parsons (ed.), D. Reidel Publishing Company, pages 185-243.

Irvine, T.N. (1976): Alaskan-type ultramafic-gabbroic bodies in the Aiken Lake, McConnel Creek, and Toodoggone map-areas, geological Survey of Canada Paper, 76-1A, pages 76-81.

Irvine, T.N. (1967): The Duke Island Ultramafic Complex, Southeastern Alaska: In: Ultramafic and Related Rocks, P.J. Wyllie (ed.); John Wiley & Sons, Inc., N.Y., pages 84-96.

Irvine, T.N. and Smith, C.H. (1967): The Ultramafic Rocks of the Muskox Intrusion, NWT, Canada: In: Ultramafic and Related Rocks, P.J. Wyllie (ed.); John Wiley & Sons,Inc., N.Y., pages 38-49.

Kakizawa, M., Yamasaki, A. and Yanagisawa, Y. (2001): A New CO2 Disposal Process Using Artificial Rock Weathering of Calcium Silicate Accelerated by Acetic Acid, Energy, v.26, pages 341-354.

Kerans, C. (1983): Timing and Emplacement of the Muskox Intrusion: Constraints from Coppermine Homocline Cover strata, Canadian Journal of Earth Sciences, 20, 5, pages 673-683.

Kilby, W.E. (1994): Mineral Potential Project-Overview, Geological Fieldwork, Paper 1995-1, pages 411-416.

Kohlmann, J., Zevenhoven, R. and Mukherjee, A.B. (2002): Carbon Dioxide Emission Control by Mineral Carbonation: The Option for Finland, Proceedings of the 6th European Conference on Industrial Furnaces and Boilers, Estoril Lisbon, Portugal.

Kohlmann, J. and Zevenhoven, R. (2001): The Removal of CO2 from Flue Gases Using Magnesium Silicates, in Finland, Proceedings of the 11th International Conference on Coal Science, San Francisco, California.

Lackner, K.S., Butt, D.P. and Wendt, C.H. (1997): Magnesite Disposal of Carbon Dioxide, Proceedings of the 22nd International Technical Conference on Coal Utilization & Fuel Systems, Clearwater Florida, pages 419-430.

MacIntyre, D., Legun, A., Bellefontaine, K. and Massey, N.W.D. (1995): Northeast B.C. Mineral Potential Project, Geological Survey Branch Open File 1995-6.

MacIntyre, D., Ash, C. and Britton, J. (1994): Nass-Skeena, Geological Survey Branch Open File 1994-14.

Le Maitre, R.W., Editor (1989): A Classification of Igneous Rocks and Glossary of Terms, Blackwell Scientific Publishing Company: 193 pages

Massey, N.W.D. (1994): Vancouver Island, Geological Survey Branch Open File 1994-6.

Mathison, C.I. and Ahmat, A.L. (1996): The Windimurra Complex, Western Australia, In: R.G. Cawthorn (ed.), Layered Intrusions, Elsevier Science, pages 485-509.

McBirney, A.R. (1996): the Skaergaard Intrusion, In: R.G. Cawthorn (ed.), Layered Intrusions, Elsevier Science, pages 147-179.

McKelvy, M.J., Chizmeshya, A.V.G., Bearat, H., Sharma, R. and Carpenter, R.W. (2002): Developing a Mechanistic Understanding of CO2 Minerals Sequestration Reaction Processes, Proceedings of the 26th International Technical Conference on Coal Utilization & Fuel Systems, Clearwater, Florida, 2001, 13 pages

Mihalynuk, M., Bellefontaine, K., Brown, D., Logan, J., Nelson, J., Legun, A. and Diakow, L. (1996): Digital Geology, NW British Columbia, Geological Survey Branch Open File 1996-11.

Monger, J.W.H. (1997): Plate Tectonics and Northern Cordillera Geology: An Unfinished Revolution, Geoscience Canada, 24, 4, pages 189-198.

Monger, J.W.H. and Journeay, J.M. (1994): Guide to the Geology and Tectonic Evolution of the Southern Coast Mountains, Geological Survey of Canada Open File 2490, 77 pages plus maps.

Monger, J.W.H. and Berg, H.C. (1984): Lithotectonic Terrane Map of Western Canada and Southeastern Alaska, In: Lithotectonic terrane maps of the North American Cordillera, Silberling, N.J. and Jones, D.L. (eds.), Open File Report - U.S. Geological Survey, pages B1-B31.

Moores, E.D. (2002): Pre-1 Ga (pre-Rodinian) Ophiolites: Their Tectonic and Environmental Implications, GSA Bulletin, v. 114, no. 1, pages 80-95.

Moores, E.D. (1982): Origin and Emplacement of Ophiolites, Review of Geophysics and Space Physics, v. 20, no. 4., pages 735-760.

Naslund, H.R., and McBirney A.R. (1996): Mechanisms of Formation of Igneous Layering, In: Cawthorn, R.G. (Ed.), Layered Intrusions, Elsevier, pages 1-43.

Nelson, J.L. and Bradford, J.A. (1993): Geology of the Midway-Cassiar Area, Northern British Columbia (104O, 104P), Geological Survey Branch, Bulletin 83, 94 pages

Nixon, G.T., Hammack, J.L., Ash, C.H., Cabri, L.J., Case, G., Connelly, J.N., Heaman, L.M., Laflamme, J.H.G., Nuttall, C., Paterson, W.P.E. and Wong, R.H. (1997): Geology and Platinum-Group-Element Mineralization of Alaskan-Type Ultramafic-Complexes in British Columbia, Geological Survey Branch, Bulletin 93, 142 pages

Nixon, G.T. (1996): Alaskan-Type Pt ±Os ±Rh ±Ir; In: Selected British Columbia Mineral Deposit Profiles, Volume 2, Metallic Deposits, D.V. Lefebure and T. Höy (eds.), British Columbia Ministry of Energy and Mines, pages 109-111.

Nixon, G.T. (1990): Geology and Precious Metal Potential of Mafic-Ultramafic Rocks in British Columbia: Current Progress, Geologic Fieldwork, 1989, Paper 1990-1, pages 353-358.

O'Connor, W.K., Rush, G.E., Dahlin, D.C., Reidel, S.P. and Johnson, V.G. (2003): Geological Sequestration of CO2 in the Columbia River Basalt Group, Proceedings for the 28th International Technical Conference on Coal Utilization &Fuel Systems**,** Clearwater, Florida, 12 pages

O'Connor, W.K., Dahlin, D.C., Nilsen, D.N., Walters, R.P. and Turner, P.C. (2000): Carbon Dioxide Sequestration by Direct Mineral Carbonation with Carbonic Acid, Proceedings of the 25th International Technical Conference on Coal Utilization & Fuel Systems, Coal Technology Association, Clearwater, Florida.

O'Connor, W.K., Dahlin, D.C., Turner, P.C. and Walters, R.P. (1999): Carbon Dioxide Sequestration by Ex-Situ Mineral Carbonation, Proceedings of the 2nd Dixy Lee Ray Memorial Symposium: Utilization of Fossil Fuel-Generated Carbon Dioxide in Agriculture and Industry, Washington, D.C.

Read, P.B. and Wheeler, J.O. (1977): Geology, Lardeau, West-half, Geological Survey of Canada, Open File 432, map scale 1:125,000.

Rublee, V.J. (1986): Occurrence and Distribution of Platinum-Group Elements in British Columbia, B.C. Ministry of Energy, Mines, and Petroleum Resources, Open File 1986-7,94 pages

Schiarizza, P., Gaba, R.G., Glover, J.K., Garver, J.I. and Umhoefer, P.J. (1997): Geology and Mineral Occurrences of the Taseko-Bridge River Area, Geological Survey Branch Bulletin 100, 292 pages

Schiarizza, P. and Church, N. (1996): (East Part) the Geology of the Thompson-Okanagan Mineral Assessment Region, Geological Survey Branch Open File 1996-20.

Schiarizza, P., Panteleyev, A., Gaba, R.G. and Glover, J.K. (1994): Cariboo-Chilcotin Area, Geological Survey Branch Open File 1994-7.

Seifritz, W. (1990): CO2 Disposal by Means of Silicates, Nature, 345, pages 486.

Simandl, G.J., Riveros, C.P. and Schiarizza, P. (2000): Nephrite (jade) deposits, Mount Ogden Area, Central British Columbia (NTS 093N 13W), Geological Survey Branch, Geological Fieldwork 1999, pages 339-347.

Simandl, G.J. and Ogden, D. (1999): Ultramafic-Hosted Talc-Magnesite, In: Selected British Columbia Mineral Deposit Profiles, Volume 3, Industrial Minerals and Gemstones, G.J. Simandl, Z.D. Hora and D.V. Lefebure (eds.), British Columbia Ministry of Energy and Mines, pages 65-68.

Simandl, G.J. and Paradis, S. (1999): Ultramafic-Related Corundum, In: Selected British Columbia Mineral Deposit Profiles, Volume 3, Industrial Minerals and Gemstones, G.J. Simandl, Z.D. Hora and D.V. Lefebure (eds.), British Columbia Ministry of Energy and Mines, pages 123-127.

Simandl, G.J. Birkett, T. and Paradis, S. (1999a): Vermiculite, In: Selected British Columbia Mineral Deposit Profiles, Volume 3, Industrial Minerals and Gemstones, G.J. Simandl, Z.D. Hora and D.V. Lefebure (eds.), British Columbia Ministry of Energy and Mines, pages 69-72

Simandl, G.J., Paradis, S. and Birkett, T. (1999b): Schist-Hosted Emeralds, In: Selected British Columbia Mineral Deposit Profiles, Volume 3, Industrial Minerals and Gemstones, G.J. Simandl, Z.D. Hora and D.V. Lefebure (eds.), British Columbia Ministry of Energy and Mines, pages 113-117.

Virta, R.L. and Mann, E.L. (1994): Asbestos, In: Donald D. Carr (ed.), Industrial Minerals and Rocks, 6th Edition, pages 97-124.

Voormeij, D.A. and Simandl, G.J. (in prep): CO2 sequestration Potential of the Tulameen Ultramafic Complex, British Columbia, Canada.

Voormeij, D.A. and Simandl, G.J. (2004): Ultramafic Rocks in British Columbia- Applications in CO2 Sequestration and Mineral Exploration, Geological Survey Branch, Geofile 2004-1.

Voormeij, D.A. and Simandl, G.J. (2003a): Geological and Mineral CO2 Sequestration Options for British Columbia: A Technical Review, Geological Fieldwork 2002, Paper 2003-1, pages 265-282.

Voormeij, D.A. and Simandl, G.J. (2003b): CO2 Sequestration Options for B.C.: Matching Sinks and Sources, Geological Survey Branch, Geofile 2003-11.

White, G.V. (1987): Olivine Potential in the Tulameen Ultramafic Complex: Preliminary Report, Geological Fieldwork 1986, Paper 1987-1, pages 303-307.

Wilson, A.H. (1996): The Great Dyke of Zimbabwe, In: R.G. Cawthorn (ed.), Layered Intrusions, Elsevier Science, pages 365-401.

Wilson, J.R., Robins, B., Nielsen, F.M., Duchesne, J.C. and Vander Auwera, J. (1996): the Bjerkreim-Sokndal Layered Intrusion, Southwest Norway, In: R.G. Cawthorn (ed.), Layered Intrusions, Elsevier Science, pages 231-255.

Wu, J.C.S., Sheen, J.D., Chen, S.Y. and Fan, Y.C. (2001): Feasibility of CO2 Fixation via Artificial Rock Weathering, Ind. Eng. Chem. Res., v. 40, pages 3902-3905.